

Facsimile Price $ 26.00
Microfilm Price $ 18.20

Available from the
Office of Technical Services
Department of Commerce
Washington 25, D. C.

NYO-9791 (Book 10)

SURVEY OF COMPONENT REQUIREMENTS AND AVAILABILITY FOR GAS-COOLED NUCLEAR REACTOR POWER PLANTS

Compressors and Turbines

By
Georgs Novickis

April 1962

Laboratories for Research and Development
The Franklin Institute
Philadelphia, Pennsylvania

UNITED STATES ATOMIC ENERGY COMMISSION • DIVISION OF TECHNICAL INFORMATION

DISCLAIMER

This report was prepared as an account of work sponsored by an agency of the United States Government. Neither the United States Government nor any agency thereof, nor any of their employees, makes any warranty, express or implied, or assumes any legal liability or responsibility for the accuracy, completeness, or usefulness of any information, apparatus, product, or process disclosed, or represents that its use would not infringe privately owned rights. Reference herein to any specific commercial product, process, or service by trade name, trademark, manufacturer, or otherwise does not necessarily constitute or imply its endorsement, recommendation, or favoring by the United States Government or any agency thereof. The views and opinions of authors expressed herein do not necessarily state or reflect those of the United States Government or any agency thereof.

DISCLAIMER

Portions of this document may be illegible in electronic image products. Images are produced from the best available original document.

Other issues of this report bear the number I-A 2392-6.

LEGAL NOTICE

This report was prepared as an account of Government sponsored work. Neither the United States, nor the Commission, nor any person acting on behalf of the Commission:

A. Makes any warranty or representation, expressed or implied, with respect to the accuracy, completeness, or usefulness of the information contained in this report, or that the use of any information, apparatus, method, or process disclosed in this report may not infringe privately owned rights; or

B. Assumes any liabilities with respect to the use of, or for damages resulting from the use of any information, apparatus, method, or process disclosed in this report.

As used in the above, "person acting on behalf of the Commission" includes any employee or contractor of the Commission, or employee of such contractor, to the extent that such employee or contractor of the Commission, or employee of such contractor prepares, disseminates, or provides access to, any information pursuant to his employment or contract with the Commission, or his employment with such contractor.

This report has been reproduced directly from the best available copy.

Printed in USA. This report consists of 2 books, total price $7.00. Available from the Office of Technical Services, Department of Commerce, Washington 25, D. C.

USAEC Division of Technical Information Extension, Oak Ridge, Tennessee

THE FRANKLIN INSTITUTE • *Laboratories for Research and Development*

I-A2392-6

SURVEY OF COMPONENT REQUIREMENTS AND AVAILABILITY FOR GAS-COOLED NUCLEAR REACTOR POWER PLANTS

COMPRESSORS AND TURBINES

by

Georgs Novickis

April 1962

Prepared for

U.S. ATOMIC ENERGY COMMISSION
Contract AT (30-1)-2512

ABSTRACT

Closed-cycle gas turbines have a great potential for producing a highly efficient nuclear power plant. Such turbines are now being developed for three applications: the HTRE program (Heat Transfer Reactor Experiment) for nuclear aircraft propulsion, the MGCR program (Marine Gas Cooled Reactor) for nuclear marine propulsion, and the ML-1 (Mobile Low-Power Gas-Cooled Nuclear Power Plant) for nuclear electric power generation in an Army mobile power plant as part of the Army Gas-Cooled Reactor Systems Program (AGCRSP).

Much information can be learned from existing non-nuclear gas turbines. We examined some characteristics of several non-nuclear gas turbines as well as gas turbine prime movers of 18 notable U.S. gas-cooled nuclear power plant projects. Turbine and compressor performance, performance improvement, full-load and part-load operation, maintenance, component life, and reliability are discussed. Consideration is given to factors affecting structural integrity of turbomachinery, such as choice of proper materials, vibrations, cooling, and construction features.

The material reported in this summary is based on information obtained in part from the references appended to the report and in part from the data requested from some 60 manufacturers.

Delete Thurnt

SUMMARY

Closed-cycle gas turbines have a great potential for producing a highly efficient nuclear power plant. Such turbines are now being developed for three applications: the HTRE program (Heat Transfer Reactor Experiment) for nuclear aircraft propulsion, the MGCR program (Marine Gas Cooled Reactor) for nuclear marine propulsion, and the ML-1 program (Mobile Low-Power Gas-Cooled Nuclear Power Plant) for nuclear electric power generation in an Army mobile power plant. The ML-1 plant, now nearing completion, will be the first U. S. nuclear power plant with a gas turbine as a prime mover. It will use nitrogen as coolant.

Much can be learned from existing non-nuclear gas turbines which are used today in practically every type of application. Compressor types are radial flow, axial flow, mixed flow, rotary piston, or free piston while turbines are radial, axial or mixed flow. Of some 700 turbine installations, we examined the characteristics of about 30. Largest turbine is a 53,000-hp unit while the smallest turbine is a 70-lb thrust unit. Largest domestic gas turbine manufacturers are General Electric Co. and Westinghouse Electric Corp. The operating experiences of interest are turbine performance, compressor performance, component life, maintenance, performance improvement, and reliability. A general trend in the future development of gas turbines is toward higher efficiency, longer life, and greater reliability combined with simplicity.

The design of nuclear turbomachines will always be more conservative compared with gas turbines in other applications. It is affected by the properties of the coolant or working fluid which must be given due consideration. We have examined gas turbine prime movers of 18 notable U. S. gas-cooled nuclear power-plant projects. Included are the turbines by Westinghouse Electric Corp. for the MGCR and by Clark Bros. Co. and Stratos Division of Fairchild Corp.* for the ML-1.

The basic process of converting kinetic energy to shaft work is expressed by Euler's equation. We have repeated the specific equations for torque, power transfer, and energy transfer for centrifugal and axial compressors as well as for axial and mixed flow turbines. Other important relationships concern turbine efficiencies. If these relationships are to be applied to models, scale factors must be introduced. Optimum performance in these machines can be attained when we understand the thermal and aerodynamic aspects of operation. To permit the designer to arrive at an optimum design, we discussed the design considerations for the various types of compressor and turbine.

*Now, Stratos Division, Fairchild-Stratos Corp.

Characteristic parameters of turbomachinery include turbine velocity ratio, pressure coefficient, flow factor, specific speed, Reynolds number, and Mach number. One method of obtaining these values from similarity relations has been employed. The use factor must also be considered to evaluate service performance. Further, compressors and turbines, being directly interrelated, must be matched in weight flows, pressure ratios, speeds, etc. A complete analysis consists not only of matching under static conditions but also under dynamic ones to make sure that operation is stable. It is also necessary to investigate part-load operation. Off-design performance conditions include compressor surging, excessive temperatures, excessive speeds, and such control functions as starting and stopping.

The factors which affect structural integrity of turbomachinery are complex. The first of these is choice of proper materials. While the technology of ceramics and refractory metals has not yet been mastered, superalloys are now available which serve up to 2000°F. In addition to temperature, both mechanical and thermal stresses affect machinery life to a large extent. Vibrations, on the other hand, are a problem which is more readily solved. The main components from a design standpoint are rotors, disks, blades, casings, and fastening devices. One way to allow for increased turbine inlet temperature beyond material imposed limitations is by cooling. Among various methods attempted, the three main ones employ rim cooling, hollow blade air cooling, and liquid cooling. Descriptions of detailed construction features of ML-1 and MGCR turbines serve as examples of current practice.

In addition to the test facilities at manufacturing plants, there exist a number of special research centers in which gas turbine tests are performed. Some of these facilities are described.

The material reported in this summary is based on information obtained in part from the references appended to the report and in part from the data supplied by manufacturers. We solicited data from some 60 manufacturers and recorded the data received on two types of blanks, Sheet A for availability and Sheet B for capability.

The list of manufacturers plus the data submitted are included in the report. Analysis of the data indicates that several areas remain for future development: materials, bearings and seals, special valves, and aerodynamics of turbomachines for gases other than air, particularly at higher reactor outlet temperatures than presently used.

TABLE OF CONTENTS

		Page
	ABSTRACT	i
	SUMMARY	ii
	NOMENCLATURE	viii
1.	INTRODUCTION	1
	1.1 General	1
	1.2 Review of Turbomachinery in Use	3
	1.2.1 Nuclear Aircraft Propulsion	3
	1.2.2 Nuclear Marine Propulsion	5
	1.2.3 Nuclear Electric Power Generation in an Army Mobile Power Plant	7
2.	NON-NUCLEAR GAS TURBINES	11
	2.1 General	11
	2.2 Summary of Features of Operating Plants	19
	2.3 Operating Experience	45
	2.3.1 Turbine Performance	45
	2.3.2 Component Performance	49
	2.3.3 Component Life	62
	2.3.4 Maintenance	63
	2.3.5 Performance Improvement	70
	2.3.6 Reliability	74
	2.4 Compressor Types	79
	2.4.1 Radial Compressors	79
	2.4.2 Mixed Flow Compressors	87
	2.4.3 Axial Flow Compressors	88
	2.4.4 Rotary Piston Compressors	89
	2.4.5 Free Piston Compressors	92
	2.5 Turbine Types	98
	2.5.1 Radial Turbines	98
	2.5.2 Axial Turbines	98
	2.6 Types of Arrangement	101
	2.7 Future Developments	104

TABLE OF CONTENTS (Cont.)

		Page
3.	NUCLEAR GAS TURBINES	110
	3.1 General	110
	3.2 Requirements of Nuclear Turbomachinery	110
	3.3 Power Plant Studies	121
	3.3.1 Plant Details	121
	3.3.2 ML-1	139
	3.3.3 MGCR	153
	3.4 Future Developments	163
4.	PHYSICAL AND MATHEMATICAL RELATIONSHIPS	165
	4.1 Basic Relationships	165
	4.2 General Relations for Compressors and Turbines	167
5.	THERMO-AERODYNAMIC ASPECTS	182
	5.1 Hydraulic Efficiency of Turbomachines	182
	5.1.1 General	182
	5.1.2 Total Efficiency	182
	5.1.3 Hydraulic Efficiency	183
	5.1.4 Optimum Obtainable Efficiency	187
	5.1.5 Evaluation of Model Tests	189
	5.2 Radial and Mixed-Flow Compressors	195
	5.3 Axial Flow Compressors	212
	5.3.1 Subsonic Compressors	212
	5.3.2 Transonic Compressors	216
	5.3.3 Supersonic Compressors	226
	5.4 Axial Flow Turbines	229
	5.5 Radial Flow Turbines	235
	5.6 Stratos TCS-670 Turbine-Compressor Set	245
	5.7 Clark CSN-1 Turbine-Compressor Set	249
	5.8 MGCR Turbine-Compressor Set	265
	5.8.1 Compressor Performance	265
	5.8.2 Compressor Development	269
	5.8.3 Turbine	272
	5.8.4 Turbine Model Test	278
	5.8.5 Turbine Inlet Scroll	282
	5.9 Influence of Gas Properties in Closed Cycles	285

TABLE OF CONTENTS (Cont.)

Page

6. CHARACTERISTIC PARAMETERS OF TURBOMACHINERY 291

6.1 General 291
6.2 Similarity Parameters for Turbine Design. 292
6.3 Similarity Parameters for Compressor Design 295
6.4 Performance Presentation. 298

6.4.1 Turbines 298
6.4.2 Compressors. 299
6.4.3 Use Factors. 299
6.4.4 Optimum Flow Rates and Tip Speeds. 303

7. MATCHING OF TURBOMACHINERY 305

8. PART-LOAD OPERATION AND CONTROL. 314

8.1 Part-Load Conditions. 314
8.2 Controls for Gas Turbine Functions. 318
8.3 Control Systems 322
8.4 Considerations for Part Load. 333
8.5 Regulation of Closed Cycle Turbines 343

9. OPERATIONAL STABILITY. 349

10. STRUCTURAL INTEGRITY 354

10.1 Materials. 354
10.2 Life, Temperature, and Load. 358
10.3 Mechanical Stress. 360

10.3.1 General. 360
10.3.2 Clark Bros. Co. CSN-1 T-C Set. 362
10.3.2 Stratos TCS-670 T-C Set. 369

10.4 Thermal Stress 379
10.5 Fatigue. 382
10.6 Vibration. 383

11. TURBINE COOLING. 406

11.1 General. 406
11.2 Blade Cooling. 409
11.3 Convective Air Cooling 414
11.4 Water Cooling. 426
11.5 Experimental Cooled Turbines 428
11.6 Other Cooling Methods. 442

TABLE OF CONTENTS (Concl.)

		Page
12.	DETAILS OF STRUCTURAL DESIGN.	451
12.1	Components.	451
12.1.1	Casings	451
12.1.2	Rotors and Disks.	457
12.1.3	Radial Flow Impellers	465
12.1.4	Turbine Blading	467
12.1.5	Integral Rotors	479
12.1.6	Stator Blading.	482
12.1.7	Compressor Blading.	483
12.1.8	Blade Fastening	487
12.1.9	Bolts	490
12.2	Gas Turbine Sets.	490
12.2.1	Clark Model CSN-1, Axial-Flow T-C Set for ML-1.	490
12.2.2	Stratos Model TCS-670, Radial-Flow T-C Set for ML-1	497
12.2.3	MGCR Turbomachinery	513
13.	AVAILABILITY AND CAPABILITY	525
13.1	Manufacturers' Information.	525
13.2	Future Development.	527
13.3	Limiting Factors.	528
13.4	List of Manufacturers, Turbine and Compressor Data Sheets.	534
14.	TEST FACILITIES	577
REFERENCES	. . . . .	587

NOMENCLATURE

A	area
b	blade length
c	absolute velocity, velocity
c_p	specific heat at constant pressure
c_v	specific heat at constant volume
D	Diffusion factor
D	diameter
d	diameter
E	rate of energy transfer
F	force, factor
f	coefficient of friction
f_b	coefficient of bearing friction
G	mass flow rate, or weight flow rate
Gr	Grashof number
g	acceleration of gravity
H	head
h	blade height
h	enthalpy
hp	horse power
J	mechanical equivalent of heat
K	coefficient
k	ratio of specific heats
L	length
L	load
Ma	Mach number
m	molecular weight
N	rotative speed
Nu	Nusselt number
n	number of blades
n	polytropic exponent
n	some number

NOMENCLATURE (Cont.)

P	power
p	pressure
Q	volume flow rate
q	pressure coefficient, stagnation pressure
R	universal gas constant
R	reaction
Re	Reynolds number
r	radius, reaction, solidity (chord-to-pitch ratio of blading)
r	ratio
s	path length, entropy
T	temperature, absolute temperature
t	thickness
t	pitch of blading
U	wetted perimeter of flow channel section
u	peripheral velocity
v	specific volume
W	work
W	weight
W	weight flow rate
w	relative velocity
Y	pressure ratio function
β	coefficient of thermal expansion
γ	specific weight
ϵ	diameter ratio
η	efficiency
μ	dynamic viscosity
ν	kinematic viscosity
λ	leakage factor
ρ	loss coefficient

THE FRANKLIN INSTITUTE • Laboratories for Research and Development

I-A2392-6

NOMENCLATURE (Concl.)

π	pressure ratio
Φ	torque
φ	flow factor
ψ	pressure coefficient
ω	angular velocity
ζ	loss coefficient

Subscripts:

1	entrance; inlet
2	exit; before turbine rotor
3	machine outlet
ad	adiabatic
C,c	compressor
e	kinetic energy
f	fluid
h	hydraulic; hub
i	inner
m	mechanical
n	net; normal, meridional
o	reference value
R	reaction
r	runner; rotor; radial
s	stage; specific; standard; separation of flow
st	static
T,t	turbine
u	circumferential
v	loss, velocity

LIST OF FIGURES

Figure		Page
1-1	A Modern Industrial Gas Turbine.	10
2-1	70 lb Thrust Jet Engine by Williams Research Corporation.	15
2-2	Growth of US Navy Gas Turbines in Ships and Boats, 1955-1961	15
2-3	GE Typical Small, Simple Cycle, One-Shaft Gas-Turbine Unit	20
2-4	GE Typical Small Simple-Cycle, Two-Shaft Gas-Turbine Unit	20
2-5	GE Typical Medium Size Simple-Cycle, One-Shaft Gas-Turbine Unit	21
2-6	GE Typical Large Simple-Cycle, One-Shaft Gas-Turbine Unit	21
2-7	Typical Cross-Section of a Westinghouse Industrial Gas Turbine.	25
2-8	Comparative Plant Costs for Different Turbines	25
2-9	The 10,000 kw Moscow Plant Shown Under Construction at the Escher Wyss Works	32
2-10	The 13,750 kw Machine Set for the Solid-Fuel-Fired Closed-Cycle Oberhausen Plant.	32
2-11	Dependency of an Open-Cycle Gas Turbine Output and Thermal Efficiency on Compressor Inlet Temperature . .	32
2-12	Promising Applications of Aircraft Gas Turbines to Industrial Power Plants.	34
2-13	One-Quarter Scale Model of Cooper-Bessemer RT-248 Gas Turbine with Gas Generator Cutaway to Show Two-Spool Deisgn	35
2-14	Pratt & Whitney Aircraft Type Gas Turbines for Industrial Application	36
2-15	GE Model 240 Turboshaft Engine	37
2-16	Bristol Siddeley 3 Megawatt Turbo-Generator.	38
2-17	Generating Station at Princetown, Bristol Siddeley Industrial Proteus	38
2-18	Theoretical Performance of Turbojet Engine	41

LIST OF FIGURES (Cont.)

Figure		Page
2-19	Specific Consumption of Modern Turbojet and By-Pass Engines.	41
2-20	Bristol Siddeley BS 75 Ducted Fan Engine	44
2-21	Bristol Siddeley Olympus BO121 Turbojet Engine	44
2-22	Progress of General Electric Co. Turbine Installations.	47
2-23	Operational Data of General Electric Industrial Gas Turbines	48
2-24	Nimonic-80 First-Stage Bucket Failure.	53
2-25	First-Stage Bucket Failure Caused by Thermal Shock . .	53
2-26	Wheel Failure in Dovetail Section.	53
2-27	Section View of Combustion Chamber with Louvered Liner.	56
2-28	View of A Two-Shaft GE Gas Turbine with Top Casings Removed.	56
2-29	Bristol Siddeley Viper ASV11 Turbojet Engine	73
2-30	Strength of Recent High-Temperature Forged and Cast Materials.	73
2-31	Improvement in Aero-Engine Overhaul Life	78
2-32	Bristol Siddeley Proteus 765 Turboprop Engine.	78
2-33	Diagrammatic Cross-Section of the Rolls-Royce Dervent 5 Turbojet Engine.	81
2-34	AiResearch Gas Turbine Compressor & Power Unit Model GTCP 85-91	82
2-35	Bristol Siddeley Marine Proteus 1270 Series.	85
2-36	Clark Isotemp Compressor Package	90
2-37	Brown Boveri Axial Flow Compressor	90
2-38	A Clark 18,000 bhp Axial Flow Compressor for Gas Turbine Application.	90
2-39	Range of Compression Ratio and of Inlet Volume Flow of One-Casing Turbo-compressor According to Current Manufacturing Practice (for Compression of Air from Atmospheric Conditions)	91

LIST OF FIGURES (Cont.)

Figure		Page
2-40	Range of Specific Work and of Inlet Volume Flow of One-Casing Turbo-Compressors According to Current Manufacturing Practice (Valid for all Gases).	91
2-41	Diagram of Elliott-Lysholm Gas-Turbine Cycle for Ship Propulsion	93
2-42	Elliott-Lysholm Compressor.	93
2-43	Performance Characteristics of Elliott-Lysholm 12,500-cfm Compressor	94
2-44	Combination Design of Three Floating-Piston Engines Serving a Gas-Turbine (Sulzer Co.).	94
2-45	Schemes of Terry and Drag Turbines.	99
2-46	Test Set-Up of Inward Flow Radial Turbine	99
2-47	Clark Bros. Co. 9000 hp Single-Shaft Industrial Gas Turbine	99
2-48	Outline of Clark Model TA Combustion Gas Turbine. . .	100
2-49	Strato Disk Turbine 6X-1.	103
2-50	Straight-Compound and Cross-Compound Arrangements . .	103
2-51	Proposed Russian Gas Turbine Power Plant.	105
2-52	Performance Predictions for Turbojet and Turboprop Engines	109
3-1	Speed of Sound as a Function of Temperature for Various Gases	112
3-2	Schematic Layout of Turbomachinery with In-Line Power Turbine	112
3-3	Cross-Sectional Drawing, 1000-psia Helium Turbo-machinery	118
3-4	Cross-Sectional Drawing, 1000-psia Carbon Dioxide Turbomachinery.	118
3-5	Cross-Sectional Drawing, 2000-psia Carbon Dioxide Turbomachinery.	119
3-6	Solar Aircraft Co. - Jupiter T-520 Turbo-Compressor Set	125
3-7	Escher Wyss TUCO 52 2000 kw Closed-Cycle Turbo-Compressor Set.	125

LIST OF FIGURES (Cont.)

Figure		Page
3-8	System Flow Sheet of Ceramic Power Breeder Reactor. . .	127
3-9	Cycle T-S Diagram of ORSORT Ceramic Breeder Reactor . .	128
3-10	General Arrangement of 60 Mw Nuclear Closed Cycle Gas Turbine Power Plant	129
3-11	Section Through Machinery Set of ORSORT Ceramic Breeder Reactor	129
3-12	Power Plant Flow Diagram - Small Gas-Turbine Cycle Reactor	132
3-13	Profile of the 5-Mw Closed-Cycle Daniels Breeding Reactor	132
3-14	Arrangement of Three-Turbine Power Plant (Studebaker-Packard).	134
3-15	Detail of Machinery (Studebaker-Packard).	135
3-16	Flow Diagram of Studebaker-Packard Power System	136
3-17	Schematic Diagram of Closed-Cycle Gas Turbine Power Plant (Turret).	138
3-18	Flow Diagram of WKNL System	140
3-19	Helium Turbo-Compressor Set of WKNL System.	141
3-20	The ML-1 Power Plant.	143
3-21	Arrangement of Equipment of the ML-1 Power Conversion Skid - Plan	144
3-22	Arrangement of Equipment of the ML-1 Power Conversion Skid - Elevation.	144
3-23	Arrangement of Equipment of the ML-1 Power Conversion Skid - Plan View of Precooler	145
3-24	Arrangement of Equipment of the ML-1 Power Conversion Skid, View From Generator Side.	145
3-25	Simplified Flow Diagram for the ML-1.	148
3-26	ML-1 Cycle Characteristics.	150
3-27	The Axial Flow Turbine Compressor Set for ML-1.	151
3-28	Arrangement for Helium-Cooled Reactor Power Plant, Plan (MGCR)	154
3-29	Arrangement for Helium-Cooled Reactor Power Plant, Elevation (MGCR).	154

LIST OF FIGURES (Cont.)

Figure		Page
3-30	MGCR Flow Diagram-LPT Driving.	155
3-31	Flow Sheet for MGCR Closed-Cycle Gas Turbine System (Helium Cooled, Graphite Moderated).	156
3-32	MGCR Turbomachinery-HPT Driving.	162
3-33	MGCR Flow Diagram-HPT Driving.	164
4-1	Radial Compressor - Basic Relations.	173
4-2	Axial Flow Compressor - Basic Relations	174
4-3	Radial Turbine - Basic Relations	175
4-4	Axial Turbine - Basic Relations.	176
4-5	Thermodynamic Process of Fluid in Turbine Stage. . . .	178
4-6	Velocity Diagrams and Schematic Blade Shapes of Normal Blade Elements.	181
5-1	Head-Loss Correction Curve	186
5-2	Wheel Proportions for Radial and Mixed Flow Compressors.	196
5-3	Stage Performance with Vaneless Diffusers.	196
5-4	Stage Performance with Vaned Diffusers	196
5-5	Obtainable Radial Compressor Efficiencies, Representative of Advanced Engines	198
5-6	Influence of Compressor Efficiency on Impeller Stress.	198
5-7	Effect of Cooling on Horsepower.	201
5-8	Effect of Cooling on Discharge Temperature	201
5-9	Intercooled Multi-Stage Radial Compressor.	203
5-10	Oerlikon Radial Compressor-Longitudinal Section. . . .	204
5-11	Oerlikon Radial Compressor-Cross-Section	204
5-12	Velocity Triangle at Impeller Exit	207
5-13	Flow Pattern in Vaneless Diffuser.	207
5-14	AiResearch Turbocharger Model T1407.	207
5-15	Compressor Wheel and Diffuser Assembly in a Torus-Type Casing - 100 hp Lightweight Gas-Turbine Unit. . .	207
5-16	Influence of Blade Curvature on Compressor Map	209

LIST OF FIGURES (Cont.)

Figure		Page
5-17	Velocity Distribution along Impeller Blade.	209
5-18	Velocity Distribution along Diffuser Vane	209
5-19	Barrel Assembly with DeLaval Mixed-Flow Impeller with Birmann-Blading for High Flow and Low Pressure Boost	213
5-20	Limitations of Conventional Subsonic Inlet Stages . .	213
5-21	Development of Diffusion Factor	215
5-22	Diffusion-Factor Correlation for Compressor Inlet Stages.	215
5-23	Performance Improvement Resulting from Better Stage-Matching.	215
5-24	Weight Flow versus Mach Number.	218
5-25	Pressure Ratio versus Mach Number	218
5-26	Performance of AiResearch Transonic Mixed Flow Compressor.	218
5-27	Over-All Performance Characteristics of the Three-Stage Transonic Compressor.	218
5-28	Cross-Sectional View of Eight-Stage Axial-Flow Compressor, Inlet Bellmouth, and Discharge Collector.	220
5-29	Effect of Reynolds Number on Multistage Performance .	221
5-30	Typical Performance Map of Eight-Stage Compressor . .	221
5-31	First-Stage Rotor of Long-Chord Compressor.	223
5-32	First-Stage Rotor of Medium-Chord Compressor.	223
5-33	Eight-Stage Axial-Flow Compressor	224
5-34	Coordinates of Tip Section of a Rotor Blade Measured On Design Stream Surface.	224
5-35	A Dimensional Comparison Between a Conventional Compressor (Atar 101), the S-1 Compressor Preceded by Three Conventional Stages, and the One-Stage S-2 Compressor.	226
5-36	A Cross-Section of the S-1 Compressor. Below this, Sections of the Blades are given with the Mean Diameter denoted by the Section Line A-B.	226

LIST OF FIGURES (Cont.)

Figure		Page
5-37	First Unshrouded Shock-in-Rotor Supersonic Compressor.	228
5-38	Typical Performance Curves of Shock-in-Rotor Type Supersonic Compressor	228
5-39	Supersonic Impulse Rotor for Shock-in-Stator Supersonic Compressor.	228
5-40	Performance of Impulse-Type Supersonic Compressor Rotor	228
5-41	Turbine Blade Characteristics	234
5-42	Test Performance of 400-hp Turbine Stage. Total-to-Static Efficiencies	236
5-43	Test Performance of 400-hp Turbine Stage. Total-to-Total Efficiencies.	236
5-44	Velocity Triangles for Three Different Reactions. . .	242
5-45	Loss Distribution for High and Low Specific Speed Turbines.	242
5-46	Comparison of 50 per cent Reaction and Impulse Blading	242
5-47	Velocity Triangles for Zero Reaction Turbines	242
5-48	Blade Passage Configuration	246
5-49	Performance of Impulse Type Radial Turbine.	246
5-50	Blade Loading for Zero Diffusion.	246
5-51	Turbine Wheel and Nozzle Ring in their Working Relationship.	246
5-52	TCS-670 Compressor Performance, Air	247
5-53	TCS-670 Compressor Performance, Nitrogen.	247
5-54	TCS-670 Turbine Performance	250
5-55	Flow Diagram for Clark CSN-1 Gas Turbine.	250
5-56	CSN-1 Compressor Blade Section Data vs. Diameter. . .	253
5-57	CSN-1 Compressor Air Angle Distribution vs. Diameter, Stage 1	253
5-58	CSN-1 Compressor Blade Efficiency vs. Incidence Parameter	254

LIST OF FIGURES (Cont.)

Figure		Page
5-59	CSN-1 Compressor Blade Profile C4 Section Ordinates.	254
5-60	Notation for Velocity Triangles on Axial-Flow Compressor Stage	256
5-61	CSN-1 Predicted Compressor Characteristic at Variable Turbine Inlet Temperature	257
5-62	CSN-1 Compressor Performance Characteristic.	257
5-63	Notation and Sign Convention for Velocity Triangles on Axial Flow Turbine Stage.	258
5-64	CSN-1 Turbine Blade Section Data vs. Diameter. . . .	262
5-65	CSN-1 Turbine Loss vs. Incidence Parameter	262
5-66	CSN-1 Turbine Velocity Triangles	263
5-67	CSN-1 Turbine Performance Characteristics.	264
5-68	MGCR Compressor Model Aerodynamic Performance vs. Combined Solidity Change with Equilibrium Boundary Layer.	268
5-69	MGCR Compressor Model Aerodynamic Performance-Flow Coefficient, Pressure-Coefficient, Efficiency. . . .	271
5-70	Influence of Recuperator Effectiveness and Relative Pressure Loss on Optimum Compression Ratio	271
5-71	MGCR Program - Compressor Diffuser and Hood Model Test Pressure Loss vs. Diffuser Inlet Mach Number. .	273
5-72	Performance Characteristics of MGCR High-Pressure Turbine (Gas-Helium; Inlet Temperature = 1,289°F). .	274
5-73	Performance Characteristics of MGCR Low-Pressure Turbine (Gas-Helium; Inlet Temperature = 1,022°F). .	274
5-74	Blade Total Pressure Loss versus Blade Length for MGCR High-Pressure Turbine Test Model at Design Point-Rotor No. II	276
5-75	Center of the Turbine Test Facility.	277
5-76	1000 Horsepower Water Dynamometer.	277
5-77	MGCR Model Turbine Test, Second Stage, Pressure Ratio = 1.25	280
5-78	MGCR Model, Turbine Test, Second Stage, Configuration 2A, Turbine Flow Constant vs. Velocity Ratio Parameter - Pressure Ratio	280

LIST OF FIGURES (Cont.)

Figure		Page
5-79	MGCR Model Turbine Test. Tested Performance Field, Second Stage.	281
5-80	HPT Inlet Scroll Model Configuration I.	283
5-81	HPT Inlet Scroll Model Configuration II	283
5-82	Turbine Inlet Cone.	284
6-1	Turbine-Velocity Triangles and Geometries	294
6-2	ND-Diagram for Single-Disk Turbines	294
6-3	Compressor Velocity Triangles and Geometries.	296
6-4	Approximate ND-Diagram for Single-Disk Pumps and Low-Pressure-Ratio Compressors.	296
6-5	General Performance Presentations of a Radial Turbine	300
6-6	Performance of Radial Turbines (50 per cent Reaction Blading).	300
6-7	Performance of Radial Turbines (High Reaction Blading).	300
6-8	Typical Performance Curves of an Axial Flow Compressor	301
6-9	Typical Performance Chart of a Centrifugal Compressor	301
6-10	Typical Performance Curves of Lysholm Positive Displacement Rotary Piston Compressor	301
6-11	TCS-670 Compressor Characteristics for Air.	302
7-1	Interrelation of Specific Speeds for Single-Spool Gas-Turbines.	309
7-2	Matching of Single-Spool Gas-Turbines	309
7-3	Interrelation of Specific Speeds in Single-Spool Turbo-Chargers (Gas Generators)	309
7-4	Torque Relations for Compressor and Turbine	310
7-5	Matched Performance Characteristics of 16-Stage Compressor and 3-Stage Turbine.	312
8-1	Schematic Diagram of the Rheinhausen Gas Turbine. . .	321
8-2	Starting Diagram of 2-Shaft Brown Boveri Gas Turbine.	321
8-3	Relative Heating Rates of Turbine Casing and Liner During a Normal Start	323

LIST OF FIGURES (Cont.)

Figure		Page
8-4	Heating Rates of the LP Turbine Disk Rims During a Normal Start.	323
8-5	Increase of Initial Torque by Boosting.	325
8-6	Gas-Turbine Unit In Two-Shaft Arrangement	325
8-7	ML-1 Start-Up Schedule-1 (Reactor Outlet Temperature vs. Time)	327
8-8	ML-1 Start-Up Schedule-2 (Compressor Inlet Pressure vs. Time)	328
8-9	ML-1 Start-Up Schedule (Speed vs. Time)	329
8-10	TCS-670 Turbine-Compressor and Gear Box Starting Torque	330
8-11	CSN-1 Speed vs. Torque for Starting	332
8-12	CSN-1 Nondimensional Starting Characteristics	332
8-13	Part-Load Performance of Nuclear Power Plant (Studebaker-Packard).	335
8-14	MGCR Estimated Basic Cycle Efficiency at Part Load. . .	337
8-15	MGCR Operating Points for Various Plant Modifications to Permit Operation at 1,500°F.	337
8-16	MGCR Program - High Pressure Drive Design, Part Load Performance	342
8-17	Closed-Gas-Cycle Temperature - Pressure Quadrants . . .	344
8-18	Time Rate of Change in Output as a Function of the System Quadrant in Which Fluid is Introduced or Withdrawn	344
8-19	Effect of Changes in System Weight Flow on Net Power Output.	347
8-20	Closed-Cycle Gas-Turbine Nuclear Power Plant with Receiver and Accumulator.	347
8-21	System Pressure Variations With Load.	347
9-1	Blade Incidences for a Small Axial Compressor	352
10-1	Oxidation of Surfaces of a Fractured Cermet Blade . . .	359
10-2	Cermet Blades After 52 Hours and 15 Minutes at an Average Gas Temperature of 2000°F	359
10-3	Temperature vs. Creep-Time From Nimonic 80A at 20 kg/mm^2 Stress and 0.2% Creep	361

LIST OF FIGURES (Cont.)

Figure		Page
10-4	Relation Between Life of Gas-Turbine EM27P Blading and Related Load.	361
10-5	Clark Turbine Blade, Stress vs. Diameter, Stage 1 . . .	363
10-6	Clark Turbine Blade, Stress vs. Diameter, Stage 2 . . .	363
10-7	Clark Compressor Balde, Stress vs. Diameter, Stage 1. .	365
10-8	Clark Compressor Blade, Stress vs. Diameter, Stage II .	365
10-9	Clark Compressor Rotor, Stress vs. Radius.	367
10-10	Clark Turbine Disk, Stress vs. Radius, Stage 2.	367
10-11	Clark Rotor Shaft Stress Picture.	368
10-12	Stress to Rupture in 50,000 Hours vs. Temperature for 19-9 DL	370
10-13	Stress to Rupture in 50,000 Hours vs. Temperature for Type 316 Stainless Steel.	370
10-14	Stress to Rupture in 50,000 Hours vs. Temperature for Incoloy 901	371
10-15	Stress to Rupture in 50,000 Hours vs. Temperature for N-155	371
10-16	Stress Values in Stratos Compressor Wheel, 1st Stage. .	372
10-17	Stress Values in Stratos Turbine Disk, 1st Stage. . . .	373
10-18	Stresses in Impeller at Overspeed	377
10-19	Wheel Stresses.	377
10-20	Typical Life-Speed Relationship for Aluminum Impeller .	378
10-21	Strength of Blade Root Fixings of Model No. 2, Steel No. 1, at 710°C	378
10-22	Cracks in Turbine Bucket.	381
10-23	Temperature Distribution for Original Blade at 4 Seconds	381
10-24	Stress Distribution for Original Blade at 4 Seconds . .	381
10-25	Maximum Blade Stress.	381
10-26	Typical Buckets Cracked by Thermal-Fatigue.	384
10-27	Bucket Stress and Temperature Distributions at Rated Conditions.	384

LIST OF FIGURES (Cont.)

Figure		Page
10-28	Number of Starts and Operating Hours When Cracks were First Found in Each Bucket.	385
10-29	Relative Proportions of Stiff and Flexible Shafts. . .	387
10-30	Effect of Rotor Support Flexibility on Second Critical Speed	387
10-31	Relation Between First and Second Critical Speeds. . .	388
10-32	Vibration of Typical Compressor Rotors	388
10-33	Clark Compressor Blade Interference Diagram.	391
10-34	Clark Rotor Shaft Shear and Moment Diagram	393
10-35	Spherical Bearing Retaining Pin and Hole Damage. . . .	399
10-36	Frequency Response of Gas-Generator Rotor Assembly in "Free" Condition.	399
10-37	Frequency Response of Gas-Generator Rotor Assembly in "Fixed" Condition	399
10-38	Frequency Response of Gas-Generator Rotor Assembly as Installed in Engine.	399
10-39	Original and Redesigned Compressor-Turbine Shafts. . .	402
10-40	Nodal Lines of Blade and Disk Vibrations	402
10-41	Spectrum of Natural Impeller Vibration Frequencies . .	402
10-42	Impeller with Mounted Strain Gages	403
10-43	A Nodal Pattern of Six Nodal Diameters and One Circular Node Indicated on a Disk at 1015 cps.	403
10-44	Principal Modes of Vibration of W2/850 Turbine Blades	403
10-45	Interference Diagram for W2/850 Turbine Blades at 700°C.	403
11-1	Jet Engine Performance as a Function of Turbine Inlet Temperature.	407
11-2	Turboshaft Engine Performance as a Function of Turbine Inlet Temperature.	407
11-3	Cross Section of Air-Cooled Turbojet Engine.	415
11-4	Three Methods of Air-Cooling Turbine Blades.	415

LIST OF FIGURES (Cont.)

Figures		Page
11-5	Air-Cooled Turbine Blade Configurations.	416
11-6	Transpiration-Cooled Blade Utilizing Orifices in Base for Metering Cooling Air	416
11-7	Effect on Metal Temperature of Special Methods of Cooling Leading and Trailing Blade Edges	416
11-8	Comparison of Relative Coolant Flow Requirements for Several Types of Air-Cooled Turbine Blades	420
11-9	Air-Cooled Turbine-Disk Configurations	420
11-10	Impeller Vanes for Air-Cooled Turbine Disks.	420
11-11	Air-Cooled Blade Cross Sections.	423
11-12	Cooling-Air Flow Path in Blading	423
11-13	Slanted-Corrugation Tip-Capped Blade	425
11-14	Air-Cooled Corrugated-Insert Turbine Rotor Blade with Leading-Edge Tip Cap	425
11-15	Air-Cooled Turbine Component and Adjacent Parts. . . .	425
11-16	Variation of Coolant Temperature Rise and Prevalent Blade Temperature with Coolant Flow Rate	430
11-17	Cross Section of Turbine Showing Cooling Air-Flow Path	430
11-18	Cross Section of Rotor Assembly Showing Cooling Passages	430
11-19	Three Stage Rotor Assembly - Radial Coolant Inlet. . .	431
11-20	Cutaway of Rotor Blade Showing Cooling Passages. . . .	431
11-21	Section Through First-Stage Rotor Blade.	431
11-22	Section Through Stator Vane.	431
11-23	Rotor-Blade Trailing Edge Temperature.	439
11-24	Cooling System Performance, Liquid Cooled Turbine. . .	439
11-25	A Part-Sectioned View of the English Electric EM85 8,000 hp Gas Turbine	444
11-26	Air Cooling System of the Orenda OT-F-2 Industrial Gas Turbine.	447
11-27	Turbine Compressor Set for ML-1, Cooling Gas Diagram .	448

LIST OF FIGURES (Cont.)

Figures		Page
12-1	Cast Casing of a Two-Stage Turbine.	454
12-2	Simple Open-Cycle Type Westinghouse 7000 hp Gas Turbine, Showing Simplified Two-Bearing Construction.	454
12-3	Turbine Casing.	454
12-4	Compressor Casing	454
12-5	Cross-Section of Horizontally-Split Centrifugal Compressor-Diaphragm Cooling is Provided.	455
12-6	Clark No. 2 10-stage Horizontally-Split Multi-Stage Centrifugal Compressor.	455
12-7	Cross-Section of Vertically-Split Centrifugal Compressor.	456
12-8	Vertically-Split Multi-Stage Centrifugal Compressor .	456
12-9	Cross-Section of DeLaval Centrifugal Compressor . . .	458
12-10	Exploded View of DeLaval Supercharger	458
12-11	Section Through the Experimental Rotor for the St. Dizier Gas Turbine of Electricite de France	459
12-12	A Suggested Built-Up Rotor Formed by Flash-Butt-Welding Disks Together.	459
12-13	Solar Jupiter Engine Compressor Rotor	462
12-14	Built-Up Compressor Rotor of the Orenda OT-F-2 Industrial Gas Turbine.	462
12-15	Elliott Co. Radial Compressor Impellers	466
12-16	Section Through DeLaval Impeller Showing Separate Forged Blades	466
12-17	DeLaval Riveted Centrifugal Impeller.	466
12-18	Section Through DeLaval Impeller Showing Blade Milled from Hub Forging	466
12-19	Sections Showing DeLaval Impeller, Forged and Machined in Halves and Welded Together	468
12-20	DeLaval Welded Compressor Wheel	468
12-21	Clark Centrifugal Impellers	470
12-22	Integrally Cast Wheel for an Exhaust-Gas Turbine. . .	470

LIST OF FIGURES (Cont.)

Figure		Page
12-23	Selection of Gas-Turbine Rotor Blade in Nimonic Alloys.	470
12-24	Combination Blade Bucket Produced for the General Electric CJ-805-23 Aft-Fan Engine	473
12-25	Extruded Blade Sections in Nimonic Alloys with Cooling Passages.	475
12-26	Cast Hollow Stator Blades for Jet Engine (Diameter 140 mm)	475
12-27	Internal Airfoil Designs for Maximum Blade Heat Transfer.	475
12-28	Rover Gas-Turbine Rotor with Integrally Machined Blades.	480
12-29	Sulzer Wheel of an Exhaust-Gas Turbine with Cast Blades	480
12-30	Integrally Cast Turbine-Blade Rings Welded to a Combined Hub and Disk of Lower Alloy	489
12-31	Selection of Gas-Turbine Stator Blades Precision-Cast in Nimocast Alloys	489
12-32	Compressor-Turbine Interstage-Seal Diaphragm and Nozzle-Vane Assembly.	489
12-33	T58 Fixed Stator-Vane Ring.	489
12-34	Clark Axial Flow Turbine Compressor Set for the ML-1. .	491
12-35	Clark T-C Set for the ML-1 Blade - 1st Stage Turbine Rotor	492
12-36	Clark T-C Set for the ML-1 Turbine Stator Layout. . . .	492
12-37	Clark T-C Set for the ML-1 Duct-Turbine Inlet	493
12-38	Clark T-C Set for the ML-1 Compressor Discharge Volute Assembly.	493
12-39	Clark CSN-1 Turbo-Compressor Set During Assembly. . . .	494
12-40	Stratos Radial Flow Turbine Compressor Set for ML-1 . .	505
12-41	Stratos T-C Set for ML-1, Second-Stage Turbine Wheel. .	506
12-42	Stratos T-C Set for ML-1, Turbine Flange Seal	507
12-43	Stratos T-C Set TCS-670	508
12-44	Second Stage Disk Assembly for MGCR	514

LIST OF FIGURES (Cont.)

Figure		Page
12-45	Westinghouse Compressor Disk and Shaft Assembly Installation of Compressor Blades.	515
12-46	Westinghouse Turbine Wheel Assemblies Showing Curvic Coupling Connection Between Rotating Stages.	515
12-47	Westinghouse Turbine Disk and Torque Assembly of Through Bolts and Blades	516
12-48	Westinghouse Turbine Blades, Fir-Tree Root	516
12-49	Westinghouse Compressor-Turbine Assembly	518
12-50	Westinghouse Compressor Cylinder Base Assembly Showing Vane Assembly Construction and Installation.	518
12-51	Support Arrangement for MGCR Machinery	524
13-1	Allis Chalmers 2,250,000 cfm Axial Flow Compressor for NASA During Assembly	531
13-2	Allis Chalmers 2,250,000 cfm Axial Flow Compressor for NASA. Rotor on a 42-Foot Vertical Boring Mill at the York Works	531
13-3	AiResearch Twenty-Horsepower Turbine Wheel Compared With the Size of a Silver Dollar	531
13-4	Delaval Ljungstrom Turbine Co. 40 Mw Turbine Plant . . .	533
14-1	Open Cycle Test Facility at Clark Bros. Co..	578
14-2	Clark Bros. Co. CSN-1 Turbine Compressor Test Installation	579
14-3	Stratos Test Arrangement for TCS-670	580
14-4	Flow Diagram of Gas Turbine Test Facility at Ft. Belvoir	581
14-5	Large GE Regenerative-Cycle, One-Shaft Gas Turbine on Factory Test	584
14-6	Orenda Rotating Blade-Cooling Rig.	584

LIST OF TABLES

Table		Page
2-1	Characteristic Data of Representative Modern Gas Turbines.	12-13
2-2	Number of Gas Turbine Installations	15
2-3	Characteristic Data of Stationary Gas-Turbine Power Plants.	16
2-4	Characteristics of Marine Gas Turbines Installed or Building, 1953 through 1957.	17
2-5	General Electric Gas Turbine Operating Experience . . .	19
2-6	General Electric Gas Turbines, Basic Designs as of 1958	22
2-7	Westinghouse Industrial Gas Turbines.	24
2-8	Westinghouse Industrial Gas Turbines, Operating Summary	27
2-9	Westinghouse Industrial Gas Turbines, Application List.	28
2-10	Main Data on Six Industrial Solid-Fuel-Fired Closed-Cycle Gas-Turbine Plants, which Have Come into Operation since 1956.	30
2-11	By-Pass Engine Comparisons.	42
2-12	General Electric Turbines in Service by End of 1957 . .	46a
2-13	Component Life of GE Turbines	62
2-14	Openings of Turbines for Examination Logged for GE 8500 hp Locomotives on the Union Pacific Railroad. .	66
2-15	Number of Interruptions of the Ravensburg Plant	67
2-16	Bristol Siddeley Viper Turbojet Engine Development. . .	70
2-17	Unscheduled Engine Removals	75
2-18	Radial Compressors from US Manufacturers.	88
2-19	Design Data on Free-Piston Gasifiers.	96
2-20	Free-Piston Gas-Turbines in Marine Installations. . . .	97
3-1	Influence of Type of Gas on a Radial Compressor	113
3-2	Influence of Type of Gas on an Axial Compressor	114
3-3	Principal Dimensions and Characteristics.	116

LIST OF TABLES (Cont.)

Table		Page
3-4	Basis for Comparing Weights of Machine Components. . . .	120
3-5	Notable US Studies of Gas-Cooled Nuclear Power Plants with Gas-Turbine Prime Movers.	122-123
3-6	Gas-Turbine Prime Movers of Gas-Cooled Nuclear Power Plant Projects	124
3-7	Characteristics of ML-1 Plant.	146
5-1	Stratos TCS-670 Compressor Performance Coordinates . . .	248
5-2	Compressor Design Chart for ML-1	252
5-3	Turbine Design Chart for ML-1.	261
5-4	Maximum Efficiencies and Corresponding Pressure Coefficients at Different Solidities (MGCR Compressor) .	267
5-5	Comparison of Mean and High Compressor Loading Configurations	269
10-1	Typical Turbine Blade and Disk Stress Levels	374
10-2	Shaft Component Data for Calculating Critical Speed of Stratos Shaft	396
10-3	Input Sheet for Computing Critical Speed of Stratos Shaft.	397
11-1	Comparison Between Normal and Air-Cooled Turbine Blading.	421
11-2	Cycle Design Data, Cooled Turbine.	429
11-3	Turbine Heat Rejection Rates in Btu/sec.	432
11-4	Design Power-Plant Performance	432
11-5	Theoretical Rotor Heat-Transfer Rates for Measured Flow	437
11-6	Design Point Heat Balance from Test Data	438
12-1	Materials Used for Turbine Disks and Rotors.	463
12-2	Advantages and Disadvantages of Ferritic and Austenitic Alloys	464

LIST OF TABLES (Cont.)

Table		Page
12-3	Blade Materials.	481
12-4	Selected Part List for Clark T-C of the ML-1	498-502
12-5	Weight of Major Components in Clark T-C Set for the ML-1	503
12-6	Table of Materials, Stratos T-C Set for ML-1	512
12-7	Piping, Flange Sizes and Locations for 1000 psia and 2000 psia CO_2 Plants (for MGCR).	521
13-1	List of Gas Turbine Manufacturers.	535
13-2	Approximate Diameters of Closed-Cycle Turbomachinery Runners for Different Outputs.	529
13-3	Compressor and Turbine Data for Russian 300 MW Gas-Turbine Plant.	530

pg. xxx [illegible]

1. INTRODUCTION

1.1 General

Little has been done in the nuclear gas-turbine field to date, but the potential is great for using gas turbines at high temperatures to produce a highly efficient nuclear power plant. Pressurizing of the closed gas-turbine cycle leads to machinery of small dimensions and to better efficiencies because of Reynolds number effects. The pressurized direct closed cycle is especially suitable for a nuclear power plant as it does not require a bulky and complex primary heat exchanger which is indispensable in closed-cycle gas-turbine installations fired with fossil fuel.

The gas-turbine cycle is limited in efficiency mainly by the maximum temperatures available from the reactor. Further, it will benefit from increases in this temperature more than does the steam cycle. Increasing the maximum temperature will increase the average temperature at which heat is added more rapidly in the case of the gas-turbine cycle than in the case of the steam-turbine cycle.[1,2*] Another advantage of the gas-turbine cycle, from the view-point of turbo-machinery, is the potential for fast thermal-stress-free start-up and maneuverability at the plant resulting from combined lack of massive components and lower heat transfer coefficients possible with the flowing coolant. These characteristics permit the application of the closed-cycle gas-turbine system to marine or other vehicle propulsion as well as to peak-shaving electric power plants. An indication of this suitability is the successful performance of a chemically-fired closed-cycle gas-turbine system already developed and now being extended to maritime use.[3]

When a direct-cycle power recovery system is used, there is a strong incentive to utilize gas temperatures as high as possible.

---

*Raised numbers refer to the references at the end of this report.

With the stainless steel clad UO_2 matrix fuel elements, 1600°F is the present maximum feasible cladding temperature. This temperature would permit a bulk reactor outlet temperature of 1400°F[4], a temperature of the same order as current gas-turbine technology permits for continuous operation. A development is in progress (MCGR) to reach a maximum fuel element cladding temperature of 1700°F, and a reactor outlet temperature of 1500°F for continuous operation. Since metal cladding imposes a temperature limitation on the fuel element, other-than-metal claddings are elsewhere in development (HTGR, PBR). However, the performance of such coatings is yet unproven. Generally, it appears that the reactor technology has greater difficulties than the turbine technology to reach higher cycle temperatures.

Contrary to the developments in this country, the British nuclear constructors have been reluctant to start the development of nuclear gas-turbine plants, being of the opinion that time has not yet come for a reliable installation which is more economical than a steam-turbine plant. In this country, developments have not been tied in with the expectancy of immediate economical advantages. First steps have already been taken in design and construction of such plants, at conservative reactor outlet temperatures.

Major needs in the gas-turbine power machinery are the development of seals and bearings[5], of aerodynamic features of compressors and turbines, of materials[6], and of special valves[7]. Unusual environments require investigations on compatibility of coolants with structural materials at high temperatures. For example, tests on certain high-strength metals for turbine blades and disks indicated a reduction of strength in a helium atmosphere. Plant efficiency is very sensitive to compressor and turbine efficiencies, about two-thirds of the work output of the turbines is used to drive the compressors. Charts in Report NYO 9787 on Cycles[2] give ratios of total turbomachinery power to net power output. For additional requirements, such as nearly

absolute gas-tightness of seals[5], the development of nuclear turbomachinery is essentially based on the experience available with non-nuclear machines. The choice of coolant also imposes specific requirements on design and on the selection of structural materials[6]. Much of the research on high-temperature materials is currently directed toward the missile program. A great deal of the Aircraft Nuclear Propulsion metallurgical research at Battelle and elsewhere is highly pertinent to high-temperature reactor development[8]. Extensive research in the aircraft industry on turbomachinery can also be applied to nuclear power systems.

Nitrogen as coolant, having practically the same density as air, permits the efficient use of conventional air compressors and air turbines. A number of studies, such as the Turret gas-turbine cycle[1], and the current reactor for the Army (ML-1) are based on the use of nitrogen. The operation of the ML-1 should resolve many of the questions regarding use of nitrogen. However, no outstanding long-term advantages are apparent for nitrogen, helium or carbon dioxide being more promising coolants.

1.2 Review of Turbomachinery in Use

1.2.1 Nuclear Aircraft Propulsion

General Electric Co. in Evendale, Ohio, has been developing a direct-cycle nuclear-powered aircraft engine and Pratt & Whitney Division of United Aircraft Corporation in Middletown, Conn., has been developing an indirect-cycle nuclear-powered aircraft engine. These developments terminated by higher decision to cancel programs for nuclear military aircraft. Effort will possibly be redirected to a new development program on high-temperature materials for non-aircraft power technology.

This use of turbomachinery may be summarized as follows. The Atomic Energy Commission has completed the last phase of testing for the Heat Transfer Reactor Experiment No. 3 (HTRE-3). This third experiment in a series has been conducted by the Aircraft Nuclear Propulsion Department of General Electric Co. in Evendale to verify aircraft nuclear propulsion reactor design factors and operating characteristics. The first milestone in the HTRE program was the successful operation of the HTRE-1 in January 1956. It was the first time a turbojet engine (a modified J-47) had been operated exclusively on heat supplied from a nuclear reactor. From September 1956 to January 1957, the HTRE-1 operated over 150 hours completely on nuclear power to demonstrate the feasibility of a direct-cycle aircraft nuclear propulsion system. The main purpose of HTRE-2 was to test new materials proposed for use in building future power plants. The HTRE-3, in a horizontal configuration as would be required for flight purposes, is capable of operating at approximately 2000°F. It is cooled by air provided from the HTRE assembly's two modified J-47 turbojets. From September 1959 until December 1960, the power plant operated for 146 hours at full power with 65 hours of continuous operation. For the first time, two jet engines were run simultaneously on nuclear energy.

During the last phase of HTRE-3 in November 1960, another objective in the HTRE program was attained when two turbojet engines were started and brought to normal operating range on nuclear power alone. In previous tests, the turbojet engines were started with chemical fuel and, once they obtained normal operating range, they were transferred to nuclear power. The all-nuclear start is considered to be important because it imposes larger thermal stresses in the reactor than by using a chemical-to-nuclear power transition.

Little is known of similar developments abroad. There are indications that USSR gas turbine developments include a prototype propulsion plant for a nuclear bomber consisting of turbojets of 35,000 pounds thrust[9].

1.2.2 Nuclear Marine Propulsion

The Maritime Gas-Cooled Reactor (MGCR) is one of two gas-cooled nuclear power plants presently developed which employs gas turbo-machinery as prime movers. The latest steps can be described briefly as follows:

The 1954 Congress appropriated a sum of money to convert four Liberty ships, two of these with gas-turbine installations. Marine-drive proposals were obtained for open-cycle, closed-cycle, and free-piston units. Finally, a regenerative open-cycle type from General Electric Co. was chosen for several reasons. It was a successful land unit, gave a favorable thermal efficiency, burned a low-cost Bunker C fuel of low vanadium content, and the Maritime Administration had a developed fuel-treatment system. This unit was installed into the John Sergeant. The second unit selected, for the William Patterson, was the free-piston type, originally developed by SIGMA, with Cleveland Diesel Division licensed as builder. The free-piston unit has a high thermal efficiency, burns Bunker C fuel without treatment, and has been used extensively in Europe. Both gas turbine units have been in service for a reasonable period at this point.

The next study of the Maritime Administration covered the closed cycle gas-turbine. In 1956, proposals were solicited on a 20,000-shp closed-cycle gas-turbine unit with a 6000-shp oil-fired heat source to be used for land testing. The project was temporarily set aside because the cost was too high. In 1957, the Maritime Administration became interested in the project again and requested proposals on a 20,000-hp closed-cycle unit with a gas-cooled reactor[10]. As a result, the Maritime Gas-Cooled Reactor Program (MGCR) was initiated on February 17, 1958 with the General Dynamics Corporation under contract AT (04-3)-187. Westinghouse Electric Corporation is subcontractor for the development of turbomachinery and has participated in the project work since August 20, 1958.

The principal goal of the MGCR Program is the development of a nuclear powered marine propulsion system utilizing a high-temperature, gas-cooled nuclear reactor, closed-cycle gas-turbine power plant. Design objectives for the power plant are high thermodynamic efficiency, simplicity of design, ease of operation, low maintenance costs, and maximum efficiency of operation over a wide range of power settings[11].

The MGCR project was divided into four phases. The first phase, now finished, was to develop unit type and to establish gas temperatures, pressures and so on. The second phase, now in progress, covers the construction of the turbine plant only. The third phase is building the entire plant, including the reactor, and the fourth phase covers testing. Initially, it was hoped that the project would be finished in 1962. It was intended to be followed by a second unit to be installed in a ship in 1965[10]. Now it is intended to complete the EBOR experiment by the spring of 1965 when testing will start. The MGCR turbomachinery will become operable probably not before 1967.

The slow progress is due in part to economic conditions and in part to the fact that the MGCR Project has been directed to change the emphasis of its development program, which has previously been one of research and development leading directly to the construction of a land-based MGCR prototype plant. In December 1960, formal authorization was received to reorient the program to include design, construction, and test operation of a 10 Mw (thermal) reactor experiment as an intermediate stage to determine the operating characteristics of BeO-moderated, gas-cooled systems so as to lend greater assurance of success to the subsequent prototype plant.

During the past year, several alphabetical designations have been generated in connection with the MGCR Program. To assist the reader in relating these concepts, we provide the following list of designations[11].

Beryllia Reactor Experiment (BRE) Beryllium Oxide Reactor Experiment (BORE) Experimental Beryllium Oxide Reactor (EBOR)	10 Mw (t) Experimental Beryllium Oxide Reactor. This is a planned test of the MGCR reactor concept utilizing full size fuel and moderator elements to be operated at design specific power. The 10 Mw (t) limitation is achieved by reducing the MGCR core diameter but not its length. A 10 Mw (t) heat dump will be substituted for the turbomachinery.
Helium Reactor Turbine Experiment (HRTE) Maritime Gas-Cooled Reactor Experiment (MGCRE) Maritime Gas-Cooled Reactor Test (MGCRT)	22,000 shp - Mw (t) varies with cycle temperature (approx. 50 Mw (t)). This is a planned test of the MGCR concept which will follow the EBOR. It will employ a full size core and Utilize turbomachinery
Maritime Gas-Cooled Reactor Prototype (MGCR-P) Mark I (MK-I)	32,000 shp - power varies dependent on temperature. These plants are alternate versions of the objective of the MGCR Program.

At the present time, tests with compressor and turbine stages are being performed at the Westinghouse Electric Corp. in Lester, Penna. After their completion, construction of the turbomachinery will be started. Parallel and prior to these extensive tests other were performed on the compatibility of helium atmosphere with structural materials[6].

1.2.3 Nuclear Electric Power Generation in an Army Mobile Power Plant

The Army Gas-Cooled Reactor Systems Program (AGCRSP) began in 1955 with the conduction of a feasibility study by the Oak Ridge School of Reactor Technology and the initiation of a conceptual design by Sanderson & Porter Engineers of a mobile gas cooled nuclear power plant, capable of trailer, flatcar and aircraft transport, to supply electric power for the Army in the field. Sanderson & Porter also studied power conversion equipment and designed a test facility, later designated the Gas Turbine Test Facility (GTTF), in which closed cycle power conversion equipment could be experimentally tested (described in Section 14).

In 1957, the Atomic Energy Commission selected a water moderated reactor concept for development and awarded Contract AT (10-1)-880 to Aerojet General Corporation for the design and fabrication of the Gas-Cooled Reactor Experiment (GCRE) in which fuel elements were to be developed and dynamic and control characteristics of the reactor system were to be determined. Earlier in 1957, the Army Corps of Engineers had awarded Contract DA-44-009-ENG-3252, also to Aerojet, for the assembly and operation of the GTTF.

In 1959, Aerojet General Nucleonics under subcontract to Aerojet General Corporation became overall systems contractor under Contract AT(10-1)880 and became responsible for the development of the closed-cycle, gas cooled mobile nuclear power plant designated the ML-1. The ultimate objective of the AGCRSP is to develop a set of plans and specifications for a field model mobile gas cooled nuclear power plant, to be designated the ML-1A. These plans and specifications are to be used by the Department of Defense to procure field plants.

Turbine compressor sets for the ML-1, were designed, developed and fabricated under Army Contract DA-44-192-ANG-8 by Stratos Division, Fairchild-Stratos Corp. and by Clark Brothers, Div. of Dresser Industries both under subcontract to Aerojet.

Aerojet is currently conducting feasibility studies on advanced gas cooled mobile nuclear power systems for the AGCRSP. GCRE-II was the name previously used for the advanced reactor system to be installed and tested in the GCRE at the National Reactor Testing Station, Idaho.

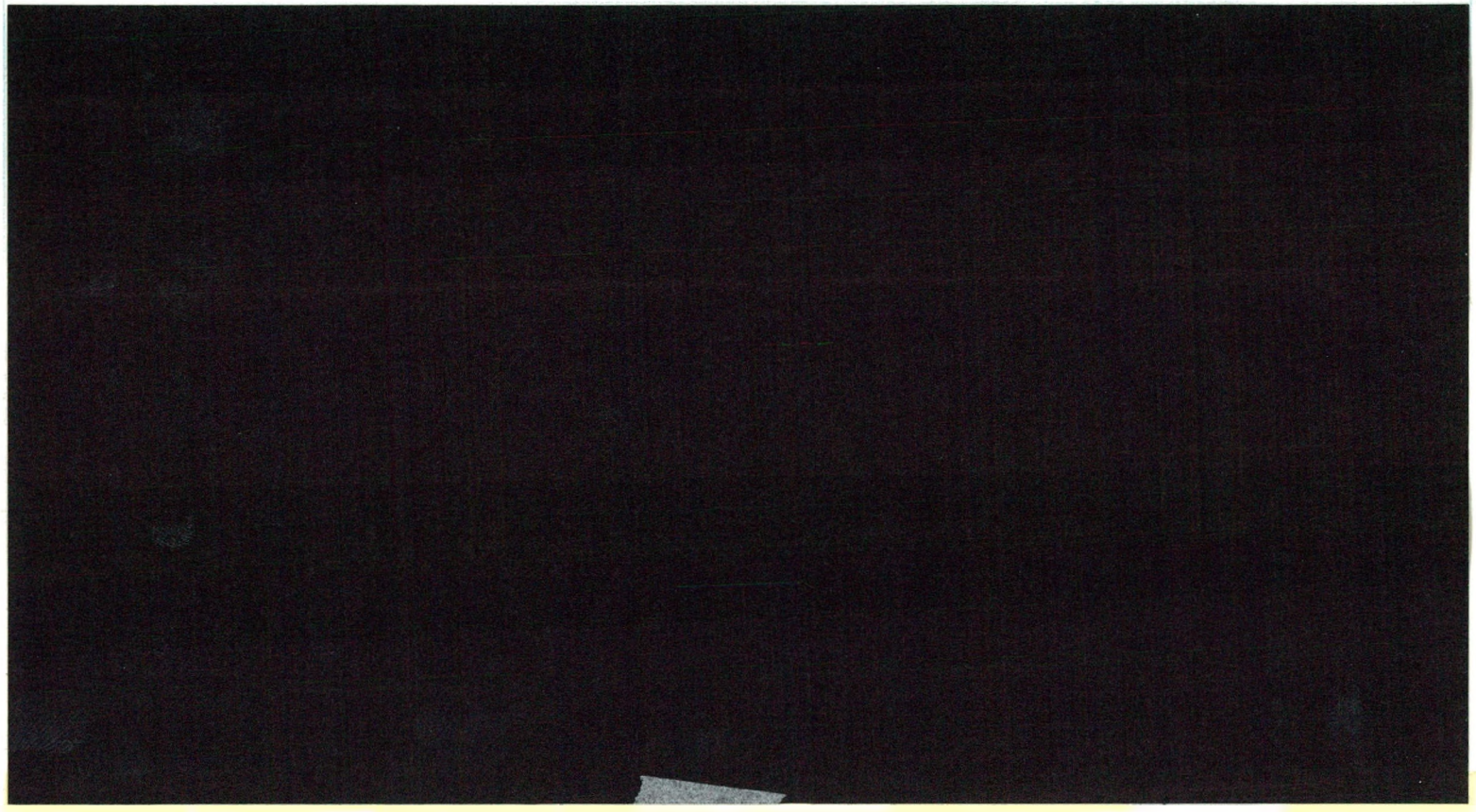
Summary of main symbols:

CGRE - Gas-Cooled Reactor Experiment
GTTF - Closed Cycle Gas Turbine Test Facility
ML-1 - Mobile Low-Power Gas-Cooled Prototype
ML-1A - Mobile Low-Power Gas-Cooled First Field Plant

The ML-1 achieved initial criticality in March 1961 and is scheduled for full power operation in the Fall of 1962. The power conversion portion of the plant was tested previously using a chemically fired heat source. The ML-1 will be the first U. S. nuclear power plant with a gas turbine prime mover and will use nitrogen as the working fluid.

The flow diagram of an open-cycle fossil-fuel heated gas-turbine unit without recuperation shown in Figure 1-1, illustrates the structural design of a modern industrial gas-turbine. Air is drawn in at the inlet, conducted through the scroll and cone insert, and compressed through the succeeding stages of a multi-stage compressor. As the air is forced into the combustion chambers, fuel is injected and ignited. Combustion is continuous and self-sustaining. The hot gases leave the combustion chambers at high velocity. The gases first pass through the compressor-turbine, where sufficient power is extracted to drive the multistage compressor to which this turbine is directly coupled. The gases then pass through the work or power turbine. Here a large portion of the remaining useful power is extracted. The power turbine is normally made separately from the compressor-turbine (or gas producer turbine) where a wide range of speeds is required. It can also be coupled directly to the gas producer when it is desired to maintain constant speed in such applications as the drive of alternating current generators.

In a nuclear gas-turbine plant, the reactor is substituted for the combustion chamber, but except for special seals, pressure level, working gas, configuration, and dimensions, the principal similarity to a conventional gas-turbine remains. Hence, Figure 1-1 may be considered as a general illustration of a gas-turbine.



Air Inlet

Fig. 1-1 - A Modern Industrial Gas Turbine

2. NON-NUCLEAR GAS TURBINES

2.1 General

A large amount of information is now available about existing gas turbines. Today gas-turbine power is being used in practically every type of application suitable as a prime mover. Depending on the compromise solution between various factors, such as life, efficiency, simplicity, cost and weight per unit of power, which are preferred for a distinct application, gas turbines may be classified tentatively in following groups:

(a) industrial (including el-power generation)

(b) lightweight industrial (also ship propulsion and locomotive)

(c) marine

(d) automotive

(e) auxiliary service

(f) aircraft accessory

(g) aircraft

(h) nuclear

(i) missile

The term "industrial gas turbine" is not sharply definable. While we are considering electric power generation as belonging to the applications of an industrial gas turbine, other investigations restrict the use of this term to such applications as supply of compressed air, hot gases, mechanical power, or various combinations of these outputs.

Table 2-1 presents a selected set of characteristic data of representative modern gas turbines for each of the above groups. Nuclear gas-turbines will be considered in more detail in Section 3. According to one source, the world-wide number of gas-turbine installations, other than aircraft, are estimated in Table 2-2.[18] The power range for the first column is from 1800 hp up, and of the second column from 1000 hp up. Therefore the first column does not include the 1000-1799 hp range in which there are only a few units such as Ruston & Hornsby, 1260 hp.

Table 2-1

CHARACTERISTIC DATA OF REPRESENTATIVE MODERN GAS TURBINES

	INDUSTRIAL							LIGHTWEIGHT INDUSTRIAL AND MARINE					MARINE		
MANUFACTURER	BROWN BOVERI CORP.	CLARK BROS. CO.	DE LAVAL-LJUNGSTRÖM	ESCHER WYSS LTD.	GEN. ELECTRIC CO.	ORENDA	WESTINGHOUSE EL. CORP.	COOPER BESSEMER	GEN. ELECTRIC CO.	LYCOMING DIV. AVCO CORP.	SOLAR AIRCRAFT CO.	ORENDA	ASSOCIATED EL. IND.	UTICA DIVISION CURTISS-WRIGHT	
	IN OPERATION SINCE 1958		BIGGEST UNIT IN THE WORLD	IN OPERATION SINCE OCT. 1960				IN OPERATION SINCE OCT. 1960	IN TEST STAGE				CURRENTLY BEING MFTR'D FOR VARIOUS SHIPS		IN DEVELOPMENT
MODEL	11 (750°C)	305 S	GT-120	15	SC-1,5	OT-C-2	W-301	RT-248	240	LTCIN	SATURN T-1000	OT-F-3	G6	210-ST	400 MV
								GAS PRODUCER GG 3C - MODIFIED JET ENGINE J-57	GAS PRODUCER CJ-805 - MODIFIED JET ENGINE J-73	BASED ON T53 AIRCRAFT ENGINE		GAS PRODUCER: MODIFIED ORENDA JET ENGINE	TESTED IN 1958. NO SEA-BORNE EXPERIENCE	LICENSEE OF DAVID TAYLOR MODEL BASIN (U.S. NAVY)	
USE	GEN. DRIVE, BLAST FURNACE	GEN., COMPR. OR PUMP DRIVE	GEN. DRIVE	GEN. DRIVE + HEAT	GEN. DRIVE (PEAKING PLANT)	GEN. DRIVE ETC.	GEN. DRIVE (PEAKING PLANT)	GEN. DRIVE, MARINE, ETC.	INDUSTR., MARINE, MOBILE POWER	INDUSTRIAL OR MARINE	GEN. DRIVE, BOAT PROPULSION	GEN. DRIVE, MARINE, ETC.	NAVAL BOOST	PATROL BOAT PROPULSION	SHIP & HIGH SPEED BOAT PROPULSION
RATING	14.0 MW 15°C, 1 at OPEN η_{th} = 27%	9000 hp 80°F, 1000 ft ALT. OPEN η_{th} = 21.0 %	30 MW 80°F OPEN	13.75 MW CLOSED, AIR, INDIRECT	20,5 MW 80°F, 1000 ft ALT. OPEN	6700 hp 80°F, 1000 ft ALT. OPEN η_{th} = 18.3	22 MW 80°F OPEN	10500 hp 80°F, 1000 ft ALT. OPEN η_{th} = 25%	18840 hp 80°F, 1000 ft ALT. AIR TRANSPORTABLE PACKAGE OPEN	700 hp 80°F, SEA LEVEL OPEN	1070 hp 80°F, SEA LEVEL OPEN η_{th} = 22 %	6700 hp 80°F, 1000 ft ALT. OPEN η_{th} = 18 %	7500 hp 59°F, SEA LEVEL OPEN	3400 hp CRUISE 59°F, SEA LEVEL OPEN	3500 hp OPEN
CYCLE								POWER TURB.: 40000 hr		POWER TURB.: 10000 hr BETWEEN OVERH.	CREEP-RUPTURE 100 000 hr MIN. BEARING				
LIFE EXPECTANCY	100 000 hr CREEP-RUPT. LIFE	12 months betw. OVERHAULS			100 000 hr CREEP-RUPT. LIFE	100 000 hr CREEP-RUPT. LIFE		GAS PRODUCER: 8000 hr BETW. OVERHAULS		GAS PRODUCER: 3500 hr BETW. OVERHAULS	LIFE 10000 hr. 3000 hr BETW. OVERHAULS		BLADING LIFE 10000 hr	2000 hr BETW. OVERHAULS (OR MORE)	5000 hr BETW OVERHAULS (SPECIFIED)
PRESSURE RATIO	5,3	5.25				5.23		10,0	12.0			5,23	6.3		7.0
TURBINE INLET PRESSURE				435 psig											
TURBINE INLET TEMP.	1380°F	1350°F		1290°F	1450-1500°F		1450°F FOR BEARING	GAS PROD. 1800°F POW. TURB. 865°F		1400°F	MAX. 1500°F 1450°F CONT. OPER.		1460°F	CRUISE 1450-1500°F MAX. 1570-1620°F	1600°F
NUMBER OF SHAFTS	2 GEARED	1	2 - GAS PROD. 1 - POWER TURB.	1	1	1	1	2 - GAS PROD. 1 - POWER TURB	2	1 OR 2 (FREE POWER TURBINE)	1 OR 2 (FREE POWER T.)	2	2	2	2
SHAFT SPEED, rpm	MAIN SHAFT 3000	5000	G.P. - 3600 P.T. - 3000	6500	3600	7500	3600	POW. T.: 0 - 5200	GAS PROD. 7460 P.T.: 3900-5500	P.T.: 18900 MAX.	GAS PR. 22300	GAS. PROD. - 7500 POWER 3750-7500	GAS P. - 6850 P.T. - 4900	G.P.: - 11250 P.T.: - 5000 MAX	S.P.: 14260 P.T.: 5900 MAX.
No. OF TURB. CYLINDERS	1	1		1	1	1	1	1	1	1	1	1	1		1
No. OF TURB. WHEELS IN SER.	7	3	2+2 GAS PROD. 3 POWER TURB	6	2	2 - GAS PROD. 1 - POWER T.	4	3 - GAS PROD. 2 - POWER TURB	3 - GAS PROD. 1 - POWER TURB	2 - GAS PROD 1 - POWER TURB	2 - GAS PROD. 1 - POWER TURB.	2 - GAS PROD. 1 - POWER T.	2 - GAS PROD. 2 - POWER T.	2 - GAS PROD. 2 - POWER T	2 - GAS PROD 3 - POWER TURB.
EXHAUST TEMP.	500°F IN STACK	840°F			830°F APPR.			700°F			850°F				870°F
No. OF COMPR. CYLINDERS	2	1	2	2	1	1	1	1	1	1	1	1	1	1	1
COMPRESS. TYPE	AXIAL	AXIAL	AXIAL	AXIAL	AXIAL	AXIAL	AXIAL	AXIAL - 2 SPOOL	AXIAL	AXIAL WITH 1 RADIAL STAGE	AXIAL	AXIAL	AXIAL	AXIAL WITH 1 RADIAL STAGE	AXIAL
No. OF STAGES		13	13+10	16	16	10	15	9+7	17	5 - AX. 1 - RAD.	8	10	13	12 - AX 1 - RAD	8
No. OF INTERCOOLERS	0	0	1	1 PRECOOLER 1 INTERCOOLER	0	0	0	0	0	0	0	0	0	0	0
No. OF HEATING STAGES	1	1	1	1	1	1	1	1	1	1	1	1	1	1	1
FUEL	GASEOUS	LIQUID OR GASEOUS	LIQUID OR GASEOUS	BITUM. COAL	LIQUID OR GASEOUS	LIQUID OR GASEOUS	LIQUID OR GASEOUS	LIQUID OR GASEOUS	LIQUID OR GASEOUS	LIQUID	LIQUID OR GASEOUS	LIQUID OR GASEOUS	LIQUID	LIQUID	LIQUID
HEAT RATE			11200 BTU/hp-hr		10600 BTU/hp-hr	14050 BTU/hp-hr	11000 BTU/hp-hr	10100 BTU/hp-hr	10400 BTU/hp-hr	13480 BTU/hp-hr	11400 BTU/hp-hr	14050 BTU/hp-hr	13500 BTU/hp-hr	12200 BTU/hp-hr	11200 BTU/hp-hr
COMBUSTOR TYPE	1 CHAMBER	2-CHAMBER	2-CHAMBER	1 AIR HEATER, 10000 hr LIFE AT FULL LOAD	16 TUBE	8 TUBE, REVERSE FLOW	12 TUBE	8 TUBE	10 TUBE	1 CHAMBER	9 ANNULAR SIMPLEX SPRAY NOZZLES	6 TUBE	6 TUBE	8 TUBE	6 TUBE
REGENER. EFFECTIVENESS	0.78	0	0		0	0	0	0	0	0	0	0	0	0	0
TURBINE COOLING		DISKS, BLADE ROOTS, STATOR				DISKS, BLADE ROOTS & STATOR						DISKS, BLADE ROOTS, CASING			DISK, BLADE Roots
DRY WEIGHT lb	640000 INCL. GENERATOR	85000	900 000 INCL. ACCESSORIES		284000 INCL. ACCESSOR.	35000	266500 INCL. ACCESSORIES	GAS GEN.: 4000 POW. TURB.: 21000	6600	1200 INCL. ACCESSORIES	1200 lb WITH REG. GEAR, 1200-1800 RPM	13000	45000	2900 INCL. ACCESS.	7000
DIMENSIONS L x W x H [in]	850x320x430	363x130x190	1200x600x500		489x186x108	220x106x90	531x174x180	260x156x167	290x65x95	76x26x38	70x45x44	196x67x86	260x79x86	112x52x49	
STARTER		250 hp APPROX.				VARIOUS TYPES POSSIBLE	700 hp WOUND ROTOR IND. MOTOR	25 hp	AIR EL.-MOT. OR FUEL-AIR GEMOUS. WEIGHT: 300 LB			VARIOUS TYPES POSSIBLE	COMPR. AIR 43 hp PEAK		
STARTING TIME TO FULL POWER		30 min. SAFE 7 min TESTED		30 min. TO 2 hours (CONSERV)		8 MINUTES	30 MINUTES		2 MINUTES		QUICK START	5 MINUTES	3½ MINUTES	60 SEC	
REFERENCES	13, 14	10, 13	13	13, 15	13, GE BULL. GED-3546	13, ORENDA BULL. DESS 207	13, WESTINGH. BULL. B-7912	13, COOP.-BESS. BULL. No. 952B, 52	G.E. BULL. GET-3044	10, 13	10, SOLAR BULL.	13, ORENDA BULL. DESS 207	13, 16	10, 13, BRISTOL SIDD. BULLETIN	17

	VEHICLE PROPULSION		AUXILIARY SERVICES		AIRCRAFT ACCESSORIES			AIRCRAFT		NUCLEAR				MISSILE
MANUFACTURER	ALLISON DIV. OF GEN. MOTORS CORP	CHRYSLER CORP	AiRESEARCH MFG. CO.	BOEING AIRPLANE CO.	AiRESEARCH MFG. CO.	GEN. ELECTRIC CO.	GEN. ELECTRIC CO.	—	—	CLARK BROS. CO.	STRATOS, A FAIRCHILD DIVISION OF CORP		WESTINGHOUSE EL. CORP	STRATO MISSILES
														UNDER OFFICIAL TESTS
MODEL	GMT-305	CR 2A EXPERIMENTAL	GTP 30	502-118	CTSP 200-1 CARTRIDGE TURBINE STARTER AND COOLING UNIT	AS-12 CARTRIDGE TURBOSTARTER	AS-185 FUEL-AIR TURBOSTARTER	IN PRESENT OPERATION		CSN-1	TCS 670	TCS 560	WN-202-IE	6X-1
										FACTORY TEST RUNS MADE	FACTORY TEST RUNS MADE	TEST RUNS UNDERWAY	PRELIMINARY DESIGN COMPLETED	DISC TURBINE
USE	HEVY DUTY VEHIC. ALSO MARINE AND GEN. DRIVE	PASSENGER CAR OR TRUCK	AUXILIARY POWER UNIT, GEN. DRIVE	AIRCRAFT TURBO-STARTER FOR GROUND SERVICE (AIR SUPPLY)	FOR J75 SIZE ENGINE	B-57	F-1018 AND SOLAR T-520J	PROPELLER TURBINE	TURBO-JET	ML-1	ML-1	GTTF	MGCR PROTOTYPE	AUXILIARY POWER DRIVE
					CARTR. CONSUMED IN 14 TO 25 SEC					MILITARY PORTABLE POWER PLANT	LIGHTWEIGHT POWER PLANT	GAS TURBINE TEST FACILITY FOR ML-1	FOR SHIP PROPULSION	
RATING	225 hp 80°F	140 hp 85°F	35.5 hp	195 Air hp	720 lb-ft 155 hp	365 lb-ft	485 lb-ft			498 kW	634 hp	400 kW	32000 hp	95 hp
					NACA STD SEALED					125°F AMBIENT CLOSED, N_2 + 0.5% O_2	120°F AMBIENT CLOSED, N_2 + 0.5% N_2			
CYCLE	OPEN	OPEN	OPEN	OPEN	OPEN	OPEN	OPEN	OPEN	OPEN			CLOSED, N_2, INDIRECT	CLOSED, He	OPEN
LIFE EXPECTANCY				OVERHAUL LIFE 3750 STARTS	OVERHAUL LIFE 100 STARTS INITIALLY 400 STARTS W/ DEVELOPMENT			2000 hr BETWEEN OVERHAULS	1500 hr OVERHAULS	50000 hr	50000 hr		SEAL 30000 hr	
										10000 hr BETW. OVERHAULS	10000 hr BETW. OVERHAULS			
PRESSURE RATIO		4.0	2.5					14 TAKEOFF 16		2.59	2.72	2.75	2.60	
TURBINE INLET PRESSURE					835 psia	1215 psia	440 psia			296.5 psia	294 psia	183 psia	1080 psia	
TURBINE INLET TEMP.	1650°F	1700°F MAX.	1550°F		2000°F	2100°F	2200°F	1790°F TAKE OFF 1920°F 1610°F) CRUISE 1730°F)		1200°F	1200°F	1150°F	HPT - 1300°F LPT - 1110°F	2500°F
NUMBER OF SHAFTS	2	2 MAX.	1	2						1	1	1		
SHAFT SPEED rpm	GAS P.: 35000 POW. T.: 24000	GAS PROD.: 44810 POW. TURB: 45730		GAS PROD: POWER T.: 28500	STARTING GEAR RATIO 23.2:1	45000				22000	18500	18000	LPT-HPC-LAC 12000 HPT - 8140	
NO. OF TURBINE CYLINDERS	1	1	1	1						1	1	1	2	
NO. OF TURBINE WHEELS IN SER	GAS PROD.: 1 POWER TURB.: 1	GAS PROD.: 1 POWER TURB: 1	1 RADIAL	GAS PROD.: 1 POWER T.: 1	1	1	1			2	2	2	HPT - 9 LPT - 7	
EXHAUST TEMP.	500°F	400°F												
NO. OF COMPR. CYLINDERS	1	1	1	1						1	1	1	2	
COMPRESSOR TYPE	RADIAL	RADIAL	RADIAL	RADIAL						AXIAL	RADIAL	RADIAL	AXIAL	
NO. OF STAGES	1	1	1	GAS PROD.: 1 AIR SUPPLY: 1						11	2	2	LPC - 15 HPC - 25	
NO. OF INTER-COOLERS	0	0	0	0						0	0	0	1	
NO. OF HEATING STAGES	1	1	1	1						1	1	1 - HEAT EXCHANGER	1	
FUEL	LIQUID	LIQUID	LIQUID	LIQUID	SOLID	SOLID	LIQUID	LIQUID	LIQUID	NUCLEAR	NUCLEAR	LIQUID	NUCLEAR	
HEAT RATE	10400 BTU/hp-hr	9700 BTU/hp-hr	15200 BTU/hp-hr	20100 BTU/hp-hr										
COMBUSTOR TYPE	2 CHAMBERS	1 CHAMBER	1 CHAMBER	2 CHAMBERS										
REGENERATOR EFFECTIVENESS	YES	92%	75%											
TURBINE COOLING											NONE	NONE		
DRY WEIGHT lb	765 lb INCL. ACCESSOR.	450 lb INCL. ACCESSORIES	481 lb WITHOUT REGENER.	410 lb	75 lb	60 lb	52 lb							
DIMENSIONS LxWxH in.	41 x 32 x 29 INCL. ACCESSOR	36 x 35 x 27 INCL. ACCESSORIES	20 x 22 x 22 WITHOUT REGEN.	50 x 28.5 x 27	18.3 x 17 x 16	21 x 9 x 9	14 x 9 x 9							
STARTER					—	—	—					ELECTRIC		
STARTING TIME TO FULL POWER	1/2 MINUTE AT −45°F				—	—	—							
REFERENCES	10	10, 18	10, 13	10, 13	AiRes. BULL. SP-5-19P	19	19	20	20	21	22		SHEET 6/1 AND 6/2	

*) ESTIMATED

Table 2-2

NUMBER OF GAS TURBINE INSTALLATIONS

Items	Prior to 1960	1960 on	Total
Manufacturers reporting sales	24	19	32
Units - total	592	156	748
Mw capacity as listed	2319.42	505.57	2824.99
Mw capacity as listed, converted to hp	3,407,080	735,427	4,142,507
hp as listed	2,264,100	463,893	2,727,993
grand total, hp	5,671,180	1,199,320	6,870,500

Another source lists over 200 models for industry and about 70 models for commercial airlines of 46 manufacturers in nine countries, as of 1961.[13] Largest model is a 53,600-hp unit built by DeLaval Ljungstrom Turbine Co., Sweden*, and the smallest, a 70-lb unit built by Williams Research Corporation, Michigan (see Figure 2-1).

These is no doubt by now that a distinct gas-turbine industry exists. While the newer models show modern development trends, the older generation of gas-turbines already offers long-term operating experience, which is particularly important for the design of long-life reliable units. Table 2-3[23] lists characteristic data on a number of such gas turbines of the early fifties. In addition, Table 2-4[24] lists information on marine gas-turbines installed or built 1953 to 1957.

Long life gas-turbines of the industrial class, particularly closed-cycle installations, are the basis for the development of nuclear gas turbines, and therefore deserve particular attention. However, experience with other gas-turbines may be of not less importance for development of nuclear gas turbines toward higher efficiency and reliability

*See Figure 13-4, page 533.

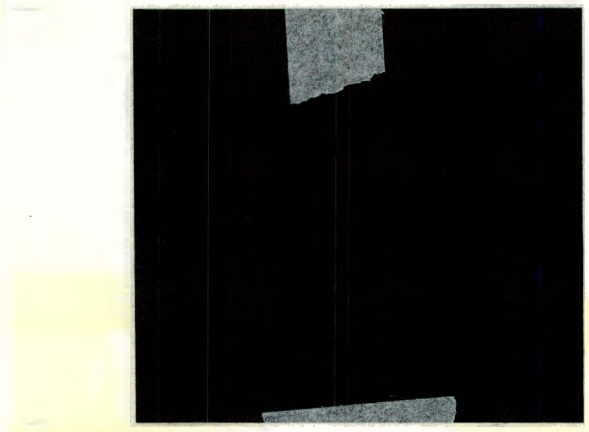


Fig. 2-1 - 70 lb Thrust Jet Engine by Williams Research Corporation

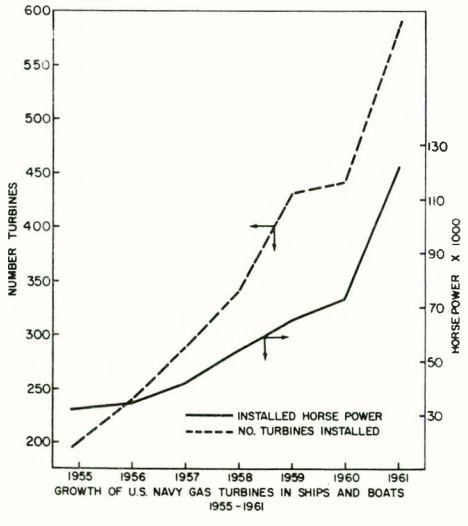


Fig. 2-2 - Growth of US Navy Gas Turbines in Ships and Boats, 1955-1961

Table 2-3

CHARACTERISTIC DATA OF STATIONARY GAS-TURBINE POWER PLANTS

Builder	General Electric Company					Westinghouse Electric Corporation				Brown Boveri Corporation				Ruston & Hornsby, Ltd.	Clark Bros. Co.
Capacity, kw, except where otherwise noted	5000	10,000	16,500	21,800	27,500	2400	3750	8500	16,500	2500	6200	20,000	27,000	650	6200
Turbine temperature, F	1450	1450	1450	1450	1450	1350	1350	1350	1350	1200	1200	1200	1100	1340	1350
Pressure ratio	6.0	6.0	6.0	6.0	6.0	4.9	4.1	6.0	6.0	4.6	4.6	16.0	8.0	4.1	4.25
Cycle	Open	Open	Open	Open	Open	Open	Open	Open	Open	Open	Open	Open	Open	Open	Open
Number of shafts	1	1	1	1	2	1	2	1	1	1	1	2	2	2	2
Shaft speeds, 1000 rpm	6.9	4.9	3.6	3.29		8.5	6.0	4.69	3.6	5.35	3.6	4.75/3.0	3.0/3.0	11.5/6.0	5.0/3.6
Number of turbine cylinders	1	1	1	1		1	1	1	1	1	1	2	3	1	1
Number of turbine wheels in series	...	...	...	...	2	...	2	...	...	...	...	...	DFTC	2	2
Number of compressor cylinders	1	1	1	1		1	1	1	1	1	1	2	4	1	1
Number of intercoolers	0	0	0	0	1	0	0	0	0	0	0	1	2	0	0
Number of heating stages	1	1	1	1		1	1	1	1	1	1	2	2	1	1
Combustor type	Multiple	Multiple	Multiple	Multiple		Multiple	Multiple	Multiple	Single	Single	Single	Single	Single	Single	Single
Regenerator effectiveness, per cent	0	0	0	0		0	75	0	0	75	0	0	80	75	0
Fuel	G, O	G	G, O	G, O	G, O	G, O	G, O	G, O	G, O	BG	G	O	O	O	O
Turbine cooling	Disk	Disk	Disk	Disk		...	...	...	...	D, S	D, S	D, S	...	D, S	D
Compressor type, number of stages	A, 15	A	A, 15	A, 15		A, 14	A, 11	A, 14	A, 15	A	A	A	A	A, 13	A, 13

Builder	English Electric Company, Ltd.	Metropolitan-Vickers Electrical Company Ltd.		Escher Wyss Ltd.	John Brown & Co.	AiResearch Manufacturing Company	Boeing Airplane Company	Solar Aircraft Company		Sulzer Brothers	David Budworth Limited	Utica Division Curtiss-Wright Corporation	
Capacity, kw, except where otherwise noted	1910	1750	2500	2000	2000	100 hp	240 hp	50 hp	520 hp	7500	45 hp	60 hp	2800 hp
Turbine temperature, F	1430	1180	1292	1220	1220	1550	1500	1100	1460	1256	1480	...	...
Pressure ratio	4.8	5.0	5.38	3.6	3.6	3.3	3.95	2.35	4.6	6.6	2.7	2.9	...
Cycle	Open	Open	Open	Closed	Closed	Open	Open	Open	Open	Open	Open	Open	Open
Number of shafts	2	1	1	1	1	1	2	1	1	1	1	1	2
Shaft speeds, 1000 rpm	8.25/7.0	7.0	7.0	12.75	12.75	6.0	35.5/2.92	38.25	20.0	4.25	45.0	46.0	...
Number of turbine cylinders	1	1	1	1	1	1	1	1	1	1	1	1	1
Number of turbine wheels in series	2	...	...	...	...	...	2	...	...	...	...	...	2
Number of compressor cylinders	1	1	1	1	1	...	1	1	1	2	1	1	1
Number of intercoolers	0	0	0	1	1	0	0	0	0	1	0	0	0
Number of heating stages	1	1	1	1	1	1	1	1	1	1	1	1	1
Combustor type	Double	Multiple	Multiple	External	Single	Single	Double	Single	Single	Single	Single	Single	Multiple
Regenerator effectiveness, per cent	60	0	0	90	87	0	0	0	0	77	0	0	0
Fuel	O	O	O	PC	Peat	DO	O	O, K	O, K	BG	O	O	O, G
Turbine cooling	D	...	...	...	None	None	...	...	...	...	...	...	...
Compressor type, number of stages	A-6, C	A, 14	A, 15	C, 3	C, 3	C, 2	C, 1	C, 1	A, 10	A, 21	C, 1	C, 1	...

A = axial flow
BG = blast-furnace gas
C = centrifugal
D = disk cooling
DFTC = double-flow l-p turbine and compressor
DO = diesel oil
G = natural gas
K = kerosene
O = oil
PC = pulverized coal
S = stator cooling

Table 2-4

CHARACTERISTICS OF MARINE GAS TURBINES INSTALLED OR BUILDING, 1953 THROUGH 1957

Country	Manufacturer	Model	Continuous power	Description[a]	Number of engines	Weight including gear, lb	Turbine-inlet temperature, deg F	Pressure ratio	Specific fuel consumption, lb per shp-hr	Hours[x] between overhauls when operated at continuous rating
England	W. H. Allen Sons & Co., Ltd.	Type C	500 kw	SPT	9	11200	1380	10.0:1	1.1[b]	5000
England	W. H. Allen Sons & Co., Ltd.	Type B-1	125 kw	SS	1	750	1300	2.5:1	2.3[b]	1000
England	W. H. Allen Sons & Co., Ltd.	Type D	350 kw	SS	6	3000	1380	2.7:1	1.93[b]	1000
England	British Thomson-Houston	...	1300 hp	SPTR	1	112000	1108	4.0:1	0.64[c]	-[xx]
England	British Thomson-Houston	...	5500 hp	PTL-R-I-W	1	376000	1200	6.0:1	0.505[c]	-
England	Blackburn	Turmo 600	350 hp	SPT	2	310	1500	4.0:1	1.15	500
England	Metro-Vickers Electric Co., Ltd.	G2/1	4500 hp	SPT	4	9700	1472	4.0:1	0.80	-
England	Metro-Vickers Electric Co., Ltd.	G2/2	4000 hp	SPT	2	9700	1436	4.0:1	0.85	300
England	Rover Gas Turbines, Ltd.	1S-60	40 kw	SS	..	...	1454	2.9:1	...	-
England	Ruston Hornsby, Ltd.	T-A	1300 hp	SPT	1	12600	1340	4.0:1	0.91	100000[xxx]
England	Ruston Hornsby, Ltd.	T-E	300 kw	SS	2	4400	1470	3.5:1	0.98	8000
England	Rolls-Royce Ltd.	RM-60	5400 hp	SPT R-I	2	26000	1510	18.0:1	0.66	-
France	Rateau	ACB	3300 hp	I-R	1	...	1290	9.0:1	0.49	-
Japan	Mitsubishi	...	2500 hp	SPT-IRH	..	77000	1290	10.0:1	0.50	-
Japan	Mitsubishi	EWJN10	10000 hp	Closed-cycle, IR	2	325000	1340	3.8:1	0.50	-
Japan	Mitsubishi	...	200 hp	SPT	..	2100	1472	3.7:1	1.20	-
U. S.	Boeing Airplane Co.	502-2	160 hp	SPT	1	236	1550	3.0:1	1.35	-
U. S.	Boeing Airplane Co.	502-6	160 hp	SPT	184	315	1550	3.0:1	1.40	500
U. S.	Boeing Airplane Co.	502-8C	160 hp	SPT	6	319	1580	3.0:1	1.37	500
U. S.	Boeing Airplane Co.	502-10C	220 hp	SPT	58	325	1535	4.0:1	1.06	500
U. S.	Boeing Airplane Co.	Fog generator 500-10C	...	SS	7	650	1500	4.0 1	...	-
U. S.	General Electric Co.	...	6600 hp	SPT R-W	1	...	1450	4.9:1	0.51	-
U. S.	Pratt & Whitney Aircraft	T-34	5000 hp	SS	4	2590	...	6.7:1	0.74	-
U. S.	Solar Aircraft Co.	T-520	500 hp	SS	5	850	1450	4.6:1	1.10	1000
U. S.	Solar Aircraft Co.	T-522	500 hp	SPT	4	1000	1450	4.6:1	1.10	1000
U. S.	Solar Aircraft Co.	T-45	46 hp	SS	95	65	1300	2.4:1	2.0	-
U. S.	Lycoming Div. of AVCO	T-53	685 hp	SPT	1	480[e]	1500	6.0:1	0.75	-

[a] PTL = power turbine driving low-pressure compressor, R = regenerator, I = intercooled, H = reheat, W = waste-heat boiler, SS = single-shaft, SPT = separate power turbine.
[b] Lb of fuel per kwhr.
[c] Lb per bhp-hr.
[d] Not including spare engines.
[e] Less reduction gear.

[xxx] Figure as per ref. 24, Table 8, appears to mean overall expected lifetime.

[xx] After 5 years of service, the turbine appeared to have a useful life if at least 20,000 hr (installed in vessel "Auris" in Oct. 1951).

[x] Completed from Table 8, Ref. 24.

dictated by competition of other prime movers. A higher turbine inlet temperature is the most effective means for obtaining higher efficiency. A second means is improvement of aerodynamic design. For both cases, experience gained with aircraft turbines is most useful. Aircraft engines represent more refined solutions and advanced technology achieved by extensive and costly development programs, economically bearable only because of large production. By approximately 1958, one-half billion horsepower had been produced by jet gas-turbines.[25] However, operating-temperature demands are more severe and operating-life demands are less stringent for jet engines than for nuclear plants. Because of these differences in requirements, careful judgement must be exercised in applying the data on jet-engine materials to nuclear turbomachinery problems.

A great deal of experience has also been accumulated in the field of small gas turbines, a large number of which is in successful operation. Many small units have been built for military applications, for auxiliary power sources providing air starts and for electric power in aircraft. Also, many gas-turbines were produced for portable generators, air conditioning, snow and ice removal, salvage operations, helicopter propulsion, and ground support equipment for commercial airlines. In addition, they have been applied to pipeline sandblasting, gas compressors, and air drilling. For example, Ai-Research Manufacturing Company, a division of the Garrett Corporation, has built more than 10,000 of such turbines of various types in the 35 to 850 hp range.[26] Figure 2-2[27] shows the growth of Navy gas-turbines in ships and boats, 1955-1961. Some data showing the progress of gas-turbine installations of individual manufacturers are also included in Section 2.3 where operating experience is discussed.

In a comprehensive article in the Bristol Siddeley Journal[26], the following interesting comparison of space taken by generating plants appeared:

Plants	Cu-ft/Mw	Percent
Steam	64,000	100
Diesel	50,000	78
Free Piston	21,000	33
B.S. Gas-Turbine	3,400	5.5

2.2 Summary of Features of Operating Plants

As of October 1960, more than 200 General Electric gas-turbines were in operation. These units have compiled more than 4,500,000 hours of actual on-the-line operation. Ten of the General Electric gas-turbines, in service by October 1960, have operated more than 50,000 hours each, 35 units have compiled over 40,000 hours each, and 64 units over 30,000 hours each (see Table 2-5). The largest GE gas-turbine, with a capacity of 25 Mw, is scheduled for 1963 for power generation for the Oklahoma Gas-Electric Company. It is a two-shaft regenerative-cycle design to be fired with natural gas.

Table 2-5

GENERAL ELECTRIC GAS TURBINE OPERATING EXPERIENCE

Application	Units*	Kw	Hours Operation	Machine Years
Locomotive	47	225,000	974,000	111
Electric Utility	41	343,900	274,000	31
Industrial-Power Generation	18	178,500	182,000	21
Industrial-Compressor Drive	27	151,000	710,000	82
Gas-Oil Transmission	87	398,000	2,350,000	268
Marine	2	7,500	10,000	1
Total	222	1,303,900	4,500,000	514

10 units each operated over 50,000 hours
35 units each operated over 40,000 hours
64 units each operated over 30,000 hours

*Shipped 10/60

Typical GE gas turbines are shown on Figures 2-3 to 2-6, which are produced for either simple-cycle or regenerative-cycle operation. Tables 2-5 and 2-6[28,29] include some descriptive data on these turbines.

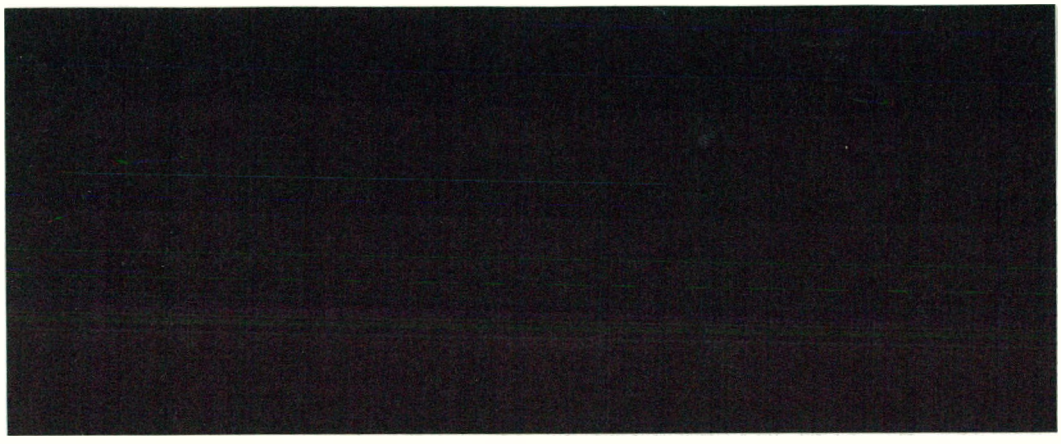


Fig. 2-3 - GE Typical Small, Simple Cycle, One-Shaft Gas-Turbine Unit

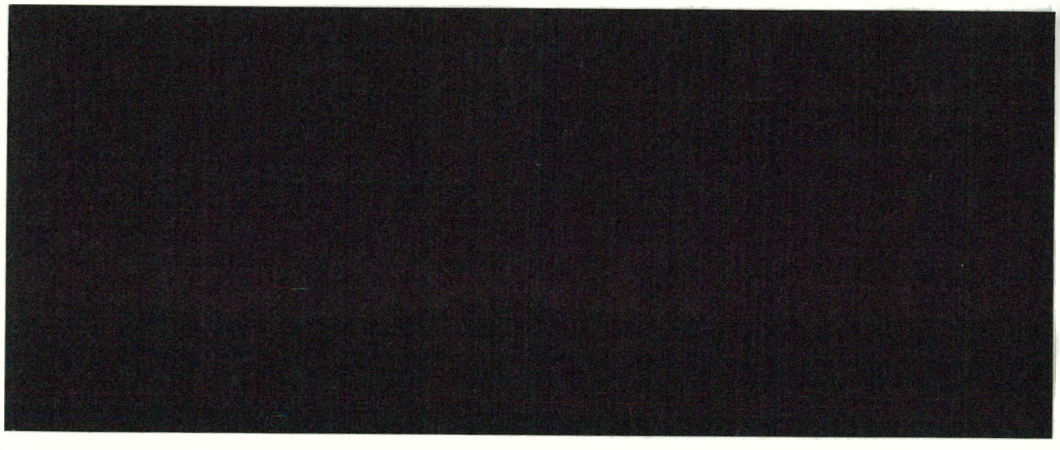


Fig. 2-4 - GE Typical Small Simple-Cycle, Two-Shaft Gas-Turbine Unit

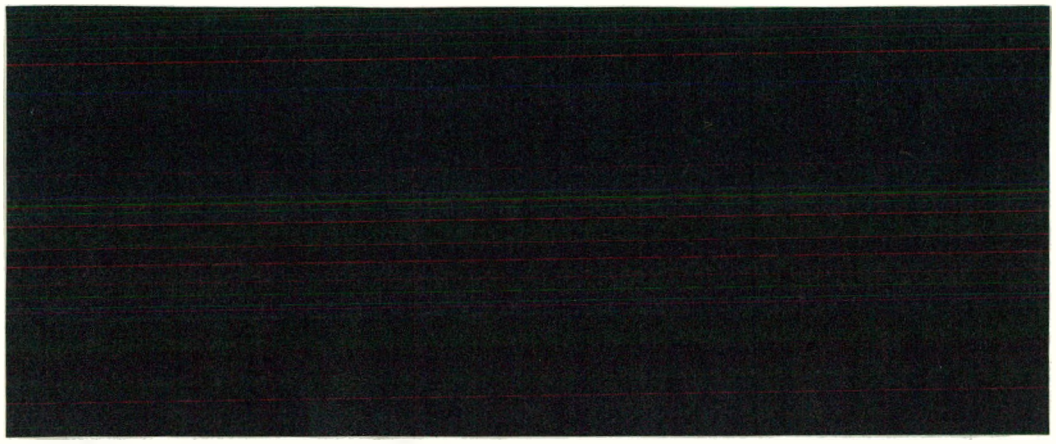


Fig. 2-5 - GE Typical Medium Size Simple-Cycle, One-Shaft Gas-Turbine Unit

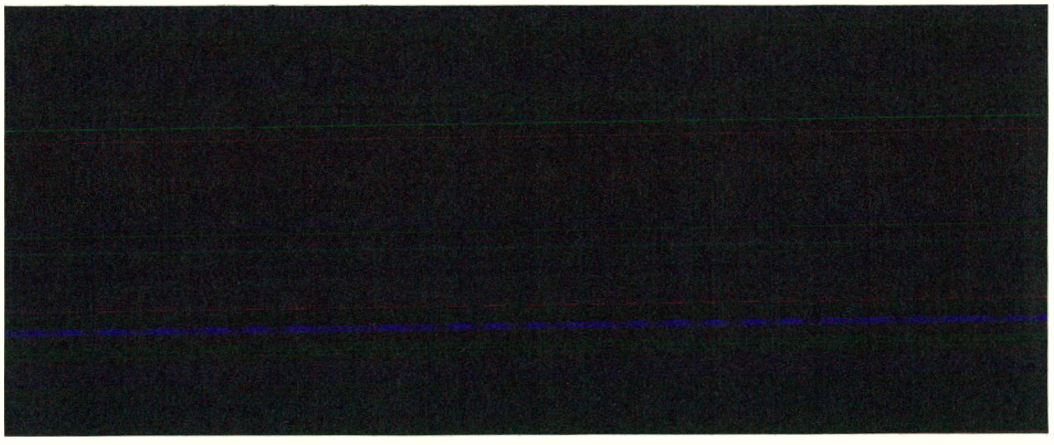


Fig. 2-6 - GE Typical Large Simple-Cycle, One-Shaft Gas-Turbine Unit

Table 2-6

GENERAL ELECTRIC GAS TURBINES, BASIC DESIGNS AS OF 1958[44,65]

Basic Design	Medium size, simple-cycle, one-shaft	Large Regenerative-Cycle, One-shaft (similar to previous large simple-cycle)	Large, simple-cycle, one-shaft
Application	Locomotives, refinery compressor drives, pipe-line compressor drives, power generation, general mechanical drives	Power generation	Power generation
Ratings	10700 hp to 14200 hp	16000 kW	21800 kW
Compression ratio	Approx. 6	Approx. 6	Approx. 6
Compressor stages	axial	axial	axial
Air mass flow, lb/sec		258	
Turbine stages	2 axial	2 axial	2 axial
Turbine inlet temp., °F	1450	1450	1450
Turbine outlet temp., °F	850	830	
Bearings	2 journal bearings, 1 thrust bearing	3 journal bearings, 1 thrust bearing	2 journal bearings, 1 thrust bearing
Output shaft at	Inlet end	Exhaust end	
Number of combustion chambers	10	8	12
Number of turbines installed or provided for installation 1961 and later	1961 - 6 turbines 1961/62 - 2 turbines 1961/63 - 4 turbines		1961 - 2 turbines

Another big gas-turbine manufacturer, Westinghouse Electric Corporation, built a prototype unit and subjected it to extensive shop testing in 1946. In 1949, this prototype unit was modified for pipeline service, driving a single-stage direct-connected compressor, and was placed on the Mississippi River Fuel Corporation pipeline. It has operated over 70,000 hours.[30]

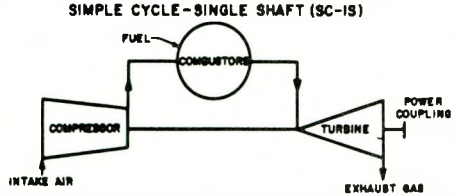
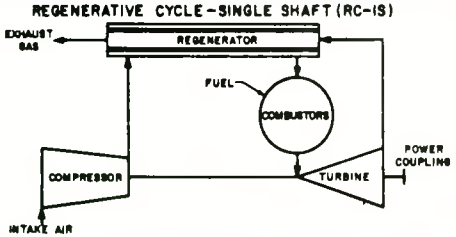
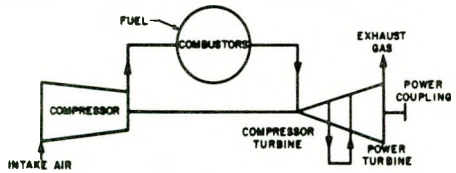
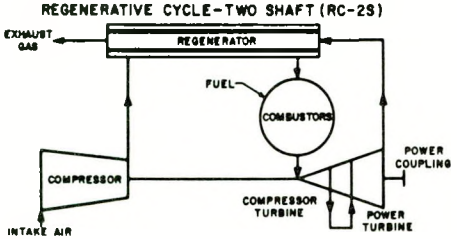
Westinghouse has developed a product line of five basic units ranging in capacity from 2250 to 25,000 kw, or roughly from 3000 hp to in excess of 30,000 hp (see Table 2-7)[10]. Figure 2-7[10] shows a typical cross-section of the Westinghouse gas-turbine line. In the main, Westinghouse units have been of the simple type without heat recovery, and are standardized on a two-bearing arrangement where the bearings are external to any of the hot gases. An axial-flow compressor is used, and six can-type combustors housed in a canted, conical housing. The units have no expansion joints and have a multi-stage, axial-flow turbine.

As typical example for the Westinghouse gas-turbine production line, let us cite a brief description of Model W-81. This gas-turbine consists of an axial flow compressor, six combustors, and a reaction turbine. The 16-stage axial-flow compressor swallows 3-1/2 tons of air per minute and compresses it to 70 psig. Approximately 11,000 kw are used by the compressor in compressing this air. At a temperature in excess of 500°F, air enters the combustion chambers where either gas or oil is burned to raise the temperature to 1350°F. At this point, it enters a 5-stage reaction turbine where it is expanded to atmospheric pressure and 740°F. The turbine extracts approximately 16,500 kw from the hot gases which is sufficient to drive the 11,000 kw axial-flow compressor and leave 5500 kw for the generator. Salient features in this gas turbine are[26]:

(a) Only two bearings support the rotating element. This minimizes alignment problems and eliminates a potential fire hazard which exists when a bearing is located between compressor and turbine.

Table 2-7

WESTINGHOUSE INDUSTRIAL GAS TURBINES

OPERATING CYCLE DIAGRAM AND NEMA DESIGNATION	MODEL DESIGNATION	RATINGS AVAILABLE	
		MECHANICAL DRIVE	POWER GENERATION
SIMPLE CYCLE-SINGLE SHAFT (SC-1S) 	W-31 W-81 W-121 W-201	3,250 HP 8,000 HP 12,000 HP 22,500 HP	2,250 KW 5,500 KW 8,500 KW 16,500 KW
REGENERATIVE CYCLE-SINGLE SHAFT (RC-1S) 	W-31-R W-81-R W-121-R W-201-R	3,000 HP 7,500 HP 11,300 HP 21,000 HP	2,000 KW 5,000 KW 8,000 KW 15,500 KW
SIMPLE CYCLE-TWO SHAFT (SC-2S) 	W-52	6,000 HP	4,000 KW
REGENERATIVE CYCLE-TWO SHAFT (RC-2S) 	W-52-R	5,000 HP	3,500 KW

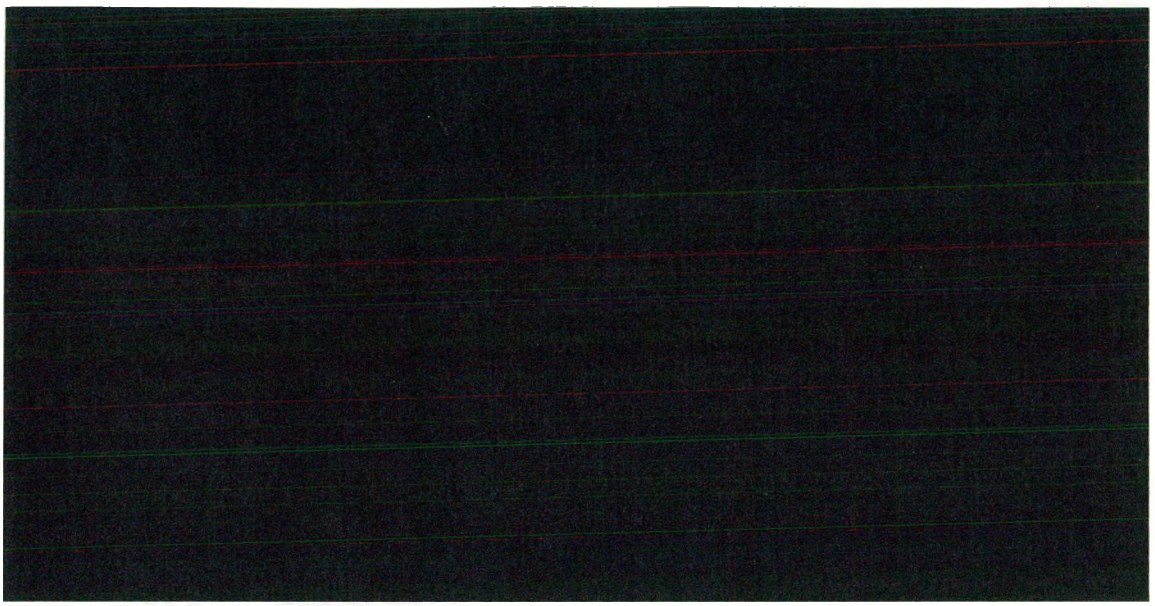


Fig. 2-7 - Typical Cross-Section of a Westinghouse Industrial Gas Turbine

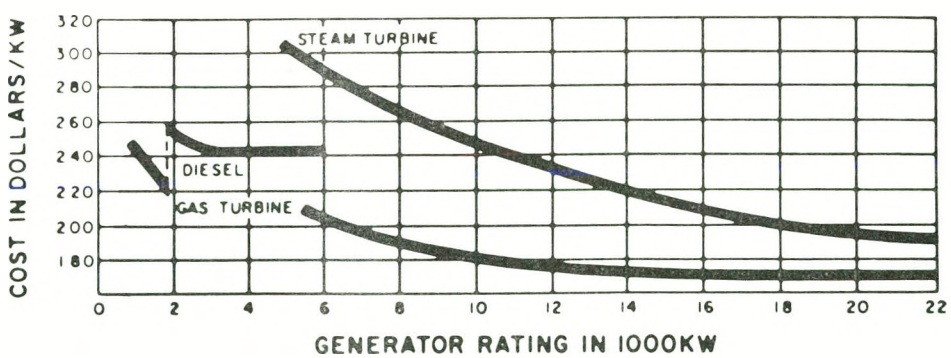


Fig. 2-8 - Comparative Plant Costs for Different Turbines

(b) Curvic couplings are used in the turbine rotor.

(c) Tangential exhaust bearing support struts. These connect the outer cylinder to the bearing housing at a tangent so that unequal heating of the struts with respect to the cylinder merely causes the bearing housing to rotate but stay coaxial to the cylinder

(d) The rotating blades of the compressor are locked in broached disk slots such that individual blade changes can be accomplished.

(e) Compressor stationary vanes are welded in removable segments to form a rigid support and to facilitate inspection.

(f) Turbine rotating blades are held in broached serrated slots, again for individual change-out.

(g) Turbine stationary blades are also welded in segments for ease of inspection.

(h) Combustor baskets are completely enclosed and have enclosed interconnection. Each combustor basket can be removed for inspection in a matter of minutes.

In addition to the eight above mentioned commercially available models, Westinghouse offers a line of gas-turbine power plants ranging from 3 to 150 Mw. The Econo-Pac Gas Turbine, a self contained plant for peaking, reserve, amd emergency, in capacities of 3000, 7000 or 12,000 kw, is a latest contribution to the production program. An operating summary of Westinghouse industrial gas turbines is presented in Table 2-8.

Another compilation, as of 1961, is shown in Table 2-9[30] giving application, number of units, and total hp of installed Westinghouse gas-turbines. Westinghouse Electric Corporation proposes a new concept - The modular concept. The modular concept employs combinations of previously developed and proven gas turbine units and unit components. Single power or gas producing sections can be mated with various output sections.

Table 2-8

WESTINGHOUSE INDUSTRIAL GAS TURBINES, OPERATING SUMMARY

Model	Rating	Number of Units in Operation	First Model in Operation	Total Operating Hours	Longest Operating Time Single Unit
W-21	1800 HP/1250 kw	4	May 1949	101,460	67,162
W-31	3250 HP/2250 kw	5	December 1956	127,800	30,252
W-52	5000 HP/3500 kw	14	December 1955	209,586	18,734
W-81	7000 HP/5000 kw	44	August 1952	681,750	54,827
W-121	14000 HP/10,000 kw	1	July 1959	9,615	9,615
W-201	125,000 SCFM	1	June 1960	175	175
		69		1,130,386	

THE FRANKLIN INSTITUTE - Laboratories for Research and Development

Table 2-9

WESTINGHOUSE INDUSTRIAL GAS TURBINES

Application	Number of Units	Total Hp
Oil Field Repressurization	28	224,000
Electric Power Generation	28	262,800
Natural Gas Transmission	23	147,300
Refinery	14	73,100
Marine Propulsion	7	65,000
Petro-Chemical	7	53,000
Crude Oil Transmission	4	32,000
Blast Furnace Blowing	1	15,000
Chemical	1	1,800
Mobile Power Generation	1	7,000
Mobile Process Air Plant	1	1,800
TOTAL	115	882,800

With the modular concept applied to gas turbine systems there is no longer a limit to the size of the gas turbines. Ratings as high as 150 Mw gas turbines can be built from standard components which could be used for peaking, and later combined with a steam plant to form a combined cycle.[30] Figure 2-8[10] shows comparative costs for gas-turbine, diesel, and steam-turbine base load power plants per kilowatt. Westinghouse Electric Corp. found that in the 20,000 kw range of capacity, a complete peak-shaving gas-turbine plant can be installed for between $100 and $125 per kw, as compared to $170, for the base load plant.

Since 1951 there has been a 5400 kw Brown Boveri gas-turbine set fired with blast-furnace gas, running in the ARBED steelworks at Dudelange, Luxembourg. It is performing well and, with a total of 63,000 hours' service, has the longest service record of all Brown Boveri gas turbines. Over 100 Brown Boveri gas turbines are now in operation with a total installed power of 1200 Mw.

The Escher Wyss Ltd. experience in design and construction of closed-cycle gas-turbine installations is of particular interest for nuclear applications. Since 1956, six solid-fuel-fired plants, rated from 2 to 13.5 Mw, have come into operation. Additional oil and gas-fired installations, both for stationary power plants and ship propulsion, have been built and operated or will soon start operation. None of these is in the U.S. A list of these plants, as of the end of 1960, is shown in Table 2-10[15].

Most of the coal-fired plants mentioned in Table 2-10 are used as combined power-production and central-heating installations. As the cooling water from precoolers of the cycle can be made available at about 190°F, a unique heat source at a convenient temperature level is provided for different industrial or domestic purposes. It should be noted that in contrast to steam plants, heat extracted from the closed cycle at the aforementioned temperature is pure waste heat. By using the heat from coal properly for both electricity and heat production, the over-all efficiency can be raised to 60 or 70 per cent. Central-heating schemes using waste heat are fast spreading in Western Europe and Russia. For combined power-production-and-heating systems, small and medium thermal power plants are best. Central heating is only economical when the distance of users from the power plant is not too great. In general, 1 kw installed may cover the needs of about one worker in industrial plants (Ravensburg 1800 kw for 1800 people). About the same amount (1 kw or about 3400 Btu per hour) may be consumed for heating purposes. Therefore, a closed-cycle plant of say 25 Mw electrical output will cover the needs of about 25,000 people with their families.

Erection in the Escher Wyss Works of the Machinery for the 10,000 kw Moscow plant is shown in Figure 2-9[31]. This plant started operation in September 1960. The gas turbine set at the Oberhausen plant began operation in October 1960 (Figure 2-10[15]).

Table 2-10

MAIN DATA ON SIX INDUSTRIAL SOLID-FUEL-FIRED CLOSED-CYCLE GAS-TURBINE PLANTS WHICH HAVE COME INTO OPERATION SINCE 1956

	Ravensburg, W. Germany	Coburg, W. Germany	Oberhausen, W. Germany	Moscow, Russia	Altnabreac, Scotland	Rothes, Scotland
Built by	EW/GHH	GHH	GHH/EW	EW	JB	JB
Purpose	E+H	E+H	E+H	E+H	E	E
Output, kw	2300	6600	13,750	10,000	2000	2000
Fuel, coal	Bitum.	Bitum.	Bitum.	Brown	Peat	Slurry
Lower heating value, Btu per lb	13,500	12,400	13,100	4500	5200	5900
Turbine-inlet temperature, deg F	1220	1255	1290	1255	1220	1220
Turbine-inlet pressure, psig	370	355	435	400	405	405
Heat production, normal, Btu per hr	7×10^6	26×10^6	65×10^6	-	-	-
Heat production, maximum, Btu per hr	12×10^6	55×10^6	85×10^6	32×10^6	-	-
Air heater tube dimensions, in.	1.3 x .1	1.3 x .13	1.3 x .11	1.6 x .16	$1\frac{1}{4}$ x 0.1	$1\frac{1}{4}$ x 0.1
Number of combustion chamber tubes	136	320	2 x 240	320	160	160
Combustion-chamber diameter, ft	9.7	15.2	2 x 14.1	17.7	9.9	9.9

E = Electricity, H = Heat, EW = Escher Wyss, JB = John Brown, GHH = Gutehoffnungshütte.

Note: John Brown Works, Clydebank, Scotland and Gutehoffnungshütte Sterrade, Oberhausen, Germany are licensees of Escher Wyss.

[Ref. 109]

Some of the operating experience gained at the Ravensburg plant is described in Section 2.3. Low cooling-water requirements and operational simplicity of isolated self-controlled plants bring about more and more applications of closed-cycle gas-turbine plants in remote areas. Experience shows that the air heater can use low-grade fuel without difficulty. For self-contained plants with widely variable load, the variable pressure-regulation system applied in closed-cycle systems leads to high efficiencies not only at full loads but also over a wide power range as compared with open-cycle gas turbines, in which the efficiency falls relatively rapidly at reduced loads.

Furthermore, as load capacity is independent of ambient air temperature, nominal load capacity is available in winter as well as in summer. Thus, plant efficiency depends only on the cooling-water temperature which varies less than ambient air temperature. This is different with the open-cycle gas turbine in which maximum load capacity is considerably reduced in summer. These facts can be seen, for example, in Figure 2-11[32], which refers to a General Electric open-cycle gas turbine and shows that the output "bonus" offered by this turbine operated at 0°F can be as great as 40 per cent over its normal rating at 80°F (standard conditions: 80°F and 14.7 psia, the latter corresponding to 1000 feet elevation). Summer operation has to be considered when evaluating the overall economy of a plant. For larger units, both maximum efficiency and part-load efficiency will be appreciably higher.[15]

Since World War II, the gas turbine has emerged as the dominant aircraft power plant for reasons of unprecedented performance and dependability. These basic assets, plus the ability to perform under all climatic conditions, to start and stop quickly, to attain full power without warm-up, and to require minimum operating and maintenance attention add up to broad technological potentials for the aircraft-type gas turbine in the industrial power field.

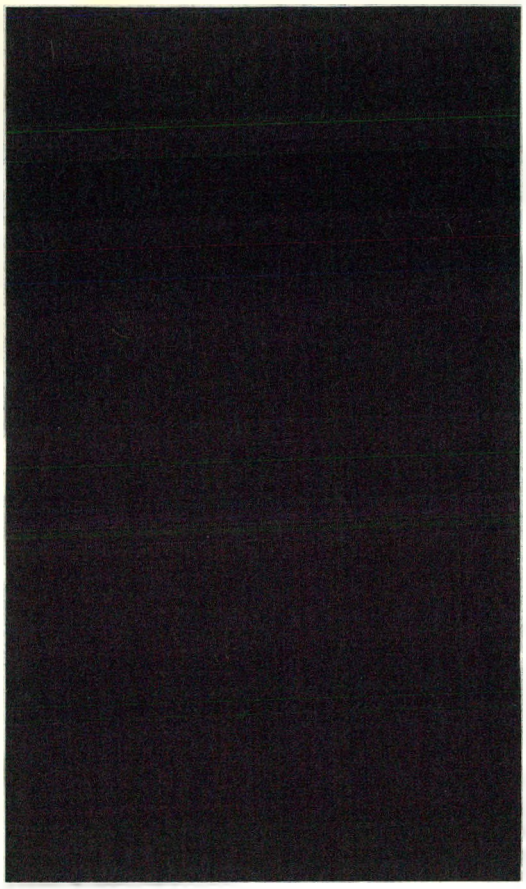


Fig. 2-9 - The 10,000 kw Moscow Plant Shown Under Construction at the Escher Wyss Works

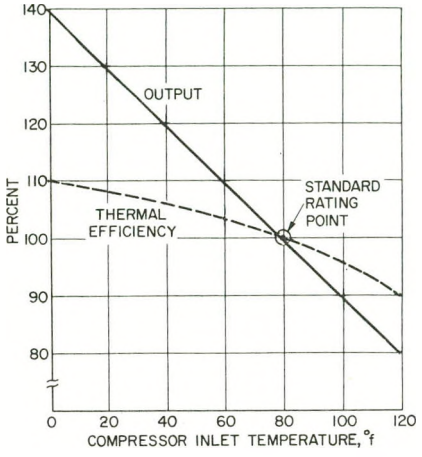


Fig. 2-11 - Dependence of an Open-Cycle Gas Turbine Output and Thermal Efficiency on Compressor Inlet Temperature

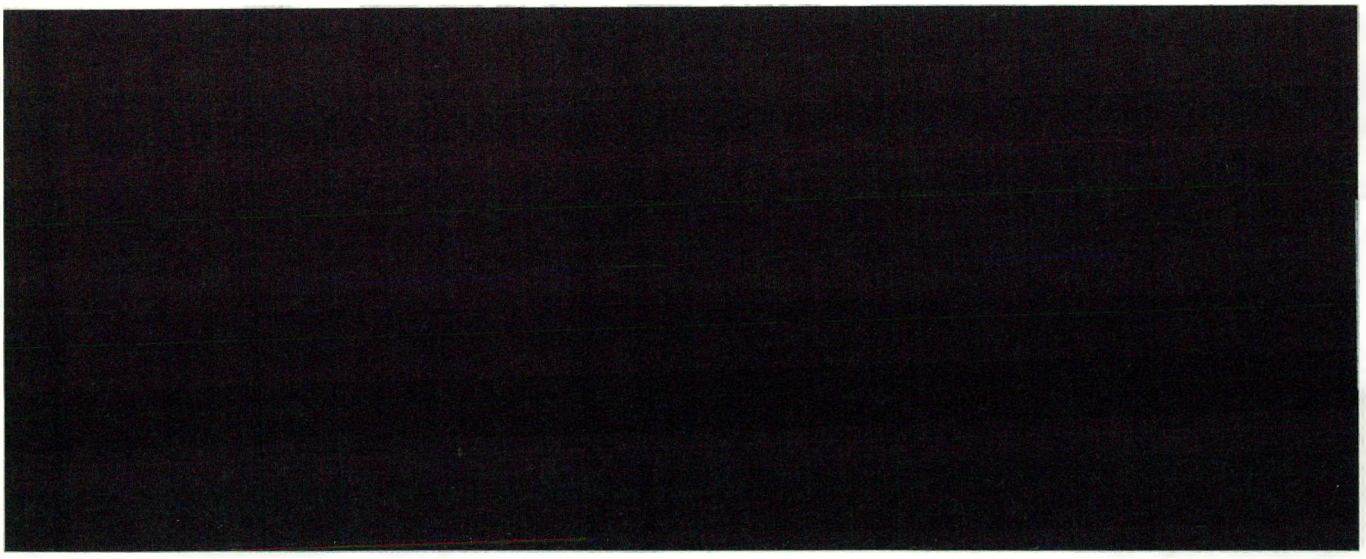


Fig. 2-10 - The 13,750 kw Machine Set for the Solid-Fuel-Fired Closed-Cycle Oberhausen Plant

Various aircraft gas turbines are promising for light-weight industrial gas-turbine installations (see Figure 2-12).

Pratt & Whitney Aircraft and Cooper-Bessemer Corporations have collaborated to produce the industrial package shown in Figure 2-13. It combines an industrialized PE WA J57, a widely-used jet engine, and a separate free-turbine unit supplied by Cooper-Bessemer (see also Table 2-1). This gas turbine already completed a 8000-hour run in a mainline compressor station[30]. Pratt & Whitney has now a series of aircraft-type gas-generators which can be used in conjunction with a free-running industrial power-turbine (see Figure 2-14).

A new line of gas turbines ranging in output from 50 to 20,000 shp with high power-to-weight ratios and the compact size of aircraft jet engines will complement General Electric's established family of land and marine gas turbines. They are designed for application where mobility and small size are required. Two models presently offered have been selected for marine and industrial applications or feasibility test in the field. They are the Model 240, rated at 20,000 shp (see Figure 2-15 and Table 2-1) and the Model 720/722 with a 900 shp output. Model 240 incorporates the basic gas generator used on the company's J79 military and CJ-805 commercial jet engine. It weighs approximately 5500 lb and operates on several types of fuel to serve as primary propulsion on an 80-ton hydrofoil boat being built for the Maritime Administration by Dynamic Developments Inc., an affiliate of Grumman Aircraft. Designed around the company's T58 turboshaft engine, Model 720/722 started service trials during 1960. It weighs 300 lb in its basic form. Typical engine packages with reduction gearing weigh about 1200 lb. Model 720 operates on kerosene, marine diesel oil, and aircraft gasolines, while the 722, similar in most respects to its sister power plant, burns natural gas.

Model 240 gas turbine is also being offered in a complete package for electric power generation, mounted on a trailer, with a total weight of 95,000 lb. Figure 2-16 shows a Bristol-Siddeley 3 Mw



Fig. 2-12 - Promising Applications of Aircraft Gas Turbines to Industrial Power Plants

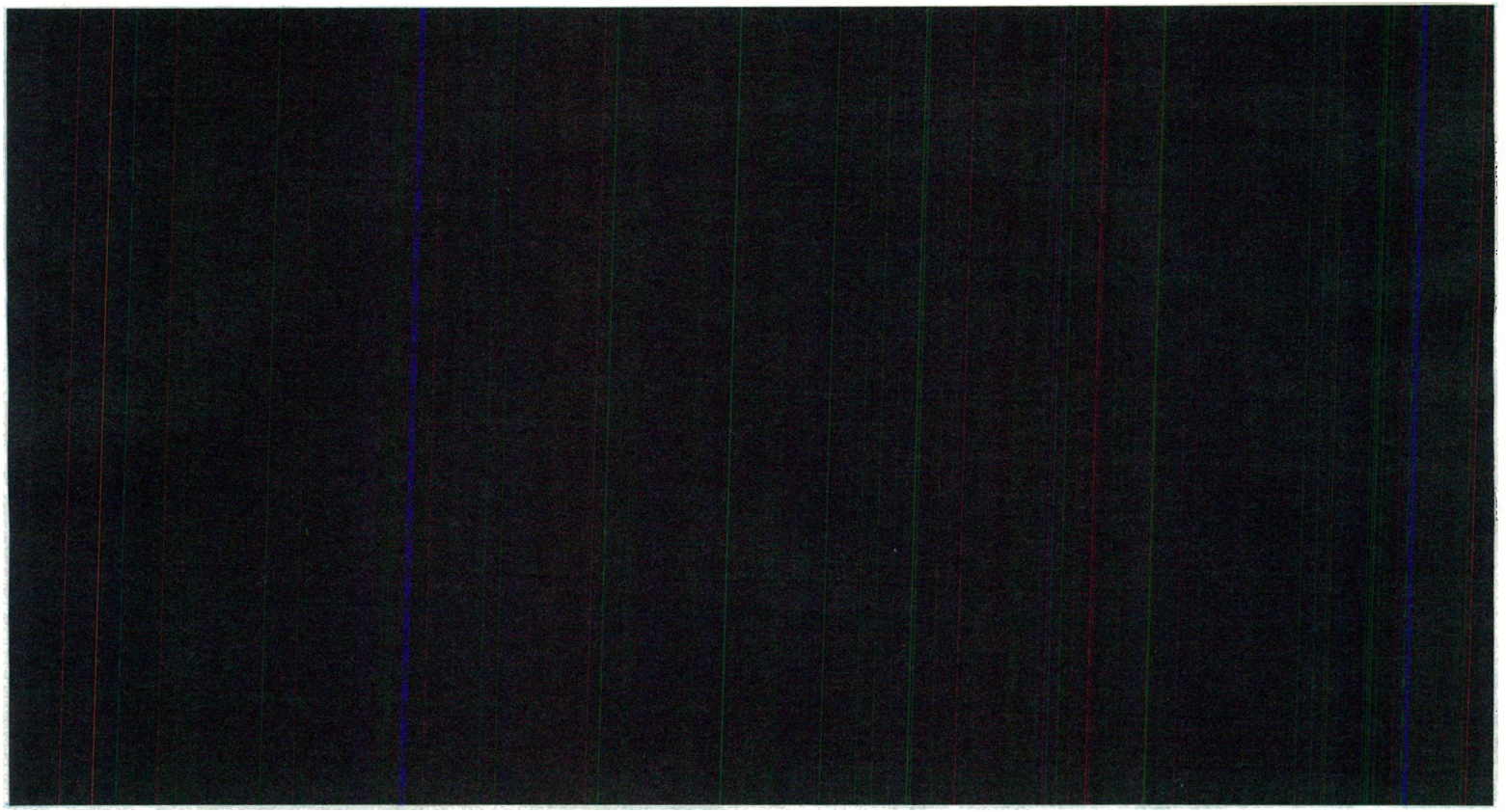
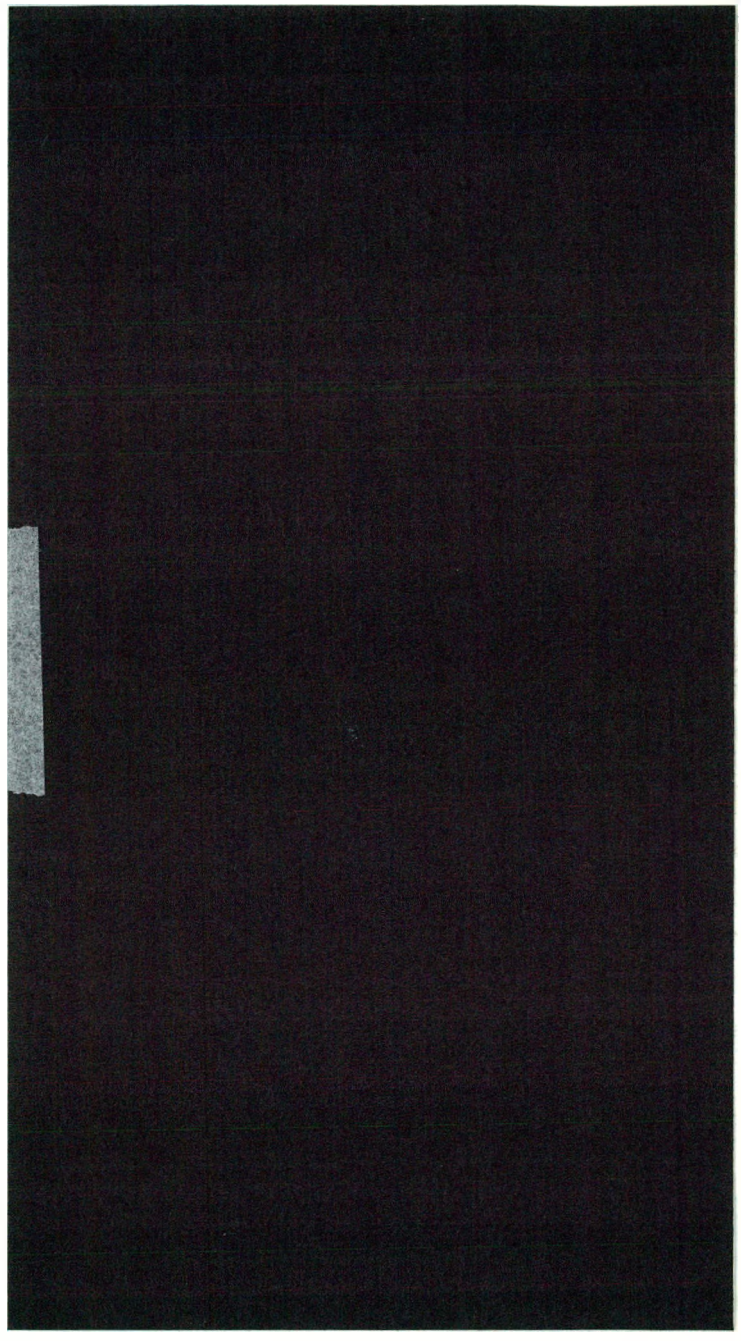


Fig. 2-13 - One-Quarter Scale Model of Cooper-Bessemer RT-248 Gas Turbine with Gas Generator Cutaway to Show Two-Spool Design.

Industrial Designation	Continuous Power	Air Flow
STG	350 hp	5 lb/sec
GG12	2500 hp	45 lb/sec
ST2	4600 hp	60 lb/sec
GG8	7000 hp	96 lb/sec
GG3	10500 hp	147 lb/sec
GG4	15000 hp	218 lb/sec



ST - Shaft Turbine

GG - Gas Generator

FT - Gas Generators with Integral Free Turbines (not shown).

Fig. 2-14 - Pratt & Whitney Aricraft Type Gas Turbines for Industrial Application

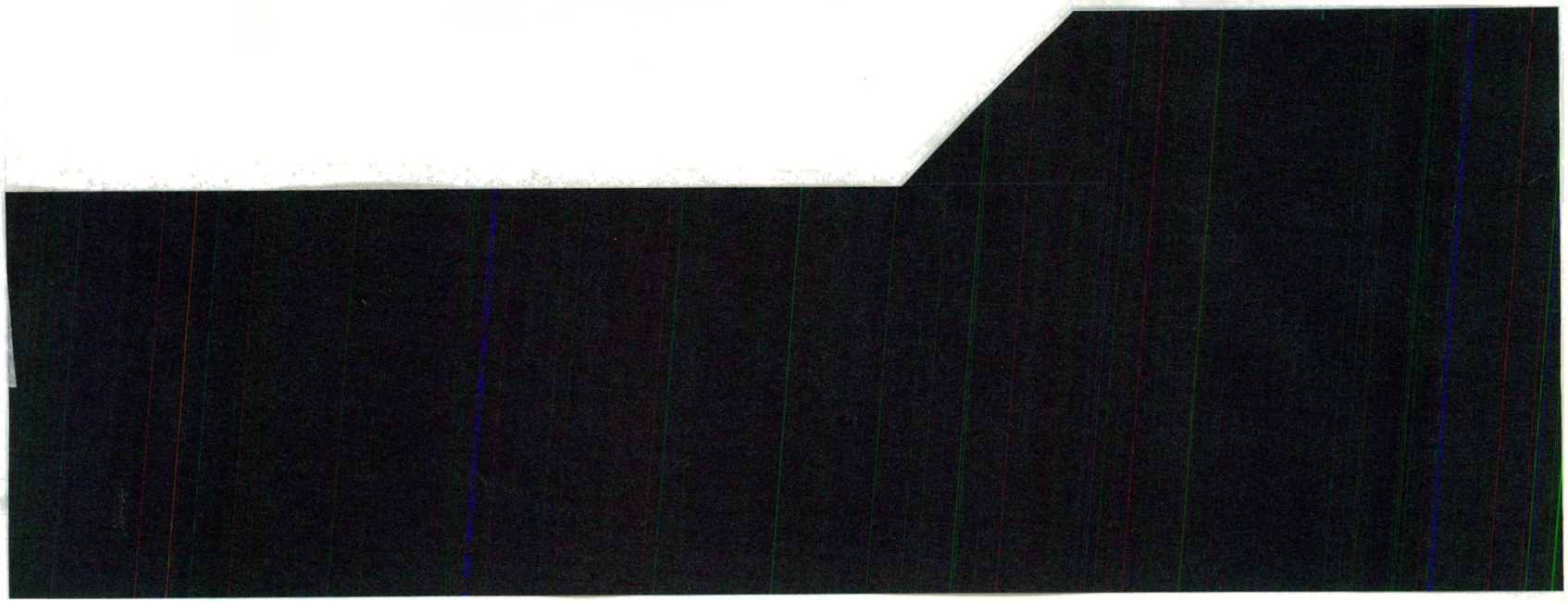


Fig. 2-15 - GE Model 240 Turboshaft Engine

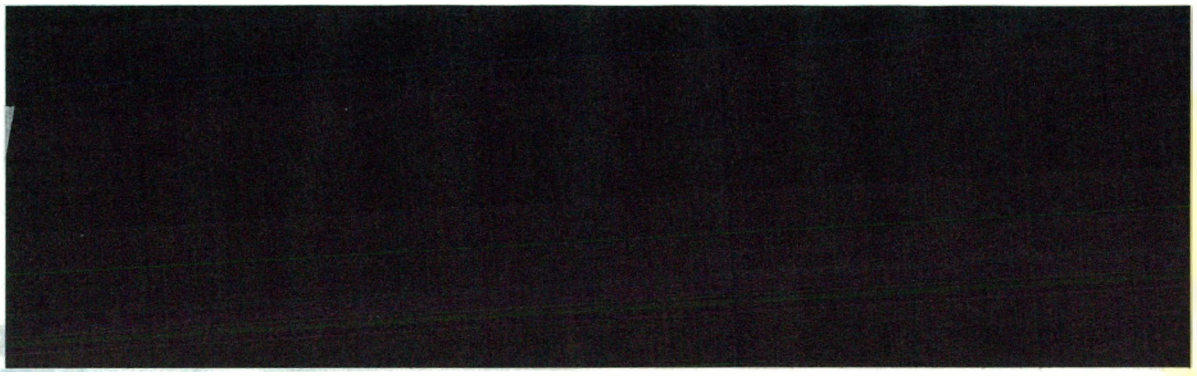


Fig. 2-16 - Bristol Siddeley 3 Megawatt Turbo-Generator

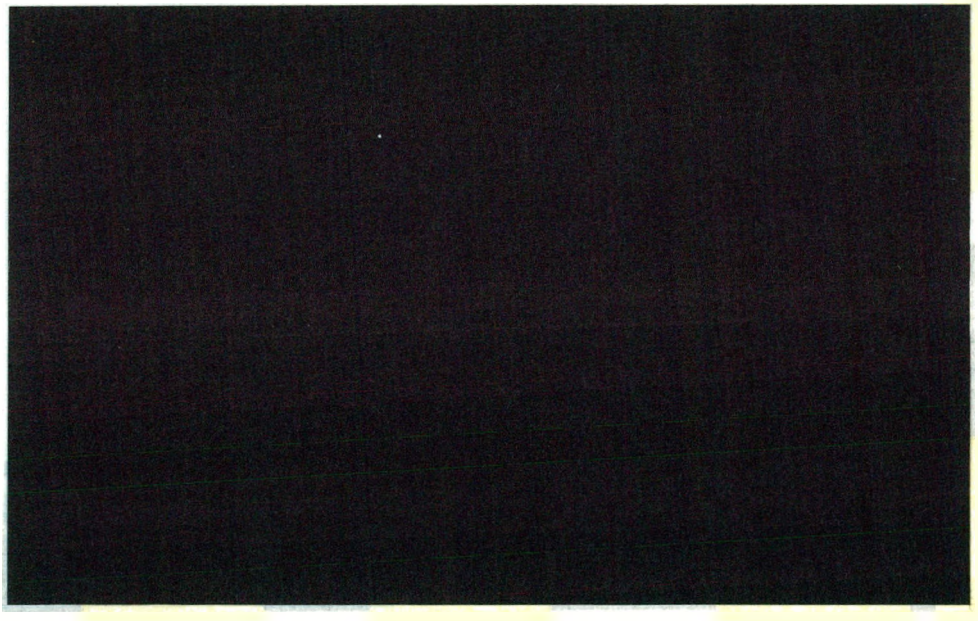


Fig. 2-17 - Generating Station at Princetown, Bristol Siddeley Industrial Proteus

turbo-generator for peaking or other non-continuous industrial application, or for a stand-by unit. The gas turbine used is a modified Bristol-Siddeley aircraft turboshaft engine. Figure 2-17 is an outside view of such small power plant.

Central Electricity Generating Board of England has placed an order for a Bristol Siddeley 15-Mw gas turbogenerator set using the Olympus jet engine as the gas producer. It is expected to go into operation in late 1962. The power turbine weighs 10 tons and the jet gas generator weighs only 2.2 tons. Similar developments exist in other parts of the world.

In describing the progress of the gas turbine, it is difficult to ascribe specific developments to a particular year. Generally they are the result of several years' evolution through stages of theoretical analysis, performance study, project design, test, and finally operating trial. Recent progress of aircraft engines embrace almost the whole flight spectrum from zero to supersonic speed. It is interesting to note that it is the two extremes of range which are receiving the most attention. In gas turbine development, it is perhaps noteworthy that all British by-pass engines are of the two-compressor type with air by-passed from the front compressor. No turbine has been made with the lift fan design which has been exploited in the U.S.

From a performance point of view, the merits of an aircraft engine depend upon achieving a high output/weight ratio, a low fuel consumption/output, and a high output/frontal area. These parameters are not always compatible with each other nor with other factors which may have important bearings on design such as cost, overhaul life, and reliability. The latter, as also for other gas-turbine applications, demands conservative design and stressing while the former call for high gas temperatures to give high specific output and high compression ratio for low specific consumption or efficiency. This is illustrated in Figure 2-18[32], for subsonic

and supersonic turbojet engines. It may be noted that the turbine temperature for the latter to achieve minimum specific consumption is on the order of 1200°K (1700°F). Hence, there is a considerable desire to operate with higher gas temperatures.

In the past, good consumption has been achieved by use of high compression ratio, or in other words, high compressor temperature rise. The compression ratio reached a limit of about 7 in single rotor engines some years ago and later development led to twin spool engines with pressure ratios of 12 and greater. More recent development has shown that the single rotor can overcome some of its limitations by the use of blow-off valves or variable stagger stator blades on one or more rows. These are now features of many high performance engines and pressure ratios of more than 10 are current in single rotors.

A still more recent approach to better consumption has been the introduction of a by-pass on turbofan engines. This improvement is basically due to the fact that, other things being equal, the thrusts from two engines with the same energy input are inversely proportional to their jet velocities or directly proportional to the square root of their gas mass flow. The by-pass augments the mass flow of a simple jet and generally retains the high pressure ratio of the twin rotor engine. There is considerable controversy on the optimum by-pass ratio and engines have been built with values of from 0.3:1 in the early Conway to 1.75:1 in BS.75. From the point of view of economy, the larger the by-pass the better, but the effect of forward speed on net thrust limits the secondary mass flow which is worth consideration. In addition, there are objections to the larger diameter and greater weight involved. Figure 2-19[32] illustrates the effect of by-pass ratio and pressure ratio in the struggle for better consumption.

Even lower consumptions are obtained, of course, if turbo-props are used. These may be regarded as the extreme limit of the by-pass engine as they accelerate the largest possible air mass flow through the propeller. They lose efficiency at much lower flight speeds.

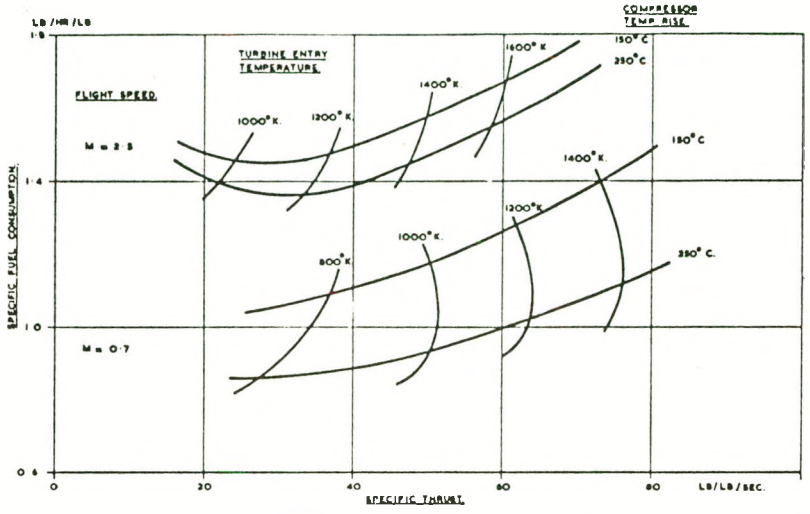


Fig. 2-18 - Theoretical Performance of Turbojet Engine

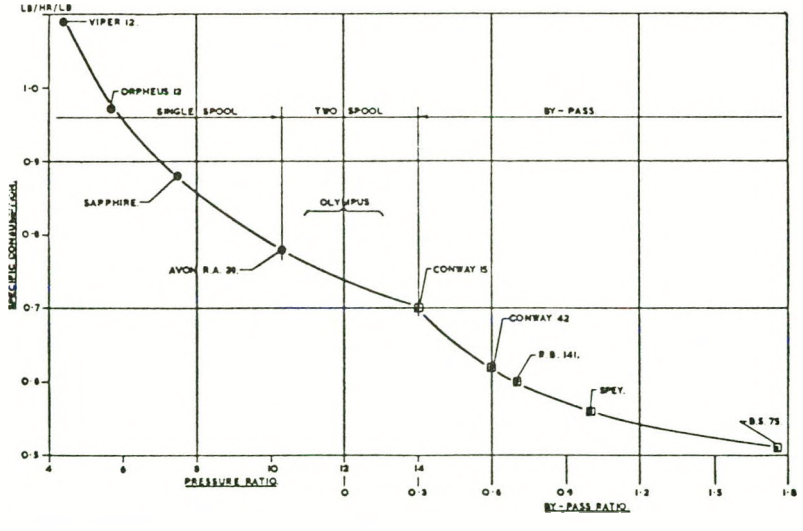


Fig. 2-19 - Specific Consumption of Modern Turbojet and By-Pass Engines

The Conway was the first modern British by-pass engine. It has been in commercial service since April 1960, and already a development program for higher ratings and better performance is well in hand. The rating of the R-Co 12 is 17,500 lb and by the end of this year the R-Co 15B will be delivered at 18,500 lb. The next development will provide a larger by-pass ratio by increasing the size of the low pressure compressor. This is a major revision but will retain the high pressure rotor system unchanged. It is designated R-Co 42 and will give 20,250 lb.

Another Rolls Royce by-pass, the Spey, incorporated much of the experience derived from the Conway. Its by-pass ratio is increased to unity and its pressure ratio to 16.75. It also has a radically changed fuel system which eliminates many of the small orifices, rubber seals, and other complications which have been troublesome in the past. There are other design differences, probably the most important being in the construction of the LP compressor which has blades pinned to flanges machined on a single drum instead of the conventional disks. A comparison with the Bristol Siddeley BS.75 is given in Table 2-11 (see also Figure 2-20[33]).

Table 2-11

BY-PASS ENGINE COMPARISONS

Engine	BS.75	Spey
Thrust (lb)	7550	9850
By-pass ratio	1.75:1	1.02:1
Pressure ratio	1.30	16.75
L.P. Compressor stages	3	4
H.P. Compressor stages	10	12
Air mass flow (lb/sec)	190	202
Thrust/frontal area (lb/sq.ft)	1040	1280
Weight/thrust (lb/lb)	0.199	0.223

The propulsion units for conventional subsonic aircraft, whether military or civil, have been developed by taking advantage of new ideas. Thus the by-pass engine is now established as a transport aircraft power plant alongside turboprop engines, and the pure jet still retains its position in the military field. The figures of transports (British) sold in the twelve months to March 1961 make this clear: 141 by-pass engine powered aircraft, 83 turbojet, and 58 turboprop.

Turbojet Engines

In the large thrust class, the Bristol Siddeley Olympus turbojet is now ahead of all others (see Figure 2-21). British turbojet engines have had more than ten years' development and "stretch" during which its thrust has grown from 10,000 lb in 1952 to 20,000 lb in 1960. The basic design of two-spool compression has remained throughout, although almost all design techniques for increasing thrust have been employed. Recently full reheat boosting has been added and more than 30,000 lb thrust is now available. Because of security classifications little further information can be published on design and performance. It is known that the Olympus has thirteen compressor stages on its two rotors and two single-stage turbines[32].

The Rolls-Royce Avon series has a similar long history and growth, although it might be more difficult to recognize the original engine as the parent of the present family. In contrast to the Olympus, the Avon has a single rotor with sixteen or seventeen compressor stages and a single turbine of three stages. Its most noteworthy feature during the past year has been an increase in overhaul life from 1600 to 2600 hours. No other turbojet has yet exceeded the former figure.

The third British engine with an interesting pedigree is the deHavilland Gyron Junior now entering production for the Blackburn Buccaneer. It was derived from the Gyron which as long ago as 1955 was approaching the 20,000 lb thrust mark and eventually achieved 30,000 lb with reheat before development stopped. The scaling-down process is

THE FRANKLIN INSTITUTE • Laboratories for Research and Development
F-A2392-

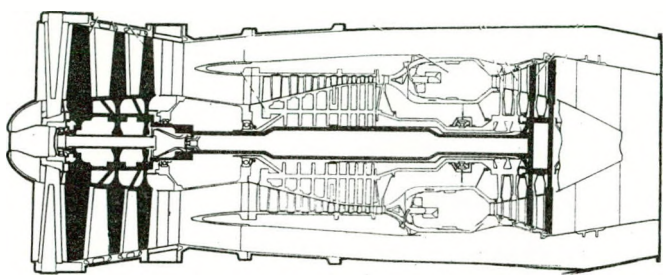


Fig. 2-20 - Bristol Siddeley BS 75 Ducted Fan Engine

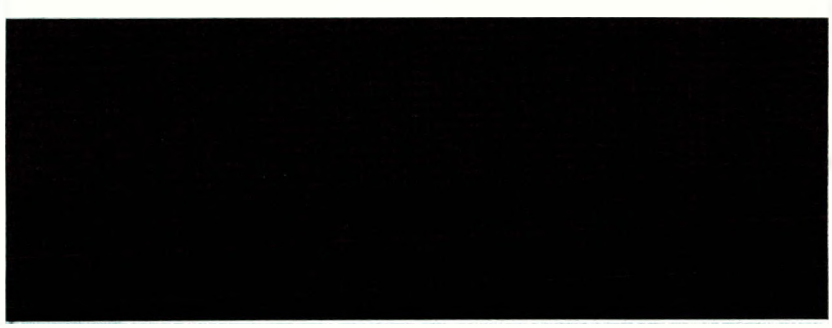


Fig. 2-21 - Bristol Siddeley Olympus BOl2l Turbojet Engine

the opposite to normal procedure but has produced an advanced engine which includes compressor air bleeding for aircraft control surfaces.

In the turboprop engine class, the Rolls Royce Dart has increased in power steadily through its life while reducing its specific consumption and specific weight. Improvements have been obtained by well-established techniques of increasing mass-flow, gas temperature, and rotational speed. The most remarkable development has been the increase in overhaul life which has continued steadily during the past few years up to the record figure of 3200 hours and is likely to be further extended. This means that overhaul is required only about once a year. All main components are good for two overhaul periods and some for three or four.

By comparison, the Tyne is a new engine with a greatly improved performance due to its double rotor layout. It has suffered a number of teething troubles, the most serious being a metallurgical fault which produced radial cracks in the compressor disks. This was traced and cured by special techniques for material production, forging, and heat treatment. A further trouble has been associated with turbine bearings and this has been manifested as vibration and oil leakage. In spite of these, development is proceeding towards larger powers.

2.3 Operating Experience

2.3.1 Turbine Performance

Operating experience has accumulated during the past ten years from the older generation of gas turbines. The main sources of such information are manufacturers' reports, published articles by gas turbine owners and operators, and reports of the various research establishments. At the same time, much important information is not available to the outsider either because the research programs are classified or because the manufacturers have a tendency not to reveal everything because of competition. In the following pages we shall present some of the information available from prominent industrial gas-turbine manufacturers.

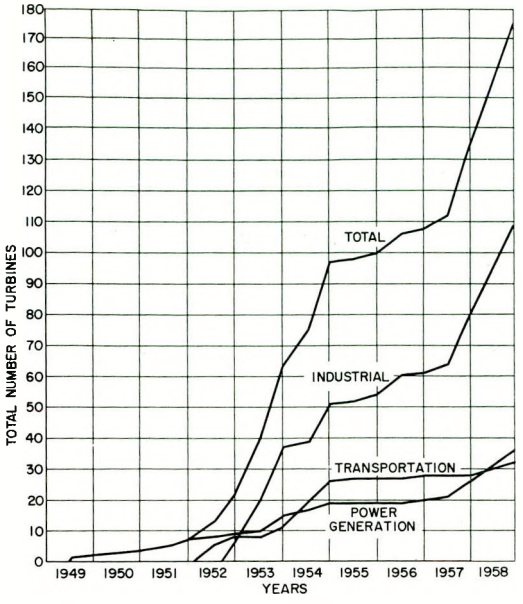
Let us begin with the operating experience of General Electric gas turbines[29]. At the end of 1957, there were 134 General Electric gas turbines installed and in operation in three basic applications: 80 industrial, mechanical drive; 28 transportation (27 locomotive and one marine); 26 power generation. The first of these turbines in commercial operation was a natural-gas-burning unit for power generation, operated in 1949. The first transportation application was a residual-oil-burning locomotive unit, operated in early 1952. The first industrial application was a gas-burning, two-shaft gas turbine for natural-gas pipe-line compressor drive, operated in the fall of 1952. The first marine application was a two-shaft, residual-oil-burning unit installed in a modified Liberty Ship hull (John Sergeant), operated in the fall of 1956. Electric utility applications include base load, end of line, peaking, and stand-by service. The industrial applications include natural-gas pipe-line compressor drive, refinery compressor drive, oilfield pressure maintenance, crude-oil pipe-line pumping and chemical-process compressor drive.

Figure 2-22[29] shows the progress of General Electric gas-turbine installations, at yearly intervals from 1949 through 1958. These turbines have been operated on five fuels: natural gas, residual oil, distillate, crude oil, and propane gas. The first natural-gas-burning unit went into service in 1949 and had accumulated 38,100 fired hours by September 30, 1957. The first residual-oil-burning unit went into service in 1950. One unit burning this fuel had accumulated 22,000 hours by September 30, 1957. At the end of 1958, 28 base-load units achieved an average of 27,000 fired hours. The 134 gas turbines in service by the end of 1957 included five different basic designs (see Table 2-12[65]). Figure 2-23[65] shows use factors, availability, and reliability of General Electric gas turbines before and through 1958. Figure 2-23 (d) contains evaluation of 28 base-load machines and gives the number of turbines considered for each year. The first five-year averages are 98.1 per cent availability and 99.3 per cent reliability.

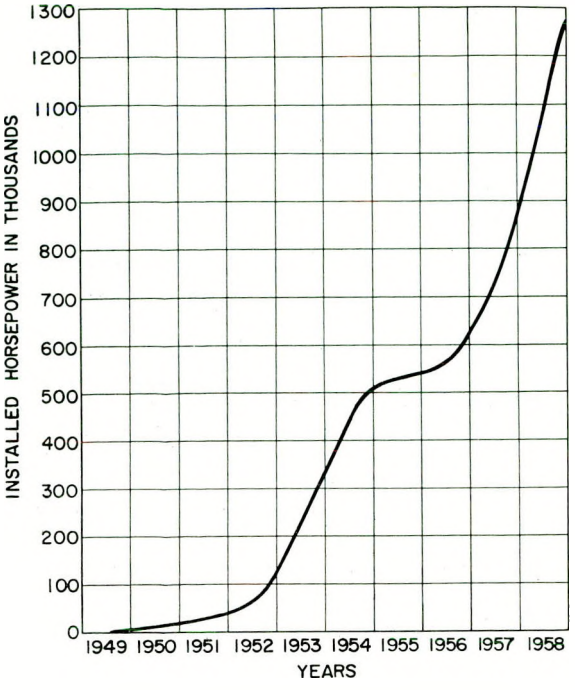
Table 2-12

GENERAL ELECTRIC GAS TURBINES IN SERVICE BY END OF 1957

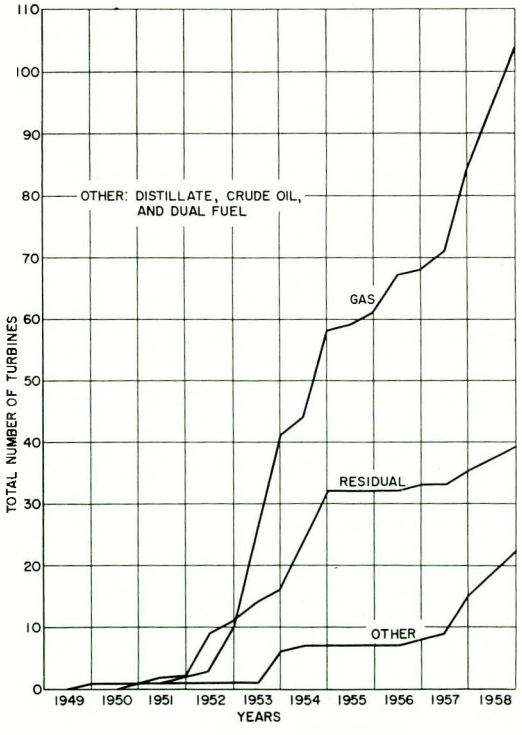
Basic Design	Small, Simple-Cycle, One-shaft	Small, Regenerative, Intercooled-Cycle, Two-shaft	Small Regenerative-Cycle, Two-shaft	Small, Simple-Cycle, Two-shaft (similar to previous, but without recuperator)	Large, Simple-Cycle, One-shaft
Application	Power generation, locomotive power plant, compressor drive	Power generation	Pipe-line compressor drives, power generation, and marine service	Crude-oil pipe-line pumping, oilfield pressure maintenance	Power generation
Ratings of built turbines	4800 to 7500 hp	normally 5000 kw	5000 to 7600 hp	6000 to 7850 hp	16,500 kw
Compression ratio	6.5		5.85	5.85	
Compressor stages	15 axial	11 axial HPC 9 axial LPC (var. speed)	14 axial	14 axial	15 axial
Air mass flow, lb/sec	98		98	98	258
Turbine stages	2 axial	First 2 axial driving HPC and output shaft, 3rd axial stage driving LPC	First 1 axial driving compressor, 2nd axial stage driving output shaft	First 1 axial driving compressor, 2nd axial driving output shaft	2 axial
Trubine inlet temp. °F	1450	1500	1450 and on some models 1500	1450 to 1500	1450
Turbine outlet temp. °F	830	820	900	900	830
Bearings	4 journal bearings, 1 thrust bearing	8 journal bearings, 4 thrust bearings	High-pressure set: 3 journal b., 1 thrust bearing. Low pressure shaft: 2 journal b., 1 thrust b.	High-pressure set: 3 journal b., 1 thrust bearing. Low pressure shaft: 2 journal b., 1 thrust b.	3 journal b., 1 thrust b.
Output shaft at	Exhaust end of Turbine	Intane of HPC	Exhaust end of Turbine	Exhaust end of Turbine	Exhaust end of Turbine
Number of combustion chambers	6	6	6	6	16
First operation	1949	1950	1952	1954	1957
Number of turbo. in service by end of 1957	42	10	61	18	4
Maximum fired hours of one turbine by Sept. 30, 1957	38,100	26,400	35,500	24,500	2500
See figure					



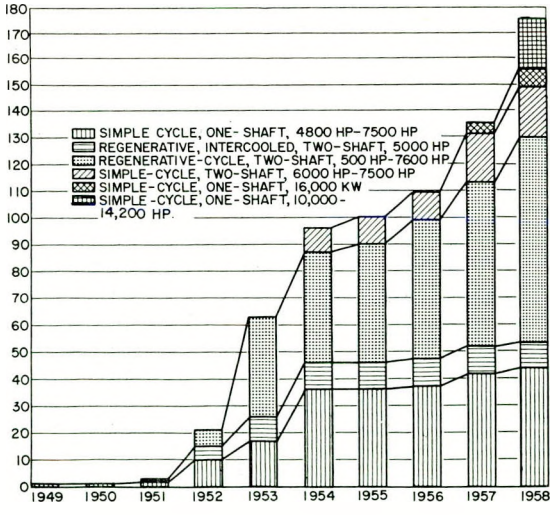
(a) Total turbines and their application



(b) Installed horsepower - total to date

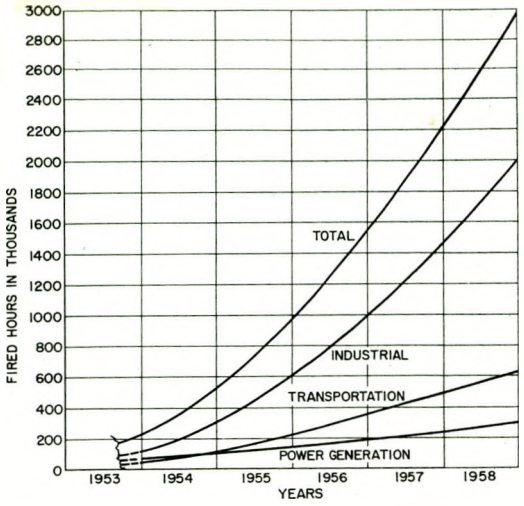


(c) Fuels burned

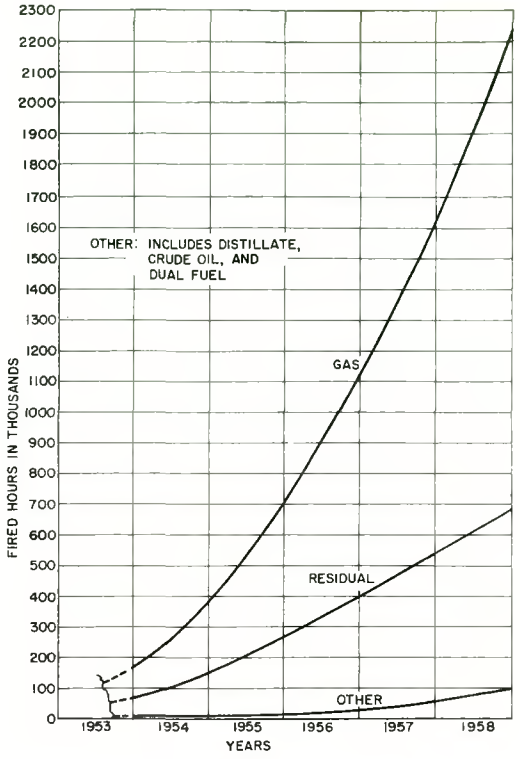


(d) Totals of each basic design

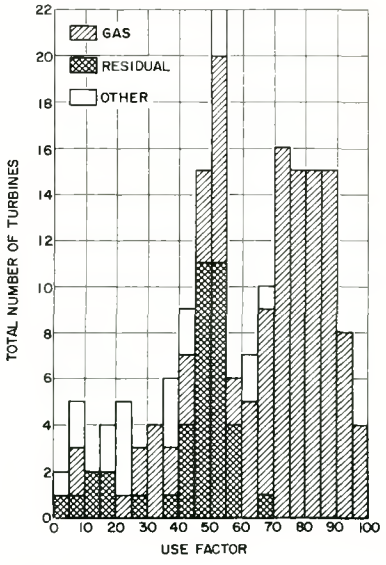
Fig. 2-22 - Progress of General Electric Co. Turbine Installations



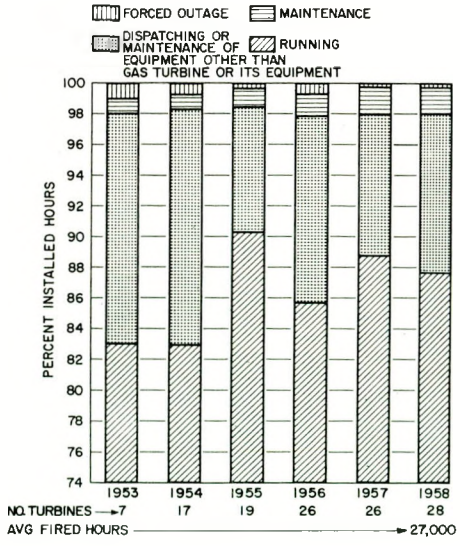
(a) *Fired hours for all General Electric gas turbines showing total hours and hours for different applications*



(b) *Fired hours for each type of fuel burned*



(c) *Chart showing use factor, and indicating fuel burned*



(d) *Chart showing use factor, availability, and reliability. Average for base-load units*

Fig. 2-23 - Operational Data of General Electric Industrial Gas Turbines

For an analysis, three units were picked out with use factors greater than 95 per cent (evaluation as per September 30, 1957). These units with little down-time, and those for reasons not chargeable to the turbine, essentially have average availability and reliability factors for the base-load group. The average for the three units follows:

Total installed hours	71,550
Fired hours	68,890
Maintenance hours	850
Forced outage hours	470
Other outage hours	1,320
Use factor	96.32%
Availability	98.17%
Reliability	99.34%

Another comparison can be made by looking at maintenance times. Machines with high use factors are usually maintained on tight schedules, working around the clock, while those with lower use factors take advantage of periods of no demand to minimize cost of maintenance. Over the long pull, however, the availability of low-use-factor machines remains at a respectable 85 per cent or higher, because maintenance is lower in proportion to use. Reliability stays about constant when the general level of maintenance is the same for high-use and low-use-factor units.

2.3.2 Component Performance

Component Failures

The accumulation of over 2,000,000 fired hours on 134 General Electric gas turbines as of September 30, 1957 has not been without component failures. Because they play a significant part in availability and reliability factors, they are listed below:

15 - First-stage bucket failures

8 - Damage due to overtemperature

6 - Second-stage bucket failures

2 - Turbine wheel failures

2 - Compressor guide vane failures.

It is interesting to note that while two of these failures occurred on one of the high-use-factor machines discussed above, its use factor is 96.6, availability 98.4, and reliability 98.8. A more detailed description and discussion of failures and part life follows.

First and Second Stage Buckets

Five of the first-stage bucket failures listed earlier were in buckets of Nimonic-80 material. Failure occurred at a point between 16,000 and 20,000 fired hours.

The buckets which failed experienced grain boundary separation. This separation was caused by slight material structural instability at operating temperatures, due to aging of the material at temperatures close to the full-load operating temperature of the bucket. It appears that the long-term stability of the material can be increased indefinitely by a special heat treatment involving double aging. This treatment combined with non-destructive testing has been used to correct all buckets of this type in service to avoid possible additional failures. Figure 2-24[29] is a photograph of a typical failure of this type.

Six second-stage bucket failures were attributed to material. These buckets were originally made of Timken material, and the failures were from fatigue due to vibration. These buckets are now made of Crucible 422 alloy and are operating satisfactorily.

Turbine Nozzles

Natural-gas-fired units have first- and second stage nozzles in operation in excess of 30,000 fired hours. Minor repair is sometimes required at inspection intervals; usually welding of small cracks in the trailing edge of the first-stage nozzle partitions. Turbines burning residual fuel in intermittent service have required some replacement of first-

stage nozzles at 5000 to 10,000 hours. The life of this nozzle is largely dependent on the condition of the combustion system, and the number of starts or heat-shock cycles it has been exposed to. The 5000- to 10,000-hour life includes operation previous to improved combustion systems, and heat-shock control modifications. Therefore, present life should be somewhat improved but how much is not established at this time. Many second-stage nozzles on residual burning units are still in operation, with minor repair, after more than 20,000 fired hours.

Heat Shock

Of fifteen first-stage bucket failures, ten were attributed to heat or thermal shock. Thermal shock occurs when the buckets are subjected to a very rapid combustion-gas temperature rise. The outer skin of the bucket attempts to expand since it feels the high temperature almost immediately. The bulk of the material toward the middle of the bucket, however, warms at a slower rate. Since the outer skin is trying to expand faster than the inner part of the bucket, it is subjected to very high compressive stresses. These high stresses (occurring at every start-up) plus minute notches on the leading edge due to corrosion, foreign particles, or both in the gas stream cause a crack to start.

The correction for this condition is, of course, to reduce temperature gradients during starting. This places a precise demand on the control system. It has been accomplished by arranging the various control systems to give small time-controlled increments of fuel during the starting cycle. Figure 2-25[29] is a photograph of a failure of this type.

Composite Turbine Wheels

Two failures were listed earlier which occurred in 1952 and 1955. One failure occurred in the dovetail area (bucket connection point) and the other failure was a separation between rim and wheel center. This wheel employed a high-temperature rim welded to a wheel center of lower alloy. The failure occurred in the weld area. Sonic

testing has been used extensively to inspect all composite wheels in service, and it is now a regular part of each scheduled maintenance inspection. With this kind of inspection there have been no further failures and the necessary control has been established to follow the sonic history of each composite wheel. Figure 2-26[29] is a photograph of the dovetail failure.

The turbine wheels are designed for at least 100,000 hours of service. There have been only two failures up to September 30, 1957. Already many gas-fired wheels have operated successfully for well over 30,000 hours. A larger number of oil-fired machines have wheels which have operated successfully for well over 20,000 hours even though they have been subjected to frequent starts and rapid variations in load. In some cases, minor repairs are required at inspection intervals. This usually consists of grinding out minute cracks in the dovetail area.

Combustion System

One of the earliest problems encountered with residual-fuel-burning units was the short life (100 to 300 hours) of combustion liners, and the short servicing interval (50 to 75 hours) of fuel nozzles.

Damage to the cap and liner consisted of the burning away of liner tabs, or liner hooks in local areas, and warping which then led to further overheating, closing off of cooling air slots, and rapid deterioration of the next section downstream. A new liner and fuel-nozzle combination was developed, usually referred to as air-swirl nozzle and louvered liner. In the louvered liner, this situation is improved by admitting air through a large number of closely spaced openings, formed by punching small portions of the liner surface outward. The use of many such openings permits a nearly continuous thin sheathing film, and by proper choice of louver size, spacing and location, cooling can be increased in local areas, which tend to run hot, and decreased in regions which run cool. Figure 2-27[29] is a cross section of the air-swirl nozzle and louvered liner combination.

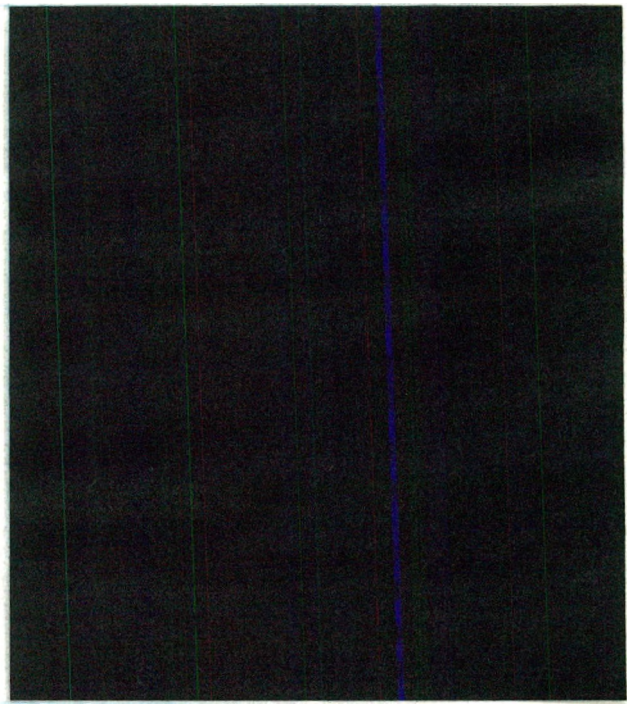


Fig. 2-24 - Nimonic-80 First-Stage Bucket Failure

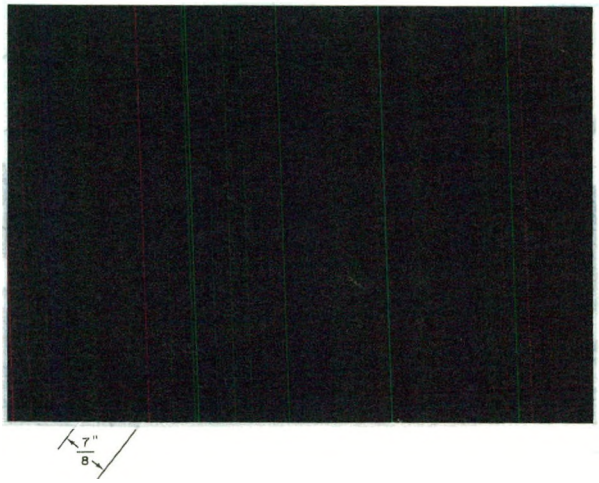


Fig. 2-25 - First-Stage Bucket Failure Caused by Thermal Shock

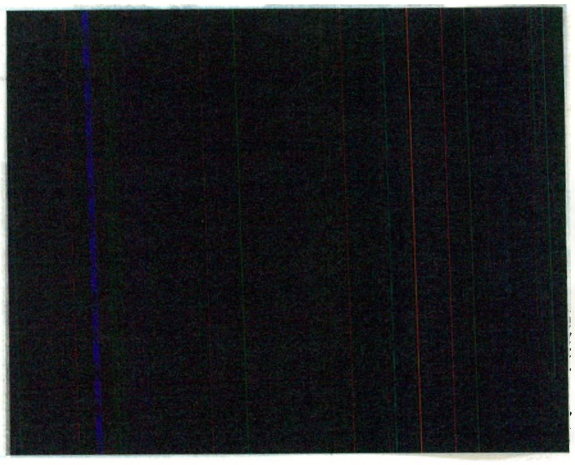


Fig. 2-26 - Wheel Failure in Dovetail Section

Fuel nozzles and combustion liners using natural-gas fuel have operated on many units in excess of 30,000 fired hours without signals of distress. In some cases, minor repair is required at the 8000 hour, or 24,000 hour inspections. Fuel nozzles, used with residual oil in intermittent service (frequent stops and starts), require cleaning at intervals of approximately 400 fired hours. This same fuel nozzle in continuous operation is expected to require cleaning at about 2500-hour intervals.

Combustion liners for intermittent residual-oil operation are operating satisfactorily for 3000 to 5000 fired hours. They are normally inspected at 400 fired-hour intervals, in conjunction with the cleaning of fuel nozzles. The life of these liners in continuous operation with residual fuel is not established but they will probably be inspected at 2500-hour intervals again in conjunction with fuel-nozzle servicing.

Fuel Treating

Early experience burning residual oils indicated that control must be maintained over the sodium, vanadium and calcium content to prevent rapid corrosion of turbine parts, and ash deposition. A treating and additive system has been developed to accomplish this control and maintain the specifications required to burn a wide range of residual oils.

Base Mounting

Early gas turbines were shipped with the turbine as an assembled unit, and oil tank, piping, wiring, and accessories were shipped as separate components. This method caused, in some cases, relatively long installation times and presented storage and handling problems.

To reduce installation time and cost to a minimum, gas turbines rated to approximately 13,000 hp, were modified to base mounting with the base containing assembled piping, wiring, auxiliaries, and the oil tank. The latest development is to deliver complete gas turbine package plants, which results in simple foundation requirements and fast installation of preassembled package components. GE estimates indicate that with nominal advance site preparation, a package plant of 10.75 kw capacity can be started within ten days after arrival at the site.

Horizontal-Split Casings

Many early gas turbines had some major casings with vertically split joints, rather than a split at the horizontal centerline. While vertical joints, in some cases, have an advantage in controlling temperature distortion, operating experience indicated disadvantages from a maintenance point of view. To keep major maintenance time as low as possible, all GE gas turbines are now built with casings split at the horizontal centerline. Figure 2-28[29] shows a typical unit with the top casings removed.

Thrust Bearings

During the early operation of the two-shaft mechanical-drive gas turbines, a series of load-turbine thrust-bearing failures occurred. The cause of these failures was found to be high static thrust loads at "break away" of the gas turbine load shaft and high-pressure (600-800 psi) single-stage centrifugal compressor. These failures were eliminated by increasing the effective area of the active thrust bearing to carry the high static loads.

Compressor Inlet Guide Vanes

Two failures were previously noted as inlet-guide-vane failures. The unshrouded guide vanes failed in fatigue. Shrouding of the guide vanes eliminated the trouble. This shrouding has been entirely successful since 1955.

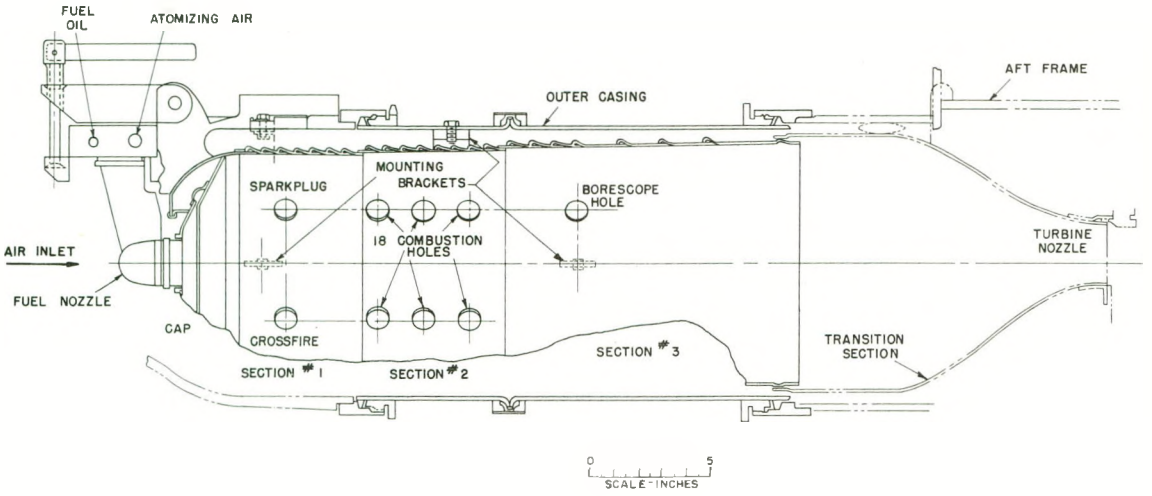


Fig. 2-27 - Section View of Combustion Chamber with Louvered Liner

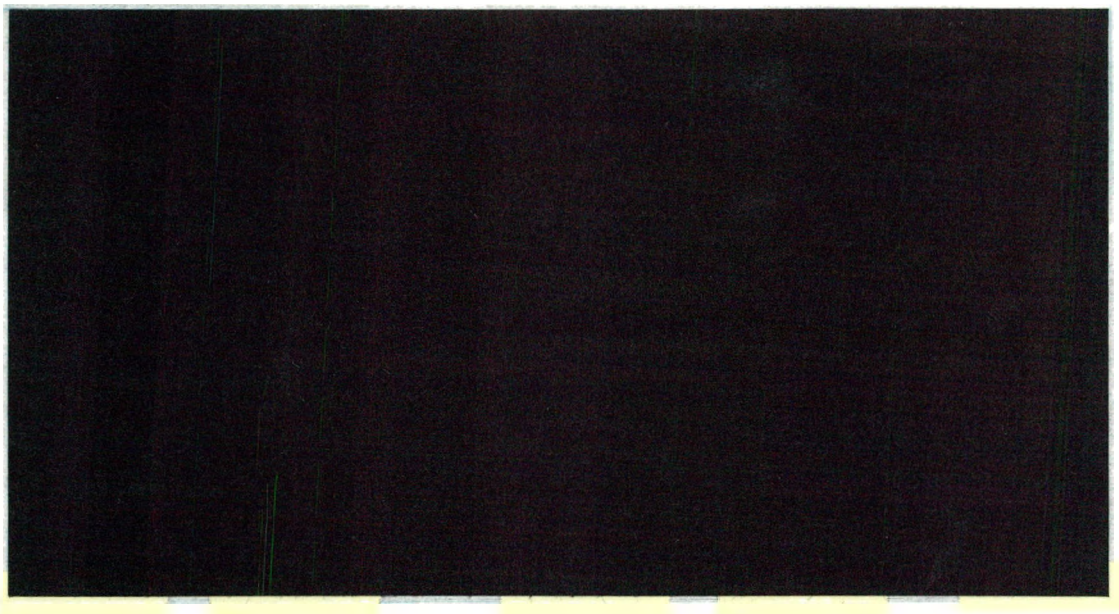


Fig. 2-28 - View of a Two-Shaft GE Gas Turbine with Top Casings Removed

Failure Experience by Air Force

An analysis of the failures in turbojet engines in U.S. Air Force[30] reveals the following information: Time to overhaul the average turbojet engines, based on three models for which considerable experience has been obtained, varied with engine model and application from 105 to 760 hours. Most frequent and consistent cause of overhaul was foreign-object damage, from 26% to 59% of the engines being overhauled for this reason. Failures in the hot section are a frequent cause for engine removal from aircraft. Failures of some engine parts have caused flight accidents. In 1953, 205 accidents were due to jet-engine failure or malfunctions. The responsible component was determined for 182 accidents. In decreasing order of frequency of accidents, there were 68 fuel-control failures, 54 compressor failures including foreign-object damage, 16 turbine bucket failures, 14 turbine disk failures, 10 main bearing failures, and finally 20 miscellaneous accidents from 16 different causes.

Of the 54 accidents resulting from compressor failure, only one involved a centrifugal compressor, although accumulated flying time for engines having centrifugal compressors was about the same as for engines having axial compressors.

Review of U.S. Air Force service records shows that foreign-object damage in jet engines is a major maintenance and safety problem. Few objects are identified; however, most damage is caused by air-base surface debris, parts of failed inlet components, and objects left by personnel. Centrifugal engines are much less vulnerable to damage than axial types. Aircraft designs providing maximum engine inlet height have minimum engine damage. Screens for axial-flow engines have not been effective in preventing damage necessitating premature overhauls but probably have prevented accidents. Personnel training, improved air-base debris removal, avoidance of mass taxi operations, improved engine screens, and engines of rugged construction are suggested as

remedial measures. Military failure statistics indicate that foreign-object damage, vibration fatigue, and stress-corrosion cracking are among the more important failure causes, placing compressor blades high on the list of engine components responsible for engine overhaul and flight accidents.

Service records for turbojet engines were studied to learn the types and causes of combustor failures and to obtain suggestions for improving engine reliability. Statistical data derived from the records show that the inner liner consistently accounted for the largest number of combustor failures in all engines studied, and several replacements of liners were usually made between major overhauls. However, liner failures rarely were the cause of an engine overhaul or an engine failure in flight. Liners usually fail because of thermal stresses induced by large temperature gradients and propagated by thermal cycling associated with starting, accelerating, and stopping the engine. Failures are accelerated by such factors as improper fuel flow, carbon deposits, and severe transients. Two serious flight accidents that occurred in 1953 were attributed to igniter and fuel-nozzle malfunctioning.

Repeated thermal stresses are the most important factor causing damage to nozzle diaphragms. These stresses arise from nonuniform temperature distributions and from constraints which prevent the nozzle diaphragm from expanding and contracting freely during heating and cooling. Repetition of these stresses occurs during starting, acceleration, and stopping and eventually causes cracks along the edges of the nozzle vanes, at the trailing edge of the vane slot in the inner ring, and in the weld joining the inner ring to the mounting flange. These cracks usually do not progress to complete failure of the unit.

Although cracks in nozzle diaphragms are frequent and add to the cost of engine maintenance, they rarely cause engine failure. Damage to nozzle diaphragms is not a problem with respect to reliability at the present time. This may be due to frequent repairs and replacements

in the field and during major overhauls for other types of damage. Cracks, because of their rate of propagation and effect on engine operation, can be safely handled by scheduled inspection. This involves costly repairs and replacements. Cracking of nozzle diaphragms can be reduced in the following ways:

(a) Incorporate provisions to allow parts to expand and contract freely.

(b) Distribute temperature more evenly throughout nozzle diaphragm and attaching parts of the engine.

(c) Use materials with better resistance to repeated thermal stressing.

(d) Eliminate vane slots in inner ring or reduce their tendency to promote cracks.

Rapid deterioration of the nozzle diaphragm occurs when, through malfunction of the combustor, severe overtemperature occurs. Overtemperature may cause sections of nozzle vanes to be burned off. Nicks and dents in the exposed surfaces are frequently caused by foreign objects.

Air Force service records indicated that for several models of the jet engine turbine-bucket, replacements are frequently necessary because of bucket cracking or fracture. Bucket fracture occasionally occurs in flight. In engines with single-stage turbines, the fragments from fractured buckets are often ejected through the discharge nozzle with no further damage and little loss in thrust. There is a risk associated with permitting bucket fracture in flight, however, as attested by the fact that in 1953, of 205 Air Force flight accidents attributed to jet-engine malfunction, 16 were traced to turbine-bucket failure. In the case of multistage turbines, the probability of catastrophe from failure of a turbine bucket is much greater. A failed bucket in an early stage may destroy the buckets in successive stages and stop or destroy the engine.

Turbine buckets are subjected to the combination of centrifugal stress, vibratory stress, high and rapidly changing temperature, and a corrosive atmosphere. Turbine buckets can fracture by stress-rupture or fatigue, or a combination thereof. Fracture can be accelerated by damage from overtemperature or overstress, or damage or cracks resulting from thermal fatigue, or perhaps from corrosion, or nicks caused by solid objects in the stream.

Disk failure in an airplane turbine can cause immediate destruction of the airplane: of the major airplane accidents caused by the engine in 1953, 8% were due to failure of turbine disks. Evidence of incipient failure is frequently found in the disks of engines being overhauled for other reasons. Disk failures encountered in service were found to have resulted from (a) tension in the serration area; (b) radial cracking of the rim, particularly at bucket-retaining pinholes; (c) fracture at weld in composite disks; or (d) failure of the shaft.

Two suggestions for avoiding flight failures have been considered. They are for design improvements in the disk-cooling system and for scheduled inspections to detect cracks, abnormal growth, and distortion in the bucket-root area. The inspection schedule for each disk type should be based on service experience with the specific disk.

Various types of bearing failure, mechanisms of failure of these various types, and possible methods of improving bearing reliability are discussed. Fatigue life, which is of primary importance to ball thrust bearings, can be increased by reducing load. At present, it appears necessary to schedule bearing replacements on the basis of expected fatigue life. Excessive wear rate indicates need for redesign. Under conditions of normal wear, bearing replacement can be based on measured clearances in the bearing at inspection periods. For extreme boundary lubrication failures, when excessive metal transfer occurs at the sliding surfaces, material change and redesign are indicated. Bearing reliability can be improved by (a) additional information, (b) better

failure detection devices and (c) better maintenance practice. Bearing temperature acceleration seems to be a parameter that can be used to warn of imminent bearing failure.

Improvements in manufacturing standards and in quality control should result in improved reliability. Reliability of fuel controls in turbojet engines has been studied on the basis of available failure statistics. In general, these statistics indicate that fuel-control systems that incorporate many functions are more subject to failure than those incorporating fewer functions.

Air Force accident records indicate that one-third of the flight accidents occurring with turbojet aircraft are caused by fuel-control malfunction. An evaluation of the performance of current fuel controls from Air Force records indicates further that nearly three-fourths of the fuel-control malfunctions are attributable to mechanical failure of control and fuel-system components and that one-fourth are due to inadequacy of the control method. Therefore, the possibility exists that a significant improvement in turbojet-aircraft reliability could be achieved by improvements in the details of mechanical design of control and fuel system components.

Effects of fuel-control malfunctions on engine performance have been examined. Evaluation indicates that fuel-control complexity results from complex requirements imposed by the dominant requirement of operational reliability of the turbojet aircraft.

Reliability of the turbojet engine can be improved by increasing the endurance of its components and by providing for removal of critical components from the engine before their failure jeopardizes the engine. Basis for the removal of engine components must come from an understanding of their failure causes and characteristics.

2.3.3 Component Life

Operating conditions have a major effect on the life of component parts. For example, gaseous fuels produce less deterioration than residual fuels. Likewise, continuous service is less severe than intermittent service. As service experience is gained, designs are being modified continuously to improve the life of the parts under all operating conditions. Table 2-13[65] shows the life which has been obtained up to September 30, 1957 under favorable conditions, such as continuous operation on gaseous fuels and also under the most severe conditions, such as railroad service where the machines are not only operated on residual fuel but also subjected to frequent starts and rapid load variations. For residual-fuel machines in normal industrial service, the life of the components should be appreciably greater than for railroad service.

Table 2-13

COMPONENT LIFE OF GE TURBINES

	Gas-fired Continuous Service (hr)	Residual-oil Intermittant Service (hr)
Combustion liners	Over 3000	3000 to 5000
Fuel nozzles	Over 3000	Over 10,000
First-stage turbine nozzle	Over 3000 (minor repairs)	5000 to 10,000 depending on service conditions
Second-stage turbine nozzle	Over 30,000	Over 20,000 (minor repairs
Turbine buckets	Over 30,000	Over 20,000
Turbine wheels	Over 30,000 (minor repairs)	Over 20,000 (minor repairs)

2.3.4 Maintenance

Maintenance practices vary greatly with the type of fuel burned and the type of service in which the gas turbine operates. In general, with gas-fired high-use-factor machines, It is recommended that partial inspections be made at yearly intervals (8000 hours), and complete inspections be made every three years (24,000 hours). In actual practice, many machines receive their only inspections at 16,000-hour intervals and in a few cases at intervals even longer. Residual-oil-fired machines in intermittent service (50 to 60 per cent use factors with frequent stops and starts) generally receive a yearly partial inspection (4000-5000 fired hours) and every two years a complete inspection (8000-10,000 fired hours). These units also receive minor combustion inspections at shorter intervals.

Gas-fired units receive combustion system inspections usually in conjunction with the partial and major inspections listed above. Residual-oil-burning units, as noted previously, require fuel-nozzle servicing at 400-fired-hour intervals. Combustion liners are inspected in conjunction with this servicing. The inspection at this time is with a borescope to keep down-time at a minimum. Further inspection is dictated by observations with the borescope.

Under certain conditions and in some applications, oil vapor, dust, sand, or water-soluble compounds may be carried into the axial-flow compressor inlet. In the case of water-soluble compounds or combination by oil vapor and dust, a build-up on compressor blades may occur, reducing compressor efficiency and capacity. The rate of build-up determines the compressor cleaning interval. An injection method has been developed of cleaning these compressors while running. In the case of sand or cinders entering compressors without inlet air filters, it has been necessary to reblade at intervals as short as 15,000 hours. The interval depends entirely on the severity of the abrasive intake.

Nozzles, buckets, and wheels are inspected partially during minor inspections and are inspected thoroughly during the major inspection. The inspection consists usually of visual, plus liquid-penetrant testing, and in the case of composite wheels, sonic testing. Necessary minor repairs are made based on the findings of these tests.

The periodic minor and major inspections mentioned apply to all gas turbines. Not much practical experience has been recorded to date as to time and manpower requirements to perform these inspections. But indications are that the minor inspection requires 350 to 450 man-hours and the major inspection, 800 to 900 man-hours. It should be expected that these requirements will decrease with practice and experience, and should approach 0.1 manhour/hp for a major inspection and 0.04 manhour/hp for a minor inspection at present turbine ratings. Regarding the GE gas turbine package power plants, access to the turbines for routine inspection and minor maintenance is achieved by swinging up the hinged side panels of the enclosure. The availability of a long-term maintenance contract from GE adds to potential reliability of the package plant.

The following running experience with GE gas turbine locomotives of 8500 hp has been reported[34]. On August 31, 1958, the first of 30 gas turbine-electric locomotives was placed in service on the Union Pacific Railroad. Four locomotives were delivered in 1958 and seven in 1959. By October 1, 1960, 19 locomotives were in service, under severe conditions, and had already totalled 95,000 fired hours. The maximum fired hours for any one turbine was 10,218, the minimum 306. The General Electric frame size 5 gas turbine used in these locomotives is a simple-cycle, single-shaft, two-bearing machine having a 16-stage axial compressor and a 2-stage turbine operating at 4860 rpm. The turbine, when ordered in 1957, was an entirely new model, and many modifications were developed on the manufacturer's test stand before the first locomotive was delivered in 1958. The need for other changes was discovered in field service, and improvements developed as a result of service problems were incorporated by the manufacturer in turbines yet to be delivered.

Prior to the delivery of the first locomotive, factory tests had revealed that a serious rotor-bow condition could develop during short shut-down periods. This was not compatible with the start-and-stop type of operation to which these locomotives would be subjected. To prevent this condition, the gas turbine is automatically cranked at 750 rpm whenever it is shut down. Cranking is performed by motoring the No. 1 generator. If this cranking should fail, the rotor would bow and cause excessive vibration when the turbine was restarted. In the event that the auxiliary diesel engine could not supply power to motor the No. 1 generator, the cool-down cranking feature would be lost. To prevent excessive rotor bow under such abnormal circumstances, an air-circulation system was developed for the distance piece located at about the mid-point of the compressor and turbine-rotor assembly. A small battery-powered, motor-driven blower provides sufficient air to keep the hot air around the distance piece from stratifying and maintains rotor bow below vibration limits.

All turbines are equipped with GE vibration detectors that shut the turbine down if vibration in the horizontal plane exceeds 3 mils. Vibrations are not measured in the vertical and axial planes because of disturbances from rail joints and run-in of train slack.

The turbine casing has a horizontal split which permits removal of the top half with the turbine in the locomotive. All parts can be removed and replaced, except compressor-rotor blades. As listed in Table 2-14[34], there have been 22 occasions to open up a turbine partially or completely. Nine turbines had unscheduled openings because of trouble originating in the turbine requiring immediate repair. Based on these nine unscheduled openings for 95,727 turbine hours, an average of 10,638 hours per turbine is obtained.

There have been some cases of compressor pulsation. On one occasion, 8 hours were spent trying to start a turbine. Each time the turbine was fired it would hang up at 2800 to 3100 rpm and have to be

Table 2-14

OPENINGS OF TURBINES FOR EXAMINATION LOGGED FOR GE 8500 HP LOCOMOTIVES ON THE UNION PACIFIC RAILROAD

Date	Turbine Serial Number	Loco. No.	Total Fired Hours	Reason
3-11-58	97664	3	437	Missing 2nd stage tie pins.
15-12-58	97666	4	200	Broken tie wire 2nd stage buckets.
5- 2-59	97666	4	900	Failed inlet silencer causing compressor damage.
5- 2-59	97661	2	1800	Failed inlet silencer causing compressor damage.
23- 3-59	97662	1	2963	Scheduled modifications and evaluation inspection.
13- 4-59	97661	2	2455	Missing 2nd stage tie pins.
2- 8-59	97666	4	3370	Excessive vibration.
29- 8-59	97669	8	2378	Scheduled modifications.
7- 9-59	97664	3	5105	Scheduled modifications.
2- 1-60	97669	8	4300	Broken 2nd stage bucket.
13- 4-60	97674	13	300	Damage to first stage nozzle and buckets from dowels lost out of transition piece holding bars.
16- 4-60	97671	10	1450	Scheduled modification of transition piece holding bars.
16- 4-60	97672	11	1500	Scheduled modification of transition piece holding bars.
16- 4 60	97673	12	750	Scheduled modification of transition piece holding bars.
16- 4-60	97675	14	50	Scheduled modification of transition piece holding bars.
18- 5-60	97672	11	1800	Broken turning vanes in inlet silencer causing compressor damage.
23- 6-60	97664	3	9034	Scheduled modification to combustion chambers and transition pieces
22- 6-60	97661	4	6359	Pulsation.
6- 7-60	97676	5	7700	Scheduled modifications.
9- 8-60	97667	6	7381	No. 1 combustion chamber casing burned through.
15- 8-60	97664	3	9661	Seized rotor caused by failure of No. 1 bearing.
16- 8-60	97662	1	9547	Scheduled inspection and repair of transition pieces.

shut down. It was eventually started by removing the orifices in the tenth stage extraction lines that supply air for turbine-shell cooling. This change was thereafter made on all turbines. The pulsation margin was improved on later machines by increasing the size of the first-stage nozzle opening by 10 per cent and slightly modifying the combustion chamber line.

At the present time, liners and caps are repaired at approximately 1600 hour intervals. All are repaired by building up with welding or welding on new sections.

Operating Experience at Ravensburg

The first industrial closed-cycle pulverized coal-fired plant at Ravensburg, West Germany, started operation at the beginning of 1956[15]. It is a combined installation for power production (2300 kw max.) and central heating (10,000,000 Btu/hr max.) in the form of 170/110°F hot water. Since 1957 it has operated practically without trouble. The availability of this pioneer plant in the different years is shown in Table 2-15[15].

Table 2-15

NUMBER OF INTERRUPTIONS AT THE RAVENSBURG PLANT

Year	1956	1957	1958	1959	1960
Operating hours (total)	3246	8885	13,531	18,444	21,625
Cause of interruption:					
Machine group	4	0	0	0	0
Air heater	11	1	0	0	0
Charging installation	2	3	0	0	0
TOTAL	17	4	0	0	0

The time for normal revisions and checks can be determined by the operator and is no longer dictated by difficulties in the plant. By the end of 1960, the plant had achieved 24,650 hours of industrial service and produced over 31.6 million kw-hr. Over 123 billion Btu of waste heat had been used for room heating and hot-water production. The power plant is extensively automated and requires only one man per shift for supervision, with another man as general help, for such work as cleaning and emptying ash buckets.

The plant is shut down on weekends, although in cold weather it is sometimes kept running to provide room heating, thus eliminating the need for a separate heat system. In the summer, the demand for electric power is very low at night and the plant was shut down every evening for a period of 3 months in 1958. Restarting in the morning was accomplished in about half an hour. An inspection of the entire plant after this period showed all elements to be in perfect condition. The cycle was absolutely clean and the air-heater tubes had no slag deposits or signs of corrosion. There was no trouble with the air heater nor with any other element of the plant. Both temperature distribution in the tubular heating system and the inlet temperatures to the turbine of 1220°F could be kept constant even under fast changes of load. From cold condition after longer shut-down periods, restart is made in about 2 hours because there is no need to hurry. Starting time is dictated by the relatively thick brick wall of the combustion chamber. After about 18,000 hours of operation in 1959, official trial tests were carried out which show that expectations concerning efficiency at various loads have been fulfilled.

The regulation of the closed-cycle gas turbine was also the subject of extensive tests. The control and self-regulating properties are remarkable for such a relatively small unit with coal firing. An average of about 1500 kw is needed during the day with a peak load of 1800 to 2000 kw. Load fluctuations are rather heavy and abrupt ($\pm$200 kw).

The regulating device is designed for sudden and unexpected interruptions. The plant then adjusts automatically to the base-load requirements and does so without any interruption of power delivery. In case of load increase, air is injected into the circuit to increase the pressure level. When the load decreases, air is discharged to decrease the pressure level. While the temperature of the working air at the turbine inlet always remains constant (in the range of $\pm$ 9°F), the output changes in direct proportion to the pressure level.

For economic reasons, the regulating device was designed to act as follows. If the plant is connected to the outside electric grid where no big load increases are to be expected, then the output is raised in such a way that a low-pressure charging compressor pumps air into the low-pressure side of the circuit. If on the other hand, the plant is supplying only the factory where bigger unexpected load increases occur in a short time, then high-pressure air is discharged from an air accumulator into the circuit ahead of the turbine. In this way, large load peaks can be regulated quickly. Load drops are also regulated quickly with a bypass valve. Thus it is possible to keep the frequency constant within $\pm$ 2 per cent = $\pm$ 1 cycle even if large load fluctuations occur in the factory requirements. The accumulator is charged by having a high-pressure charging compressor take air from the high-pressure aide of the circuit. Two overspeed trips (one hydraulic, one mechanical) work in parallel to assure that the maximum overspeed of 10 per cent will never be exceeded. These overspeed trips act directly on the quick-closing device.

There is a great deal of operating experience with industrial turbines of other notable manufacturers as, for instance, Westinghouse and Brown Boveri, showing good reliability of their installations. However, the previous example was chosen as sufficiently representative.

2.3.5 Performance Improvement

It is useful to take a look at the continuing improvement of aero-engine performance and at the explanation of how it came about. The two main contributing factors are design improvements and new materials. The former is now based on many years of engine development, component research and operational experience while the latter were caused by the constant stimulus of designers' demands.

Almost all new engines are designed with some capacity for increased performance in mind. The "stretch" of an engine, for purpose of illustration, may be typified by the data shown in Table 2-16[32] which indicate existing and projected developments of the successful Bristol Siddeley Viper engine, originally designed as a short-life power unit (see Figure 2-29).

The first column gives details of what may be regarded as the standard engine although, in fact, it has almost 50 per cent more thrust than its predecessor, the ASV.8, without significant difference in dimensions.

Table 2-16

BRISTOL SIDDELEY VIPER TURBOJET ENGINE DEVELOPMENT

Column	1	2	3	4	5
Engine	ASV.11	ASV.12	ASV.20	BS.209	BS.86
Sea level static thrust (lbt)	2500	2700	3240	3830	3700
Maximum engine speed (rpm)	13800	13800	14400	14400	13800
Maximum static air mass flow (lb/sec)	44	44	55	55	121
Turbine entry temperature (°F)	1530	1630	1545	1700	1530
Specific consumption (lb/hr-lbt)	1.07	1.11	1.01	0.975	0.722
Dry weight (lb)	549	549	575	593	
Overall length (in.)	64.0	64.0	66.7	68.5	
Maximum diameter (in.)	24.5	24.5	24.5	24.5	

The second column shows the effect of increasing the turbine inlet temperature by approximately 100°F. Engine dimensions and weight remain unaltered, thrust increases by 8 per cent, but there is a consumption penalty of nearly 4 per cent. The third column is the performance when a zero stage is added to the compressor. In some engines this involves a slight increase in intake diameter but the maximum diameter is not necessarily the intake. In this case, the larger intake area associated with a zero stage is obtained by continuing the rotor taper so that the hub to tip ratio is increased within a cylindrical casing. The air mass flow is increased by 25 per cent and the thrust by 30 per cent compared with column 1. The gas temperature has been reduced from column 2 and the rotor speed increased. The latter, together with the zero stage, produces a greater compression ratio and a reduced specific consumption. The additional compressor stage has pushed up the length and weight slightly, but the specific weight is reduced.

Column 4 is a development of column 3 which embodies a two-stage turbine and a higher gas temperature. These again increase length and weight but reduce specific consumption and increase thrust. Variants of this arrangement will give still lower specific consumption at the expense of less thrust by reducing the gas temperature. The final column shows that the best way of reducing consumption is to convert the engine to a by-pass arrangement. In this case, an aft-fan is proposed. Note that rpm and gas temperature are down to their original values.

Another feature of recent aero-engines is the effort to incorporate well-proven components of previous engines, both to reduce development effort and to insure reliability. The Bristol-Siddeley BS.75 ducted fan engine (Figure 2-20), for example, has a three-stage fan based on the first three stages of the Olympus low pressure compressor. Its compressor is similar to the Orpheus compressor, its combustion system is influenced by Siddeley experience with vaporizing systems in the Sapphire, and its turbine stages are similar to those of the Proteus.

The effect of gas temperature in increasing output has been greatly used by designers and engine temperatures of the order of 1970°F are now used (for take-off). This demands first-class materials and turbine blade cooling. Much ingenuity has been expended in providing cooling passages in blades so that the maximum effect is achieved by the minimum of cooling air (see Section 11.2).

Compressor performance has been improved by increasing air inlet velocities and reducing blade hub to tip ratios. During the past five years, mass flow ratio has increased from about 30 to 36 lb/sec per ft^2 of inlet area. This has increased blade design problems to maintain efficiency over a range of rotational speed. High performance engines use variable stagger on inlet guide vanes and, in some cases, on one or more rows of stator blades. It is noticeable, too, that blade chords have been reduced and this permits a reduction in overall compressor length and weight. In some engines, compressor casings have been made as complete drums without the normal axial split into two halves. This eliminates the joint flanges and bolts and reduces weight appreciably. Weight is also reduced by the use of titanium in the high pressure stages and by improved materials elsewhere.

One of the most critical components in a gas turbine is the turbine blading. It is subjected to high temperatures and stresses and is liable to fail through creep or fatigue if conditions become too onerous. Much work has been done through the years to give better properties to blade materials and this has not slackened during recent times. The Nimonic series of chromium-nickel alloys has been a remarkable demonstration of this. The most recent additions to this series, Nil05 and Nill5, are compared with the earlier Ni90 in the stress temperature curves of Figure 2-30. These alloys begin to melt about 2370°F, but it can be seen that they can sustain a substantial load even at an operating temperature more than 80 per cent of the melting point. This feature has resulted in difficulties arising in the forging of the material, and a somewhat reluctant consideration of casting.

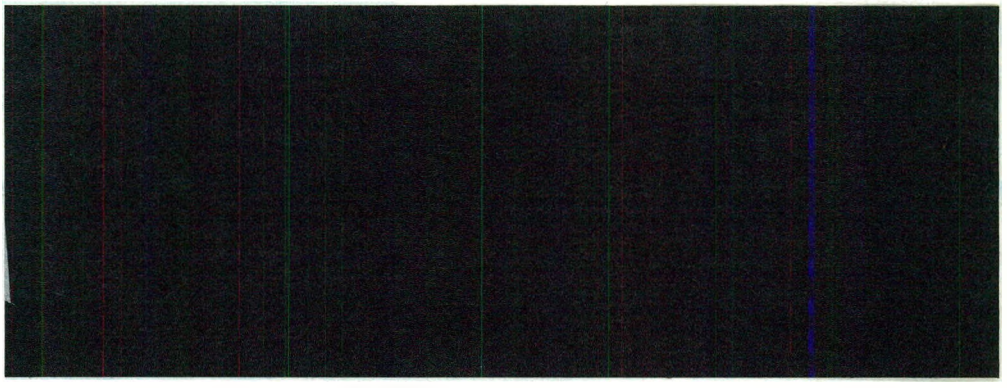


Fig. 2-29 - Bristol Siddeley Viper ASV11 Turbojet Engine

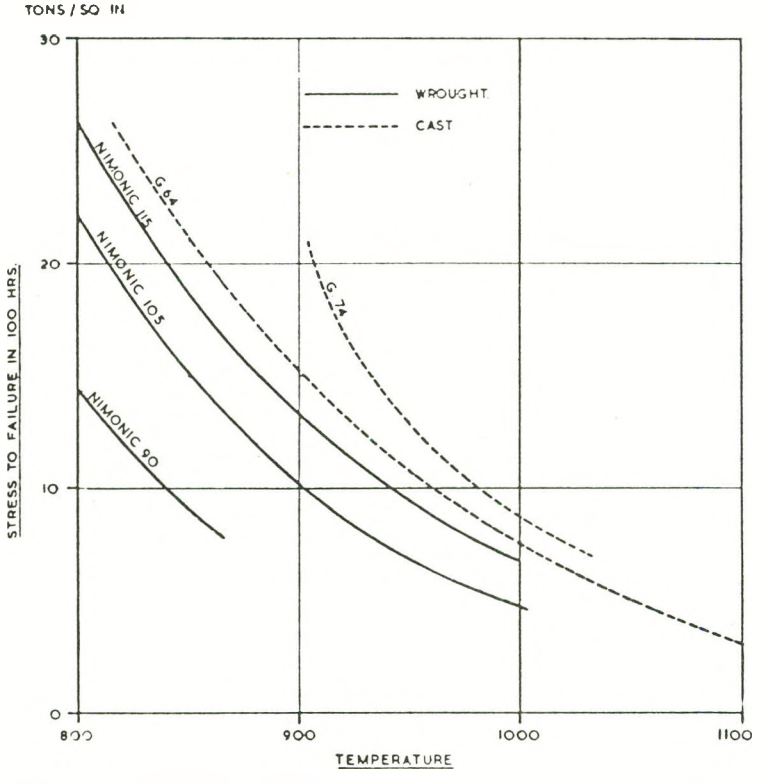


Fig. 2-30 - Strength of Recent High-Temperature Forged and Cast Materials

Cast alloys are able to operate at a higher temperature for a given stress but have been regarded with suspicion in case the scatter in performance should offset this gain. With the introduction of vacuum melting techniques, this problem is largely overcome as has been demonstrated by the Proteus which has been operating with G.64 alloy blades for thousands of hours. It is compared with the wrought alloys in Figure 2-30[35], as is the still more advanced G.74. Further in the future, refractory metals may be introduced. Research is proceeding on alloys of molybdenum, niobium and tungsten, but no satisfactory results are available yet.

In the other major hot component, the turbine disk, British practice has been to use a martensitic steel as temperatures have been below 930°F. The demand for higher blade temperatures and the higher temperatures of cooling air, especially in supersonic flight, for the disk rim will force the introduction of vacuum-melted austenitic steels in order to cope with temperatures approaching 1100°F.

In the compressor, titanium alloys will also become a necessity as the air temperature rises higher with higher forward speed conditions. Such alloys are already good for use up to 840°F. In the cold end of the compressor or in very light engines, plastic blading is now being discussed. It is satisfactory for temperatures up to 480°F, and has a strength to density ratio more than twice that of aluminum alloy. See also Report NYO 9793 on materials[6].

2.3.6 Reliability

Improvements in design or materials can be converted into improved life or reliability. In many cases, both have been combined but the picture would not be complete without some examination of this factor.

The Rolls-Royce Conway by-pass jet engine, which has been in service only since April 1960, is an interesting example. Already its overhaul life has reached a figure of 1600 hours, and unscheduled

engine removals from BOAC aircraft have dropped from an initial figure of 0.67 per 1000 flying hours to less than one-third of this. These figures are compared with those for some earlier fully developed engines in Table 2-17[32].

Table 2-17

UNSCHEDULED ENGINE REMOVALS

Engine	Removals per 1000 hrs. Flight
Wright Turbo Compound	0.69
Rolls-Royce Merlin	0.46
Rolls-Royce Dart	0.078
Rolls-Royce Conway	0.20

One recent problem, that of take-off noise, has led to new operating techniques which, in turn, have improved engine reliability. Full power (and full turbine inlet temperature) were originally used on Douglas DC-8 engines for 1 min 50 sec and the turbine blade failure rate was 0.133 per 1000 hours. In the Boeing 707, take-off power was applied for only 1 minute before throttling back. This reduction in time at full temperature was reflected in a blade failure rate of only 0.041 per 1000 hours. Later proposals by TCA to operate for only 45 seconds will be still more effective as, in this short time, the air-cooled turbine blades will not reach the full permissible temperature at all. The other factor which helps to give a long reliable life is that the engines are used on long haul flights so that maximum temperature is required less frequently than in some other operations.

One year of DC-8 operation and over 42,000 Conway engine hours have been accumulated by Trans-Canada Airlines. The Conway is one of the new turbofans, utilizing the bypass principle, of the type now appearing on the American market. This RCO12 Conway engine as used in TCA operation has an average take-off thrust of 18,000 lb at ISA conditions at sea level. This increases to 20,000 lb as colder conditions

are encountered. These thrusts are the highest being achieved by any gas turbine engine in civil flight operation to date.

Combustion in these engines is very clean. The combination of high-pressure fuel system and fuel burner design (particularly when operated on JP-4 fuel) is providing a remarkably clean, carbon-free operation. Another feature is that the Conway engine is fully adaptable to fuels of different specific gravity without need for adjustment. Gravity changes only require a corresponding change in the calculated fuel loaded for a given flight.

One problem that has been more severe than anticipated has been that of bird ingestion. A great deal of work and planning is required to combat the bird ingestion problem. TCA has experienced a large number of cases of bird ingestion, to the point that nearly all engines in the fleet are believed to have ingested a bird at some stage of their operation. As it is now, the Conway engine has coped reasonably well with ingested birds[36].

This problem has always been of reasonable concern, and centrifugal compressors doubtless are less sensitive to hazards provoked by bird ingestion as illustrated by the following occurrence. In Canada a squadron of Vampires in a formation take-off flew through a dense flock of hundreds of birds and continued on its mission. The official report stated that the engines operated normally after a short period of rough running, and concluded with the words: "It appears therefore that the Goblin II engine can swallow birds without damage or effect on performance."[20]

TCA's basic philosophy is that time between overhauls of an engine and the period considered maximum service life of its components should be increased as fast as proof becomes available that no hazard will exist due to the time extension. Failure not related directly to service time should not limit time extension between overhauls.

A rapid overhaul life development has been achieved with the Conway engine. By means of a planned sampling program, TCA reached 1500-hr on its sample engines as of last March. The gas turbine engine is potentially adaptable to high overhaul life as compared to piston engines and a philosophy of engine life development matched to the potential of this type engine is required.

TCA believes that the program as practiced by the airline and approved by the Canadian Department of Transport permit exploitation of potential engine overhaul life without increasing risk of failure. It believes in the validity of a small number of samples seen at short time increments such as 100-hr. In general, on the gas turbine engine, the airline is probing for component total-time limitations rather than limitations which could be linked with time between overhaul.

Development of the engine to 1500-hr overhaul life within the period of one year of operation is a sign of the potential of the Conway engine, as well as confirmation of the validity of the program. Nothing is evidenced in the engine to date which could limit overhaul life development. Unless something unexpected occurs, TCA proposes to continue the life development program by following the sampling program with a continuous-type trial, 2000-hr overhaul life being the immediate objective.

Overhaul life of other engines has been rising rapidly as can be seen from Figure 2-31[32]. The Dart, with 3200 hours, is outstanding but the Avon is climbing quite rapidly toward this figure. The Proteus (see Figure 2-32) is also in the long life category and should proceed to 3000 hours, in due course. They all substantiate the claim, made many years ago, that gas turbines would be simpler to maintain and more reliable than piston engines. Progress towards this state has been based on many hours of development and service operation. To achieve 1000-hour overhaul life requires about 100,000 hours of running experience, 2000-hours overhaul needs about 300,000 hours, and 2500 hours requires

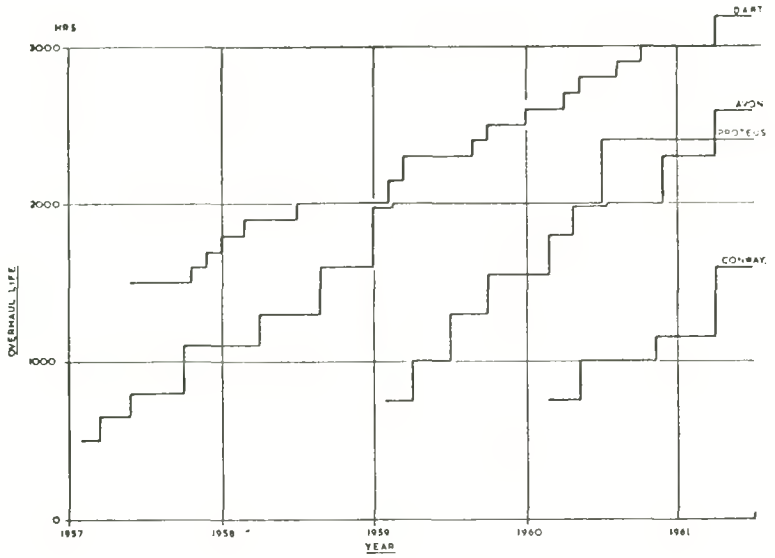


Fig. 2-31 - Improvement in Aero-Engine Overhaul Life

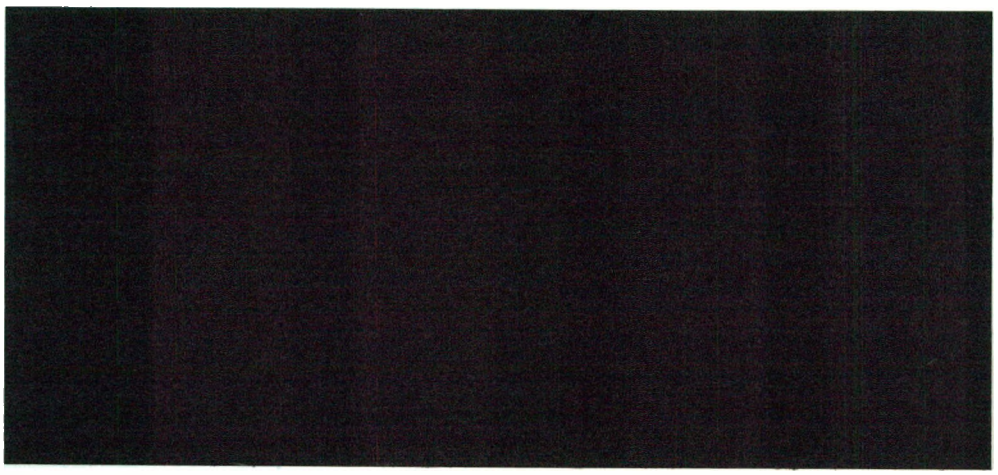


Fig. 2-32 - Bristol Siddeley Proteus 765 Turboprop Engine

some 450,000 hours[32]. However, it is known that by November, 1959, Proteus aero-engines had completed nearly 900,000 hours, being still in the 2000-hour overhaul life level. Only by July, 1960, this engine reached the 2400-hour line (see Fig. 2-31).

2.4 Compressor Types

Gas turbines need compressors which can handle large volumes economically, compressing them generally to moderate pressures. Compression ratios in the whole range of gas turbines vary approximately from 2.5 to 16 for a single compressor, depending on the type of installation. Only some of the various existing types of compressors found application to operate together with a gas turbine.

Compressors of regenerative type are not discussed in this report because of their low efficiency. However, such compressors have been successfully used where high pressure ratios per stage are required and efficiency is of secondary importance (see NYO Report No. 9790, on Circulators[37]).

2.4.1 Radial Compressors

While the centrifugal or radial-flow compressor does not occupy a position of comparable importance with the axial-flow machine, it nevertheless possesses some desirable characteristics with respect to applications to gas turbine plants. The principal comparative advantages of the radial compressor are light weight in small sets, simplicity, compactness (short length), rugged construction, high pressure ratio per stage, and a wider range of stable operation. However, lower peak efficiencies, bulky multistage construction, and greater frontal area (large diameter) are serious disadvantages, the latter in particular for aircraft power plants.

This disadvantage becomes more pronounced when the attempt is made to find optimum designs for the channels of flow of the radial compressor. For, while it is actually possible to design these channels to give an efficiency only very little inferior to that of the axial

compressor, the diffusers then take up a great deal of space, and the resulting machine can become disproportionately heavy and expensive.

The radial compressor has been closely associated with gas turbine development since the earliest days of investigation. However, the modern radial compressor bears little resemblance to its predecessor. Both stage and overall performances have been improved through better knowledge of gas dynamics, more careful selection of wheels and other stage components, and cooling of the gas being compressed by either internal or external means. The use of radial compressors in the future is dictated by recently achieved improvements in efficiency (see Fig. 5-5 in Section 5.2).

Although the axial compressor has already been substituted for the radial in many gas-turbine applications, it was sometimes the result of a remarkable struggle. For example, the radial compressor which has been developed to a highly reliable unit in British aircraft engines gave up its strong positions only slowly to the axial compressor after the World War II period[38]. Figure 2-33[39] shows an obsolete British jet-propulsion engine of the Whittle type, the Rolls-Royce Dervent V, extensively used in the beginning of the fifties. H. Schelp, of the turbomachinery Ai-Research Manufacturing Division of Arizona, Garrett Corporation, expresses the opinion that for gas turbines up to 1000 hp output, the radial compressor, used as one stage or two stages, will prove to be the best design approach[10].

Figure 2-34 shows the Ai-Research gas turbine compressor and power unit model GTCP85-9 which is used for the Ai-Research 120 kva power package. It has a service life of 1250 hours or 5000 starts, whichever occurs first. This lightweight power package provides all the electrical and pneumatic power to meet the increased ground support requirements of the newest jet transports. It can be installed on nearly any vehicle or carried as an onboard unit. The compressor section is designed to provide a source of compressed air for the turbine and

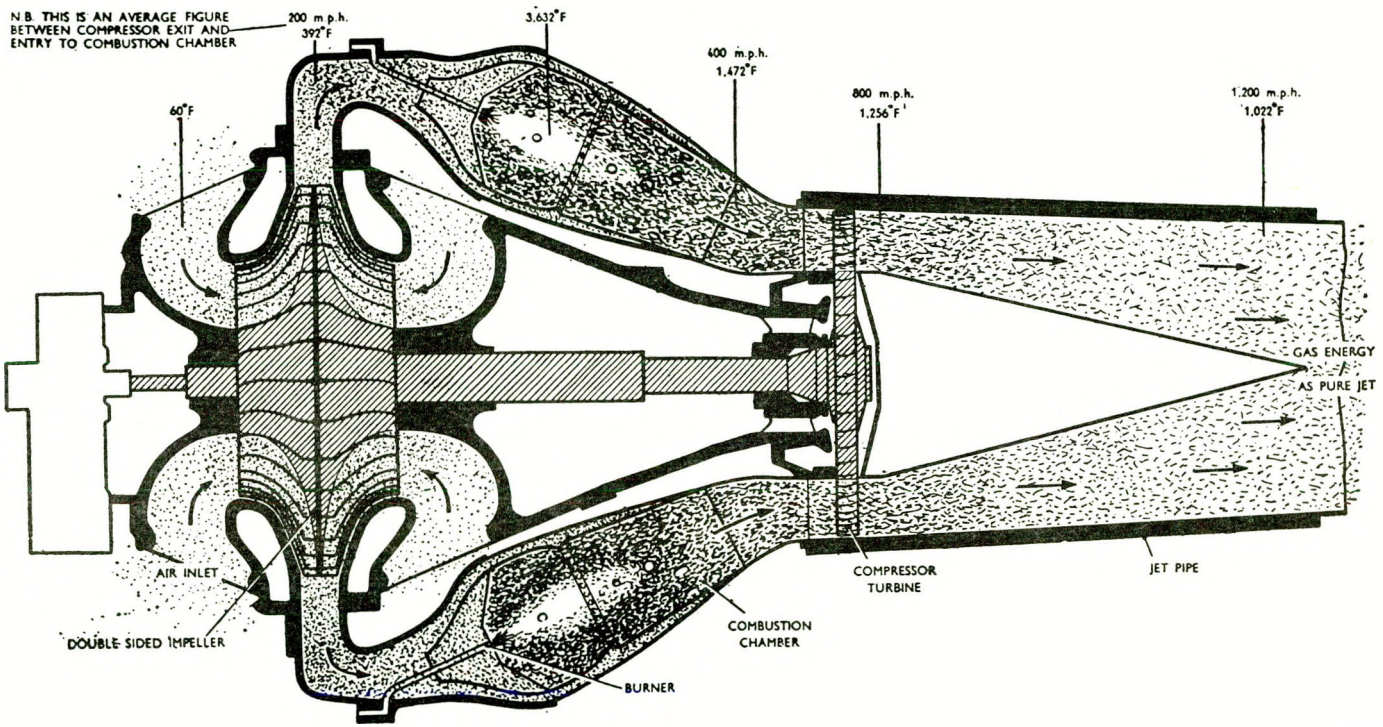


Fig. 2-33 - Diagrammatic Cross-Section of the Rools-Royce Dervent 5 Turbojet Engine

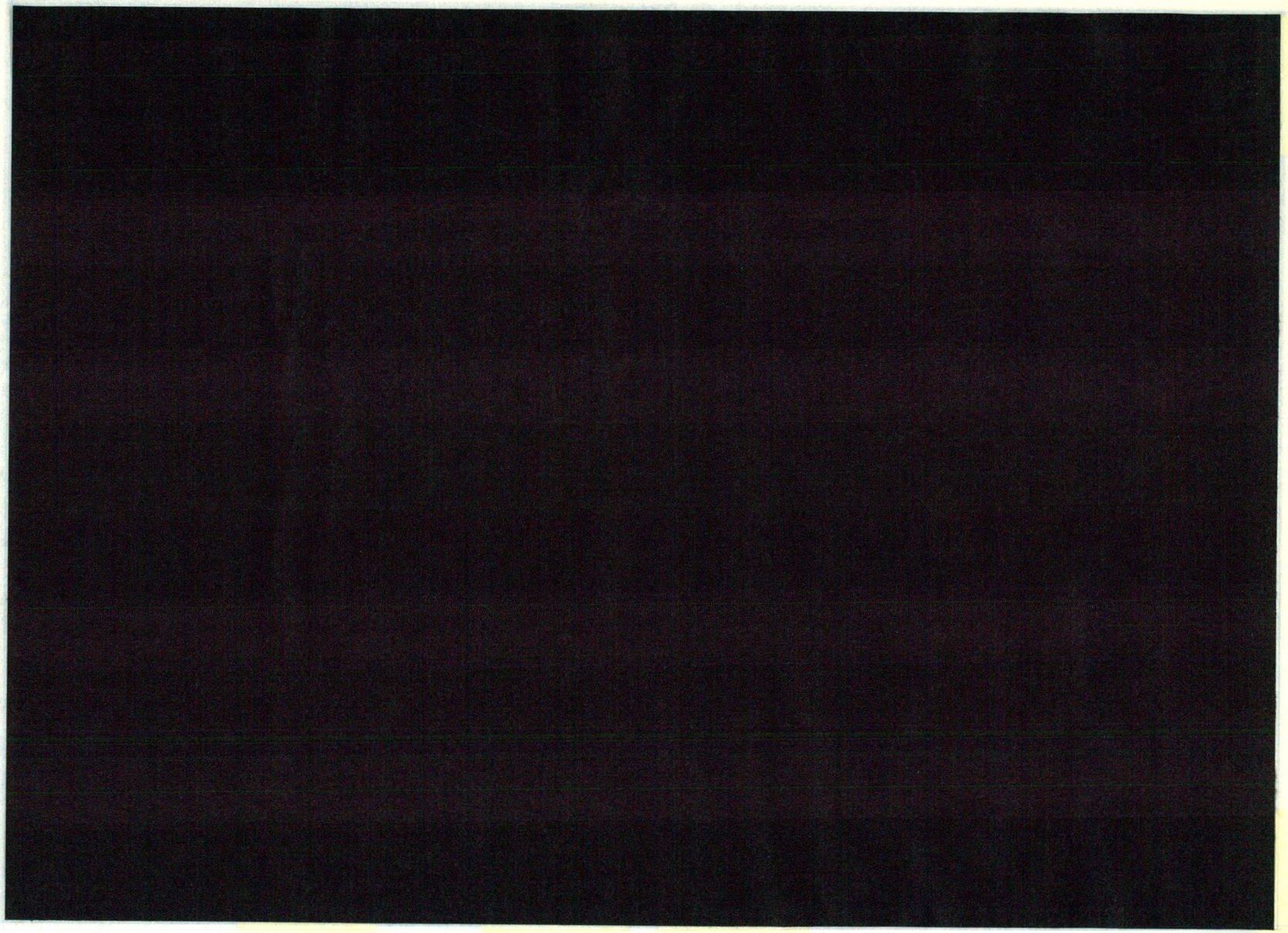


Fig. 2-34 - AiResearch Gas Turbine Compressor & Power Unit Model GTCP 85-91

for pneumatic power. The compressor is a two-stage centrifugal type utilizing two radial outward flow impellers. Air enters the double entry first stage impeller through a compressor inlet plenum, flows through a vaned diffuser into crossover ducts leading into the inlet of the single entry second stage. Air discharges from the second stage compressor through a vaned diffuser into the turbine plenum. The impellers are mounted on a common shaft coupled to the turbine rotating assembly and to the accessory assembly by means of quill shafts.

The radial compressor has unquestionably conquered a unique position in the field of small gas turbines for light-weight power units of numerous applications, such as aircraft ground support, air supply to various types of pneumatically operated equipment, vehicle propulsion, and turbocharging.

Competition between radial and axial compressors exists at some outputs depending on type of application. A recent example of such competition are the two closed-cycle gas-turbine units, one as standby unit for the other, ordered for the 300-500 kw Army Mobile Low-Power Nuclear Power Plant ML-1 (see Section 3.3.2). One of these units, manufactured by Clark Bros. Co., has an axial compressor, and the other, manufactured by Stratos Division, Fairchild-Stratos Corporation, has a radial two-stage compressor (see Figures 12-33 and 12-38).

In other places, the radial compressor can still be encountered in connection with gas-turbine installations, where a successful design stems from earlier days. Thus we see that in 1960 the construction of a 2 Mw coal slurry-burning closed-cycle gas turbine was completed by Messrs. John Brown & Co. (Clydebank) Ltd. for the National Coal Board at Rothes Colliery, Fife, Scotland[40]. The gas turbine for this installation is basically an at least 10 years old Escher Wyss design (Tu-Co 52) and has a 3-stage radial compressor (see Fig. 3-7). Generally, for a closed cycle, the pressure level of the coolant causes a corresponding reduction of turbomachinery size, and the compromise between many

design considerations might favor the radial compressor against the axial at different outputs than for an open cycle. Individual manufacturers' experience may also establish different preferences. Another Escher Wyss designed and built closed-cycle plant, that of 12,500 kw at Saint Denis Station, Paris, is equipped with two-stages of axial-flow and two-stages of centrifugal compression[35].

Another place for using radial stages is in axial-flow compressors at the high pressure and as an additional stage to the axial rows. This last radial stage cuts down the number of pure axial stages required for a given compression ratio and increases the critical speed of the shaft. Another feature of such arrangement is the increase of the stable region of operation in the axial-flow portion in single-spool compressors. A typical example is shown in Figure 2-35, giving the longitudinal section of the Bristol Siddeley Marine Proteus 1270 series gas turbine. In the compressor of this engine, air flows through a twelve-stage axial compressor to a single radial stage. Such compressors are sometimes called axial-centrifugal compressors.

Continental has a series of centrifugal compressors that can be assembled into engines to produce from 300 to 1200 hp as shaft turbines and from 1.4 to 6.3 lb/sec of compressed air, and a series of combined transonic axial and centrifugal compressors that can be assembled into engines to produce from 425 to 2100 hp as shaft turbines and from 1.8 to 9.3 lb/sec of bleed air. Such on-the-shelf availability of components can sometimes result in an important short-cut in development time for new engines[10].

It is not too difficult to predict the future trends for the combined transonic axial and centrifugal stage compressor. Undoubtedly, higher pressure ratios will be efficiently achieved in both the transonic stage and the centrifugal stage. It is more difficult to predict the maximum attainable stage pressure ratio because nothing to date has indicated that higher pressure ratios are unfeasible. This upper limit

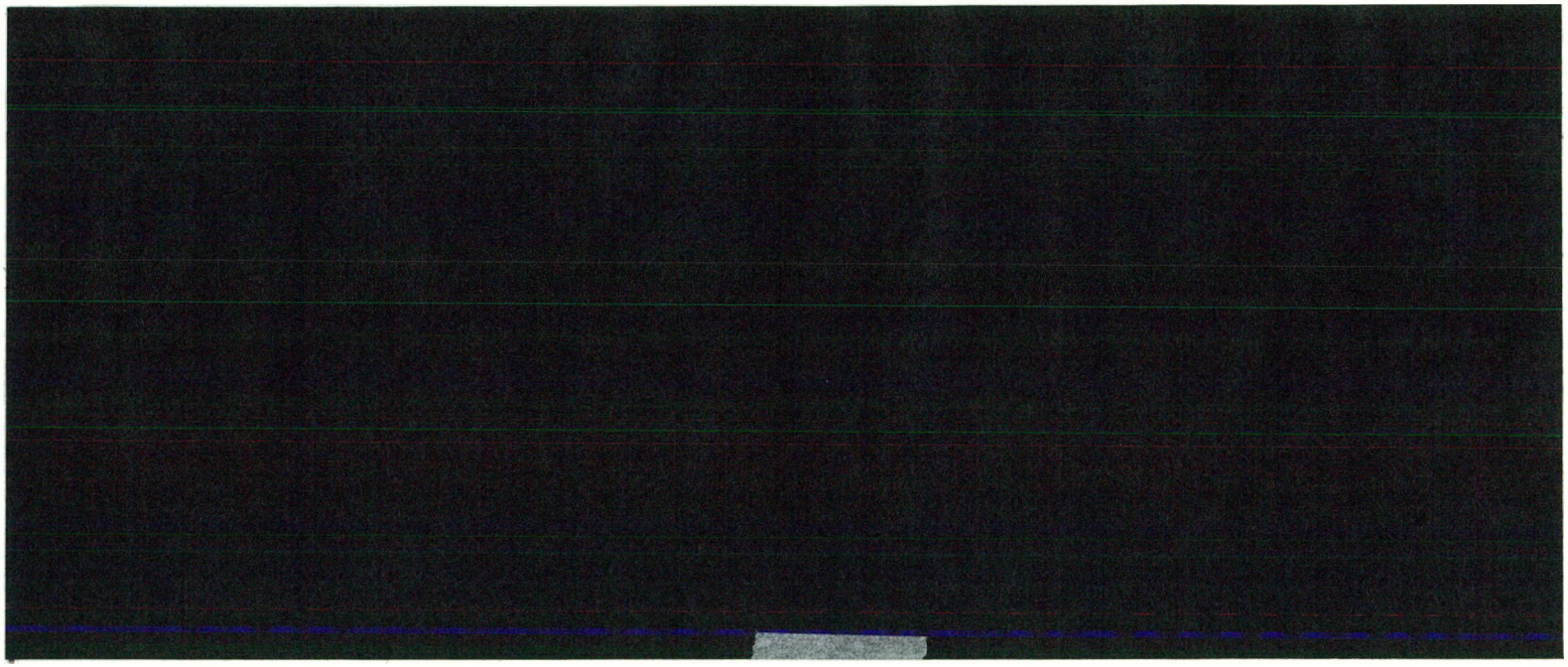


Fig. 2-35 - Bristol Siddeley Marine Proteus 1270 Series

on pressure ratio will, certainly, be influenced by engine size and application. The higher pressure ratios for a single transonic stage combined with a centrifugal stage will be achieved in the smaller engines where frontal area is not so critical, and this pressure ratio will probably be well above 7.0:1. Two transonic stages matched with a centrifugal stage will, of course, develop even higher pressure ratios and do it more efficiently than the single transonic-centrifugal compressor. These higher overall pressure ratio configurations will undoubtedly require some form of part-speed assistance, such as interstage bleed or variable geometry, to provide good acceleration.

The increase in stage pressure ratio will come about as a direct result of more development and experimental investigation. The 1.5:1 pressure ratio transonic stage is at the same point in the state of the art that the subsonic axial flow stage was 15 years ago. Since then, both the subsonic axial flow stage pressure ratio and the overall compressor pressure ratio have increased substantially. At the same time the small gas turbine will encourage more and more interest in the centrifugal stage. As a result, improvements in the centrifugal stage will also be realized.

Certainly, current experience has indicated that a single transonic axial compressor stage can be matched to a centrifugal compressor and operated in an engine so that pressure ratios of 5.0:1 to 6.0:1 can be achieved with reasonable efficiencies. Two transonic stages have been matched with a centrifugal stage and have demonstrated the practicality of using this type of compressor to obtain pressure ratios above 6.0:1. Current experience has also indicated that transonic stages with pressure ratios of over 1.7:1 are feasible. Although the transonic axial-centrifugal stage principle has not yet been fully exploited, the cost and performance aspects of this type of compressor have encouraged Continental to continue on in this field.

In the general trend to simplify gas-turbine installations, turbines and compressors are usually combined in common casings. This feature also cuts down transfer losses. Nonetheless separate compressors can be coupled with turbines as parts of a gas-turbine installation. In any case, design experience invested in separately built compressors can be utilized in a joint compressor-turbine design.

Interstage cooling of radial multi-stage compressors is sometimes applied to increase efficiency of compression. An example for such an isothermal compressor may serve the new Clark Isotemp centrifugal multi-stage-compressor package with intercoolers built into the compressor base (see Figure 2-36). These compressors are built in six frame sizes with horsepowers ranging from 1000 to 8000 shp and capabilities, from 5000 to 38,000 cfm.

Such interstage cooling is feasible only for radial multi-stage compressors but not for axial machines because of the character of the flow passages. Table 2-18 lists typical ranges of capacities of radial compressors available from U.S. manufacturers.

2.4.2 Mixed Flow Compressors

Mixed flow compressors fall between radial and axial types and have shown good performance for certain applications, especially in the field of turbochargers. Combined with the Birmann blading (see Section 5.2), the mixed flow impellers (see Figure 5-19) are suitable for very high tip speeds.

Table 2-18

RADIAL COMPRESSORS FROM U.S. MANUFACTURERS

Manufacturer	Inlet Volume cfm	Pressure psig	Note
De Laval	1000 to 150,000	to 1000, and more	horiz. split casing
Clark	From 2000 discharge for high-pressure cases to 150,000 suction for low-pressure cases	to 800, and more	horiz. split casing, 7 frame sizes
Clark	From 200 discharge for high-pressure cases to 20,000 suction for low-pressure cases	to 5000	vert. split casing 4 frame sizes
Clark	5000 - 38,000	100	Multi-stage isotemp compressor, horiz. split casing, 6 frame sizes
Elliott	Up to 150,000	to 500	Multi-stage
Elliott	700 to 10,000	7.0	single-stage

2.4.3 Axial Flow Compressors

Axial flow compressors are the dominating type of compressor for present use with gas-turbines because of the large flow rates they can handle and because their efficiency is higher than that of a radial compressor. In aircraft applications, the lesser frontal area and lesser weight gives an axial a better chance. It may be noted that there are about 100 aircraft gas turbines for every other gas-turbine engine in use at the present time. If jet engines are excluded and only shaft engines in aircraft are counted, then the ratio is still about one to one[10].

Figure 2-37[42] shows a section through a typical industrial axial-flow compressor (Brown Boveri) and Figure 2-38 shows one of Clark Bros. Co. for gas turbine application. Manufacturers indicate that they can build axial-flow compressors of large capacities. Elliot Co. cites a value of more than 300,000 cfm, for example. According to current manufacturing practice, Figure 2-39[42] indicates the range of compression ratio and of inlet volume flow of one-casing turbocompressors for compression of air from atmospheric conditions. Figure 2-40[42] gives the range of specific work and of inlet volume flow of one-casing turbocompressors which is valid for all gases.

Allis Chalmers designed and built several of the world's largest axial-flow compressors at the York Works for the National Advisory Committee for Aeronautics. Figure 13-1 shows a 2,250,000 cfm machine during installation. Three electric motors, totalling 89,000 hp, drive this compressor at a maximum speed of 900 rpm. Figure 13-2 shows the 150-ton, 10-stage rotor redied for facing the shaft connections in a 42-foot vertical boring mill. Individual rotor disks are completely machined from steel forgings and spacer rings are fabricated from alloy steel. All welds are radiographed. Parallelism and runout of the entire assembly, when completed, are accurate to one thousandth of an inch. The largest compressor designed by Allis Chalmers develops inlet volumes of 4,300,000 cfm with a 150,000 hp drive.

2.4.4 Rotary Piston Compressors

A key feature of a rotary piston compressor is that it has no surge troubles. The advantages of high efficiency and stability of performance, normally associated with reciprocating compressors, are introduced into the high-speed rotary field. Two helical rotors transport air from inlet to outlet while simultaneously effecting compression. Since the rotors are driven through timing gears, metallic contact is avoided, thus eliminating the need for lubrication. However, we know of only one gas-turbine installation which uses this type of compressor.

FRANKLIN INSTITUTE - Laboratories for Research and Development
I-A23925

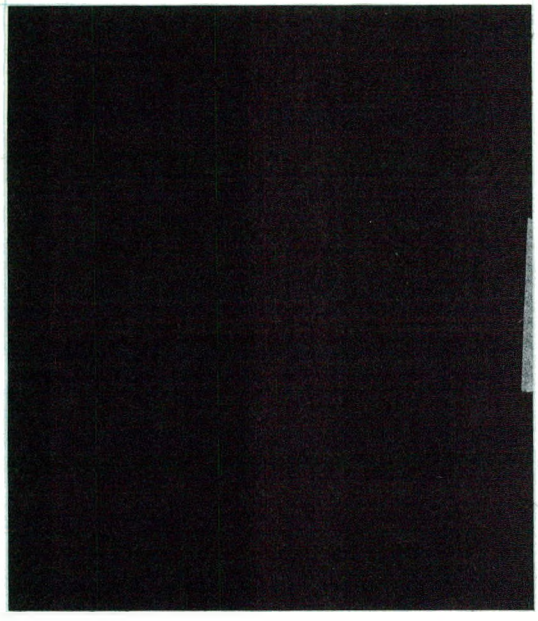


Fig. 2-36 - Clark Isotemp Compressor Package

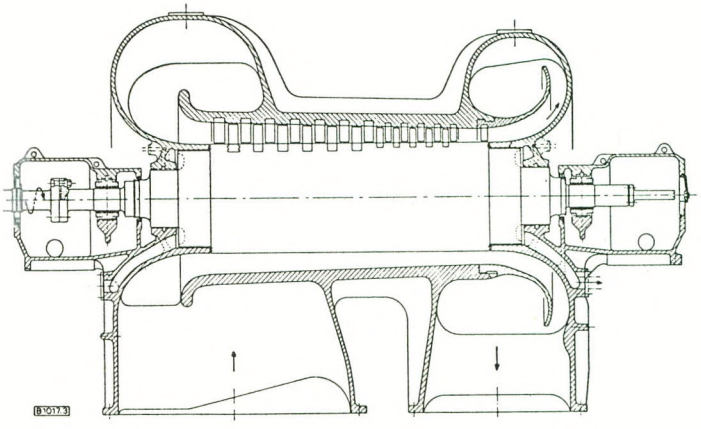


Fig. 2-37 - Brown Bovery Axial Flow Compressor

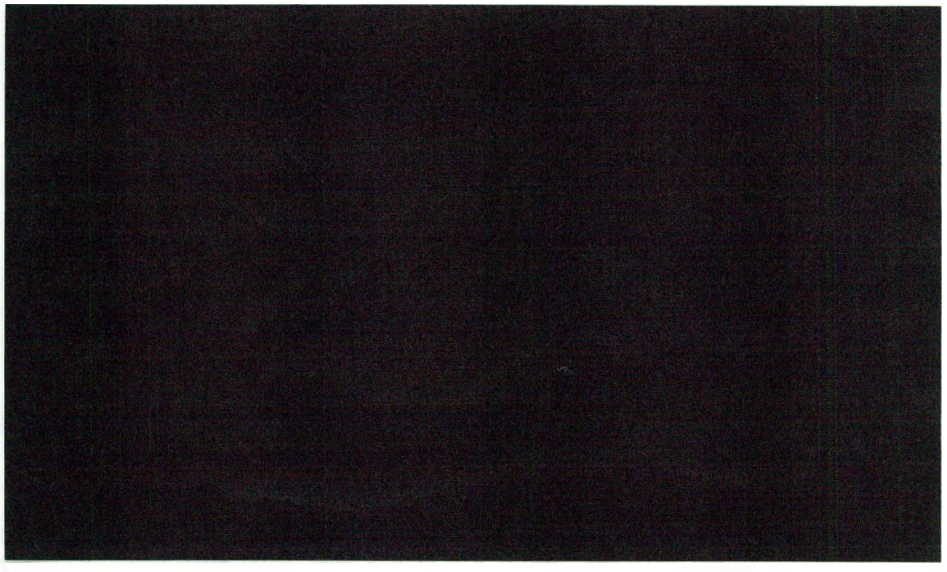


Fig. 2-38 - A Clark 18000 bhp Axial Flow Compressor for Gas Turbine Application

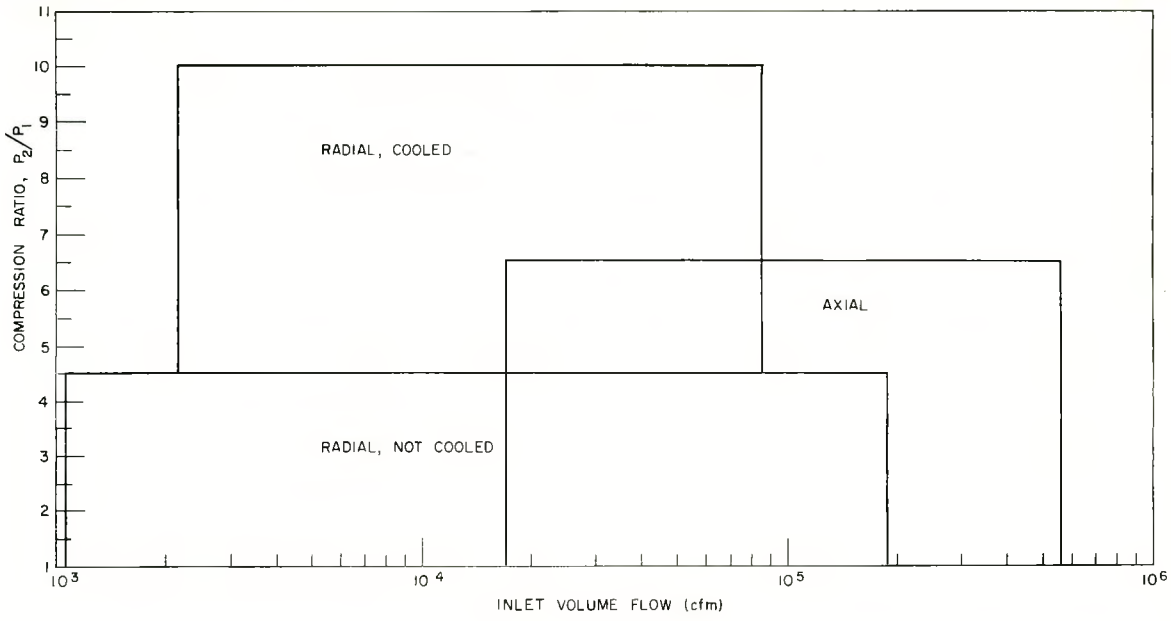


Fig. 2-39 - Range of Compression Ratio and of Inlet Volume Flow of One-Casing Turbo-compressors According to Current Manufacturing Practice (for Compression of Air from Atmospheric Conditions)

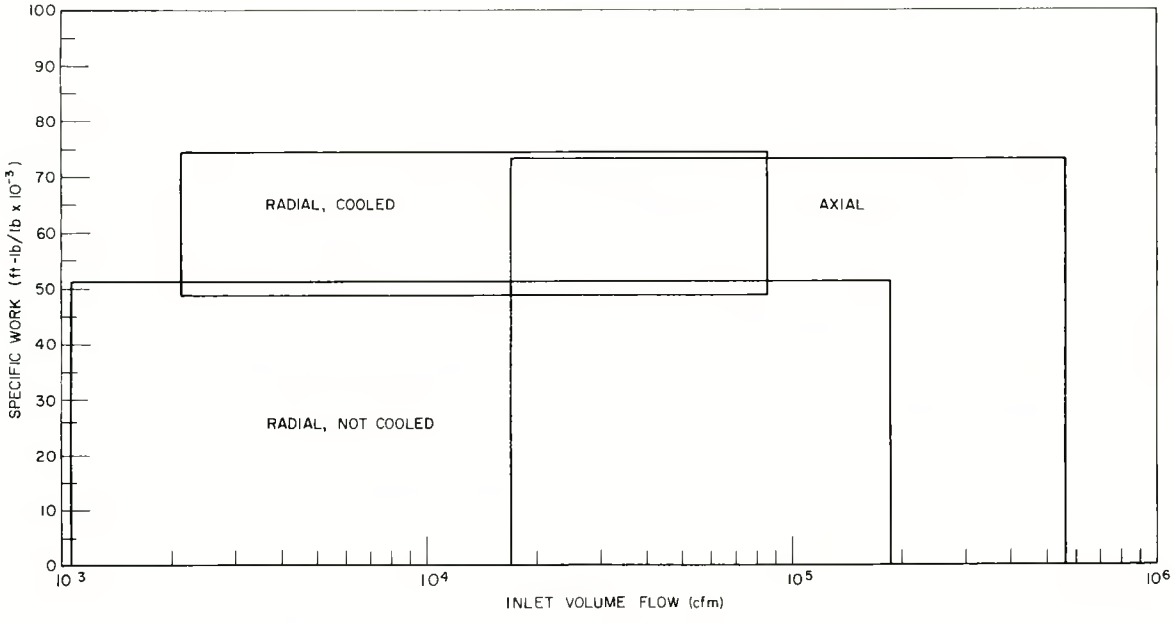


Fig. 2-40 - Range of Specific Work and of Inlet Volume Flow of One-Casing Turbo-compressors According to Current Manufacturing Pratice (Valid for all Gases)

This is the Elliott-Lysholm gas-turbine for ship propulsion. Figure 2-41[43] shows the flow diagram and some other pertaining information of this cycle. Figure 2-42[43] illustrates an Elliott-Lysholm compressor separately, and Figure 2-43[43] shows the performance characteristics of such compressors.

2.4.5 Free Piston Compressors

Free piston compressors are another type of compressor used successfully in gas-turbine installations, particularly for marine applications. In the event that the free-piston engine is to serve a conventional open cycle gas-turbine system, the total output of the engine is usually arranged to come from the exhaust of the diesel engine and feed directly into the turbine. In this case, the dimensions of the engine are made such that exhaust pressure and temperature from the diesel engine are in the desired range for operating the gas turbine.

Figure 2-44[44] illustrates a design developed by Sulzer in Switzerland for a 7000-hp gas turbine which receives its gas supply from three floating-piston engines. The bounce cylinders are shown at the extreme ends of each of the floating-piston engines. The exhaust from each engine feeds into a common header which serves the exhaust-gas power turbine. A charging compressor, also driven from the hot gas supplied by the free-piston engines, is used to supercharge the gas supply to the free-piston engines. A synchronization system, which can be controlled by fuel-injection timing and the resonance conditions of the compressors, can provide a uniform flow of gases to the exhaust-gas turbine. It is thought that the Sulzer design has an over-all efficiency in excess of 40 per cent based on the lower heating value of the fuel. The starting of any free-piston unit can be accomplished by supplying compressed air to the far face of the compressor cylinder so as to provide the initial compression stroke for the opposed piston diesel or even by supplying air to the bounce cylinder for the same purpose. It is, of course, necessary to see that the bounce cylinder under operating conditions is provided with an adequate amount of air to give the spring action required for effective operation of the unit.

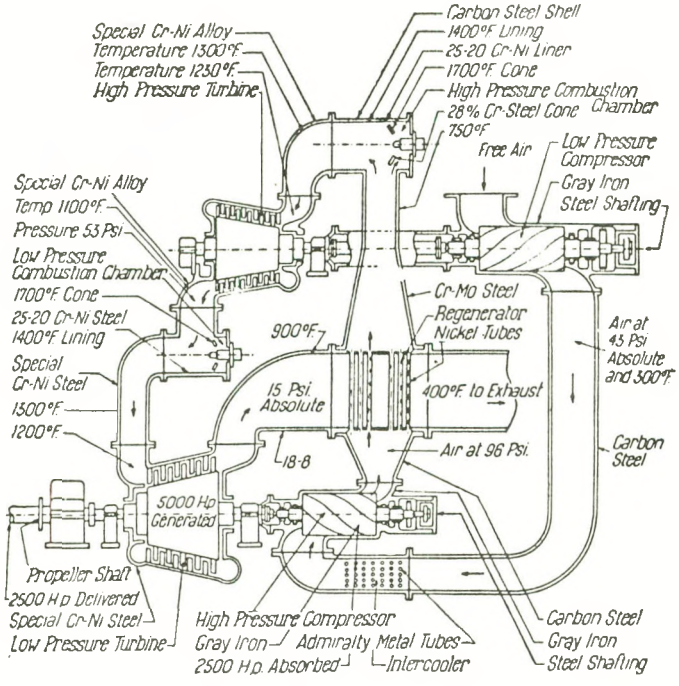


Fig. 2-41 - Diagram of Elliott-Lysholm Gas-Turbine Cycle for Ship Propulsion

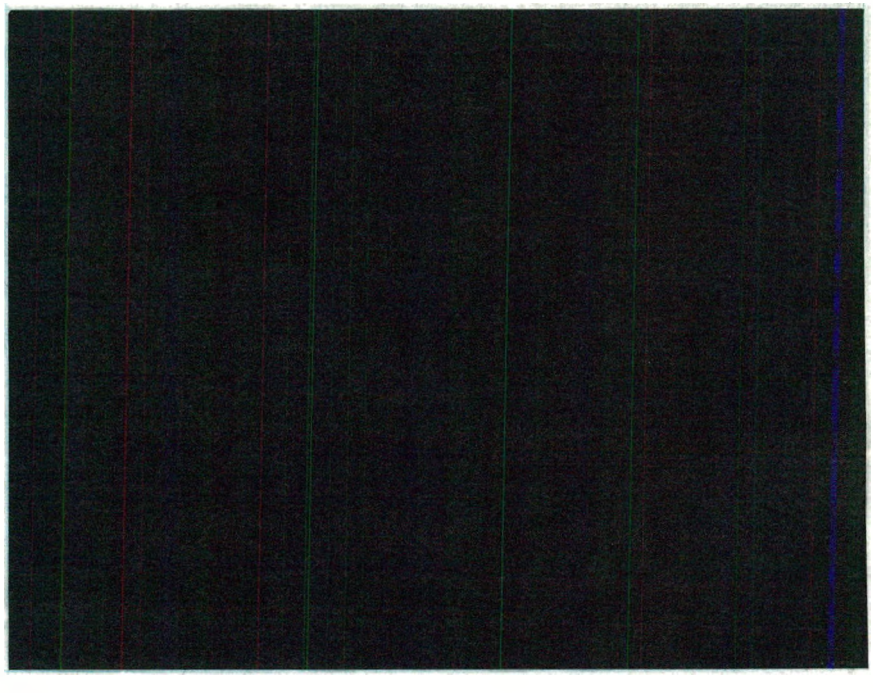


Fig. 2-42 - Elliott-Lysholm Compressor

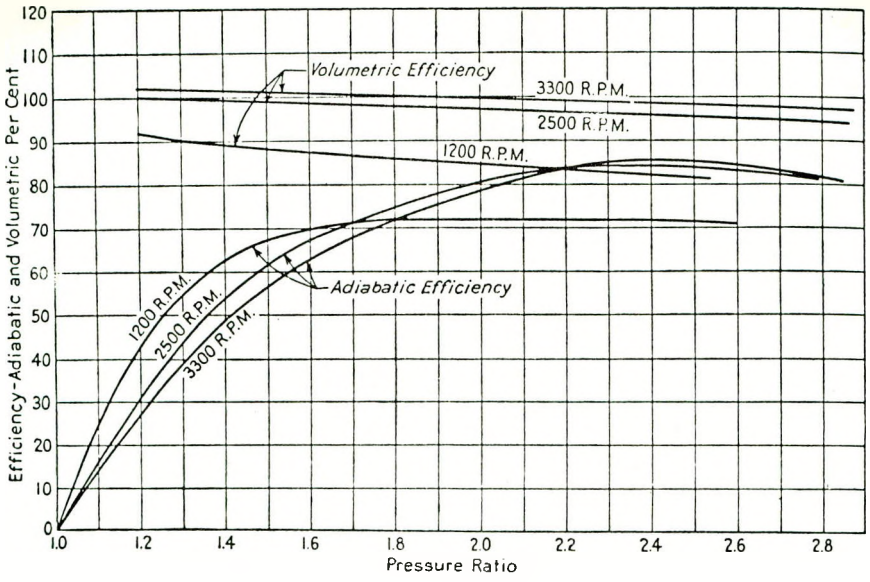


Fig. 2-43 - Performance Characteristics of Elliott-Lysholm 12,500-cfm Compressor

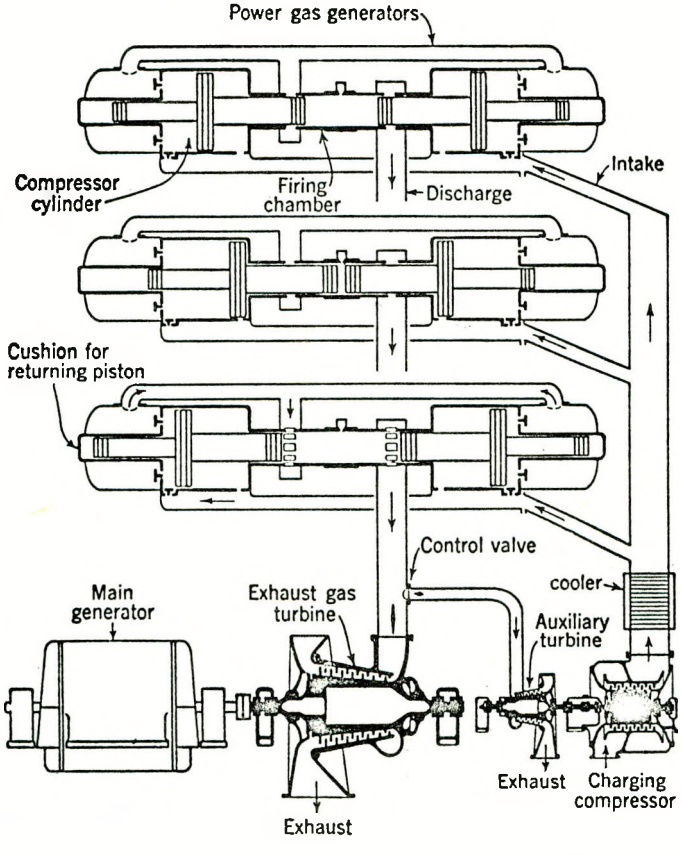


Fig. 2-44 - Combination Design of Three Floating-Piston Engines Serving a Gas-Turbine (Sulzer Co.)

The high efficiency of the power unit can be explained in terms of the effectiveness of the diesel engine, which serves as the gas-generation stage of the process. In a normal gas-turbine system, approximately two-thirds of the turbine output is required to compress the gases used in the turbine, leaving one-third of the power available for useful external output. The free-piston design eliminates this compressor tax and supplies the gases at high pressure and high temperature almost as a by-product. The turbine can be of conventional design. The free-piston engines, having no cranks or external shafting and operating in a horizontal plane with no side thrust, can keep wear to a minimum[44].

It is not likely that a free-piston engine will ever be used in nuclear gas-turbine installations. In this case, the arrangement would have to be with flow-wise separated diesel engine and compressor. Leakage problems would arise between nuclear and diesel circuits. Contamination of the nuclear circuit by lubricants would be an additional serious problem.

Free-piston engines have been applied in this country by William Patterson for the Maritime Administration[10]. The propulsion plant of the William Patterson consists of six free-piston gas generators, each rated at approximately 1250 gas hp, and two 3000-shp reversible gas turbines connected to the ship's propeller through a double-reduction, locked train, marine reduction gear. The ship had sailed approximately 70,000 miles, completing six voyages, as of March 1959. The early performance of the Patterson, from a maintenance and reliability standpoint, has not been too encouraging. However, it must be remembered that the use of free-piston machinery for marine propulsion in this power range is a new concept. It is too soon to draw any conclusions on the suitability of free-piston machinery for marine propulsion. Much was learned, and the modifications that have been made to improve reliability are encouraging.

Some data on free-piston gas-generators and their application are given in Tables 2-19[24] and 2-20[24].

The French Navy, in 1953-1955, installed free-piston gas-turbine propulsion plants in 21 mine-sweepers. These ships are 2-shaft and each shaft is driven by a free-piston gasifier combined with a gas turbine. The gasifiers are GS-34 units. Turbines are by Rateau. The power per shaft is 900. Astern power is supplied by astern stages in the turbine. These installations are the only publicized naval propulsion plants using free-piston gasifiers combined with turbines[24].

Also, four 4570-gross tonnage Soviet bulk carriers are being built with free-piston gas turbine propulsion plants. Four GS 34 gasifiers, built by SIGMA (Societe Industrielle Generale de Mecanique Appliquee, France), deliver gas at 3.1 atmospheres and 842°F, to a gas turbine of Alsthom (France) manufacture. The turbine is geared from 5500 down to 115 rpm and delivers 4000 shp to the propeller[9].

Table 2-19

DESIGN DATA ON FREE-PISTON GASIFIERS

Item	GM-14, or GS-34	CS-75
Engine cylinder bore, in.	13.4	7.5
Compressor cylinder bore, in.	35.4	20.75
Over-all length, ft.	14	7.5
Stroke, cmr*	2 x 18 in.	2 x 9.5 in.
Number cycles per min., cmr	600	1000
Mean piston speed, fpm	1800	1580
Gas temperature, cmr	840 F	470 C
Gas horsepower, cmr	1230	420
Weight, tons	7.5	2.25
Gas flow, lb per sec.	8.5	-

*cmr = continuous maximum rating.

Table 2-20

FREE-PISTON GAS TURBINES IN MARINE INSTALLATIONS

Country	Manufacturer	Gasifier made	Power/ plant shp	Plants/ ship	Service	Ship	No. of ships	Status	Gasifiers-turbines/ plant*	Astern power
England	Free Piston Engine Co.	GS-3	2500	1	MP	Ore carrier	1	Building	G3/T1	Turbine
England	A. Stephens Sons	GS-34	4000	1	MP	Ormara	1	Building	G4/T1	Turbine
England	-	GS-34	4000	-	MP	-	1	Building	-	-
England	-	GS-34	2000	1	MP	-	1	Building	-	-
England	Free Piston Engine Co.	GS-34	7000	1	MP	Crest Ship Co.	1	Building	G-/T2	-
England	Smiths Dock	GS-34	-	-	-	Bolton S.S. Co.	1	Building	G4/T-	-
England	Free Piston Engine Co.	CS-75	200 kw	1	MA	-		Building	G1/T1	-
France	SIGMA	GS-34	900	2	NP	Minnesweep	21	Installed	G2/T1	Turbine
France	-	GS-34	8000	2	MP	-	2	Building	G2/T4	CPP
France	-	GS-34	2000	1	MP	Goodwood	1	Building	G2/T1	-
France	SIGMA	GS-34	2000	1	MP	Merignac Cantenac	2	Installed	G2/T2	Turbine
France	SIGMA	GS-34	600 kw	1	MA	Bethsabee	1	Installed	G1/T1	-
Germany	Demag Modag	GS-34	1400	1	MP	Sagitta	3	1 in operation, 2 building	-	Turbine
U.S.	SIGMA-GM	GM-14	6000	1	MP	W. Patterson	1	Installed	G6/T2	Turbine

Plant includes gasifiers and turbines supplying power to a single load.

M = merchant, N = naval, P = propulsion, A = generator.

G = gasifiers, T = turbines.

2.5 Turbine Types

Only two basic turbine types have proved to be successful when applied to gas turbines, radial and axial. We consider the diagonal centripetal type to be included in the radial centripetal. The radial centrifugal, of the Ljungstrom type, successful as steam turbine, has not found application as gas turbine. In the following descriptions, the term radial is used to mean radial centripetal.

Terry and drag turbines developed for low power outputs, and for low specific speeds are not considered in the following discussion. Incomplete test information is available on these types of turbines. Figure 2-45[45] shows the Terry and drag turbines schematically.

2.5.1 Radial Turbines

Radial turbines have established their place in industry, especially in the field of small turbomachinery, because of their simplicity, ruggedness and reliability. Although in most cases the field of application is tailored to use the usual 50 per cent reaction, there are many applications for turbines which operate at much smaller reactions in order to approach the performance range of impulse-type axial turbines. More and more applications are also found in the fields of low specific speeds where the radial turbine's competitor, the axial turbine, may operate with partial admission. A typical example of a small radial-inflow turbine is shown in Figure 2-34. Figure 2-46 shows a glowing inward flow radial turbine at a temperature of 1600°F and a wheel speed of 40,000 rpm during test at Ai-Research.

2.5.2 Axial Turbines

The axial turbine is by far the predominant type of turbine presently used. To illustrate the general design of industrial gas turbines, Figure 2-47 shows a section through a single-shaft gas turbine, and Figure 2-48[52] shows a section through a two-shaft gas turbine with a free power turbine.

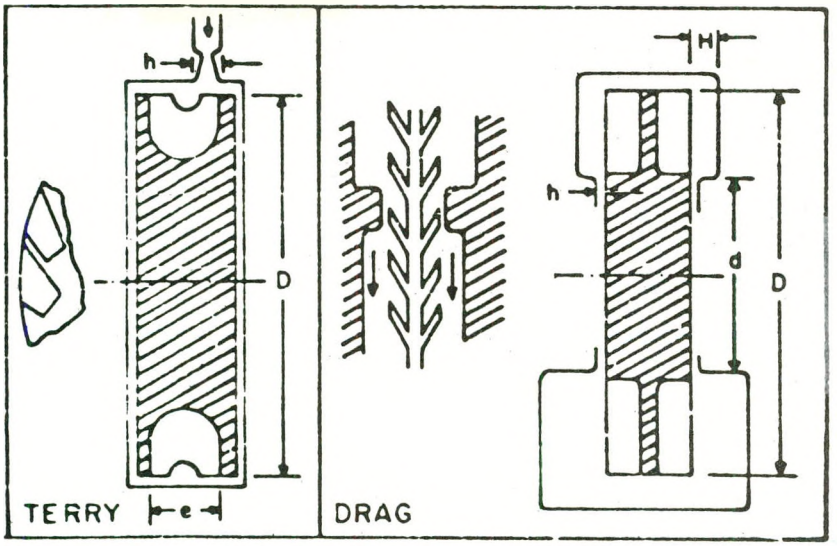


Fig. 2-45 - Schemes of Terry and Drag Turbines

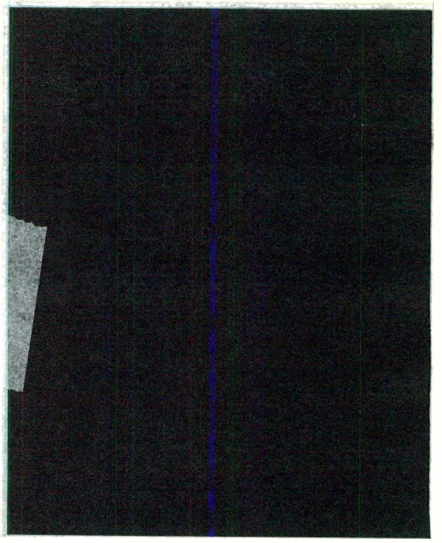


Fig. 2-46 - Test Set-Up of Inward Flow Radial Turbine

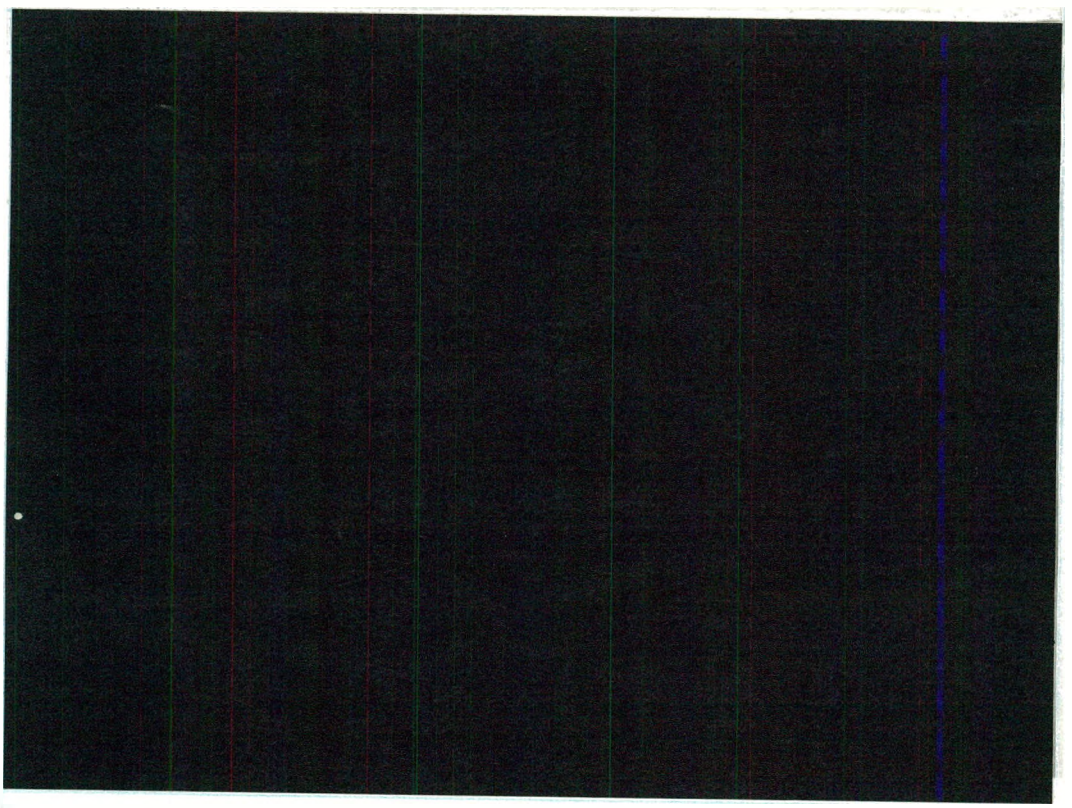


Fig. 2-47 - Clark Bros. Co. 9000 hp Single-Shaft Industrial Gas Turbine

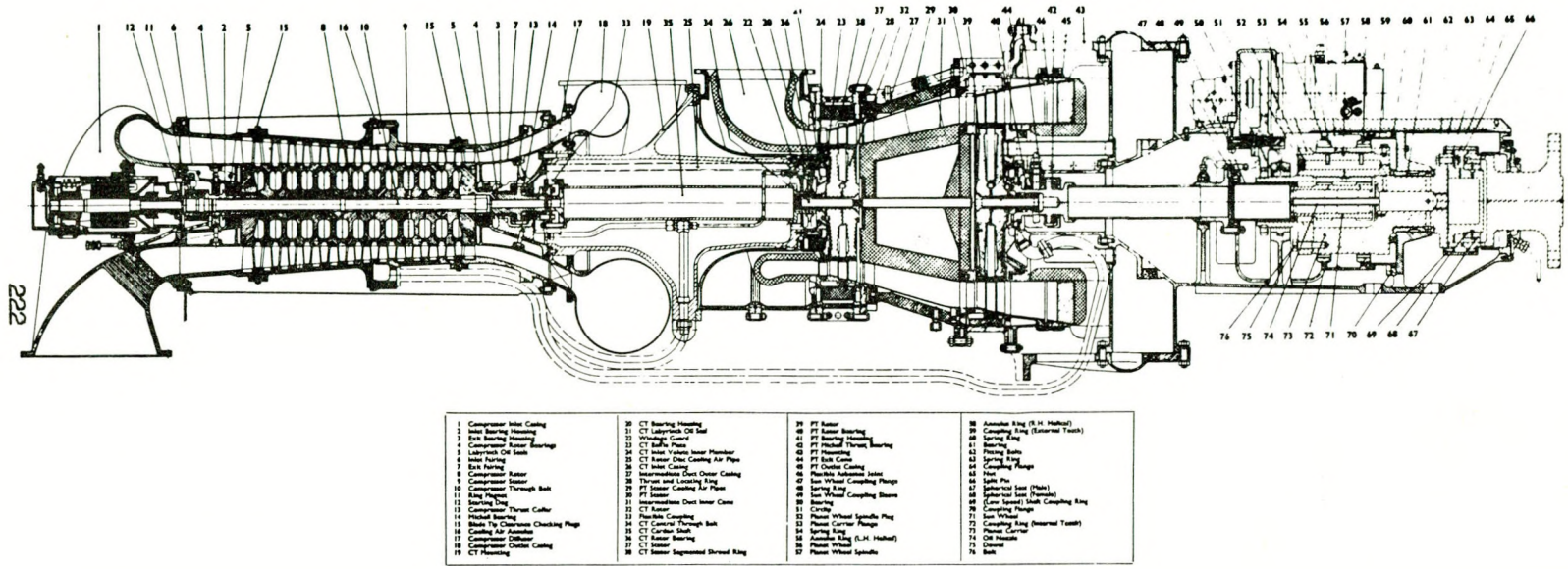


Fig. 2-48 - Outline of Clark Model TA Combustion Gas Turbines

As an unusual turbine type, we mentioned the Strato-Missiles Unique Disk turbine shown in Figure 2-49. A light-weight design, it is now being considered by the Air Force at Wright Field because of its claimed advantages when compared with existing axial, radial, and drag type turbines. The 6X-1 shown is 6 inches in diameter with 10 disks rated at 95 hp.

The turbine is driven by high-velocity combustion gas products, introduced into the turbine chamber by two split nozzles. As the gas particles impinge on the disks, they create a drag force which drives the disks. Since the gas can only escape at the center, virtually all energy in the gas particles is expended in turning the disks before it is exhausted. Efficiency is estimated to be 70%. This efficiency is coupled with the simplicity of design, low cost, light weight (1/5 pound per HP), silent operation and ability to operate at 2500°F gas temperature. The turbine may be designed as an integral part of the device it is driving and therefore, can be used as an accessory power drive or as a main power source.

For high temperature applications, it might be interesting to look into a design of a multi-stage turbine where the first stage would be a disk turbine. Disks might better resist the impact of the hottest streams of gases with present materials. The following stages might be of conventional design. The loss in efficiency in the first stage would presumably be recuperable in the last stages.

2.6 Types of Arrangement

When it is considered that there are many possible mechanical arrangements which can be made for each of the many thermodynamic cycles, and that, even with component performance fixed at a design point, the characteristics of each component may vary widely under different operating conditions, it will be realized that it is not practicable to present a general investigation of all possible arrangements. A total of about forty different mechanical layouts of a simple cycle are possible (although

by no means equally desirable) without having more than two compressor rotors, and without considering the extraction of useful power from more than one shaft at a time[46]. Not all of the possible arrangements need be seriously considered when deciding on a layout for a particular duty. Many of them are obviously unsuitable because of limitations in component design, and others are known to be difficult to operate satisfactorily. In a paper by Mallinson and Lewis[47], many arrangements are examined and compared for operating stability and efficiency variation. We suggest that this paper be consulted as a guide to the choice of a layout.

A number of general conclusions can be stated simply concerning the qualities of the various arrangements. First, schemes involving parallel compressors are undesirable for several reasons. There is generally little point in splitting the air flow into two parallel streams because compressor size is not usually a limiting factor. A higher pressure ratio than can be obtained from a single shaft compressor is often desirable, and this in fact constitutes one of the main reasons for series schemes with two or more compressors. While it is possible to obtain, with an axial compressor, a compression ratio of up to 12, the characteristic of such a compressor would require a speed to start a turbine as high as 1.5 times of the normal operating speed, if no regulation of the compressor stator blades is provided[48]. It is not probable that a compression ratio higher than 6, or perhaps 8 with further development, will be used in a single-spool axial compressor for an industrial gas turbine, where compressor surge must be avoided over a wide range of operation[48]. Most important of all is the inherent difficulty of operating two compressors in parallel without encountering prohibitive instability and control problems. Secondly, it may fairly be said that in general the cross-compound schemes (see Figure 2-50) are more difficult to operate successfully than the straight-compound ones.

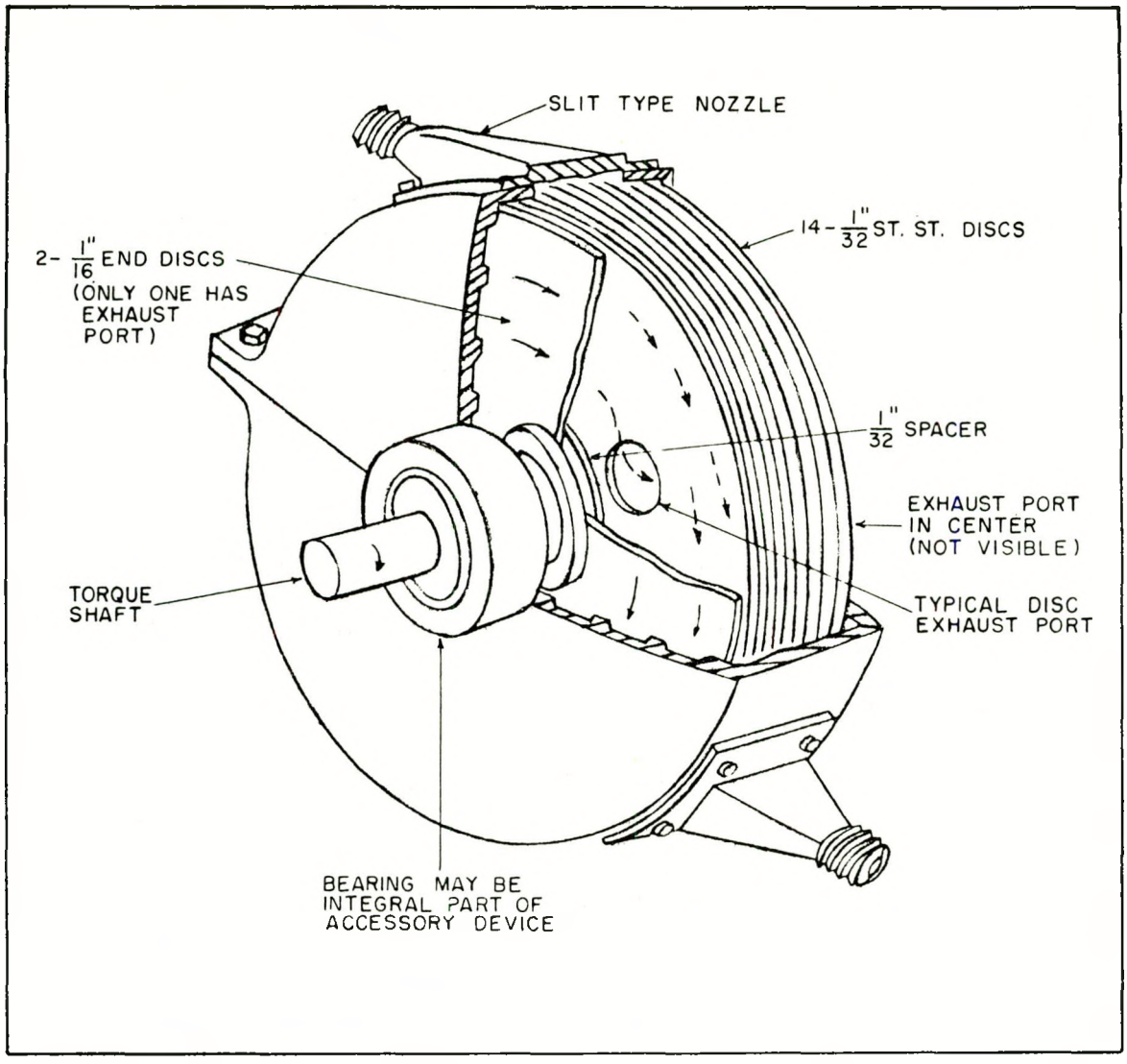


Fig. 2-49 - Strato Disk Turbine 6X-1

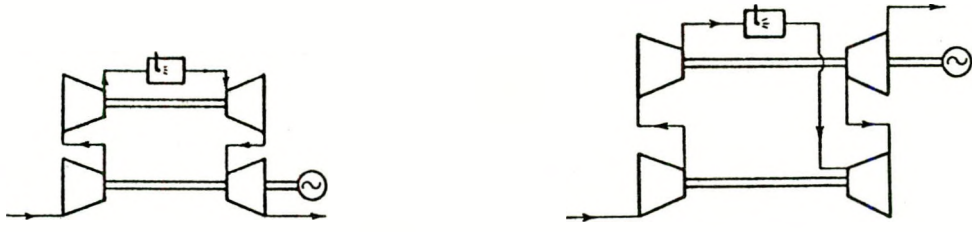


Fig. 2-50 - Straight-Compound and Cross-Compound Arrangements

The presently used gas turbine arrangements have a trend toward simplicity. One-shaft turbo-sets are frequently used as base-load units or as peaking units for electric power generation. Where partial load operating conditions are important, two-shaft machines have to be used because gas turbines whose compressors run at constant speed have a high fuel consumption at partial load. Depending on economical feasibility, the selected schemes of cycle may be simple or regenerative, and both of them are widely used. However, great capacity one-unit gas-turbine power plants may require a quite complex arrangement when a high pressure ratio is used to reduce the size of machinery and to increase the efficiency, particularly when flexibility of operation is an important factor. A three-shaft arrangement, shown in Figure 2-51[9] proposed for a Russian 300 Mw gas turbine power plant may serve as an example.

2.7 Future Developments

A general trend in the future development of gas turbines is toward higher efficiency, longer life and greater reliability combined with simplicity. The achievement of higher efficiency is generally visualized by raising the turbine inlet temperatures rather than by complicating the cycle, although the second way is also extensively studied and has been considered in certain industrial applications, such as combined steam and gas turbine installations. Steam and gas turbines can be combined to produce mechanical power in such a way that the combined installation achieves a higher efficiency than the steam or gas turbine running alone. Several different arrangements are feasible. For example, it is possible to incorporate a gas-turbine cycle in the combustion circuit of the boiler of a steam system; alternatively, a waste-heat boiler and steam turbine can be made to follow a gas-turbine. In the first arrangement the main stress is laid on the steam turbine, in the second on the gas turbine.[49] Apart from such special developments, the general tendency for simplicity leads to a prevailing abandonment of recuperation in small-to-medium size industrial open-cycle gas-turbine installations.

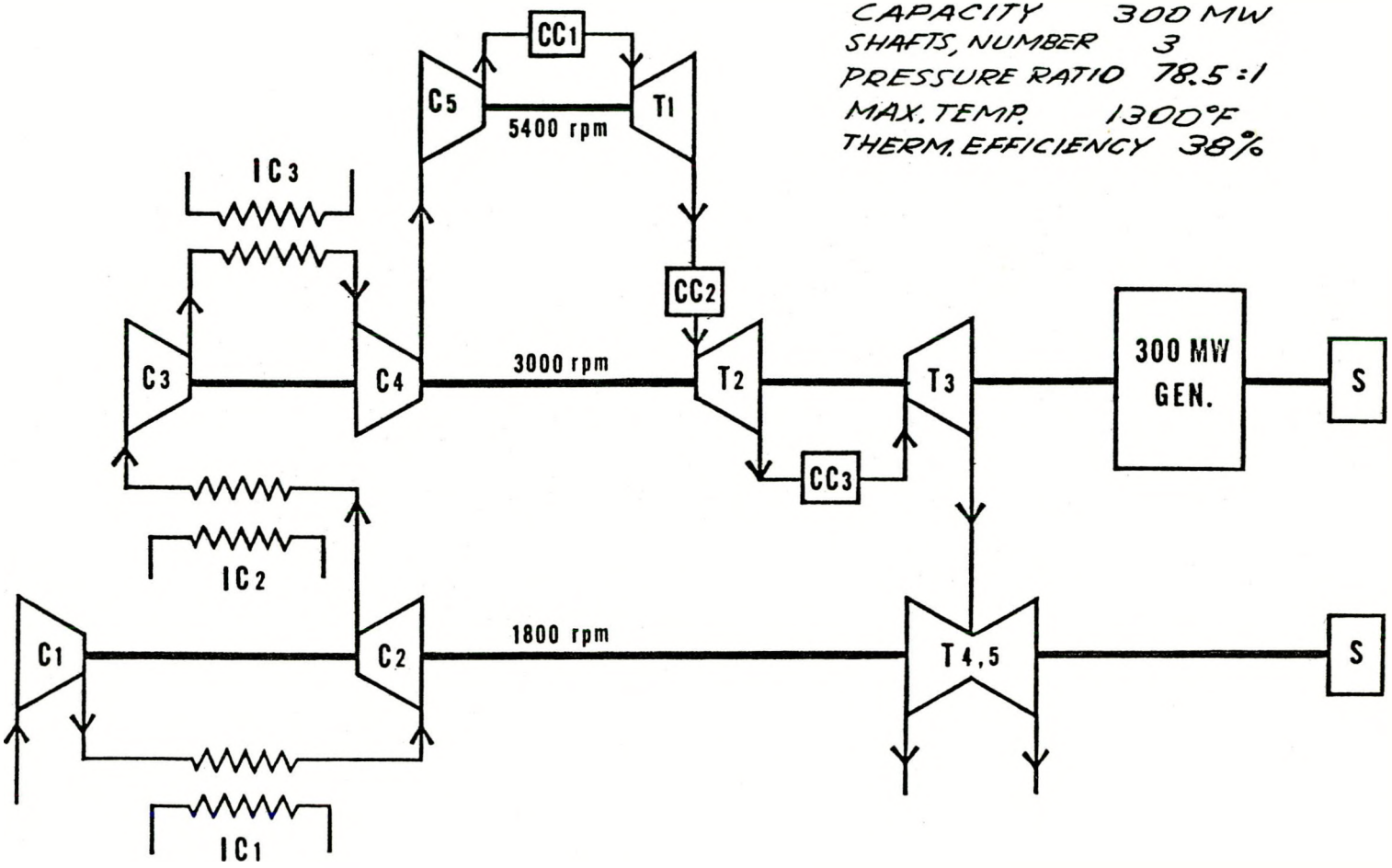


Fig. 2-51 - Proposed Russian Gas Turbine Power Plant

Turbine inlet temperatures are increasing consistently but at a rather slow rate, hand in hand with the development of high-temperature-resisting alloys for turbine blading. While some industrial turbines have already achieved long-life inlet temperatures in the order of 1500°F, the general tendency is to remain on the conservative side. The maximum capacity of gas-turbines for electrical power plants is continuously growing, paralleling the growth of industrial plants and 50 Mw units are probably coming into this field during the next decade. Lightweight medium size units, of approximately 10 Mw, are being produced by some manufacturers as complete power-packages, and this tendency will probably continue, having the aim to cut down installation time and costs.

Operational experience is accumulating at a fast rate and many developments in the immediate future will consist of minor but essential improvements based on such experience. These improvements will contribute to greater reliability and life of gas turbine.

Except for nuclear applications, future large gas-turbine installations will probably be of the open-cycle type because of their greater simplicity. However, solid-fuel fired plants will be restricted to the closed-cycle type. The general picture is that the gas-turbine is gradually replacing all other thermal prime movers, the automotive field being the only one where such a trend cannot yet be observed.

Predictions, five years ago, put 300,000 turbine-powered automobiles on the road by 1965. This has proved to be considerably optimistic. Except for one manufacturer, which may possibly have a turbine model in quantity production by that time, the gas turbine would seem to be another 10 years away. In fact it may never see widespread automotive use (trucks excepted) if break throughs occur in fuel-cell development or in other power sources now in research and prototype. A general statement from one side was made several years ago: in appraising the potential of any powerplant, we should keep in mind that, in order to supplant present piston engines, the new engine must

(a) occupy less space

(b) weigh less

(c) operate more economically

(d) be cheaper to produce

(e) be cheaper to maintain

(f) give better vehicle performance

To succeed the new engine cannot merely break even, but must surpass present achievements and it must do so in the face of continued improvement of present engines[50].

Development programs exist for cooled turbines and test facilities. One of such programs, at the General Electric Company, has the following objectives[51]:

(a) Development of a fully convective air-cooled, flight-type, single-stage turbine to demonstrate the feasibility of operation at an average inlet temperature pf 2000°F, with 4.3 per cent of compressor-discharge cooling air.

(b) Development of a test facility capable of testing the turbine under controlled conditions for cooling effectiveness, aero-thermodynamic performance, and mechanical reliability.

Demands for higher jet engine thrust-to-weight ratios to satisfy the needs for high Mach number and vertical take-off aircraft are continuously increasing. Since World War II, the three-fold increase in thrust-to-weight ratio can be attributed almost entirely to the development of light-weight construction and of the axial-flow compressor, and little credit can be given to the meager 200°F increase in turbine-inlet temperature. Increasing the turbine-inlet temperature, beyond present-day material limits of 1600-1700°F, by convective air cooling, will increase the jet-engine thrust-to-weight ratio and will markedly improve the performance of the turboprop and by-pass engines[51].

Small turboshaft engines for private airplanes develop slowly and are not yet competitive in price with the conventional piston engine.

Material development is keeping pace with turbine development. Forecasts have been made for British aircraft engines that around 1968 turbine inlet temperatures at cruising range would be as high as now at take off. This will require using of turbine-blade cooling.

Figure 2-52[20] shows past progress and extrapolation for the future of combustion temperatures, pressure ratios, and blade temperatures for turbojet and turboprop engines.

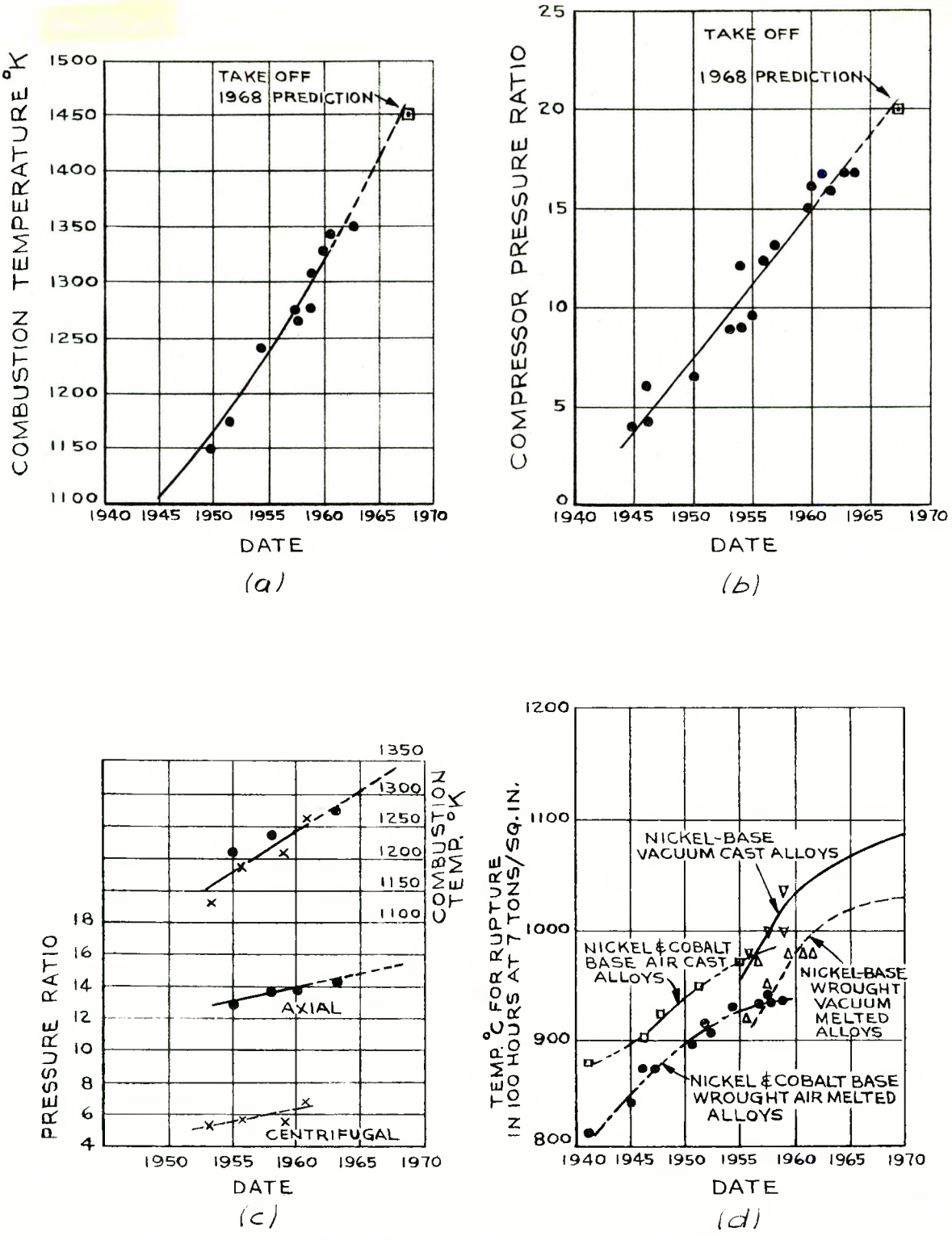


Fig. 2-52 - Performance Predictions for Turbojet and Turboprop Engines

3. NUCLEAR GAS TURBINES

3.1 General

Nuclear gas turbines, as compared with gas turbines for most other applications, will be always more conservative in design because of the graver consequences of a failure. Such a failure might cause a dangerous contamination of the atmosphere or at least require a prolonged down-time necessary for decontamination of surfaces before dismantling and overhaul of a unit can be accomplished. Both safety and maintenance reasons will markedly influence the development of nuclear gas turbines causing a lag behind other modern industrial gas-turbine installations especially in application of higher gas temperatures. Accumulation of operating experience with smaller units will be mandatory, gradually stepping up the inlet temperature to reasonably high values before construction of large nuclear gas-turbine plants can be attempted.

3.2 Requirements of Nuclear Turbomachinery

The construction of turbomachines in connection with the exploitation of nuclear energy presents the designer with new problems and at the same time renders more difficult the solution of problems with which he is already familiar because numerous limitations are imposed upon the design. The turbomachines must withstand effects of temperature, corrosion, and radiation, and must offer every guarantee in respect to hermetic sealing. The avoidance of contamination by harmful substances such as oil or the exclusion of humidity from the atmosphere, raise the problems of dry friction of moving parts, of virtually absolute gas tightness, and of the treatment and degassing of surfaces. The machines must further offer a maximum of operational reliability with a minimum of maintenance, which must be as simple and straightforward as possible[37,52,53]. As the machines must often work under completely new conditions, extensive laboratory tests are necessary in order to ascertain the effects of the factors involved, whether they act singly or simultaneously[52].

The properties of the coolant, or working fluid, in a direct closed-cycle gas-turbine reactor power plant affect the design of system components in a variety of ways. Some of these effects are obvious, while others are subtle but nevertheless important. All must be given due consideration in determining optimum power plant and better coolant. Molecular weight and heat capacity of the coolant together with cycle pressures and temperatures determine volumetric flow rates and linear velocities and, consequently, the size of all components including the turbomachinery. The possible leakage of coolant from the systems is affected by its molecular weight and its solubility in lubricating and sealing liquids[1]. Size and weight of turbomachine are affected by the sonic velocity and volumetric flow of the working fluid. (See also reports NYO 9786 on Coolants[54] and NYO 9792 on Bearings and Seals[5].)

A glance at Figure 3-1[52] shows that the speed of sound for heavy gases, such as uranium hexafluoride or Freon 12, is relatively low. It follows that at high pressure ratios the peripheral speed at the inlet to the machine may be fixed by the Mach number. For light gases, on the other hand, such as hydrogen and helium, the tensile strength of the material used for the rotor will be the limiting factor.

Let us consider first a single-stage radial compressor with open impeller which is used for compressing light or heavy gases, and the diameter of which we may take for reference purposes as unity. We assume that the peripheral speed does not exceed the limit set by the maximum permissible stress in the rotor and that the Mach number at the inlet diameter of the impeller is limited to the maximum value of 0.9. From these given values, the other characteristics of the machine may be determined, i.e., discharge rate and pressure ratio. All data relating to nitrogen will be regarded as reference values with which those for other gases may be compared. As soon as a value reaches the prescribed limit it will be marked with an asterisk, for such values that restrict the speed of the rotor and thereby determine the size of the machine.

THE FRANKLIN INSTITUTE • Laboratories for Research and Development
I-A2392

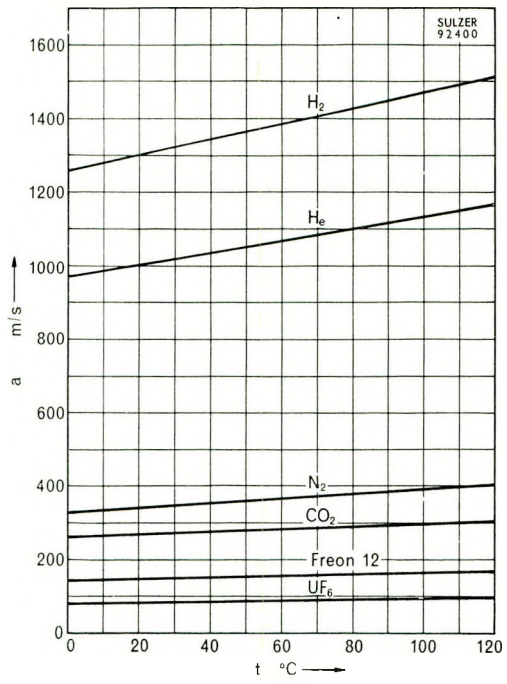


Fig. 3-1 - Speed of Sound as a Function of Temperature for Various Gases

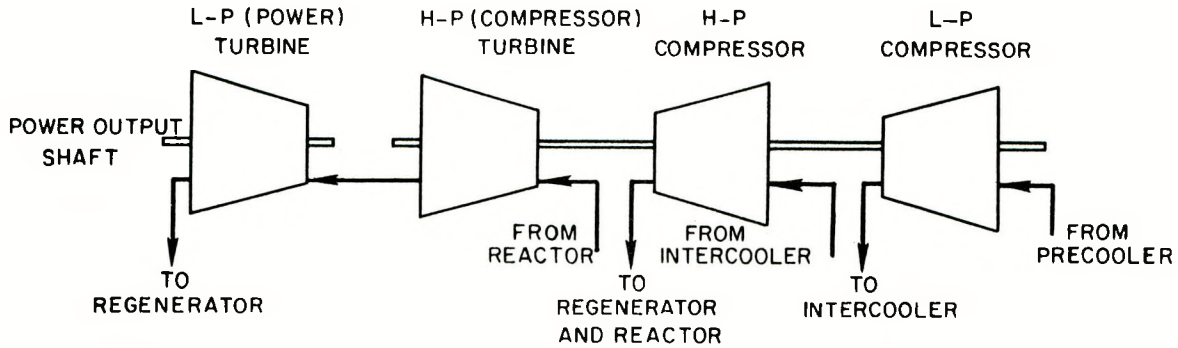


Fig. 3-2 - Schematic Layout of Turbomachinery with In-Line Power Turbine

Table 3-1[52] shows that in the case of the heavy gases in question it is the minimum Mach number at the impeller inlet which limits the number of revolutions. With uranium hexafluoride, however, the low ratio of the specific heats, $k = 1.06$, and the high pressure ratio of 7.5 result in a relatively small volume of gas at the outlet. The ratio between the width of the impeller at the outlet and the outside diameter is therefore 2.2%, which is regarded as the lower limit.

With CO_2 the strength limit of the rotor is reached almost at the same time as the specified Mach number. In the case of N_2 and the light gases, the limit is determined solely by the strength of the rotor.

Table 3-1

INFLUENCE OF TYPE OF GAS ON A RADIAL COMPRESSOR

Gas	Mach No.	Stress Ratio	Speed Ratio	Pressure Ratio	Vol. ratio of gas aspirated	
UF_6	0.90*	0.14	0.37	7.5	0.21	
CF_2Cl_2 Freon 12	0.90*	0.42	0.65	7.5	0.37	
CO_2	0.90*	1.0*	1.0	5.0	1.0	Steel rotor
N_2	0.70	1.0*	1.0	3.0	1.0	
H_e	0.28	1.0*	1.0	1.2	1.2	
H_2	0.21	1.0*	1.0	1.1	1.2	
H_e	0.42	1.35*	1.5	1.5	1.8	Titanium
H_2	0.32	1.35*	1.5	1.25	1.8	alloy rotor

450 m/sec rotor tip speed

Temperature at inlet of machine = 353°K

* Limiting values

If materials are used for which the ratio of permissible stress to specific mass assumes a progressively smaller value, it will be clear that the limit based on the strength of the impeller will be displaced toward the heavy gases. If a titanium alloy is chosen as material for the impeller, the peripheral speed can be increased toward 700 meters per second for the light gases, as can be seen from the last two figures in Table 3-1.

A similar comparison can be made with axial compressors. Table 3-2[52] gives details of results obtained with a ten-stage compressor having a radius ratio at the inlet of 1.5. The Mach number at the blade tip at the inlet was limited to 0.9.

Table 3-2

INFLUENCE OF TYPE OF GAS ON AN AXIAL COMPRESSOR

Gas	Mach No.	Stress Ratio	Speed Ratio	Pressure Ratio	Vol. ratio of gas aspirated	
UF_6	0.9*	0.06	0.25	3.8	0.25	
CF_2Cl_2 Freon 12	0.9*	0.2	0.45	4.2	0.45	
CO_2	0.9*	0.6	0.77	4.3	0.75	Steel rotor
N_2	0.9*	1.0	1.0	4.5	1.0	
H_e	0.45	2.2*	1.5	1.9	1.5	
H_2	0.35	2.2*	1.5	1.4	1.5	
H_e	0.7	3.0*	2.3	3.8	2.3	Titanium
H_2	0.55	3.0*	2.3	2.1	2.3	alloy rotor

Number of stages = 10
210 m/sec rotor tip speed
Temperature at inlet of machine = 353°K
* Limiting values

It is interesting to note that it is the Mach number which limits the peripheral speed of the rotor for the first four gases, while with the light gases the maximum number of revolutions of the machine depends on the strength of the material. Here also materials with a more favourable permissible stress to specific mass ratio can be used to advantage in order to raise the pressure ratio or reduce the number of stages[52].

Generally, smaller volumetric flows tend to require machines with smaller flow annulus area, all other conditions being equal. The effect of volume is modified, however, by the properties of the gas. Gases having high molecular weight and low sonic velocity require lower velocities through the machine than do the lighter gases which have higher sonic velocities. Gases having low sonic velocity therefore, require larger flow annulus areas than lighter gases for a given volumetric flow. In this respect the lighter gases tend to give a smaller, lighter weight turbomachinery than the heavier gases. However, power cycle thermodynamics call for greater compressor work input for optimum performance with the lighter gases (see Charts B-30 and B-31 in NYO Report 9787 on Cycles[2]). This, in turn, necessitates more compressor and turbine stages.

Higher system pressures result in lower volumetric flows for a given weight flow of working fluid, and the area of the flow annuli of the turbomachinery will be reduced proportionately. At the same time, the thickness of the machinery casings will have to be increased to carry the greater pressure loads. It can be seen from the above discussion that, in order to estimate the effect of coolant composition and pressure on the turbomachinery, it is necessary to lay out preliminary designs of the machinery for the different conditions under consideration and then to estimate the respective weights from these designs. This step was taken in preliminary studies for the MGCR for helium at 1000 psia and carbon dioxide at 1000 and 2000 psia. The resulting pertinent information is listed in Table 3-3[55].

Table 3-3

PRINCIPAL DIMENSIONS AND CHARACTERISTICS

	1000 PCI He				1000 PSI CO_2				2000 PSI CO_2			
	LPC	HPC	HPT	LPT	LPC	HPC	HPT	LPT	LPC	HPC	HPT	LPT
Speed (RPM)	15000	15000	15000	10000	10500	10500	10500	8000	18750	18750	18750	15900
No. Stages	14	18	7	5	6	9	3	2	6	10	2	2
Hub Dia.	14.5	11.4	13.4	17.0	12.7	11.1	11.6	16.5	5.5	4.5	8.4	8.7
Tip Dia. (in)	18.1	14.3	17.8	22.7	18.1	14.4	14.8	20.7	9.1	7.1	10.5	12.1
Tip Dia. (out)	18.1	14.3	20.2	25.0	15.2	12.6	18.1	24.6	8.0	6.0	12.1	14.6
Tip Speed (ft/sec)	1185	935	1320	1095	830	660	830	875	745	580	990	1015
Axial Vel. (ft/sec)	490	488	539	453	363	329	335	364	391	257	371	383
Stage Press. Ratio	1.035	1.027	1.074	1.06	1.14	1.12	1.31	1.41	1.14	1.11	1.47	1.48
Comp. Eff. Fl. to Fl.	85.2	85.2	89.8	87.2	83.6	84.1	89.8	84.3	82.6	83.6	88.7	84.0
Hub Tip Ratio First	.8	.8	.753	.75	.70	.77	.785	.797	.605	.634	.80	.72
Hub Tip Ratio Last	.8	.8	.663	.68	.835	.88	.64	.67	.688	.750	.695	.595
Overall Length		24 ft 11 in.				21 ft 6 in.				20 ft 5 in.		
Overall Weight		35,500 lbs				38,300 lbs				32,000 lbs		
Stage Efficiency	89	89	90	90	89	89	90	90	89	89	90	90

All the machinery is assumed to be in an arrangement in line as shown in Figure 3-2, and the sections through the three compared lay-outs are shown in Figures 3-3 to 3-5[29]. The arrangement in line results in lower total weight, fewer shaft seals, and slightly higher efficiency than the alternate arrangement where the power turbine is in a separate casing. However, the latter arrangement permits a shorter overall length. Since the helium machinery requires more stages, it is expected to be longer and more likely to require the separate power turbine arrangement, than the CO_2 machinery. This has a detrimental effect on power-plant efficiency because of aerodynamic losses in the connecting piping between compressor turbine and power turbine, but it may be necessary if machinery compartment space is limited.

Table 3-4[1] will enable one to consider machinery weights in their proper perspective in relation to the other components of the gas-turbine plants. For all practical purposes, the weights of the three rotating machinery units, 1000 psia helium, 1000 psia carbon dioxide, and 2000 psia carbon dioxide, are the same.

The reactors considered in Table 3-4 are not the latest that may be considered for this application; nor do the performance estimates reflect technological advances that may improve the performance of the subsequent plants over that expected for the prototype. For example, successful development of higher-temperature materials for the reactor structure, such as niobium alloys, and successful development of long-burn-up solid-homogeneous fuel structures could result in significant reductions in the capital and operating costs of such a plant. Therefore, the data presented serve principally to illuminate differences in plant performance relating to choice of coolant and moderator.

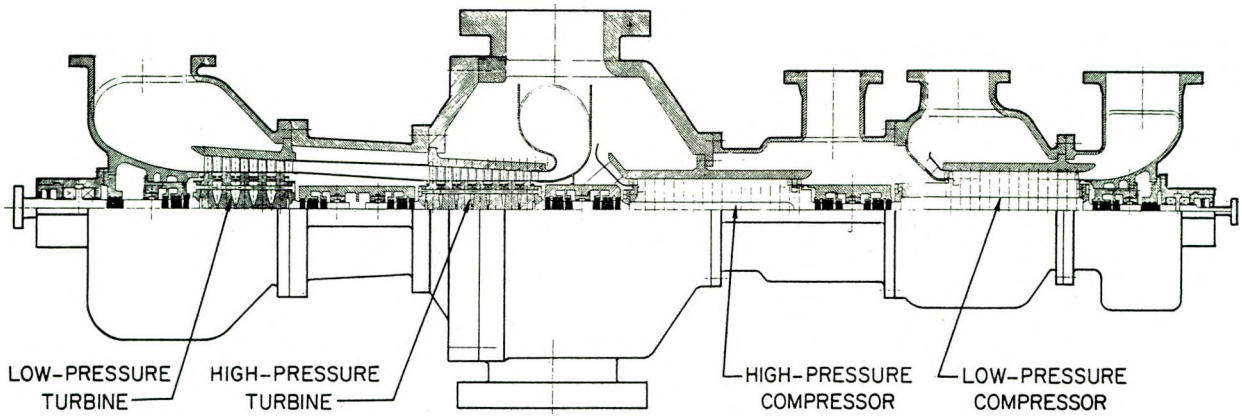


Fig. 3-3 - Cross-Sectional Drawing, 1000-psia Helium Turbomachinery

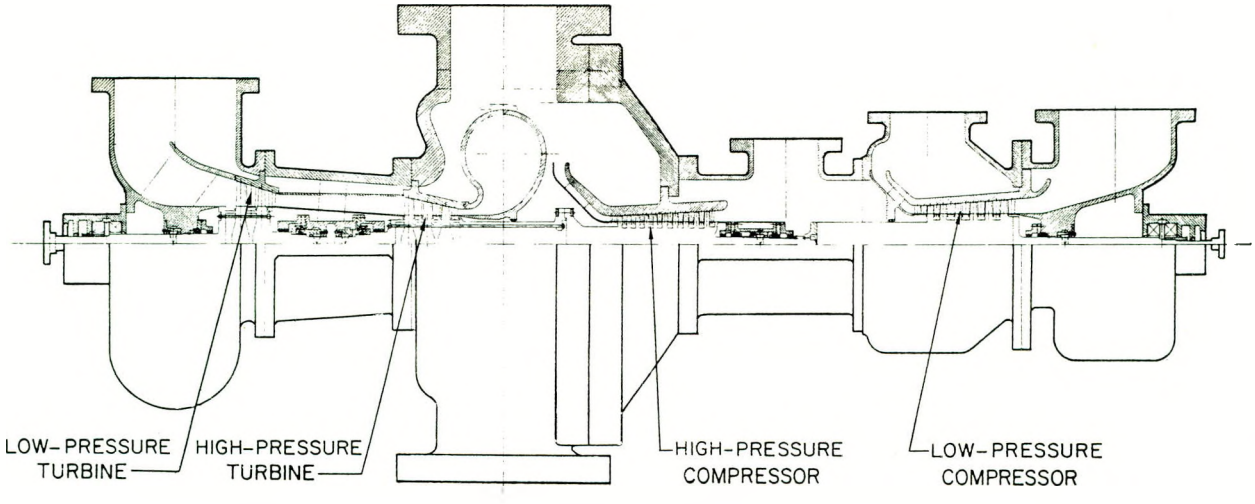


Fig. 3-4 - Cross-Sectional Drawing, 1000-psia Carbon Dioxide Turbomachinery

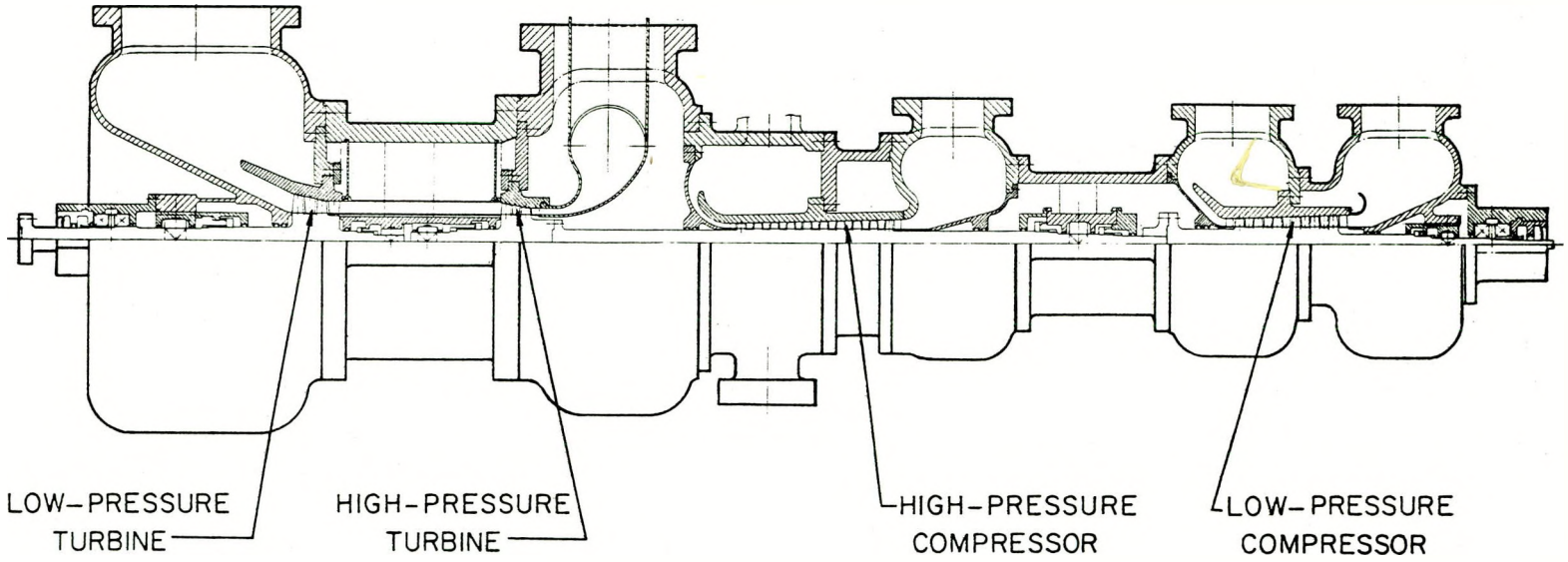


Fig. 3-5 - Cross-Sectional Drawing, 2000-psia Carbon Dioxide Trubo-machinery

Table 3-4

BASIS FOR COMPARING WEIGHTS OF MACHINE COMPONENTS

(Shaft Output = 20,000 hp)
Weights in long tons

	Graphite Helium	Graphite CO_2	H_2O CO_2	ZrH CO_2
Net Plant Efficiency, %	30.0	32.5	31.4	33.1
Reactor Heat Output				
Heat Input to Coolant Mw	49.7	45.9	44.7	44.7
Heat Loss to Moderator, Mw	-	-	2.8	-
Maximum Coolant Pressure, psia	1000	1000	2000	2000
Exit Temperature of Coolant from Reactor, °F	1300	1300	1300	1300
Diameter and Height of Reactor Core and Reflector, ft	8.37	8.37	5.08	5.00
Reactor Vessel Diameter, ft (O.D.)	10.4	10.4	7.43	7.28
Reactor Vessel Height, ft	21.1	21.1	16.7	15.0
Reactor Vessel Wall Thickness, in.	5.75	5.75	7.58	7.44
Reactor Weight, tons	173	173	80	99
Primary Shield, tons	572	566	410.5	353
Secondary Shield, tons	404	438	470	460
Moderator Cooling Systems, tons	-	-	7.5	-
Turbomachinery, tons	15.8	17.1	14.3	14.3
Regenerator, tons	37.1	71.5	60.7	60.7
Intercooler and Precooler, tons	27.0	38.2	26.9	26.9
Valves and Piping, tons	26.8	35.7	30.4	30.4
Coolant Storage System, tons	24.7	35.2	29.0	29.0
Reduction Gear, tons	134.0	111.5	175.0	175.0
Fluid Load, tons	235.8	244.5	241.6	241.6
Auxiliary Systems and Equipment, tons	367.8	377.8	369.1	367.0
Total Machinery Weight, tons	2017.5	2018.5	1915.1	1869.1
Specific Weight, lb/SHP	201	214	192	187

3.3 Power Plant Studies

3.3.1 Plant Details

Beginning with the early fifties, a number of studies were performed by different industrial and research groups, mostly under the sponsorship of the AEC, envisaging the utilization of gas-turbines as prime movers in gas-cooled nuclear power circuits. Table 3-5 lists the notable U.S. power plants, having gas-turbines as prime movers, which have been studied. Their characteristics are identified in Table 3-6.

With the achievement of sufficiently high gas temperatures in gas-cooled nuclear power reactors, this concept materialized in this country in two developments, the ML-1, a prototype of a mobile low-powered nuclear power plant for the Army, and the MGCR, a maritime gas-cooled reactor power plant for the Maritime Administration. The ML-1 is near completion, and the MGCR program is in full development at this time.

Let us now examine some of these studies in more detail.

Gallagher Open Cycle

The Gallagher open cycle is to be considered only as a purely theoretical cycle because of the possible contamination of the atmosphere by fission products in the stream through the stack. A Solar Aircraft Company Jupiter T-520 gas-turbine was selected as prime-mover for this hypothetical plant (see Fig. 3-6)[56]. It has 400 shp at 75°F at the compressor inlet. Turbine inlet temperature is 1325°F.

Gallagher Closed Cycle

The closed cycle utilizes an Escher Wyss Tuco-52 (Turbo-Compressor) set, designed for a closed cycle (see Fig. 3-7)[56].

ORSORT Ceramic Breeder Reactor Power Plant

In 1954 a power breeder was investigated by a study group headed by J. F. Smith to which J. R. Johnson of Minnesota Mining &

Table 3-5

NOTABLE U.S. STUDIES OF GAS-COOLED NUCLEAR POWER PLANTS
WITH GAS-TURBINE PRIME MOVERS

1. Gallagher Open Cycle
   Naturally Enriched Uranium (UO_2), BeO Moderated, Air 1325°F 64.7 psia, 0.2 MWe, 1954.

2. Gallagher Closed Cycle
   Naturally Enriched Uranium (UO_2), Graphite Moderated, N_2 1220°F 396 psia, 2 MWe, 1954.

3. Oak Ridge School of Reactor Technology
   ORSORT Ceramic Breeder Reactor, UO_2 in SiC-Si and ThO as Breeder Material, Graphite Moderated, Single Cycle He 1400°F 1000 psia, 60 MWe, 1954.

4. Daniels
   Uranium-Thorium Breeding Cycle (UC_2), Graphite Moderated, He 1350°F 225 psia/air 1250°F 420 psia, 5 MWe, 1956.

5. Studebaker Packard Corp.
   Enriched Uranium (UC_2) in Graphite, Graphite Reflector-Moderated, He 1740°F 294 psia/open cycle air 1400°F 78.6 psia, 17 MW (3 units), 15 MWe, 1956.

6. Ford Instrument Company
   FICO Partially Enriched Uranium (UO_2), Graphite Moderated, Single cycle N_2 1300°F 535 psia, 15 MWe, 1956/1957. The cycle used is known as the Jarvis cycle.

7. Ford Instrument Company
   FICO Marine Enriched Uranium (UO_2) Graphite-Moderated, Single cycle He 1150°F 600 psia, 22000 shp, 1957.

8. General Motors Corp.
   Maritime Power Plant, Highly Enriched Uranium (UO_2), Graphite Moderated, Single Cycle He 1300°F 1000 psia, 22,000 shp, 1957.

9. Los Alamos Scientific Laboratory
   Turret Exper. Plant, Highly Enriched Uranium in Graphite, Graphite Moderated, Single Cycle N_2 1300°F 530 psia, 20 MWe, 1957/1958.

10. General Dynamics General Atomic Division and Electric Boat Division for MGCR (Maritime Gas-Cooled Reactor) Program of AEC and U.S. Maritime Administration
MGCR, Partially Enriched Uranium (UO_2), Graphite Moderated, Single Loop He 1300°F 1000 psia, 20,000 shp, 1958.

11. MGCR, Partially Enriched Uranium (UO_2), Graphite, D_2O, BeO, or H_2O Moderated, Single Loop CO_2 1300°F 1000 psia, 20,000 shp, 1958.

12. MGCR, Partially Enriched Uranium (UO_2), H_2O, ZrH, or Graphite Moderated Single Loop CO_2 1300°F 2000 psia, 1958.

13. MGCR, Partially Enriched Uranium (Heterogeneous-UO_2 in BeO or Al_2O_3, or semihomogeneous - UC in graphite, or UO_2 in BeO), Graphite Core, Single Loop He 1300°F 800 psia, 22,000 shp mas., 1959.

14. MGCR Preliminary Design, Partially Enriched Uranium (UO_2 or UO_2-BeO), BeO-Moderated, Single Loop He 1300°F 1150 psia, 32,000 shp, 1960.

15. WKNL
(Walter Kidde Nuclear Laboratories), Portable Army Reactor, Highly Enriched Uranium (UO_2), Graphite Moderated, Single Cycle He 1150°F 164 psia, 0.125 Mwe, 1955.

16. Alco Products - Sanderson & Porter
Closed Cycle Gas Turbine Test Facility for Army Portable Nuclear Power Plants, H_2O Moderated, N_2 1150°F 210 psia, 0.4 Mwe, 1957.
(Forerunner of ML-1).

17. Aerojet - General Nucleonics for AGCRSP (Army Gas-Cooled Reactor Systems Program)
ML-1 - Prototype of a Mobile Low-powered Nuclear Power Plant, Partially Enriched Uranium, H_2O Moderated, Single Cycle N_2 1200°F 310 psia, 0.4 Mwe, in Construction (First Location at Idaho Falls).

18. GTTF - Gas Turbine Test Facility for ML-1 at Fort Belvoir, Virginia. Operating since 1959.

Table 3-6

GAS-TURBINE PRIME MOVERS OF U.S. GAS-COOLED NUCLEAR POWER PLANT PROJECTS

TABLE

1		PLANT OR PROJECT	GALLAGHER OPEN CYCLE	GALLAGHER CLOSED CYCLE	ORSORT CERAMIC REG. & RECUP. OF AFTURB. C.	DANIELS BREEDING CYCLE	STUDEBAKER PACKARD POWER PLANT	FICO STATIONARY POWER PLANT (BRAYTON CYCLE)	FICO MARINE POWER PLANT	G.M. MARINE POWER PLANT	TURRET EXPERIMENTAL POWER PLANT	MGCR	MGCR	MGCR	MGCR TENTATIVE PROTOTYPE	MGCR PRELIMIN. DESIGN	WKNL PORTABLE POWER PLANT	S&P TEST FACILITY	ML-1	ML-1	GTTF AT FT. BELVOIR
2		OWNER			AEC	DANIELS	AEC	AEC	AEC	AEC	AEC	AEC	AEC	AEC	AEC	AEC	AEC	ARMY ENGINEERS	ABC	ABC	ARMY ENGINEERS
3		USE	EL. POWER GENERATION	EL. POWER GENERATION	EL. POWER GENERATION AND BREEDING	EL. POWER GENERATION AND BREEDING	EL. POWER GENERATION	EL. POWER GENERATION	TANKER PROPULSION	TANKER PROPULSION	EL. POWER GENERATION	SHIP PROPULSION	SHIP PROPULSION	SHIP PROPULSION	SHIP PROPULSION	SHIP PROPULSION	ARMY PORTABLE POWER PLANT	GAS TURB. TEST FACILITY	ARMY MOBILE POWER PL.	ARMY MOBILE POWER PL.	GAS TURB. TEST FACILITY
4		STATUS	STUDY 1954	STUDY 1954	STUDY 1964	STUDY 1956	STUDY 1956	STUDY 1956/57	STUDY 1957	STUDY 1957	STUDY 1957/58	STUDY 1958	STUDY 1958	STUDY 1958	STUDY 1959	PREL. DESIGN COMPL. 1960	STUDY 1955	STUDY 1957	IN TURBO TEST	MACHINERY STAGE	IN OPERAT. SINCE 1959
5		DESIGNER	GALLAGHER (AM. LOC. CO.)	GALLAGHER (AM. LOC. CO.)	ROBINSON CYCLE	DANIELS	STUDEBAKER PACKARD CORP.	FORD INSTRUMENT CO.	FORD INST. COMPANY	GENERAL MOTORS CORP.	LOS ALAMOS SCIENT. LAB.	GENERAL	DYNAMICS CORP. -		G.A. & EL. BOAT DIV.	WALTER KIDDE NUCL. LAB.	SANDERSON & PORTER	AEROJET - GEN. NUCLEONICS			
6		TOTAL THERM. POWER	2 MW	7 MW	149.6 MW	20 MW	60 MW	44 MW	64 MW	55 MW	66 MW	50 MW	46 MW	45 MW	54.2 MW		1.112 MW		3.3 MW	3.3 MW	
7		TOTAL NET POWER	0.2 MW	2 MW	60 MW	5 MW	15 MW	15 MW	22000 shp	22000 shp	20 MW	20000 shp	20000 shp	20000 shp	22000 shp	32000 shp	0.125 MW	0.4 MW	0.33 MW	0.33 MW	0.4 MW
8		PLANT EFFICIENCY	10.2%	28.6%	40.1%	25%	25%	34%	25.7%	29.8%	30.3%	30.0%	32.5%	33.1%	30.3%		11.2%	16%	10.0%	10.0%	
9		CYCLE	DIRECT OPEN	DIRECT CLOSED	DIRECT CLOSED	INDIRECT CLOSED	INDIRECT OPEN	DIRECT CLOSED	DIRECT CLOSED	DIRECT CLOSED	DIRECT CLOSED	DIRECT CLOSED	DIRECT CLOSED	DIRECT CLOSED	DIRECT CLOSED	DIRECT CLOSED	DIRECT CLOSED	DIRECT CLOSED	DIRECT CLOSED	DIRECT CLOSED	INDIRECT CLOSED
10		GAS	AIR	N_2	He	He/AIR	He/AIR	N_2	He	He	N_2	He	CO_2	CO_2	He	He	He	N_2	N_2+0.5% O_2	N_2+0.5% O_2	COMB. GASES / N_2
11		NUMBER OF PRIME MOVERS	1	1	1	1	3 SECTIONALIZED AND INTERCONNECTED	1	1	1	1	1	1	1	1	1	1	1	1	1	1
12		MANUFACT. OF TURBINE	SOLAR, JUPITER T-520	ESCH. WYSS TU-CO 52	ESCH. WYSS (NORDBERG CO.)		STUDEBAKER PACKARD	ESCHER WYSS (NORDBERG CO.)	ESCH. WYSS (NORDBERG CO.)		ESCH. WYSS	WESTINGHOUSE ELECTRIC CORPORATION					CLARK BROS. CO.	ESCH. WYSS DESIGN	CLARK BROS. CO.	STRATOS OF FAIRCHILD CORP.	DIVISION OF
13		SHAFT ARRGT.	SINGLE	SINGLE	TWO-SHAFT LPT FREE	SINGLE	TWO-SHAFT LPT FREE	SINGLE	SINGLE	TWO-SHAFT	SINGLE	TWO-SHAFT LPT FREE	TWO-SHAFT LPT FREE	TWO-SHAFT LPT FREE	TWO-SHAFT LPT FREE	TWO-SHAFT HPT FREE	SINGLE	SINGLE	SINGLE	SINGLE	SINGLE
14		MASS FLOW lb/sec	8.25	54	219.4	130.5	104 PER SET	305.6	131.7	81.9	411	74.6	327.5	284.9	72.8	112	2.844	18.5	COMB 28.3 TURB 26.0	26.0 25.3	16.6
15	LPC	INLET PRESS. psia	14.6	~119	426	110	14.4	125	300	362		385	167	333	308	445	105	76	116.2	118.2	68.6
16	"	INLET TEMP. °F	75		90	72	80	90	90	100	90	100	100	100		85	120	100	132.9	133.7	100
17	"	OUTLET PRESS. psia	64.7	396	661	420	78.6		600	3 COMPRESS. IN SERIES		624	368	739	524	690	165		321.3	322.8	188.5
18	"	OUTLET TEMP. °F			210	244	465		295			239	224	228		206			369.7	368.4	
19	"	TYPE AND NO. OF STAGES	AXIAL-10	RADIAL-3	AXIAL-10		AXIAL-8 TRANSONIC					AXIAL-14	AXIAL-6	AXIAL-6	AXIAL-17	AXIAL-15	RADIAL-5		AXIAL-11	RADIAL-2	RADIAL-2
20	"	ISENTROPIC EFFICIENCY			88%		86%	86%				85.2%	83.6%	82.6%			75%				
21	"	SPEED RPM	20000	12750	11600							15000	10500	18750	12200	12000	15000	18000	22000	18000	18000
22	HPC	INLET PRESS. psia	—	—	656	—	—		—			616	362	721	519	680	—		—	—	—
23	"	INLET TEMP. °F	—	—	90	—	—		—		90	100	100	100		85	—		—	—	—
24	"	OUTLET PRESS. psia	—	—	1015	—	—	535	—	1000	530	1000	1000	2000	800	1155	—	210	—	—	—
25	"	OUTLET TEMP. °F	—	—	210	—	—	235	—	196		239	268	269		236	—	329	—	—	—
26	"	TYPE AND NO. OF STAGES	—	—	AXIAL-10	—	—		—			AXIAL-18	AXIAL-9	AXIAL-10	AXIAL-21	AXIAL-25	—		—	—	—
27	"	ISENTROPIC EFFICIENCY	—	—	88%	—	—	86%	—			85.2%	84.1%	83.6%			—		—	—	—
28	"	SPEED RPM	—	—	11600	—	—		—			15000	10500	18750	12200	12000	—	18000	—	—	—
29	HPT	INLET PRESS. psia	62.8	384	985	400	74.2	510	578	962	520	923	851	1764		1080	161	203	290.4	291.8	183
30	"	INLET TEMP. °F	1325	1220	1400	1250	1400	1300	1150	1300	1300	1300	1300	1300	1300	1300	1150	1150	1193.5	1193.5	1150
31	"	OUTLET PRESS. psia	15	120	665		28.8	130		552		554	373	852		820	106.2		120	122	71.5
32	"	OUTLET TEMP. °F	878	829	1160	794	1053	820	835			1008	1106	1123		1120	952.5	844	899.2	907.8	848
33	"	TYPE AND NO. OF STAGES	AXIAL-3	AXIAL-5	AXIAL-6		AXIAL-2					AXIAL-7	AXIAL-3	AXIAL-2	AXIAL-7	AXIAL-9	AXIAL-4		AXIAL-2	AXIAL-2	AXIAL-2
34	"	ISENTROPIC EFFICIENCY			89%		87%	89%				89.8%	89.8%	88.7%			80%				
35	"	SPEED RPM	20000	12750	11600							15000	10500	18750	12200	8140	15000	18000	22000	18000	18000
36	LPT	INLET PRESS. psia	—	—	665	—	28.7	—	—	552	—	554	373	852		814	—	—	—	—	—
37	"	INLET TEMP. °F	—	—	1160	—	1053	—	—	997	—	1008	1106	1123		1110	—	—	—	—	—
38	"	OUTLET PRESS. psia	—	—	440	—	15.3	—	—		—	404	179	367		460	—	—	—	—	—
39	"	OUTLET TEMP. °F	—	—	942	—	852	—	—	832	—	852	948	940		825	—	—	—	—	—
40	"	TYPE AND NO. OF STAGES	—	—	AXIAL-15	—	AXIAL-3	—	—		—	AXIAL-5	AXIAL-2	AXIAL-2	AXIAL-6	AXIAL-7	—	—	—	—	—
41	"	ISENTROPIC EFFICIENCY	—	—	89%	—	87%	—	—		—	87.2%	84.3%	84.0%			—	—	—	—	—
42	"	SPEED RPM	—	—	3600	—		—	—		—	10000	8000	15900	8000	12000	—	—	—	—	—
43		TOTAL COMPR. RATIO	4.43	3.30	2.38	3.82	5.45	4.28	2.00	2.76		2.60	6.00	6.01	2.62	2.60	1.57	2.76	2.77	2.73	2.75
44		TOTAL EXPANS. RATIO	4.19	3.20	2.24		4.86	3.92				2.28	4.75	4.81	2.38	2.35	1.52		2.42	2.39	2.56
45		WEIGHT lb CT. MACHINE	854									35500	38300	32000	35200				2000	3450	
46		SIZE L x W x H in.	75x32x42									299 LONG	252 LONG	245 LONG	360 LONG x 96 DIA.						
47		HEAT EXCHANGERS	R	PC, IC, R	PC, IC, R	PHE, PC, IC, R	PHE (η=87.7%), PC, IC, R		PC, R	PC, IC, R	PC, IC, R	PC, IC, R	PC, IC, R	PC, IC, R	PC, IC, R	PC, IC, R	PC, R	PC, R	PC, R	PC, R	PC, R
48		RECUPER. EFFECTIVENESS			92%		72%	90%			80%	90%	90%	90%	90%						
49		REFERENCES	13, 56, 57	13, 56, 57	53, 57	53, 56	58	59	53	53	60	1, 55	1, 55	1, 59	61	Sheets 4/1, 6/2	48	53	Sheets 4/4, 6/4, 6/5	62, Sheets 6/4, 6/5	62, Sheets 6/4, 6/5

PC - PRECOOLER, IC - INTERCOOLER, R - RECUPERATOR, PHE - PRIMARY HEAT EXCHANGER

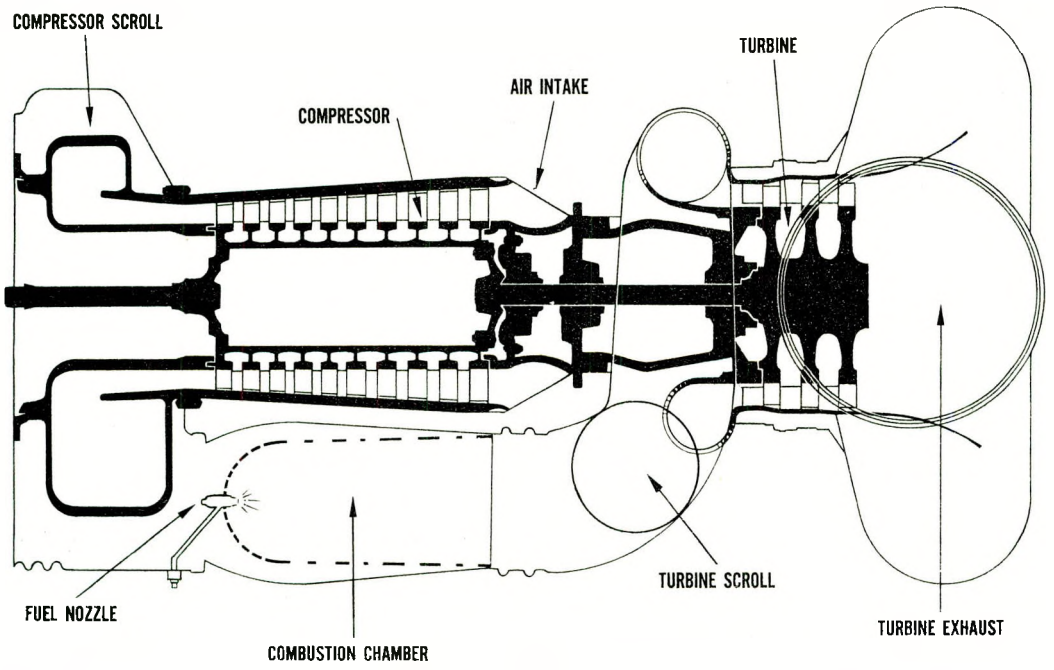


Fig. 3-6 - Solar Aircraft Co. - Jupiter T-520 Turbo-Compressor Set

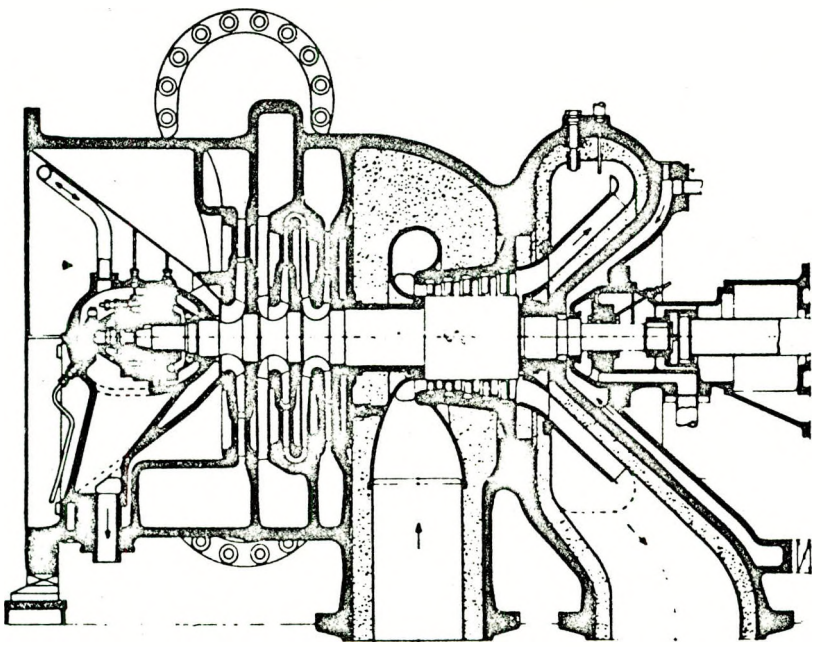


Fig. 3-7 - Escher Wyss TUCO 52 2000-kw Closed-Cycle Turbo-Compressor Set

Manufacturing Co., was an adviser. The power system was designed by S. T. Robinson and R. Bennenati of Sanderson and Porter Co., N. Y. This design was preceded by a smaller system designed by a group headed by J. G. Gallagher, ORSORT, 1953. The same cycle, was analyzed by The American Turbine Corporation in a separate design study. A flow diagram of the system is shown in Figure 3-8[56]. Figure 3-9[63] shows the cycle in the T-S diagram, Figure 3-10[63], the general arrangement of the proposed power plant and Figure 3-11[64], the turbomachinery set. The turbine-compressor set and the turbine-generator set are located above ground in the open air. The remainder of the equipment is located below ground level for shielding purposes. The activity of the gas stream is kept to such a level that turbines and compressors need not be shielded. This is accomplished by bleeding off about 1% of the working medium from the outlet of the compressor, sending it through a liquid nitrogen cold trap and putting it back through the regenerator to the inlet of the compressor set. In the cold trap any volatile fission products are condensed that may excape from the fuel elements. This purification system causes a very small loss in station efficiency, approximately 1/4 of one per cent[56].

Fluid mechanics and gas dynamics, upon which turbomachinery design is based, are founded upon the concepts of perfect fluid, potential flow, and real fluid corrections to this flow. Both theoretical and experimental developments of the science are expressed in terms of kinematic non-dimensional parameters and such non-dimensional groups as Reynolds number and Mach number. Therefore, if the effects of these non-dimensional variables are properly applied, much of the existing work on turbo-machinery for air can be used for the design of units for another gas such as helium.

The use of helium as a working fluid results in two major changes, one advantageous and one disadvantageous. The fact that the sonic velocity in helium is about three times that in air results in practical release from Mach number (compressibility) restrictions.

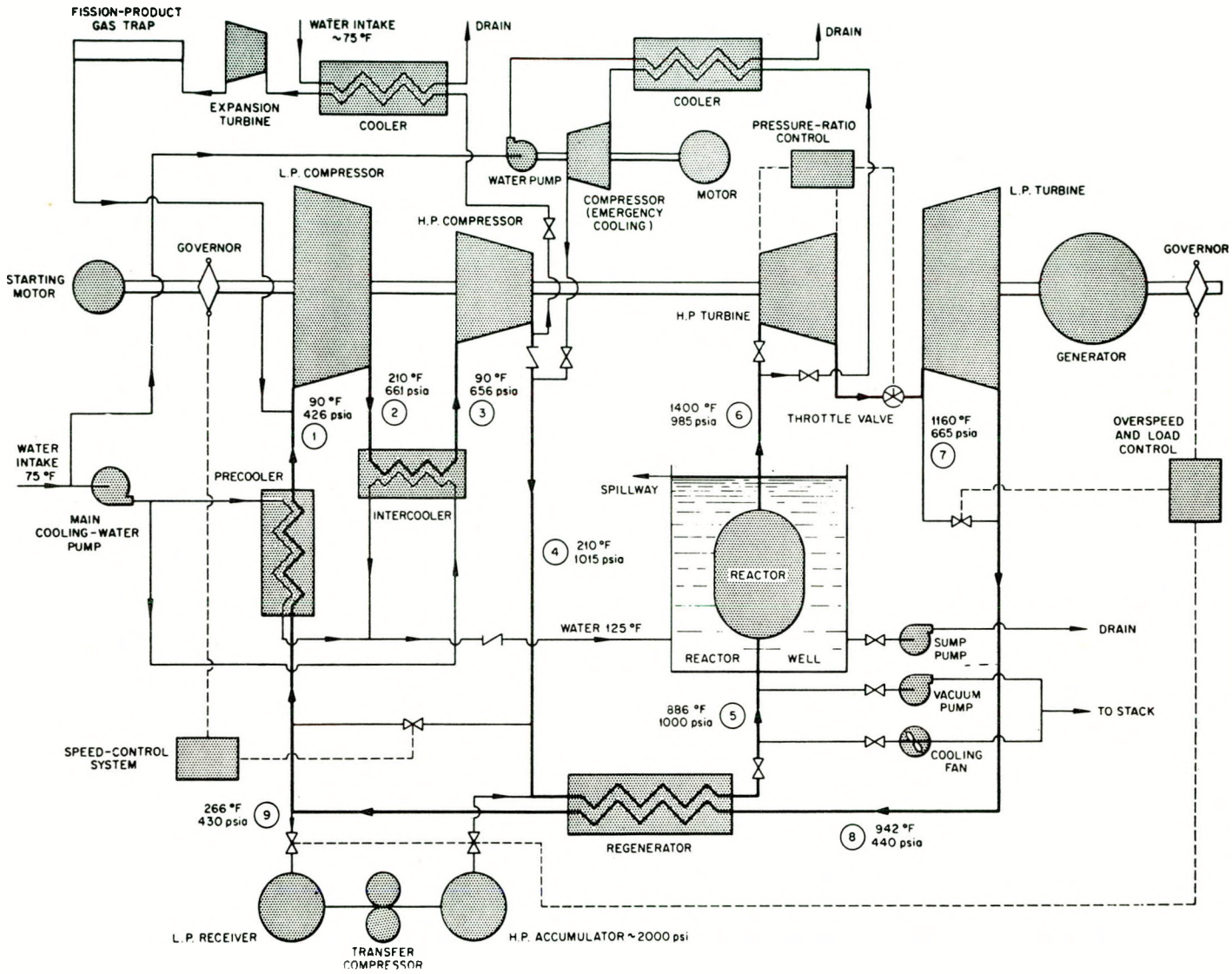


Fig. 3-8 - System Flow Sheet Ceramic Power Breeder Reactor

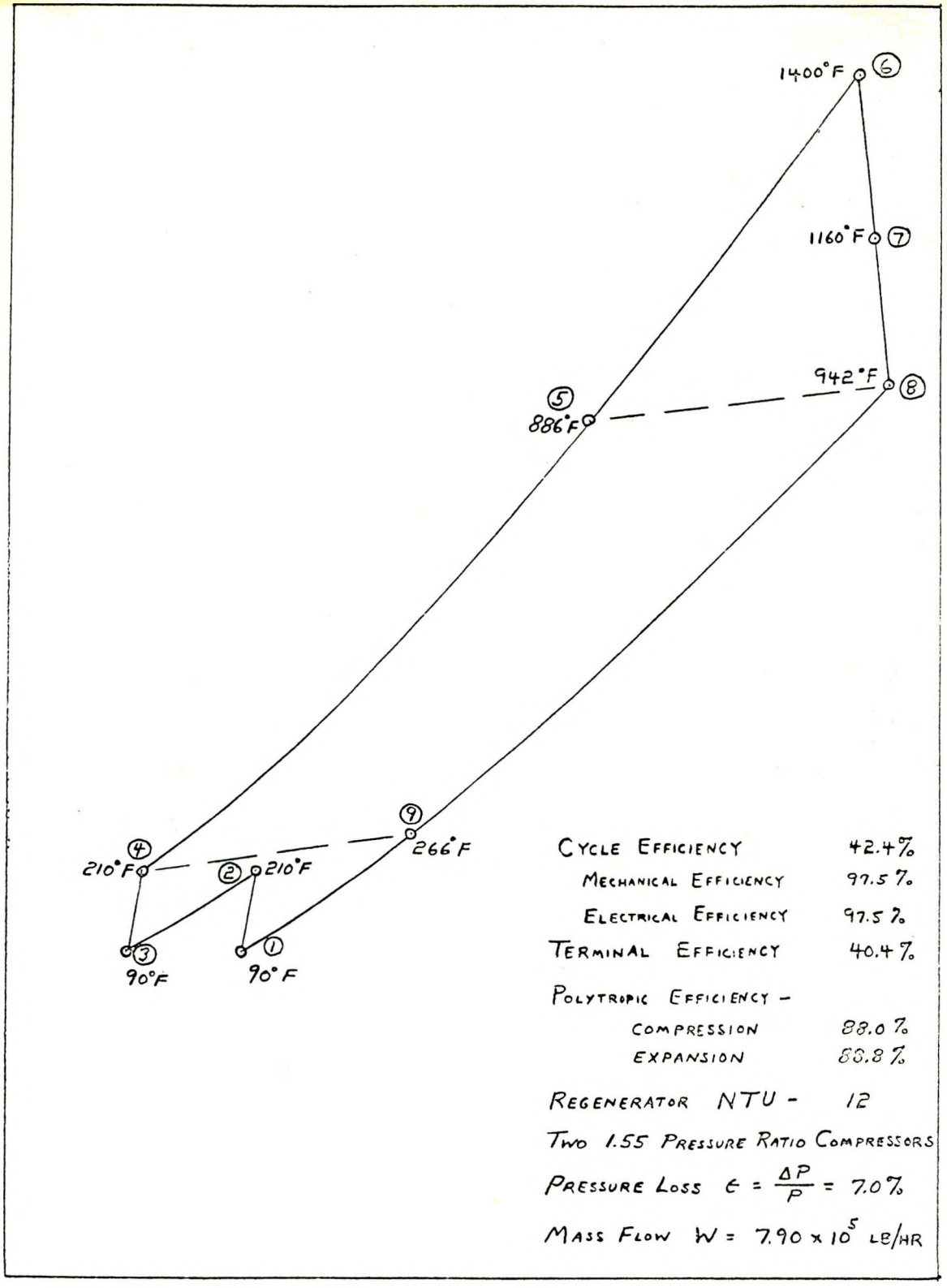


Fig. 3-9 - Cycle T-S Diagram of ORSORT Ceramic Breeder Reactor

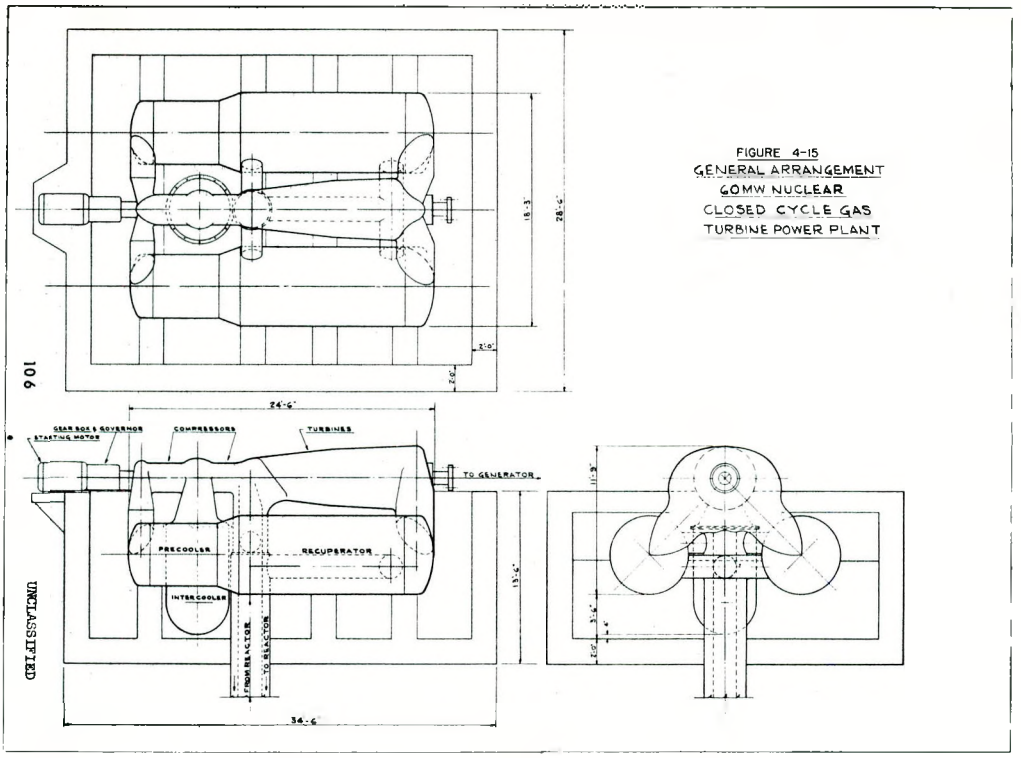


Fig. 3-10 - General Arrangement of 60 Mw Nuclear Closed Cycle Gas Turbine Power Plant

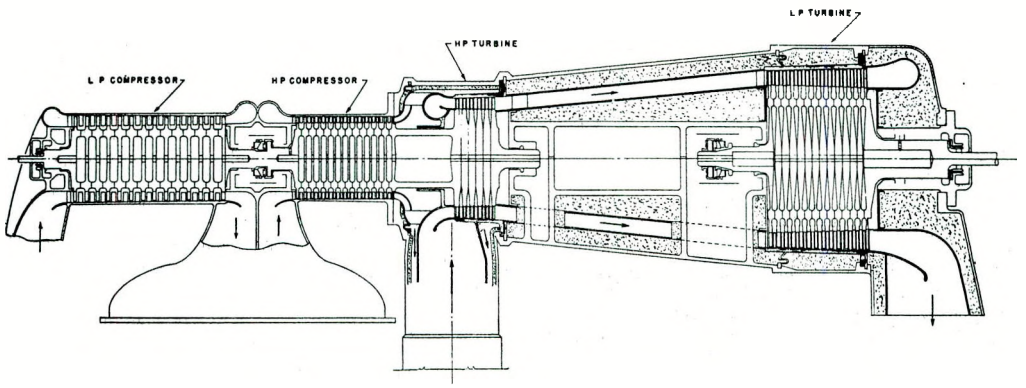


Fig. 3-11 - Section Through Machinery Set of ORSORT Ceramic Breeder Reactor

Therefore, tip speeds are limited only by structural considerations. On the debit side, the high c_p of helium (about 1.25 against 0.24 for air) results in a temperature rise per stage of only one-fifth that of air for the same blading diagram and enthalpy input per stage ($c_p \Delta T$).

In spite of the low ΔT per stage, the required number of stages as compared to present day air practice is low. This is because of the overall optimum pressure and temperature ratios for the nuclear helium plant. Thus, the resulting mechanical design of a nuclear helium machine bears a close resemblance to its air counterpart[63]. In order to give the proposed 60 Mw machine performance a strong foundation in reality, blading and proportions of the set have been closely patterned on an existing successfully tested research compressor and on a successful turbine. Tip speeds, solidity ratios, and blade diagrams are essentially identical to those of the test machines. Hub-tip diameter ratios are made similar to those of the models (except where modifications are needed to match speed and volume flow of the helium machine).

The compressor and turbine were designed for and tested in air, with air Mach number limitations being an important factor. The helium design is so closely patterned on the air machine that no attempt was made to take advantage of the release from Mach number limitations. Hence, there should be a slight unaccounted-for performance bonus, which follows the conservative design pattern adopted for this unit with the idea of providing as nearly guaranteed performance as possible in the preliminary design of an unconventional machine.

When considering helium as a real frictional fluid capable of separation from boundary walls in an adverse pressure gradient, the question of being able to maintain the same blade velocity diagram without flow separation arises. The answer is that for a given velocity diagram, the ability to resist separation is directly proportional to a fractional power of the Reynolds number ($Re^{\frac{1}{n}}$). Now $Re = uL/\nu$ and we assume u is the same for air and helium machines, then

$$\frac{L}{\upsilon_{helium}} \geq \frac{L}{\upsilon_{air}}$$

if we expect to utilize the same velocity diagram. Since υ takes values in the helium machine roughly 1/3 of that for the usual air machine then the characteristic length, say, blade chord, must be at least 1/3 that of a comparable air plant. This condition is greatly exceeded with the result that this 60 Mw plant operates with a Reynolds number higher than the test machines and, therefore, can be expected to equal or exceed the test efficiency, if all other factors are equal[63].

Daniels Breeding Cycle Power Plant

Figure 3-12[56] shows the power plant flow diagram, and Figure 3-13[65] a section of the plant. The proposal emphasizes the use of an intermediate heat exchanger. Daniels pointed out that much higher efficiency could be obtained using refractory metal turbines in future power plants[56]. A 5 Mw nuclear turbine was fully designed at that time as a closed cycle unit and could be delivered by Escher Wyss within 18 months.

Studebaker Packard Corporation Nuclear Power Plant

This study has been based on the use of a nuclear reactor to supply heat to an open-cycle gas turbine. The gas turbine, and its heat exchangers, uses conventional gas turbine materials operating under conditions (turbine inlet temperature 1400°F) which are presently attainable. This indirect open-cycle nuclear gas turbine is able to operate with relatively good efficiency (28 to 30%) over the operating range from one-fourth to full power, and requires no supply of water for cooling purposes. The reactor itself uses helium as a coolant in the primary loop.

The off-design (part load) operation of the gas turbine results in poor performance because the cycle must be operated at reduced turbine temperatures and under off-design operating conditions for the various components. There are two standard ways of handling this problem.

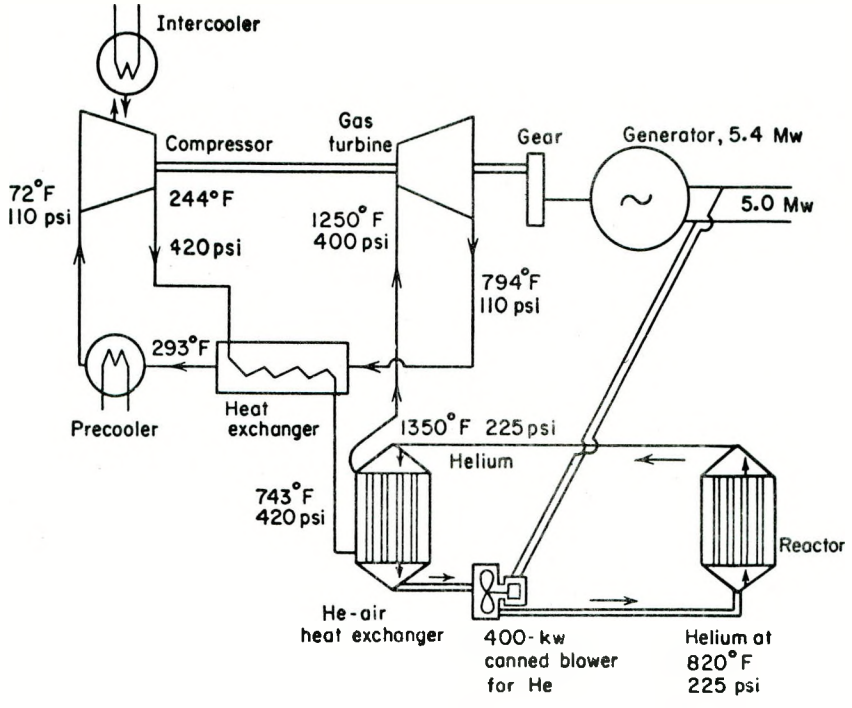


Fig. 3-12 - Power Plant Flow Diagram - Small Gas-Turbine Cycle Reactor

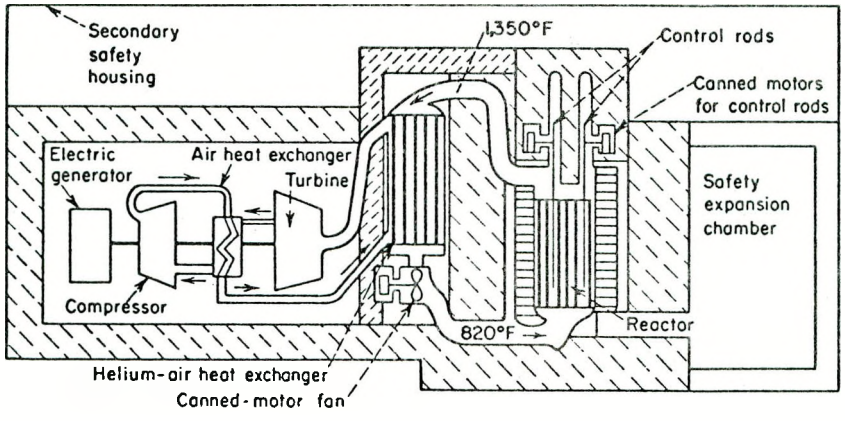


Fig. 3-13 - Profile of the 5-Mw Closed-Cycle Daniels Breeding Reactor

One is by use of a closed cycle in which the output is varied by varying the density of the gaseous power medium in the cycle. Studebaker-Packard chose not to use this method because of the requirement which it imposes for a large supply of cooling water into which to dump waste heat from the cycle. It was rather decided to use three parallel gas turbine power plants, any number of which can be operated simultaneously to satisfy given conditions of loading, thus operating reasonably close to optimum design conditions.

An alternative power plant, actually an adaptation of the one considered here, would allow a high temperature of operation, and hence, a higher efficiency, if certain component developments can be carried out. In this power plant, a high temperature turbine is placed directly in the inert-gas, reactor-cooling, stream. This turbine is built from graphite or other high temperature material, such as a high strength alloy of molybdenum. The exhaust heat from this high temperature turbine is used by the intermediate heat exchanger to heat air in the air-turbine cycle. The materials for such a high-temperature cycle are not now available[58].

The arrangement of the three-turbine power plant is partly shown in Figure 3-14[58]. An enlarged detail of the machinery is shown in Figure 3-15. The flow diagram is given in Figure 3-16[58]. The gas-turbine plant used for this study was scaled as directly as possible from a Packard designed 10,000 hp marine-propulsion power plant designated MGT-10. This plant has the same general requirement of high thermodynamic efficiency over a wide range of performance as is required for the stationary power plant for this investigation. The helium circulator and helium-air heat exchanger required new designs. The power plant is composed of three independent units (each having a compressor, a turbine, and a recuperator) operating in parallel. The compressor is an eight-stage, axial flow machine based on an NACA transonic compressor. The turbine consists of two parts, one coupled to the compressor, the other to the external power plant load. The compressor turbine has two axial stages, the power turbine three[58] (see also Table 3-6).

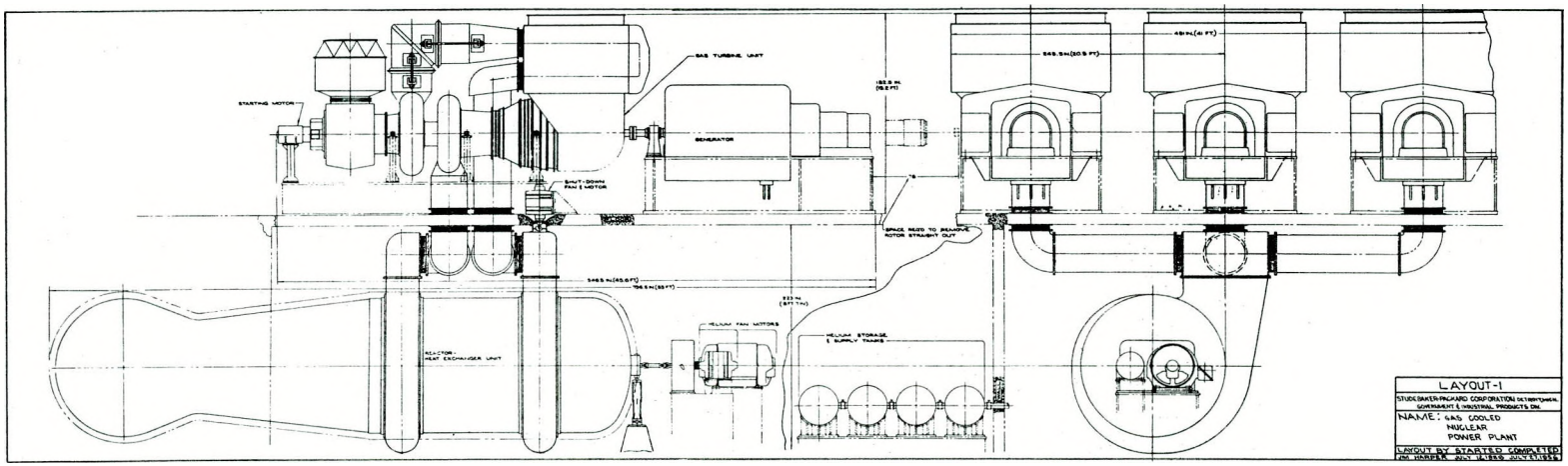


Fig. 3-14 - Arrangement of Three-Turbine Power Plant (Studebaker-Packard)

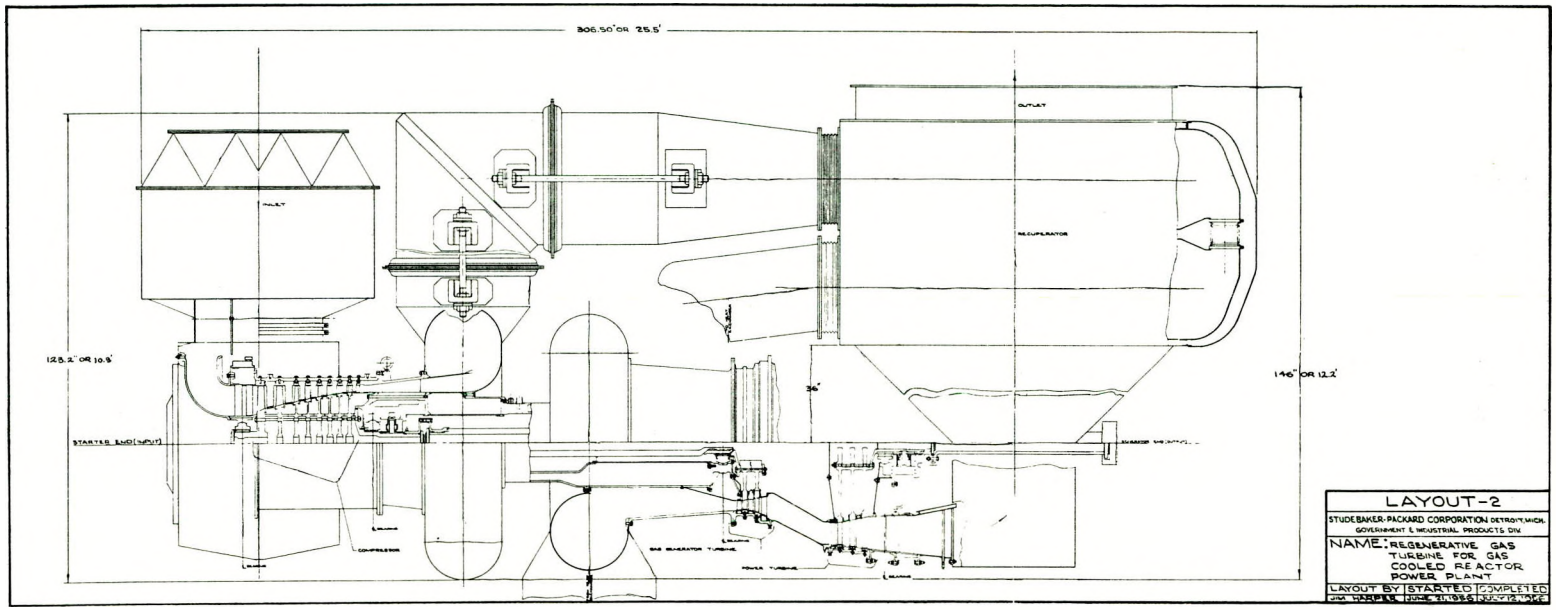


Fig. 3-15 - Detail of Machinery (Studebaker-Packard)

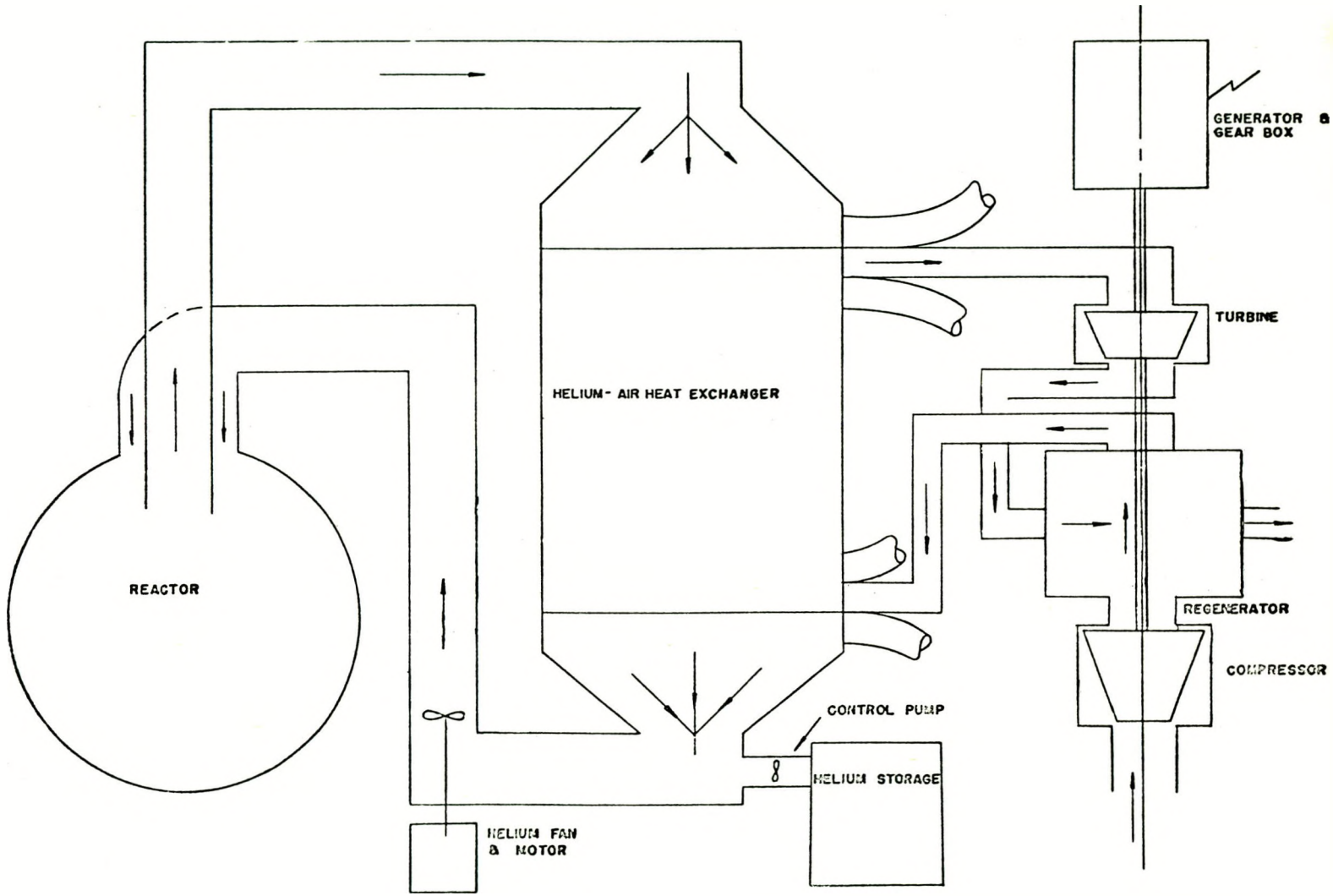
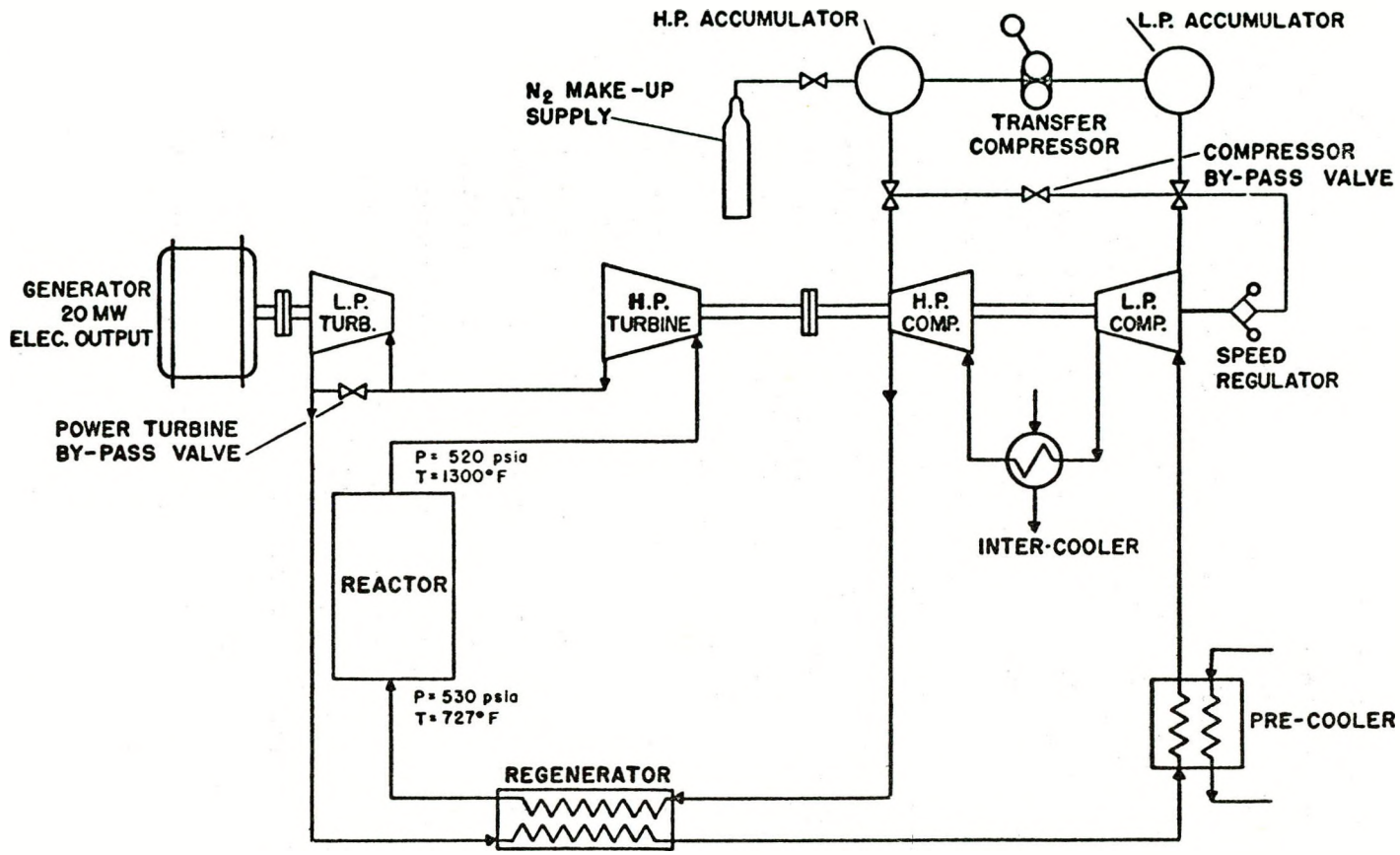


Fig. 3-16 - Flow Diagram of Studebaker-Packard Power System

Turret Experimental Nuclear Power Plant

A nitrogen-cooled graphite-moderated nuclear reactor experiment is proposed to drive a closed-cycle gas turbine power plant at 1300°F[60]. The indicated compatibility of graphite with nitrogen coolant allows the use of presently existing air turbine-compressor equipment instead of waiting for the development of helium turbomachinery. The prime mover chosen for purposes of this study is an Escher-Wyss plant of 20 Mw electrical capacity. The turbine consists of a two-stage compressor with intercooler driven by a high-pressure turbine and, on a separate shaft, a low-pressure turbine driving the useful generator load. A schematic diagram of the cycle is given in Figure 3-17[66].

Studies indicate that the power cycle is relatively unaffected by the nature of the working fluid[2,67]. Helium, nitrogen and carbon dioxide have all been shown to be usable with only minor variations in cycle efficiency, assuming of course, that turbomachinery and heat exchangers are properly designed for the working fluid selected. The many papers on this subject usually select helium for the working fluid because of its low neutron cross section and inert nature[54]. These characteristics are postulated to ease the reactor design problems. Nitrogen has been selected as the working fluid for other reasons, it eases turbomachinery design problems. Air-cycle machinery operating today is suitable for use with nitrogen and could be adapted to the Turret reactor with a minimum of delay and development expense. The use of helium would reduce reactor control problems, would result in smaller heat-transfer equipment, and would produce a higher net cycle efficiency. It is expected that Turret reactors would adopt the helium cycle as soon as practical[60].



ELECTRICAL OUTPUT —20 MW
REACTOR OUTPUT —66 MW
N_2 FLOW RATE —1,480,000 LBS/HR
CYCLE EFFICIENCY —30.3%

Fig. 3-17 - Schematic Diagram of Closed-Cycle Gas Turbine Power Plant (Turret)

Walter Kidde Nuclear Laboratories Portable Nuclear Power Plant

The Walter Kidde study and proposed design calls for a gas-cooled nuclear reactor suitable for supplying 100 kw of electrical energy and 400 kw of heat to a distant early warning (DEW) radar station. The plant is designed for packaging in the continental United States, shipment by air to a remote base and erection on a permafrost site during the four-month summer construction season.

A flow diagram of the system is shown in Figure 3-18[68]. The main components in the gas cycle are the reactor, turbine, recuperator, water heater, helium cooler, and compressor (see Figure 3-19[68]). About 78 per cent of the turbine power is used to drive the compressor which is mounted on the same shaft. The remaining power is converted to electricity in a generator driven by the turbine through a gear train. An electrical dumping system is provided which automatically compensates for instantaneous changes in demand load by diverting excess power to a series of resistors.

3.3.2 ML-1

The ML-1, the first US direct-and closed-cycle gas-cooled nuclear power plant, has been under development for nearly six years. In such a system the gas, heated in the reactor core, is used to drive a turbine and is then recycled to the reactor. The turbine is coupled to the electrical generation system. Operation of a prototype of this power plant which will be known as the Mobile Low-Power Nuclear Power Plant No. 1 (ML-1), was scheduled for this year.

The ML-1, transportable in four packages totalling less than 38 tons, combines the gas cooled reactor system with a direct- and closed-cycle gas turbine-driven power conversion system. The plant will generate about 300 net kilowatts of electricity and when fully developed will operate at least one year at full power without refueling. The power plant is designed to be operable 12 hours after delivery at a site.

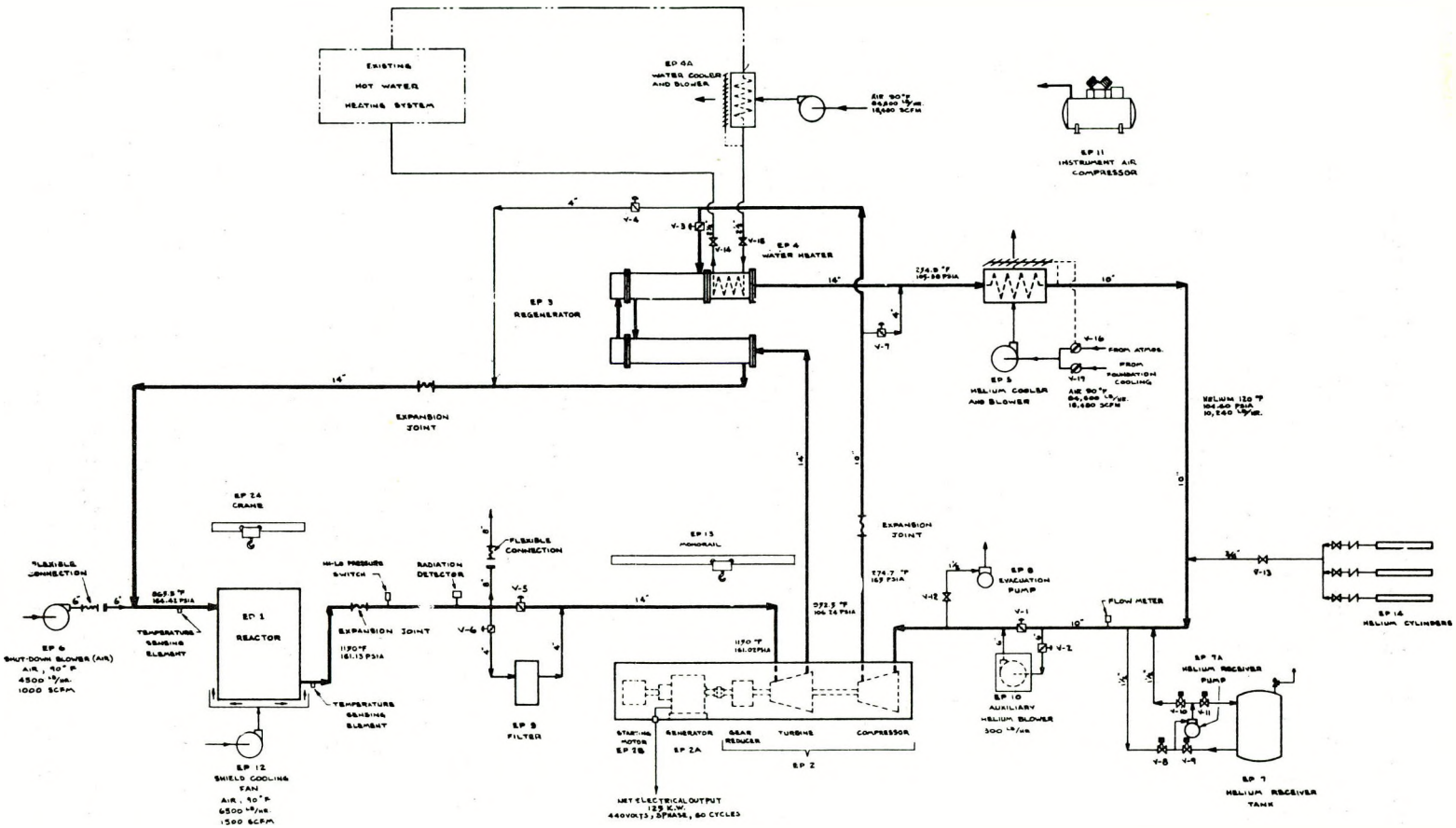


Fig. 3-18 - Flow Diagram of WKNL System

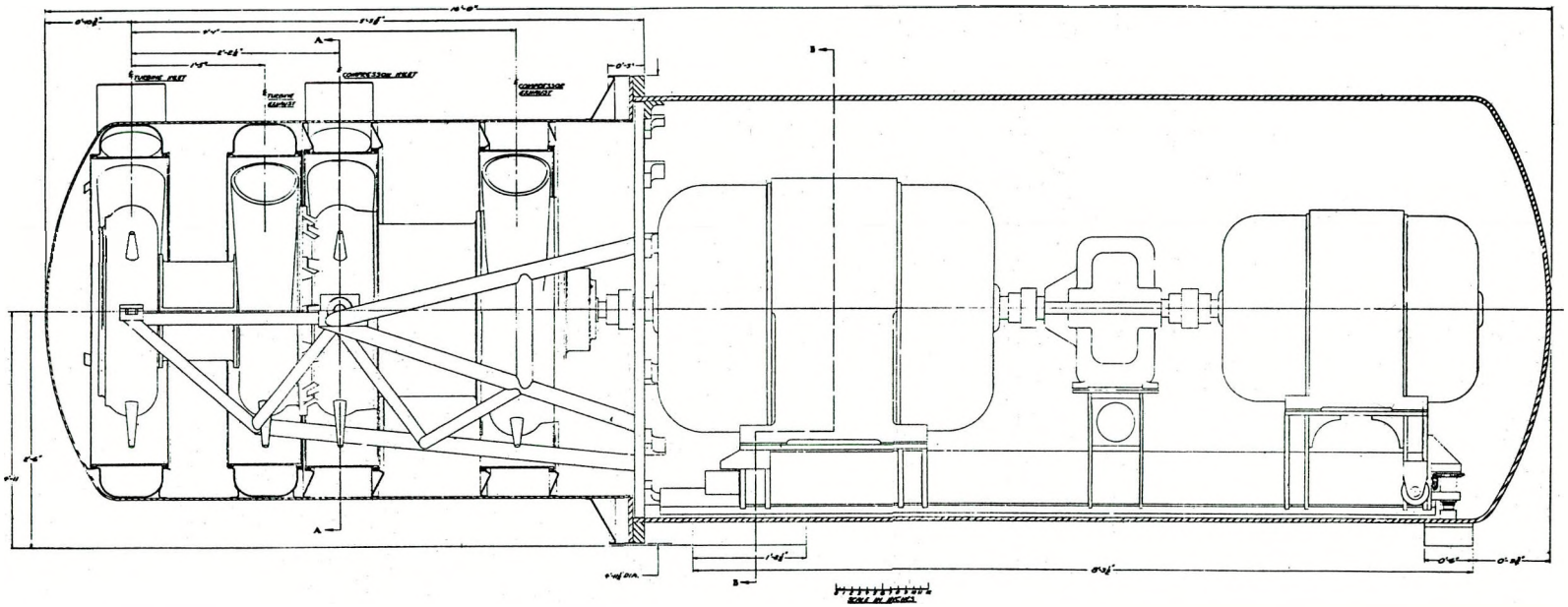


Fig. 3-19 - Helium Turbo-Compressor Set of WKNL System

Adequate shielding will permit relocation 24 hours after shut-down. Figure 3-20[69] shows a cutaway view of the power plant in perspective.

The power conversion skid supports and encloses the power conversion equipment during both operation and shipment. The three major items of equipment are the turbine-compressor set (T-C set) which includes a reduction gearbox, the alternator and starting motor, and the recuperator and precooler. The skid also contains a lubrication system for the T-C set and alternator, a vacuum pump for purging all interconnecting piping, including the control by-pass, and electrical switchgear. The general arrangement of equipment on the skid is shown in Figures 3-21 to 3-24[69].

The rotating equipment is located in-line and the outlet from the turbine is connected directly to the recuperator. The reduction gearbox is mounted to the compressor at the high-speed end, and the 500 kva alternator at the low-speed end. The gearbox also provides a drive for the lubricating oil pump. The recuperator is rigidly fixed to the structure of the skid floor on the vertical centerline of the rotating equipment. The alternator is mounted on sliding feet to accommodate thermal expansion. The equipment is self-supporting between alternator and recuperator. The precooler forms the roof of the skid (see Figure 3-22).

The general non-nuclear characteristics of the plant are listed in Table 3-7[12,62,69]. The T-C set includes a compressor, a gas turbine, and a reduction gearbox. Two types of T-C set are being developed for the ML-1, an axial flow set manufactured by Clark Bros. Co. and a radial flow set manufactured by Stratos Division, Fairchild-Stratos Corp. The rotational speed is 22,000 rpm for the axial flow set and 18,000 rpm for the radial flow set.

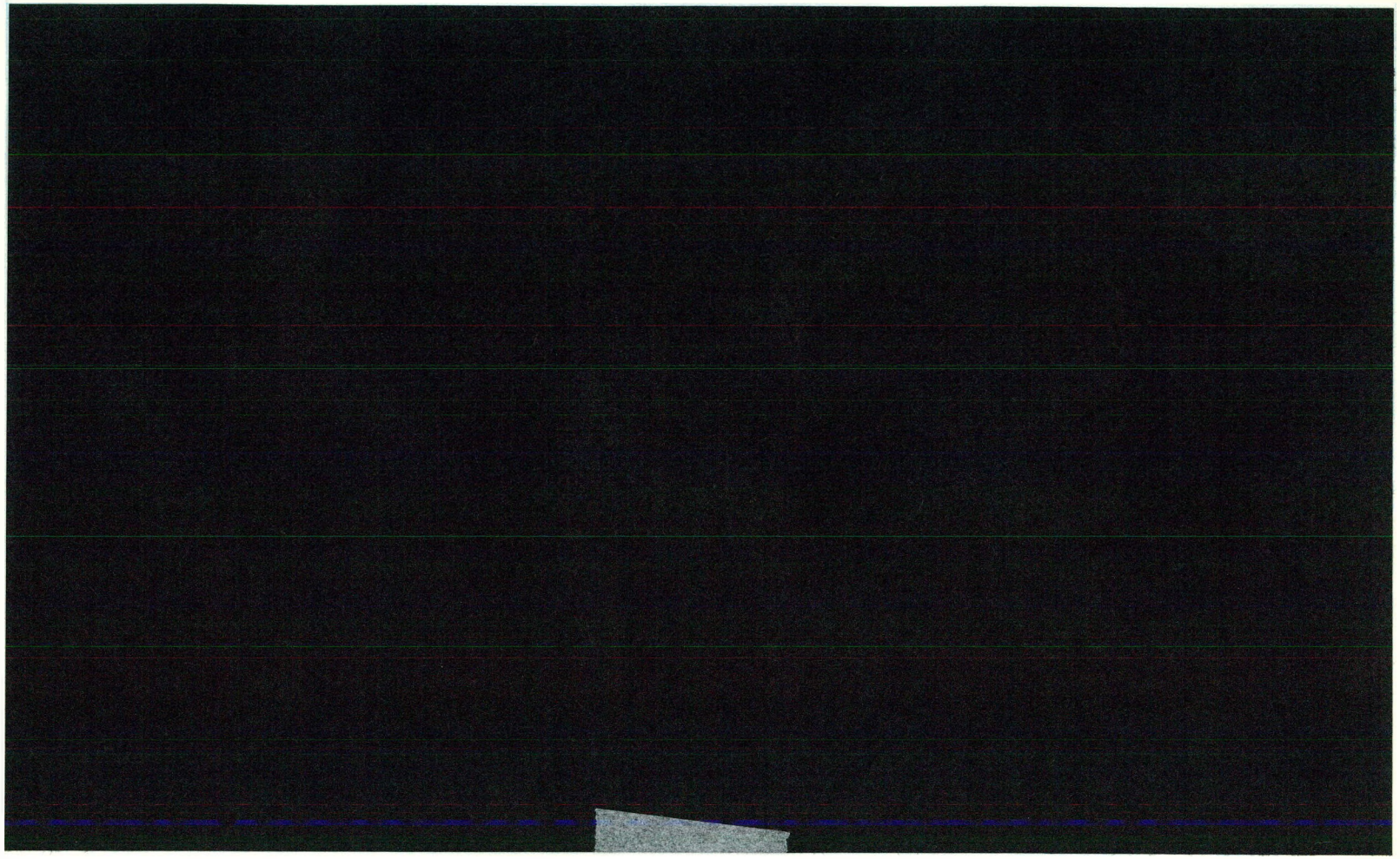


Fig. 3-20 - The ML-1 Power Plant

THE FRANKLIN INSTITUTE • Laboratories for Research and Development
I-A2352

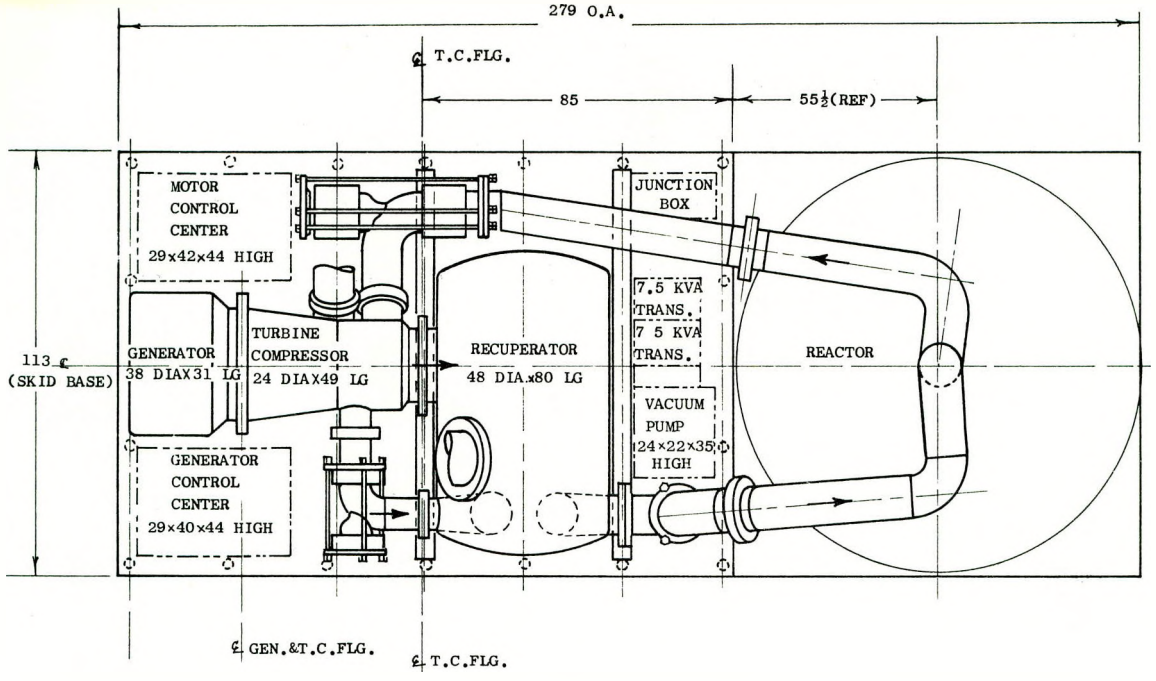


Fig. 3-21 - Arrangement of Equipment of the ML-1 Power Conversion Skid-Plan

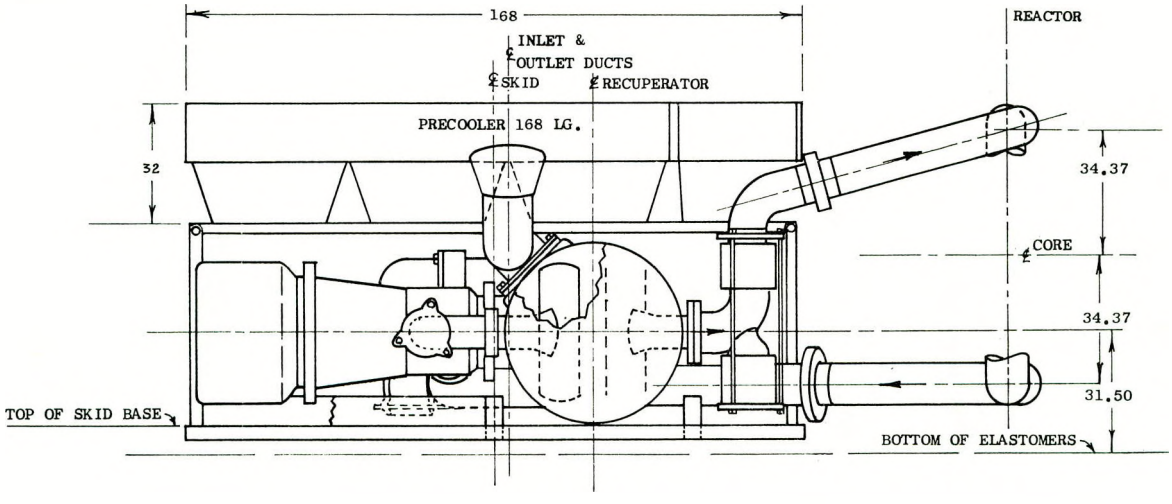


Fig. 3-22 - Arrangement of Equipment of the ML-1 Power Conversion Skid-Elevation

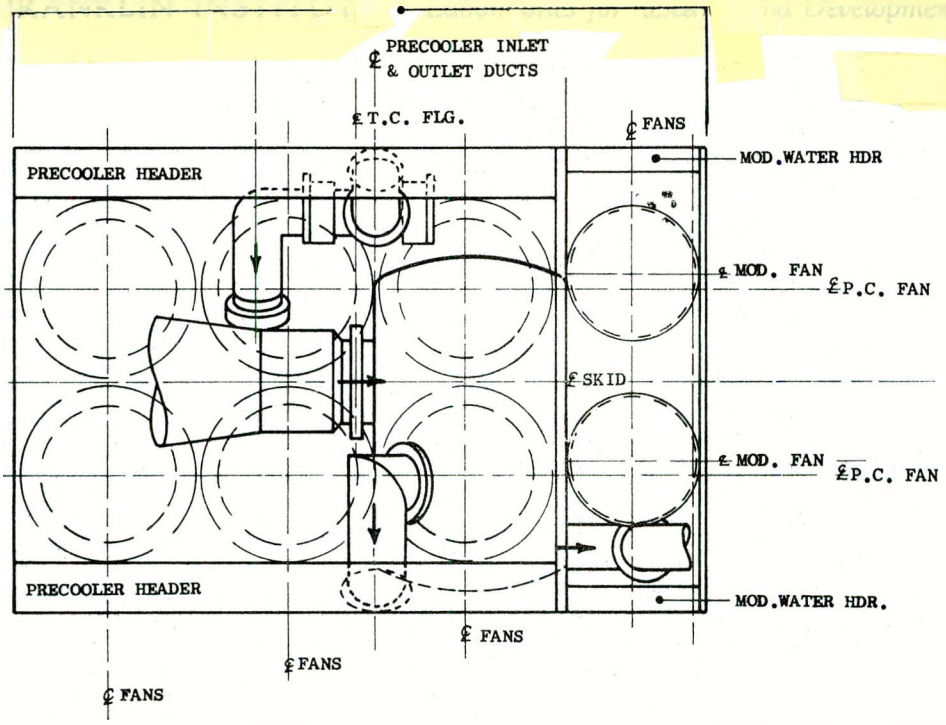


Fig. 3-23 - Arrangement of Equipment of the ML-1 Power Conversion Skid-Plan View of Precooler

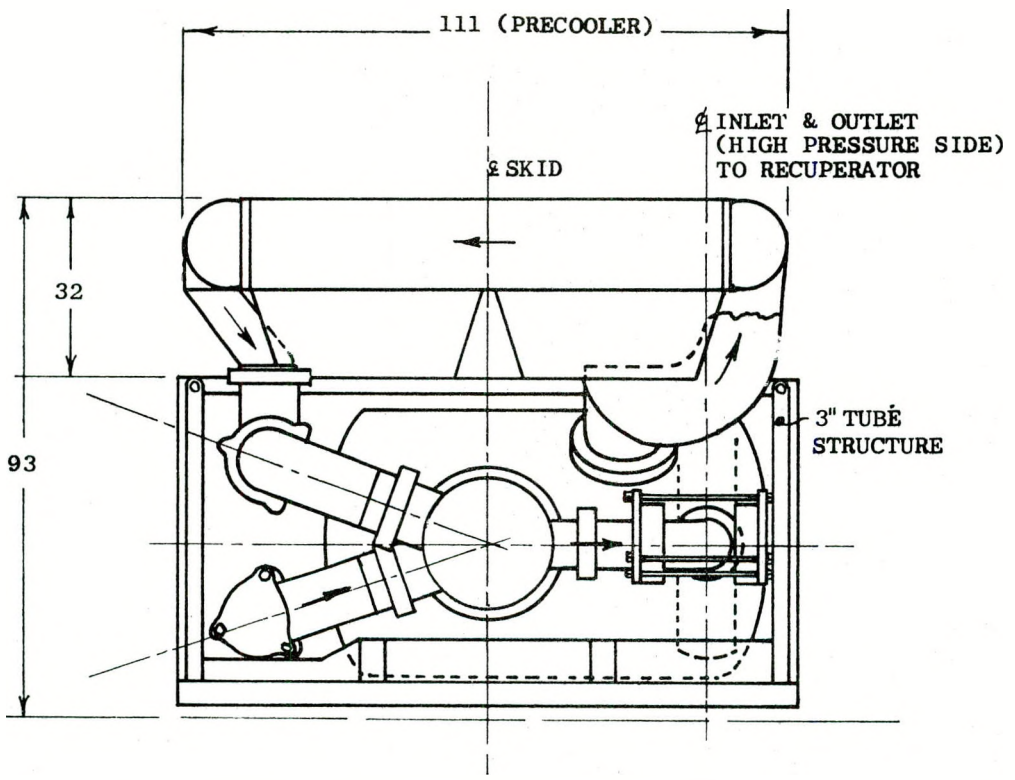


Fig. 3-24 - Arrangement of Equipment of the ML-1 Power Conversion Skid, View From Generator Side

(Generator, T-C Set, and Control Panels not shown)

Table 3-7

CHARACTERISTICS OF ML-1 PLANT

Design performance at 100°F		
Gross electrical output	400 kw	
Net electrical output	330 kw	
Reactor thermal power	2.9 Mw to gas; total - 3.3 Mw	
Cycle efficiency	13.8%	
Plant thermal efficiency	13.3%	
Coolant flow	92,000 lb/hr	
Working fluid	99.5 vol % N_2 + 0.5 vol % O_2	
Reactor inlet temperature	800°F nominal	
Reactor mixed-mean outlet temperature	1200°F max	
Maximum velocity	180 ft/sec	
Inlet pressure	315 psia (max.)	
Core Δp	15 psi	
Reactor Δp	22 psi	
Type of Cycle	Brayton cycle with regeneration	
Total volume of working fluid system	120 cu ft	
Total system working fluid inventory, full load at 100°F	52 lb	
Working fluid transit time	2.0 sec	
Cycle characteristics		
Ambient temperature	100°F	
Net power, kw	330	
Reactor inlet, °F	791	
Turbine inlet, °F	1200	
Compressor inlet °F	132	
Compressor inlet, psia	117	
Compressor outlet, psia	320	
Reactor inlet, psia	313	
Alternator Characteristics	60 Cycle Operation	50 Cycle Operation
Output		
Rating, kva	500	417
Voltage, volts	2400/4160	2000/3467
Rotor shaft speed, rpm	3600	3000
Case		
Diameter	40.6 inches	
Length	32.75 inches	
Weight	5500 lb	
Temperature, operating	275°F internal max (hot spot)	

pg 147 blank

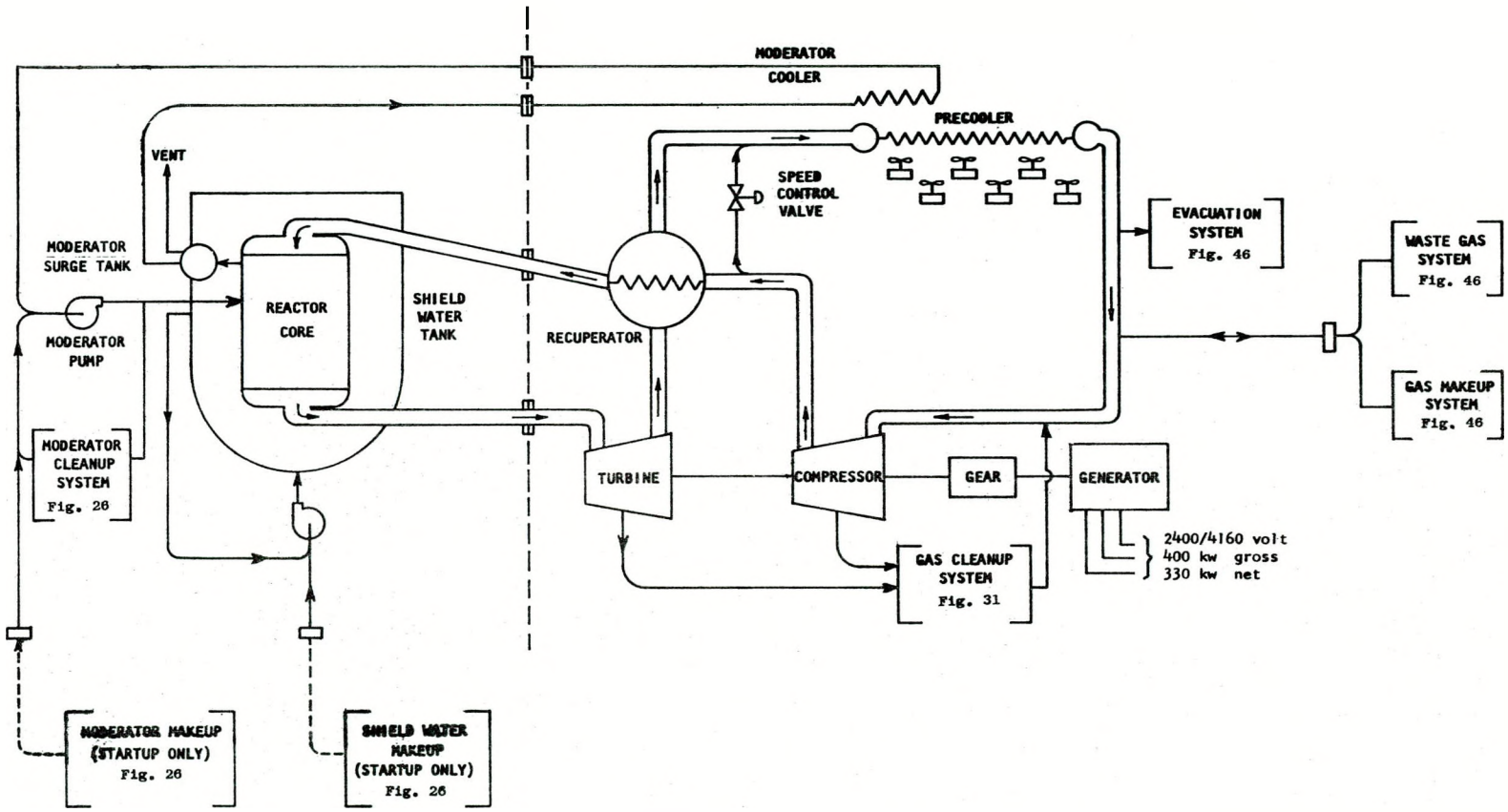
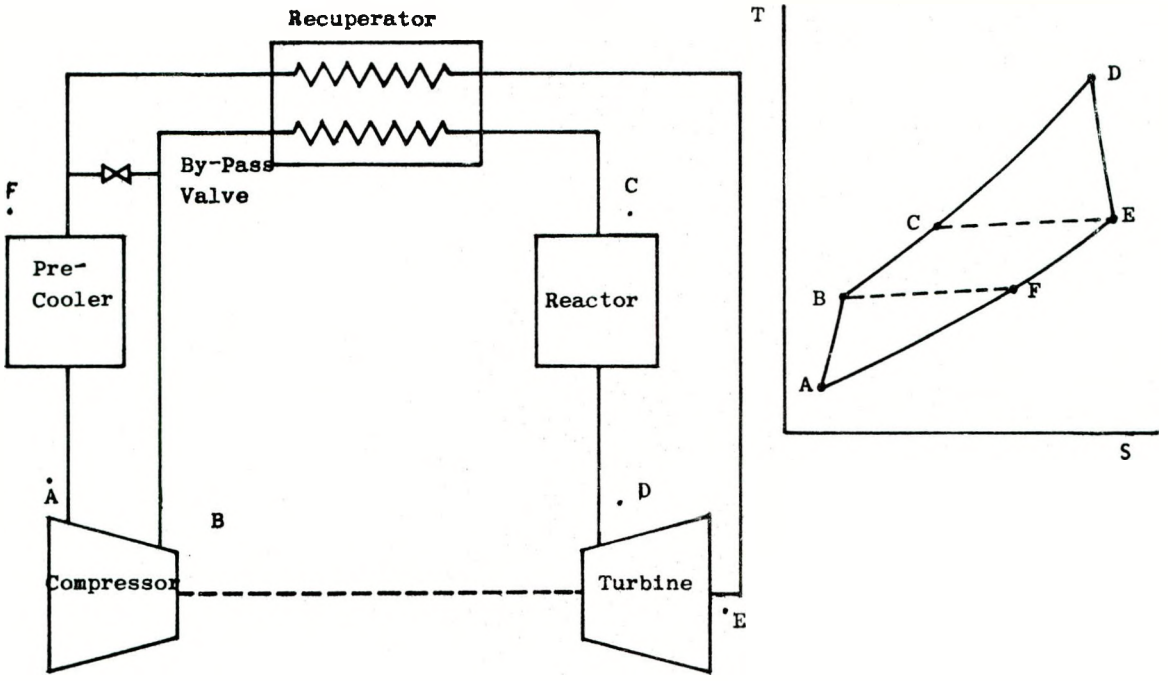


Fig. 3-25 - Simplified Flow Diagram for the ML-1

(Page 149 omitted)

page 149 blank



Ambient Temperature		125°F	100°F
kw		276	330
mass, lb		52	52
by-pass %		1	1
A	P, psia	123	117
	T, °F	156	132
B	P	321	320
	T	388	366
C	P	312	313
	T	819	791
D	P	292	289
	T	1200	1200
E	P	128	120
	T	922	901
F	P	125	118
	T	495	479

Fig. 3-26 - ML-1 Cycle Characteristics

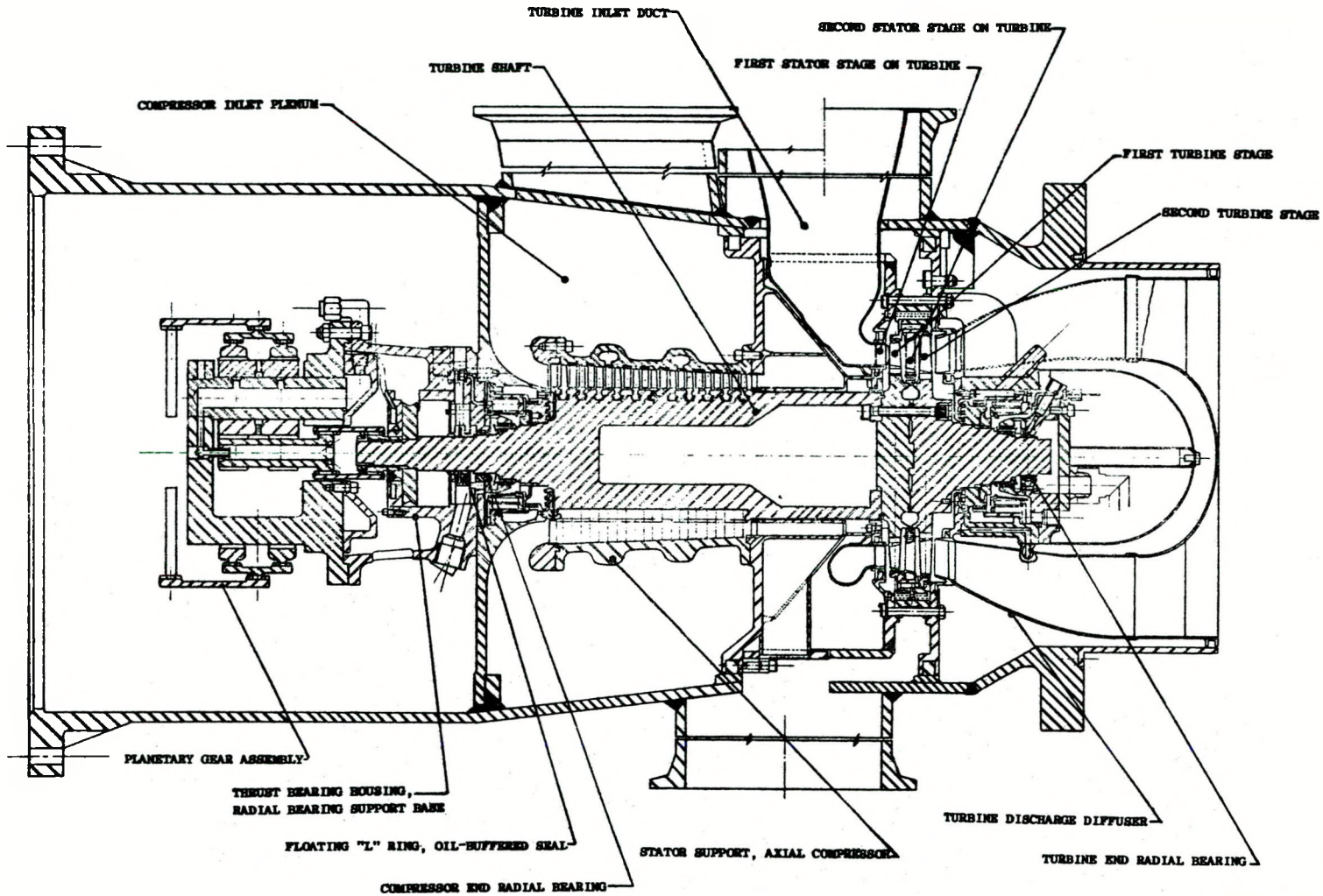


Fig. 3-27 - The Axial Flow Turbine Compressor Set for ML-1

Figure 3-25[69] shows the simplified diagram of the ML-1, and the cycle characteristics illustrated by the scheme on Figure 3-26[69]. The turbo-compressor set itself is described in more detail in Section 12.2.1 (see also Figure 3-27[62]).

The T-C unit is designed to operate at least 5000-6000 hours with no more than field maintenance service, and 10,000 hours between major overhauls. The total design life of the unit is 50,000 hours[70].

The ML-1 reactor is now limited to an outlet coolant temperature of 1200°F to maintain a maximum allowable hot-spot fuel-element surface temperature of 1750°F. Calculations were made to determine the gains possible through advancements in high-temperature materials technology. The results showed that a 50°F increase in turbine inlet temperature would increase the plant thermal efficiency 0.75 percentage points and would decrease the weight of the power conversion skid by about 1000 lb. Calculations based on advancements in turbomachinery technology showed that a one percentage point change in turbine or compressor efficiency produces about a 0.6 percentage point change in cycle efficiency and a reduction in weight of the power conversion skid of 600 to 800 lb[12].

3.3.3 MGCR

Compressor and turbine model stages of the MGCR are being tested at the Westinghouse Electric Company as well as models of some other essential parts such as compressor diffuser and turbine exhaust hood. Figures 3-28[1] and 3-29[1] show the arrangement of the power plant in the ship, and Figures 3-30[71] and 3-31[1] show the cycle flow diagram in the version with the low-pressure turbine driving. Lack of funds has extended the realization of this project further than anticipated.

(Pages 147 and 149 omitted).

The turbomachinery layouts developed during the course of the evaluation study were of a preliminary nature and were principally intended to illustrate the effect of working-fluid composition and pressure on the size and speed of the machinery (see Section 3.2). On completion of the evaluation phases, more detailed examination of the turbomachinery and related subjects was begun by Electric Boat Division and by Westinghouse Electric Corporation, the turbomachinery subcontractor.

The greater part of the development work for the rotating machinery was assigned to Westinghouse Electric Corporation under subcontract. This includes aerodynamic and mechanical development of turbines and compressors as well as start-up and control analysis. The subcontract also includes work in metallurgy and work on sealing and lubrication systems.

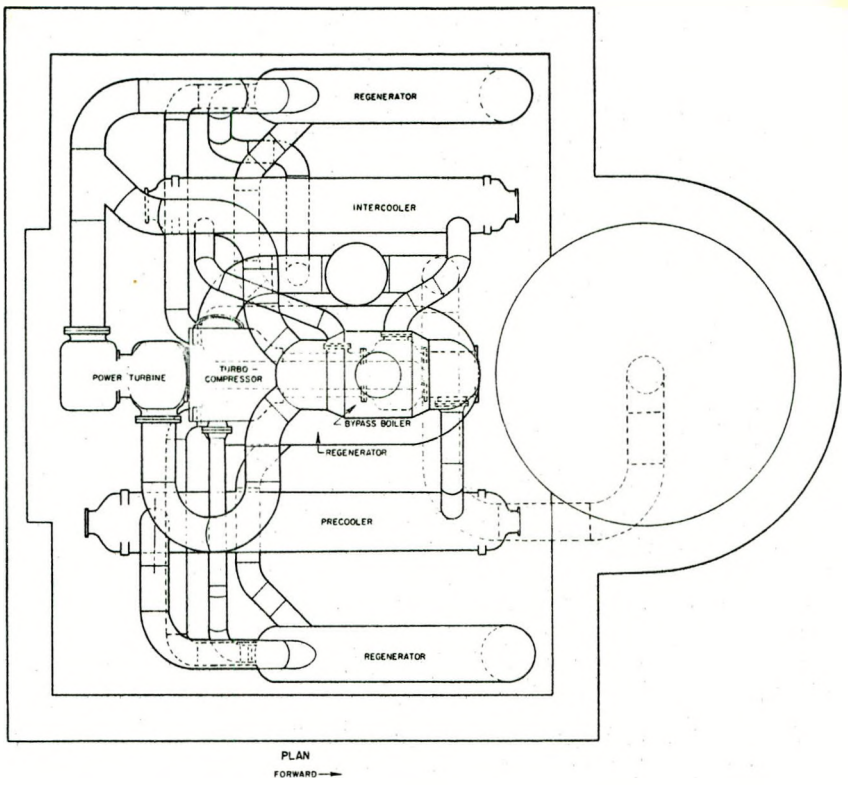


Fig. 3-28 - Arrangement for Helium-Cooled Reactor Power Plant, Plan (MGCR)

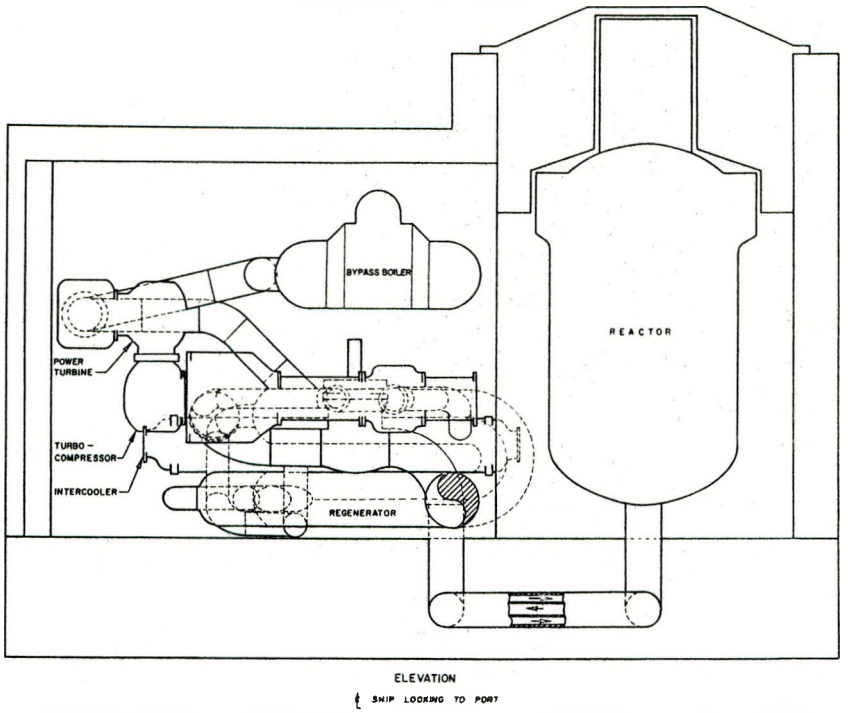


Fig. 3-29 - Arrangement for Helium-Cooled Reactor Power Plant, Elevation (MGCR)

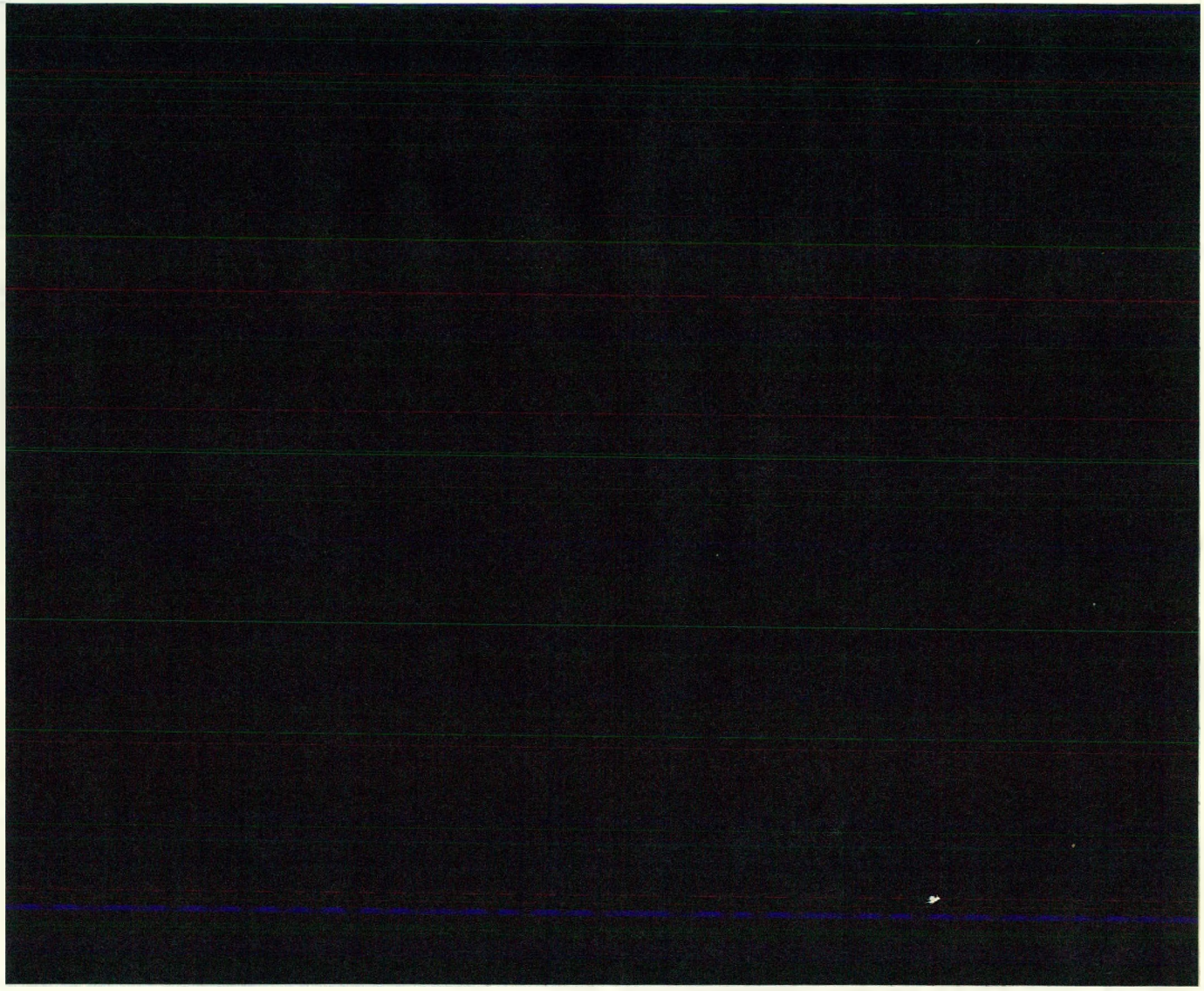
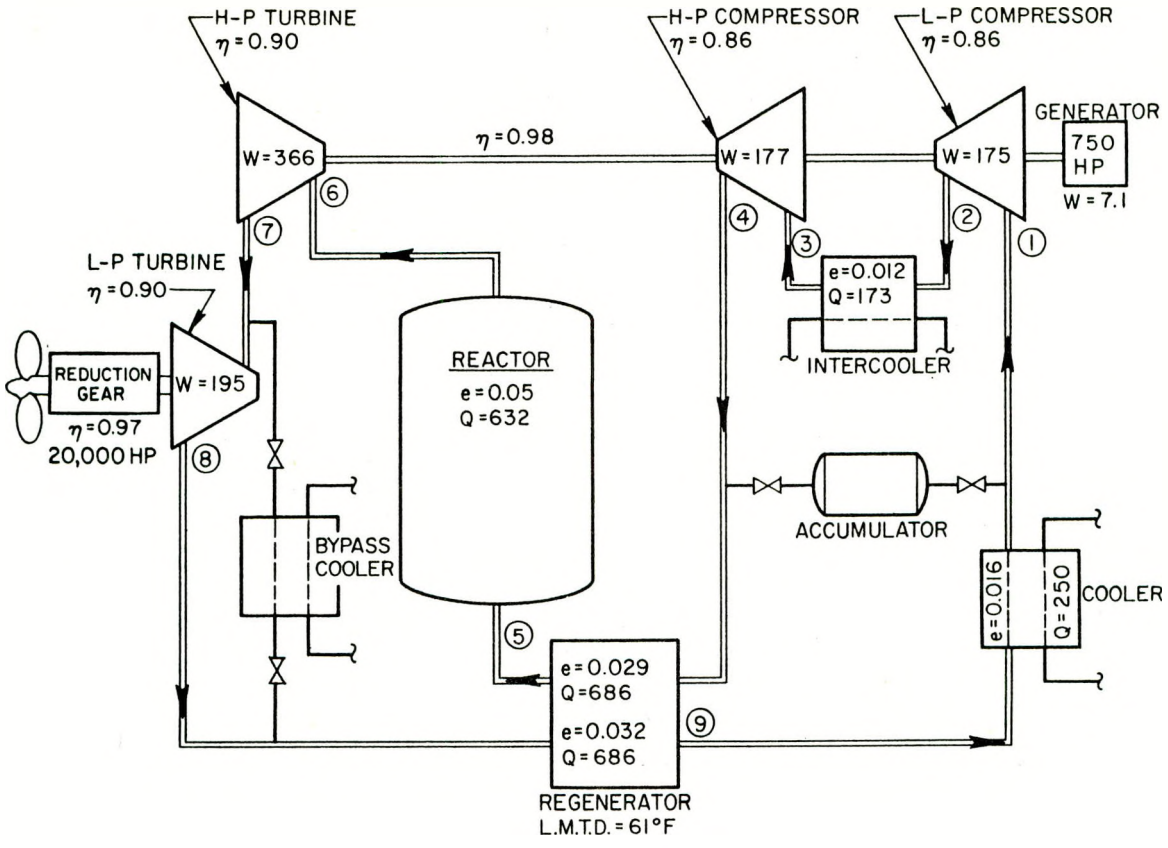


Fig. 3-30 - MGCR Flow Diagram LPT Driving



FLOW RATE, 74.6 LB/SEC
NET OVER-ALL CYCLE EFFICIENCY, 30.0%
BASIC CYCLE EFFICIENCY, 32 %
PRESSURE RATIO, 2.6
e_T = 0.14
ALL W AND Q IN BTU/LB

	TEMPERATURE (°F)	PRESSURE (PSIA)	VOLUME FLOW RATE (FT^3/SEC)
①	100	385	295
②	239	624	228
③	100	616	186
④	239	1000	144
⑤	791	971	262
⑥	1300	923	386
⑦	1008	554	535
⑧	852	404	654
⑨	301	391	393

Fig. 3-31 - Flow Sheet for MGCR Closed-Cycle Gas Turbine System (Helium Cooled, Graphite Moderated)

Work at Electric Boat in connection with the rotating machinery consists of monitoring the Westinghouse effort in aerodynamic and mechanical development, coordinating this work with other parts of the program, studying machinery performance, and assisting in cycle and control analysis in relation to turbomachinery performance.

It soon developed that critical shaft speed was an important consideration in the detail design of the machinery. The relatively large numbers of compressor and turbine stages and the high rotational speeds resulting from the use of helium result in machine rotors which are long and flexible and have a high ratio of running speed to first critical speed. In previous experience at Westinghouse, the maximum value obtained for this ratio was 2.8, whereas the first designs of the MGCR machinery yielded ratios between 3 and 4. Different ways were therefore investigated to decrease the bearing span in order to stiffen the shaft and decrease the running to critical speed ratio. One possibility investigated was to vary the division of pressure ratios between the two compressors. By using a higher pressure ratio in the low-pressure compressor, fewer stages would be required in the high-pressure compressor, thereby decreasing its length and increasing its critical speed. However, a study of the effect on cycle efficiency of varying the pressure ratios indicated that the highest cycle efficiency was obtained with a higher pressure ratio in the high-pressure compressor. Unfortunately, this lowers the critical speed. The study also showed, however, that thermodynamic efficiency was not a strong function of pressure-ratio split and that a sufficient number of stages could be shifted from the high-pressure compressor to the low-pressure compressor to obtain a significant reduction of the critical-speed problem with an efficiency penalty of less than one percentage point.

Also in connection with the critical-speed problem, the maximum cycle pressure level was decreased from 1000 to 800 psia. This decrease results in rotors of greater diameter, which are therefore stiffer, turning at lower rpm, thus decreasing the running to critical-speed ratio. Maximum design pressure level has been set at 800 psia and design power level has been kept at 20,000 shp.[72]

As a result of the various studies carried out, the speed of the main shaft was set to approximately 12,200 rpm, which allows a factor of approximately 2.75 times first critical speed. Although a higher factor could be tolerated, it was felt that other design considerations, such as minimum hub diameter, stage work, number of stages and shaft stiffness, made optimization at the foregoing speed highly desirable. In addition, the required seal welding of casing joints and the generally limited access to the shaft, after operation of the machinery, preclude any fine field balancing; therefore, it was believed advisable to keep the ratio of operating speed to critical speed within the limits of experience.

After analyzing various possible stage types, the symmetrical-staging, constant-axial-velocity, free-vortex design appeared to be best for the compressors. With this stage type, one, or at the most two, master blade patterns will be sufficient for blading each compressor[72]. As for the compressors, decisions favoring the free-vortex, symmetrical-staging design having constant axial velocity, with slight divergence along the tip diameter, have been made for the high-pressure turbine.

Further study has been made on the low-pressure, or power turbine because of additional problems. Because the power turbine must be capable of variable speed, it was desired to hold maximum design speed below the first critical speed. However, as design speed was reduced, the required number of stages was increased, thus increasing the shaft length and lowering the first critical speed. Simultaneously, however, speed ratio and size of the reduction gear were reduced. Since the reduction gear is a major power-plant item from the standpoint of both cost and weight, this reduction tended to offset the increased number of turbine stages.

A rotor study by Electric Boat demonstrated the effect of bearing and seal diameters on critical speed. It was found that 4-inch-diameter bearings with 5- or 6-inch-diameter shafting at the seal labyrinths will provide satisfactory stiffness[73].

Westinghouse completed a design analysis of the power turbine similar to one previously conducted, for the high-pressure rotor. Included in the optimization of the turbine was a study of the corresponding marine-type reduction gear. It was found that the minimum total cost of turbine and reduction gear occurs at a turbine speed of 8500 rpm. The power turbine blades are similar to those used in the high-pressure turbine, thus enabling both turbines to be designed from the same test data[74].

One of the most promising methods of absorbing power generated by the MGCR plant in a test facility is by means of an air compressor. A survey was conducted by Westinghouse to determine what compressors are available and which ones could be used for this purpose without extensive

development. Aircraft engine compressors appeared especially promising because their high running speed may obviate reduction gears[74]. Investigations were started on the suitability of using both compressors of a twin-spool turbojet which would be operated with the shaft locked together in order to attain the required capacity of a load absorber for the prototype. Since the altitude of the test site may affect the power-handling capability of any compressor designed for given sea-level characteristics, it may be necessary to introduce water injection and air preheating in the inlet duct[75].

It has been found that an eddy-current absorption dynomometer, made by Eaton Dynamtic Co. for the Air Force, is well suited in terms of speed and capacity for use as a load absorber for the MGCR prototype. Commercial compressors were found to be much more expensive to purchase and adapt than the aircraft engine[61]. Information is being obtained on other types of power absorbers, such as water brakes and electric dynamometers[74].

Tests are continuing at Westinghouse to establish creep-rupture and fatigue strength of structural metals in high-temperature helium. Tests on high-strength metals for turbine blades and disks are particularly important. Information available at the beginning of the project indicated an approximately 25% fall-off of strength of these metals in a helium atmosphere. Subsequent tests run in pure helium, helium with oxygen-carrying impurities, and air indicate a slight difference in favor of pure helium. Future tests will include runs at 1500°F to enable further advances in the power plant[75].

Early in 1960, the power cycle was changed resulting in an increase in output power from 22,000 shp to 30,000 shp maximum and an increase in peak pressure from 800 psia to 1150 psia. The latter figure was chosen to preserve the compressor volume flow. Compressor size was thus not changed but the blade-bending loads were increased approximately 40%.

In the case of the compressor blades, it was found that sufficient bending strength could be achieved by increasing root thickness from 15% to 18% of the chord. A similar change is not practicable in the turbine because[75]:

(a) The low fatigue strength of Inconel 713C as observed in earlier tests was confirmed.

(b) A sufficient change in thickness would change the contour of the blade path so much that a new blade model would be required.

(c) Aerodynamic performance of the thicker blades would be inferior. Increasing the blade chord could solve some of these problems but this would in turn result in a longer rotor with too low a critical speed.

The following design modifications to the rotating machinery are being studied simultaneously[75]:

(a) To relocate the turbine-compressor rotor bearings so that the high-pressure turbine is supported on separate bearings. Turbine-blade chord can then be increased, or other changes can be made, e.g., decreasing diameter and increasing number of stages in order to obtain the required blade bending strength.

(b) To interchange the high-pressure and low-pressure turbines. The advantage of this arrangement is that the high-pressure turbine is run at low speed, and the low-pressure turbine rotor is larger in diameter and hence stiffer than the high-pressure turbine rotor. Several inherent difficulties presented by this arrangement are receiving study prior to giving it more serious consideration.

The concept of high-pressure drive machinery results in many changes in the machinery compartment arrangement. The major difference between the high-pressure drive and the low-pressure drive is the location of the four basic units which comprise the rotating machinery, see Figure 3-32[11]. The flow diagram for the high-pressure drive is shown

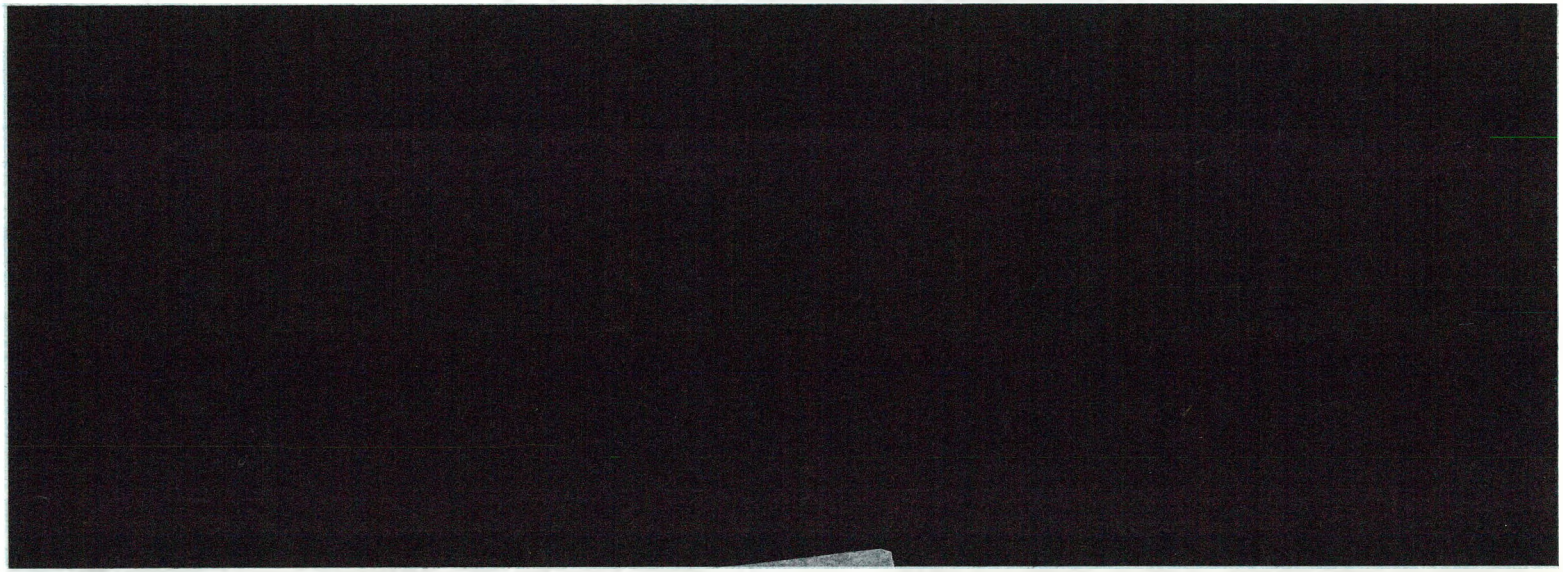


Fig. 3-32 - MGCR Turbomachinery HPT Driving

in Figure 3-33[11]. A major problem associated with the high-pressure drive system is the increase in piping length required. Various alternate schemes are now being worked out to reduce piping to a minimum[71].

3.4 Future Development

For a number of years, future development will be confined to gaining experience with experimental power plants such as the ML-1 and later the MGCR. This experience will direct the future development. It is too early to look for specific trends at this time. The seal and bearing problems as well as the problem of selecting and developing of adequate structural materials for the critical parts such as turbine disks, turbine blading, valves, and hot ducts will certainly require continuous attention and effort.

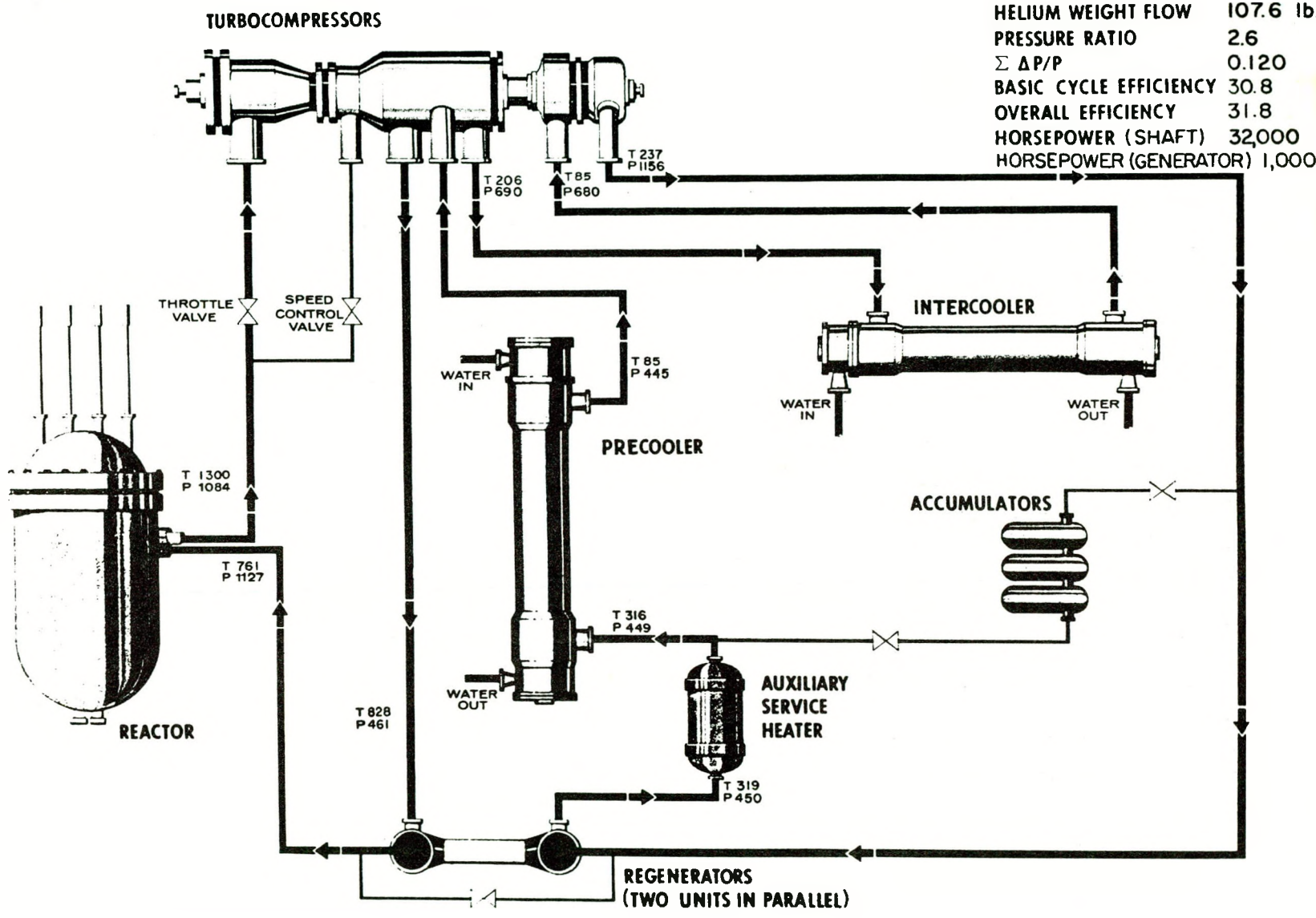


Fig. 3-33 - MGCR Flow Diagram HPT Driving

THE FRANKLIN INSTITUTE • Laboratories for Research and Development

4. PHYSICAL AND MATHEMATICAL RELATIONSHIPS

4.1 Basic Relationships

The problems with turbomachinery center around the process of converting kinetic energy into shaft work or vice versa. This process, although but one link in the chain of various states of energy, concerns the question of thermodynamic availability of energy which is the controlling factor influencing stage characteristics. We are dealing primarily with a flow process subject to the laws of fluid dynamics. Basic relations may be stated as follows: if the flow through a stage is assumed to be rotationally symmetrical, an element of this stage, bounded by two neighboring coaxial stream surfaces, may be considered, for which the rate of energy transfer is given by Euler's equation

$$E = \frac{G}{g}\,\omega\Delta\,(rc_u)$$

For pure axial flow this equation reduces to

$$E = \frac{G}{g}\,u\Delta\,c_u$$

where
- E = rate of energy transfer
- G = weight flow rate
- g = acceleration of gravity
- ω = angular velocity
- r = blade radius
- c = absolute velocity
- u = peripheral velocity
- c_u = circumferential component of absolute velocity

The equations may be applied to an entire stage only if the circulation about the blade sections is the same in all stream surfaces. We make this assumption in the relations given in this section furthermore, the connection between thermodynamic and mechanical quantities will be presented neglecting irreversible losses. While crude, this approach is nevertheless useful at times for estimating and for understanding basic principles. The function of the blading, whether for compressor or turbine, is to change momentum flow. The torque on the fluid exerted by the blades

is equal to the change in angular momentum of the fluid between entrance and exit sections, and is measured by the mass rate of flow times the change in velocities between entrance and exit sections. By the law of action and reaction, there is a corresponding torque reaction exerted by the flow on the blades.

If c_{1u} and c_{2u} are the whirl entrance and exit velocities, i.e. the absolute tangential entrance and exit velocities of the flow passing through the blades, then

$$\Phi = \frac{G}{g} (c_{2u} r_2 - c_{1u} r_1) \text{ lb-ft}$$

is the torque exerted on the flow and

$$\Phi = -\frac{G}{g} (c_{2u} r_2 - c_{1u} r_1) = \frac{G}{g} (c_{1u} r_1 - c_{2u} r_2) \text{ lb-ft}$$

is the torque exerted on the blades

If ω is the angular velocity of the rotor, then $u_1 = \omega r_1$ = entrance peripheral velocity (ft/sec) and $u_2 = \omega r_2$ = exit peripheral velocity (ft/sec). The power or rate of energy transfer from moving blades to the fluid flow is

$$\Phi \omega = \frac{G}{g} (c_{2u} r_2 - c_{1u} r_1) \omega = \frac{G}{g} (u_2 c_{2u} - u_1 c_{1u}) \frac{\text{ft-lb}}{\text{sec}}$$

The power or rate of energy transfer from the fluid to the moving blades

$$\Phi \omega = -\frac{G}{g} (c_{2u} r_2 - c_{1u} r_1) \omega =$$

$$= \frac{G}{g} (u_1 c_{1u} - u_2 c_{2u}) \frac{\text{ft-lb}}{\text{sec}}$$

let

$$\left| c_{2u}\, r_2 - c_{1u}\, r_1 \right| = \Delta(c_u\, r)$$

Thus $\frac{G}{g}\,\Delta\,(c_u\, r)$ is the angular momentum of the flow. It is increased in passing through the compressor and decreased in passing through the turbine. The function of the fixed blades or nozzles is to accelerate the flow to a given angular momentum, thus creating the initial whirl velocity c_{1u}.

4.2 General Relations for Compressors and Turbines

For Centrifugal Compressors

The fluid flow enters the moving blades or rotating channel near the shaft hub at a small radius r_1 and leaves radially at radius r_2 so that, across the moving blade system

$$\Phi_C = \frac{G}{g}\left[c_{2u}\, r_2 - c_{1u}\, r_1 \right] \quad \text{torque, lb-ft}$$

$c_{1u} = 0$ in most radial flow compressors

$$P_C = \Phi_C\, \omega = \frac{G}{g}\left[u_2\, c_{2u} - u_1\, c_{1u} \right] \text{ power transfer, } \frac{\text{ft-lb}}{\text{sec}}$$

and $h_2 - h_1 = \frac{P_C}{JG} - \frac{1}{J}\,\frac{c_2^2 - c_1^2}{2g}$ energy equation, $\frac{\text{BTU}}{\text{lb}}$

For Axial Compressors $r_1 = r_2$ $\therefore\ u_1 = u_2 = \omega r$; hence for moving blades,

$$\Phi_C = \frac{G}{g}\,(c_{2u} - c_{1u})\, r \quad \text{torque, lb-ft}$$

$$P_C = \Phi_C\, \omega = \frac{G}{g}\left[c_{2u} - c_{1u} \right] u \quad \text{power transfer, } \frac{\text{ft-lb}}{\text{sec}}$$

and

$$h_2 - h_1 = \frac{P_C}{JG} - \frac{1}{J}\frac{\left(c_2^2 - c_1^2\right)}{2g} \quad \text{energy equation,} \quad \frac{BTU}{lb}$$

For Turbines

In general, for moving blades of mixed flow or axial flow turbines, respectively

$$\Phi_T = \frac{G}{g}\left[c_{1u}\, r_1 - c_{2u}\, r_2\right] = \frac{G}{g}\left[c_{1u} - c_{2u}\right] r \qquad \text{torque, lb-ft}$$

$$P_T = \frac{G}{g}\left[u_1\, c_{1u} - u_2\, c_{2u}\right] = \text{power transfer}$$

$$= \frac{G}{g}\left[c_{1u} - c_{2u}\right] u \qquad \frac{\text{ft-lb}}{\text{sec}}$$

$$h_1 - h_2 = \frac{P_T}{JG} + \frac{1}{J}\frac{c_2^2 - c_1^2}{2g} \quad \text{energy equation,} \quad \frac{BTU}{lb}$$

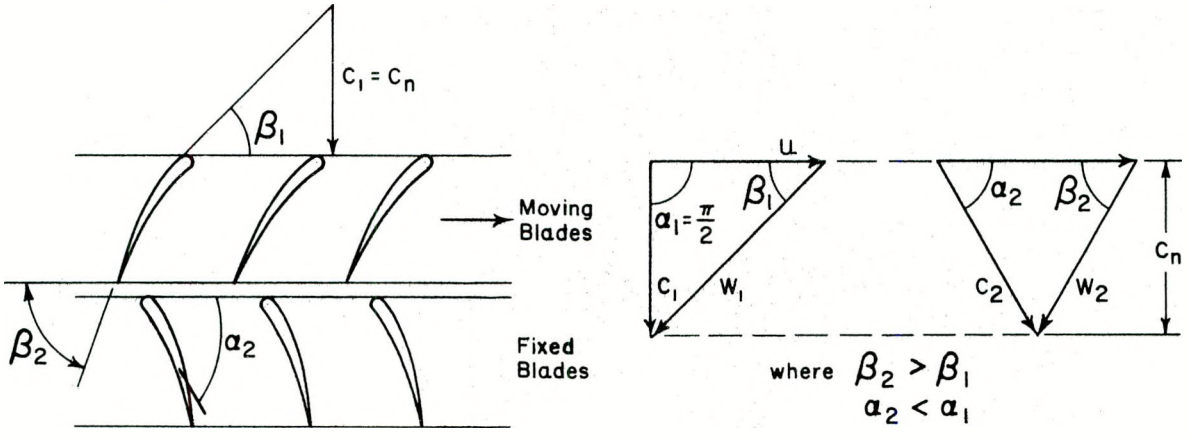
Any turbine must always have stationary guide blades or nozzles for accelerating the flow and thereby increasing the initial whirl velocity to the moving blades. It is important to note that although a torque is exerted on the flow and likewise reacts on the nozzles or stationary blade system (increasing the angular momentum of flow), no work is done on the flow, except for friction losses. In compressor stationary blades there is a torque decreasing the angular momentum of the flow.

The fluid flows through any compressor or turbine either in an axial or radial direction or in combination of both. A whirl or angular momentum is important to the flow and is proportional to the torque exerted by the blading. The momentum change through any set of blading is always determined by the preceding blading, that is, for the initial momentum to a set of blading by the preceding stationary nozzles, and for the exit momentum by the velocity conditions of the blading under consideration at exit.

The entrance velocity to a set of blades has three absolute components, namely an axial component, a radial component, and a whirl or tangential component. The same holds for the exit velocities. In a radial flow turbine, we are mainly concerned with the radial and tangential components.

The volume flow rate is determined by the normal component velocity, i.e., the axial or radial components above mentioned, multiplied by the effective cross section to the flow, i.e., a section normal to the flow. The weight flow rate must equal the volume flow rate times the specific volume at the section under consideration.

For Multi-Stage Axial Compressors



With n stages, the torque Φ_c is

$$\Phi_c = \sum_1^n \frac{G}{g} (c_2 \cos \alpha_2 - o)r \quad \text{where r is the mean radius}$$

but $c_2 \cos \alpha_2 = u - c_n \cot \beta_2$ and $w_2 \sin \beta_2 = c_n$

$$\Phi_c = \sum_1^n \frac{G}{g} (u - c_n \cot \beta_2)\, r$$

THE FRANKLIN INSTITUTE Laboratories for Research and Development

with $u = r\,\omega$

the corresponding power is

$$\Phi_{c\,\omega} = \sum_{1}^{n} \frac{G}{g}\ (u - c_n \cot \beta_2)\ u$$

c_n may be obtained from the condition of continuity of the gas flow.

With blade height = h

Annular area = $2\pi\ r\ h$

Further, with

Leakage factor = λ

Specific volume = v

the weight flow per second through blades is

$$2\pi\ r\ h\ \ c_n = (1-\lambda)\ Gv$$

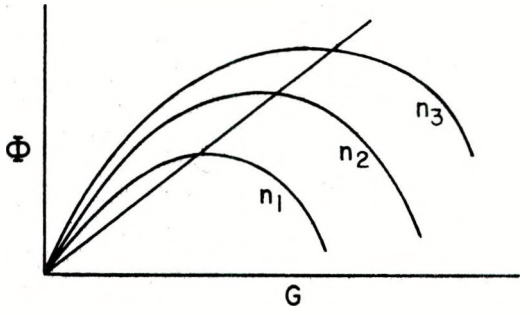
and $$c_n = \frac{(1-\lambda)\ Gv}{2\pi\ r\ h}$$

Or substituting in the power equation

$$P_c = \Phi_{c\,\omega} = \sum_{1}^{n} \frac{(1-\lambda)\ G}{g}\ (u - BG)\ u$$

where $B = \frac{(1-\lambda)v}{2\pi\ r\ h}\ \cot \beta_2$ for any blade pair (complete stage).

From this relation, we see that the compressor torque increases directly with speed u. On the other hand it increases as a parabolic function of the flow rate G.



$$\Phi = \Sigma \frac{G}{g} \left(u - BG \right) r$$

The maximum torque occurs when

$$\frac{d\,\Phi}{d\,G} = 0 = \sum_{1}^{n} (u - 2\,BG) = 0$$

so that with n stages

$$G = \frac{nu}{2 \sum_{1}^{n} B}$$

and

$$\Phi_{max} = \frac{ru^2}{g} \sum_{1}^{n} \left[\frac{n}{2 \sum_{1}^{n} B} \left(1 - \frac{Bn}{2 \sum_{1}^{n} B} \right) \right]$$

The torque curves are spaced as the square of the speed. The corresponding power curves vary as the cube of the speed.

In a compressor, the torque exerted on the flow by the blades decreases beyond an optimum flow rate G_{opt}, where

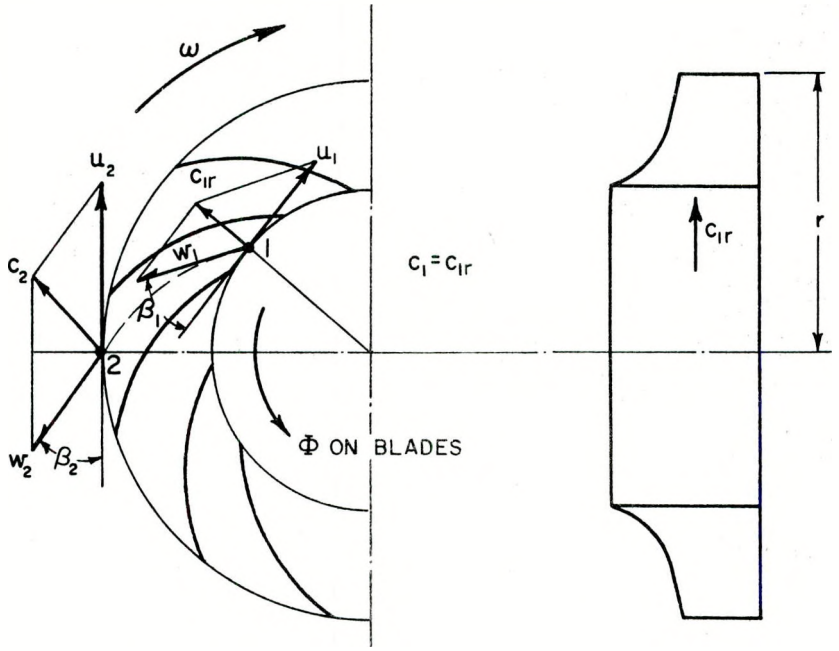
$$G_{opt} = \sum_{1}^{n} \frac{\pi u r h}{(1-\lambda) v \cot \beta_2}$$

In the region where the flow rate $G > G_{opt}$, a decrease in flow results in an increase in torque and power exerted on the flow, or an increase in flow rate results in a decrease in torque. Thus, if due to external causes, the flow rate suddenly drops, the torque and power both automatically increase and we have a stabilizing effect. Therefore, for stability, the compressor should operate at a flow rate $G > G_{opt}$, and for best efficiency and maximum output G should (though larger) approximate G_{opt}.

Figures 4-1 to 4-4 give some basic relations in a concentrated form for compressors and turbines. The questions of efficiency of a turbomachine were not touched in this section, and if we would have to deal with an isentropic flow without irreversible losses, all velocity triangles, satisfying the equations of angular momentum and of continuity, would be equivalent regarding efficiency. In such a case the design of the blading would have the only purpose; to assure the necessary changes of flow direction. However, the true flow is not isentropic due to irreversible losses. The magnitude of the losses depends on friction, on the Mach number, and on the degree of diffusion, particularly in compressors because of decelerated flow.

At this point there begins the refinement of design considerations and various characteristic values have been introduced to aid in the selection of optimum velocity triangles. One of the important characteristic values is the degree of reaction.

The degree of reaction determines largely the velocity diagram, the losses and the blade shape. However, the difficulty of choosing the optimum degree of reaction or its distribution along the blade and along the stages still remains regardless of such a statement because of the



Tip Speed $u_2 = r\omega$

Torque on Blades $$\boxed{\Phi = \frac{G}{g}(u_2 - w_2\cos\beta_2)r} \qquad (1)$$

$$u_2 - w_2\cos\beta_2 = c_u$$

Power $$\boxed{\Phi\omega = \frac{G}{g}(c_u u_2)} \qquad (2)$$

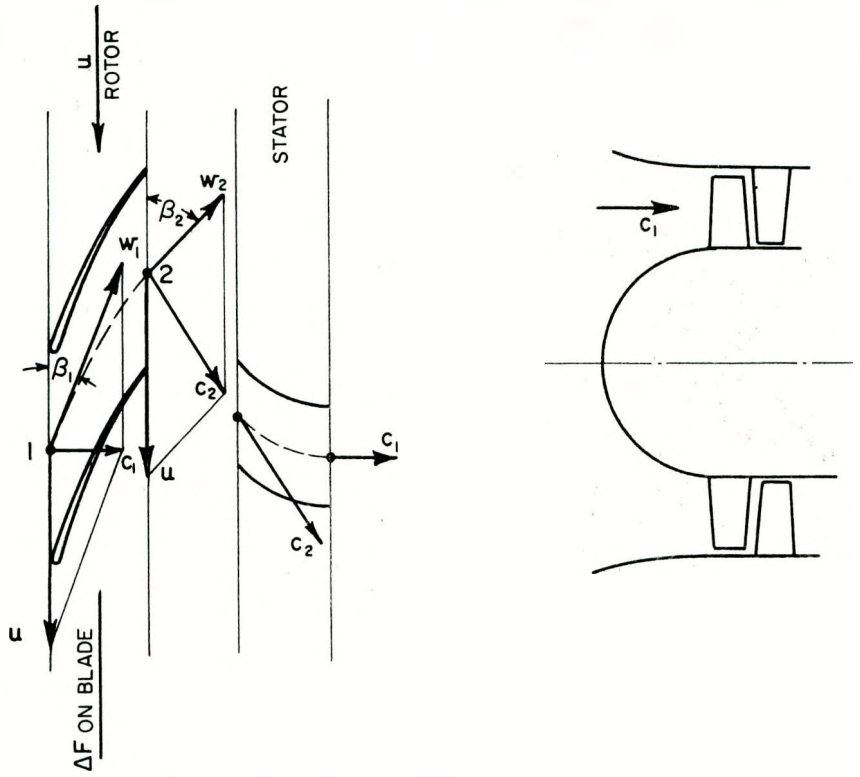
Energy Equation $$\frac{k}{k-1}p_1v_1\left[\left(\frac{p_2}{p_1}\right)^{\frac{k-1}{k}} - 1\right] = \frac{1}{g}c_u u_2$$

per unit weight assuming isentropic compression ($\eta_{ad} = 1$)

$$k = \frac{c_p}{c_v} \quad \text{and since} \quad \frac{k}{k-1}p_1v_1 = Jc_pT_1$$

Pressure Ratio (compression ratio) $$\boxed{\frac{p_2}{p_1} = \left(\frac{u_2c_u}{gJc_pT_1} + 1\right)^{\frac{k}{k-1}}} \qquad (3) \quad p_2 > p_1$$

Fig. 4-1 - Radial Compressor - Basic Relations



$$w_2 \sin\beta_2 = c_1$$

Tangential Force on Blades

$$\boxed{\Delta F = \frac{G}{g}\left(u - w_2 \cos\beta_2\right) = \frac{G}{g} u \left(1 - \frac{c_1 \cos\beta_2}{u \sin\beta_2}\right)} \quad (1)$$

$$e = \frac{c_1}{u} = \tan\beta_1$$

Power

$$\boxed{\Delta F \times u = \frac{G}{g} u^2 \left(1 - e \cot\beta_2\right)} \quad (2)$$

Energy Equation $\frac{k}{k-1} p_1 v_1 \left[\left(\frac{p_2}{p_1}\right)^{\frac{k-1}{k}} - 1\right] = \frac{u^2}{g}\left(1 - e \cot\beta_2\right)$

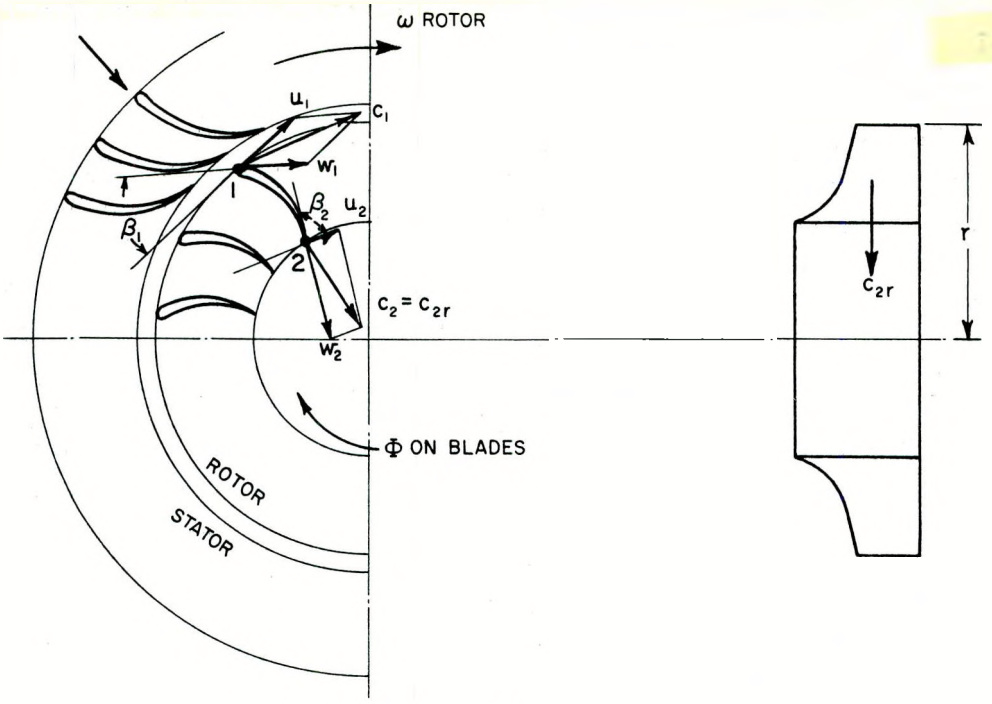
per unit weight assuming isentropic compression ($\eta_{ad} = 1$)

$k = \frac{c_p}{c_v}$ and since $\frac{k}{k-1} p_1 v_1 = J c_p T_1$

Pressure Ratio (compression ratio)

$$\boxed{\frac{p_2}{p_1} = \left[\frac{u^2(1-e\cot\beta_2)}{g J c_p T_1} + 1\right]^{\frac{k}{k-1}}} \quad (3) \quad p_2 > p_1$$

Fig. 4-2 - Axial Flow Compressor - Basic Relations



Tip speed $u_1 = r\omega$

Torque on blades $$\boxed{\Phi = \frac{G}{g}\left(u_1 - w_1 \cos\beta_1\right)r} \qquad (1)$$

$$u_1 - w_1 \cos\beta_1 = c_u$$

Power $$\boxed{\Phi\omega = \frac{G}{g}\left(c_u u_1\right)} \qquad (2)$$

Energy equation per unit weight, assuming isentropic expansion ($\eta_{ad} = 1$)

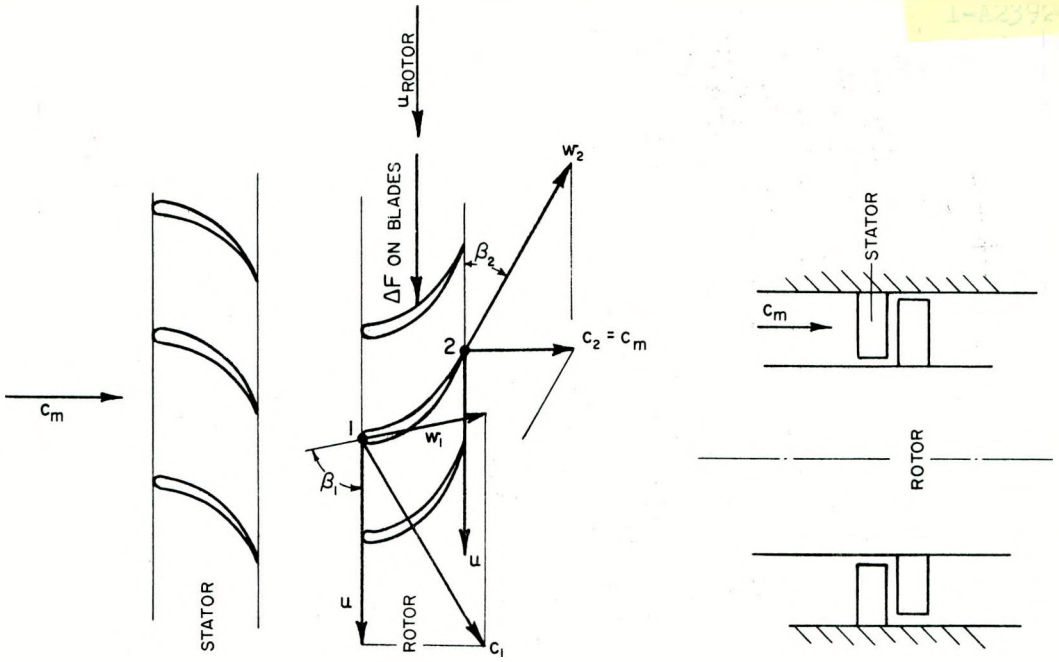
$$\frac{k}{k-1}\, p_1 v_1 \left[1 - \left(\frac{p_2}{p_1}\right)^{\frac{k-1}{k}}\right] = \frac{1}{g}\, c_u u_1$$

$k = \frac{c_p}{c_v}$ and since $\frac{k}{k-1}\, p_1 v_1 = J c_p T_1$

Pressure ratio (Expansion ratio) $$\boxed{\frac{p_1}{p_2} = \left(1 - \frac{u_1 c_u}{g J c_p T_1}\right)^{\frac{k}{1-k}}} \qquad (3) \qquad p_1 > p_2$$

Fig. 4-3 - Radial Turbine - Basic Relations

THE FRANKLIN INSTITUTE — Laboratories for Research and Development
I-A2392-4



$$w_1 \sin\beta_1 = c_m$$

Tangential force on blades

$$\Delta F = \frac{G}{g}\left(u - w_1 \cos\beta_1\right) = \frac{G}{g} u \left(1 - \frac{c_m}{u}\frac{\cos\beta_1}{\sin\beta_1}\right) \qquad (1)$$

$$e = \frac{c_m}{u} = \tan\beta_2$$

Power

$$\Delta F \times u = \frac{G}{g} u^2 \left(1 - e \cot\beta_1\right) \qquad (2)$$

Energy equation per unit weight, assuming isentropic expansion ($\eta_{ad} = 1$)

$$\frac{k}{k-1} p_1 v_1 \left[1 - \left(\frac{p_2}{p_1}\right)^{\frac{k-1}{k}}\right] = \frac{u^2}{g}\left(1 - e \cot\beta_1\right)$$

$$k = \frac{c_p}{c_v} \text{ and since } \frac{k}{k-1} p_1 v_1 = J c_p T_1$$

Pressure ratio (Expansion ratio)

$$\frac{p_1}{p_2} = \left[1 - \frac{u^2 (1 - e \cot\beta_1)}{g J c_p T_1}\right]^{\frac{k}{1-k}} \qquad (3) \quad p_1 > p_2$$

Fig. 4-4 - Axial Turbine - Basic Relations

many factors involved and their complex interaction in three-dimensional flow.

From two-dimensional flow considerations, the following discussion holds. The degree of reaction of the turbine stage can be defined in two ways. One method relates the isentropic enthalpy drop necessary in the rotor to the total isentropic enthalpy drop of the stage. This so-called isentropic or theoretical degree or reaction r^* is defined by Fig. 4-5[76].

$$r^* = \frac{h_1^* - h_2^*}{H_e - h_2^*} = \frac{h_1^* - h_2^*}{\Delta h_{is}}$$

where the asterisks refer to the enthalpies at the pressures p_1 and p_2 ahead and after the rotor at the entropy s_e of the conditions at the entrance, and H_e is the total enthalpy ahead of the stage. The effective degree of reaction r is

$$r = \frac{h_1 - h_2}{H_e - h_2}$$

where h_1 and h_2 are the actual static enthalpies ahead and after the rotor. With the kinetic energies there is also[76]

$$r = \frac{w_2^2 - w_1^2 + u_1^2 - u_2^2}{c_1^2 + w_2^2 - w_1^2 + u_1^2 - u_2^2}$$

This degree of reaction is therefore completely determined by the velocity diagram. This condition is contrary to those which are used for the incompressible flow through an axial-flow compressor cascade, where the theoretical degree of reaction can be determined from the velocity diagram.

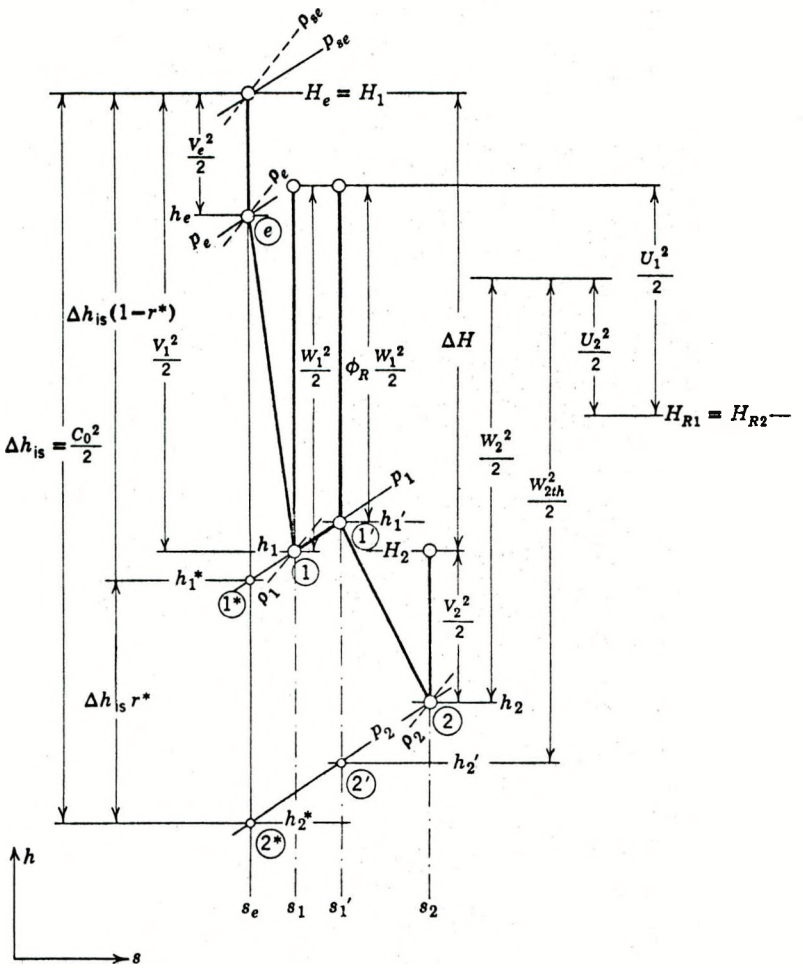


Fig. 4-5 - Thermodynamic Process of Fluid in Turbine Stage

$$r^* = \frac{w_{u1} + w_{u2}}{2u}$$

however if, in the thermodynamic treatment of axial-flow compressor stages, the degree of reaction is expressed by enthalpy drops also, the same situation will arise as with the turbine stages.

Both the theoretical and the effective degree of reaction are of interest in turbines. The first divides the isentropic drop of the stage in the parts used up by the stationary and rotating row, the other is a means of judging whether accelerated or decelerated flows occur in the rotating cascade. Experience shows that the relative velocity w_2 at the rotor exit should not be smaller than w_1. As a limit then, if $w_2 = w_1$ the effective degree of reaction should not be less than

$$r_{min} = \frac{u_1^2 - u_2^2}{c_1^2 + u_1^2 - u_2^2}$$

hence, for axial turbines, the effective degree of reaction must be larger than zero to produce accelerated flows in the rotor cascades.[76]

The efficiency of an axial-flow compressor stage has a maximum value for particular values of r^*. For equal drag/lift coefficients for stationary and rotating rows, the optimum degree of reaction r^* is 0.5. However, for particular applications and because of manufacturing and operational problems, it is frequently advantageous to build stages with degrees of reaction different from 0.5.

The velocity diagram is completely defined by three values, the flow coefficient, the pressure coefficient, and the degree of reaction. They may be used as parameters to establish the direction of flow at inlet and outlet of both fixed and moving rows of the normal stage (normal stages

are those stages for which conditions of flow, whether compressible or incompressible, are identical at inlet and outlet as to direction and velocity of flow, except for a difference in head, i.e. $c_o = c_2$). Hence, they define the ideal blade angles for any given operating condition of a blade element.

A tabulation of the velocity diagrams and of the shape of blade of the fixed and moving rows, in schematic presentation, is shown in Figure 4-6[77] for various values of pressure coefficient and degree of reaction and for a consistent value of flow coefficient because the latter is of secondary importance.

The simple one-dimensional approach is not sufficient particularly where decelerated flow occurs and the two-dimensional analysis of the cascades, which is based on the assumption of axisymmetric fluid motion through a turbomachine, has to be corrected by three-dimensional considerations, according to actual flow in the passages of turbomachines. Experimental data are indispensable for an effective design of turbomachinery and such data are being produced continuously according to specific needs of application. All these considerations make the aerothermodynamic design of turbomachinery rather complicated and this fact is reflected in the vast literature on the subject.

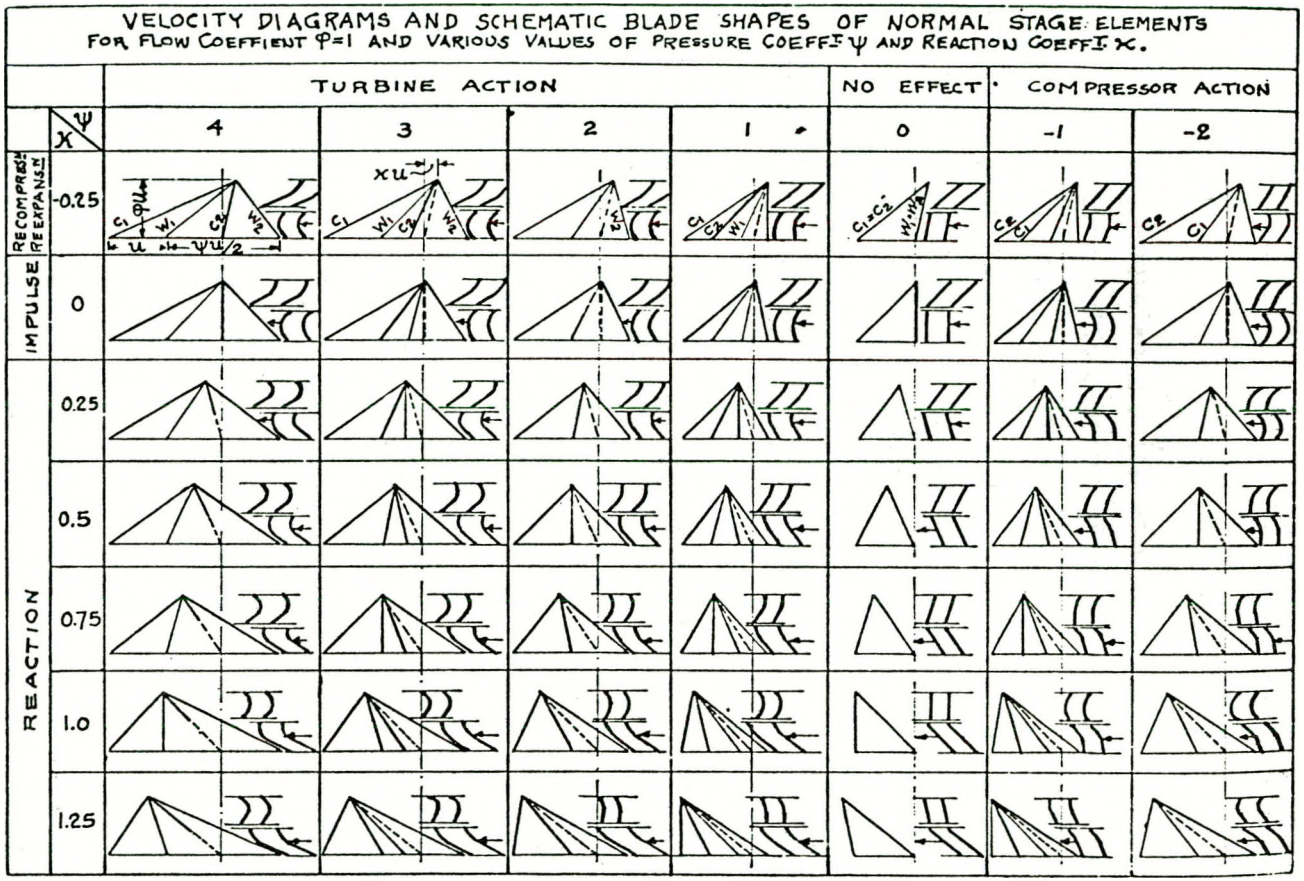


Fig. 4-6 - Velocity Diagrams and Schematic Blade Shapes of Normal Blade Elements

5. THERMO-AERODYNAMIC ASPECTS

5.1 Hydraulic Efficiency Of Turbomachines

5.1.1 General

By means of design and manufacturing provisions, it is possible to reduce the losses in the flow across a turbomachine practically to those of wall friction and of those occurring in transforming kinetic energy into pressure energy. Machines having only these two types of losses can be brought to an optimum obtainable efficiency. Simple expressions for such efficiency can be derived for one-stage machines and can be used, with corresponding amendments, also for multi-stage arrangements. Besides, the expressions can be applied in the evaluation of model tests.

The difference between the optimum efficiency, accounting for unavoidable losses, and the actual efficiency of a machine is the yardstick for determining its quality of design and precision of construction.

5.1.2 Total Efficiency

Denoting the circumferential power at the blades, the power of runner friction, and the power of mechanical losses (bearing and seal friction, auxiliary drives) by P_u, P_r and P_m, respectively, the available power of a turbine, or the required power of a compressor will be

$$P = P_u - P_r - P_m \qquad \text{for the turbine, and}$$

$$P = P_u + P_r + P_m \qquad \text{for the compressor.}$$

And if P_o is the power of an ideal machine without any losses, the total efficiencies are

$$\eta = \frac{P_o}{P} \qquad \text{for compressors, and}$$

$$\eta = \frac{P}{P_o} \qquad \text{for turbines.}$$

Frequently the ideal power of a compressor is based on the discharge mass flow, and not on the mass flow in the inlet pipe, as it is difficult to determine the leakage mass flows at guarantee tests. Furthermore, when entering into the details of determination of P_u, it is usual for gas turbines to omit the inlet and outlet absolute velocity energy members. The inlet member is always a negligible value, and the outlet member is considered to be a flow loss. The latter for compressors is also considered as flow loss which results in a slightly reduced value for efficiency.

5.1.3 Hydraulic Efficiency

Denoting by H_r the head due to a runner (per pound of mass flow), and by ΔG_e and ΔG_i the leakage mass flows at the inlet side of the machine (seal) and in the stages, respectively, the expressions for peripheral power at the runner is

$$P_u = (G - \Delta G_e + \Delta G_i)\, H_r \qquad \text{for compressors, and}$$

$$P_u = (G - \Delta G_e - \Delta G_i)\, H_r \qquad \text{for turbines.}$$

The negative sign at ΔG_e for the compressors is for the case when ambient pressure is smaller than the inlet pressure to the machine, which is practically true in most nuclear applications. Methods for calculating leakages at given conditions exist but are not discussed here.

If H is the head, H_v the head loss in the machine, c_u the peripheral component of absolute velocity and η_h the hydraulic efficiency, we can write the Euler energy equations

$$H_r = \frac{H}{\eta_h} = H + H_v = \frac{c_{u2}\, u_2 - c_{u1}\, u_1}{g} \qquad \text{for compressors, and}$$

$$H_r = H\eta_h = H - H_v = \frac{c_{u1}\, u_1 - c_{u2}\, u_2}{g} \qquad \text{for turbines}$$

With $\zeta = \frac{H_v}{H}$ or $H_v = \zeta H$ the hydraulic efficiency appears in the form $\eta_h = \frac{1}{1+\zeta}$ for the compressors, and

$\eta_h = 1 - \zeta$ for turbines.

The hydraulic efficiency is sometimes called internal efficiency and expressed by the symbol η_i[76].

The problem is how to determine ζ. It is convenient to split the losses into losses before the entrance to the stages, losses in the stages themselves, and losses after the stages.

$$\zeta H = H_{v,I} + H_{v,II} + H_{v,III} = \zeta_I \frac{c_1^2}{2g} + \zeta_{II} \frac{w_1^2}{2g} + \zeta_{III} \frac{c_2^2}{2g}$$

where the values of ζ_I to ζ_{III} can be determined with sufficient accuracy from experience and geometric relations.

$$f \frac{\gamma c^2}{2g} \quad Uds$$

is the expression for an elementary friction force. We now obtain for the separate head losses, assuming one-stage machines:

$$H_{v,I} = f_I \frac{c_1^2}{2g} \int_e^1 \left(\frac{c}{c_1}\right)^2 \frac{Uds}{A}$$

$$H_{v,II} = f_{II} \frac{w_1^2}{2g} \int_1^2 \left(\frac{w}{w_1}\right)^2 \frac{Uds}{A} + \zeta_s (w_1^2 - w_2^2)/2g, \text{ and}$$

$$H_{v,III} = f_{III} \frac{c_2^2}{2g} \int_2^a \left(\frac{c}{c_2}\right)^2 \frac{Uds}{A} + \zeta_s (c_2^2 - c_a^2)/2g$$

A is here the cross section of the flow channel, U its wetted perimeter, and s the length of the path along the mean streamline. The boundaries of the integrals have the same meaning as the subscripts introduced before, with the addition that "a" means outlet. The integrals can be evaluated knowing the geometry of the flow channels and the flow velocities at each point. The retardation losses characterized by ζ_s (separation of flow) should enter in above

expressions only when $\frac{w_2}{w_1} < 0.95$ (as in compressors in most cases but never in turbines) and when $\frac{c_a}{c_2} < 0.95$ (as in compressors). For well designed flow channels we may use $\zeta_s = 0.10$, and for wall friction at smooth walls, as usual in good machines, $f = 0.004$ may be used according to old experience. These values correspond to moderate Reynolds numbers, approximately $Re_o = 2 \times 10^5$ which can be considered as a reference condition (subscript o).

To account for other Reynolds numbers, the following expression can be used

$$\frac{H_v}{H_{vo}} = \frac{\zeta}{\zeta_o} = \left(\frac{Re_o}{R_e} \right)^m$$

in which $\zeta_o = \frac{H_{vo}}{H}$, and H_{vo} is assumed to be calculated with $f_l = f_{ll} = f_{lll} = 0.004$ and $\zeta_s = 0.10$. A recommended form for the Reynolds number is

$$Re = \frac{tc_m}{\nu} = \frac{\pi d c_m \gamma}{ng\mu} = \frac{G}{ng\mu b}$$

where

t = mean pitch of blading

c_m = mean meridional velocity at the inlet to the turbine runner, or at the outlet of the compressor runner

ν = kinematic viscosity

μ = dynamic viscosity

n = number of blades

d = mean runner diameter (mean stage diameter in axials)

b = width of runner canal (length of blade in axials)

γ = specific weight of gas at considered location.

The exponent m is variable (see Figure 5-1[78]). It is assumed to follow the empirical expression (base of log = 10)

$$\frac{1}{m} = 5 + \log_{10}\left(\frac{R_e}{R_{eo}}\right) \quad \text{generally } 4 < \frac{1}{m} < 10$$

For rough surfaces, f may be increased; besides, in turbomachines wall friction develops under not stationary conditions, and f is therefore greater than at stationary flow in pipes.

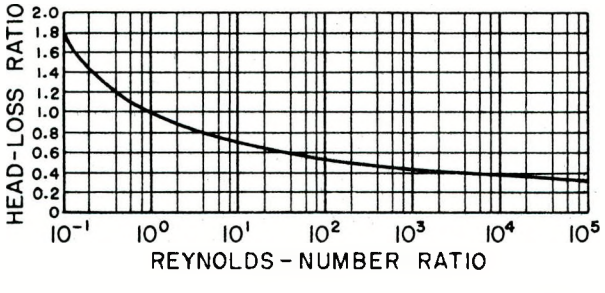


Fig. 5-1 - Head-Loss Correction Curve

Finally, the adjustable expressions for the hydraulic efficiency become

$$\frac{1}{\eta_h} = 1 + \zeta_o \left(\frac{Re_o}{Re}\right)^m \quad \text{for compressor, and}$$

$$\eta_h = 1 - \zeta_o \left(\frac{Re_o}{Re}\right)^m \quad \text{for turbines}$$

where ζ_o is to be computed from

$$\zeta_o H = H_{v,I} + H_{v,II} + H_{v,III} \text{ with } \zeta_s = 0.10 \text{ and } f = 0.004$$

5.1.4 Optimum Obtainable Efficiency

All foregoing expressions are derived for one-stage machines and, under the assumption of best design and manufacturing, the above approximate procedure also leads to high efficiency values for compressors. Comparison of calculated and test values has shown that such high figures are possible. It seems to be established that even compressors are possible with a 90% efficiency, provided the flow retardation across the machine is so small that no noticeable flow separation occurs anywhere. Particular care must be taken at the conversion of kinetic energy into pressure in the diffuser. In good agreement with calculations, one carefully designed fan working at Re = 2.23 x 10^5 gave a total efficiency of 90.3%[78,79].

For multi-stage machines, each stage must be separately considered when the Reynolds numbers of the stages are different, and must account for additional losses $H_{vz} = \sum_{i=1}^{i} H_{vzi}$, as for example in turbocompressors the pressure losses Δp_i in the intercoolers $\left(H_{vz} = \sum_{i=1}^{i} \frac{\Delta p_i}{\gamma_i}\right)$ or in gas turbines in interconnecting ducts between stage groups. The thermodynamic increase in head due to reheat is accounted for by the coefficient ρ. Thus, the specific work (head) done or absorbed by a multi-stage runner is

$$H_r = H(1 + \rho) + H_{vz} + \Sigma\left[H_{vo}\left(\frac{Re_o}{Re}\right)^m\right] =$$

$$= H\left[1 + \rho + \zeta + \left(\frac{H_{vz}}{H}\right)\right] \quad \text{for compressors, and}$$

$$H_r = H(1 + \rho) - H_{vz} - \Sigma\left[H_{vo}\left(\frac{Re_o}{Re}\right)^m\right] =$$

$$= H\left[1 + \rho - \zeta - \left(\frac{H_{vz}}{H}\right)\right] \quad \text{for turbines.}$$

The total peripheral power of a multi-stage runner is

$$P_u = (G - \Delta G_e + \Delta G_{im})H_r \quad \text{for compressors, and}$$

$$P_u = (G - \Delta G_e - \Delta G_{im})H_r \quad \text{for turbines,}$$

where ΔG_{im} is the mean inner leakage mass flow over all stages, calculable from separate stage values. Proceeding in the above indicated manner, it is possible to get the total efficiency for multi-stage machines. The conditions in multi-stage machines are considerably less favorable for obtaining high efficiencies than in single-stage machines.

The efficiency is here reduced not only by partial admission, narrow runner widths (or short blades in axials), and additional losses, but also the inner leakage losses are greater in multi-stage machines. Additional losses are often caused by considerable gaps in the axial direction to permit the safe thermal expansion of long runners. Short-pitched blading exerts a particularly unfavorable influence, not only because of smaller Reynolds numbers but also because the ratio of blade tip thickness to width of passage increases which in turn increases the tip losses. In turbine stages, the enthalpy drop per stage is relatively high, which leads to high blade loadings, therefore, to high flow deflections, which particularly in impulse turbines cause perceptable losses. However, the conditions in gas turbines are more favorable than

in steam turbines, and it is still possible to use airfoil blading similar to those used in compressors, without necessitating an exaggerated number of stages. The blades in gas turbines can be built relatively short and strong because, in the gas turbine, the change in volume of the driving medium reaches 1:10 at the most while in the steam turbine this value can be as high as 1:1500.

5.1.5 Evaluation of Model Tests

The foregoing method of calculations can also be applied for an evaluation of model tests. Let us denote the values referring to the model with a dash. For Compressors

$$\frac{1}{\eta_h} = 1 + \frac{H_v}{H} = 1 + \zeta \text{ or } \frac{1}{\eta'_h} = 1 + \zeta', \text{ respectively}$$

For Turbines

$$\eta_h = 1 - \frac{H_v}{H} = 1 - \zeta \text{ or } \eta'_h = 1 - \zeta', \text{ respectively}$$

According to previous equations

$$\zeta = \zeta' \frac{\zeta}{\zeta_o} \frac{\zeta_o}{\zeta'} = \zeta' \left(\frac{Re_o}{Re}\right)^m \left(\frac{Re'}{Re_o}\right)^{m'}$$

$Re_o = 2 \times 10^5$ and m' follows from $\frac{Re'}{Re_o}$

The value of ζ' is obtainable from the total efficiency.

For Compressors

$$\frac{1}{\eta'} = \frac{P'}{P'_o} = \frac{P'_u + P'_r + P'_m}{G'H'} =$$

$$= (1 + \zeta')\left(1 - \frac{\Delta G'_e}{G'} + \frac{\Delta G'_{im}}{G'}\right) + \frac{P'_r + P'_m}{P'_o}$$

For Turbines

$$\eta = \frac{P'}{P_o'} = \frac{P_u' - P_u' - P_m'}{G'H} =$$

$$= (1 - \zeta')\left(1 - \frac{\Delta G_e'}{G'} - \frac{\Delta G'_{im}}{G'}\right) - \frac{P_r' + P_m'}{P_e'}$$

Computing the values of P_r', P_m', $\Delta G_e'$, $\Delta G'_{im}$, and the corresponding values for the prototype, the efficiency of the full-size machine can be determined:

For Compressors

$$\frac{1}{\eta} = (1 + \zeta)\left(1 - \frac{\Delta G_e}{G} + \frac{\Delta G_i}{G}\right) + \frac{P_r + P_m}{P_o}, \text{ and}$$

For Turbines

$$\eta = (1 - \zeta)\left(1 - \frac{\Delta G_e}{G} - \frac{\Delta G_i}{G}\right) - \frac{P_r + P_m}{P_o}$$

For these values, other transformation formulae are valid. For example, for the friction in the bearings

$$\frac{P'_m}{P_m} = \frac{f_b LDN}{f'_b L'D'N'}$$

where

L = load on bearing

f_b = coefficient of bearing friction

D = bearing diameter

N = speed of shaft rotation.

Values for impeller friction can be determined from literature sources[80].

Usually the gaps, determining the leakage losses, are not in the same proportion to the main machine dimensions. Therefore, it is

always advisable to separate the influence of secondary losses on the total efficiency, as above, because it is most important to recognize each of the losses.

For multi-stage arrangements, a slightly different expression may be used

For Compressors

$$\frac{1}{\eta} = \left[1 + \rho + \zeta + \left(\frac{H_{vz}}{H}\right)\right]\left(1 - \frac{\Delta G_e}{G} + \frac{\Delta G_{im}}{G}\right) + \frac{P_r + P_m}{P_o}$$

For Turbines

$$\eta = \left[1 + \rho - \zeta - \left(\frac{H_{vz}}{H}\right)\right]\left(1 - \frac{\Delta G_e}{G} - \frac{\Delta G_{im}}{G}\right) - \frac{P_r + P_m}{P_o}$$

together with $$\zeta = \frac{1}{H} \Sigma \left[H_{vo} \left(\frac{Re_o}{Re}\right)^m\right]$$

Corresponding equations should be used for the model.

However, it is seldom that pronounced model tests are performed for multi-stage machines. Nevertheless, the expressions are useful for comparing and evaluating typical multi-stage series.

Different definitions exist of efficiencies, and one has to watch carefully to select or interpret the right one. Generally, the internal or hydraulic efficiency includes all inner losses in the turbomachine, not considering shaft friction loss nor losses due to driving of auxiliary equipment. This efficiency is equivalent to the known adiabatic efficiency of a turbomachine if no intercooling of the stages is used and no external leakage losses occur. To compare the efficiency of uncooled stages (blading), the polytropic efficiency is frequently employed and is called stage efficiency. The polytropic efficiency can be represented as a function of a polytropic and adiabatic exponents n and k respectively, where $k = \frac{C_p}{C_v}$ is the specific-heat ratio[48]

$$\eta_{pol} = \frac{1 - \frac{1}{K}}{1 - \frac{1}{n}} \quad \text{for a compressor, and}$$

$$\eta_{pol} = \frac{1 - \frac{1}{n}}{1 - \frac{1}{K}} \quad \text{for a turbine}$$

The adiabatic efficiency, in turn, is connected with the polytropic efficiency by following expressions, with r as compression or expansion ratio, respectively[85]

$$\eta_{ad} = \frac{1 - r}{1 - r^{\frac{1}{\eta_{pol}}}} \quad \text{for a compressor, and}$$

$$\eta_{ad} = \frac{1 - \left(\frac{1}{r}\right)^{\eta_{pol}}}{1 - \frac{1}{r}} \quad \text{for a turbine}$$

The following considerations show how another expression for the stage efficiency, different from polytropic efficiency, can be derived for the case of a turbine stage, as an example, without further analyzing the difference between the two efficiencies[76]. The internal efficiency η_i can be considered as the stage efficiency if the kinetic energy of the absolute velocity c_2 after the rotor is lost. This is usually the case for single-stage turbines. In multi-stage turbines, however, part of this kinetic energy will increase the isentropic enthalpy drop of the next stage because it constitutes the kinetic energy $c_e^2/2$ at its entrance. For the last stage of a stationary turbine the energy $c_2^2/2$ represents a loss, whereas in aircraft turbines or other propulsive devices the velocity c_2 can be used in part to produce useful thrust.

Let

$$\frac{c_e^2}{2} = K_e \frac{c_2^2}{2}$$

be that part of the kinetic energy of the exit velocity c_2 that contributes to the total isentropic energy of the next stage or which can be considered as useful energy. The carry-over coefficient K_e will be close to unity for the intermediate stages of a multi-stage turbine, and is zero for the last stage. For propulsive units, the factor K_e will depend on the flow angle α_2 also, because the axial component of c_2 can usually be used only to produce thrust. The actual isentropic enthalpy drop of stages where $K_e c_2^2/2$ represents useful energy is then $\Delta h_{is} - c_e^2/2$, and the stage efficiency η_s of such stages is more properly defined as

$$\eta_s = \frac{\eta_i}{1 - K_e\left(\frac{c_2^2}{c_o^2}\right)}$$

For $K_e = 0$, the stage efficiency η_s is equal to the internal efficiency η_i. It is advantageous to express the performance of a turbine stage by means of dimensionless coefficients. The peripheral speed u_1 at the rotor inlet is mainly limited by stress considerations, hence its value is usually fixed. To estimate the number of stages, it is necessary to know the isentropic enthalpy drop which can be handled by a stage at different speeds u_1. If a turbine has to generate a specified power, the work that a stage can produce per unit mass of fluid at given peripheral speeds u_1 must also be known. For these reasons the following coefficients are introduced

$$K_{is} = \frac{\Delta h_{is}}{u_1^2/2} = \left(\frac{c_o}{u_1}\right)^2 \qquad \text{head coefficient}$$

$$K_w = \frac{\Delta H}{u_1^2/2} \qquad \text{work coefficient}$$

Where Δh_{is} is the total isentropic enthalpy drop and ΔH the total energy change of the gas. The head coefficient relates the total isentropic drop of the stage to the kinetic "energy" of the peripheral speed at the rotor entrance, and the work coefficient is a measure for the actual work that the stage generates per unit mass of fluid. In

$$\Delta h_{is} = K_{is} \frac{u_1^2}{2}$$

$$\Delta H = K_w \frac{u_1^2}{2}$$

the enthalpy drop and the work of the stage have the dimension foot-pounds/slug. These quantities can be converted into Btu/lb by multiplying with the factor 3.994×10^{-5}.

For the calculation of the kinetic energy $c_2^2/2$ at the stage exit, there is introduced the leaving loss coefficient K_v

$$K_v = \left(\frac{c_2}{u_1} \right)^2$$

The work factor is then obtained from

$$K_w = \eta_i K_{is} = \eta_s \left(1 - K_e \frac{K_v}{K_{is}} \right) K_{is}$$

and the stage efficiency is

$$\eta_s = \eta_i \frac{1}{1 - K_e (K_v / K_{is})}$$

The performance of a turbine stage is therefore determined by the head coefficient K_{is}, the leaving loss coefficient K_v, and the stage efficiency η_s for a given carry-over coefficient K_e[76].

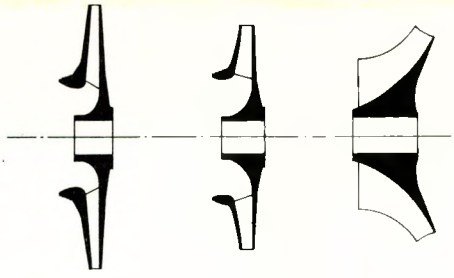
5.2 Radial and Mixed-Flow Compressors

The most significant developments in recent years have been better performance, higher tip speeds and successful use of "flexible" rotors. Better stage performance has been achieved through increased knowledge of internal gas dynamics. Better overall performance has resulted from the proper application of improved stages and by increased use of cooling during the compression. Higher tip speeds, particularly in closed wheels, have been made possible by significant metallurgical advances and the development of high strength welded wheels. The use of "flexible" rotors has been essential to large numbers of stages at high speed and has succeeded through improved balancing techniques and increased knowledge of rotor dynamics.

In many high compression applications, the discharge volume is only a fraction of the inlet volume. This requires careful attention to wheel design because the specific speed of the first wheels is much higher than that of the last wheels. The specific speed is a useful parameter from which the designer can estimate the performance of a stage, the proportions of the wheel, its blade configuration, and the stress level to be expected. Figure 5-2[81] shows typical proportions of low, medium, and high specific speed wheels.

Some designers prefer other parameters than specific speed to describe the general characteristics of a wheel or stage. Two typical flow coefficients are listed in Figure 5-2 in addition to the specific speed. Any of these characteristic numbers serves primarily as a guide and a means of comparison rather than a rigorous numerical design tool.

The performance of a single stage with vaneless diffuser can be calculated quite accurately. Many tests have been run over a wide range of speed, flow, and head, giving results as shown in Figure 5-3[81]. The fact that a band must be shown on this curve rather than a single line indicates simply that the specific speed is not adequate for a



SPEC. SPEED $N_s = N\sqrt{Q_1}/H^{.75}$	460	720	1310
1 $Q1/ND^3$	.064	.120	.343
2 C_{m2}/U_2	.181	.249	.387
STAGE ISENTR. EFFICIENCY	81%	82.5%	87.5%

Fig. 5-2 - Wheel Proportions for Radial and Mixed Flow Compressors

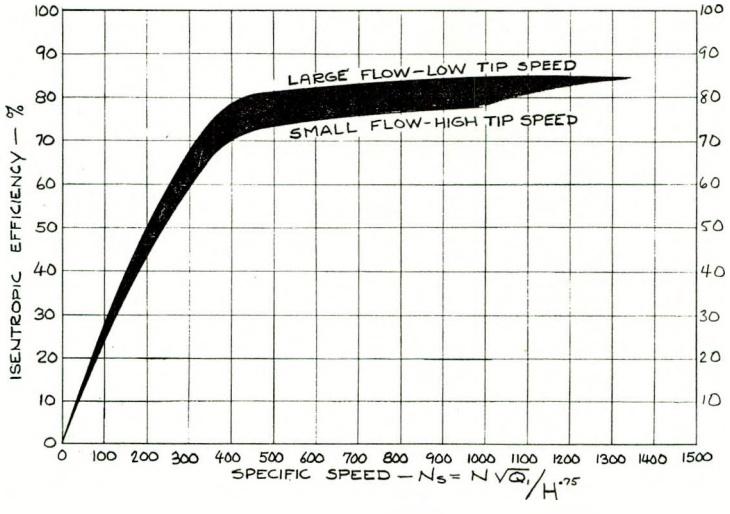


Fig. 5-3 - Stage Performance with Vaneless Diffusers

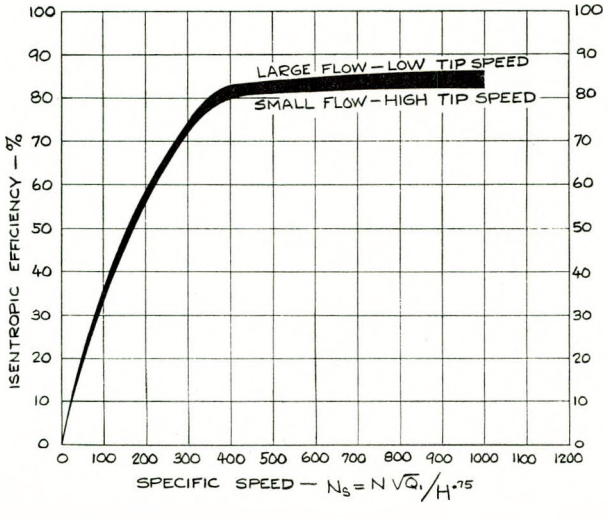


Fig. 5-4 - Stage Performance with Vaned Diffusers

rigorous definition of performance. When tip speeds and Mach numbers are high, efficiency is lower at any specific speed. Also it is always true that large machines are more efficient than small ones. Lesser variations in the band may be attributed to Reynolds number and heat transfer differences.

Figure 5-3 is drawn for vaneless diffusers. Considerable improvement in peak stage efficiency can be obtained with special vaned diffusers, particularly at lower specific speeds. Although they tend to reduce the operating flow limits of the stage and may sometimes cause high-pitched noise, such diffusers are extremely attractive in some applications. Figure 5-4[81] shows stage performance with vaned diffusers. Again a band must be shown because specific speed cannot include the effects of all design variables.

AiResearch reports efficiencies of 1-, 2-, and 3-stage designs as shown in Figure 5-5[10] plotted against compressor pressure ratio. AiResearch uses radial compressors exclusively, one stage for very small prime movers and two or three stages for larger prime movers. Major improvements in efficiency were achieved as a result of intensive research programs and of establishing efficient aerodynamic design criteria[82]. Although single-stage compressors with a 7:1 pressure ratio were developed and tested, it is preferred to limit the designs to a much lower pressure ratio per stage in order to obtain maximum reliability and performance. For the same pressure ratio, a one-stage compressor has to operate with 1.414 times the top speed of a two-stage compressor, which causes twice the stress in the rotating wheel and, in turn, requires much better and more expensive materials.

The design philosophy of using two or three stages for the compressor appears to be even more justified when possible burst failures of the rotating compressor wheels are considered. Such a failure may not necessarily occur because of material fatigue; it may also be caused by casting or forging flaws not detected by normal

THE FRANKLIN INSTITUTE • Laboratories for Research and Development

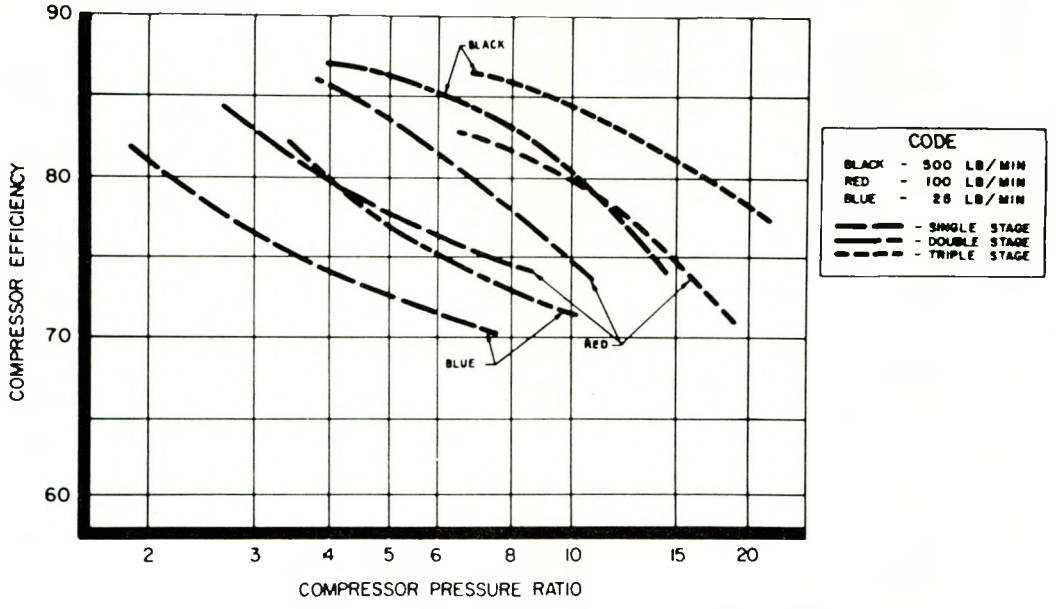


Fig. 5-5 - Obtainable Radial Compressor Efficiencies, Representative of Advanced Engines

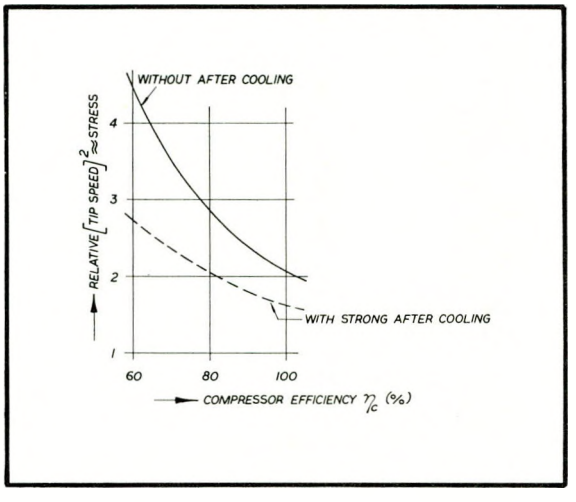


Fig. 5-6 - Influence of Compressor Efficiency on Impeller Stress

quality control. AiResearch investigations show that the rotational energy of a double-entry, single-stage compressor is seven times higher than the energy of a two-stage compressor, if the impellers are titanium. Of course, steel impellers are less expensive. For steel, the ratio is more favorable to the two-stage compressor.

Rotational energy is an extremely important design factor because so many applications require containment and protection against such a failure[10]. Furthermore, there is an inherent influence of compressor efficiency on its impeller stresses. High compressor efficiency is not only desirable for the engine itself but also for the compressor proper, requiring lower tip speeds of the impeller. The reason for this reduction is two-fold, first because the pressure ratio is smaller and second because for any pressure ratio, a highly efficient compressor requires a smaller tip speed assuming the same basic compressor blading type. Since the tip speeds of compressors are high anyway, the resulting reductions in impeller stresses due to centrifugal forces are really significant. Figure 5-6[83] shows the influence of compressor efficiency on impeller stress for a turbocharger, for a density ratio of 1:6. For a selected impeller material and process of manufacturing, there is a definite upper limit of acceptable stress level in the impeller. It is obvious that low compressor efficiency will require an impeller design which is heavier, has a large moment of inertia, contains more stored kinetic energy of rotation, results in higher bearing loads, and in the case of overhung rotor arrangement, will also increase the overhung rotor bending moment on the shaft[83].

For each application, a careful balance of gas dynamics, mechanics, metallurgy, strength of materials, and vibration analysis is vital to achieve the desired result of a good compressor every time. The variety of applications and the typically brisk production schedules do not permit extensive analysis or prototype evaluation for each compressor. Instead of this classical approach, several standard frame

sizes or casings are frequently used; for each frame, a family of wheels, diaphragms, and guide vanes is designed to encompass the complete range of flows and pressures the frame may be expected to handle.

In a multistage compressor, the designer's objective is, of course, to keep all stages within the good efficiency range shown in Figures 5-3 or 5-4. This is not always possible when the compression ratio is high or when the application falls near the lower limit of a particular frame size. In any case, the first stages will be more efficient than the last stages. This leads to the conclusion that more work must be done in the more efficient first stages and that these wheels should be larger in diameter and run at higher tip speeds than the last stages. Until recently, wheel stress limitations precluded such an arrangement and most rotors were designed with the same wheel diameter for all stages.

Another means of improving overall performance is intermediate cooling during compression. Water cooled diaphragms were first used over thirty years ago. Originally, liquid cooling was intended only to keep metal temperatures down. Later, improvements in design led to considerable performance improvement as well as metal cooling. Limits on this method of cooling are fixed by the restricted heat transfer surface that can be obtained in the internal gas passages of the compressor.

To obtain further improvement from cooling, special compressors have been designed from which the air or gas is withdrawn from the compressor case at several intermediate points and led through large-surface heat exchangers. The ultimate in such designs is cooling after each stage of compression. The benefits of cooling in air compressors are shown in Figure 5-7[81]. Figure 5-8[81] shows the reduction in discharge temperature which can be accomplished by cooling. Besides improving efficiency, cooling can be extremely helpful in handling special gases wherein high temperatures are dangerous or harmful to the process.

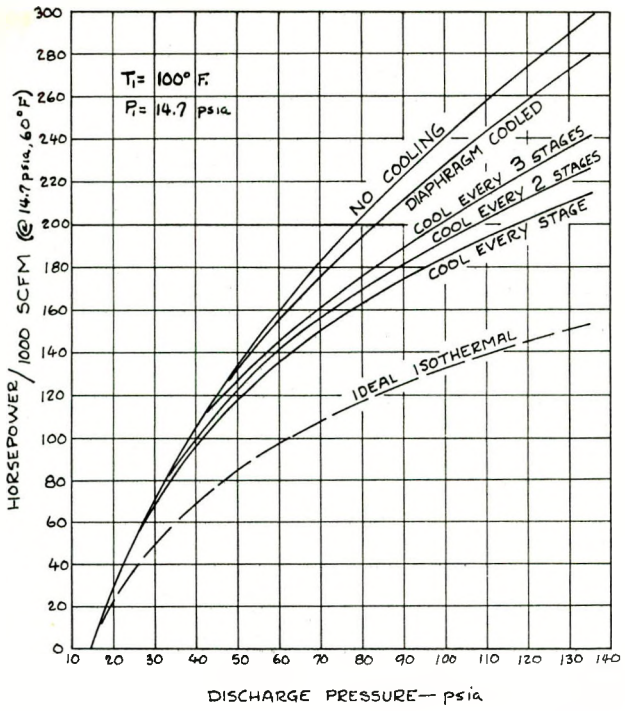


Fig. 5-7 - Effect of Cooling on Horsepower

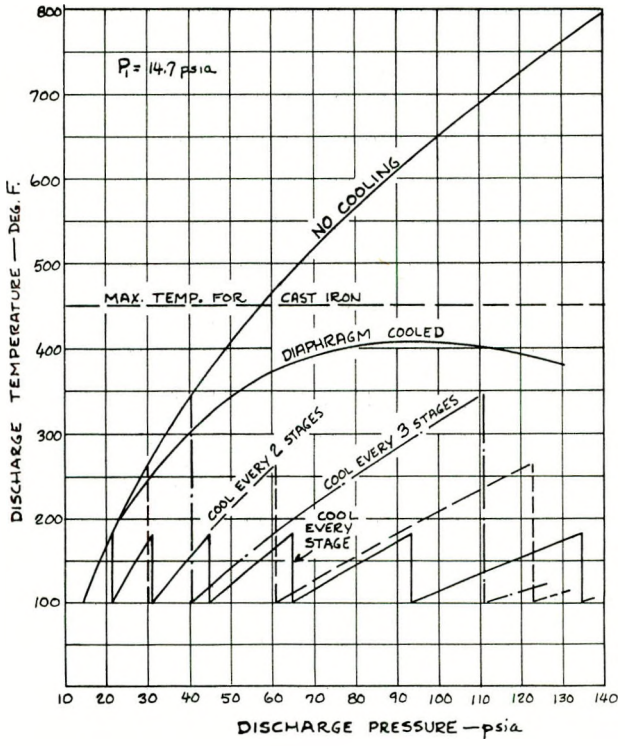


Fig. 5-8 - Effect of Cooling on Discharge Temperature

Intermediate cooling results in higher pressure ratios per stage and increased compression in a single compressor body. This increases the change in specific speed from the first to the last stage and makes it more imperative that as much work as possible be done in the efficient early stages. The arrangement of an intercooled multi-stage radial compressor is shown in Figure 5-9[42].

Systematic tests carried out by Oerlikon, Switzerland, on improvement of radial compressors intended for a 1000 kw gas-turbine installation led to a special design of a scroll with a multiple-diffuser discharger (see Figures 5-10 and 5-11[48]). With this arrangement, Oerlikon improved the stage efficiency from 76% of the basic design with the single-diffuser discharger to the value of 88% at a stage-pressure ratio of 1:63. For the 3-stage compressor, this resulted in 86% adiabatic efficiency, or 74% isothermal efficiency at the optimum operation point because of intercooling. The Oerlikon tests proved that the main origin of losses in a conventional radial compressor is the stationary scroll and not the impeller[48].

Figure 5-12[83] shows how the radial compressor works. Swirl-free air, i.e. air which does not rotate around the axis of the machine, is aspirated, and enters the bladed impeller through the inlet eye. The blades impart a swirling motion upon the air which leaves the impeller at its O.D. The work which has been put into the air is equal to $u\, c_u/g$ for every pound of air, where u is the impeller tip speed and c_u is the circumferential component of the velocity vector c of the air at the impeller discharge. It is to be noted that quite a sizeable portion of this work input is in the form of kinetic energy $c^2/2g$ at the impeller exit. Another part is therefore necessary, the diffuser, which converts this kinetic energy into useful rise of static pressure by slowing the high velocity air carefully down to an acceptable value.

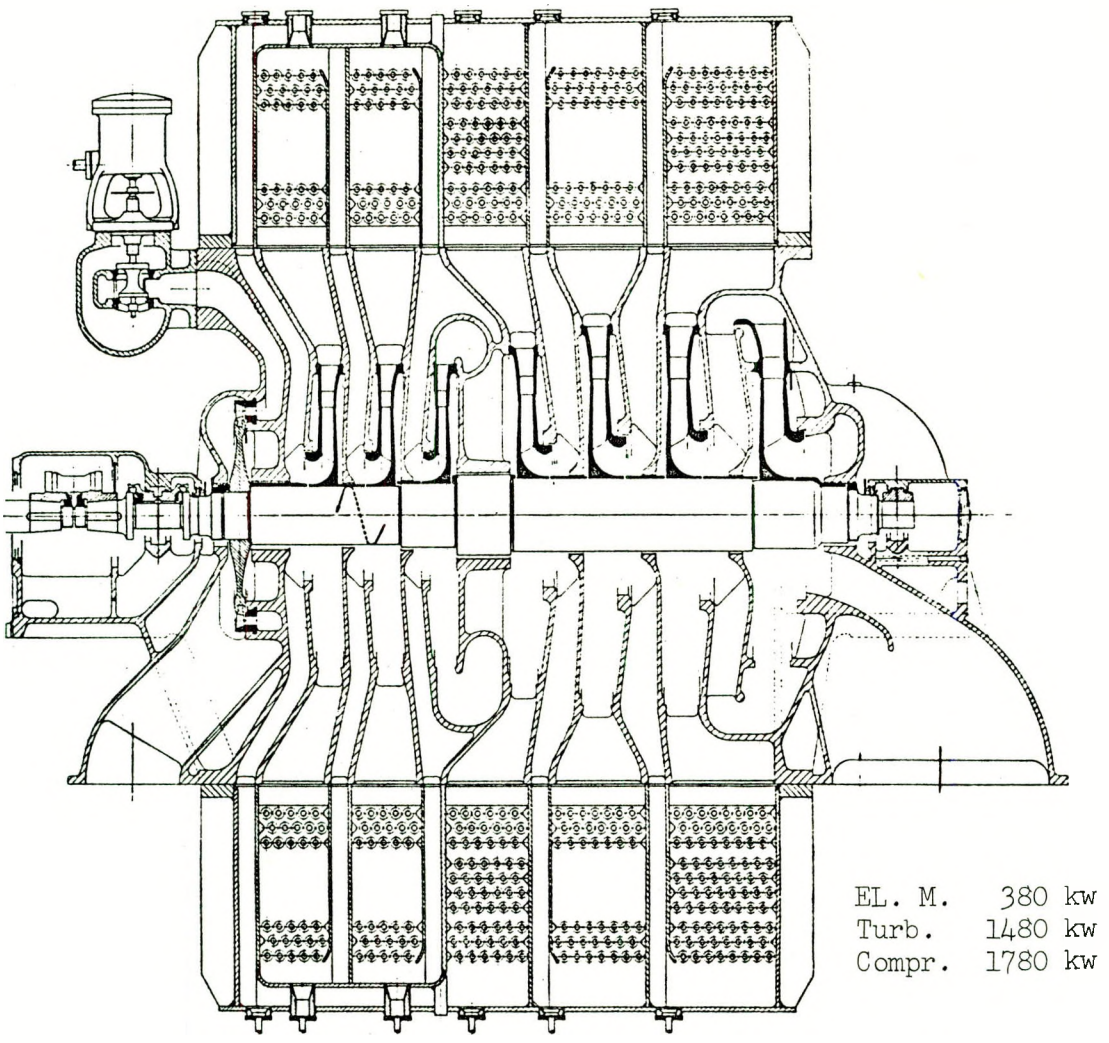


Fig. 5-9 - Intercooled Multi-Stage Radial Compressor

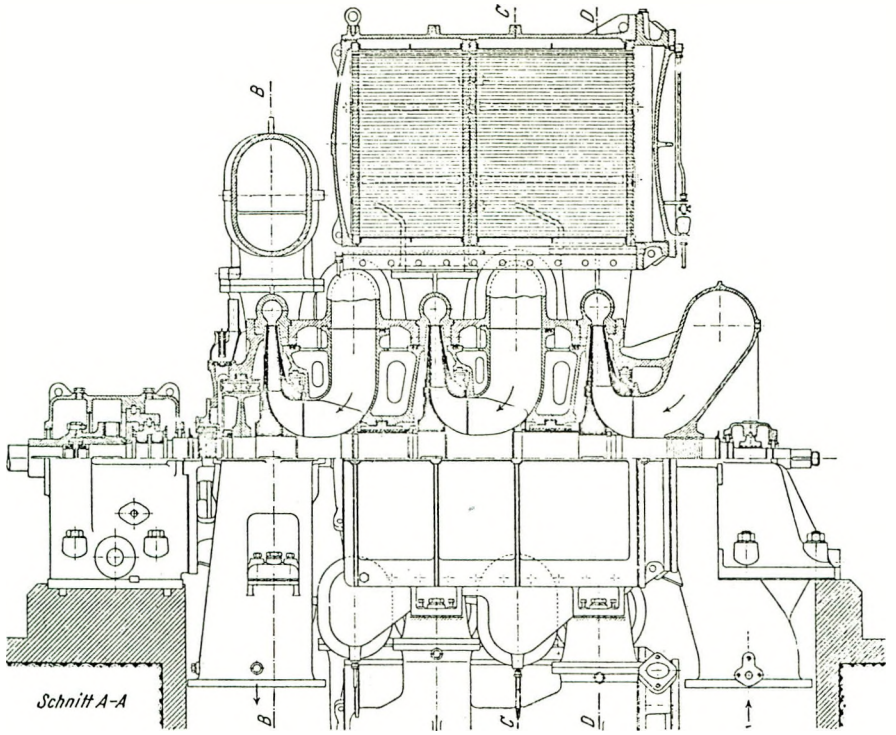


Fig. 5-10 - Oerlikon Radial Compressor Longitudinal Section

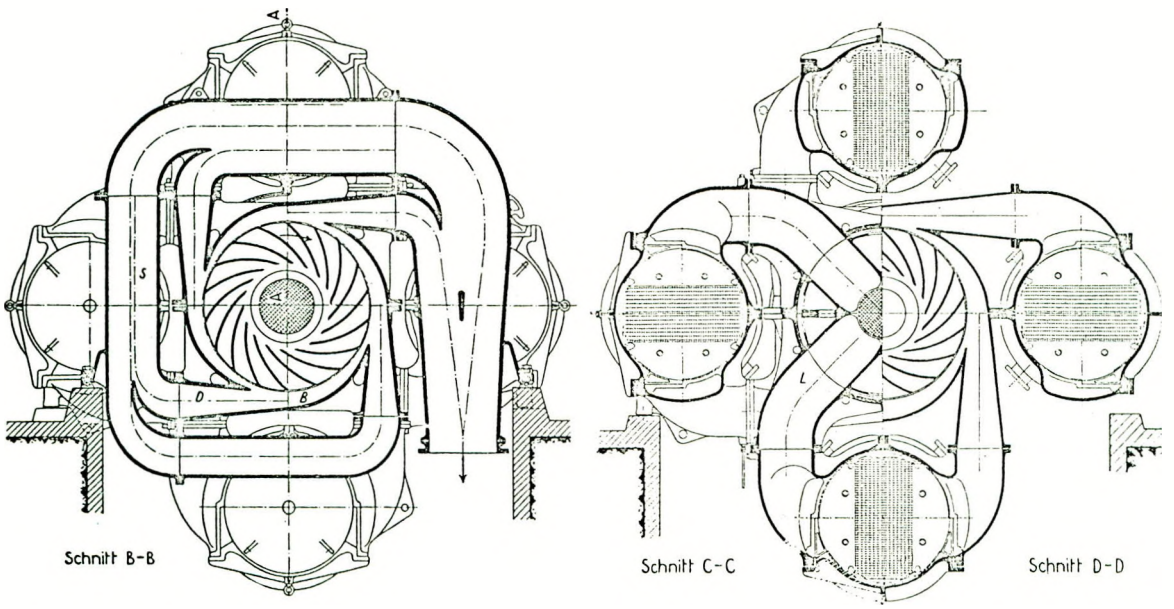


Fig. 5-11 - Oerlikon Radial Compressor Cross-Section

Different types of impeller blades are in use. The impeller exit velocity triangle at the left of Figure 5-12 corresponds to a 90° blading, the one at the right to a backward curved blading. Both blade types have their advantages and disadvantages. In comparison to the 90° blading, the backward curved blading requires a higher tip speed, the leaving velocity c, however, is smaller which means that a larger percentage of the overall pressure rise takes place within the impeller itself, and the diffuser becomes less important (high degree of reaction). This has two major consequences. First, the maximum pressure ratio for impellers of similar disk shapes is lower because of strength considerations, and second, the operating range is wider. In addition, peak compressor efficiency is usually higher.

Both blade types have been widely and successfully used, for example, in turbochargers. A single turbocharger model using a backward curved bladed impeller can cover a wide range of engines of different air flows for medium pressure ratio turbocharging. This is quite significant when it comes to questions of total production volume, spare part stock, and maintenance. The 90° compressor turbocharger will require more turbocharger models to cover the same range of engines. It will, however, permit a larger power boost.

The simplest type of diffuser design is a so-called vaneless diffuser. It does a good job in conjunction with backward curved impeller blades for compressors requiring a wide operating range. Vaned diffusers are usually used together with 90° compressors. Because the air leaves a 90° impeller with high velocity, approaching or even exceeding the velocity of sound, vaned diffusers are often combined with short vaneless diffusers in order to improve the operating range.

The small graph at the bottom of Figure 5-12 illustrates the pressure rise, the losses in the impeller and in the diffuser, the total work input, and the useful output, of a 90° compressor running at constant speed, as a function of air flow.

Figure 5-13[83] shows one side plate of a vaneless diffuser. The picture indicates the spiraling motion of the air which has been made visible by injecting a lamp black-petroleum mixture into the compressor intake while running. The air, after leaving the diffuser has to be collected. Two types of housings have been widely used, volute type or torus type. Figure 5-14[83] shows a volute housing and Figure 5-15[26] a torus type.

Figure 5-16[83] shows the performance maps of three different compressors. They are all of similar peak efficiency, have impellers of the same diameter, however, with different degrees of blade backward curvature, and have also approximately the same air flow at the same pressure ratio (similar gulp capacity). The operating ranges are bound at the left by the surge line and at the right, for comparative purposes, by a 70% efficiency line. The dotted speed lines correspond to the same impeller tip speed. The figure illustrates drastically the statements made above about range and pressure ratio. In fairness to the 90° compressor map shown it should be said, however, that this compressor has been developed for a high compressor peak efficiency and that the range could be improved by sacrificing peak efficiency.

Referring back to Figure 5-12, the work input equation shown there is simple. It is only a consequence of basic fluid mechanics and has nothing to do with aerodynamics. It for sure does not give any information on how to achieve high efficiency and it does not help to determine optimum shapes of blades, meridional contours, blade numbers, etc. Certainly average performance turbomachines can be built with nothing more than basic mechanical engineering sense. To build high performance machines of high gulp capacity and of fairly small absolute dimensions, however, a lot of aerodynamical work of an analytical and experimental nature is required. Even with today's aerodynamical know-how, electronic high speed computing machines, etc. there is still a lot of feel left which makes an aerodynamicist a half-artist. Figure 5-17[83],

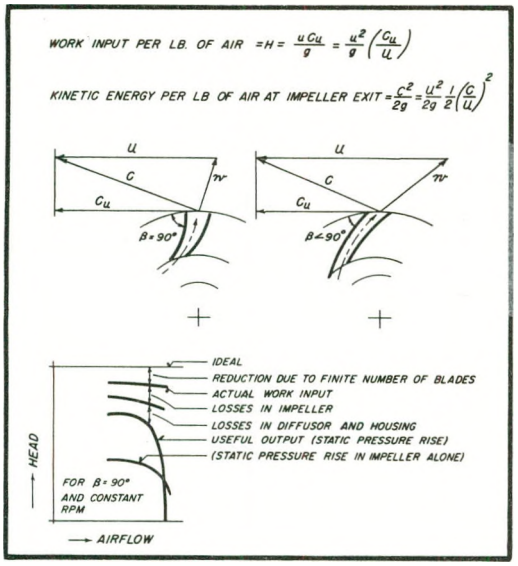


Fig. 5-12 - Velocity Triangle at Impeller Exit

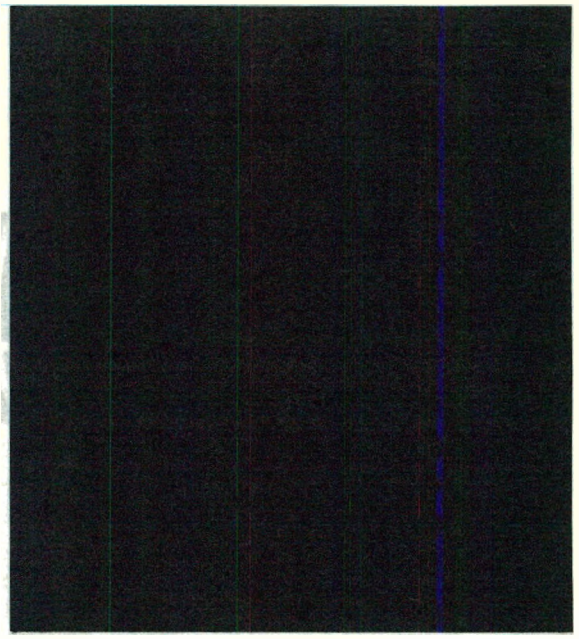


Fig. 5-13 - Flow Pattern in Vaneless Diffuser

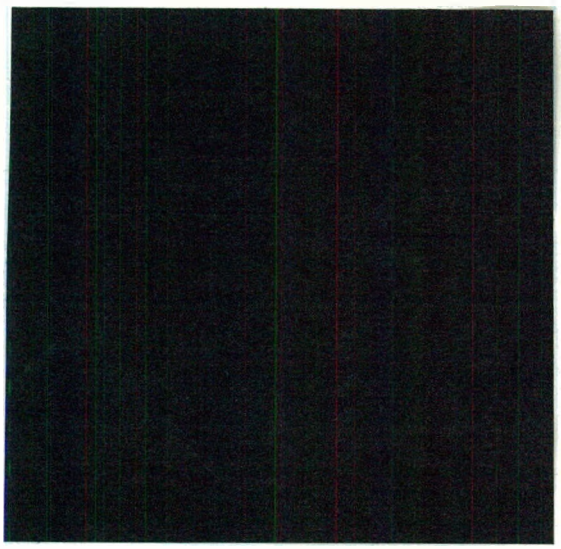


Fig. 5-14 - AiResearch Turbocharger Model T1407

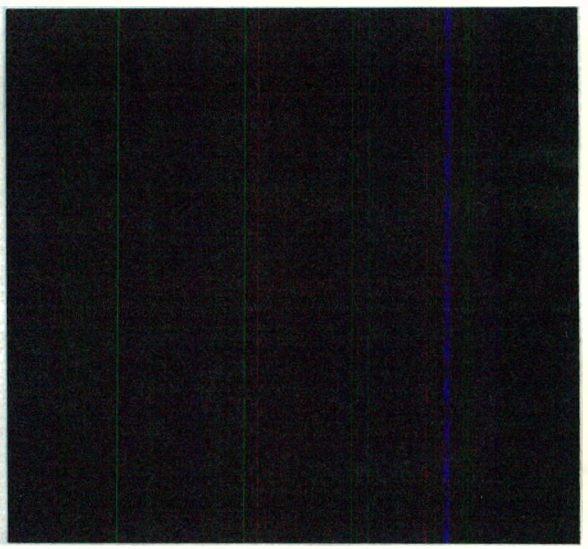


Fig. 5-15 - Compressor Wheel and Diffuser Assembly in a Torus-Type Casing - 100 hp Lightweight Gas-Turbine Unit

for example, shows calculated local velocity distributions within the impeller for its design point of rpm and air flow. The velocities are shown for three streamlines, shroud, mean and hub, and for both sides of the blades, pressure and suction side. It is worth while to note the high velocities on the suction side along the shroud streamline which come close to the velocity of sound. Fortunately today's computing machines permit quick calculations of velocity distributions of different geometrical shapes and for off-design points of operation from which a design can be chosen which appears most promising for manufacturing and testing of actual parts. Figure 5-18[83] shows a similar velocity distribution for the suction and pressure side of a diffuser vane operating near the design point.

One possibility to work at high tip speeds and hence to attain high stage pressure ratios without surpassing the sonic velocity is offered by the Birmann-blading used by DeLaval. This Birmann-blading results in a type of mixed flow compressor. Because of the backward curved blade, the relative entrance velocity of the compressed gas remains subsonic even when the tip velocity of the blade is transonic. In addition, the blade is positioned radially regardless of its negative curvature and is, therefore, favorably stressed[48]. Figure 5-19 shows a mixed-flow compressor rotor of DeLaval with Birmann-blading.

Procedures for designing hub-shroud contour and blade shape of mixed-flow and radial impellers were worked out by various investigators. Experimental results in general indicate that these design procedures are reliable. Also, results of the experimental work indicate that a good level of performance can be obtained with the design procedures. However, detailed studies of the flow in the impeller seem to indicate that the boundary-layer build-up does not occur in the manner supposed, so that a different means of allowing for boundary-layer build-up might well result in better performance. Tests with vaned diffusers indicate, that, in order to avoid the performance penalties incurred by use of vaned diffusers, more information is needed concerning viscous effects and diffuser-impeller interactions[84].

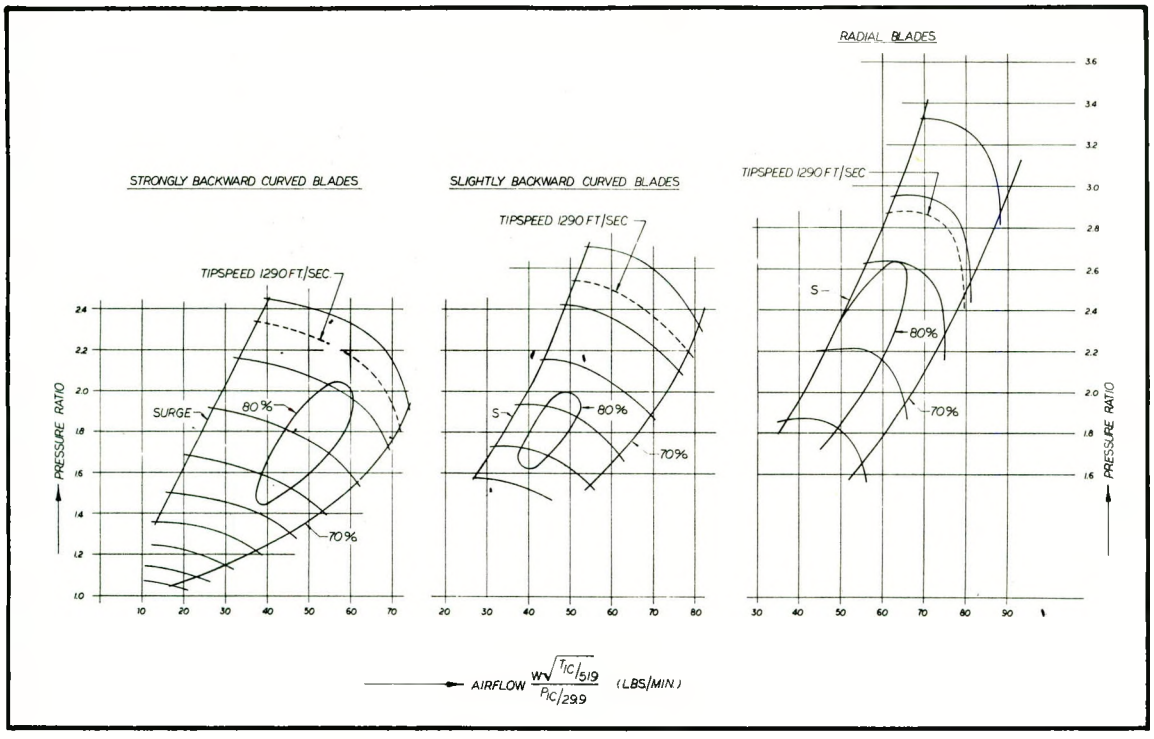


Fig. 5-16 - Influence of Blade Curvature on Compressor Map

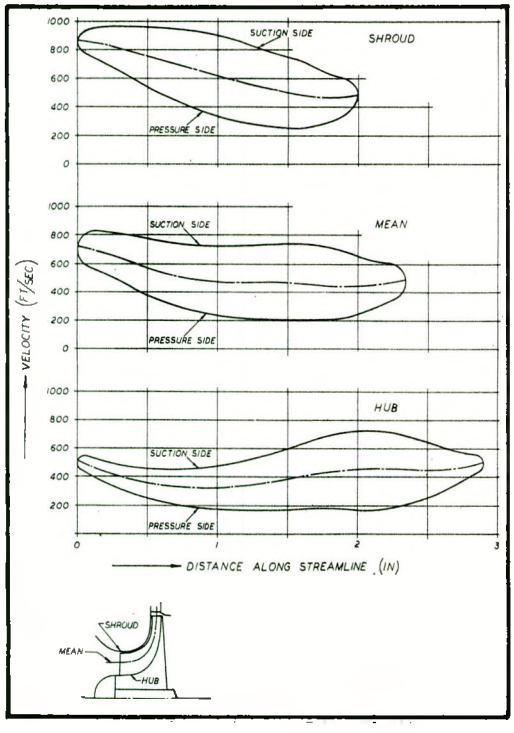


Fig. 5-17 - Velocity Distribution Along Impeller Blade

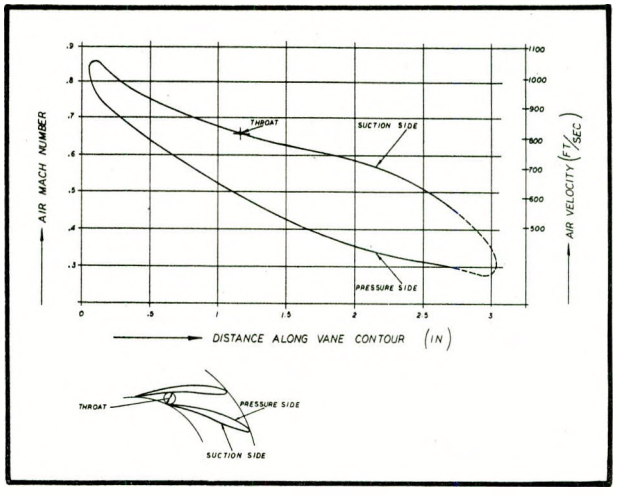


Fig. 5-18 - Velocity Distribution Along Diffuser Vane

The performance of a radial compressor is a function of the impeller and diffuser characteristics, and their relative matching and interaction.

A critical problem in the design of radial compressors is the diffusion of high air velocities leaving the impeller tip, to the low velocities normally required at the compressor outlet. For pressure ratios less than 2.5:1, it is advantageous to employ vaneless, free vortex diffusion because efficiency is comparable with vaned diffusers and the flow range is wider. The latter is extremely desirable when more than one stage of compression is required because the matching problem between the stages becomes less acute. For higher pressure ratios, diffusion is most efficiently accomplished with vane diffusers preceded by an intermediate vaneless space. Diffuser vanes exert greater flow control and, in addition, advantage may be taken of their presence to apply an outward deflection to the flow, thereby obtaining an increased rate of static pressure. Vaned diffuser profile selection is a compromise between the incident Mach number, the vane number required to avoid impeller excitation within operating speed range, and the diffuser entry to exit diameter ratio. Tests on four types of vaned diffusers of equal camber have shown that vane profile has only a minor effect on diffuser efficiency at an impeller tip speed of 1400 fps and air angle of 80°; whereas, decreasing camber together with increased intermediate, vaneless, space diffusion improved efficiency considerably. Maximum diffuser efficiency was attained with a blade camber of 15° and impeller tip air angle of 75°. Vaneless space diffusion has a smoothing effect on the distributed flow emitting from the impeller tip and tends to improve vaned diffuser operation.

The recommended development procedure is to conduct tests with at least three diffuser capacities in order to cover the complete impeller characteristic; alternatively, at lower tip speeds a vaneless diffuser test may be conducted. A vaneless diffuser test at high tip speeds is not recommended because such a diffuser exhibits a positive

pressure characteristic; that is, efficiency increasing with increasing flow, the gradient of which increases with increasing speed. Accordingly, vaneless diffusion becomes less stable and premature surge may occur before the complete impeller characteristic is obtained.

If, after completing a matching development program on a particular compressor, it is still not possible to attain the desired efficiency level, extensive internal flow research supported by cascade model tests on the particular blading profiles selected may indicate component design modification by which efficiency may be raised[85].

The design of the diffuser influences the surge characteristics of a compressor. This is particularly important in the vehicular gas turbine affecting the acceleration response of such an engine. The Allison Division of General Motors had difficulties with the original diffuser for its GT-305 engine. The installation of a subsequently designed new diffuser resulted in a large increase in compressor surge margin, without entailing any reduction in compressor efficiency during equilibrium operation of the engine[86].

Sometimes transonic flow problems may arise in centrifugal compressors. They are indicated by changes in the performance characteristics of a compressor that occur when operating in the neighborhood of Mach one somewhere in the machine. In general, for the centrifugal compressors used with gas turbine engines, the "somewhere" is limited to the impeller inlet and exit. The performance characteristics that can indicate "Mach number trouble" are over-all compressor efficiency, air flow rate, and the flow range between pulsation and maximum flow of the compressor, any one of which may be more important than the others, depending upon the particular application[87].

5.3 Axial-Flow Compressors

5.3.1 Subsonic Compressors

Past designs of subsonic axial flow compressors were generally based on the use of symmetrical velocity diagrams and thick-nose blade profiles of approximately 10 per cent maximum thickness ratio. These design practices were developed primarily from considerations of isolated-airfoil and two-dimensional low-speed concepts. As a result, serious limitations were imposed on attainable specific weight flow and stage pressure ratio. First, the use of thick blade profiles required that relative inlet Mach numbers be limited to about 0.70 or 0.75 to avoid serious loss penalites or possible choking of flow[88,89]. A typical variation of loss coefficient with Mach number for a conventional 10 per cent thick blade in cascade is illustrated in Figure 5-20(a)[88].

Second, the use of prerotation to maintain the relative inlet Mach number of the rotor within the limiting values or to establish the symmetrical velocity diagram restricted the maximum values of tip speed and inlet velocity, and consequently restricted specific weight flow. In addition, the design velocity diagrams involved such large magnitudes of tangential velocity leaving the rotor that the condition of radial pressure equilibrium resulted in large reductions in axial velocity at the tip of the rotor for low hub-to-tip radius ratio designs. A sample calculation of design values of this relative velocity ratio is shown for a typical subsonic inlet stage in Figure 5-20(b)[88].

The poor flow conditions in the rotor tip region resulting from this velocity deceleration reduced the allowable blade circulation that could be tolerated across the rotor tip sections, so that this effect, in conjunction with the low tip speeds (generally $\leq$ 1000 ft/sec), would allow only a relatively low stage pressure ratio. As a consequence, a typical variation of inlet-stage design pressure ratio with weight flow per unit frontal area might appear as in Figure 5-20(c)[88]. Compressor design procedures at that time were, therefore, basically incapable of producing both high weight flow and high stage pressure ratio.

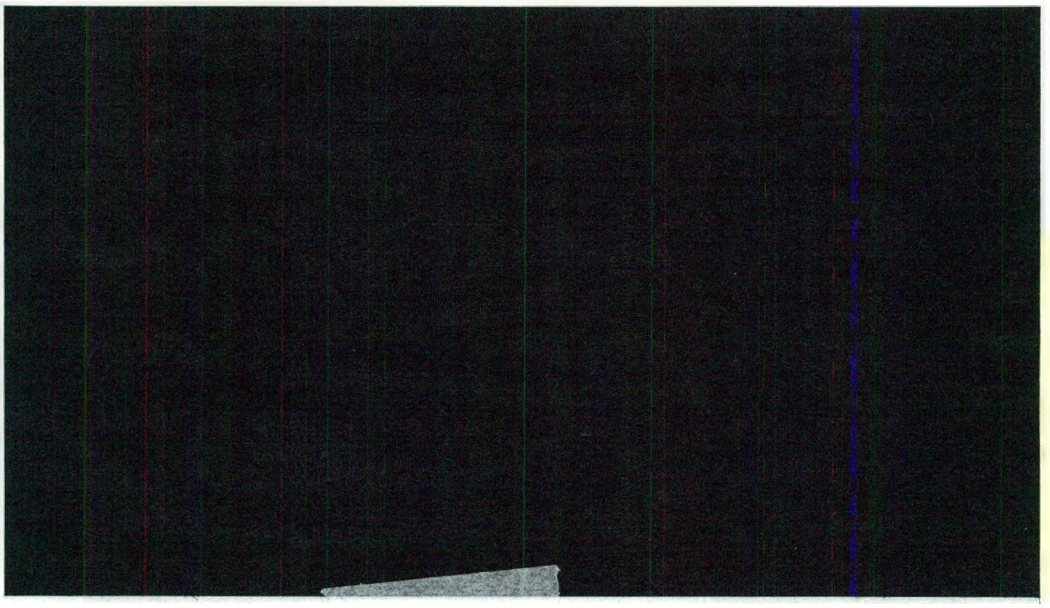


Fig. 5-19 - Barrel Assembly with DeLaval Mixed-Flow Impeller with Birmann- Blading for High Flow and Low Pressure Boost

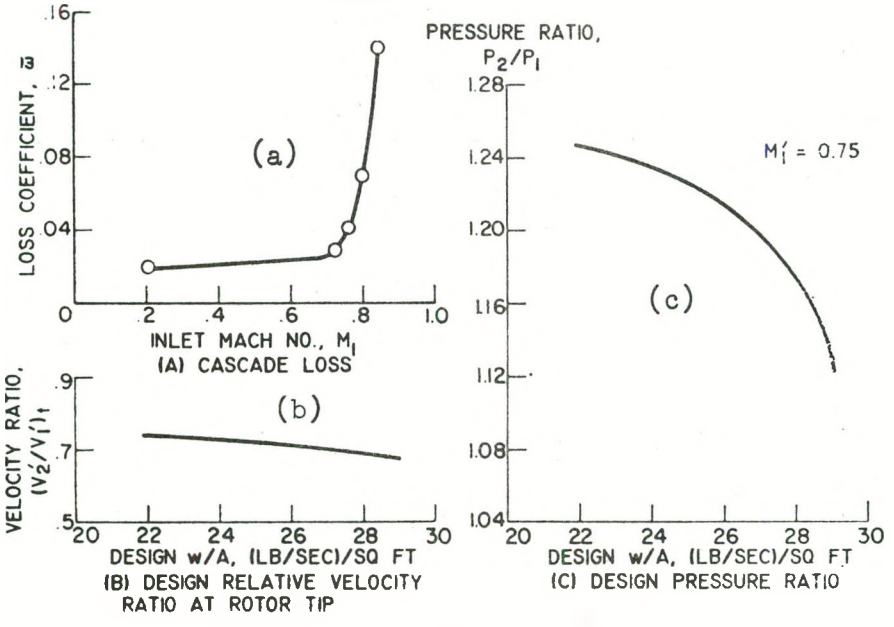


Fig. 5-20 - Limitations of Conventional Subsonic Inlet Stages

Advanced compressor requirements resulted in fundamental research involving[88]

(a) Study of tip-flow conditions and the development of better blade-loading parameters,

(b) Development of blade sections that would allow efficient operation at higher Mach numbers.

(c) Re-evaluation of basic velocity diagrams to get a better relation between weight flow and pressure ratio.

The investigation of blade-loading parameters for compressor sections resulted in the development of the diffusion factor (D-factor) as a criterion of the allowable design blade loading (see Figure 5-21[88]). This parameter was based on the diffusion velocity on the blade suction surface, so that

$$D = 1 - \frac{w_2}{w_1} + \frac{\Delta w_\theta}{2 r w_1}$$

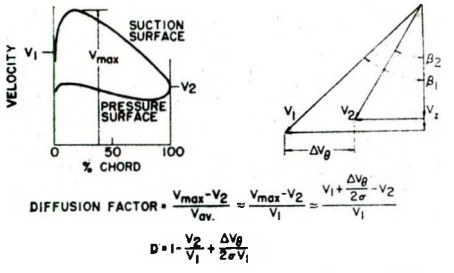
where

r = solidity (ratio chord to pitch)

w_1, w_2 = relative flow velocity at inlet and outlet, respectively

Δw_θ = change in tangential relative velocity across blade element.

The loss coefficient is $(p_2 - p_1)/(p_1 - p_{1i})$ where p_1, p_2 = total pressure at inlet and outlet, respectively, and p_{1i} = static pressure at inlet. Correlation of loss coefficient for rotor and stator sections (Figure 5-22[88]) showed that excessive losses were likely for rotor and stator sections if the diffusion factor in the tip region of the rotor exceeded a value of about 0.4. A simple gross means for relating the limiting blade loading to the velocity diagram was thus obtained for use in design and analysis. Later work on loss and stall characteristics of compressor cascade blade lead to a more refined parameter called the equivalent diffusion ratio. These blade-loading parameters were found to be generally applicable as long as the maximum Mach numbers on the blade surfaces were subsonic or transonic (Mach number less than about 1.2[88]).



Note: On this figure, velocity is designated by V in place of w.

Fig. 5-21 - Development of Diffusion Factor

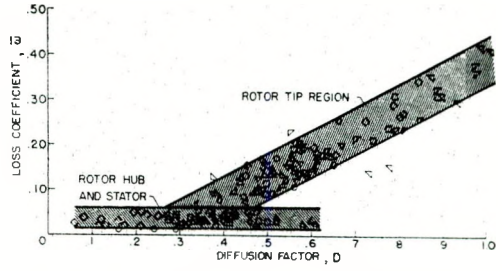
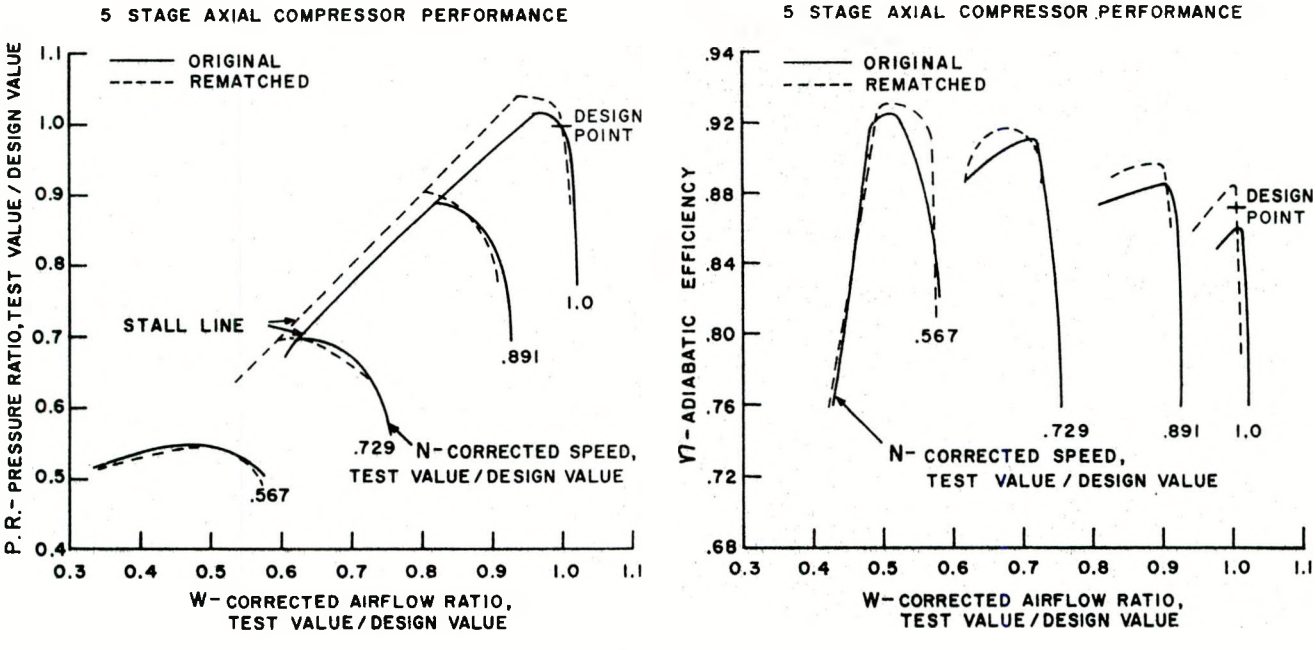


Fig. 5-22 - Diffusion-Factor Correlation for Compressor Inlet Stages



(a) (b)

Fig. 5-23 - Performance Improvement Resulting from Better Stage-Matching

Various methods for predicting off-design performance of subsonic axial-flow compressor blade rows are in existence and may prove to be useful to designers for estimation[90,91]. Other methods and considerations published are aimed to help the designer in pattering effective wide-range axial compressors[92,93].

A method based on the use of experimental interstage performance data has been developed to present graphically the performance of the individual stage together with the over-all compressor performance so that the matching characteristics can be compared with the ideal criteria[94]. For cases where mismatching exists, application of the method makes it possible: to determine which stages contribute to stage matching troubles, to trace the troubles to specific radial locations, and finally, to determine what kinds of changes are needed to correct the troubles. As experimental testing is pursued to determine the effect of compressor changes, whether they be major ones such as redesign or simple ones such as restaggering of existing airfoils, the mentioned method can always be applied to evaluate the performance of the new configuration. In this way, the experimental program always follows from a logical extension of the previous test results. In Figure 5-23[94], performance improvements are shown that resulted from applying this three-dimensional stage-matching technique to a five-stage compressor.

5.3.2 Transonic Compressors

Further development of axial-flow compressors lead to the transonic compressor. For some time, the results obtained with transonic compressors were a mixture of success and failure. We now have a clearer picture of the state of the art.

In gas turbine engines there has been an increasing incentive to raise the Mach number at which axial-flow compressors could operate efficiently. Increasing the Mach number increases the flow capacity of a compressor and thus reduces its frontal area and weight. Increasing the Mach number also raises the pressure ratio a stage can produce.

This effect reduces the number of stages required and the weight. A typical example of this trend is shown in Figures 5-24[95] and 5-25[95].

The various transonic compressor studies indicate that transonic compressors can be designed which are at least comparable in efficiency to conventional subsonic designs. The same basic techniques are used in both designs. Many of the design data correlations are apparently identical.

Transonic compressors do not impose any penalities in the useful operating flow range. In fact, blade shapes similar to those recommended for transonic compressors at high subsonic Mach numbers have been used in Europe to achieve a wide range of flow. (This is done in stationary gas-turbine-power generating stations where a wide range of flows at constant speed are required to efficiently meet a wide range of power demand.) When the compressors do stall, they develop the usual rotating stall. No unusual characteristics of this stall have been observed. Transonic compressors do not appear to require exceptionally uniform inlet flow. From some considerations, they may be less sensitive to flow aborrations than are the conventional subsonic variety.

Thin blades, having their maximum thickness near the midchord point, seem to be needed. The solidities must be high (or, what is probably more significant, the distance between the leading edge of one blade and the suction surface of the next must be small in comparison to the radius of curvature of the suction surface) to avoid large losses in the passage shock. The trailing edges should be thin to minimize wake losses which become more severe at high subsonic Mach numbers.

Excellent dimensional reliability is required for transonic compressors. This is especially true when the hub to tip ratios are high and the Mach numbers are very close to 1. An outstanding example is an experimental mixed-flow compressor designed at the AiResearch

THE FRANKLIN INSTITUTE - Laboratories for Research and Development
I-A2392-0

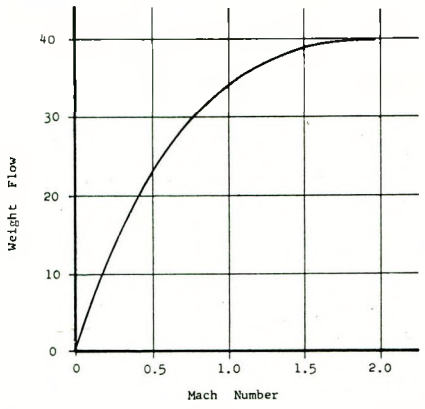


Fig. 5-24 - Weight Flow Versus Mach Number

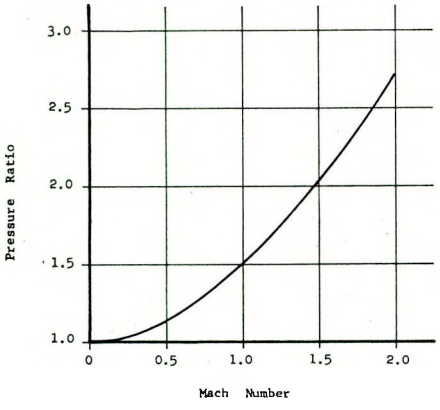


Fig. 5-25 - Pressure Ratio Versus Mach Number

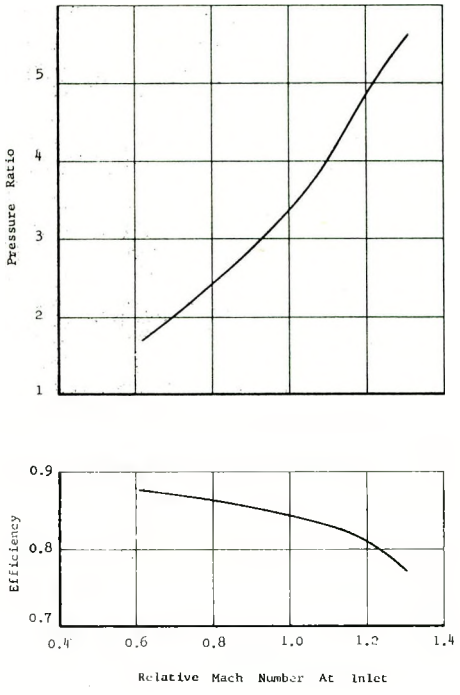


Fig. 5-26 - Performance of AiResearch Transonic Mixed Flow Compressor

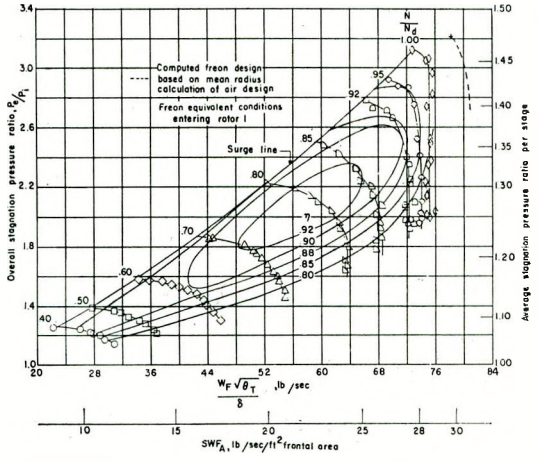


Fig. 5-27 - Over-All Performance Characteristics of the Three-Stage Transonic Compressor

Manufacturing Company of Arizona under a research contract from WADD. As shown by the curve in Figure 5-26[95], this compressor efficiently produces high-pressure ratios in a single stage, with relative inlet Mach numbers well above 1. Here, again, the radial and tangential flow distributions were studied as completely as possible to minimize undesirable velocity peaks.

In view of these experiences, the detailed study of the radial-flow distributions and of possibly even the chordwise distribution of velocity is recommended for designs that extrapolate the results of proven blade rows. In other circumstances, the less time-consuming techniques are adequate.

One transonic rotor tested at the NACA Langley Laboratory is reported to have obtained an overall efficiency of 0.91 at the design point. The measured relative Mach number at this condition was 1.08. The high efficiency was attributed to a lower maximum thickness, a reduction in static pressure rise, the transonic type thickness distribution, and the meanline selection which varied with radial station.

Transonic rotors had already been shown to be capable of producing pressure ratios of 1.3-1.65 and specific flows of 30-36.5 lb/sec ft^2 frontal area at efficiencies of 0.90. The performance of such rotors when combined with stators indicated high-stage efficiencies.

From tests of a three-stage transonic compressor it was deduced that high efficiency performance can be realized in transonic multi-stage compressors (see Figure 5-27[96]). The effect of Reynolds number on the performance of a modified eight-stage transonic compressor was studied by reducing inlet pressure at a constant inlet-air temperature (see Figure 5-28[97]). As shown in Figure 5-29[88], sizable reductions in peak efficiency, maximum weight flow, and surge pressure ratio were observed at the design speed as the Reynolds number (based on blade chord at tip of the first rotor) decreased from 1.05×10^6 to 9.6×10^4. In addition, rotating stall was found to exist up to higher equivalent compressor speeds as chord Reynolds number was reduced[88,97,98]. A typical performance map of the eight-stage compressor is shown in Figure 5-30[88].

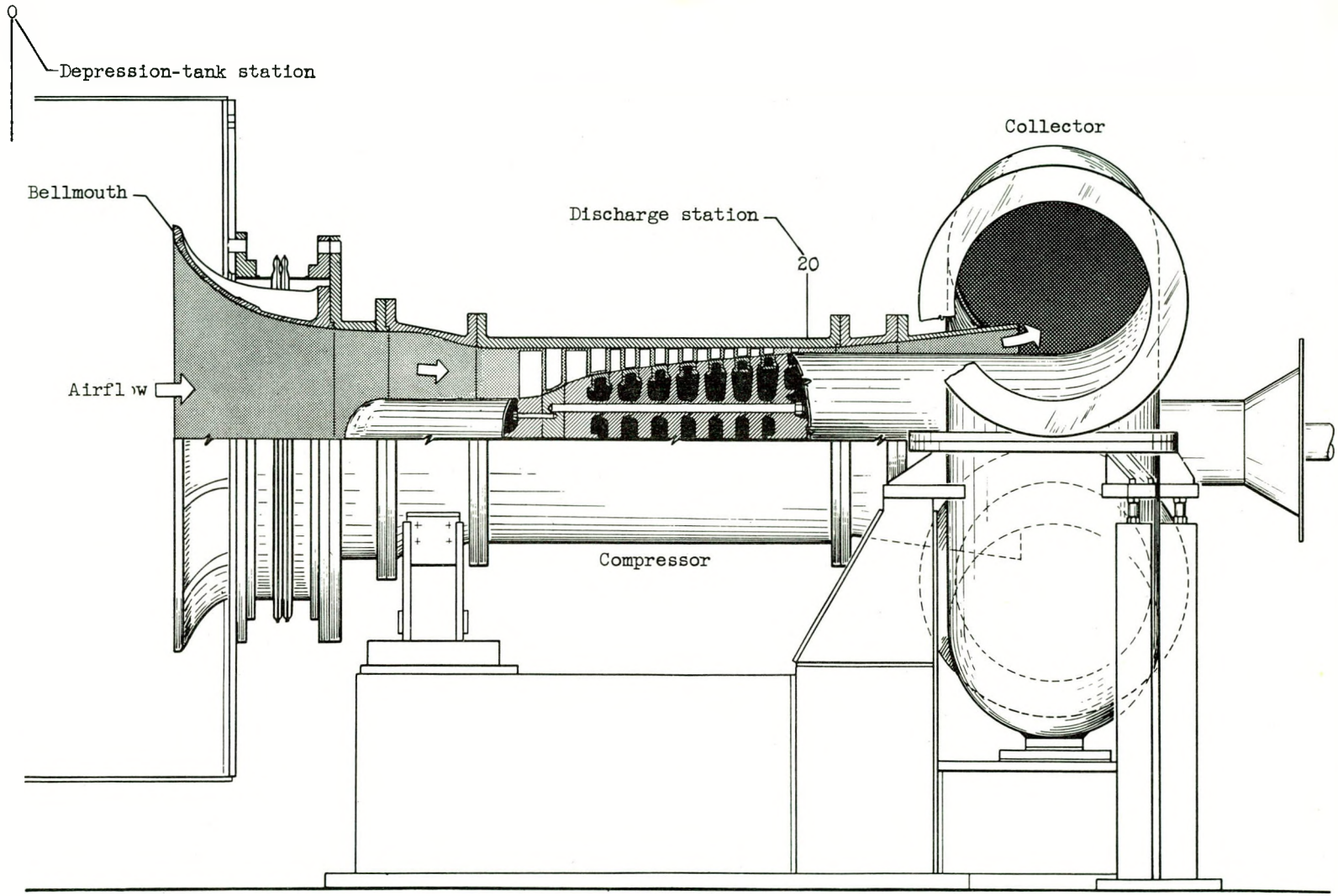


Fig. 5-28 - Cross-Sectional View of Eight-Stage Axial-Flow Compressor, Inlet Bellmouth, and Discharge Collector

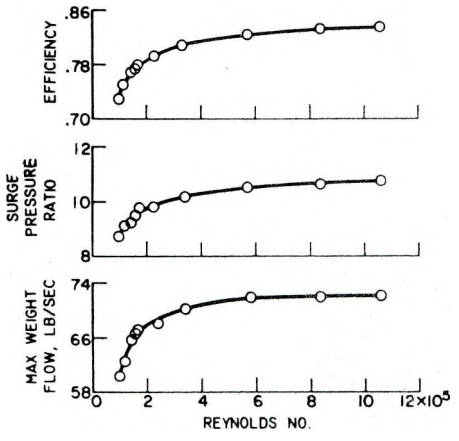


Fig. 5-29 - Effect of Reynolds Number on Multistage Performance

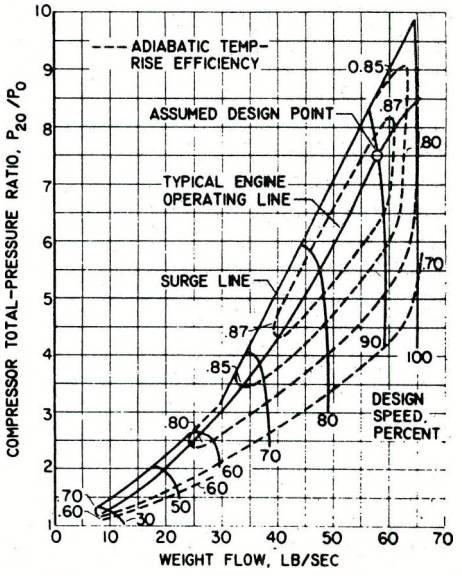


Fig. 5-30 - Typical Performance Map of Eight-Stage Compressor

Additional tests were made with the same eight-stage compressor, doubling the chord of the first two transonic inlet stages. Figures 5-31[99] and 5-32[99] show the difference between both first-stage rotors, the original (medium-chord) and the modified (long-chord). The obtained results showed that the long-chord compressor has an increased stable operating range from 60 per cent to design speed over that of the medium-chord compressor. The greatest improvement in operating range was obtained at 75 and 80 per cent of equivalent design speed. Furthermore, the long-chord compressor attains higher efficiencies than the medium-chord compressor at lower compressor speeds and approximately the same efficiency at higher compressor speeds.

A peak efficiency of 0.82 was obtained with the long-chord compressor for design speed at values of total-pressure ratio ranging from 9.0 to 10.2[99]. The rotor with the installed long-chord transonic stages is shown in Figure 5-33[88] and a typical blade section of transonic rotor is shown in Figure 5-34[100].

An approach to the design of transonic compressors on the principles of Schicht fans (axial flow fan with a low degree of reaction) was attempted by the SNECMA (Societe Nationale d'Etudes et de Construction des Moteurs d'Aviation, Paris, France). Work at SNECMA was not continued but the results seem to be encouraging. A compressor S-1 was run as a single-stage compressor, with an outlet pressure ratio equal to that of an orthodox compressor with four stages. The S-1 compressor consisted of a rotor wheel having a degree of reaction approaching zero followed by a stator operating in supersonic flow. The outlet guide vane is exposed to Mach numbers of more than 1.3. The single stage version S-2 shows Mach numbers up to 1.5 in both rotor and stator. Figure 5-35[101] shows the two transonic compressors and a conventional type, and Figure 5-36[101] shows a cross section of the S-1 compressor. The need for more detailed measurements in multi-stage transonic compressors for use in the design systems and for an understanding of the

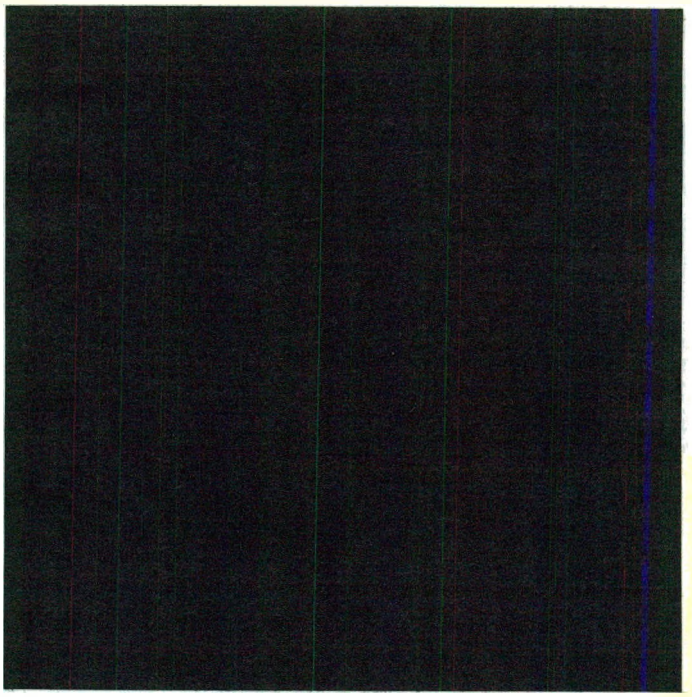


Fig. 5-31 - First-Stage Rotor of Long-Chord Compressor

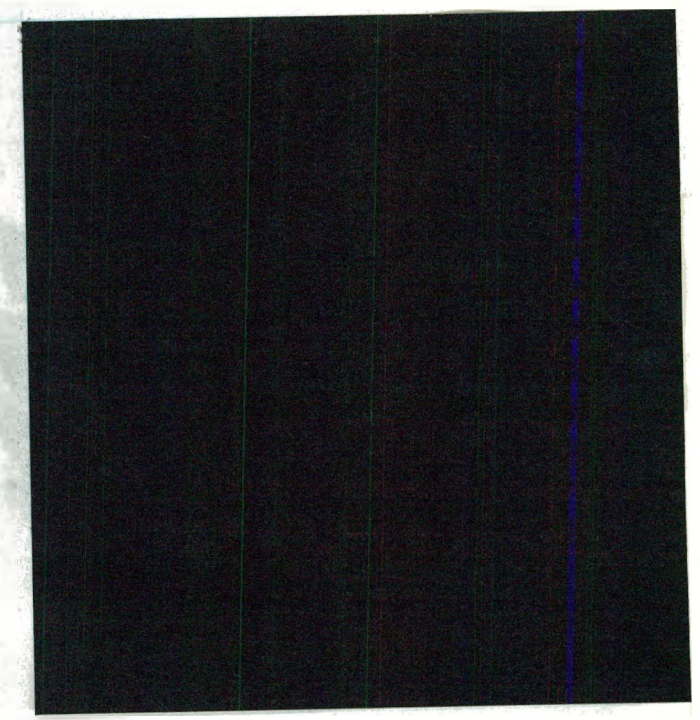


Fig. 5-32 - First-Stage Rotor of Medium-Chord Compressor

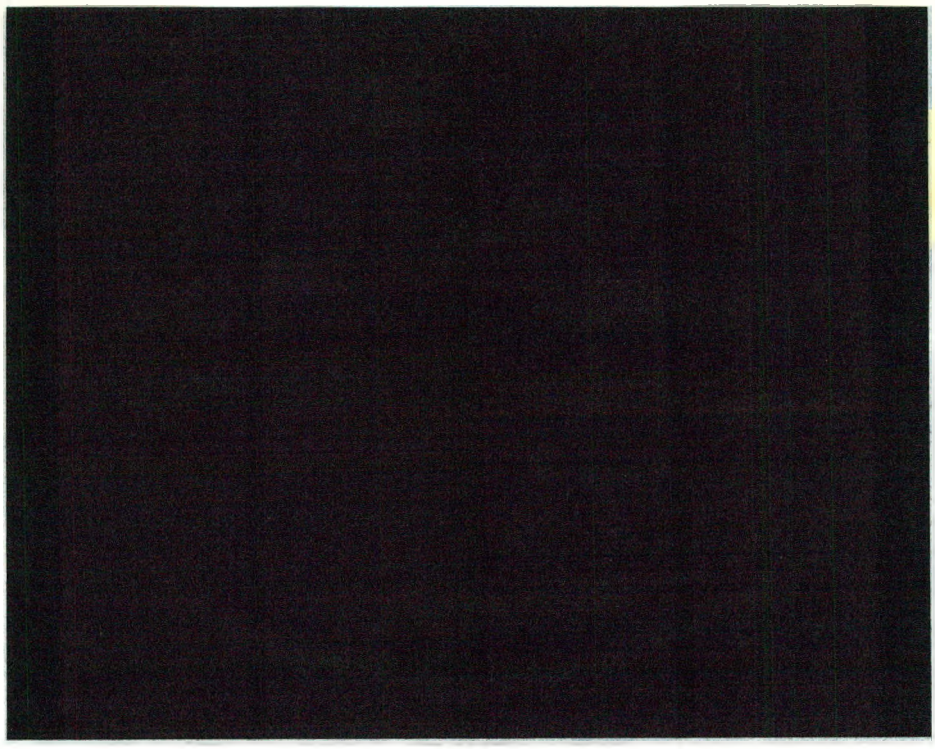
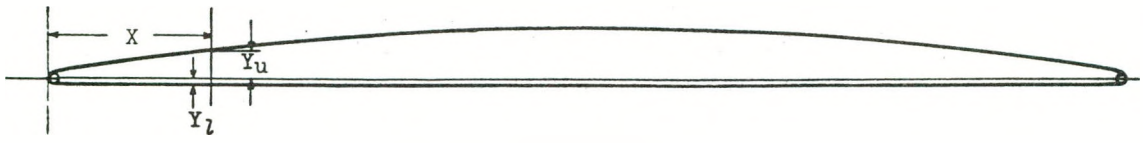


Fig. 5-33 - Eight-Stage Axial-Flow Compressor

[r_3, 8.000 in.; r_4, 7.750 in.; leading- and trailing-edge radii, 0.010 in.]



X	Y_u	Y_l	X	Y_u	Y_l
0	0	0	1.000	0.082	0.006
.100	.028	.014	1.100	.078	.006
.200	.041	.012	1.200	.076	.006
.300	.053	.010	1.300	.071	.006
.400	.063	.009	1.400	.065	.007
.500	.071	.009	1.500	.057	.010
.600	.077	.009	1.600	.046	.011
.700	.082	.009	1.700	.027	.012
.800	.084	.008	1.750	.009	.010
.900	.084	.007	1.762	0	0

Fig. 5-34 - Coordinates of Tip Section of a Rotor Blade Measured on Design Stream Surface

internal flow in a multi-stage compressor is recognized. Some insight has been gained into the applicability of inlet-stage data to the design of later stages[102,103].

Attempts have been made to summarize a real-fluid, three-dimensional performance method for a transonic-compressor single stage, suitable for programming in a digital computer. Test comparisons suggest that this practical approach may be of some value in examining single stages prior to proceeding with the usual stage-stacking practices. Methods of performance estimation for turbomachinery must receive continued attention if the cost of development of gas-turbine units is to be reduced[104].

5.3.3 Supersonic Compressor

The supersonic compressor has generally been considered as any compressor utilizing supersonic flow relative to one or more of the blade rows. As a rule, this is applied only to those designs which have supersonic velocities along the entire blade span. Those designs which utilize Mach numbers ranging from supersonic to subsonic along the span are generally classified as transonic[84].

The first supersonic compressors were designed from supersonic-diffuser concepts and data obtained by Kantrowitz and associates[105]. The first unshrouded shock-in-rotor supersonic compressor produced a pressure ratio of 2.20, and an efficiency of 84.5 per cent at an air equivalent tip speed of 1610 ft/sec when tested in Freon gas (see Figure 5-37[96]). Typical performance curves of the shock-in-rotor compressor are shown in Figure 5-38[96].

The high turning all-supersonic impulse type rotor, in conjunction with efficient shock diffusion in the stators, has the potential capability of producing in a single stage the pressure rise associated with multi-stage compressor components of present day turbojet engines. Cascade studies revealed that turning angles as great as 120 degrees could be obtained with relatively low total pressure loss, provided that little or no diffusion of the flow was required.

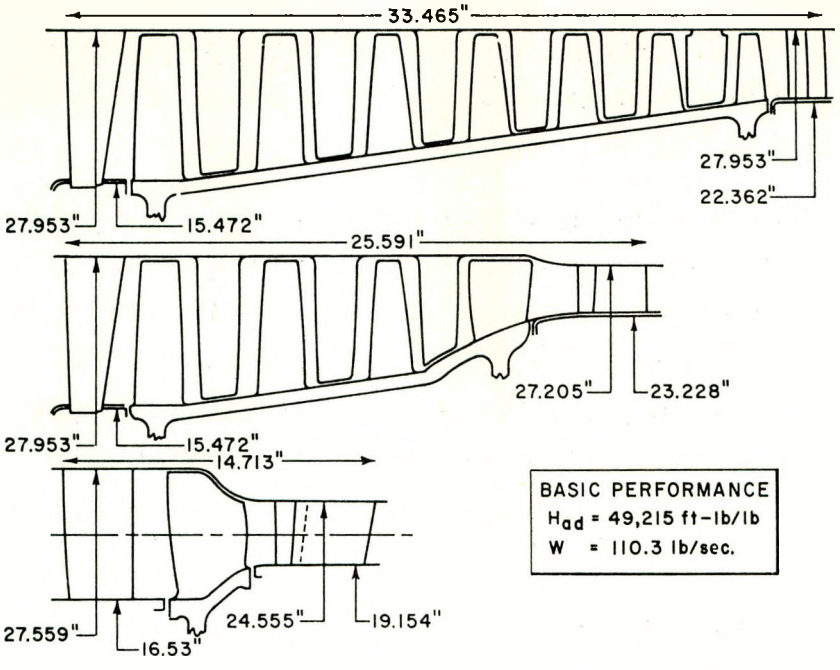


Fig. 5-35 - A Dimensional Comparison Between a Conventional Compressor (Atar 101), The S-1 Compressor Preceded by Three Conventional Stages, and The One-Stage S-2 Compressor.

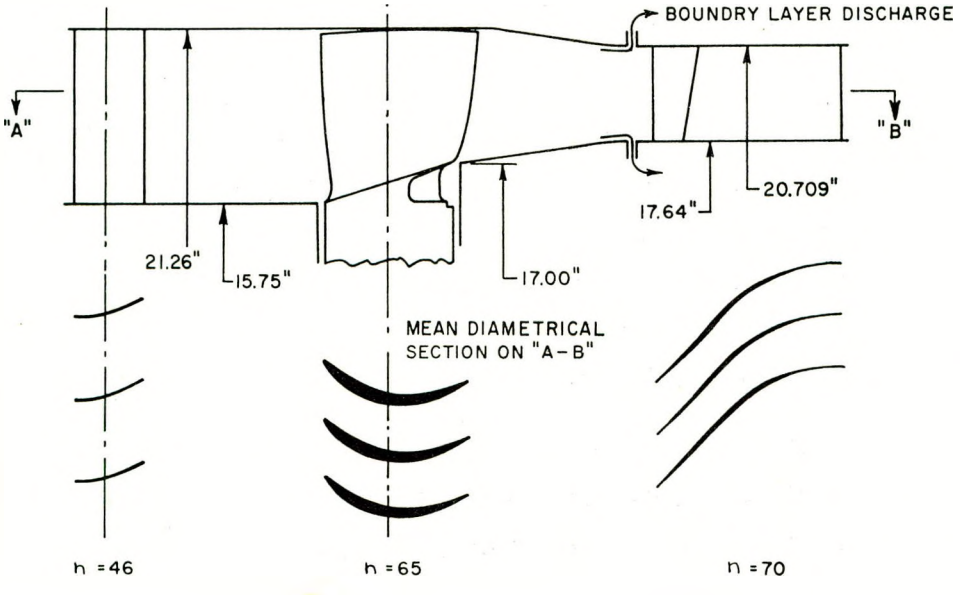


Fig. 5-36 - A Cross-Section of the S-1 Compressor. Below This, Sections of the Blades Are Given With The Mean Diameter Denoted By The Section Line A-B

The rotor of a shock-in stator compressor, shown in Figure 5-39[96], produced a pressure ratio of 7.2 with an efficiency of 90 per cent at an air equivalent speed of 1450 ft/sec (see Figure 5-40[96]). Although destruction of this plastic rotor prevented the complete stage performance evaluation from being made, cascade tests indicated that turning and diffusion could not be accomplished efficiently in a single stator.

It would appear desirable to turn the rotor exit flow back to the axial direction by means of a supersonic stator and diffuse in an annular passage which has provision for boundary-layer suction and movable components to vary the throat area. Such stators were designed and constructed; however, they were never tested because all compressor research at the NASA was terminated prior to reconstruction of the rotor[96].

A tip speed of 1600 ft/sec was used in almost all of the initial NACA supersonic compressor development. Inlet axial Mach numbers from 0.7 to 0.85 were used. The potential of supersonic compressors using reasonable blade loadings, an effective balance between blade rows, and aerodynamic blading consistent with the separation hypothesis has not yet been adequately evaluated.

Efficiency measurements on shock-in-rotor compressors at design speed ranged between 75 to 84 per cent. Maximum efficiency at part speed was generally 3 to 4 per cent higher than design speed performance. In general, removing the inlet guide vanes improved the overall performance of the rotor. More effective positioning and control of the normal shock was anticipated by placing it in the stator passage (impulse rotor). Also, boundary layer control devices might be incorporated in the stator. In general, design rotor-pressure ratio was nearly achieved or even exceeded. However, it was observed, that in all cases acceptable rotor alone performance was so severely compromised as to make stage performance unsatisfactory. The stator development programs, in general, did not attempt to apply boundary layer bleed or other means of controlling the shock-boundary-layer interaction[84].

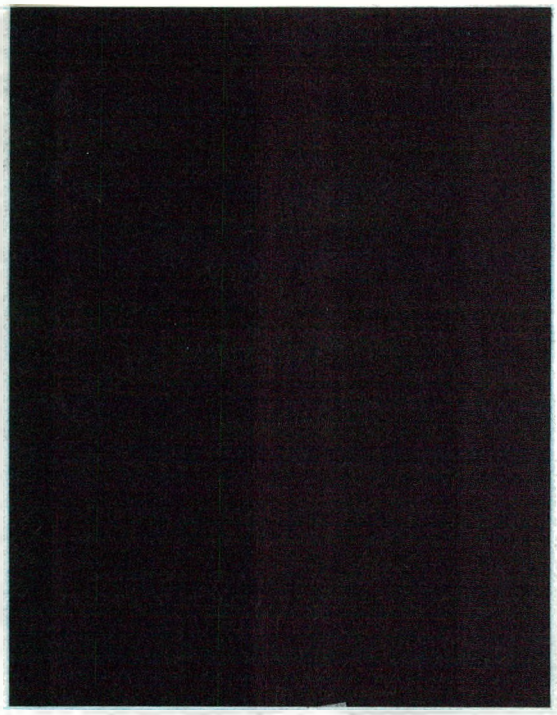


Fig. 5-37 - First Unshrouded Shock-in-Rotor Supersonic Compressor

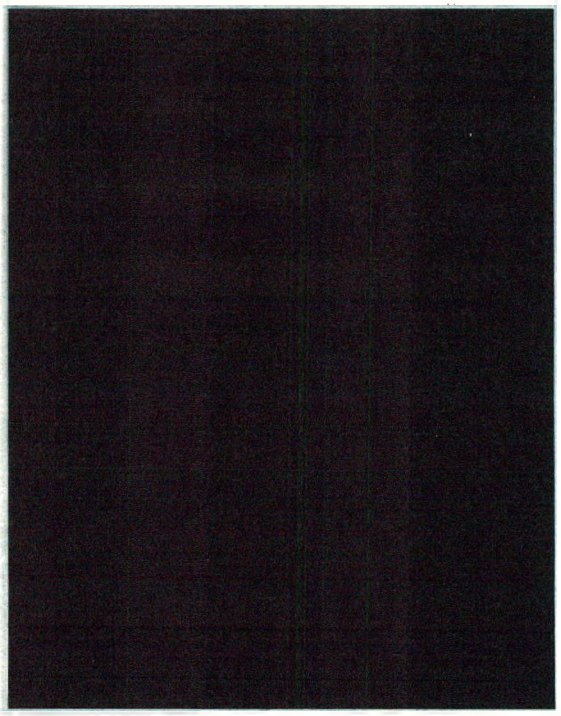


Fig. 5-39 - Supersonic Impulse Rotor for Shock-in-Stator Supersonic Compressor

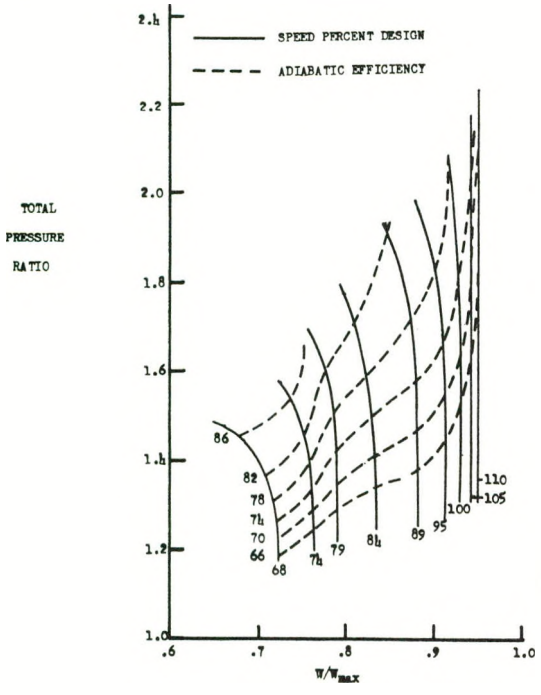


Fig. 5-38 - Typical Performance Curves of Shock-in-Rotor Type Supersonic Compressor

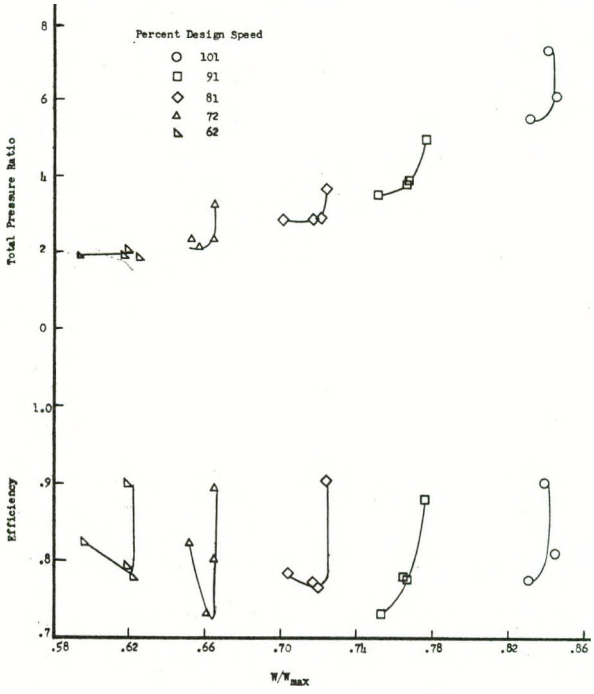


Fig. 5-40 - Performance of Impulse-Type Supersonic Compressor Rotor

Although the supersonic-compressor program at the NACA Lewis Laboratory did not result in the widespread application for this type of compressor to turbojet engines, the knowledge and benefits derived from this work were considerable. It has become obvious that the high performance values indicated in early analytical studies are not obtainable in practical compressors. Applications may result where the compact, lightweight arrangement of supersonic compressors may be useful, especially when the medium being compressed is a fluid with a low sonic velocity. Perhaps the most important result of the supersonic compressor research program was the development of the transonic compressor[105].

5.4 Axial Flow Turbines

The design parameters for a preliminary layout of a turbomachine are usually established with approximate methods prior to detailed investigations of the blading. These preliminary calculations are required in order to determine the number of stages, their peripheral speed, and the blading arrangements that produce optimum efficiencies. Economical considerations must also be taken into account. It is frequently necessary to limit the number of stages to a minimum, and such preliminary investigations must be used to evaluate the drop in efficiency which occurs if the number of stages is reduced. Similar studies must be made for aircraft propulsion units where weight is of prime importance. Cutting down of the number of stages must also be considered sometimes when the length of the rotor has to be reduced in order to increase the critical speed. Furthermore, it is often necessary to investigate the relative merits of axial flow or radial flow machines, be it because of cost or because of design and manufacturing considerations[37].

For axial flow compressors, these preliminary investigations can be carried out with the two-dimensional approach. Such calculations help to formulate a design which then can be analyzed for its three-dimensional aspects. For turbine stages, axial or radial, where the

flow is accelerated in the rows of blades, it is frequently sufficient to establish design parameters with a one-dimensional approach. The flow through the machine is supposed to have axisymmetric stream surfaces, and the behavior of the flow on a mean stream surface is considered to be representative of the whole stage. In contrast to the two-dimensional approach, the rows of blades are simulated by discontinuities. They deflect the flow on the mean stream surface and exert frictional forces, but the conditions ahead and after a row of blades are assumed to be axisymmetric. It is therefore sufficient to analyze the flow at the entrance and the exit of a cascade without investigating the conditions in the channels between the blades. For this reason it is not necessary to apply cascade theories, and the frictional losses in the cascades are simply reflected in entropy changes that the flow experiences as a whole. With this approach, the analysis is reduced to the determination of the flow properties along a particular streamline that lies on the chosen surface of revolution.

The classical theory of axial turbines differentiates between impulse and reaction stages only. In the latter, the enthalpy drop of the stage is equally divided between rotating and stationary rows of blades, whereas in impulse stages, the total enthalpy drop of the stage is converted into kinetic energy in the stator and the rotor blades exert forces in peripheral direction only because they deflect the flow. The degree of reaction of impulse stages is therefore zero and that of reaction stages is 50 per cent. Experience has shown, however, that stages with other degrees of reaction can also be used. Actually, most so-called impulse stages work with a small degree of reaction, and for many turbines it is advantageous to change the degree of reaction from stage to stage to obtain the best performance with a minimum number of stages. For small gas turbines and special applications, the radial flow turbine is of great interest because of its sturdy design. Such stages do not only have excellent efficiencies but the rotors can be overhung on the shaft, which simplifies the design of the bearings, their seals, and lubricating and cooling circuits.

To facilitate such preliminary calculations of turbine stages, general relations are established in text books which cover all types of turbine stages on a one-dimensional basis[76]. These relations are quite involved and do not permit the evaluating of optimum efficiencies with simple differentiations. For axial turbines where the losses are fairly well established by experience, and where they can be related to the stage parameters in a simple manner, the optimum operating conditions have been determined and tabulated by means of an electronic computer[76]. Such tables give sufficient information for calculating the performance of different stage combinations without having to solve complicated equations. They also make it possible to establish the arrangement that produces the highest efficiency at specified operating conditions. Similar computations have been carried out for radial turbine stages also. A large number of tables of results is necessary, however, to cover the whole range of applications because the losses cannot be related to the stage parameter by simple relations.

Brown Boveri discussed axial-flow-turbine blading as follows[14]:

At high input capacities, the reaction turbine has a better efficiency than the impulse turbine. But since it is not the efficiency alone, but the permissible temperature before the turbine which decides whether a machine with high output and low fuel consumption can be built, the following factor must not be overlooked. The impulse turbine utilizes almost the whole of its pressure drop in the fixed row of blades. Since these are not subjected to centrifugal force, they can be designed for lower stresses than the subsequent row of moving blades.

Thus for the same temperature of the moving blades it is possible to raise the inlet temperature. On the other hand, since it is easier to cool an impulse turbine, one might be led to believe that it would be preferable for the gas turbine to be built as an impulse turbine. But this is only interesting and only benefits from the above advantages when the pressure drop can be utilized in a small number of stages.

THE FRANKLIN INSTITUTE • Laboratories for Research and Development
L-A2392-E

Attaining a reasonable efficiency is only possible with high peripheral speed. But the latter leads, on the one hand, to high gas speeds and appreciable losses and, on the other, to increased centrifugal stresses in the blades and the rotor, and so to lower safety factors. Hence, the gain from higher gas temperature is mostly offset by poorer utilization of the pressure drop. In the limiting zone of the moving blades, the gas is retarded and the corresponding energy converted into heat. At high gas velocities, as are experienced with impulse blading, the temperature rise in the boundary layer is considerable. This increases the temperature of the material well above the mean gas temperature in the blade chamber, thereby reducing the advantage of impulse blading still further.

Summarizing, it may be said that, although the impulse turbine permits a higher gas temperature than the reaction turbine, the latter attains practically the same performance as regards limiting output and fuel consumption for equal material conditions and at a much lower inlet temperature. Moreover, the machine with the lower inlet temperature is more reliable.

For these reasons, Brown Boveri decided to adhere to the reaction turbine, after carrying out numerous experimental investigations into both systems. With lower stresses and gas inlet temperatures, but admittedly with slightly more material, it allows an economical machine with low maintenance costs to be built.

Having examined all these factors, the Company decided that, for certain applications, gas turbines would be built as reaction turbines for an inlet temperature of 750°C, but for installations burning heavy oil, the temperature of 620°C would be adhered to, as before. Thus, in contrast to other manufacturers, Brown Boveri produce two different types of gas turbine, one for 750°C, the other only suitable for 620°C.

Figure 5-41 shows another principal difference between impulse and reaction blading of turbines, disregarding any irreversible losses. Reaction blading, apart from being slightly more efficient than the impulse blading, has also a wider range of higher efficiency over the blade speed ratio.

A blade-design method has been developed by Boeing Airplane Company, Seattle, that takes into consideration the basic theoretical concepts of fluid dynamics as well as experimentally established design parameters. The method can be applied by the average turbine designer after a short period of special training. No special computing equipment is required to establish the blade profiles unless a comprehensive study is undertaken to show how the blade profiles change for given variations of aerodynamic blade loadings. The integrations necessary to calculate blade profiles can be carried out with sufficient accuracy in finite steps according to conventional methods if the blade chord is divided into at least ten equal increments.

By applying the method to a specific case, it is explained how well-proportional blades can be obtained that satisfy aerodynamic as well as structural requirements. The basic blade profile is fully determined from aerodynamic considerations, while experience factors are utilized only for refinements. The blade shapes are defined in a co-ordinate system that lends itself readily to manufacturing purposes. Test data, obtained from a turbine, designed according to this method, show that a close approximation of the design flow pattern can be obtained. Specifically, it was demonstrated that nearly ideal free-vortex flow can be maintained across the blading with suitably designed blade profiles. Aerodynamic performance of the turbine stage exceeded expectations.

Success of any specific blade design, of course, still depends to a large extent on the good judgement of the designer, but the described method provides him with a powerful design tool which virtually eliminates all guesswork.

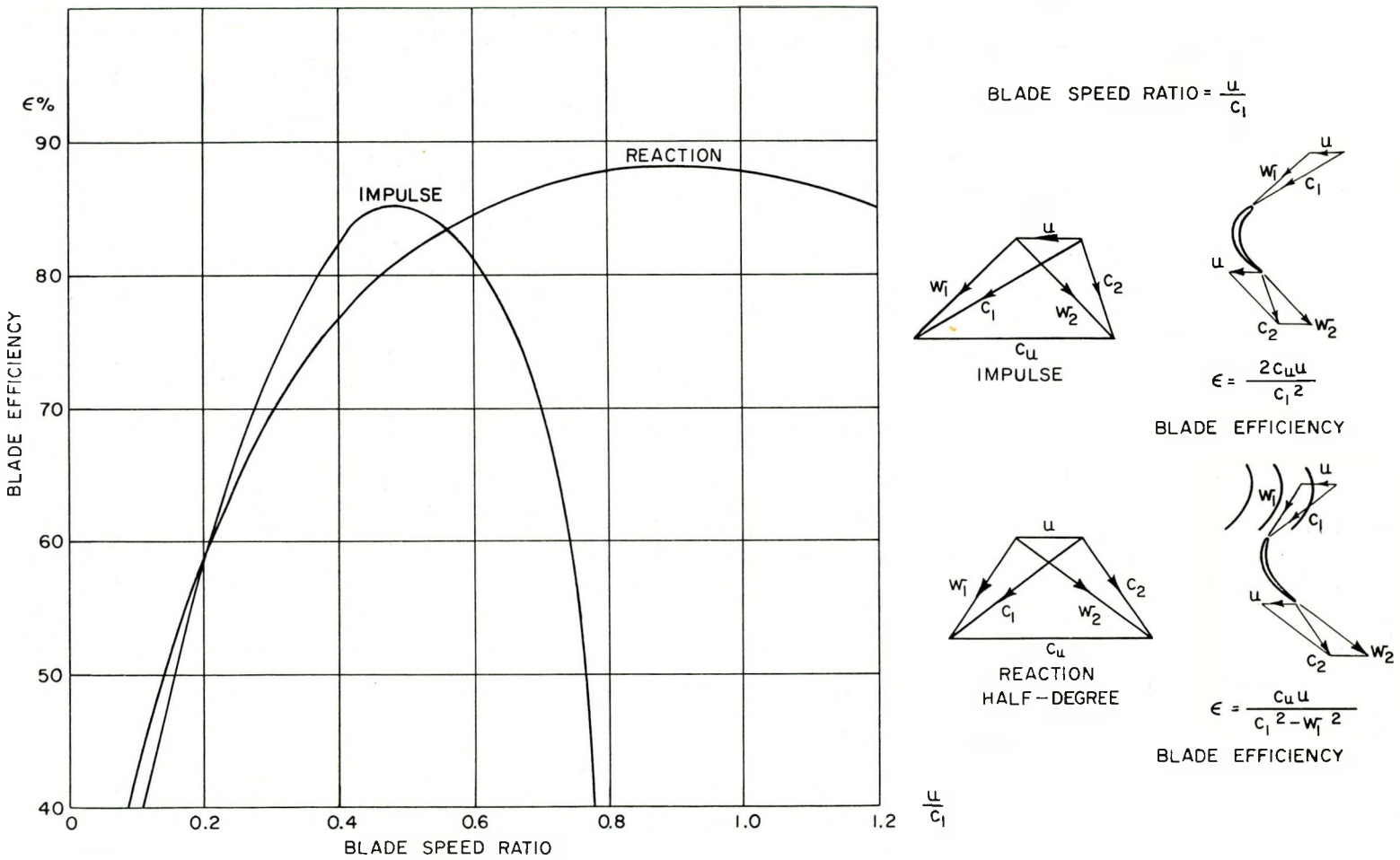


Fig. 5-41 - Turbine Blade Characteristics

The above method has been used by Boeing for many years to design the blading of axial-flow turbines. One application was the power output stage of a 400-hp two-shaft, gas-turbine engine.

Figures 5-42[106] and 5-43[106] indicate that some high efficiencies were obtained at lower than design expansion ratios. It must be mentioned, however, that these favorable results are not beyond question, because at low expansion ratios the test readings become relatively less accurate. Of more significance is the fact that the efficiencies do not decrease at expansion ratios considerably higher than design. This means that the oblique nozzles of the diaphragm assembly can produce higher than sonic velocities efficiently in the vaneless space between stator and rotor blades.

5.5 Radial Flow Turbines

The general equation for the Euler work of a turbine H_e can be written

$$H_e = \frac{u_1 c_{u1} - u_2 c_{u2}}{g}$$

The adiabatic head H_{ad} available in the turbine is determined by the pressure ratio (total inlet to static-exit pressure) and the total inlet-gas temperature and is related to the Euler work by

$$H_{ad} = H_e + \text{losses}$$

Introducing the reaction as a ratio between the head drop in the wheel and the head drop across the turbine (total-to-static) yields

$$r = \frac{H_{wheel}}{H_{ad}}$$

From the velocity triangles w_1, the relative velocity entering the blading, is obtained. The relative leaving velocity w_2 follows from the equation

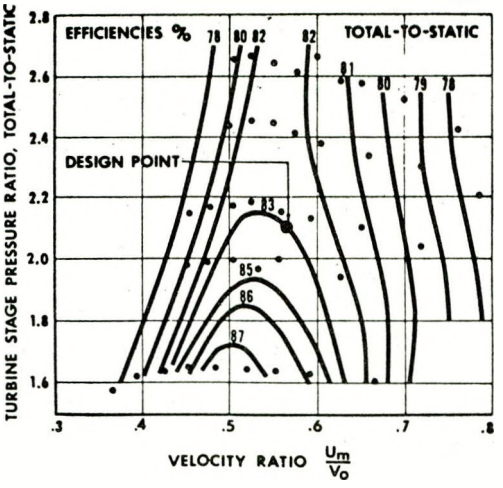


Fig. 5-42 - Test Performance of 400-hp Turbine Stage. Total-to-Static Efficiencies

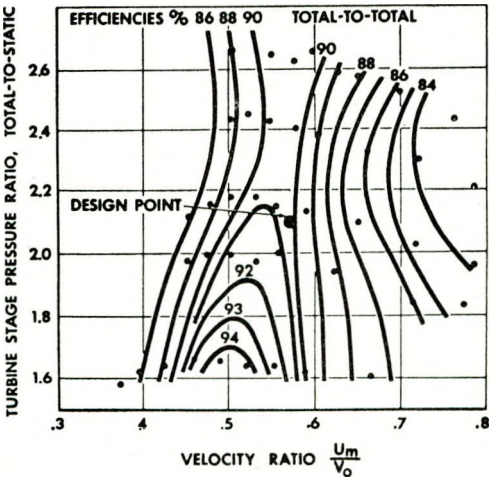


Fig. 5-43 - Test Performance of 400-hp Turbine Stage. Total-to-Total Efficiencies

$$\frac{w_2^2}{2g} = \frac{w_1^2}{2g} + rH_{ad} - \frac{u_1^2 - u_2^2}{2g} - \text{losses}$$

This equation expresses the fact that the relative leaving energy is equal to the energy entering the wheel plus the reaction head, minus the head required to counterbalance the centrifugal forces in the wheel minus the losses in the wheel. In general, the losses which have to be considered from the inlet plenum to the impeller are

(a) nozzle-friction loss

(b) momentum loss due to nozzle blockage

(c) friction loss in the vaneless space between nozzle and wheel.

The last two losses can be combined. Accurate prediction of the flow losses through a radial wheel requires consideration of a three-dimensional flow just as in a radial compressor. Owing to the generally accelerated flow pattern in a turbine wheel, however, a two-dimensional analysis often may be sufficient up to the exducer. In the axial part of the turbine, the exducer, radial equilibrium plays an important role in the flow picture, and the correct evaluation of the flow pattern and the velocity triangles at the exit require due consideration of three-dimensional flow. The losses which have to be considered in the wheel are

(a) incidence loss

(b) passage-friction loss

(c) blade-loading loss

(d) leakage loss.

The incidence loss is assumed proportional to a fraction of the incidence component of the velocity triangle with due consideration of the slip effect. Test data indicate that this fraction is close to 1.0.

THE FRANKLIN INSTITUTE • Laboratories for Research and Development

The passage friction loss may be treated as a friction loss in a channel of variable geometry.

The blade-loading loss is known to be a function of the so-called diffusion parameter, which relates the velocity difference through which the flow is decelerated on the suction side or the pressure side to some revelant mean relative velocity.

Hence

$$\text{pressure-side diffusion parameter} = \frac{\text{inlet relative velocity - minimum relative velocity}}{\text{inlet relative velocity}}$$

$$\text{suction-side diffusion parameter} = \frac{\text{maximum relative velocity - outlet relative velocity}}{\text{maximum relative velocity}}$$

The flow is generally accelerated in turbine passages. Hence, the diffusion parameters are small and the blade-loading loss may be negligible. However, certain configurations, particularly designed for low-velocity factors, produce decelerated flow in the wheel because of the necessity to reduce reaction. Blade-loading losses may then become considerable. Similar conditions occur at low-specific-speed designs where the throughflow velocities are made as small as possible.

The performance of a radial turbine is determined to a large extent by the ratio of two throat areas, the nozzle throat area and the exducer throat area. When the pressure ratio across the turbine is steadily increased for example, by reducing the back pressure while the inlet pressure is maintained constant, all velocities in a turbine increase. The highest velocities are established in the two throats, with the highest absolute velocity in the nozzle throat, and the highest relative velocity in the exducer throat. At the critical pressure ratio, the nozzle may choke and further drop of the back pressure will only reduce the pressure after the nozzle, resulting in supersonic flow in the nozzle section. A further pressure drop leads to choking conditions at the exducer, which results in a fixed flow pattern upstream. Still further

back-pressure drop produces a supersonic flow pattern at the exducer exit. If the exducer is choked before the nozzle is choked, further drop of the back pressure no longer influences the flow conditions in the turbine. The efficiency changes, however, because it is expressed as the ratio of the Euler work, which is almost constant, divided by a steadily increasing adiabatic head.

Whether the turbine nozzle or the exducer throat chokes first depends, to a large extent, on the turbine reaction. The amount of head drop in the wheel compares to the total head drop in the entire turbine. If a larger fraction of the available head is utilized in the wheel, less is available across the nozzle, or in other words, the inlet-peripheral-velocity component declines. If now the wheel-tip speed is adjusted for obtaining optimum Euler work,

$$H_e = \frac{u_1 c_{u1} - u_2 c_{u2}}{g}$$

it can be shown that the velocity triangles lead to less turning in the wheel. Since losses in the wheel diminish considerably with reduced turning, higher efficiencies are to be expected with an increase in reaction.

Figure 5-44[107] shows three sets of velocity triangles for different reactions. Constant work $u\Delta c_u$ is assumed for all three cases. In this example, the turning of an axial impulse turbine, $r = 0$, is approximately 120°. For 50 per cent reaction, the turning decreases to approximately 70°. For a reaction of 70 per cent, the turning is only 20°. These turning values can be further decreased if a radial-inflow turbine is used as shown by the dotted exit triangles in Figure 5-44. For a radial turbine with a reaction of 0.7, the turning can be made zero. This reduction in turning is an inherent advantage of the radial-inflow turbine as compared with the axial turbine.

The condition of constant work $u\Delta c_u$ = const, naturally requires that the tip speed increase with a decrease in turning. With increased tip speed, the disk friction and ventilation losses rise and their influence may offset a potential gain from reduced turning losses. If a turbine has low disk-friction losses, as is the case with a high-specific-speed machine, high tip speed and high reaction may lead to optimum performance. Inversely, low-specific-speed machinery has comparatively high disk-friction losses, and the potential gain from high reaction may become unavailable.

Speed restrictions from stress in many cases may not allow the optimum layout. If a maximum tip speed u is given and the head drop (pressure ratio) is specified, the desired value of $u\Delta c_u$ may require the highest turning Δc_u possible. This is equivalent to going to an impulse-type machine where almost all of the head drop occurs in the nozzle.

These considerations are more generally shown in Figure 5-45[107]. The two main losses, turning loss and disk friction, are plotted as a function of tip speed for an optimum layout of the turbine. As the turning losses drop with increasing u, the disk friction rises. The minimum of the losses strongly depends upon the magnitude of disk friction. Since disk friction (in ft-lb per lb of working medium) is inversely proportional to the through-flow of a turbine, the magnitude of disk friction is a function of the through-flow possibilities of a turbine which is also expressed as the specific speed. High-specific-speed turbomachinery has relatively low disk friction. Hence it should utilize high reaction, as shown in Figure 5-44. Inversely, high reaction machinery is sensitive to size.

By a correct choice of exit blade angle as a function of the radius, it is possible to permit approximately the same work to be drawn from the fluid at hub and shroud line in spite of different peripheral speeds at hub and shroud. However, at some reduced reaction, the head

available to maintain discharge flow at the shroud may not suffice to do so at the hub, and part of the hub section may not have any flow at all or even backflow. That is, some fluid may enter the turbine at the hub and flow toward the wheel tip, as in a compressor. The three-dimensional character of the flow in the exducer comes to light, especially if the exducer is overloaded. Flow distortion also shows up in the temperature distribution.

Radial turbines have been built successfully for 50 per cent reaction. But often the problem arises of designing a radial turbine for such a low tip speed relative to the spouting velocity, in other words for such a low velocity factor, that the regime of the impulse-type turbine is approached. In such cases, the inlet triangles must look like those for impulse-type turbines, and the inlet blade angles should be accommodated to these conditions. The second step is to adapt blade angles to the flow angle, as shown in Figure 5-46[107].

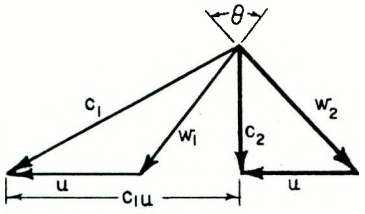
If the reaction is made equal to zero, the maximum efficiency (neglecting losses in the wheel) for axial and radial turbines is the same, (see Figure 5-47[107]). The actual loss picture changes this statement. The energy balance requires that

$$\frac{w_2^2}{2g} = \frac{w_1^2}{2g} + rH - \frac{u_1^2 - u_2^2}{2g} - \text{losses}$$

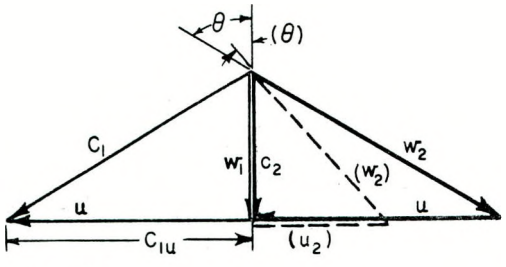
Hence, for no reaction ($rH = 0$), the centrifugal field has to be balanced by a deceleration of the relative velocity. If the losses are neglected, then

$$w_1^2 - w_2^2 = u_1^2 - u_2^2$$

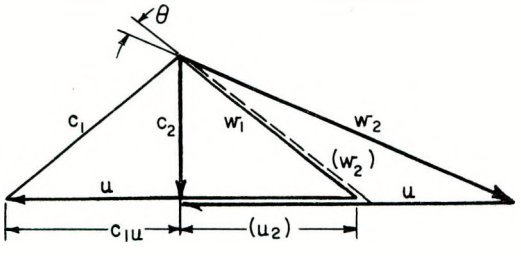
This means a deceleration of the relative velocity is on the order of u_2/u_1 because $u_1 = w_1$ approximately. In addition, the flow has to turn through a considerable angle, as shown in Figure 5-48[107], and the resultant general configuration is about the worst which could be selected from an aerodynamic standpoint, namely, a strong deceleration while turning the flow. High losses are, therefore, unavoidable.



$c_{2u} = 0$
$R = 0$
$\theta_{AXIAL} = 100° - 130°$



$c_{2u} = 0$
$R = 0.5$
$\theta_{AXIAL} = 60° - 80°$ $\theta_{RADIAL} = 30° - 40°$



$R = 0.7$
$\theta_{AXIAL} = 10° - 20°$ $\theta_{RADIAL} \longrightarrow 0$

Fig. 5-44 - Velocity Triangles for Three Different Reactions

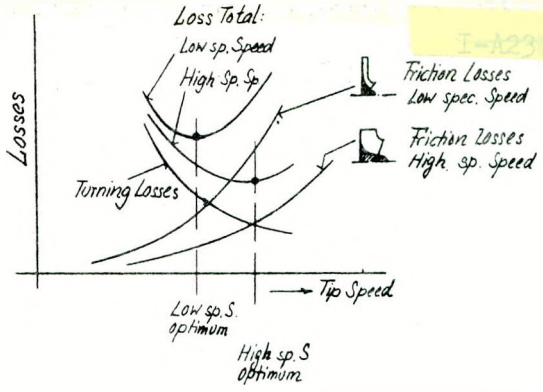


Fig. 5-45 - Loss Distribution for High and Low Specific Speed Turbines

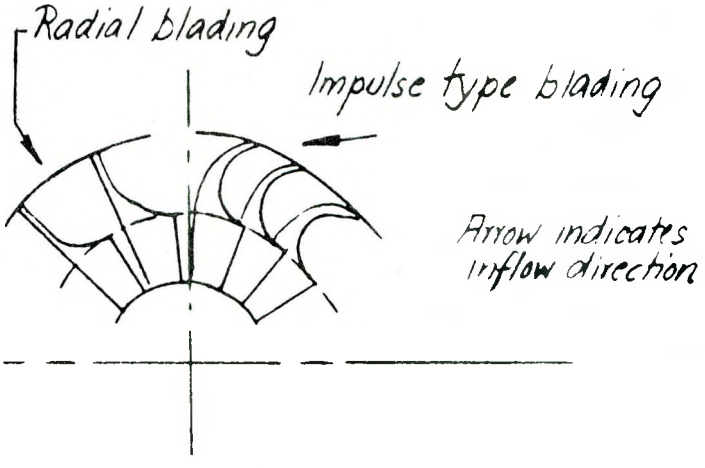


Fig. 5-46 - Comparison of 50 per cent Reaction and Impulse Blading

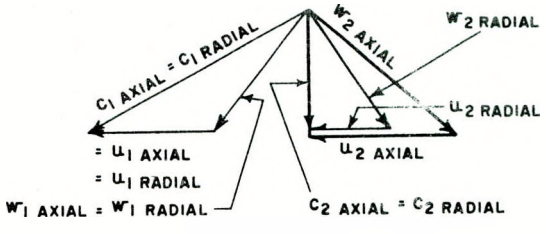


Fig. 547 - Velocity Triangles for Zero Reaction Turbines

Reaction can be reduced by increasing the exducer throat area relative to the nozzle throat area, which allows the head drop to take place mostly in the nozzles. Rise of losses and backflow near the hub limits this procedure. The combined effect is that the centrifugal field decreases and the losses increase with decreasing velocity factor, and a true impulse design is difficult to establish. Hence, the overall efficiency for a turbine designed for low velocity factor is only a few efficiency percentage points better than that of one running at this off-design condition. This was confirmed to a certain degree by the test data shown in Figure 5-49[107].

The concept of the specific speed relates weight flow and head of a turbomachine to a rotational speed by means of the equation

$$N_s = N\sqrt{Q}/H^{3/4}$$

A low specific speed means that for a given rpm the weight flow is small or the head is high.

Adaption to low specific speed in the field of axial turbines is normally accomplished by use of partial admission. Partial admission may also be considered with radial turbines. However, because of the centrifugal field in the impeller, the passages not subjected to through-flow will have a large eddy motion, which may induce higher losses than are encountered in axial turbines. Hence, let us consider only full-admission radial turbines and the steps to be taken to design an optimized radial turbine for small weight flows, assuming that the rotational speed is fixed.

Consider a turbine of a given diameter and rpm which has to be redesigned to accommodate a smaller weight flow. First, wheel-passage width is decreased as far as possible. All velocity triangles would remain unchanged; only the weight flow drops proportional to the width. The influence of leakage losses through gaps becomes relatively more important. Next to be considered is a decrease in

through-flow velocity because the mass flow is also proportional to this velocity. This can be accomplished by positioning the nozzle vanes at a flat angle to the peripheral direction (6 to 10 degrees). However, flat angles lead to problems of impeller loading. The best design from the blade-loading point of view has no appreciable deceleration on suction or pressure side, as expressed by the suction and pressure-side diffusion parameters discussed earlier. This can be accomplished by having the mean relative velocity rising uniformly from inlet to exit, as shown in Figure 5-50[107].

The pressure-side velocity would stay constant in the region where the flow enters the wheel and from the mid-section or would rise sharply, its maximum value approaching the mean relative velocity. Similarly, on the suction side, the velocity will rise strongly until about the mid-section of the profile. From this point on, the velocity should stay constant and equal to the mean velocity at the turbine exit. This velocity distribution could be produced by correspondingly shaping the meridional passage of the turbine, especially by blade-thickness distribution, and by increasing the number of impeller blades at the same time, thus reducing the velocity span between mean-relative and suction or pressure surface velocities[107].

Just a few words about the turbine nozzle. The nozzle is the counterpart of a vaned diffuser in a radial compressor. Its job is to create a swirling motion of the gas before entering the turbine wheel. In general, the gas increases its velocity while passing through the nozzle vanes. Because of weight reasons, and also because subdivided exhaust manifolds for best pulse utilization require small cross sections for the turbine inlet port or ports, the inlet velocities to the turbine housing become high and sometimes there remains only a relatively small amount of flow acceleration for the nozzle passage. In the case of nozzles for radial turbines, this fact becomes even more pronounced and there is little work left for the nozzle vanes. It appears only natural in such a case to reduce the number of nozzle vanes or to dispose of the

vanes entirely. In this last case, the turbine housing has to be shaped properly so it can take over the nozzle's function. Such a housing then becomes actually a one-vane nozzle[83]. See also Figure 5-51[26] which shows a turbine wheel and nozzle ring of a lightweight 100-hp gas turbine.

5.6 Stratos TCS-670 Turbine-Compressor Set

The compressor for the ML-1 is a two-stage radial design while the turbine is a reaction type, two-stage axial flow design[22]. The turbine is designed with a constant blade root diameter of 12.14 inches. The mean diameters of the first and second stage rotors are 12.90 and 13.20 inches, respectively. Each turbine rotor uses 83 blades. The nozzle rings each use 79 blades (see also Section 12.2.1).

Since the axial length available at the turbine exit is short, some alternate method was necessary to diffuse the discharge efficiently. Effective diffusion is also required for proper flow distribution into the recuperator. As a result of exhaustive tests at Stratos, a set of vortex generator vanes has been developed. With these vanes installed at the diffuser, it is claimed that satisfactory results have been achieved.

Initially, the Stratos T-C design was not acceptable because of undesirable surge characteristics during the starting transient. This condition was corrected by redesigning the second-stage compressor diffuser[12]. Compressor calculated performance coordinates are given in Table 5-1[22], and performance charts are shown in Figures 5-52[22] and 5-53[22], one for air and the other for nitrogen. Efficiency for air at the same mass flow factor and speed of rotation is slightly higher. Figure 5-54[22] shows the turbine performance.

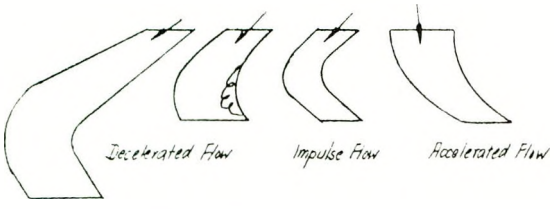


Fig. 5-48 - Blade Passage Configuration

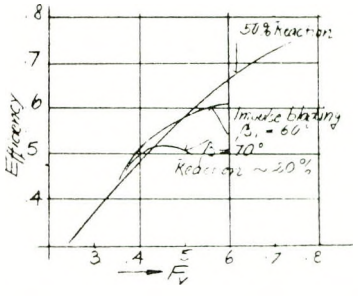


Fig. 5-49 - Performance of Impulse Type Radial Turbine

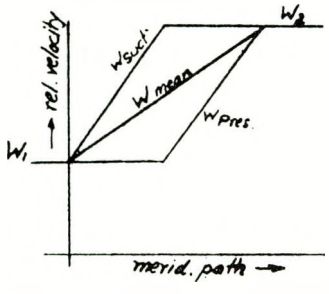


Fig. 5-50 - Blade Loading for Zero Diffusion

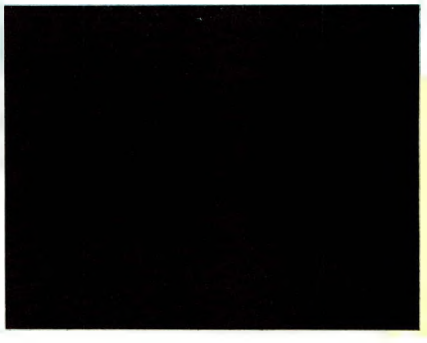


Fig. 5-51 - Turbine Wheel and Nozzle Ring in Their Working Relationship

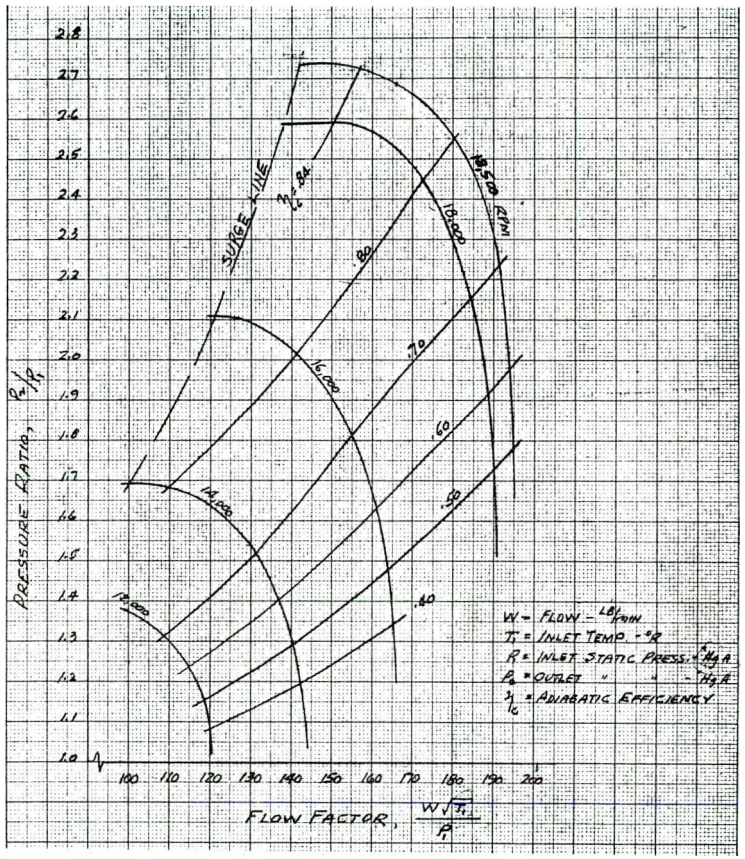


Fig. 5-52 - TCS-670 Compressor Performance, Air

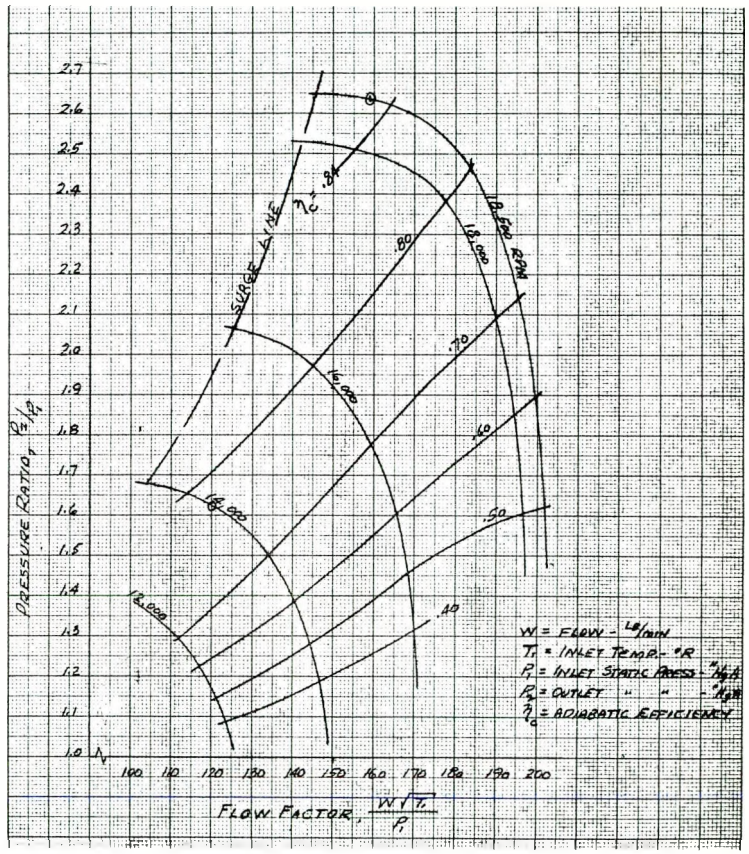


Fig. 5-53 - TCS-670 Compressor Performance, Nitrogen

Data from Stratos Division, Fairchild Corp., Report SRC-104

Table 5-1

STRATORS TCS-670 COMPRESSOR PERFORMANCE COORDINATES

Speed RPM	Efficiency η_{ad}	Nitrogen Pressure Flow Ratio P_2/P_1	Nitrogen Pressure Flow Factor $W\sqrt{T_1}/P_1$	Air Pressure Flow Ratio P_2/P_1	Air Pressure Flow Factor $W\sqrt{T_1}/P_1$
12,000	.75	1.380	98.5	1.380	101.5
	.70	1.315	108.8	1.295	111.8
	.60	1.238	115.0	1.227	117.1
	.40	1.082	120.0	1.088	123.8
14,000	.82*	1.690	100.0	1.680	103.8
	.80	1.683	109.7	1.655	114.0
	.70	1.518	131.3	1.500	134.0
	.40	1.195	142.3	1.188	146.8
16,000	.83	2.100	128.5	2.055	129.0
	.80	2.016	141.3	1.973	145.0
	.70	1.815	155.0	1.756	159.3
	.40	1.343	165.2	1.315	170.0
18,000	.84	2.590	150.6	2.512	155.3
	.80	2.450	172.5	2.385	177.5
	.70	2.155	184.3	2.090	190.0
	.50	1.728	190.0	1.607	196.5
18,500	.84	2.725	157.0	2.622	164.0
	.80	2.553	180.4	2.465	183.5
	.70	2.236	191.5	2.143	195.5
	.50	1.782	194.8	1.620	201.7

*Surge Point

Data from Stratos Division of Fairchild Engine & Airplane Corp., Report SRC-104

5.7 Clark CSN-1 Turbine-Compressor Set

The Clark CSN-1 set for the ML-1 has already undergone tests in a fossil-fuel fired open-cycle operation at the factory. Also, as part of the ML-1 power conversion skid, the set has operated in closed-cycle configuration with a fossil-fuel fired heater. The CSN-1 will be part of the ML-1 during initial operation at the National Reactor Testing Station, Idaho. The flow diagram for compressor and turbine is shown on Figure 5-55[21].

The design of the axial flow compressor is based on the original concept of a constant stator efflux angle with 50% reaction close to the inside diameter. The compressor is designed for constant temperature rise along the length of the blade on the assumption that constant axial velocity will exist along the length of the blade. This cannot be true for radial equilibrium to occur, but considerable experience has shown that for inside to outside diameter ratios used in this compressor, the influence of radial equilibrium is small. In fact, ignoring radial equilibrium in this type of design has shown that the optimum efficiency is equivalent to a free vortex (special case of radial equilibrium) or equilibrium design, but that the optimum efficiency occurs much closer to the operating line of the turbine.

The original proposal for the axial compressor showed 10 stages. However, calculations have been performed (with limited knowledge of the pressure losses in the various components in the cycle) which indicate that considerable benefit will be derived in the cycle from a specific output viewpoint in operating at a higher compression ratio than the 2.59/1 specified. For this reason it was deemed advisable to add an additional stage of compression making the axial 11 stages with slightly lower loading per stage.

The temperature rise distribution in the compressor and the deflection requirements in rotor and stator have been chosen bearing in mind the specification requirements of 125% overspeed and good low speed starting characteristics allowing ample margin between the operating and surge lines.

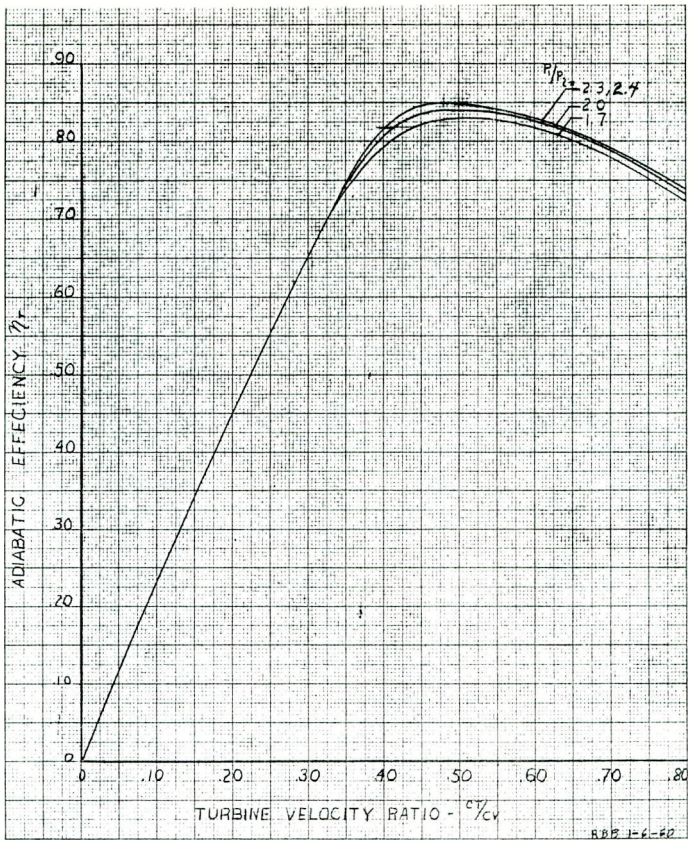


Fig. 5-54 - TCS-670 Turbine Performance

Data from Stratos Division, Fairchild Corp., Report SRC-104

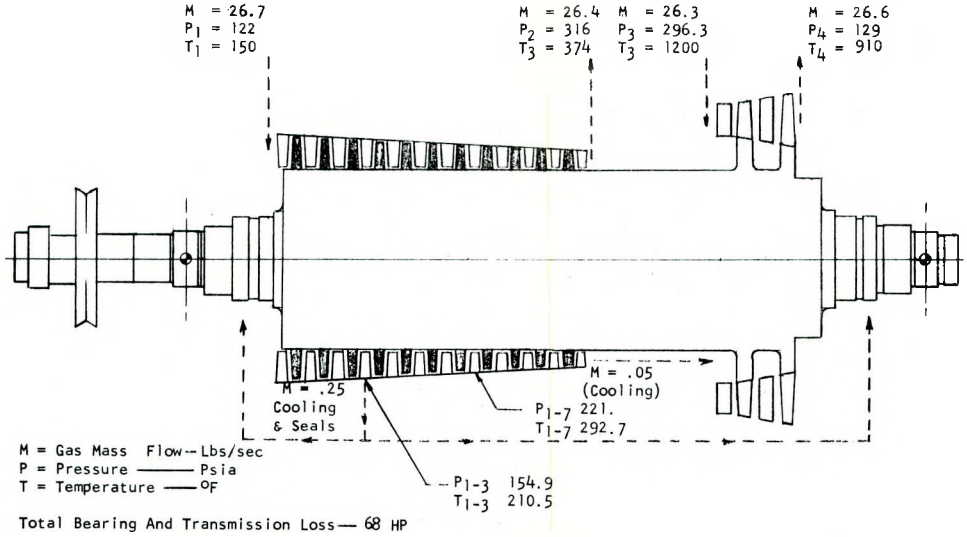


Fig. 5-55 - Flow Diagram for Clark CSN-1 Gas Turbine

Table 5-2[21] gives comprehensive design data for the axial flow compressor, showing blade section data, velocities, pressures, temperatures, etc. From this design sheet it is possible to reconstruct the entire aerodynamic design concept and the physical characteristics of the aerofoil sections.

Figure 5-56[21] gives the compressor blade section data variations with diameter, including maximum and minimum moments of inertia of the sections, areas, etc. These values are presented to enable checks of the CF and gas bending stresses to be made. Figure 5-57[21] shows the gas angle variation with radius to give a pictorial representation of the deflection through rotors and stators. Figure 5-58[21] shows the efficiency for the various blade sections based on a 0.010-inch radial clearance between blades and casing. From this characteristic, an approximate mean curve was obtained to feed into the predicted performance computation of the compressor on a digital computer.

Figure 5-59[21] gives the ordinates for the blade section designated as a C-4 section. This section has been tested by NACA and it has been found to compare favorably with the NACA-65 series aerofoil section of the same mean camber height. A C-4 section aerofoil on a circular arc camberline was selected in preference to the NACA-65 series aerofoil primarily for mechanical reasons, but also for a slight increase in incidence range of the C-4 section. The NACA profile has a distinct hook close to the trailing edge of the blade, (especially with high cambers) making it difficult to manufacture without "burning" or overheating the trailing edge section of the aerofoil. Moreover, for similar thickness/chord ratios and performance the C-4 section has a greater minimum moment of inertia and hence strength.

All 11 stages have similar blading, except for length, and the rotor has a constant inside diameter, making the rotor blade fastening similar in every stage. Stator blades are untwisted constant section rolled airfoils with shrouds on the inside diameter for minimum effect

Table 5-2

COMPRESSOR DESIGN CHART

ROW	ENTRY ANNULUS DIMENSIONS	SECTION DIA. in	$\beta_1°$	$\beta_2°$	CAMBER $\theta°$	STAGGER $\gamma°$	CHORD c in	MAX. THK. / CHORD t/c	No. of BLADES	PITCH / CHORD s/c	ENTRY ANNULUS AREA in²	ENTRY VELOCITY ft/sec	U ft/sec	T_{tot} °R	P_{tot} psia	STAGE ΔT °F	$\varepsilon°$	$\delta°$	$i°$	Ω	$\frac{i-i^*}{\theta}$	η_{adia}	$\alpha_{1-3}°$	$\alpha_{2-4}°$	SECTION DATA	
I.G.V.	6.750 9.000	7.0 7.5 8.0 8.5 9.0									27.818			610.0	122.0								40.00		
1st ROTOR	6.750 9.000	7.0 7.5 8.0 8.5 9.0	59.0 59.0 59.0 59.0 60.0	33.80 41.20 47.70 52.70 56.25	25.20 17.80 11.30 6.30 3.75	46.40 50.10 53.35 55.85 58.12	.500	.150 .1375 .125 .1125 .100	61	.721 .772 .824 .875 .927	27.818	271.0	719.9	610.00	122.00	21.21	13.50	7.30	2.45	.97	-.0269	.849	61.09	48.44	15.00 C4 13.75 C4 12.50 C4 11.25 C4 10.00 C4	25.2 C 30 17.8 C 30 11.3 C 30 6.3 C 30 3.78 C 30
1st STATOR	6.750 8.958	7.0 7.5 8.0 8.5 9.0	58.7	34.70	24.00	46.70	.500	.150	58	.812	27.227	266.4					15.53	8.25	-2.20		-.0633	.841	57.50	42.93	15.0 C4	24.0 C 50
2nd ROTOR	6.750 8.916	7.0 7.5 8.0 8.5	59.0	33.80 41.20 47.70 52.70	25.20 17.80 11.30 6.30	46.40 50.10 53.35 55.85	.500	.150 .1375 .125 .1125	61	.721 .772 .824 .875	26.637	264.4	719.9	631.21	135.17	19.34	13.50	7.30	2.45	.95	-.0512	.847	60.76	48.44	15.00 C4 13.75 C4 12.50 C4 11.25 C4	25.2 C 30 17.8 C 30 11.3 C 30 6.3 C 30
2nd STATOR	6.750 8.875	7.0 7.5 8.0 8.5	58.7	34.70	24.00	46.70	.500	.150	58	.812	26.065	261.7					15.53	8.25	-2.20		-.0141	.849	58.26	42.96	15.0 C4	24.0 C 50
3rd ROTOR	6.750 8.836	7.0 7.5 8.0 8.5	59.0	33.80 41.20 47.70 52.70	25.20 17.80 11.30 6.30	46.40 50.10 53.35 55.85	.500	.150 .1375 .125 .1125	61	.721 .772 .824 .875	25.494	259.5	719.9	650.55	147.92	19.91	13.50	7.30	2.45	.93	-.0017	.850	61.43	48.45	15.00 C4 13.75 C4 12.50 C4 11.25 C4	25.2 C 30 17.8 C 30 11.3 C 30 6.3 C 30
3rd STATOR	6.750 8.702	7.0 7.5 8.0 8.5	58.7	34.70	24.00	46.70	.500	.150	58	.812	24.915	257.3					15.53	8.25	-2.20		+.0319	.855	58.97	42.96	15.0 C4	24.0 C 30
4th ROTOR	6.750 8.750	7.0 7.5 8.0 8.5	59.0	33.80 41.20 47.70 52.70	25.20 17.80 11.30 6.30	46.40 50.10 53.35 55.85	.500	.150 .1375 .125 .1125	61	.721 .772 .824 .875	24.335	255.2	719.9	670.46	161.95	20.33	13.50	7.30	2.45	.91	+.0399	.856	61.99	48.46	15.00 C4 13.75 C4 12.50 C4 11.25 C4	25.2 C 30 17.8 C 30 11.3 C 30 6.3 C 30
4th STATOR	6.750 8.709	7.0 7.5 8.0 8.5	58.7	34.70	24.00	46.70	.500	.150	58	.812	23.774	253.4					15.53	8.25	-2.20		+.0726	.861	59.61	42.99	15.0 C4	24.0 C 30
5th ROTOR	6.750 8.668	7.0 7.5 8.0 8.5	59.0	33.80 41.70 47.70 52.70	25.20 17.80 11.30 6.30	46.40 50.10 53.35 55.85	.500	.150 .1375 .125 .1125	61	.721 .772 .824 .875	23.214	251.3	719.9	690.79	177.29	20.58	13.50	7.30	2.45	.89	+.0782	.861	62.51	48.49	15.00 C4 13.75 C4 12.50 C4 11.25 C4	25.2 C 30 17.8 C 30 11.3 C 30 6.3 C 30
5th STATOR	6.750 8.626	7.0 7.5 8.0 8.5	58.7	34.70	24.00	46.70	.500	.150	58	.812	22.645	250.1					15.53	8.25	-2.20		+.1058	.864	60.12	43.04	15.0 C4	24.0 C 30
6th ROTOR	6.750 8.584	7.0 7.5 8.0	59.0	33.80 41.70 47.70	25.20 17.80 11.30	46.40 50.10 53.35	.500	.150 .1375 .125	61	.721 .772 .824	22.076	248.4	719.9	711.37	193.88	20.66	13.50	7.30	2.45	.87	+.1057	.864	62.88	48.53	15.00 C4 13.75 C4 12.50 C4	25.2 C 30 17.8 C 30 11.3 C 30
6th STATOR	6.750 8.543	7.0 7.5 8.0	58.7	34.70	24.00	46.70	.500	.150	58	.812	21.562	247.7					15.53	8.25	-2.20		+.1301	.866	60.50	43.07	15.0 C4	24.0 C 30
7th ROTOR	6.750 8.502	7.0 7.5 8.0	59.0	33.80 41.70 47.70	25.20 17.80 11.30	46.40 50.10 53.35	.500	.150 .1375 .125	61	.721 .772 .824	20.976	246.1	719.9	731.97	211.87	20.69	13.50	7.30	2.45	.86	+.1268	.866	63.16	48.55	15.00 C4 13.75 C4 12.50 C4	25.2 C 30 17.8 C 30 11.3 C 30
7th STATOR	6.750 8.460	7.0 7.5 8.0	58.7	34.70	24.00	46.70	.500	.150	58	.812	20.418	246.1					15.53	8.25	-2.20		+.1457	.867	60.74	43.10	15.0 C4	24.0 C 30
8th ROTOR	6.750 8.418	7.0 7.5 8.0	59.0	33.80 41.70 47.70	25.20 17.80 11.30	46.40 50.10 53.35	.500	.150 .1375 .125	61	.721 .772 .824	19.860	245.2	719.9	752.66	230.95	20.58	13.50	7.30	2.45	.85	+.1638	.867	63.38	48.57	15.00 C4 13.75 C4 12.50 C4	25.2 C 30 17.8 C 30 11.3 C 30
8th STATOR	6.750 8.372	7.0 7.5 8.0	58.7	34.70	24.00	46.70	.500	.150	58	.812	19.320	245.6					15.53	8.25	-2.20		+.1512	.868	60.83	43.11	15.0 C4	24.0 C 30
9th ROTOR	6.750 8.336	7.0 7.5 8.0	59.0	33.80 41.70 47.70	25.20 17.80 11.30	46.40 50.10 53.35	.500	.150 .1375 .125	61	.721 .772 .824	18.781	245.0	719.9	773.24	250.33	20.58	13.50	7.30	2.45	.85	+.1374	.867	63.30	48.57	15.00 C4 13.75 C4 12.50 C4	25.2 C 30 17.8 C 30 11.3 C 30
9th STATOR	6.750 8.296	7.0 7.5 8.0	58.7	34.70	24.00	46.70	.500	.150	58	.812	18.262	245.7					15.53	8.25	-2.20		+.1512	.868	60.83	43.11	15.0 C4	24.0 C 30
10th ROTOR	6.750 8.256	7.0 7.5 8.0	59.0	33.80 41.70 47.70	25.20 17.80 11.30	46.40 50.10 53.35	.500	.150 .1375 .125	61	.721 .772 .824	17.740	245.5	719.9	793.82	271.36	20.35	13.50	7.30	2.45	.85	+.1325	.867	63.24	48.56	15.00 C4 13.75 C4 12.50 C4	25.2 C 30 17.8 C 30 11.3 C 30
10th STATOR	6.750 8.213	7.0 7.5 8.0	58.7	34.70	24.00	46.70	.500	.150	58	.812	17.185	247.4					15.53	8.25	-2.20		+.1346	.867	60.87	43.08	15.0 C4	24.0 C 30
11th ROTOR	6.750 8.170	7.0 7.5 8.0	59.0	33.80 41.70 47.70	25.20 17.80 11.30	46.40 50.10 53.35	.500	.150 .1375 .125	61	.721 .772 .824	16.631	248.4	719.9	814.17	293.31	19.86	13.50	7.30	2.45	.85	+.1042	.864	62.86	48.52	15.00 C4 13.75 C4 12.50 C4	25.2 C 30 17.8 C 30 11.3 C 30
11th STATOR	6.750 8.127	7.0 7.5 8.0	58.7	34.70	24.00	46.70	.500	.150	58	.812	16.146	250.1					15.53	8.25	-2.20		+.1081	.865	60.16		15.0 C4	24.0 C 30
DIFFUSER INLET											15.661	250.3		834.03	315.77										

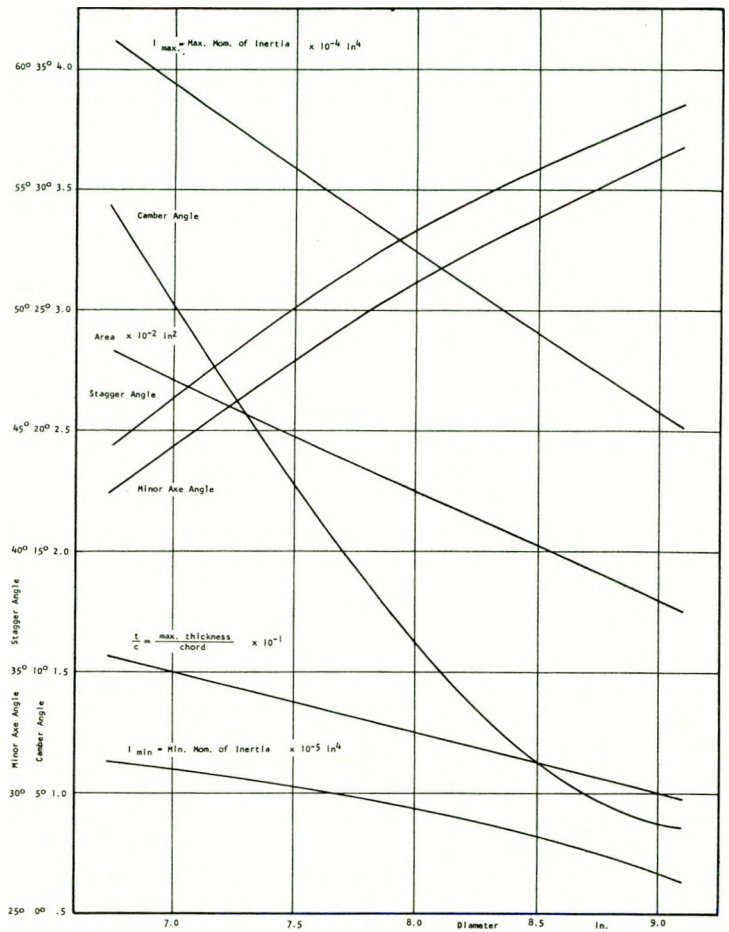


Fig. 5-56 - CSN-1 Compressor Blade Section Data vs. Diameter

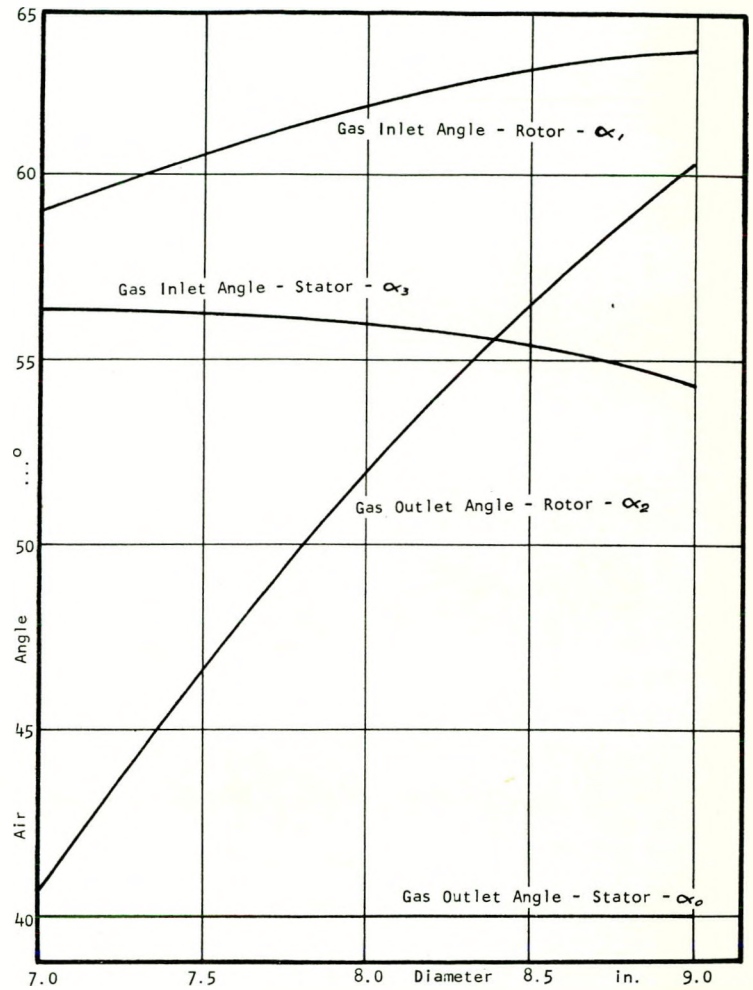


Fig. 5-57 - CSN-1 Compressor Air Angle Distribution vs. Diameter, Stage 1

Note: See Notation on Figure 5-60

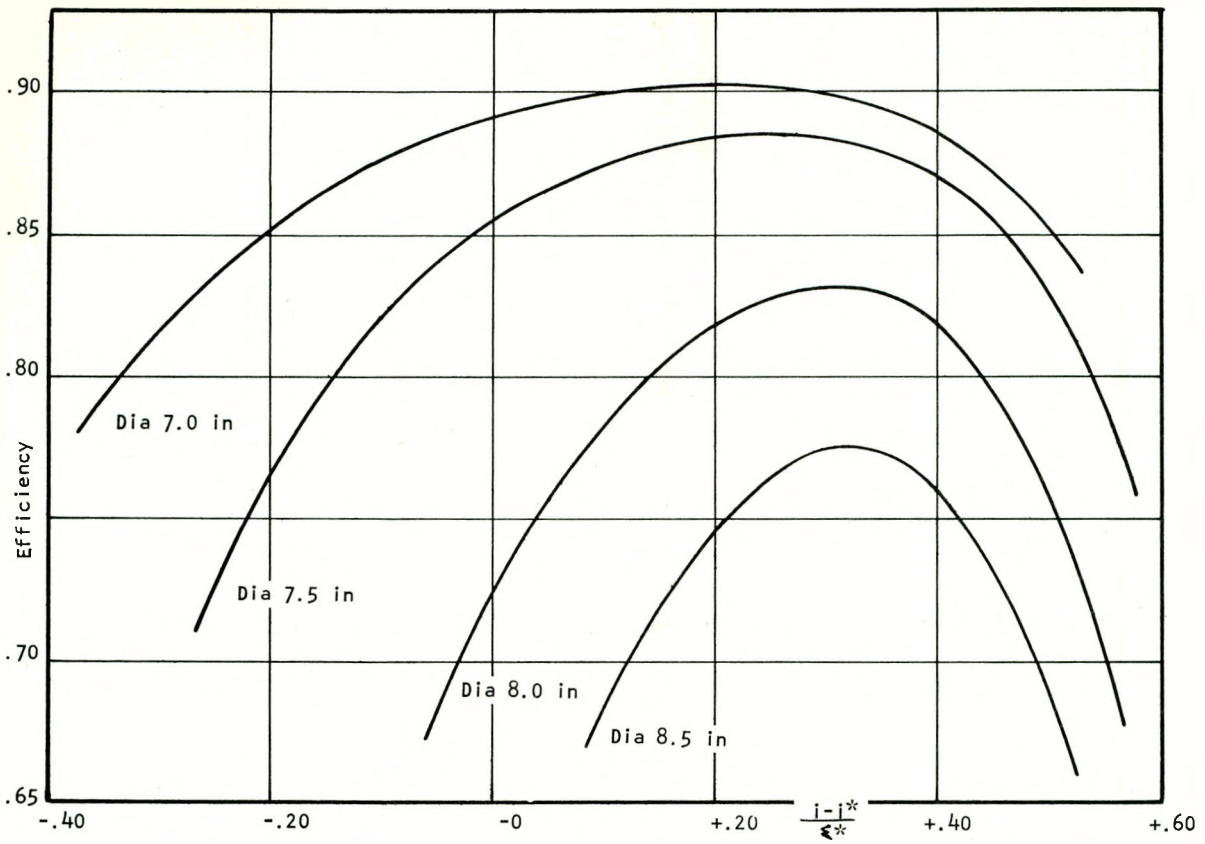
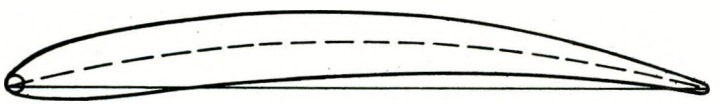


Fig. 5-58 - CSN-1 Compressor Blade Efficiency vs. Incidence Parameter



Base Form C4

Station	Upper Ordinate	Lower Ordinate
0	0	0
1.25	1.65	1.65
2.5	2.27	2.27
5.0	3.08	3.08
7.5	3.62	3.62
10	4.02	4.02
15	4.55	4.55
20	4.83	4.83
30	5.00	5.00
40	4.89	4.89
50	4.57	4.57
60	4.05	4.05
70	3.37	3.37
80	2.54	2.54
90	1.60	1.60
95	1.06	1.06
100	0	0
Leading Edge Radius 12%t Trailing Edge Rad. 6%t		

Fig. 5-59 - CSN-1 Compressor Blade Profile C4 Section Ordinates

of end losses and circulation around the blade tip. Provision has been made to bleed small quantities from the third or seventh stage or both, depending upon the final requirements. This gas will be used for buffer seal gas and cooling of turbine disks and casings.

The conservative design of the compressor has ensured that by small changes to the compressor stator blading, the mass flow and pressure ratio can be altered by about 10% to suit possible changes in cycle requirements. If any change in the flow requirements of the cycle are foreseen, then early provision should be made to produce stator rings of different stagger to those described here.

The anticipated performance characteristics of the axial flow compressor is shown in Figures 5-61[21] and 5-62[21]. These characteristics are based on approximately mean diameter conditions, and indicate an overall efficiency of 83.8%. Previous use of the prediction method for other compressors has shown a high degree of accuracy especially around the design point.

Flow tests were made of a full-scale model of the compressor discharge volute for the Clark T-C set. Since the discharge volute is the most critical aerodynamic section with respect to compressor efficiency, aerodynamic model tests are the most practical solution for proper design of the diffuser[12]. Figure 5-60[21] shows the notation for velocity triangles on axial-flow compressor stage.

The compressor discharge volute receives gas directly from the 11 stage stator blade at swirl angle of approximately 44°. Keeping the distance between bearings to a minimum is absolutely essential if the critical speed requirements of the specification are to be met. For this reason, the design of the compressor discharge volute has been quite difficult.

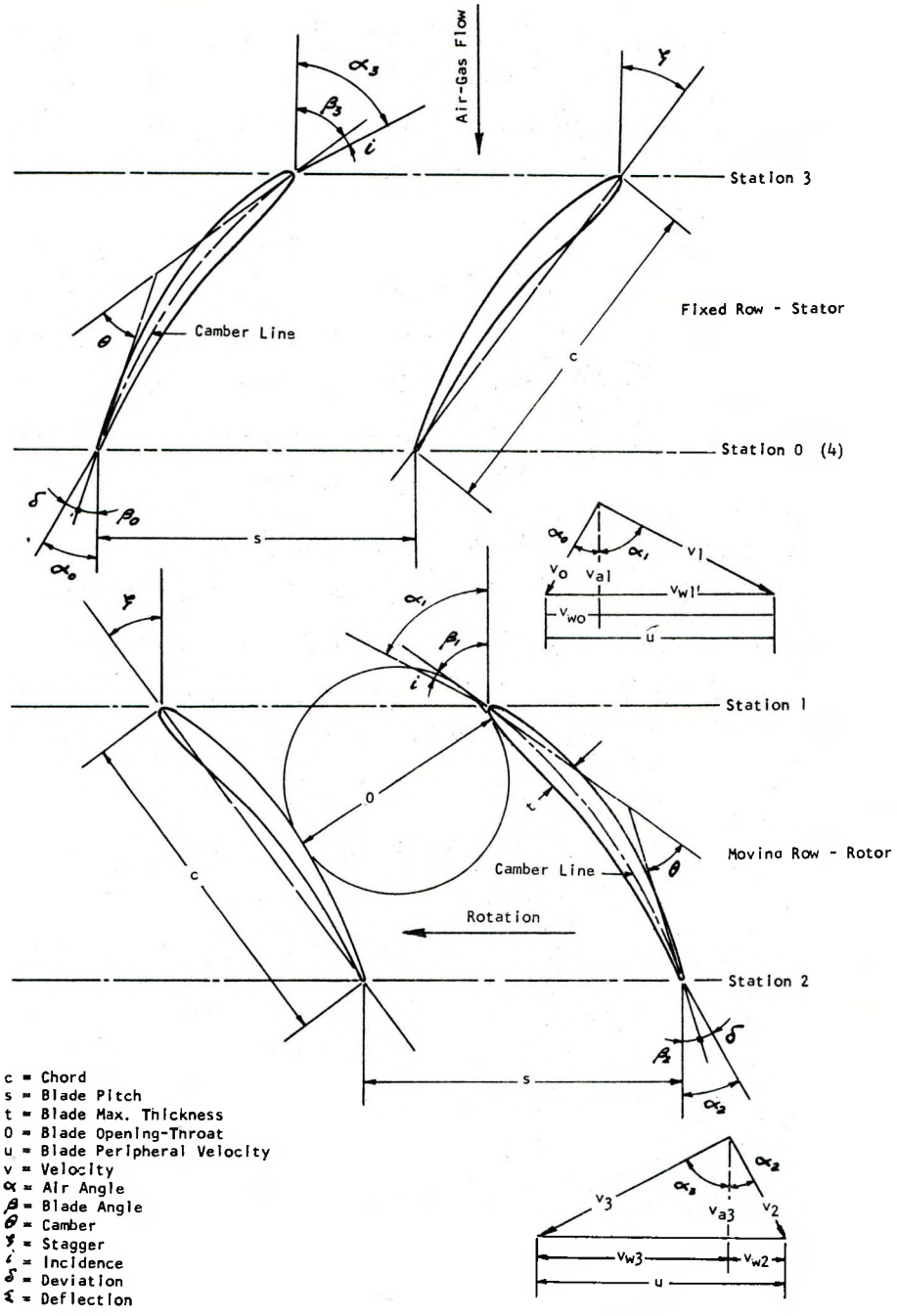


Fig. 5-60 - Notation for Velocity Triangles on Axial-Flow Compressor Stage

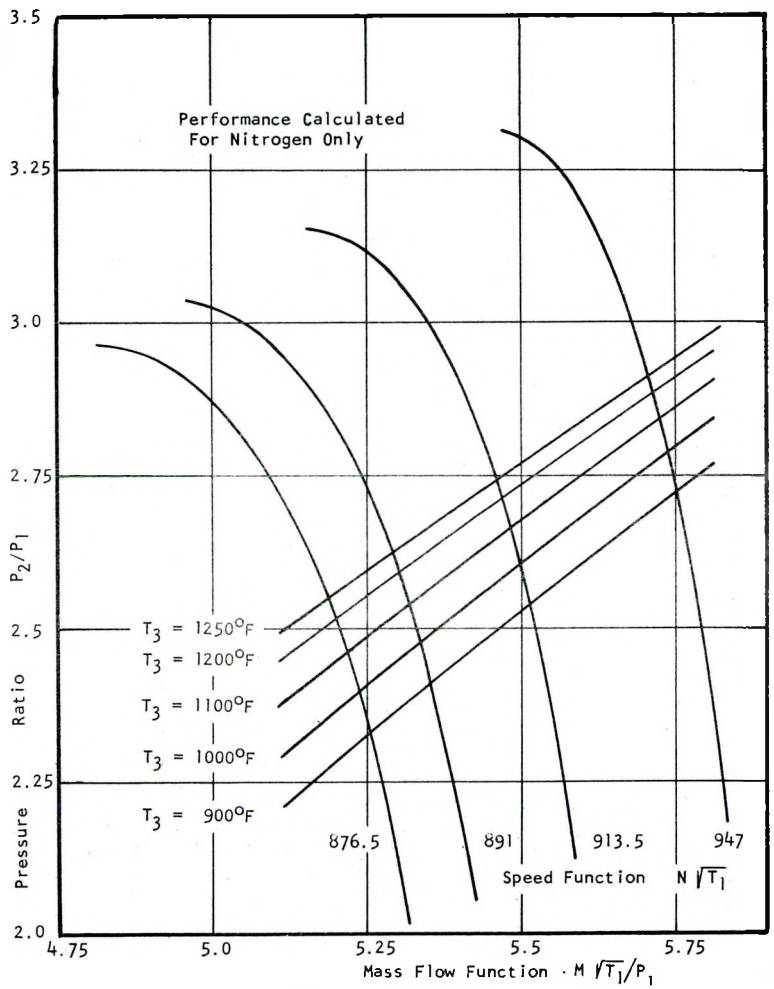


Fig. 5-61 - CSN-1 Predicted Compressor Characteristic at Variable Turbine Inlet Temperature

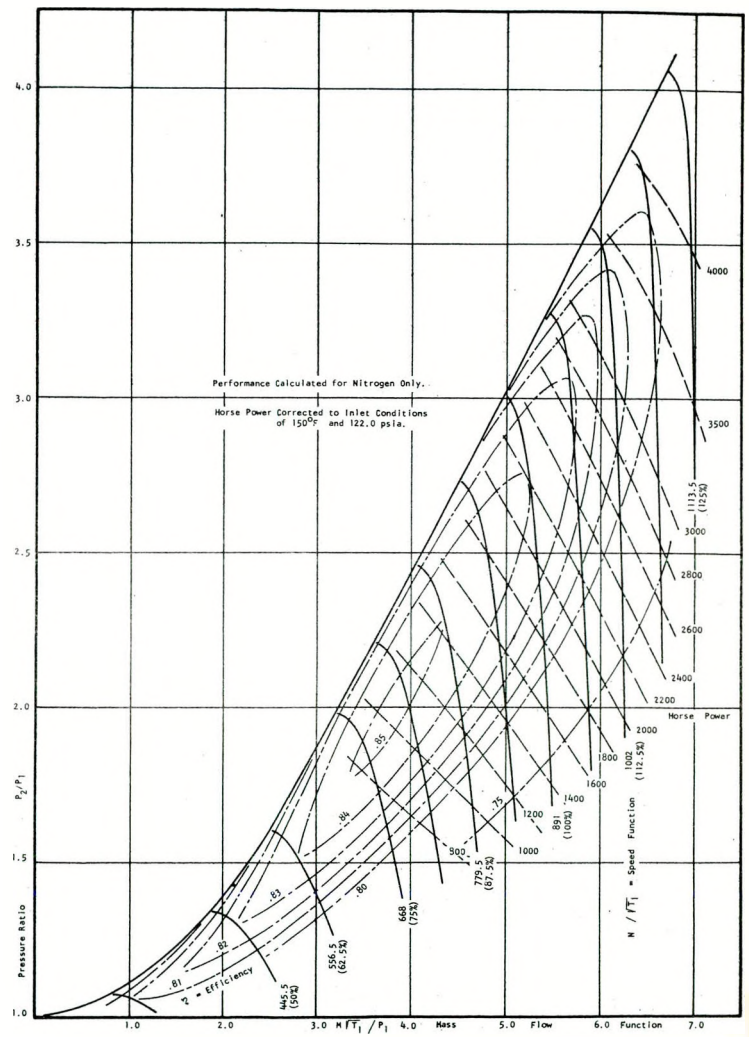


Fig. 5-62 - CSN-1 Compressor Performance Characteristic

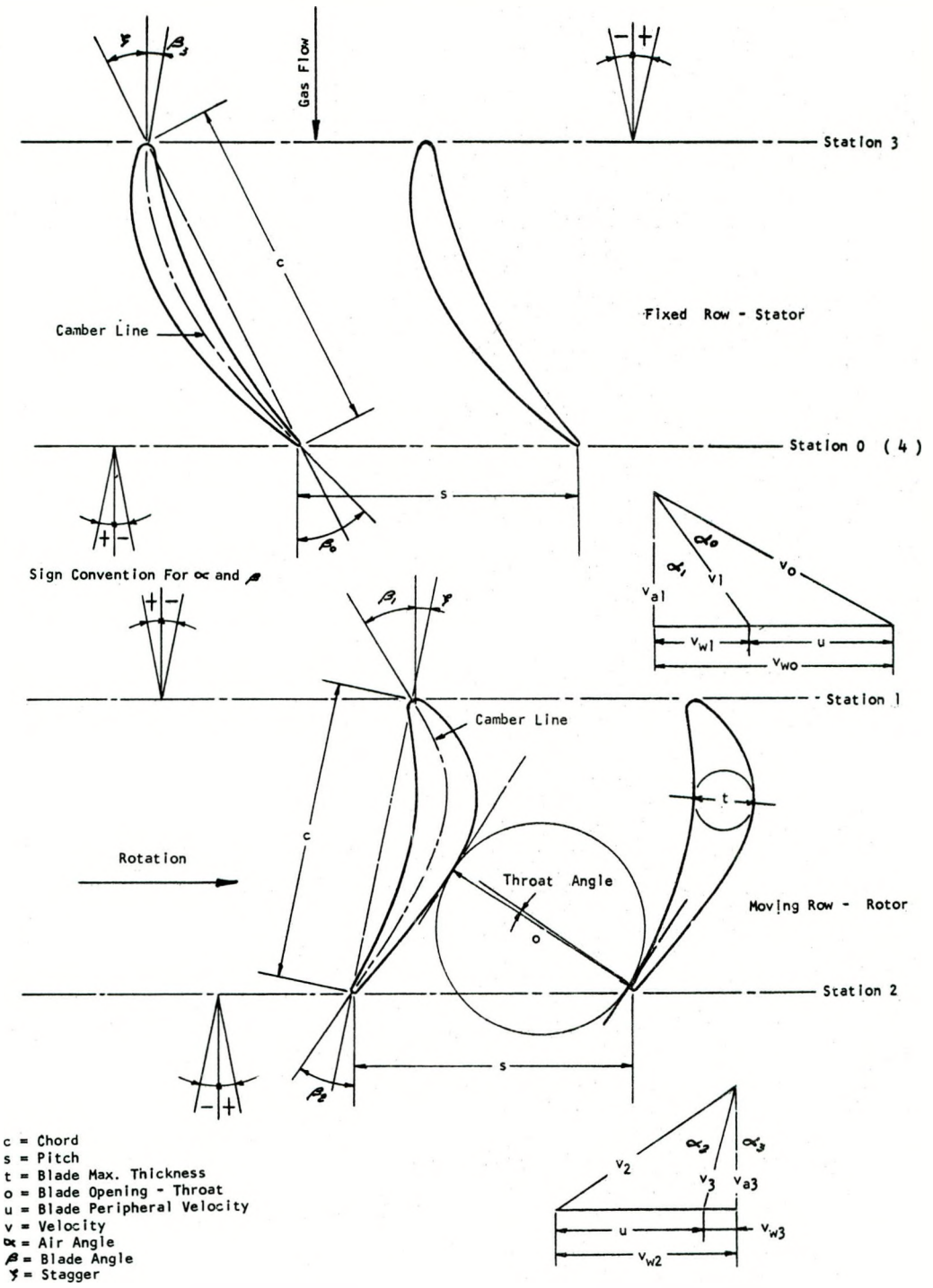


Fig. 5-63 - Notation and Sign Convention for Velocity Triangles on Axial Flow Turbine Stage

It is well known that adverse pressure gradients, which are formed in a scroll diffuser for radial equilibrium to exist, can cause high diffusion losses. For this reason, the compressor discharge volute has been designed as a variable-area constant-velocity collector. Diffusion is accommodated outside the barrel of the TC set in the ducting between compressor discharge and regenerator inlet, where improved diffusion rate can be obtained. However, even with a constant velocity collector of this type, the performance cannot be assessed accurately.

The turbine inlet duct is an accelerating passage with rapid acceleration taking place close to the first stage nozzle blades of the turbine. Because of the acceleration of the turbine inlet volute, no serious difficulty is expected in obtaining low loss characteristics in this section.

Because of the extremely limited space available for diffusion in the exhaust of the turbine and because of the lack of knowledge concerning the recuperator gas side header, it was impractical to attempt to fulfill the original requirements of AGN Specification TM-353 for maximum velocity profile variation of 50%. If improved distribution is required from the turbine exhaust (which incidentally will be affected by the header arrangement of the recuperator), then much more detailed information would be required from AGN and the recuperator manufacturer, and more length for the overall unit would be required.

The turbine design is a conventional two-stage design with 50% reaction at the mean diameter. It conforms to the special radial equilibrium design case of constant work done, and constant axial

velocity along the length of the blade. This special design case is commonly called "free vortex," and required the whirl velocity after the nozzle blades to vary inversely proportional to radius. The turbine is unchoked as critical pressure drop does not occur over any one row of blades.

Table 5-3[21] gives the design data applicable to the turbine, such as gas angles velocities, pressures, and temperatures for each stage. Figure 5-64[21] gives relevant blade section data versus diameter including maximum and minimum moments of inertia, cross-sectional areas, etc., enabling independent calculations for CF and gas bending stresses. Figure 5-65[21] shows the turbine blade section loss characteristic versus incidence parameter for the turbine blade sections for 0.015 inch clearance between shroud and stator rings.

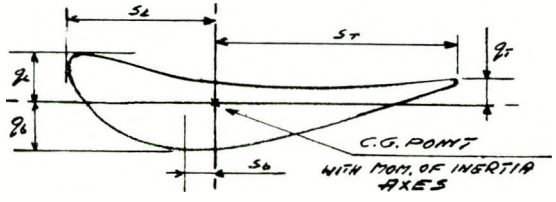
Figure 5-66[21] is a pictorial representation of the turbine velocity triangles for the turbine. In this figure, the inlet and discharge gas angles are shown together with the absolute and relative velocities.

It should be noted that the mass flow parameter, shown in Figure 5-67[21] which give the turbine performance prediction, is approximately 2% low. The areas of the turbine are deliberately left slightly undersize to allow for matching between compressor or turbine. Up to a 5% increase in turbine area can be accomplished by the simple expedient of machining trailing edges of the blading, but a decrease in area would require a new stagger for the blading. On this premise, it was considered advisable to deliberately undersize the turbine areas. A suitable correction factor has been introduced into the integrated performance characteristic to allow for this discrepancy from the design value.

Table 5-3

TURBINE DESIGN CHART

ROW	ROTOR							STATOR
DIAMETER	8.48	9.20	9.50	10.20	10.90	11.20	11.92	10.2
CHORD C IN	.7065	.7045	.7565	.8012	.8490	.8775	.9025	.8350
max. THICKN. $t_{max.}$ IN	.2770	.2315	.2110	.1655	.1255	.1095	.0850	.1655
PITCH S IN	.5668	.6149	.6350	.6818	.7286	.7486	.7968	.6818
THROAT OPEN. O IN	.1870	.1870	.1870	.1880	.1892	.1893	.1961	.1820
THROAT ANGLE °	3.20	4.87	3.15	4.30	3.87	1.98	5.30	4.30
T.E. RADIUS R_{TE} IN	.0150	.0125	.0125	.0125	.0125	.0125	.0125	.0125
L.E. RADIUS R_{LE} IN	.0670	.0600	.0555	.0400	.0325	.0340	.0340	.040
SECT. INL. $\&$ β_{1-3} °	45.08	36.78	30.97	16.37	-17.62	-29.04	-43.83	0
SECT. OUTL. $\&$ β_{2-4} °	-71.22	-71.73	-72.12	-73.25	-74.75	-75.43	-79.05	-73.25
SECT. C.G. COORD. X_c IN	.3307	.2987	.2767	.2345	.1968	.1818	.1632	
SECT. C.G. COORD. Y_c IN	.4237	.4545	.4593	.4786	.4903	.4926	.5009	
MOM. OF INERTIA / min. IN^4	.0006743	.0005188	.0004483	.0003032	.0002053	.0001814	.0001300	
MOM. OF INERTIA / max. IN^4	.0052103	.0044371	.0041271	.0037089	.0033395	.0032855	.0030933	
AREA IN^2	.1390	.1173	.1067	.0857	.0693	.0640	.0539	
MINOR AXE $\&$ α °	32.03	37.62	42.275	52.76	61.55	64.67	68.39	
DISTANCE S_L IN	.277	.283	.287	.311	.347	.365	.383	
DISTANCE q_L IN	.185	.152	.144	.118	.078	.066	.056	
DISTANCE S_T IN	.501	.510	.510	.516	.520	.521	.522	
DISTANCE q_T IN	.202	.187	.187	.120	.075	.065	.054	
DISTANCE S_b IN	.065	.075	.082	.125	.170	.210	.230	
DISTANCE q_b IN	.177	.162	.147	.116	.084	.070	.051	



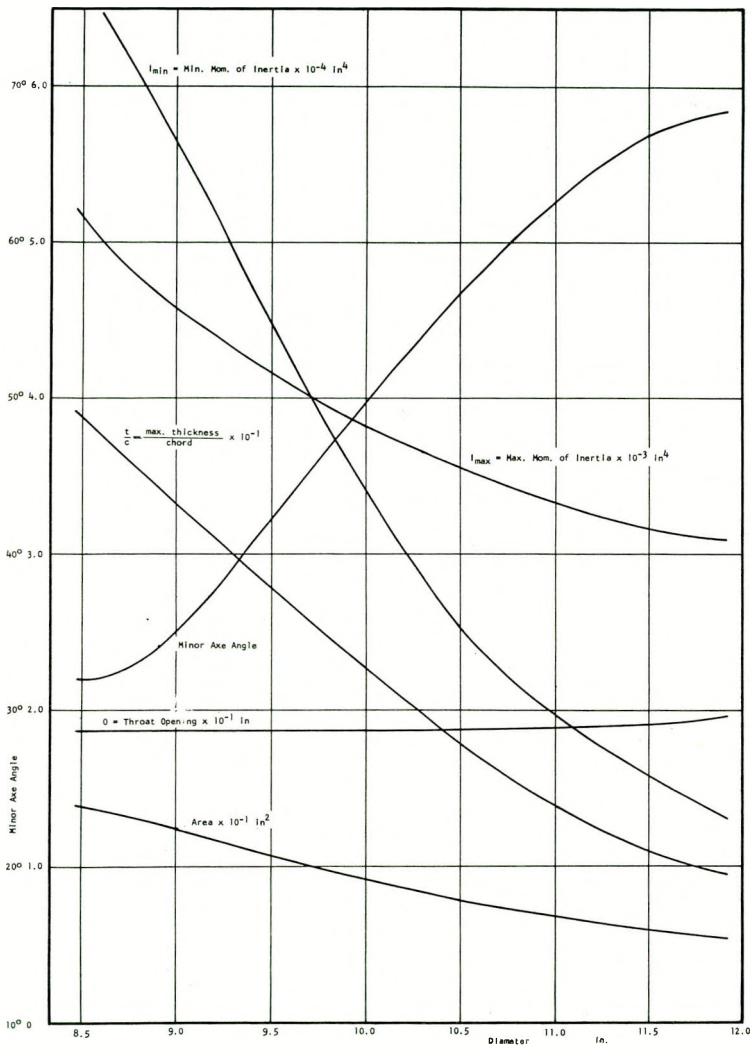


Fig. 5-64 - CSN-1 Turbine Blade Section Data vs. Diameter

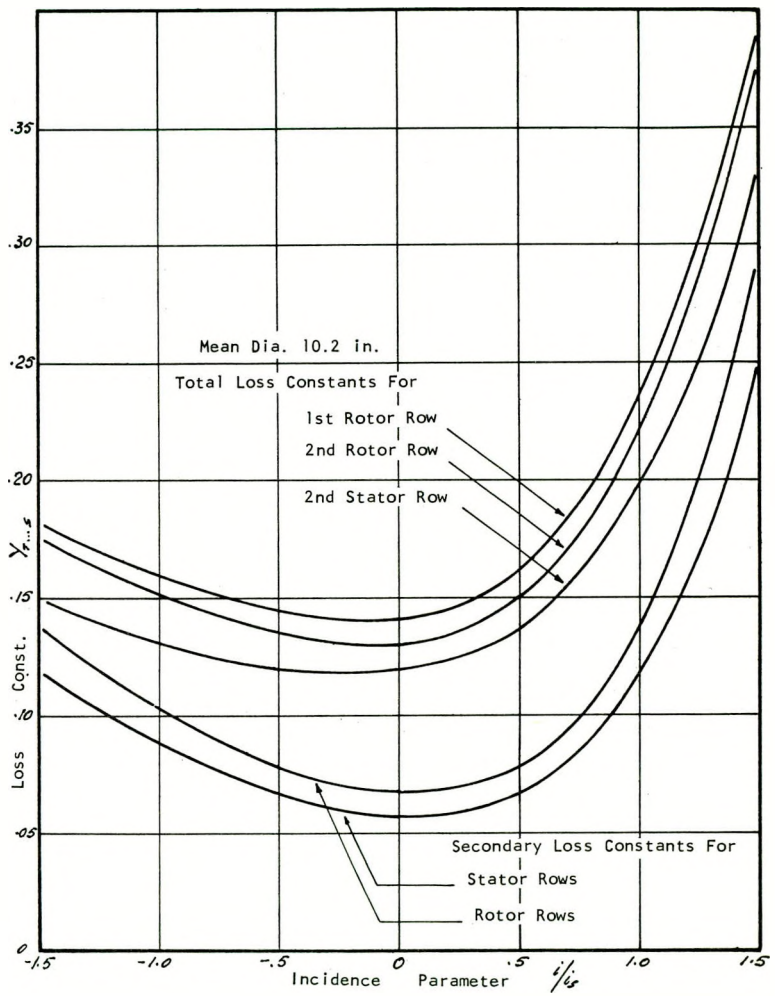


Fig. 5-65 - CSN-1 Turbine Loss vs Incidence Parameter

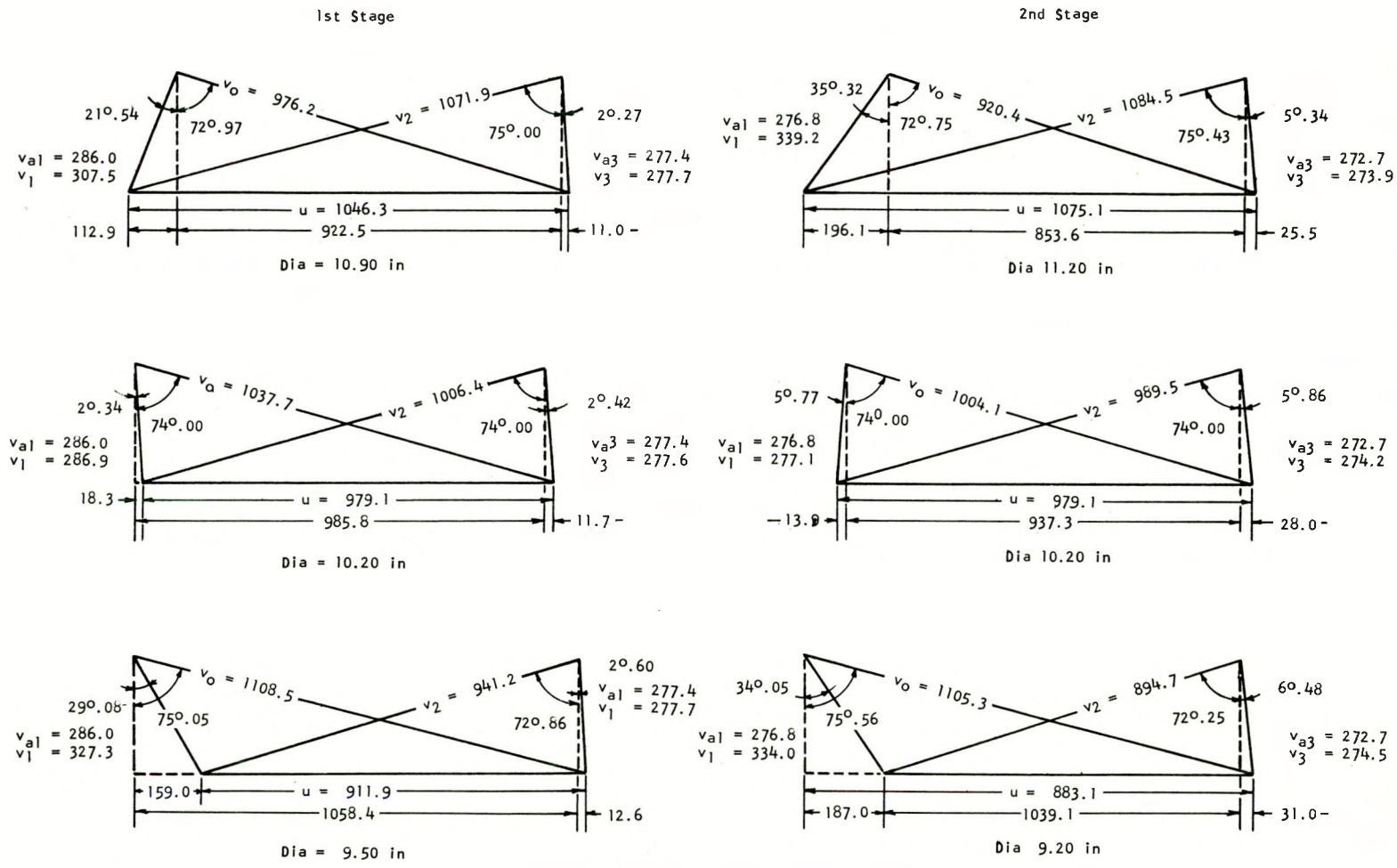


Fig. 5-66 - CSN-1 Turbine Velocity Triangles

Note: See Notation on Figure 5-63

THE FRANKLIN INSTITUTE • Laboratories for Research and Development
F-A2392-

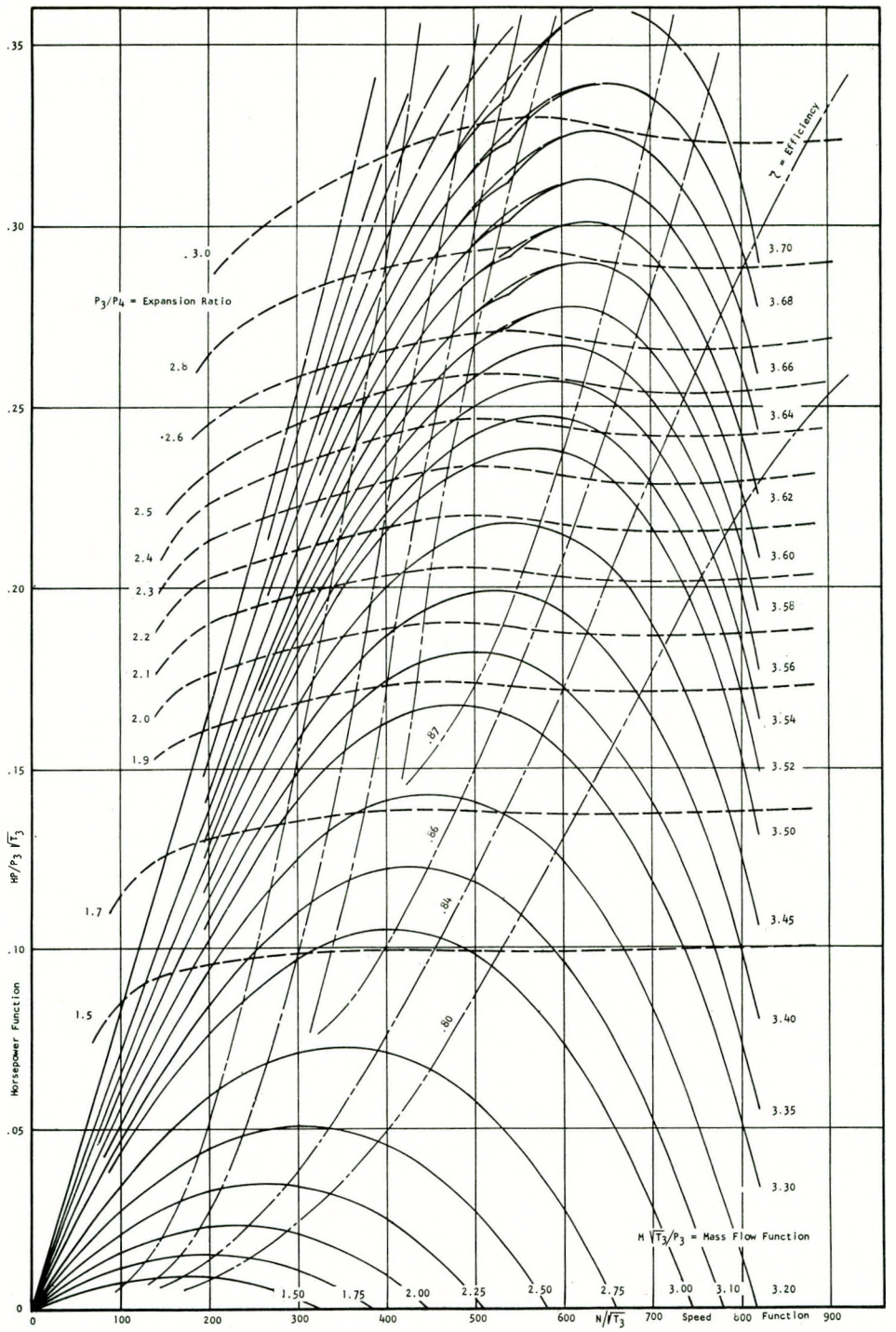


Fig. 5-67 - CSN-1 Turbine Performance Characteristics

5.8 MGCR Turbine-Compressor Set

5.8.1 Compressor Performance

Tests are underway at the Westinghouse Electric Corporation on compressor and turbine stage models to provide stage performance data[71]. Furthermore, tests are being conducted on compressor diffuser and exhaust hoods and also on turbine inlet scroll models. The compressor test model represents the ninth, tenth, eleventh, and twelfth stages of the 21-stage high-pressure compressor[73].

The study of compressor aerodynamics has centered on the question of blade loading. It has been established that the range of loading of interest for the MGCR compressor can be covered in the test program by small variations in blade stagger angle[74].

An analysis of off-design compressor performance has been carried out to determine the effect of changes in stagger angle and in solidity on cascade and stage characteristics. It was shown that rotors and stators are matched for any stagger angle. The wall-stall factor was calculated for a range of stagger angles. The methods of analysis developed in the course of this study will be applied to the interpretation of test results[61].

A decision has been made to design the MGCR test compressors with a wall-loading factor, $\frac{p}{q} = 1 - \left(\frac{w_2}{w_1}\right)^2$, representing a diffusion factor, limited to 0.45. The wall loading factor is defined as the difference between the squares of the inlet and outlet row velocity divided by the square of the inlet velocity. Because wall-stall is generally thought to occur when the wall-loading factor is between 0.45 and 0.50, this limit represents a compromise between possible improvements in compressor design (e.g., reduction of the number of stages) and a design which might be subject to excessive wall stall[61].

After shakedown runs, data were obtained on the inlet-guide vanes, as well as on the operation of rotor and stator sections of the model[75]. The four-stage compressor model, running in the variable density tunnel at Westinghouse, has provided data which give the pressure coefficient and efficiency as a function of flow coefficient. Curves of pressure coefficient vs. flow coefficient have been experimentally established on each side of the design point with adjustments of the blade setting angle. Maximum efficiency is 0.88 to 0.89.

It was found that increasing the Reynolds number brought about a decrease in pressure coefficient at a given value of flow coefficient. This is the opposite effect from that predicted from turbomachinery experience. A number of runs were made in which the Reynolds number was changed by changing speed of rotation instead of loop pressure. The resulting data indicate that the effect is a function of pressure instead of Reynolds number per se. Attempts are being made to locate the source of this anomaly by checking the instrumentation and the flow distribution entering the model[71].

The performance of the compressor model design configuration which incorporates 63 blade rotors and 56 blades stators has been previously determined. Using this performance as the basis of comparison, other rotor and stator solidity combinations have been tested and their performances compared. Table 5-4[108] gives some of the results.

If we call combined related solidity

$$r_{comb} = \frac{n_r L_r + n_s L_s}{63 L_r + 56 L_s}$$

which is related to configuration with 63 rotor blades and 56 stator blades

where

n_r = number of rotor blades

n_s = number of Stator blades

Table 5-4

MAXIMUM EFFICIENCIES AND CORRESPONDING PRESSURE COEFFICIENTS AT DIFFERENT SOLIDITIES

(MGCR Compressor)

Configuration	Maximum Efficiency	Pressure coefficient at max. efficiency
63 rotor blades, 56 stator blades Rotor solidity at hub 1.19 Stator solidity at hub 0.89	88.6	0.580
63 rotor blades, 66 stator blades Rotor solidity at hub 1.19 Stator solidity at hub 1.05	88.4	0.593
75 rotor blades, 66 stator blades Rotor solidity at hub 1.41 Stator solidity at hub 1.05	88.3	0.630
51 rotor blades, 56 stator blades Rotor solidity at hub 0.960 Stator solidity at hub 0.890	88.8	0.570
51 rotor blades, 46 stator blades Rotor solidity at hub 0.96 Stator solidity at hub 0.73	88.6	0.550

L_r = rotor blade chord length

L_s = stator blade chord length

we can plot the related pressure coefficients and related efficiencies over the combined related solidity (see Figure 5-68[108]). From this curve it can be seen that as the solidity is increased, the efficiency falls off slightly but the pressure coefficient at the point of maximum efficiency increases considerably. With decreased solidity, the efficiency increases slightly to a maximum with a considerable fall-off in pressure coefficient. As the solidity decreases further, however, the efficiency begins to fall-off with a greater decrease in pressure coefficient[108].

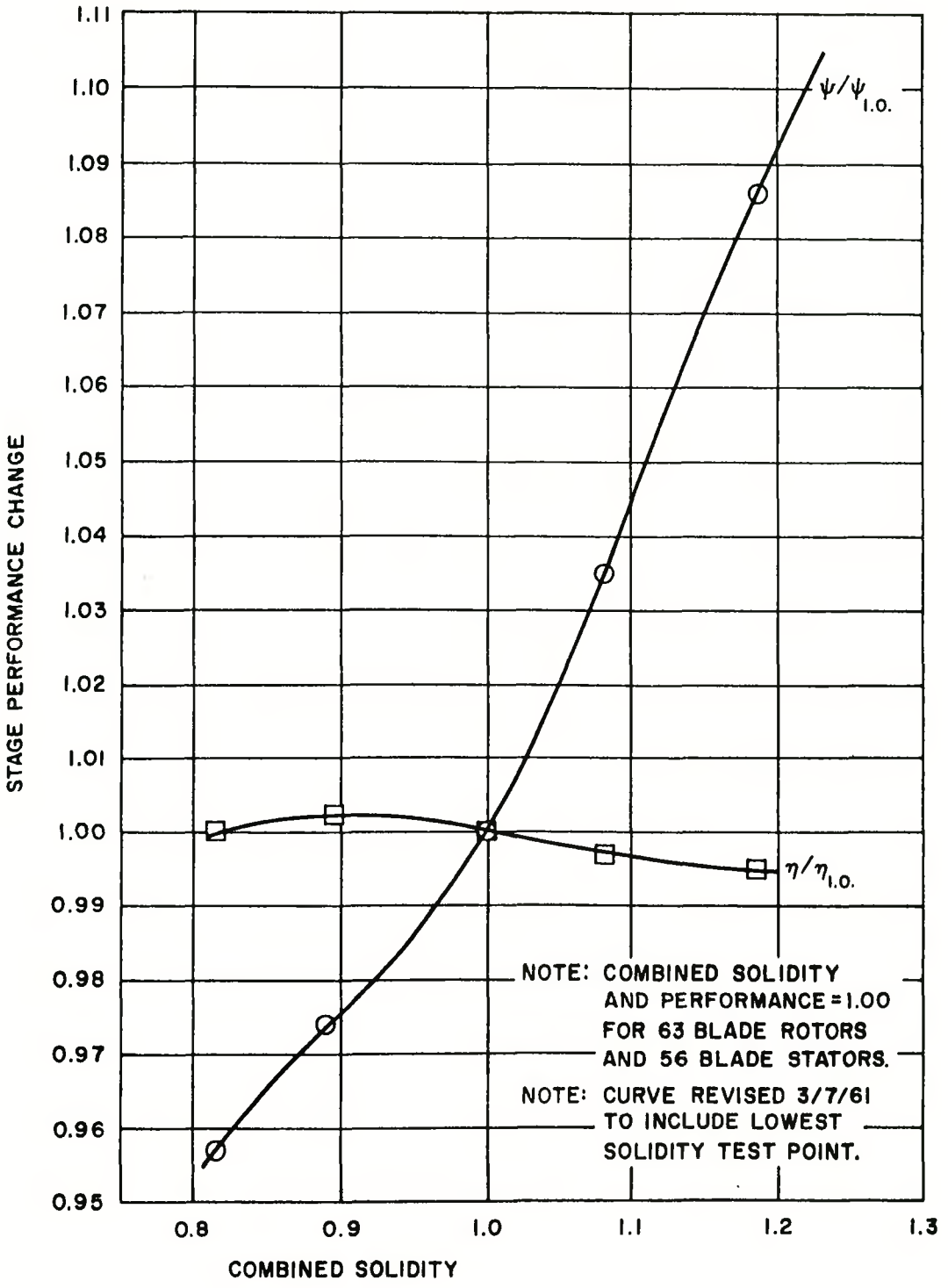


Fig. 5-68 - MGCR Compressor Model Aerodynamic Performance vs. Combined Solidity Change with Equilibrium Boundary Layer

5.8.2 Compressor Development

Tests were conducted to study the effect of stage loading in the compressor. Three basic loading configurations are planned with possible variations in solidity (blade chord to pitch radio) to optimize each configuration. Two loading configurations were completed:

(a) mean loading with a 75 blade rotor solidity and a 66 blade stator solidity, and

(b) high loading, 10% higher than mean, at the same solidities as item (a) above.

These tests showed that peak efficiency fell off 0.8% for the high loading configuration (see Table 5-5[11]).

Table 5-5

COMPARISON OF MEAN AND HIGH STAGE LOADING CONFIGURATIONS

Configuration	Mean	High
Stagger angle		
Rotor	29°00'	26°30'
Stator	43°18'	40°18'
Maximum efficiency	88.4%	87.6%
Pressure coefficient (at maximum efficiency)	0.620	0.625

Stagger angle is measured between meridional plane and camber line chord of the blades. Figure 5-69[11] summarizes the performance data obtained for the high and mean loading configurations.

A low loading configuration, to be tested for comparative purposes, was theoretically optimized with a 66 blade stator and 63 blade rotor. This configuration can be compared to a mean loading configuration at the same solidity.

The higher loaded stage configuration would permit the saving of a few compressor stages if a compromise in efficiency could be justified. It appears, however, that this is not economically warranted in this compressor design. Unless substantial savings exceeding 30% of the capital investment in compressor component costs can be achieved in staging, it becomes difficult to justify even small losses in compressor efficiency.

It appears that the compressor design is optimized approximately at the mean loading configuration for blades having the test blade camber. Blades having higher camber could be expected to optimize at higher loads[11]. Consideration was given to a possibility of compressor-stage number reduction by employing a higher recuperator effectiveness[108].

While it is not known what decisions were obtained, such a possibility might be illustrated by Figure 5-70, based on a cycle analysis performed in NYO 9787 on Cycles[2]. (See charts B-10 and B-11 of the referenced report.) The decrease of the cycle pressure ratio, required for maximum thermal efficiency, with an increase of recuperator temperature effectiveness is obvious.

For the proposed turbomachinery, evaluation tests were started on following stationary components:

(a) the low-pressure and high-pressure compressor diffuser and exhaust hoods, and

(b) the compressor turbine diffuser and exhaust hood.

The compressor diffuser considered provided satisfactory overall performance results over the speed range. Static pressure recovery was almost constant at 0.470 inlet velocity heads with total pressure losses within the original estimated values. Only the high pressure compressor shape was tested as both diffusers in the MGCR turbomachinery are geometrically similar with equal area ratios. However, each of the exhaust hood collectors was tested. These tests indicated

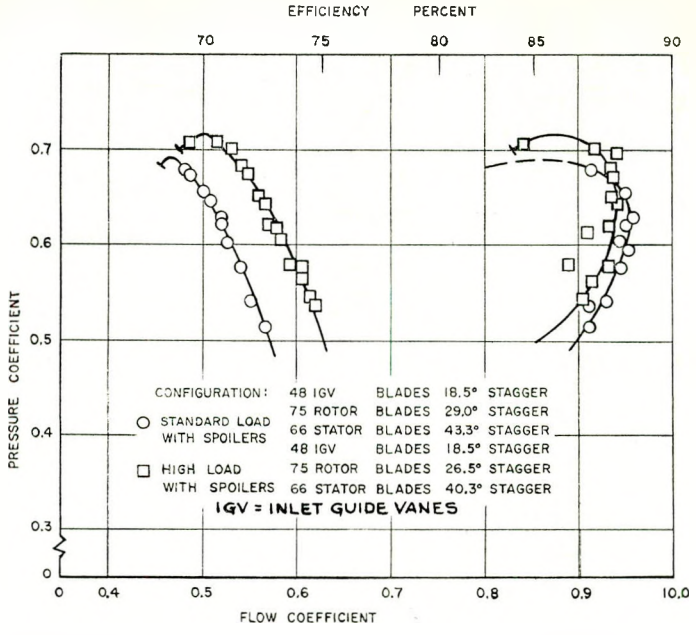


Fig. 5-69 - MGCR Compressor Model Aerodynamic Performance-Flow Coefficient, Pressure-Coefficient, Efficiency

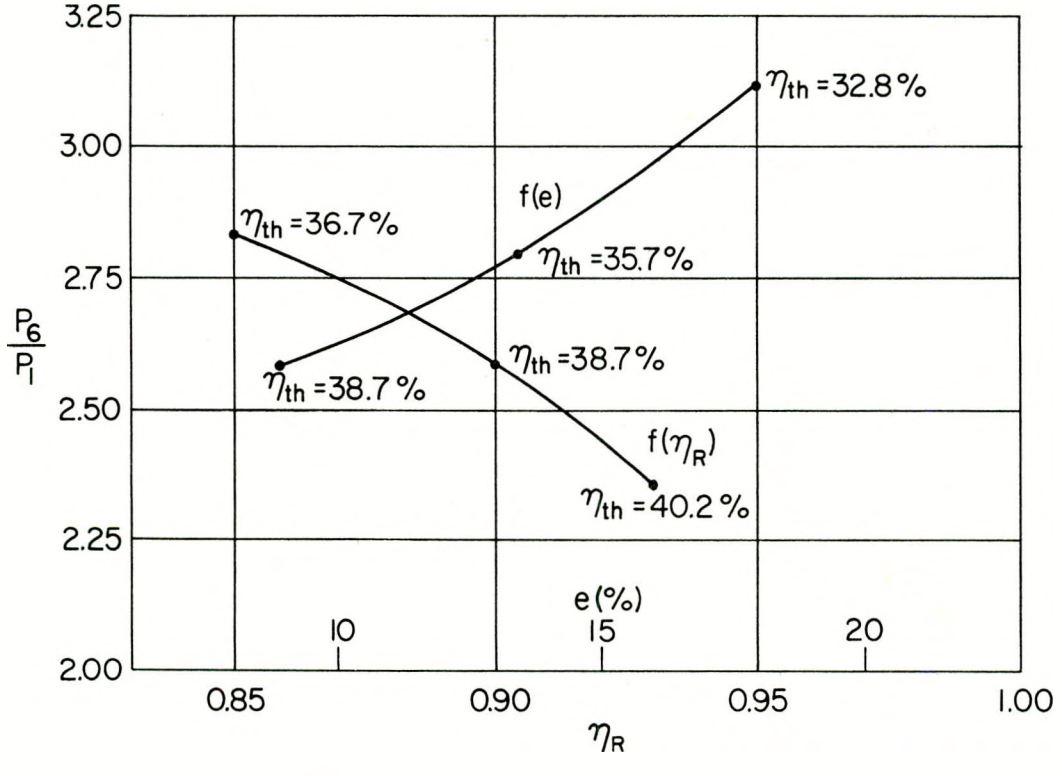


Fig. 5-70 - Influence of Recuperator Effectiveness on Optimum Compression Ratio

that no adverse conditions will result because of hood shape, exhaust pipe size, or pipe location. Inlet velocity profiles remained uniform with no perceivable circumferential variations in flow. The overall characteristics are shown in Figure 5-71[11]. It can be seen that the hood represents only 1/5 of the total loss for the combined diffuser-hood combination. These results, which are indicative of hoods adequately sized for the associated machinery, show that no difficulty should be experienced in the prototype machine.

Evaluation testing of the compressor turbine diffuser model was started. Runs were made at different inlet flows to determine the effects of Reynolds number or performance, with undistributed axial inlet flow. Future testing of this model will be concerned with hood effects and investigations into the effects of diffuser inlet-flow whirl angles and inlet-flow turbulance levels[11].

5.8.3 Turbine

The turbine test model consists of two high-pressure turbine stages, with the blade-path modified to permit testing in air. Figure 12-44 shows the second stage disk assembly of the model turbine. An analysis of the turbine-blade-path flow field has been completed by Electric Boat Division. Results were in general agreement with the Westinghouse results and indicated that the turbines will meet the design conditions. The blades for the turbine test model have consequently been approved for manufacture[46].

Performance characteristics of the MGCR turbines have been computed in accordance with an IBM program for off-design-point conditions, and turbine maps have been compiled on the basis of these results (see Figures 5-72[61] and 5-73[61]).

The configuration of these maps represents results which are typical for the case of lightly loaded turbomachinery operating at low Mach numbers. The maps indicate, with good accuracy, that both turbines will meet the MGCR efficiency requirements. This is further confirmed

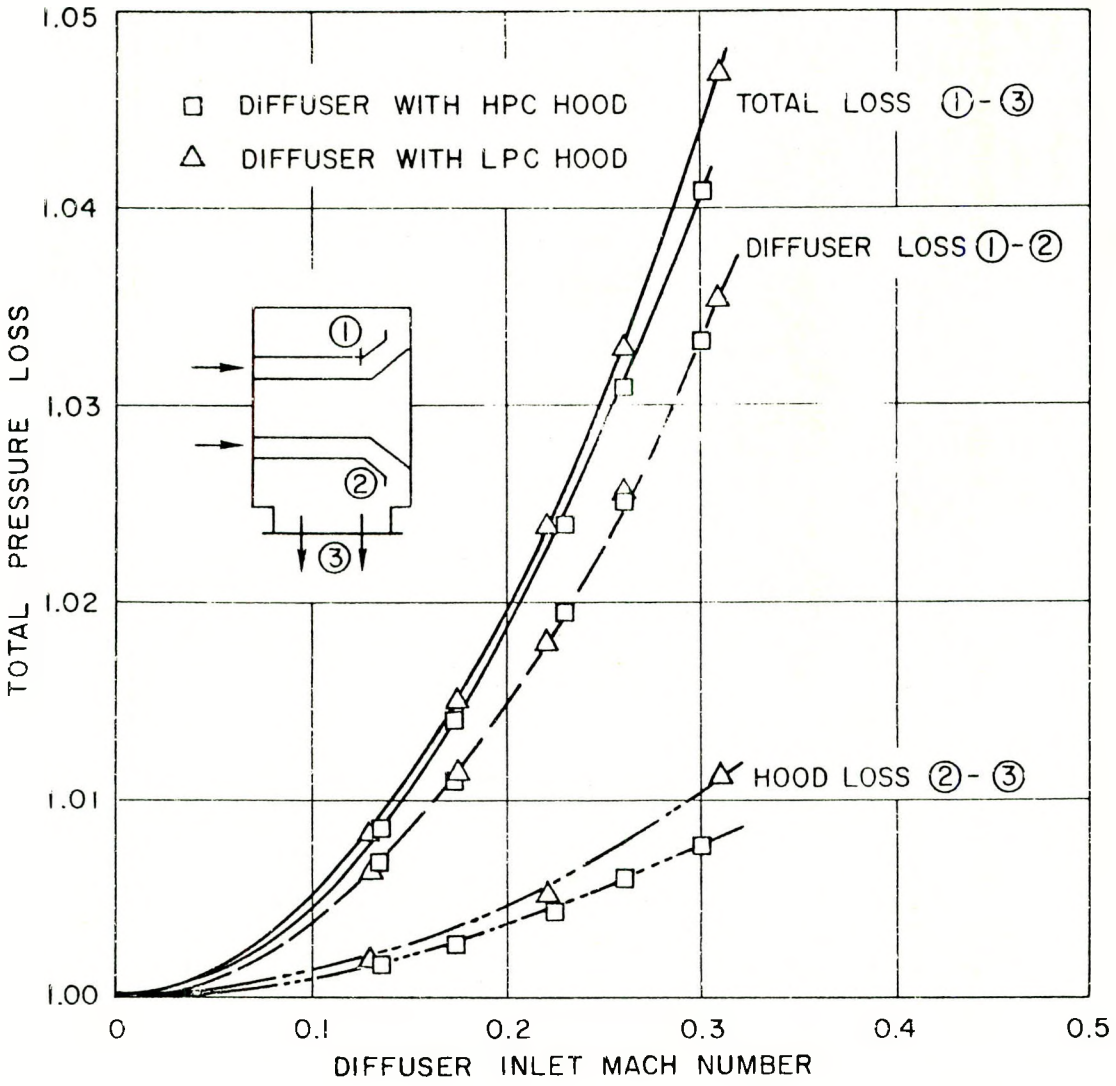


Fig. 5-71 - MGCR Program - Compressor Diffuser and Hood Model Total Pressure Loss vs. Diffuser Inlet Mach Number

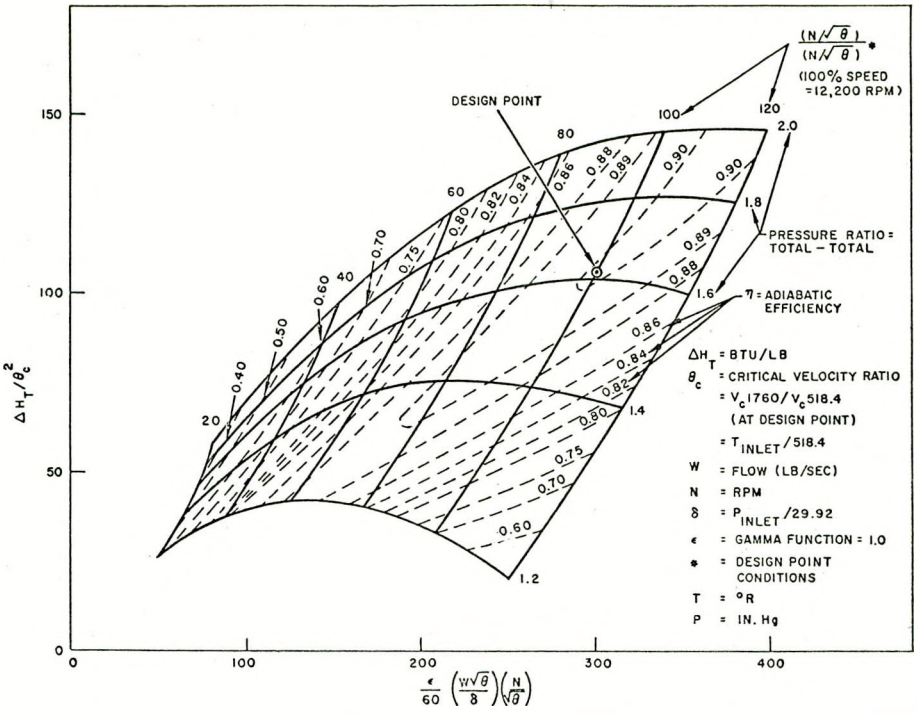


Fig. 5-72 - Performance Characteristics of MGCR High-Pressure Turbine (Gas-Helium; Inlet Temperature = 1,289°F)

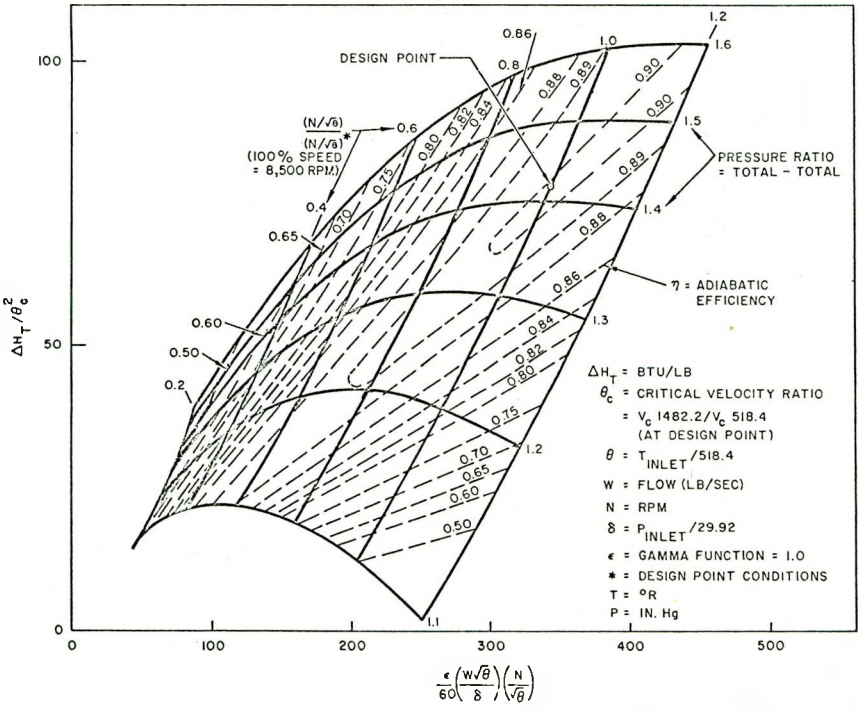


Fig. 5-73 - Performance Characteristics of MGCR Low-Pressure Turbine (Gas-Helium; Inlet Temperature = 1,022.2°F)

by a design-point blade analysis which shows that, with the existing blade design, an efficiency of approximately 90% can be attained in both turbines at their design points. Further analytical work with the turbine-blade flow-field analysis, on the basis of associated boundary layer characteristics, has yieldedpressure-loss coefficients, including the effect of downstream mixing loss (see Figure 5-74[61]). Since three independent NACA methods were used to check the analysis, these calculated losses are considered to be quite accurate[61].

Further study on the design of the prototype low-pressure turbine has resulted in a reduction of the connecting-shaft overhang from 48 inches to 24 inches, with accompanying changes in the critical shaft speed[61].

A successful trial run of the turbine-test facility has been made. The turbine was run up to 6000 rpm, on critical speed and through, with little vibration being observed. Figure 5-75[75] is a view of the center of the test facility where the model will be located. The instruments located above the shaft are vibration pickups used in operational check runs. Figure 5-76[75] shows one of the 1000 hp water dynamometers in place.

Single-stage turbine tests were performed and preliminary tests indicate good aerodynamic performance. The turbine test stand has been modified and improved. Among the changes made were:

(a) changing water brake and turbocompressor couplings to reduce vibration,

(b) use of lighter oil in turbine model and dynamometer bearings to reduce tare correction, and

(c) improvement in the accuracy of instrumentation and controls.

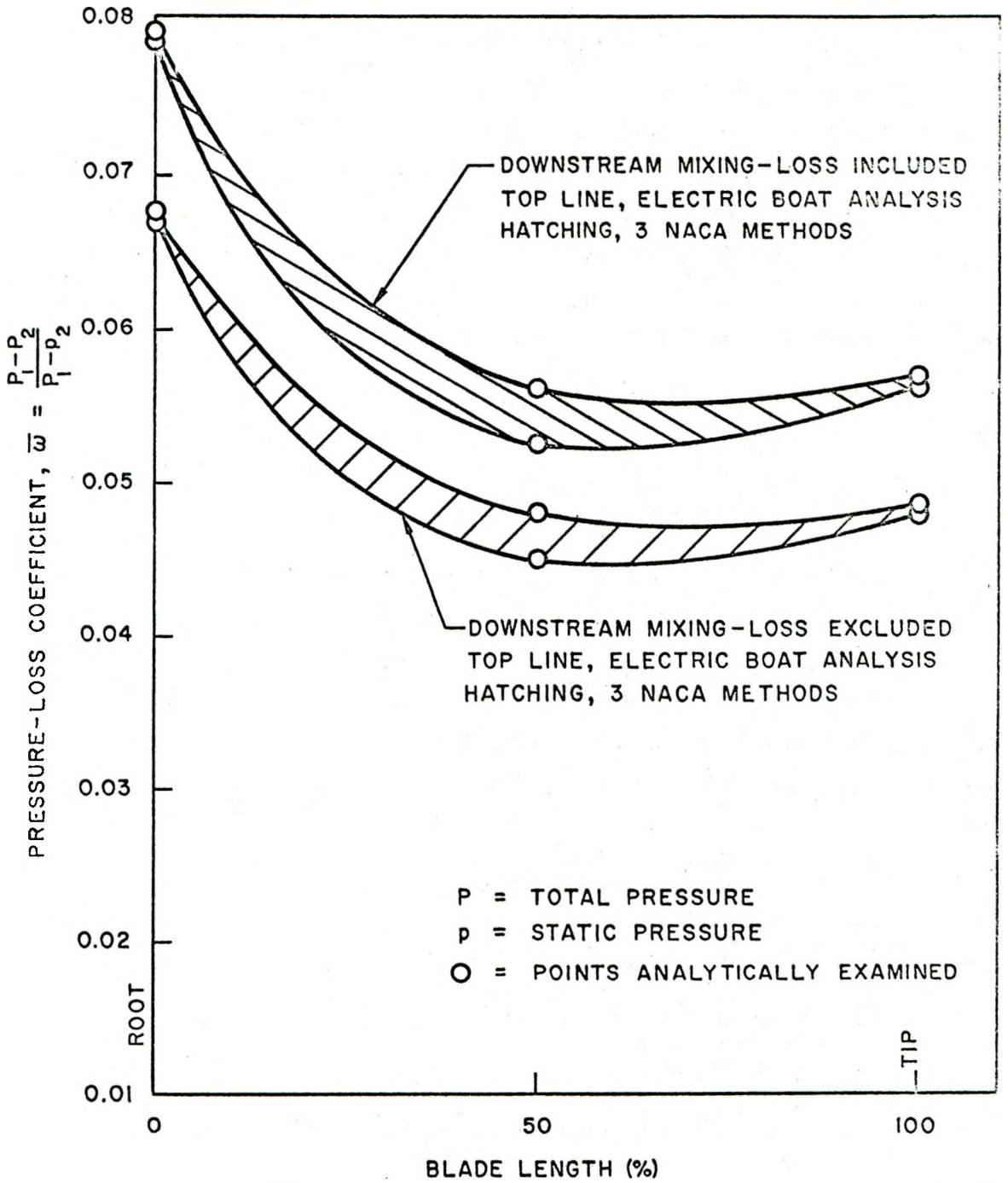


Fig. 5-74 - Blade Total Pressure Loss vs. Blade Length for MGCR High-Pressure Turbine Test Model at Design Point Rotor No. II

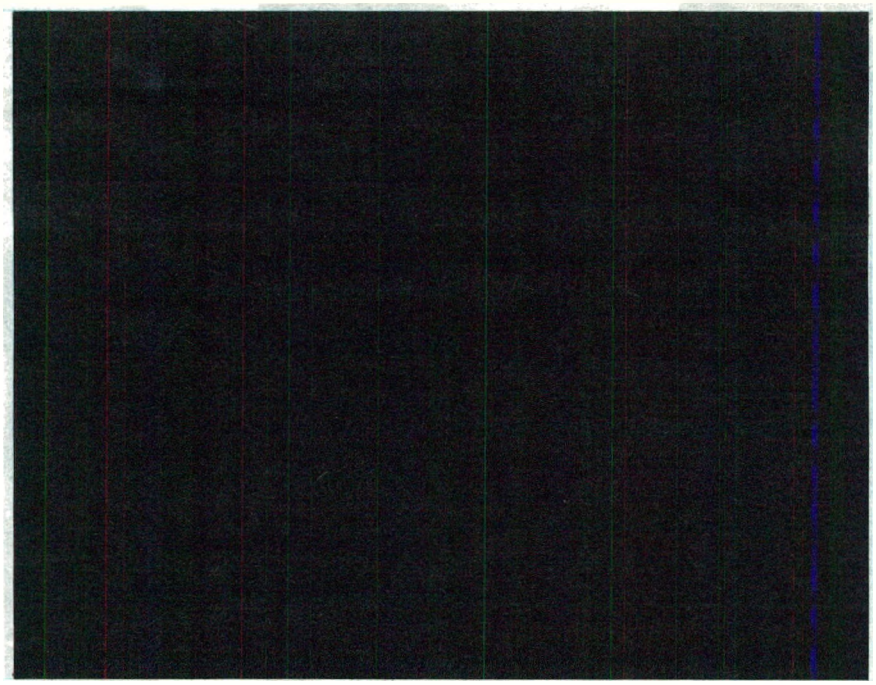


Fig. 5-75 - Center of the Turbine Test Facility

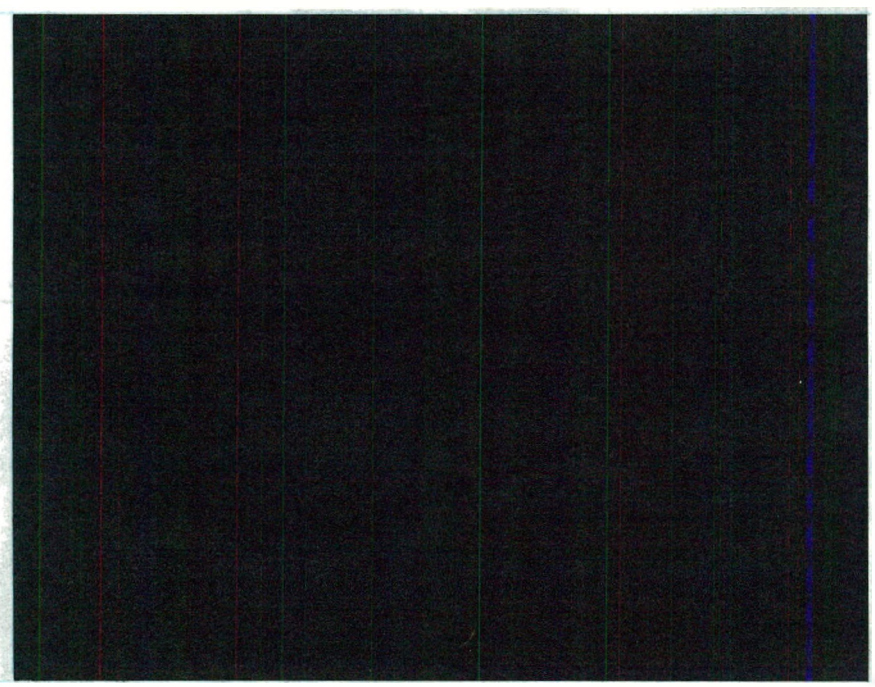


Fig. 5-76 - 1,000 Horsepower Water Dynamometer

5.8.4 Turbine Model Test

Good efficiency was obtained over a broader range than was expected which is a desirable feature in a variable-speed drive machine. The flow capacity of this model was 11% less than predicted. This was attributed mainly to the estimate of flow deviation used in the turbine design. The deviation is the amount of underturning of the flow relative to the blade exit angle and is normally estimated from cascade tests. Although new blade sections were used in this design, cascade tests were not run because any mismatch of the machine due to an incorrect deviation estimate could be corrected by adjustment of the stator blade angle.

In the second turbine test model configuration, stator angles were adjusted to improve the matching of the turbine stage. Efficiency and flow characteristics obtained in initial tests with the second configuration are shown in Figure 5-77[108], where they are compared with the results of the first configuration. A peak turbine efficiency of 91% was attained with efficiencies above 90% over a range of velocity ratio from 0.9 to 1.3. The efficiency increase of Configuration 2 over Configuration 1 was 1-1/2 points.

General conclusions can be made from these exploratory tests:

(1) An efficiency level above 90% is attainable for the second stage over a range of velocity ratios from 0.9 to 1.3.

(2) High loss regions are evident in the turbine although over-all performance is good. A significant improvement in performance could be obtained if these losses could be minimized.

(a) A high loss region, existing at the stator tip, might be improved by increasing the stator solidity from 50 to 60 blades per row. The rest of the stator shows better loss characteristics than expected.

(b) As anticipated, a high loss region exists near the rotor hub. This is the critical blade section that has the highest blade surface diffusion. Improvements on this region would require redesign of the rotating blade. It is expected that more specific recommendations can be made as the test program progresses.

Tests were completed on the second stage shrouded turbine blades (Configuration 2^{108}). A statistical analysis was made of data obtained at pressure levels of two and three atmospheres, at a pressure ratio of 1.25, and a velocity ratio of 1.0. A weighted average of these results gives an efficiency of 92.1% $\pm$ 0.5%.

Since the mean efficiency of the tests carried out at two atmospheres is within the tolerance of the three atmosphere results, the validity of the dynamometer tare values used in the calculation of the turbine power output was confirmed. The composite field of the second stage blading based on the results of the test performed is shown in Figure 5-78[11]. Figure 5-79[11] shows the variation in flow characteristics over the range of pressure ratios from 1.15 to 1.35. This curve will be important in establishing the part-load performance for matching the components of the MGCR cycle.

With the conclusion of these tests, the second stage components were replaced with first stage components (Configuration 3^{108}). This configuration consisted of shrouded rotating blades with a hub-tip ratio of 0.69 compared to 0.72 for the first stage blades. Stator solidity was set at 50 blades and rotor solidity was set at 45 blades. The tip clearance was established to 0.001 inches per inch of diameter.

Preliminary tests were run with this configuration at pressure levels of two and three atmospheres at a pressure ratio of 1.25. The limited data obtained to date appear consistent with those obtained on the second stage (Configuration 2). However, it will be necessary to complete testing over the full range of velocity ratios and pressure ratios to confirm performance characteristics.

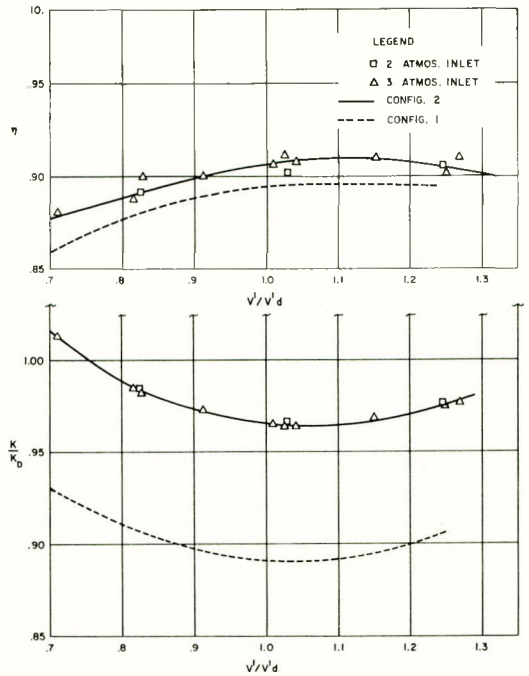


Fig. 5-77 - MGCR Model Turbine Test, Second Stage, Pressure Ratio = 1.25

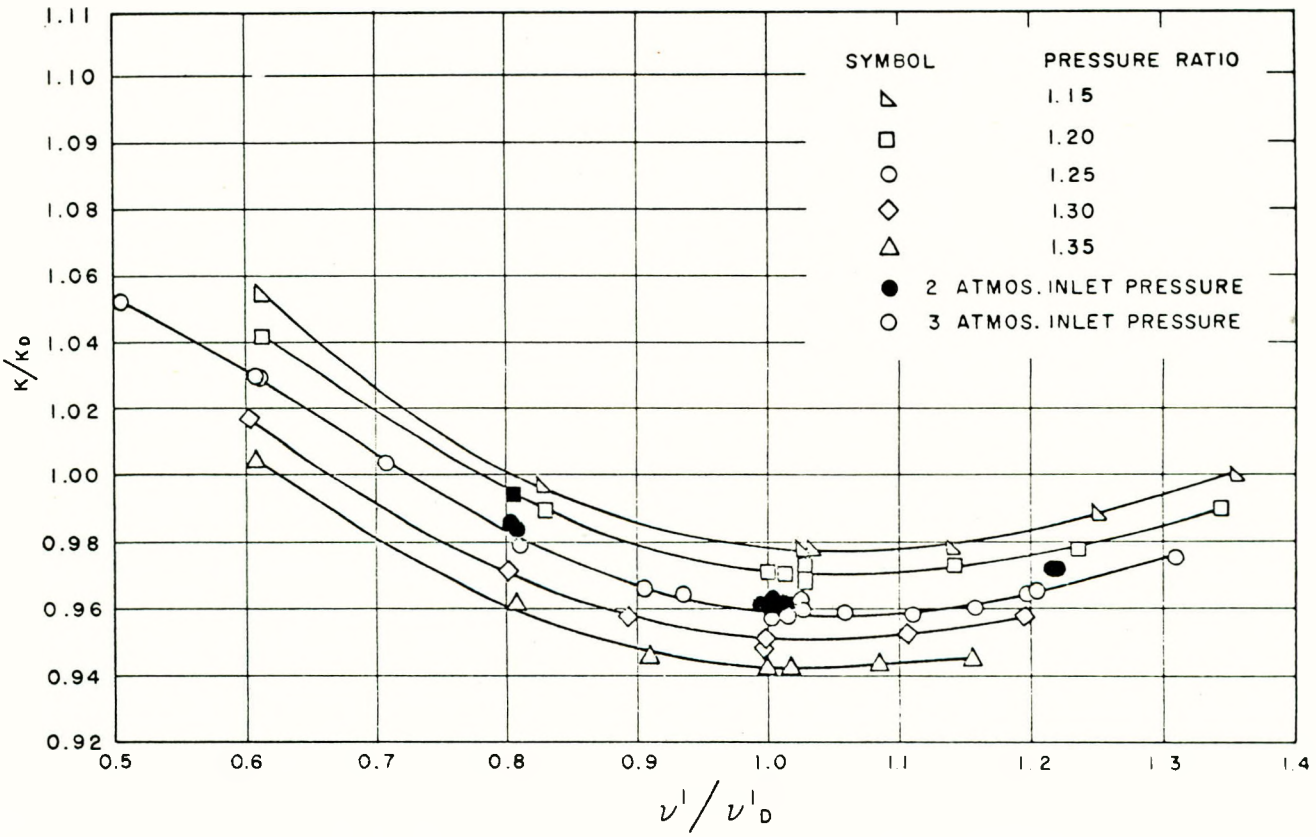


Fig. 5-78 - MFCR Model, Turbine Test Second Stage, Configuration 2A, Turbine Flow Constant vs. Velocity Ratio Parameter - Pressure Ratio

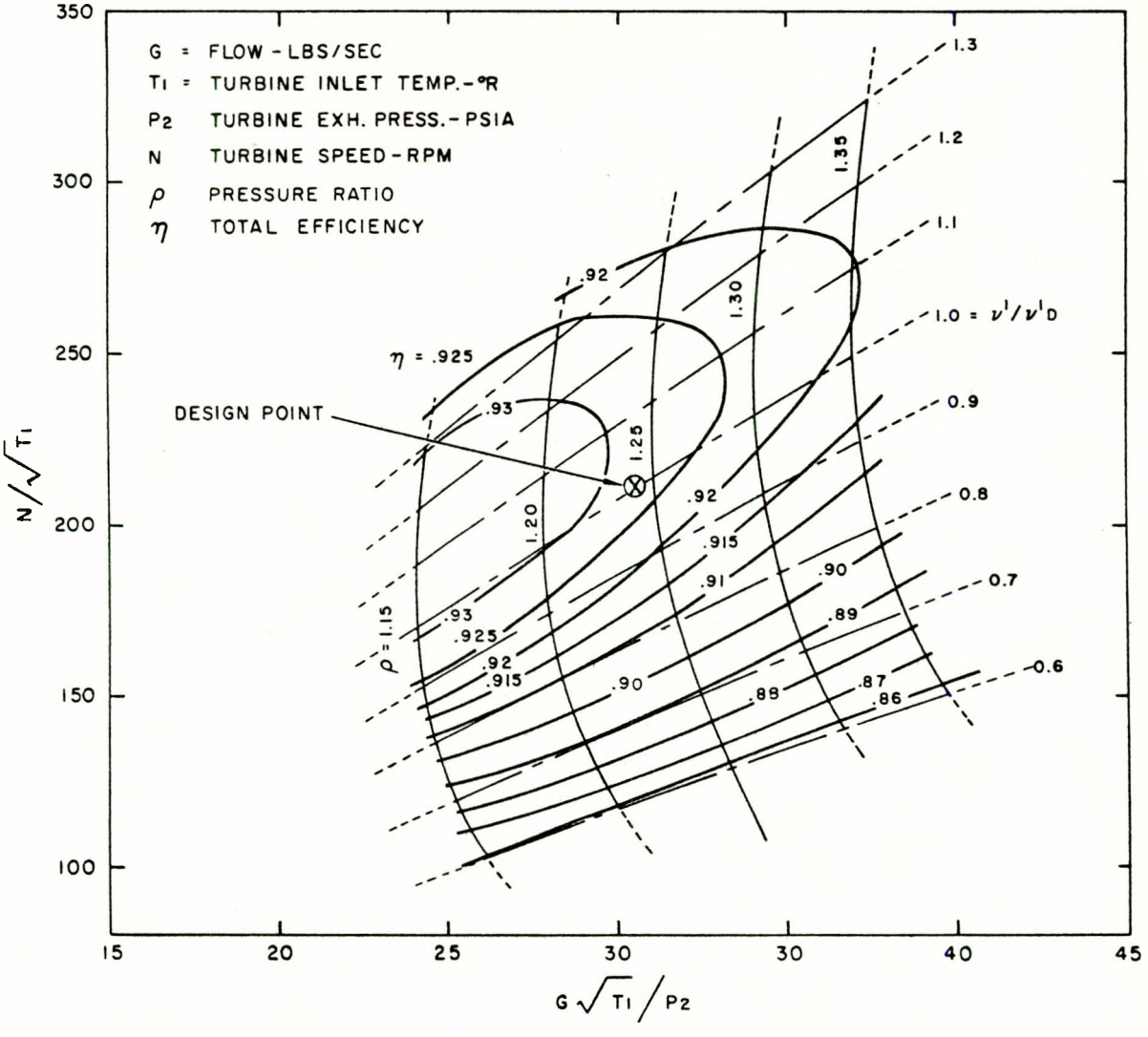


Fig. 5-79 - MGCR Model Turbine Test Tested Performance Field, Second Stage

Subsequent plans involve evaluation of unshrouded blades, clearance effects, solidity effects, and turbine flow characteristics to establish design criteria for a compatible design to match components in the 1300°F to 1500°F range.

5.8.5 Turbine Inlet Scroll

The high-pressure turbine inlet scroll is a critical portion of the machine, because of its effect on both turbine performance and on the length of the rotor and hence, on critical speed[74].

Development of a high-pressure turbine inlet scroll for obtaining an optimum flow configuration has been confined to investigation of two basic models, designated Configuration I and II (Figs. 5-80[108] and 5-81[108]). A uniform, circumferential, inlet flow distribution with flat velocity profiles and incidence angles within 10 degrees is required to obtain an acceptable scroll[108]. The models were made of wood. Tests were performed using Westinghouse Laboratory air supply and exhausting to the atmosphere[74].

Tests of one configuration of the model turbine-inlet scroll showed that the pressure losses encountered were lower than expected. The scroll was also tested as an exhaust collector and favorable loss values were obtained. A second model of the turbine-inlet scroll, a more compact configuration, has been designed afterwards[75]. After testing both configurations, the following conclusions were made[108]:

(a) Configuration I scroll gives superior performance primarily because it has a larger inlet area.

(b) A cone insert (see Figure 5-82[108]) is required in either configuration to obtain minimum whirl and equal flow distribution along the circumference.

(c) A rounded inlet edge is required on the cone insert to prevent separation at the outer wall.

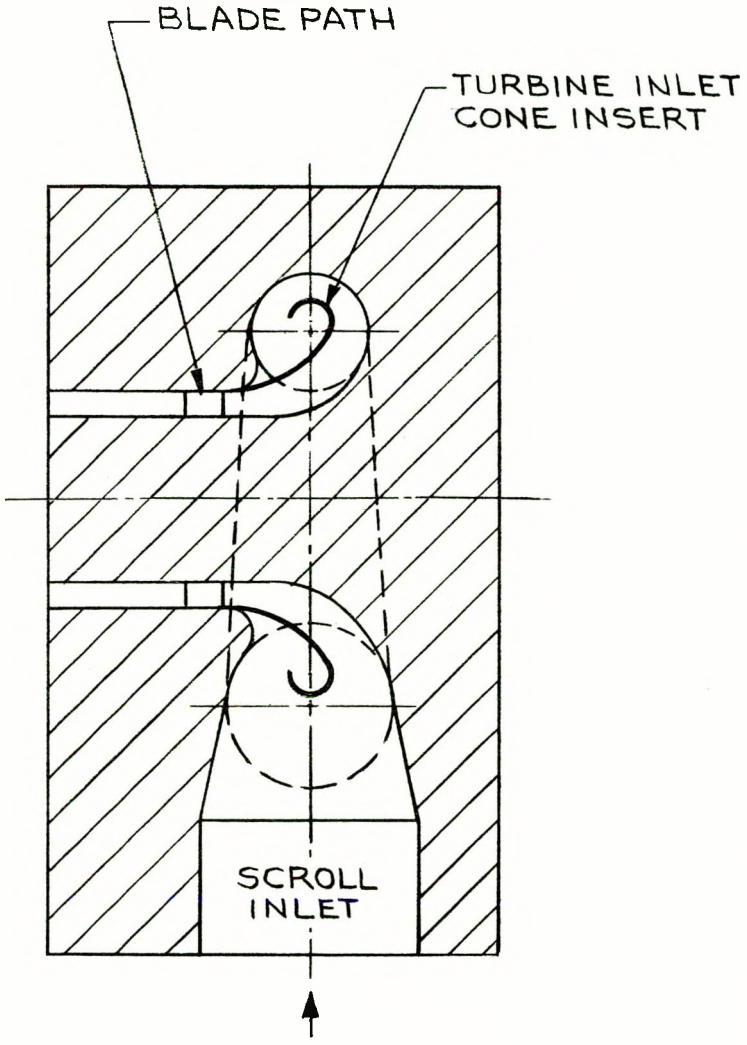


Fig. 5-80 - HPT Inlet Scroll Configuration I

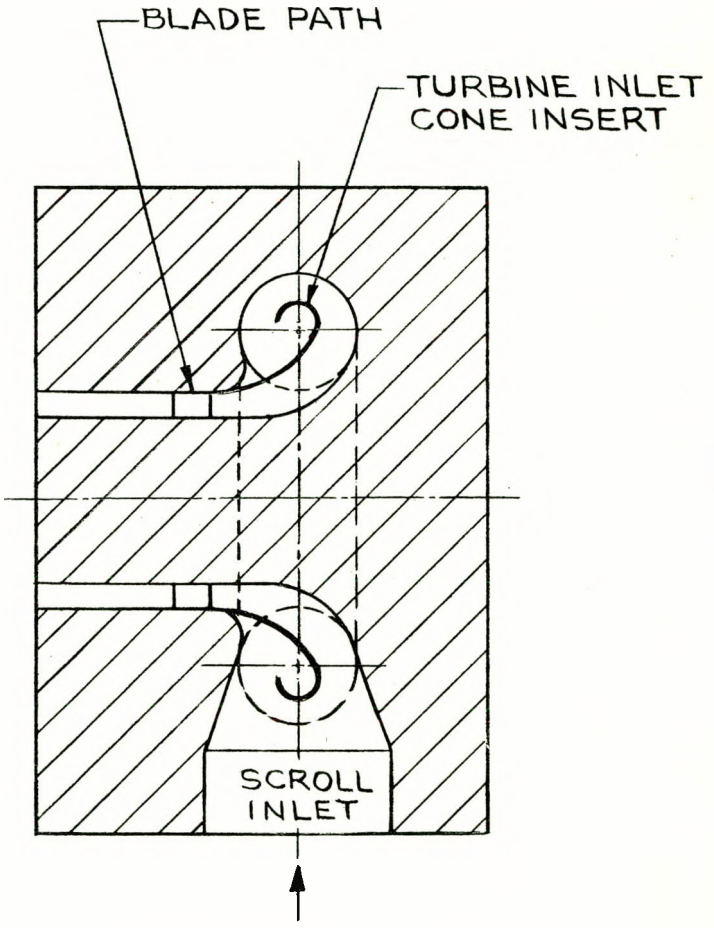


Fig. 5-81 - HPT Inlet Scroll Model Configuration II

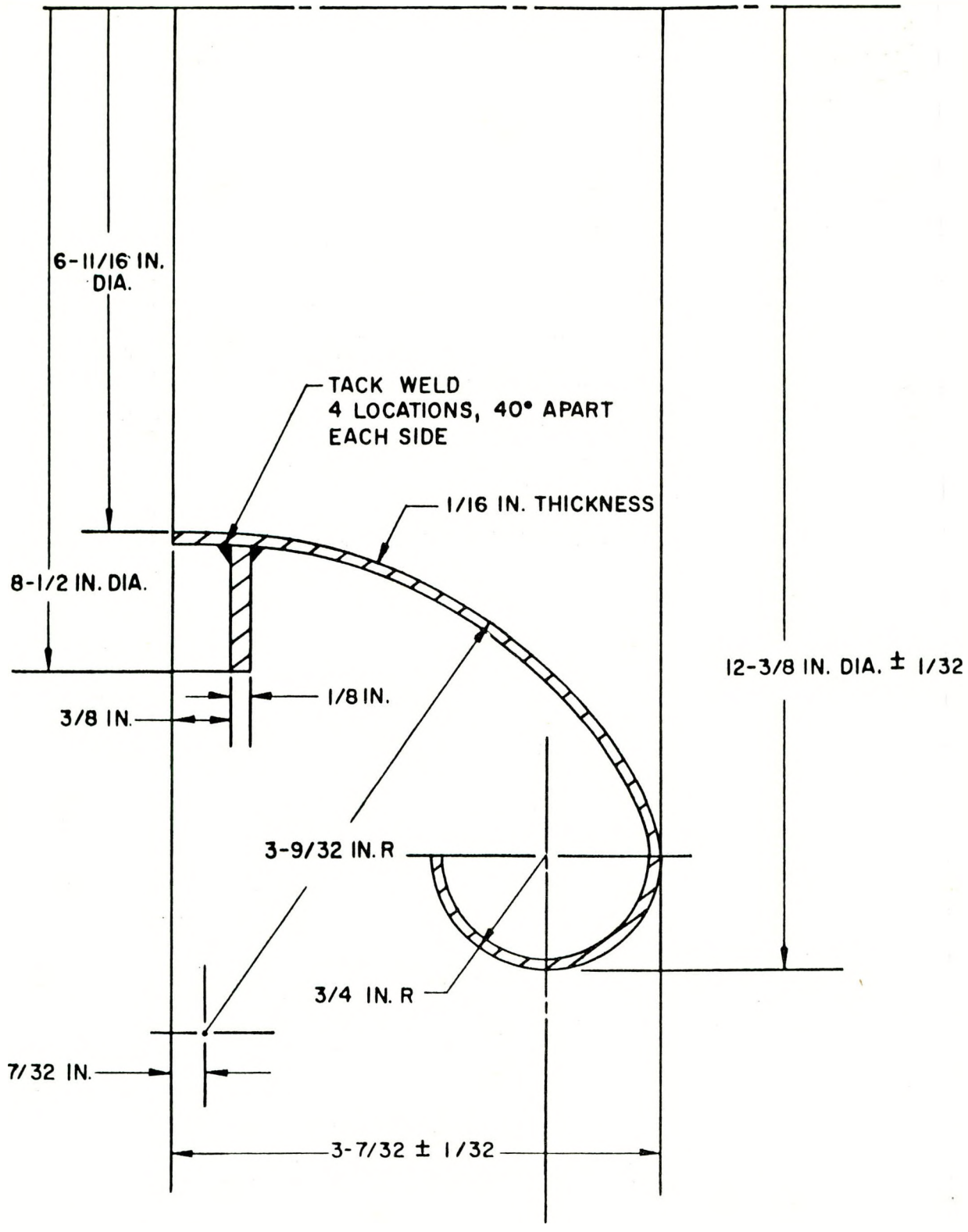


Fig. 5-82 - Turbine Inlet Cone

Both scroll models, without the inlet cones, showed variations in flow distribution of 40 to 50% and whirl angles of 20 to 30 degrees (measured from meridional plane). To remedy these conditions, the scrolls were modified by adding a sharp-edged conical insert at the blade path inlet on each of the models. Although much improvement was obtained, separation at the outer wall of the scrolls was still evident and further improvement was desirable.

The conical inserts, therefore, have been modified to include a rounded or tubular lip. With lips added to the conical inserts, circumferential flow distribution on Configuration I scroll was reduced to a maximum variation of 12% and to a 25% variation on Configuration II scroll. Whirl angles on both configurations were reduced to 10 degrees of incidence. Over-all losses in both models were well within acceptable limits.

Considering the power turbine machinery design, it is advantageous to use the smallest uniform inlet scroll possible; the scroll determines the casing size and thickness. A uniform shape is simple to manufacture. Therefore, effort has been directed toward making Configuration II acceptable by using conical inserts with various size rounded inlet lips and by optimizing the over-all cone shape. Figure 5-82 shows one of several tested cones.

5.9 Influence of Gas Properties in Closed Cycles

The relative size of turbomachinery required to effect a given network output is a function of the physical properties of the circuit gas employed. For the same cycle temperatures and compressor pressure ratio, the net work output per pound of gas flow varies with the gas that is used because each gas has a unique value for gas constant, R, and a unique value for specific heat ratio, $k = c_p/c_v$. Maximum turbine dimensions occur at turbine exhaust, where the gas has expanded to maximum volume. The relative flow areas required per unit of work can be compared for various gases by computing their specific volumes at turbine

exit, then correcting for the net output per pound of flow; all compared at the same compressor pressure ratio, compressor inlet temperature, and turbine inlet temperature. The validity of this comparison is based on the assumption that the flow velocities will be held constant among the several gases in order to maintain similar blading-velocity diagrams with machinery whose blade velocities are stress-limited by particular values.

Assuming isentropic conditions, a perfect gas, and no pressure loss for the turbomachinery, comparisons can be approximated for air, hydrogen, helium, and neon as follows[109]:

(a) Assume a pressure ratio of 4:1, compressor inlet temperature of 70°F, and turbine inlet temperature of 1700°F.

(b) Assume the following physical properties:

Gas	c_p(Btu/lb°R)	k	r(ft/°R)
Air	0.242	1.40	53.3
H_2	3.41	1.408	772
He	1.25	1.66	386
Ne	0.247	1.66	76.5

(c) Compute compressor delivery temperature, T_2

$$\frac{T_2}{T_1} = \frac{T_2}{530} = \left(\frac{p_2}{p_1}\right)^{\frac{k-1}{k}} = \left(\frac{4}{1}\right)^{\frac{k-1}{k}}$$

(d) Compute turbine exhaust temperature, T_5

$$T_5 = T_4\left(\frac{p_1}{p_2}\right)^{\frac{k-1}{k}} = 2160\left(\frac{1}{4}\right)^{\frac{k-1}{k}}$$

(e) Compute net work per pound of flow, W_n

$$W_n = c_p (T_4 - T_5) - c_p (T_2 - T_1)$$

The resultant values for net work per pound of flow, W_n, become:

Gas	W_n(Btu/lb)
Air	107.6
H_2	1545
He	652
Ne	132

(f) Compute the specific volume of gas at turbine exit, v, using $p_1 = 14.7$ psia

$$v = \frac{RT}{p}$$

The resultant values for the specific volume at turbine exit become:

Gas	$v(ft^3/lb)$
Air	36.7
H_2	526
He	228
Ne	45

(g) Divide the gas specific volume, v, by the work output per pound of flow, W_n, to yield a comparison of the machinery size required per unit of net output.

Gas	Volume Flow/Btu Net Work
Air	$\frac{36.70}{107.6} = 0.342$ ft^3/Btu
H_2	0.341 ft^3/Btu
He	0.349 ft^3/Btu
Ne	0.342 ft^3/Btu

Because the flow areas per unit of work are about equal for the several gases, the most important machinery design factor becomes the gas sonic velocity because this value is significant in determining the number of stages of compression and expansion required for the given design pressure ratio. Without consideration of the thermodynamics of turbomachinery, it may be stated in general that, as sonic velocity increases, more stages are required. Following is a comparison of sonic velocities computed at 70°F, the compressor inlet temperature of the preceding example:

Gas	Sonic Velocity, ft/sec at 70°F
Air	1113
H_2	4260
He	3260
Ne	1455

This comparison partially illustrates why air has been the working fluid for all closed-cycle gas-turbine designs that have been built so far. It also shows that the sonic velocity of neon is not significantly greater than that of air. The higher ratio of specific heats in the monatomic gas nearly equalizes the effect of this difference in sonic velocity for air and neon in terms of the pressure-ratio-per-stage that can be achieved with given blading velocities.

The power plant dimensions are influenced not only by the effect of the physical properties of the gas working fluid, but also by the gas density or operating pressure level. For a given gas at given compressor and turbine inlet and outlet temperatures, with the same compressor-blade and turbine-blade velocities, the mass (weight) flow of gas, and therefore the energy transport, is proportional to the product of flow area and pressure at any point, i.e.,

$$G \propto Ap$$

For a given flow,

$$A_1 p_1 = A_2 p_2$$

or

$$d_1^2 p_1 = d_2^2 p_2$$

where d represents turbomachinery diameter and p the cycle pressure level. If p_1 is taken as the datum (1 atmosphere), and d_1 as the corresponding turbomachine diameter, then p_2/p_1 is the operating pressure (or pressure ratio) relative to the datum, and the diameter ratio becomes

$$d_2/d_1 = 1/\sqrt{p_2/p_1}$$

Hence, the diameter of the compressor or turbine, d_2, varies inversely as the square root of the operating pressure p_2.

Conversely, because the peripheral velocities of the rotating parts remain the same, a higher speed, N_2, is required as a compensating compromise;

$$N_2 = N_1 \frac{d_1}{d_2} = N_1 \sqrt{p_2/p_1}$$

In the same manner as indicated by the diameters of the inlet and outlet pipes, the lengths, L_2, of the compressor and turbine rotors and casings are decreased as

$$L_2 = L_1/\sqrt{p_2/p_1}$$

The higher operating pressures appear to require increased thickness of tube walls for the pipes in the power plant as well as increased thickness of casing for the turbomachinery. To retain the same stress in the tube-wall materials, the thickness, t_2, would be increased as

$$t_2 = t_1 (p_2/p_1)$$

However, because the tube diameters, d_2, are decreased to $1/\sqrt{p_2/p_1}$, as indicated above, the increase in wall thickness by $\sqrt{p_2/p_1}$ would be retained and there is no net change in weight of tubes per unit length.

The torque of the compressor and turbine rotors is affected by pressure level for the condition of constant work output. For this condition

$$\Phi_1 N_1 = \Phi_2 N_2$$

where Φ = torque.

By substitution

$$\Phi_2 = \Phi_1 / \sqrt{p_2/p_1}$$

Assuming an optimum pressure ratio for optimum efficiency, the influence of various gases on different operational and dimensional parameters of the compressor and turbine was investigated by D. Reiher,[110] a generator of 3-Mw output being taken as the basis for calculation. The preference of coolant gases from the viewpoint of compressor and turbine parameters is indicated in the order CO_2, N_2, D_2, He, Ne, H_2. Overall considerations, as pointed out by this author, lead to a conclusion that helium is the best gaseous medium for use in a closed circuit comprising a nuclear reactor and a gas turbine. The following table gives an evaluation of some dimensional parameters, assuming the values for nitrogen to be unity.

Conditions of evaluation:

P_{gen} = 3 Mw; compressor inlet values p_1 = 147 psia,
t_1 = 68°F; $\pi = \left(p_2/p_1\right)_{opt}$; turbine inlet temperature
t_4 = 1292°F; relative pressure loss e = 0.1

Investigated Relative Values	GAS					
	N_2 $\pi = 2.4$	He $\pi = 2$	Ne $\pi = 2$	H_2 $\pi = 2.4$	D_2 $\pi = 2.4$	CO_2 $\pi = 4$
AXIAL COMPRESSOR						
Outside Diameter,						
1st stage	1	1.049	1.089	0.840	0.876	0.912
last stage	1	1.075	1.115	0.833	0.863	0.833
Radial Blade Length,						
1st stage	1	1.045	1.083	0.806	0.845	0.903
last stage	1	1.230	1.283	0.806	0.870	0.571
Number of Stages	1	2.620	0.656	6.400	3.280	1.640
Weight Flow	1	0.209	1.052	0.071	0.146	0.965
AXIAL TURBINE						
Outside Diameter,						
1st stage	1	1.043	1.086	0.823	0.865	0.865
last stage	1	1.038	1.098	0.836	0.870	0.910
Radial Blade Length,						
1st stage	1	1.229	1.329	0.825	0.882	0.521
last stage	1	1.021	1.071	0.808	0.849	0.879
Number of Stages	1	2.760	0.621	7.240	3.520	1.655
Weight Flow	1	0.209	1.052	0.071	0.146	0.965

The Reynolds number for the blading in the turbomachinery increases as pressure is elevated, varying as $\sqrt{p_2/p_1}$ for constant weight flow and velocity. Thus, unless blade height is so reduced that efficiency is limited by clearance problems, the upper limit to operating pressure is probably established elsewhere in the system, such as by casing thicknesses, reactor pressure vessel strength, or the duct (pipe) walls.

Increasing the pressure level is advantageous because the coolant flow volume, essentially a void in the reactor, may be reduced, or the pressure drop reduced if the same volume is maintained. As a result, the reactor can be built with a lower fuel inventory if the void is partially filled with moderator; reactor size and, consequently, shield size and weight may be reduced; or the reactor may be designed for a lower temperature difference between fuel element and flow discharge temperature by including more surface area without causing a greater percentage pressure loss. In any event, increasing the operating pressure level in a reactor-heated closed-cycle system is even more important than in a conventional fired system[109].

The efficiency of turbomachine is almost always increasing with an increase in Reynolds number. In closed cycles with high operating pressure level, the Reynolds number is increasing despite the decrease of turbo-machinery size, and influences the hydraulic efficiency of the machines (see Section 5.1.3). Apart from this, the bearing friction losses decrease because of the decreased weight of runners despite greater rotational speeds[48].

6. CHARACTERISTIC PARAMETERS OF TURBOMACHINERY

6.1 General

The basic characteristic values of turbomachines are the similarity parameters which are derived from similarity relations. Various methods of presenting such parameters are in use.

Several characteristic values are commonly used for defining significant performance criteria of turbomachines, such as turbine velocity ratio, pressure coefficient, flow factor, specific speed, Reynolds number, Mach number, and so on. Each of these parameters represents important aspects and is used to express, in a dimensionless form, significant criteria. Similarity considerations show that actually only four parameters are needed to describe completely the characteristics of turbomachines handling compressible medii; namely, Mach number, Reynolds number, and two characteristic velocity ratios. These velocity ratios can either be the flow factor and turbine-velocity ratio or equivalent values.

Practical considerations, dealing with design aspect of turbomachines, would indicate that parameters which contain rotative speed and rotor diameter would be desirable terms for the equivalent values.

Such values can be provided by similarity concept in the form of specific speed N_s and its correlate, specific diamter D_s. This concept is used to present the available information on turbine-performance data in convenient design diagrams which show the maximum obtainable efficiency together with optimum design geometry. However, because knowledge of the interrelation between geometry and losses is still incomplete, such diagrams must be labeled preliminary.

6.2 Similarity Parameters for Turbine Design

It is the purpose of the similarity parameters to define operating and design conditions for which turbines of similar design geometry experience similar fluid dynamic conditions.

Assuming $Q_3 \approx c\ A \approx c\ D^2 \approx uD^2 \approx ND^3$

and $H_{ad} \approx c^2 \approx u^2 \approx N^2D^2$

and comparing volume flow and turbine head with volume flow and head of a standard turbine (subscript s), we obtain

$$N_s = \frac{NQ_3^{1/2}}{H_{ad}^{3/4}} \qquad \text{specific speed}$$

and

$$D_s = \frac{DH_{ad}^{1/4}}{Q_3^{1/2}} \qquad \text{specific diameter}$$

These values are truly dimensionless. Specific speed and specific diameter are interrelated with other frequently used turbine parameters, velocity ratio and flow factor. Their numerical interrelations can also be expressed in terms which cover radial machines

$$N_s = \varphi^{1/2} \left(\frac{u}{c_o}\right)^{1.5} 387 \left(\epsilon^{-2} - \epsilon_h^{-2}\right)^{1/2}$$

$$D_s = \frac{0.4}{\varphi^{1/2}\left(\frac{u}{c_o}\right)^{1/2}\left(\epsilon^{-2} - \epsilon_h^{-2}\right)^{1/2}}$$

$$\frac{u}{c_o} = \frac{N_s D_s \pi}{\sqrt{2g'60}}$$

THE FRANKLIN INSTITUTE • Laboratories for Research and Development

where ϵ_h denotes the hub ratio, ϵ the rotor-diameter ratio, as defined in Figure 6-1[66], c_o the spouting velocity, and φ the flow factor, defined as ratio of axial leaving velocity and wheel speed, i.e.

$$\varphi = \frac{c_{m-3}}{u_2}$$

The frequently used "gulp factor" is also interrelated with specific speed and specific diameter. This relation reads for full-admission turbines

$$\varphi^* = \frac{Q}{ND^3} = \varphi \frac{\left(\epsilon^{-2} - \epsilon_h^{-2}\right)\pi^2}{240} = \frac{1}{N_s D_s^3}$$

The specific speed interrelates the net output hp and rotative speed of the turbine as follows

$$N_s = \frac{N}{H_{ad}^{5/4}} \sqrt{\frac{550 \text{ hp } R\, T_{3-st}}{\eta\, p_{3-st}}}$$

that is, the specific speed increases with decreasing turbine back pressure.

Figure 6-2[66] shows the maximum obtainable efficiencies in the present state of the art for single-stage turbines, including radial and axial and impulse and reaction. The shaded line in this diagram indicates the region where partial-admission and full-admission impulse turbines yield about the same efficiency, thus revealing that the operating region to the left of the shaded line is covered best by partial-admission turbines, whereas the operating region on the right of the shaded area requires full-admission designs. The numerical values quoted for the efficiency are only valid for the Reynolds numbers quoted in Figure 6-2 and for $Ma_{w-2} < 1.0$ when subsonic rotor-blade designs are used; i.e., for corresponding pressure ratios and turbine back pressures. Corrections are required when operating beyond the quoted limits. It is important to note that the data for high-specific-speed designs are

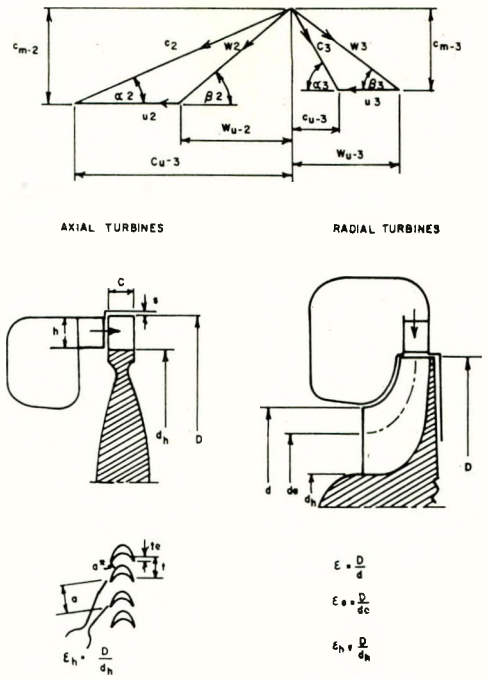


Fig. 6-1 - Turbine-Velocity Triangles and Geometries

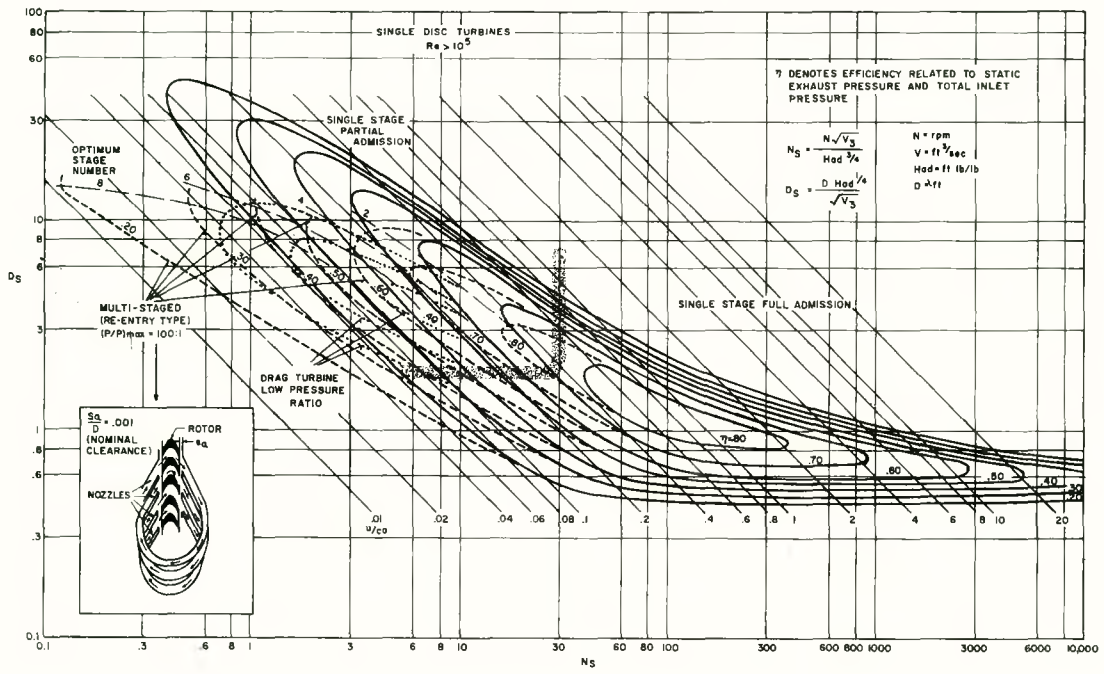


Fig. 6-2 - ND-Diagram for Single-Disk Turbines

considerably more tentative than the data for low-specific-speed designs because they are extrapolated by considering generalized trends instead of being calculated by a more rigorous optimization procedure.

6.3 Similarity Parameters for Compressor Design

The specific speed is defined as

$$N_s = \frac{N\sqrt{Q_1}}{H_{ad}^{3/4}}$$

with Q_1 denoting the volume flow at the inlet of the machine, and H_{ad} the head, actually produced by the pump or compressor. Likewise, the definition of the specific diameter reads

$$D_s = \frac{DH_{ad}^{1/4}}{Q_1^{1/2}}$$

These parameters are again interrelated with other commonly used characteristic values, such as the head coefficient

$$\psi_{ad} = \frac{H_{ad}}{u^2/g} = \frac{g\,60^2}{N_s^2 D_s^2 \pi^2}$$

and "gulp factor"

$$\varphi^* = \frac{Q_1}{nD^3} = \varphi \frac{\left(\varepsilon^{-2} - \varepsilon_h^{\,2}\right)\pi^2}{240} = \frac{1}{N_s D_s^{\,3}}$$

where

$$\varphi = \frac{c_{m-1}}{u_2}$$

denotes the flow factor (see Fig. 6-3[111] for notations).

Figure 6-4[111] is a summary of the data computed for axial compressors, radial compressors, and pumps, drag compressors, and rotary-displacement compressors in terms of specific speed and specific diameter.

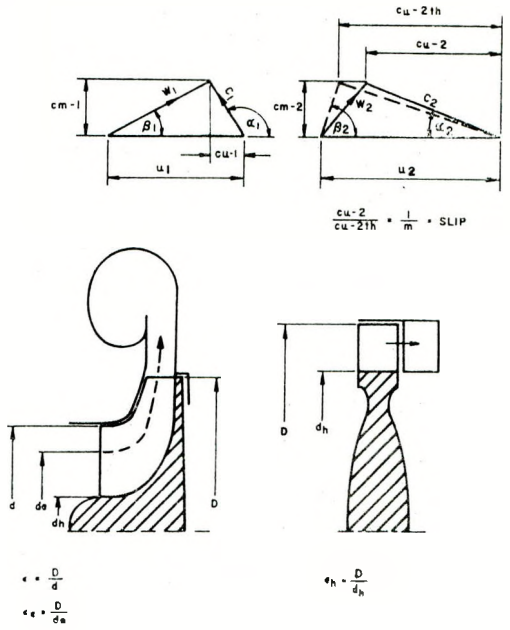


Fig. 6-3 - Compressor Velocity Triangles and Geometries

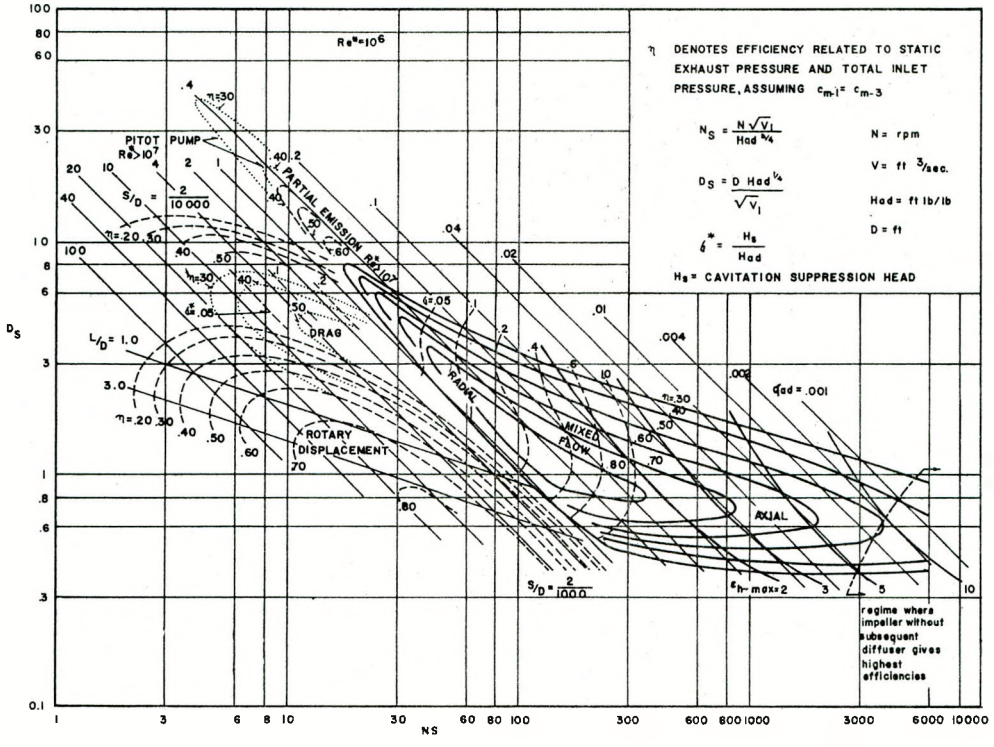


Fig. 6-4 - Approximate ND-Diagram for Single-Disk Pumps and Low-Pressure-Ratio Compressors

This diagram reveals a situation quite similar to Figure 6-2 ($N_s D_s$-diagram for single-disk turbines), namely, optimum efficiencies of pumps and compressors for specific speeds between 60 and 400, whereby for the high-specific-speed region, the axial type is optimum, whereas for the lower specific speeds, in contrast to turbines, the radial machine yields maximum efficiencies. It is to be expected that the mixed-flow compressor will yield optimum solutions for specific speeds between 150 and 300. For specific speeds below 30, the drag compressor or drag pump yields higher efficiencies than the conventional centrifugal machines, whereby head coefficients in excess of unity are obtained. This demonstrates the multistage character of drag compressors.

The data for axial compressors, shown in Figure 6-4, are adapted from (112), which quotes good agreement between test values and calculated data for the D_{s-opt} region. The optimum geometry is indicated in the form of ϵ_{h-max}-values revealing that the optimum hub ratio increases with increasing specific speeds. It is interesting to note that for extreme high specific speeds ($N_s > 3000$) axial machines consisting only of a rotor (i.e., without subsequent diffuser grid) give better efficiencies according to (112) than rotors with subsequent diffusers. The dash-dotted line in Figure 6-4 indicates the region where both arrangements have equal efficiencies.

In comparing Figures 6-4 and 6-2 in more detail, it appears logical that the counterpart of the partial-admission turbine, namely, the partial-emission pump, or its special version, the spoon-type or pitot pump, should show acceptable efficiencies in the specific-speed region of 10 to 20. In analyzing briefly the flow mechanism in these pump types, it appears that head coefficients in the vicinity of 0.5 to 0.6 should be expected from these devices. Since the flow passing through these pump types is considerably smaller than the flow passing through full-admission centrifugal pumps, optimum efficiencies for these devices should be expected at comparatively large specific diameters.

Some tentative values for the performance criteria of these pumps are shown in Figure 6-4 by dashed lines and dotted-lines.

Lines of constant efficiencies for rotary-displacement machines, operating as compressors or pumps, should be expected at comparatively low specific speeds and comparatively small specific diameters. Therefore, it may be expected that these devices show better efficiencies than drag pumps or centrifugal or pitot pumps in the low-specific-speed regions. Calculated values for Roots type compressors and gear pumps are shown in Figure 6-4 by dashed lines.

6.4 Performance Presentation

6.4.1

The performance of a turbine is usually presented in a graph where the efficiency is plotted versus either the velocity ratio

$$\frac{u}{c_o} = \frac{u}{(2g\,H_{ad})^{1/2}}$$

or the velocity factor

$$F_v = \frac{u}{(g\,H_{ad})^{1/2}}$$

also the reciprocal of F_v^2, that is a pressure coefficient,

$$q_{ad} = \frac{g\,H_{ad}}{u^2}$$

For radial turbines, a convenient over-all picture of the performance in design and off-design regions is obtained if the parameter used is the actual turbine speed. Thus, points of variable pressure ratio can be plotted as shown in Figure 6-5[107]. For a given rotational speed u or rpm, the efficiency rises if the pressure ratio is increased, while the operating point moves to smaller values of F_v until the exducer chokes. The pressure ratio at which this occurs depends on the

geometry. As soon as the exducer chokes, the efficiency starts dropping and a pronounced corner appears in the efficiency curve. By plotting these curves for a range of rpm, one can interpolate lines of constant pressure ratio. The efficiency for constant pressure ratio increases with increasing pressure ratio until an optimum is reached, and for high pressure ratios, the efficiency drops again as shown in Figure 6-5. Additional insight into the behavior of a radial turbine is obtained by plotting the reaction for the different speeds. The reaction is generally lower for lower speeds. For a given speed, the reaction drops with increasing pressure ratio until a distinct minimum occurs. When the exducer chokes, the reaction increases again. Figures 6-5 to 6-7[107] show these trends.

6.4.2 Compressors

Typical performance presentation of compressors is shown in Figures 6-8 to 6-10[35], for an axial, a radial, and a rotary-piston positive-displacement type.

Several other types of performance presentation are also in use. Figure 6-11[113] shows, for example, a non-dimensional presentation of Stratos TCS-670 compressor characteristics for air.

6.4.3 Use Factors

In order to make an evaluation of performance in service, it is necessary to analyze use factors. The many different applications impose a wide variety of demands on gas turbines. These demands vary from seldom-operated emergency power units, intermittent operation of peaking and transportation units, to the continuous operation of base-load units. A measure of this service is the use factor.

$$\text{Percent Use Factor} = \frac{\text{Total fired hours}}{\text{Total installed hours}} \times 100$$

This factor serves to place machines into one of three categories. These are: zero to 20 per cent - standby, emergency, or peaking units; 20 to 80 per cent - transportation and seasonal units;

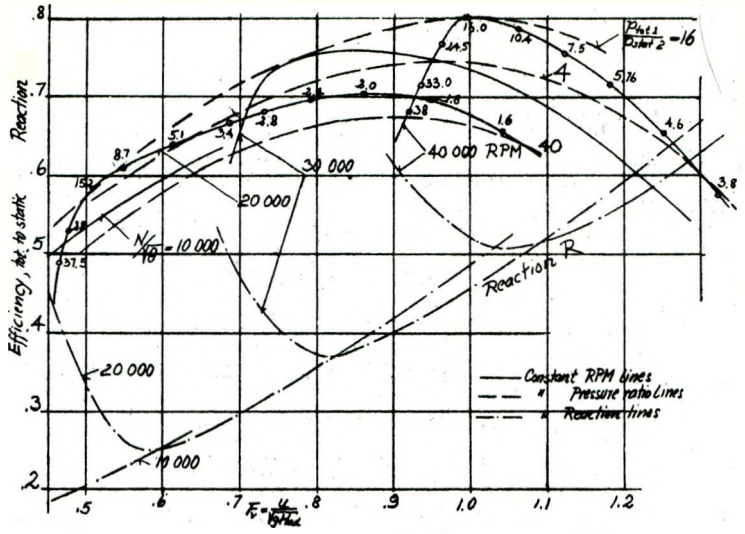


Fig. 6-5 - General Performance Presentations of a Radial Turbine

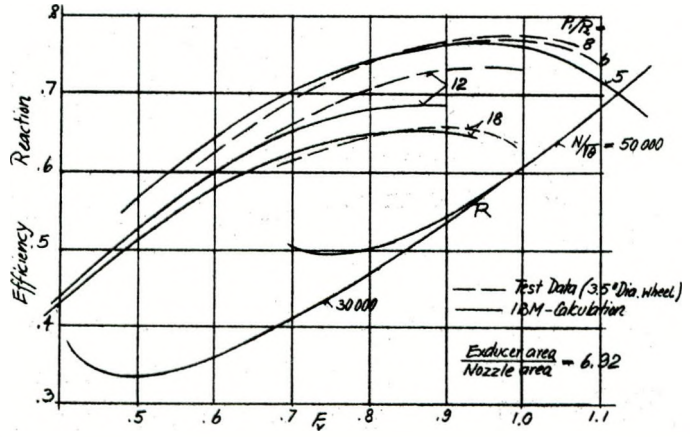


Fig. 6-6 - Performance of Radial Turbines (50 per cent Reaction Blading)

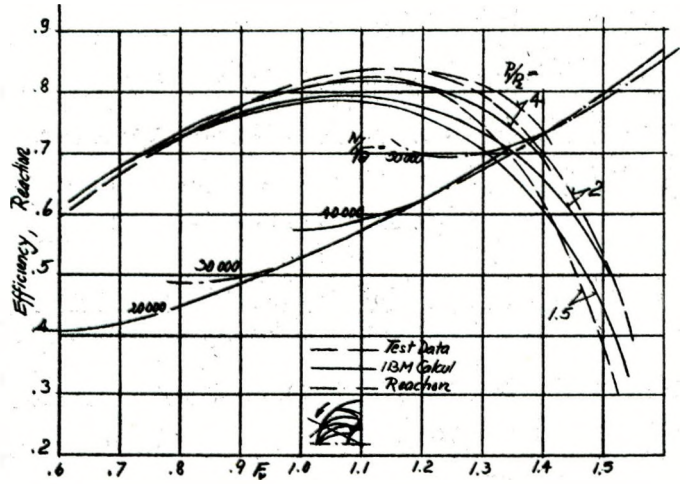


Fig. 6-7 - Performance of Radial Turbines (High Reaction Blading)

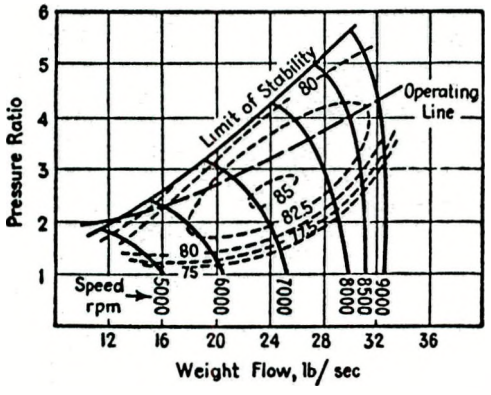


Fig. 6-8 - Typical Performance Curves of an Axial Flow Compressor

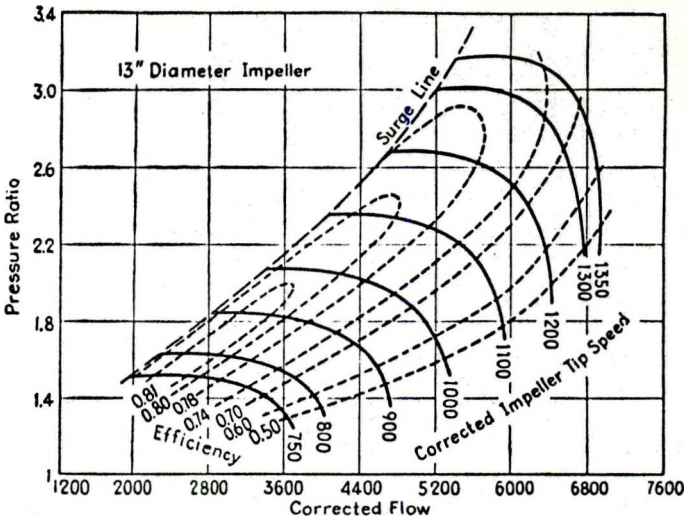


Fig. 6-9 - Typical Performance Chart of a Centrifugal Compressor

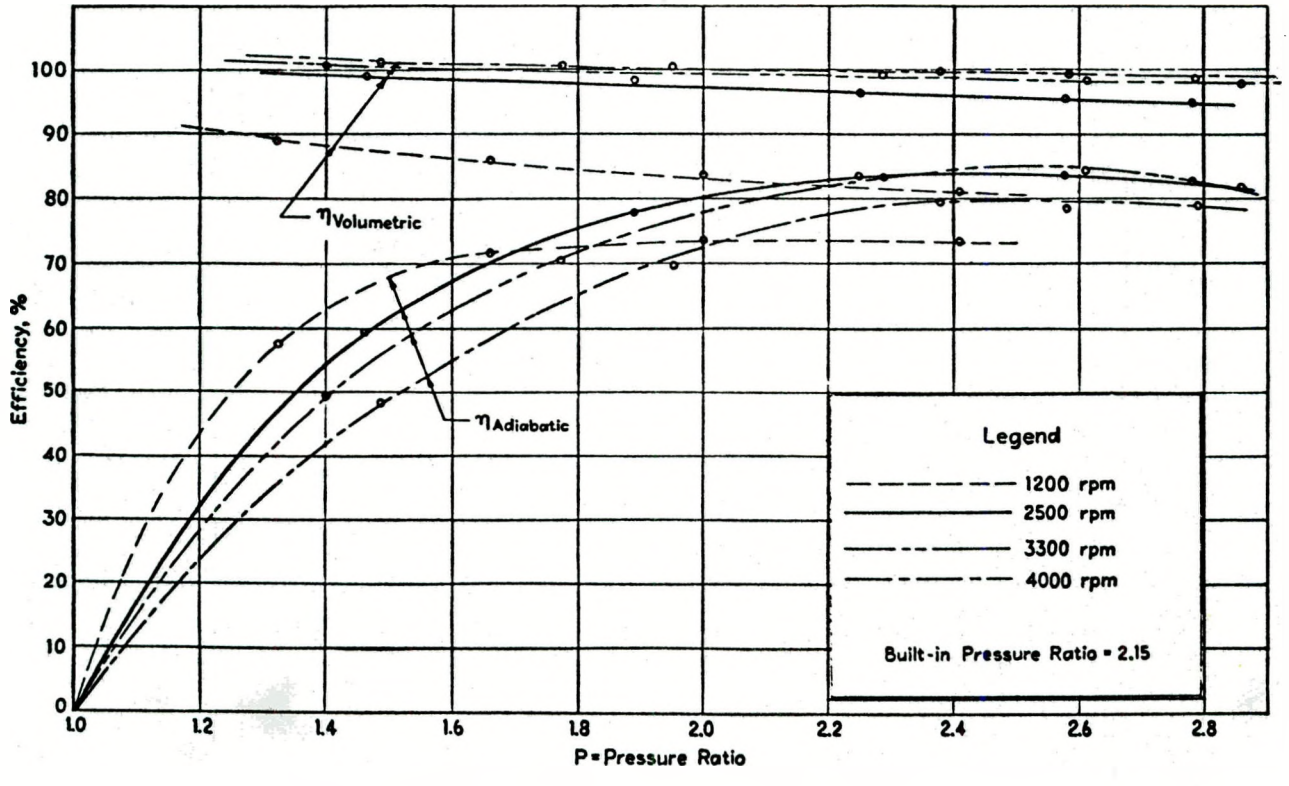


Fig. 6-10 - Typical Performance Curves of Lysholm Positive Displacement Rotary Piston Compressor

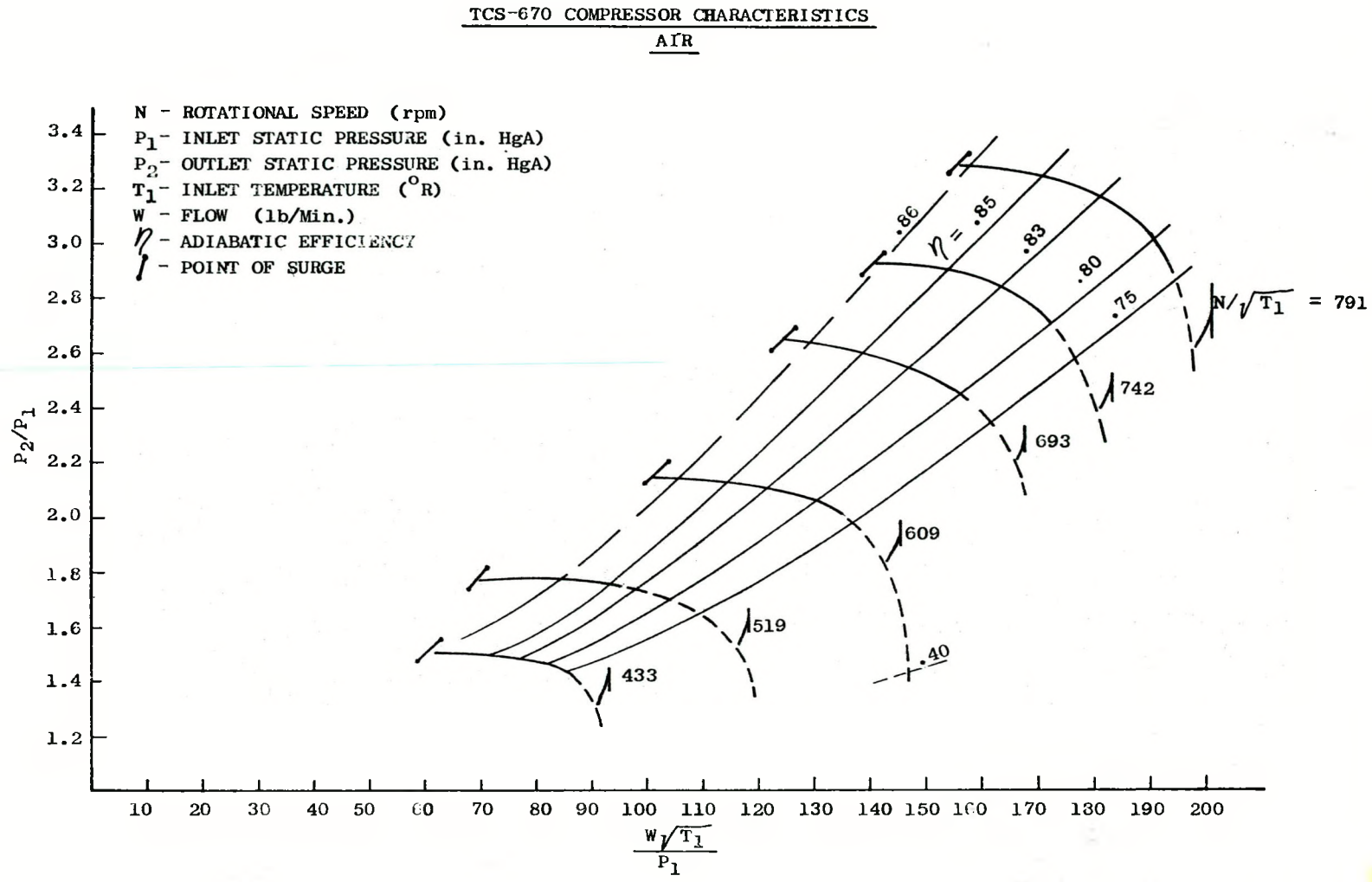


Fig. 6-11 - TCS-670 Compressor Characteristics for Air

80 to 100 per cent - base-load units. Figure 2-23c in Section 2.2 shows use factors for all General Electric industrial gas turbines before and through 1958.

Other criteria necessary to evaluate performance are availability and reliability factors. These are defined as

$$\text{Per cent availability} = \frac{\text{Installed hours} - (\text{Forced outage} + \text{maintenance})\text{hours} \times 100}{\text{Installed hours}}$$

$$\text{Per cent reliability} = \frac{\text{Installed hours} - \text{Forced outage hours}}{\text{Installed hours}} \times 100$$

Figure 2-23d in Section 2.2 shows availability and reliability factors for all General Electric industrial gas turbines before and through 1958. These factors are more easily obtained in base-load gas turbines because more accurate records are kept for them.

6.4.4 Optimum Flow Rates and Tip Speeds

Optimum flow rates and tip speeds for radial and axial compressors have been obtained by the Solar Aircraft Co. For both radial and axial compressors, the optimum flow rate can be approximated from the equations

$$W = \frac{c_w D^2 u p_1}{R T_1} \quad \text{lb/sec}$$

where c_w varies with tip-to-eye diameter ratio and flow coefficient in radial compressors and hub-to-tip ratio and flow coefficient in axial compressors. Values used here, 13.6 for radial compressors, and 33.8 for axial compressors.

D = tip diameter - ft
u = tip speed - fps
p_1 = inlet total pressure - psia
T_1 = inlet total temperature - °R
R = universal gas constant - ft lb/lb °R

Tip speed can be presented as a function of first stage pressure ratio and adiabatic efficiency as follows

$$u = c_v \sqrt{\frac{c_p T_1}{\eta_{ad}} \left[(r_{stage})^{\frac{k-1}{k}} - 1 \right]} \qquad \text{ft/sec}$$

Values for c_v used here are 166.7 for radial compressors and 304 for axial compressors.

c_p = specific heat at constant pressure. Btu/°R.lb

r_{stage} = stage pressure ratio

$k = c_p/c_v$

Note that for the assumed values of c_v and c_w for a particular stage pressure ratio and gas, the tip speed of an axial compressor will be 1.82 times the tip speed of the radial compressor and, therefore, weight flow will be 4.53 times greater in the axial based on equal tip diameters. Also note that for the same tip speed, the centrifugal will swallow 0.4 the flow rate of the axial.

According to Solar, tip speed for long life in both radial and axial compressors must be limited to a maximum value of approximately 1400 fps because of stress and fatigue, and in the case of nitrogen compressor, the relative blade Mach number will limit the tip speed to 1000 fps. It may be mentioned that in a turbo-compressor set, the compressor usually dictates the design.

7. MATCHING OF TURBOMACHINERY

It is not usually possible to choose arbitrarily such variables as variation of maximum cycle temperature, of mass flow rate, and of shaft speeds with load because there are definite limitations imposed by the relationships of mass flow-speed-pressure ratio for both compressors and turbines. These relationships are the characteristics of the components, which are of fundamental and far-reaching importance to operation of gas turbine plant of all kinds.

A problem designers are frequently facing is to find the optimum match of compressor and turbine in, for example, a gas turbine. Since in such an arrangement, both components have the same weight flow and about the same pressure ratio, it is apparent that the specific speeds of compressor and turbine are directly interrelated. Let us describe a convenient method for matching compressor and turbine. For a typical single-spool arrangement, where the compressor is directly coupled with the turbine, the interrelation is

$$\frac{N_{sc}}{N_{st}} = \sqrt{\frac{p_{3t}}{p_{1c}}} \left(\frac{T_{1t}}{T_{1c}}\right)^{1/4} \left(\frac{Y_t}{Y_c}\right)^{0.75} \frac{1}{\sqrt{1 - Y_t \eta_t}}$$

when line losses are neglected and where $Y_t = 1 - \left(\frac{p_3}{p_1}\right)^{\frac{k-1}{k}}$ and $Y_c = \left(\frac{p_3}{p_1}\right)^{\frac{k-1}{k}} - 1$ are pressure ratio functions.

In cases where these losses become of significant magnitude, they can be accounted for by reducing Y_t and η_t in above expression correspondingly. Plotting this expression as a function of the compressor pressure ratio for different temperature ratios, whereby temperature ratio refers to the ratio of turbine-inlet temperature to compressor-inlet

temperature, the diagram of Figure 7-1[111] is obtained, indicating that the specific speed of the compressor is always larger than the specific speed of the turbine when the line losses are comparatively small. Having established the interrelation of the specific speeds of both components, it is possible to obtain more detailed information for the optimum match by superimposing a transparent copy of the compressor $N_s D_s$-diagram over the turbine $N_s D_s$-diagram as shown in Figure 7-2[111] for radial compressors and radial turbines. Since the N_{st}/D_{sc} relation is fixed by the design condition $\left(\left(p_3/p_1 \right)_c = 3;\ T_t/T_c = 4;\ Re > 10^6 \right)$ in Figure 7-2, the only remaining variables are the specific diameters. These can now be adjusted by the overlay technique, until the maximum efficiency region of the turbine coincides with the maximum-efficiency region of the compressor. Thus, it is found that both components match well and that the optimum match occurs at N_{sc} values of 80 to 90 (for example) and that $D_{sc} < D_{st}$. This information can now be converted for finding the optimum rotative speed as a function of the passing weight flow, yielding after some simplifying assumptions

$$N = \frac{\sqrt{p_{1c}} \left(RT_{1c} \right)^{1/4} \left(\frac{k}{k-1} Y_c \right)^{0.75} N_{sc}}{W^{1/2}}$$

which can be rewritten in terms of net output, hp_{net}

$$N = \frac{\sqrt{p_{1c}} \sqrt{\left(\eta_t \frac{T_{1t}}{T_{1c}} \frac{Y_c}{Y_t} - \frac{1}{\eta_c} \right) \left(\frac{k}{k-1} Y_c \right)^{1.25} \left(RT_{1c} \right)^{0.75}} \times N_{sc}}{\sqrt{hp_{net}} \quad \sqrt{550}}$$

Introducing the specific design condition, quoted previously, and selecting $T_{1c} = 520°R$ and $p_{1c} = 15$ psia, there results $N = \frac{470{,}000}{\sqrt{hp_{net}}}$

This relation reveals that optimum speed of single-spool gas turbines decreases with increasing net outputs. The equation also indicates that the optimum speed increases with increasing temperature ratios, increasing compressor-inlet pressures, and increasing inlet temperatures. Since optimum rotative speed is described as a function of several parameters, including pressure ratios and component efficiency, the relation $N = 470{,}000/\sqrt{hp_{net}}$ can only be correct as long as $p_3/p_1 = 3$ represents the optimum pressure ratio. This is true only for a limited hp-range (because of Reynolds number and Mach number influences) so that in fact an additional optimization is required which indicates the optimum pressure ratio as a function of component efficiency. These considerations reveal that for power ranges below 50 hp, the optimum pressure ratio tends to be smaller than 3:1 so that the optimum speed in this region is smaller than indicated in the foregoing with respect to, for example, single-stage radial machines.

A somewhat different situation exists for turbosuperchargers and gas-turbine cycles with a free-wheeling power turbine. In these arrangements the rotative speeds and weight flows are the same (gas-generator turbine-compressor set), but not the pressure ratios of the components. With some simplifications, i.e., by neglecting the change of the ratio of specific heats, the pressure ratio required by the turbine in a turbosupercharger can be expressed by the relation

$$\frac{p_{3T}}{p_{1T}} \cong \frac{p_{3c}}{p_{1c}} \left(1 - \frac{Y_c}{\eta_c \, \eta_T \, \frac{T_{1T}}{T_{1c}}} \right)^{3.5}$$

With this relation, the interrelation of the specific speeds of compressor and turbine in a turbocharger can be quoted in the form

$$\frac{N_{sc}}{N_{st}} = \sqrt{\frac{p_{3T} \, T_{1c}}{p_{1c} \, T_{1T}}} \times \frac{1}{\sqrt{1 - \frac{Y_c \, T_{1c}}{\eta_c \, T_{1T}}} \; (\eta_c \, \eta_T)^{0.75}}$$

Representing this relation graphically as a function of pressure ratio and temperature ratio, (see Figure 7-3[111]), it is found that the specific-speed ratio is smaller than unity, increasing somewhat with the pressure ratio and decreasing with temperature ratio. It is found that the ratio of specific speeds is too small to afford an optimum match between radial compressor and radial turbine, so that, most likely, a slight efficiency sacrifice has to be anticipated as long as η (related to the static pressure) is the optimization criterion. It is also evident that the radial compressor should be of the "low-specific-speed type" and the radial turbine of the "high-specific-speed type".

The same conclusions are valid for an axial gas-generator turbo-compressor set. There is also the implication, as is apparent from Figure 6-2, that an axial turbine may offer a better match for a centrifugal compressor of the high-specific-speed type with $\beta_2 = 90°$. It may be pointed out also that efficiency alone is not always the most decisive criterion and that the difficult matching problem in many cases may be compensated for by the low cost of the radial turbine and the comparative ease of providing variable nozzles, a feature which increases the performance range of the unit. With growing flow rates, i.e., size of a turbocharger, as for example for free-wheeling power turbines, there is a limit where both turbine and compressor are best of the axial-flow type. Such limit is considered by manufacturers, skilled in radial turbomachinery, to be around 1000 hp.

Equilibrium-running of turbine and compressor can be investigated also by torque curves over flow rates, with rotational speed as a parameter, as shown in Figure 7-4. For stable operation, the operating points of the compressor must not fall on or beyond the surge line. Note that an increase of turbine inlet temperature may cause unstable operation of the compressor in a one-shaft arrangement at a given gas flow rate. More generalized, the following conditions must be satisfied in equilibrium running of turbine and compressor[114]:

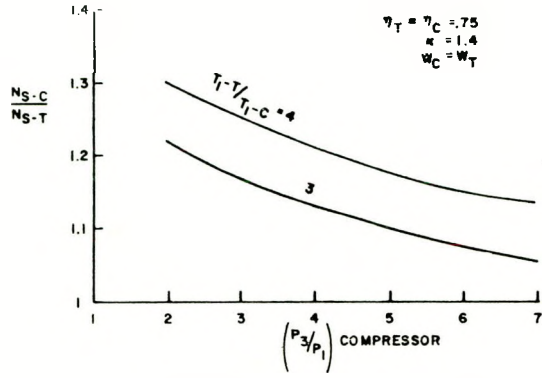


Fig. 7-1 - Interrelation of Specific Speeds for Single-Spool-Gas-Turbines

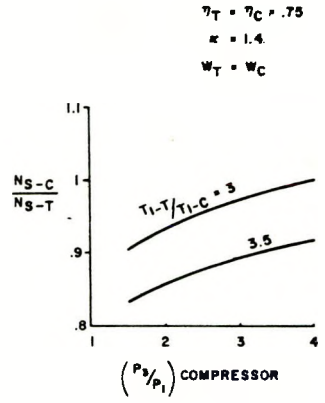


Fig. 7-3 - Interrelation of Specific Speeds in Single-Spool Turbo-Chargers (Gas Generators)

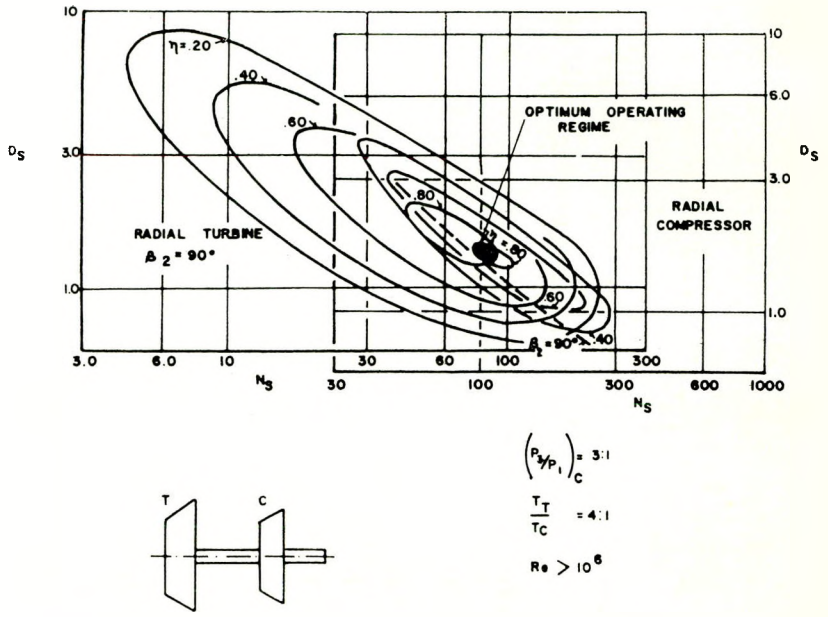
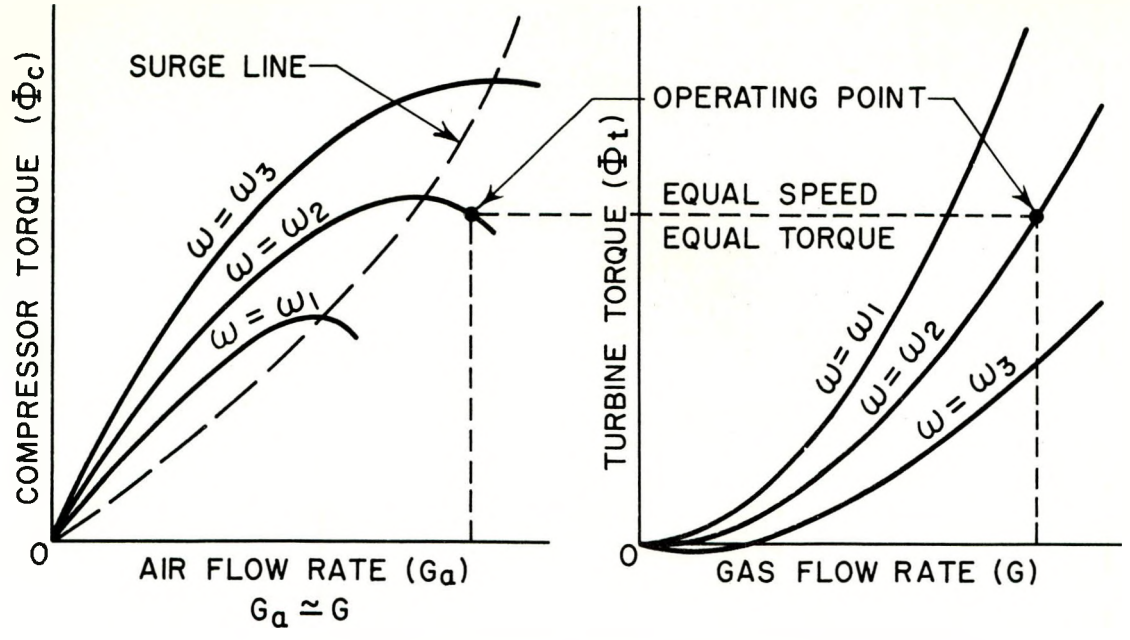


Fig. 7-2 - Matching of Single-Spool Gas-Turbines



TORQUE CURVES FOR SPECIFIED TURBINE INLET TEMPERATURE, T_{30}

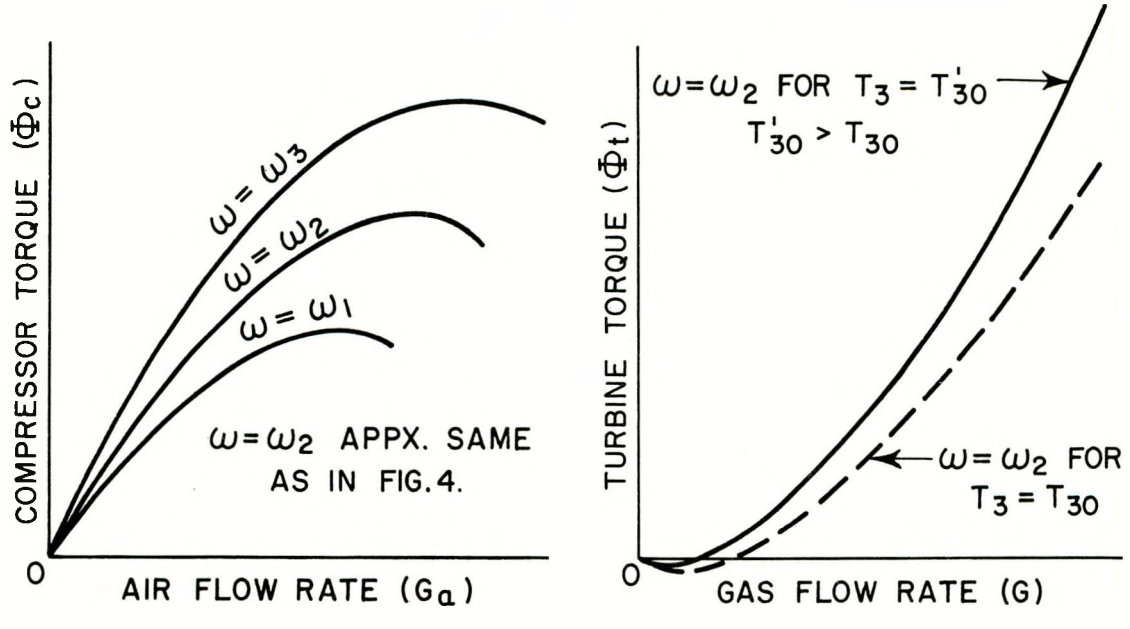


Fig. 7-4 - Torque Relations for Compressor and Turbine

(a) the ratio of turbine to compressor speed must be constant,

(b) the turbine work must equal the compressor work, and

(c) the gas mass flow through the turbine must equal the air plus fuel mass flow less any leakage.

In Figure 7-5[115] are shown the matched characteristics of a 16-stage compressor and a 3-stage turbine according to studies carried out by NACA on the basis of component performance data. These investigations were made to point out problems encountered in matching a single-spool compressor with a turbine in a high-pressure-ratio engine.

Equilibrium operation of a compressor and a turbine as a directly coupled unit in a turbojet engine requires that four conditions be satisfied:

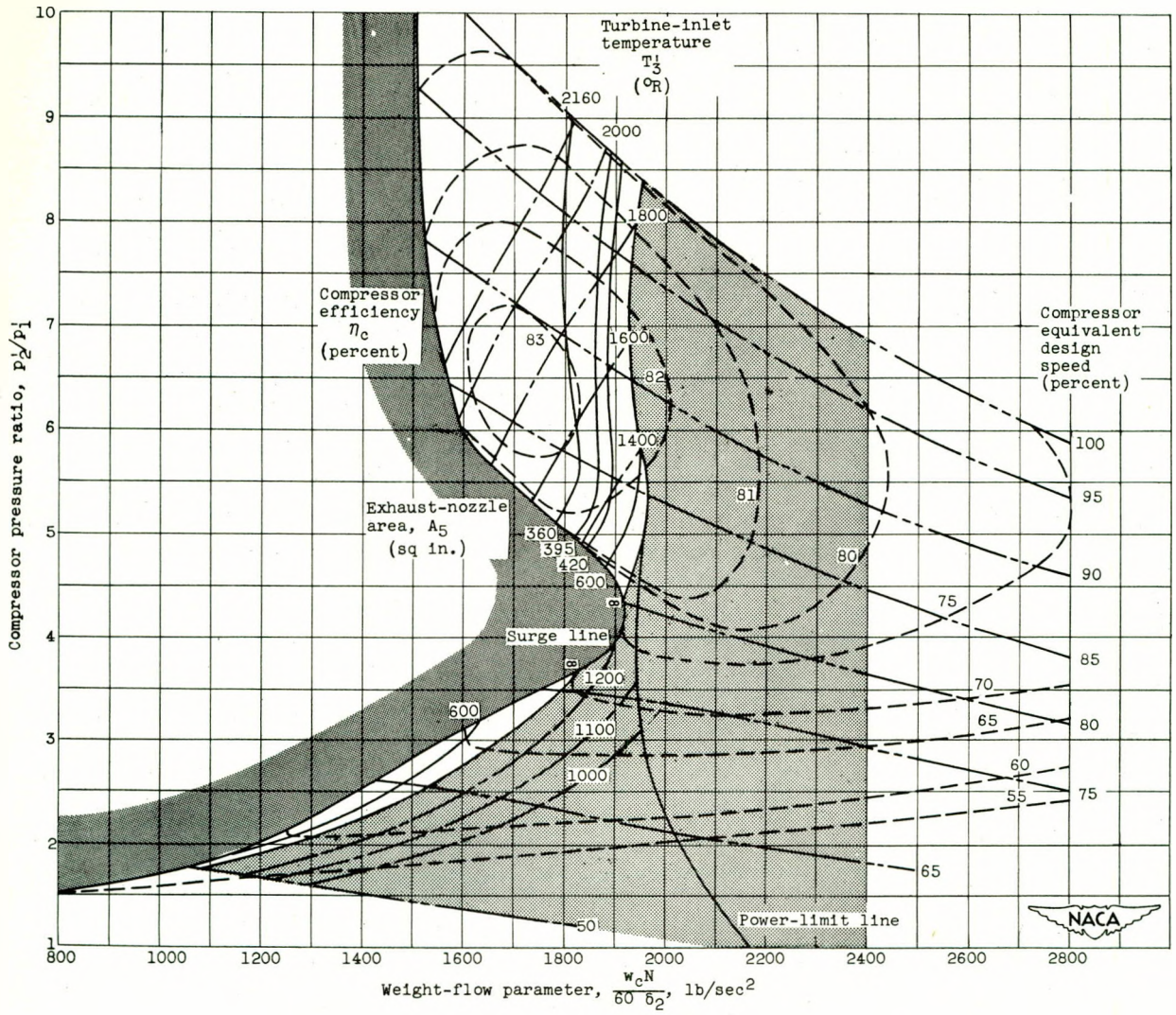
(1) The compressor rotative speed must equal the turbine speed.

(2) The air weight flow into the compressor plus the fuel weight flow added in the burners minus any leakage between compressor and turbine must equal the weight flow into the turbine when no air is bled from the engine.

(3) The turbine power (or torque) must equal the power (or torque) required to drive compressor and auxiliary equipment and to overcome mechanical losses.

(4) The over-all pressure ratio resulting from ram, compressor compression, and pressure loss in the burners must equal the over-all pressure ratio across the turbine, the tail pipe, and the jet nozzle.

Equilibrium operating lines are determined from the component performance characteristics for assumed engine operating conditions of zero flight speed, various effective exhaust-nozzle areas, and various values of leakage between compressor and turbine. Intersections of



(a) No leakage.

Fig. 7-5 - Matched Performance Characteristics of 16-Stage Compressor and 3-Stage Turbine

THE FRANKLIN INSTITUTE • Laboratories for Research

compressor and turbine speed lines define possible operating points (turbine speed lines are not shown in Figure 7-5). The region of possible engine operation without bleed lies to the right of the compressor surge line and to the left of the infinite exhaust nozzle area and turbine power-limit lines. Above approximately 83 per cent speed, the infinite-area operating line coincides with the turbine power-limit line. Operation in the region to the left of the surge line is usually undesirable, or even impossible, when the turbine pressure ratio corresponding to the required power exceeds the available compressor pressure ratio. Operation to the right of the turbine power-limit line is impossible because in this region the power required exceeds the power available from the turbine. Below approximately 83 per cent speed, operation in the region between the infinite-area (exhaust nozzle) line and the turbine power-limit line is impossible for $p_1'/p_o = 1.0$ (p_1' = stagnation pressure at compressor inlet, p_o = static pressure at NACA standard sea-level conditions) because the turbine pressure ratio corresponding to the required power exceeds the available compressor pressure ratio. Some means, such as compressor-outlet bleed, would be required for this engine to accelerate through the intermediate speed range to that of matched normal operation[115].

THE FRANKLIN INSTITUTE · Laboratories for Research and Development

8. PART-LOAD OPERATION AND CONTROL

8.1 Part-Load Conditions

Investigation of part-load operation is necessary to make sure that an engine, as designed, will operate stably and safely under all conditions it is likely to encounter. This means that the extremes of ambient conditions (and in the case of aircraft engines, of forward speed as well) must be taken into account, together with the full range of rotational speeds. While calculations are, in general, carried out for steady operating conditions, sometime it may be necessary to accelerate the plant at some predetermined rate.

The limits to satisfactory operation which must be taken into account are the following[116]:

(a) Compressor surging-Although the immediate effects of surging are not disastrous, running under surging conditions for any appreciable length of time should be regarded as impracticable. If it is found that surging is encountered under starting conditions, this may be accepted. On the other hand, if the normal running of the plant involves running any compressor very near, or on, the surge line, some modification must be made to the cycle layout or detailed design, in order to avoid the difficulty. If a particular project is shown to encounter surging at a transient condition, such as starting, this can often be dealt with by some relatively simple palliative measure, not involving changes in the main design. The simplest method of achieving this is by means of one or more blow-off valves fitted to the compressor which encounters the trouble. By this means the flow through the compressor is kept sufficiently high to avoid surging while the turbine is prevented from receiving too large a quantity of gas, by jettisoning the surplus. This is done, of course, at the expense of some power and hence results in a loss of efficiency, which does not matter under conditions which are not sustained for any long period.

Another method is the use of some variable component such as intake guide vanes or stator blades in an axial flow compressor, diffusers in a centrifugal compressor, turbine nozzles, or, in a jet engine, propelling nozzle. Any of these may result in a considerable loss of efficiency, which is acceptable for short periods, to make possible the operation of the plant without sacrifice of performance under normal operating conditions.

Acceleration of the engine necessitates higher cycle temperatures than would be necessary under steady conditions at the same rpm. As will be seen presently, this means that the operating point while accelerating moves nearer to the surge line, so some allowance should be made for this effect, especially in cases where rapid acceleration is necessary. Some margin should also be allowed for the effects of manufacturing tolerances on the relative positions of the operating line and the surge line.

(b) Excessive temperatures-The temperatures reached by the turbine blading are obviously of great importance to the safety of the plant, and definite limits are set by the properties of the materials used. Again transient conditions represent a special case and temperatures higher than would be acceptable for long period running may be preferable. The limiting temperature may not be a single fixed value but may be related to the stress imposed and hence to rotational speed. It may be found necessary to impose operational limitations in certain conditions in order to avoid excessive performance penalties in others. For example, turbine entry temperatures may rise too high when tropical ambient temperatures occur and this may necessitate acceptance of a lower maximum rpm when such conditions are encountered.

(c) Excessive rotational speeds-It is equally important that no shaft speed should become so high as to cause stresses which might be dangerous. The actual limits are to some extent linked to the temperatures occurring in the turbines at the same time, but usually high rotational speeds are accompanied by high temperatures.

In neither case is the design point value (of temperature or speed) necessarily the limit, as allowance can be made in the design for some degree of excess temperature and stress, if necessary.

(d) Excessive loading-This is a less serious aspect which is not often of great importance but which should not be entirely overlooked. Under certain operating conditions, especially combinations of high ambient pressure, high rpm and low ambient temperature, the output increases, along with blading and shaft loadings and internal pressures. These can result in a failure of some kind either in the plant itself or in gearing or driven machinery (especially electrical generators) associated with it. Again it may be necessary to impose an operational limitation to avoid such dangers.

The second object of off-design performance calculations is to enable the performance to be predicted under all conditions of operation likely to be encountered. Generally,the net output and the thermal efficiency are the quantities which it is desired to know, but others, such as various internal pressures and temperatures, may be of interest as well. The stability and safety investigations may not necessitate the completion of calculations to the point where actual performance figures are obtained. For example, having fixed an operating point on a compressor characteristic, it may not be necessary to continue any further if only the stability aspect is being dealt with.

In choosing a particular cycle layout from among the many possibilities, both aspects are important. The stability and safety question is of over-riding importance and is often decisive, but given satisfactory operation in this respect a choice will generally depend on the relationship between efficiency and output, apart from purely physical considerations such as weight, space, cost or accessibility.

The actual calculations involved in off-design performance estimation are frequently somewhat involved and laborious. This is because of the necessity to link together in the correct manner the performance of

several different components, most of whose characteristics cannot be expressed mathematically. Usually one or more iteration processes are involved and these add greatly to the complication of the process. However, the principles on which all such calculations are based are extremely simple, so much so that it is almost a formality to state them. They are as follows[116]:

(a) Continuity of mass flow-The mass flow rates through all components in series must be the same, subject to any necessary allowances for additions of fuel or leakage, cooling flows or other causes of change. The sum of the flows through any components in parallel must also obey this rule.

(b) Compatibility of speeds-The rotational speeds of all components on the same shaft must be the same, except where gearing is interposed between them, when due allowance must be made for its ratio, whether fixed or variable.

(c) Compatibility of pressures and temperatures-The pressures throughout the cycle must vary consecutively and in accordance with the characteristics of the components. The product of all the pressure increasing pressure ratios must equal the product of all the expansion pressure ratios. Similarly, the temperatures must vary consistently with heat or work input or extraction.

(d) Compatibility of powers-In steady state operation, the powers produced and absorbed on any shaft must be in balance. Especially where a turbine is driving a compressor only, with no external load (or power supply) its output must equal the power absorbed by the compressor, with allowance for such small effects as bearing losses and auxiliary drives.

In this report we cannot describe in detail the actual procedures used to investigate a complete given cycle for conditions of part-load operation, but it may be said that the arrangement of the components in the cycle has a great influence on operation characteristics.

THE FRANKLIN INSTITUTE • Laboratories for Research and Development
F-A2392-6

A general rule is that in compound cycles the part-load cycle efficiency increases as the part of compression work of turbines on the low-pressure side of the expansion increases. However, a general limitation also exists that each procedure increasing the part-load efficiency is shifting the operation line in the compressor map closer to the surge line.[48] Surge-free compressors would be a solution to this problem.

The difficulty in compound systems is to obtain surge-free operation of all compressors, in series at all matched part-load conditions. It is not an absolute requirement to have intercooling between two compressors and reheat between two turbines in a compound system. Such systems can be also operated as a compound system. Furthermore, if in such case the high-pressure turbine is driving the high-pressure compressor, and the low-pressure turbine is driving the low-pressure compressor, the system becomes very stable, because with decreasing load, the speed of rotation of the low-pressure compressor decreases much more than that of the high-pressure compressor. When intercooling is introduced, such a system is more affected by surge phenomena than without intercooling. A cross-compound arrangement is obviously worse because the low-pressure compressor, being connected to the high-pressure turbine, will easily enter the surge region already at a relatively small drop of load, as its speed of rotation remains high. The only successful cross-compound arrangement known to date is the 2500 hp Elliot-Lysholm marine installation with positive-displacement Lysholm compressors which remain stable at any point of operation. The efficiencies of this installation at part-load operation are high.

8.2 Controls for Gas Turbine Functions

The following general operational functions of gas-turbines are performed at any load:

(a) Starting and stopping control

(b) Speed or load control

(c) Temperature and rate of temperature control

(d) Emergency shutdown control.

To meet the variety of necessary requirements, the components used for the functions indicated are electrical, mechanical, hydraulic, pneumatic, or suitable combinations. For example, General Electric Co. has five basic designs (see Table 2-12). These gas turbines are used in three different applications with varied use in each. They burn four different fuels (natural gas, residual oil, distillate, and crude oil), and operate in a wide range of geographic locations. This range of conditions has placed varied requirements on the turbine starting means.

Five different starting means have been employed. These are:

(a) Expansion turbine, operating on steam, connected through a clutch to the turbine shaft.

(b) Diesel engine, operated through a torque converter, clutch, and speed-increasing gear to the turbine shaft.

(c) Diesel-engine-driven generator, connected to a motor, geared to the turbine shaft.

(d) Electric motor, with or without speed-increasing gear connected through a clutch to the turbine shaft and

(e) Expansion turbine, operating on natural gas, connected through a clutch to the turbine shaft.

A tabulation of these starting means as of (September 30, 1957) shows[29]:

Expansion turbine - steam 6 machines

Diesel engine-torque converter	7 machines
Diesel engine-generator	27 machines
Electric motor	35 machines
Expansion turbine-natural gas	59 machines
total	134 machines

A particular arrangement for starting the blast-furnace gas-turbine plant at Rheinhausen Steelworks, Germany, was devised by Brown Boveri. Because of a lack of space, the starting motor was omitted, the generator being provided with a special starting winding. By reducing the length of the machine in this way it was possible to accommodate two gas-turbine sets in the existing space. The layout is shown schematically in Figure 8-1[14]. Terminal output is 15,000 kw. Figure 8-2[117] shows the starting diagram of the Brown Boveri 13 Mw 2-shaft gas turbine in the 40 Mw Beznau power plant, Switzerland. The gas turbine, with its inherent simplicity, is very suitable for quick starting compared only with starting time required by a diesel engine.

Associated Electrical Industries, England, carried out some experimental development of starting motors on its complete G6 boost naval gas turbine in addition to a good deal of initial development done by the Admiralty at the National Gas Turbine Establishment and elsewhere.

Lubrication of these motors is by means of oil carried in with the air supply, and shortage of oil leads to excessive piston wear. In the final system, "prewetting" of the motors is employed for an instant before the application of full air pressure, so that the motors always start in the "wetted" condition.

One of the desirable features of a boost naval gas turbine is its facility for rapid starting and loading. The starter motors of the G.6 are in engagement for only about 20 seconds during a normal start, and full

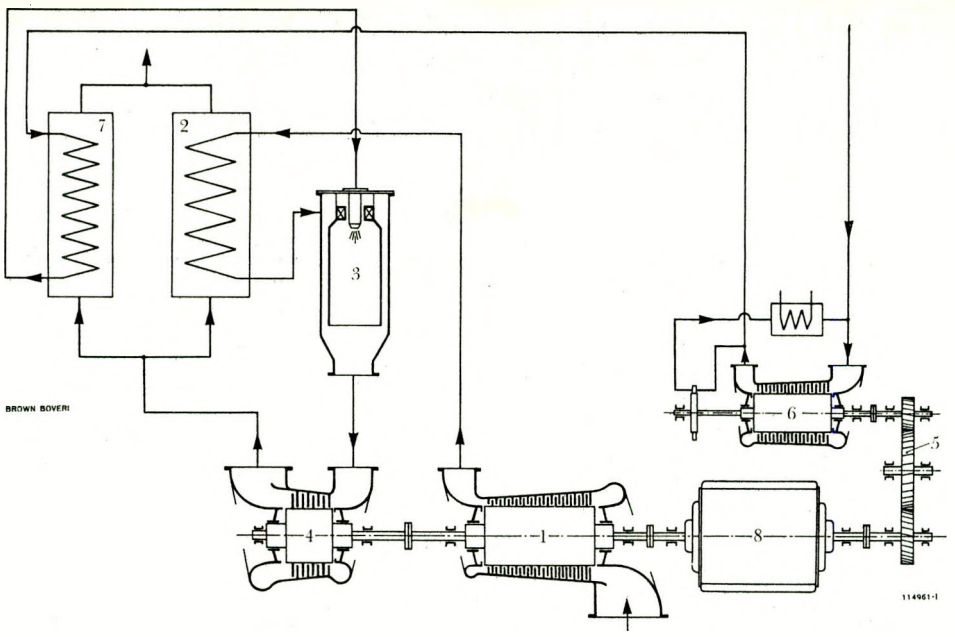


Fig. 21. – Schematic diagram of the Rheinhausen gas turbine — Terminal output 15 000 kW

1 = Air compressor	5 = Gear
2 = Air pre-heater	6 = Gas compressor with recuperation turbine
3 = Combustion chamber	7 = Gas pre-heater
4 = Gas turbine	8 = Generator

Fig. 8-1 - Schematic Diagram of the Rheninhausen Gas Turbine

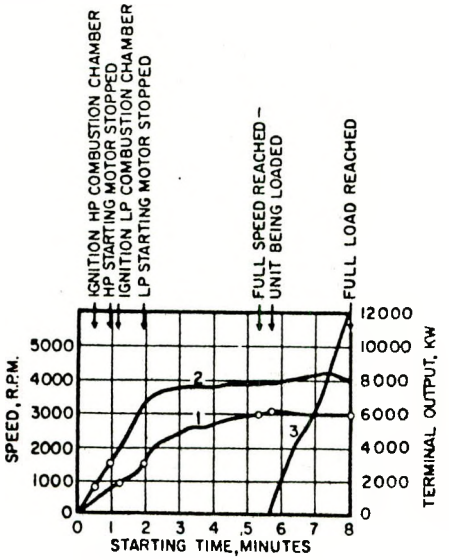


Fig. 8-2 - Starting Diagram of 2-Shaft Brown Boveri Gas Turbine

power has been achieved from a cold machine in 3 1/2 min. Some temperature variations associated with rapid starting are shown in 8-3 [16], which depicts temperatures of cylinder casing and liners of the HP turbine during a start. The interesting feature is the relatively slow heating rate of the casing itself, even though the liners, which are subjected to the full gas temperature, heat quickly. Similar results are obtained for heating rates of turbine disk rims (Fig. 8-4)[16].

8.3 Control Systems

The use of a variety of fuels over a wide range of operating conditions, and with many uses within an application, has placed a wide range of demands on the gas turbine control system. To meet these demands, a variety of systems must be employed. Those of General Electric Co. will serve as examples[29]. The control systems can be broken into four major categories:

(a) Manual Control - The operator energizes auxiliaries, engages the clutch, and starts the cranking device. He adjusts firing speed, fuel, and ignition. He controls acceleration of cranking device and increases fuel feed to bring the machine to operating speed.

(b) Semi-Automatic Control - The operator energizes auxiliaries, engages the clutch, and starts the cranking device. The remainder of cycle, fire and accelerate to speed, is automatic.

(c) Automatic Control - The operator initiates one control switch. The auxiliaries, cranking device, and acceleration are all automatic.

(d) Remote Control - A master switch is energized by a suitable communication such as wire or wireless relay.

A tabulation of General Electric units in operation as of September 30, 1957 shows:

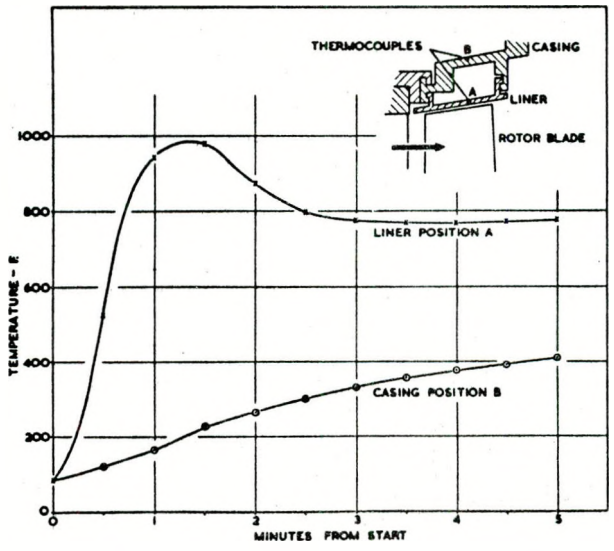
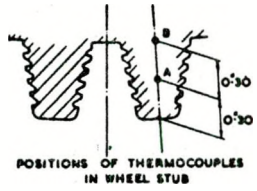


Fig. 8-3 - Relative Heating Rates of Turbine Casing and Linear During A Normal Start



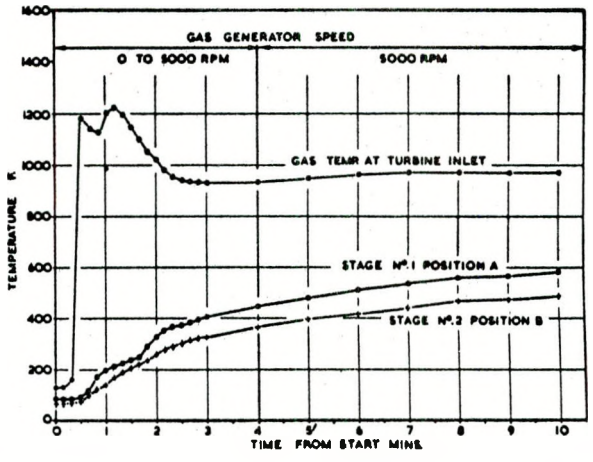


Fig. 8-4 - Heating Rates of the LP Turbine Disk Rims During a Normal Start

Manual	3 machines
Semi-automatic	19 machines
Automatic	55 machines
Automatic with remote provisions	50 machines
Remote	7 machines
Total	134 machines

An interesting method of increasing starting torque in a gas-turbine plant, proposed for a locomotive, is shown in Figures 8-5 and 8-6. By boosting both compressor turbine and load turbine, it is possible to obtain an initial torque of 3 times the rated T-C-set torque. Such initial torque is comparable with those achievable by high-initial torque electric motors.

The net power of any gas-turbine system is merely the excess of turbine power over that required by the compressor. Consequently, any provision whereby the power requirement of the compressor can be reduced will increase the net power of the system and, in general, the efficiency of cycle. However, such expected increase in efficiency must be proved more thoroughly, as mass-flow changes occur simultaneously. A large number of intercoolers in the compression phase can create the conditions of isothermal compression, representing a minimum work-input condition. Water injection into the moving air stream undergoing compression can also reduce the work required to compress the air[44].

The Puerto Rico Water Resources Authority is interested in a different way of water injection in the gas-turbine units of the 40 Mw plant, Mayaguez, Puerto Rico, in order to raise the output of the unit momentarily[118]. Highly demineralized water is injected into both combustion chambers of the two-shaft units, thus increasing weight and volume of the mass flow coming to both gas turbines appreciably. A gain

THE FRANKLIN INSTITUTE • Laboratories for Research and Development

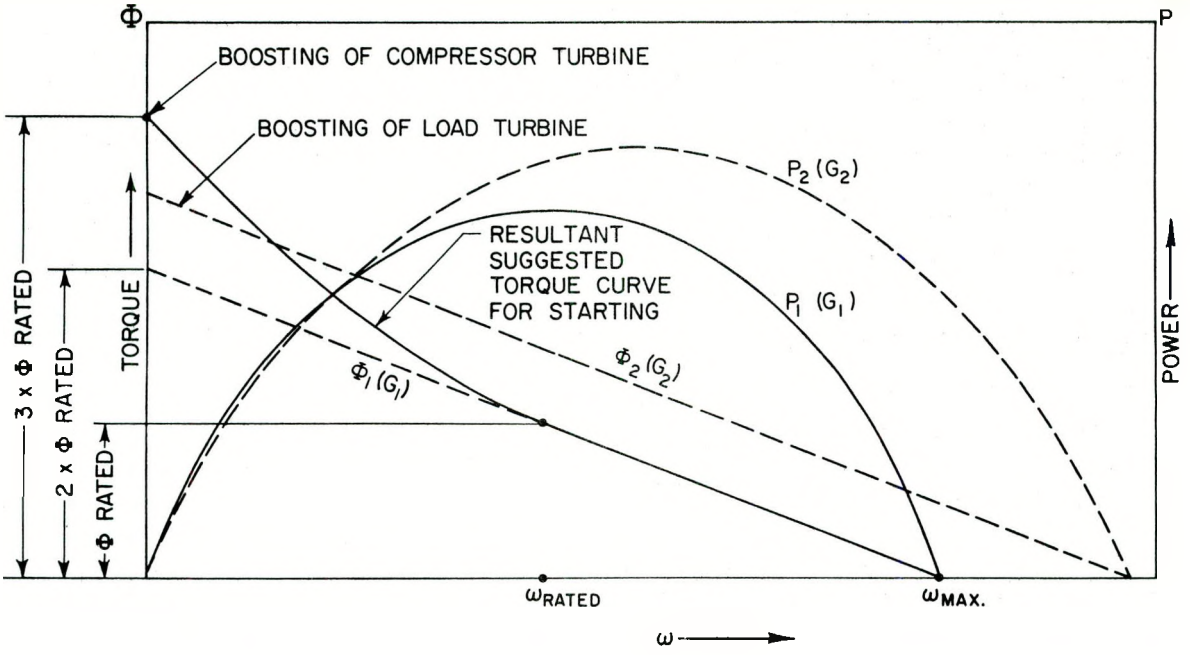


Fig. 8-5 - Increase of Initial Torque by Boosting

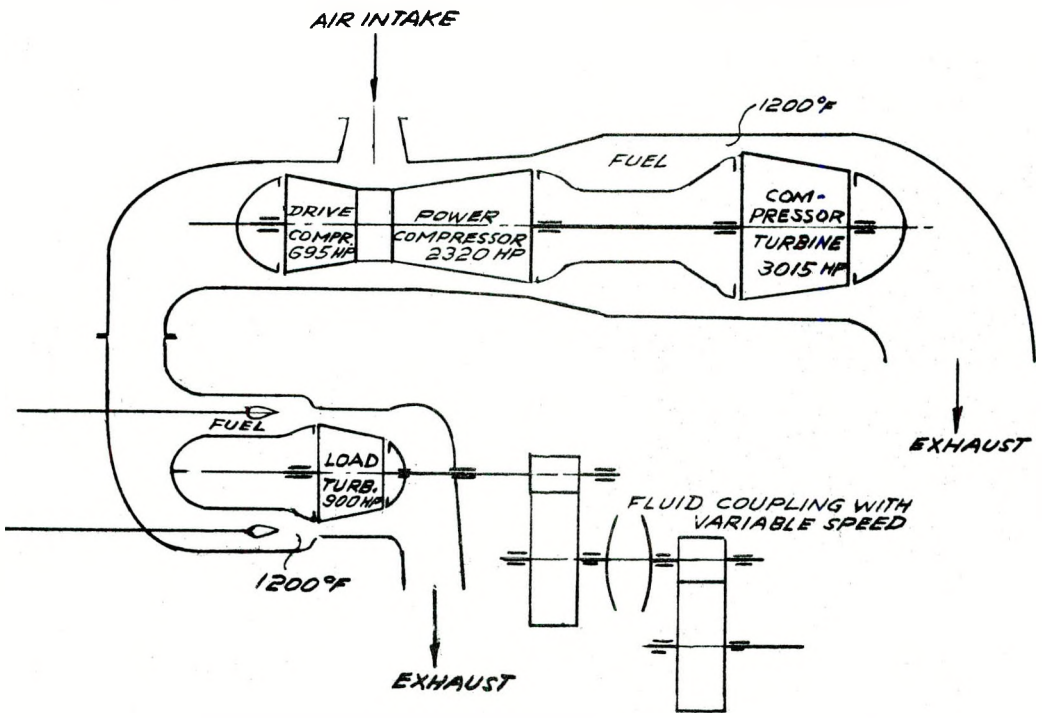


Fig. 8-6 - Gas-Turbine Unit in Two-Shaft Arrangement

in output between 10 and 15 per cent can be expected from this injection. However, the efficiency drops correspondingly because the passages of the gas turbine obviously have been designed for the normal mass flow.

Water injection has been tried successfully on a single-shaft unit during factory tests and there is no reason to believe that the application to the two-shaft unit should not be successful also. However, to prevent any deposits on the blading, it is necessary that the water be highly demineralized and it must be recognized that the produced steam is a total loss after it leaves through the stack to the atmosphere. It is rather a question of economics, if the cost of demineralization is worth the extra amount of kilowatts which the gas turbine can give momentarily.

Of course, one must also take precautions while operating the unit at this point in order not to get into the surge conditions of both axial-flow compressors, which have inherently quite a steep characteristic.

The cycle of the ML-1 nuclear power plant (see Section 3.3.2) has been simulated in an analog circuit, and many runs have been made to test different control schemes or various designs of major loop components. Transient temperature data for heat exchanger specifications were derived for various shutdown conditions. An axial compressor map was installed and compared as an alternate to the radial compressor. The analog showed that the proposed control scheme worked equally well for the two types of compressor. A modification to the control scheme was proposed to prevent driving the compressor into a surge during a load increase. The ML-1 start-up schedule is described by Figs. 8-7 to 8-9[12].

The required starting torque for the Stratos turbine-compressor set and gear box is shown in Fig. 8-10[22]. The torques required by starting motor and generator must be added to the values shown. The curves are based upon system pressure drops proportional to those at the original design condition and 0.1 pounds per second by-pass. When more accurate data are available on system pressure drops, a new set of curves can be made.

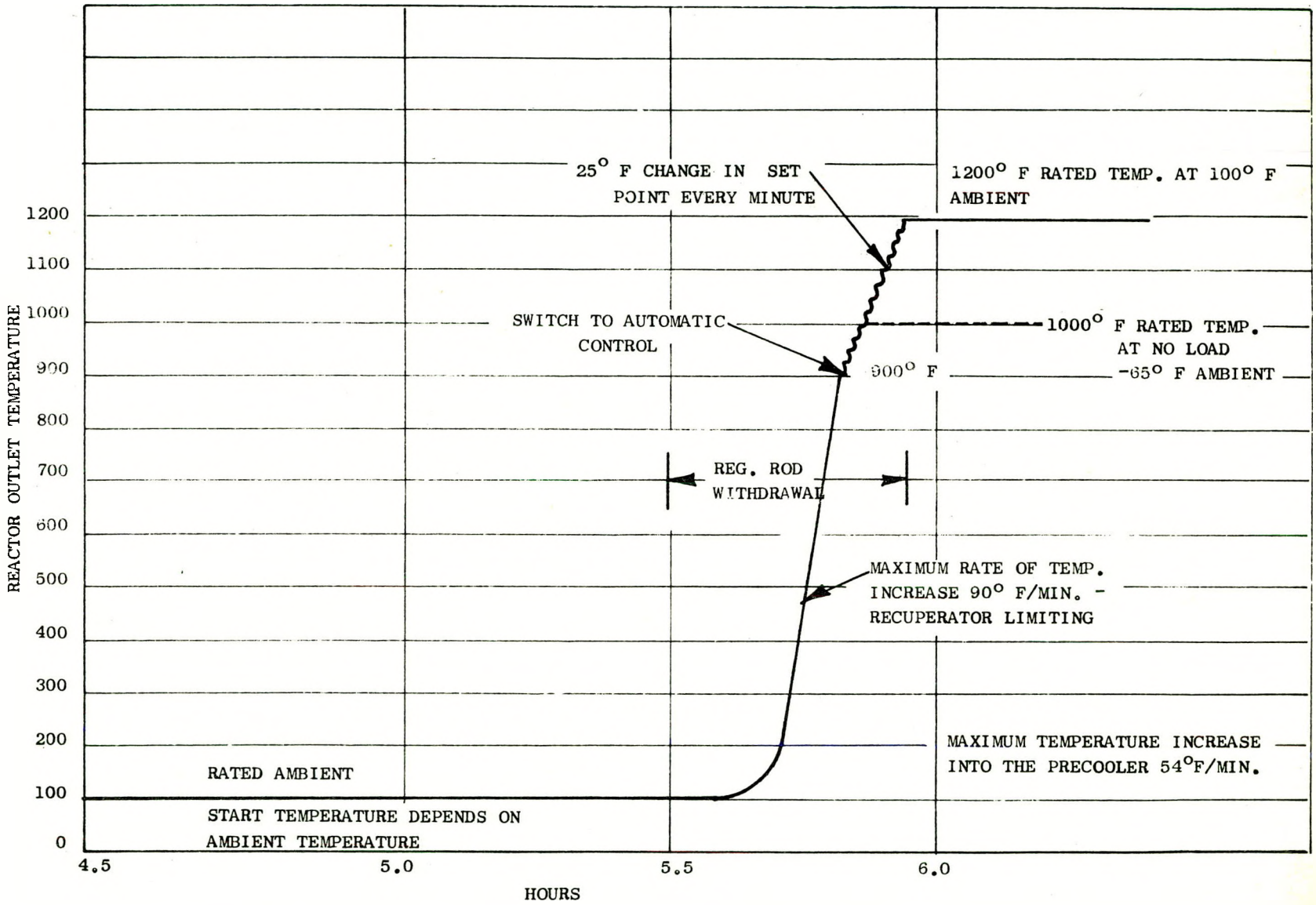


Fig. 8-7 - ML-1 Start-Up Schedule-1 (Reactor Outlet Temperature vs. Time)

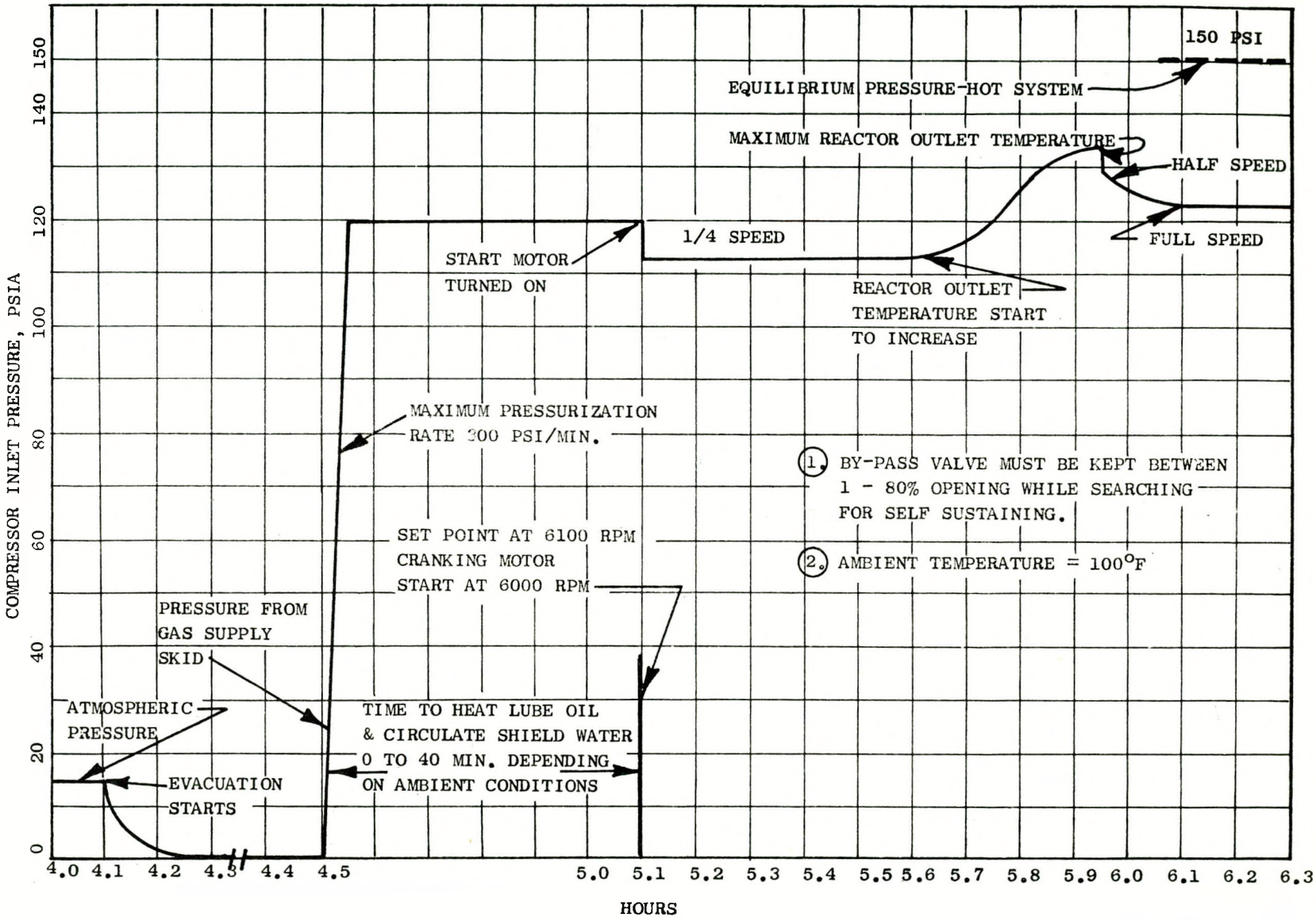


Fig. 8-8 - ML-1 Start-Up Schedule-2 (Compressor Inlet Pressure vs. Time)

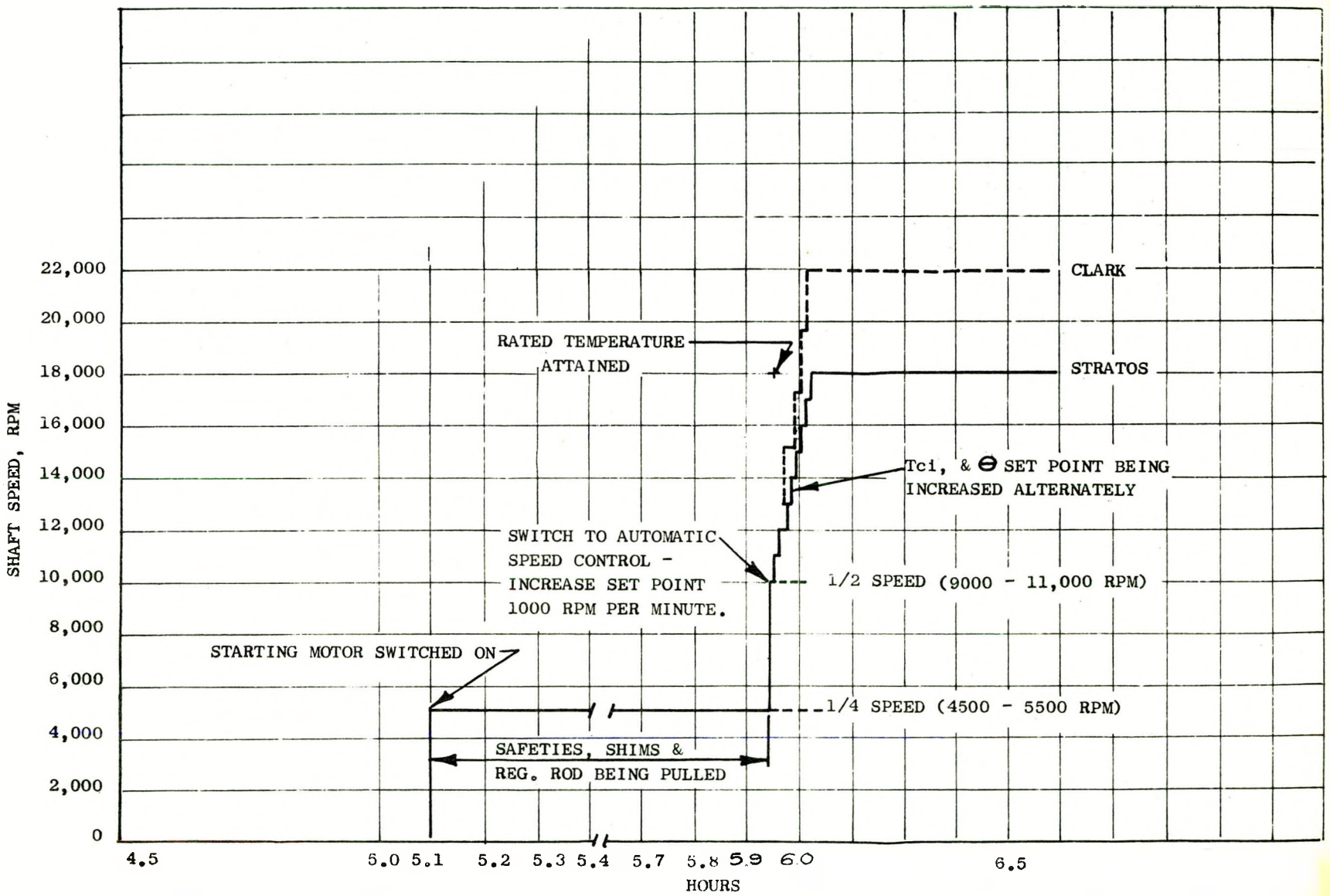


Fig. 8-9 - ML-1 Start-Up Schedule (Speed vs. Time)

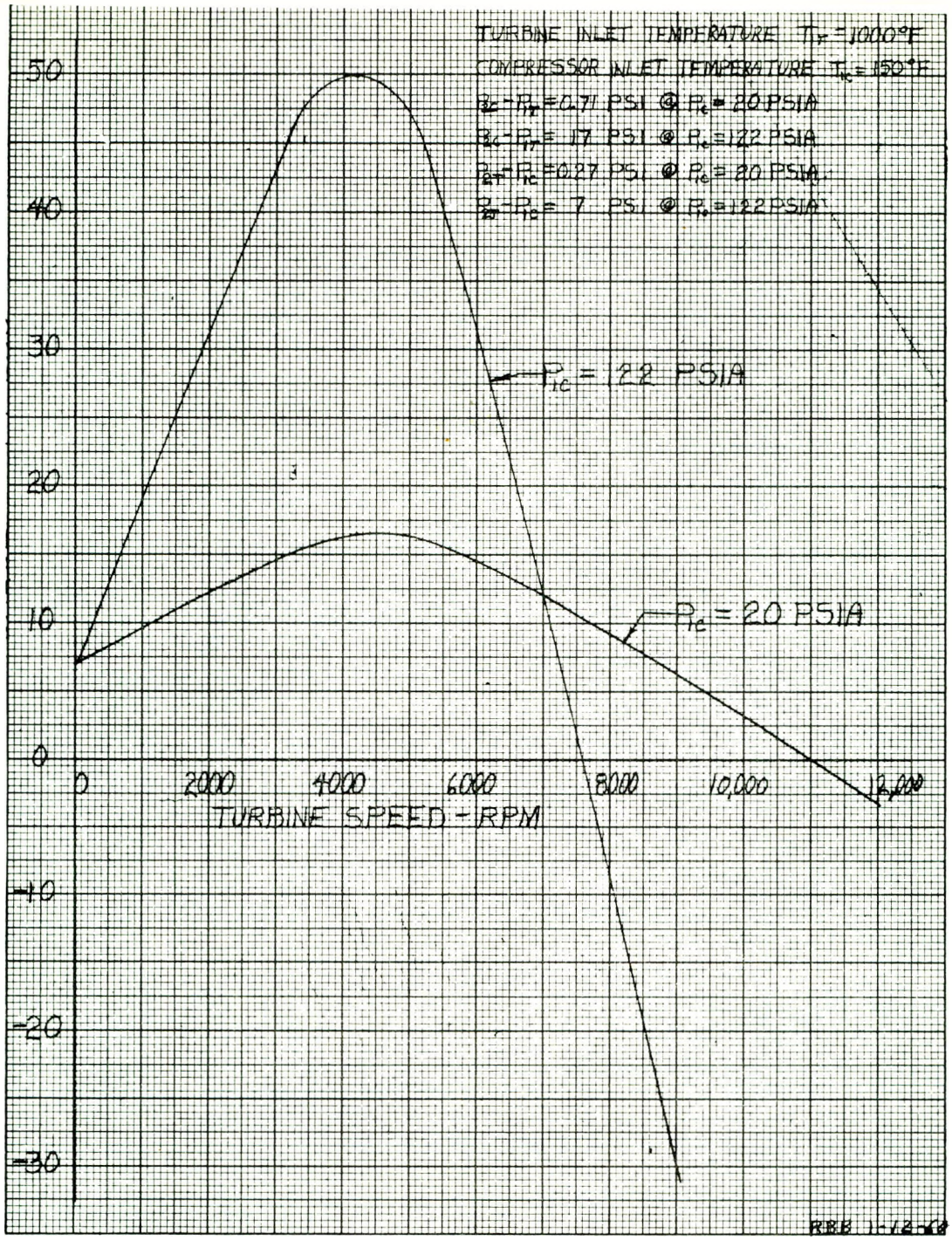


Fig. 8-10 - TCS-670 Turbine-Compressor and Gear Box Starting Torque

Data from Stratos Division of Fairchild
Engine & Airplane Corp., Report SRC-104

The steady state torque characteristics for the Clark TC set are given in Figure 8-11[21] for design compressor inlet temperature and pressure conditions of 150°F and 122 psia respectively. The torque characteristics are also given in non-dimensional form in Fig. 8-12[21] to enable the torque to be calculated for inlet conditions other than design.

Torque figures in excess of those shown in the characteristics will be required to accelerate the turbine compressor set. This is normally accomplished by making a starter motor with a two or three step starting characteristic, but may be accomplished in a variety of ways. Alternate means of starting, such as cartridge starting, compressed air or nitrogen starting, or small gasoline engine may be considered as satisfactory from TC set standpoint. Mass moment of inertia of the TC set rotor is 0.237 lb-ft-sec^2 while mass moment of inertia of the reduction gear is 0.218 lb-ft-sec^2.

Basically, turbine speed control of the ML-1 plant is accomplished through bypassing a portion of the coolant flow from the compressor discharge to the precooler inlet. The turbine speed is sensed by a pickup tachometer that transmits a voltage signal induced when a ferro-magnetic steel gear tooth passes the magnetized tip of the pickup. Speed is controlled by a position-feedback loop, with the voltage arriving at the summing point induced from a potentiometer or from a feedback amplifier. If the voltage from the valve potentiometer is sufficient, no amplifier is used. The power amplifier driving the valve will be a magnetic-type, for reliability and ruggedness.

A safety loop is included to protect the turbine from overspeeding. A shaft breakage causing the electrical load to be lost, or a malfunction in the bypass valve allowing it to stick open, would accelerate the turbine to a dangerous speed within a fraction of a second. The protective device is a second induction-pickup tachometer that operates from the gear box.

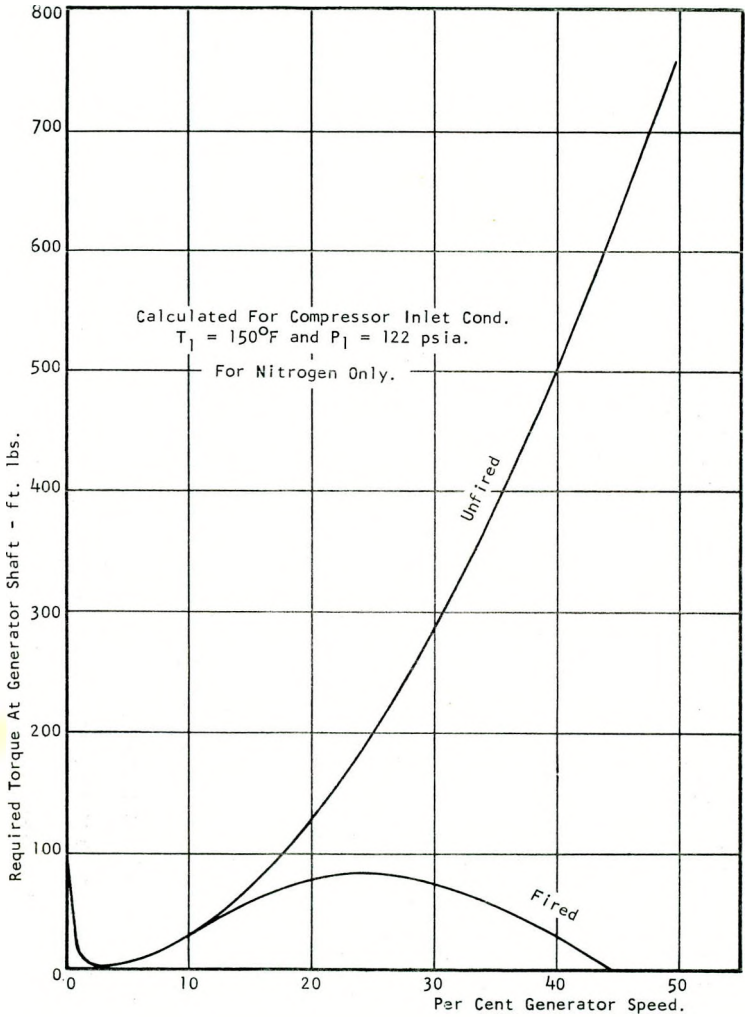


Fig. 8-11 - CSN-1 Speed vs. Torque for Starting

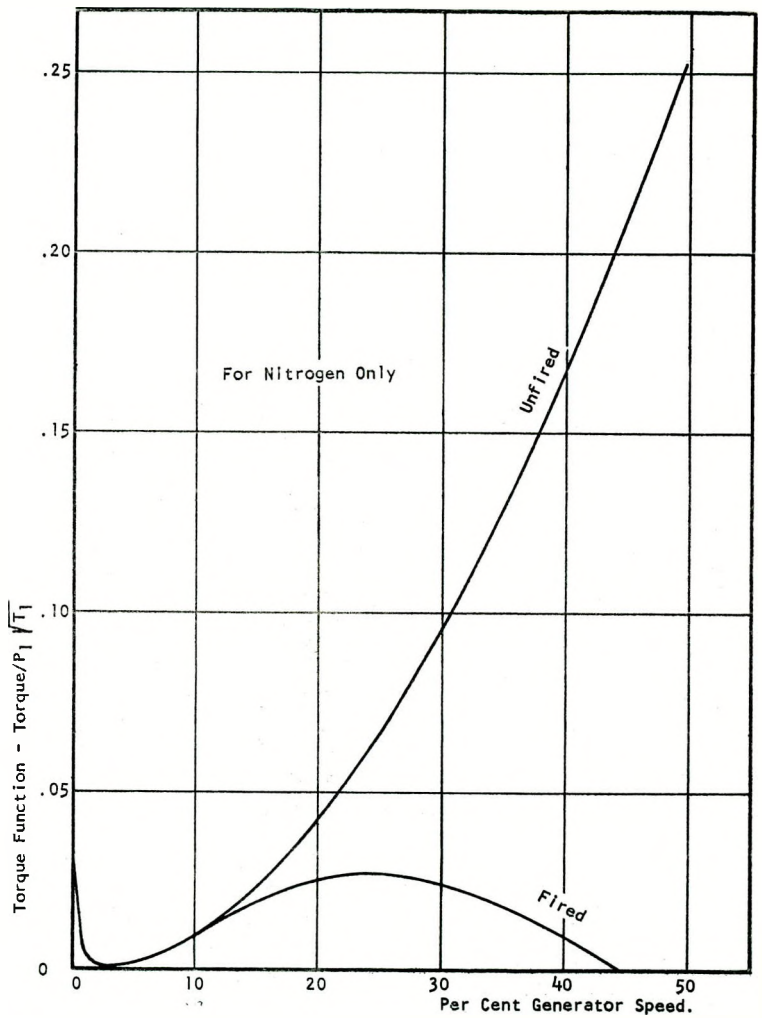


Fig. 8-12 - CSN-1 Nondimensional Starting Characteristics

This tachometer senses overspeeds from 110-125% and trips a relay, which, in turn, opens the overspeed solenoid valve. The turbine attains the 110% or 125% overspeeds in 0.16 and 0.40 second, respectively. Thus, the solenoid valve has a time constant in this range.

The overspeed bypass valve is in parallel with the control bypass valve and, hence, materials requirements and operating conditions are the same. The speed of response demanded of this valve is even shorter. The most critical time when this valve is expected to operate is in the event of a shaft breakage. The turbine-compressor set would speed up and approach critical speed in a short time: 0.16 second to reach 110% speed and 0.40 second to reach 125% speed. The overspeed valve design specifies a 0.1 second opening time. Thus, approximately 0.12 second remains for various delays in the tripping circuits. Because of the lag in reversing the turbine speed by decreasing the system pressures, this valve is tripped open when the speed reaches 110% to prevent the shaft reaching 125% speed. The valve is somewhat larger than the normal bypass control valve. Flow through the valve is 10 lb/sec, with an upstream pressure of 300 psia[62].

8.4 Considerations for Part Load

Some problems in startup and shutdown of a nuclear, gas-turbine power plant are described by Studebaker-Packard for its design of an indirect open cycle plant[58] (see also Section 3.3)

Special equipment and procedures are required to start and stop a nuclear, gas-turbine, power plant. Because the 1000-hp drive motor is not capable of stable operation below one-half speed, it is necessary to provide a smaller motor on the same shaft to drive the fan at lower speeds. Because it is not feasible to operate a complete gas-turbine unit for minor cooling purposes, a separate cooling fan is needed for circulation of air through the intermediate heat exchanger. In addition, a starting motor is needed for each of the three parallel, gas turbine units

THE FRANKLIN INSTITUTE • Laboratories for Research and Development

The starting procedure is probably about as follows. The helium loop is filled with the desired amount of helium and purged of contaminants. With the helium fan turning slowly to circulate a small amount of helium, the reactor is made critical and brought to the approximate operating temperature. During this time, the cooling fan in the air stream is also operated to prevent overheating of the intermediate heat exchanger. Next, the starting motor on one of the gas-turbine units is engaged to bring it up to idle speed, the helium fan being kept under proper operating conditions in the process. From this point, one gas-turbine unit can be brought to operating speed and power or additional units can be started. A control system is needed which will prevent excessive temperatures in the reactor and intermediate heat exchanger, as well as control the speeds of the helium fan and gas-turbine units.

After shutdown of the reactor, a significant amount of power is generated by gamma and beta radiation. After the reactor has been in operation for a year or so at full power, about six percent of full power is generated immediately after shutdown decreasing to about one-half of one percent at the end of a day. This production of power after shutdown requires that the reactor core be provided with cooling to prevent overheating. In the present helium circuit cooling is achieved by running the helium fan and the air cooling fan at low speeds. The rate of cooling is controlled by the amount of helium and air circulated which are functions of helium density and speeds of helium and air fans.

In regard to part load efficiency, a three-unit scheme is adopted for this plant. Because of the three units working in parallel, part load efficiency of the whole plant can be maintained at near optimum values over a wide range of load, regardless of the open cycle.

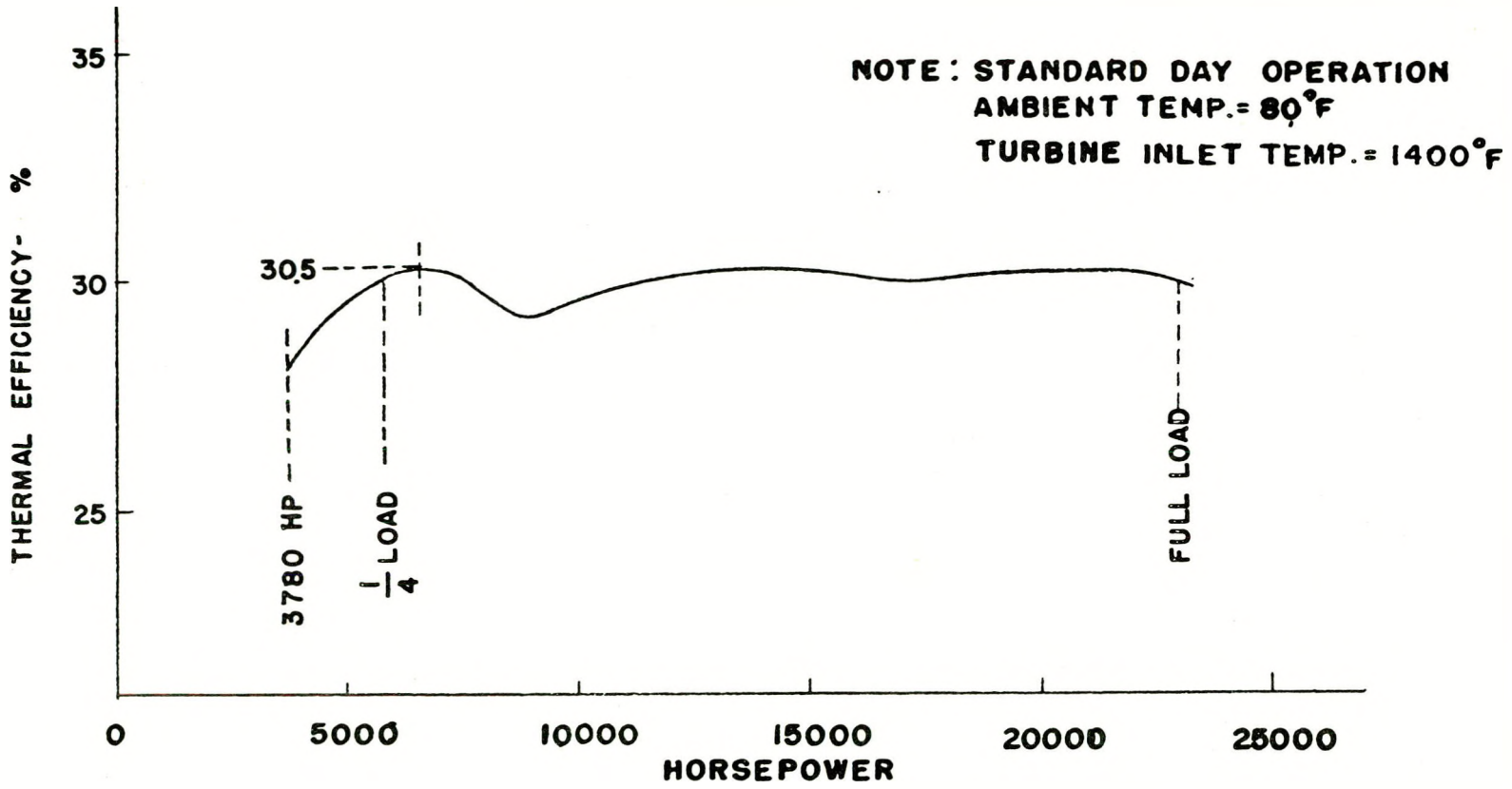


Fig. 8-13 - Part-Load Performance of Nuclear Power Plant (Studebaker-Packard)

THE FRANKLIN INSTITUTE • Laboratories for Research and Development

In the current MGCR project, in its various phases, considerable attention was given to part-load performance characteristics (Maritime Gas Cooled Reactor, see also Section 3). One of the main considerations now is whether to use the low-pressure turbine or the high-pressure turbine as the drive turbine for ship propulsion. Although reports indicate that the high-pressure drive has been given preference, there is no certainty that it will be finally selected.

A digital computer program was used to predict off-design plant performance with two bleed flows, power turbine bypass, and a steam generator (heat dump). The part-load performance characteristics for the plant with the low-pressure turbine drive arrangement were generated using the program. Figure 8-14[49] shows the estimated basic cycle efficiency at part load.

The feasibility was investigated of operating the plant at 1500°F using the part-load program. The following modifications were considered:

(a) Reblading the high-pressure turbine to maintain design speed and present design points on the compressor characteristics,

(b) Reblading the low-pressure turbine to maintain design speed,

(c) Bleeding from the high-pressure compressor discharge to the low-pressure compressor inlet to maintain design speed,

(d) Throttling the low-pressure discharge to maintain design speed, and

(e) Increasing rotational speed.

The operating point for each of these modifications is shown in Figure 8-15[73]. In each case, inventory is adjusted to maintain 22,000 shp. Accordingly, low-pressure turbine speed remains constant.

The IBM 704 code for the analysis of plant transient behavior has been modified later to include reactor thermal equations and neutron kinetic equations.

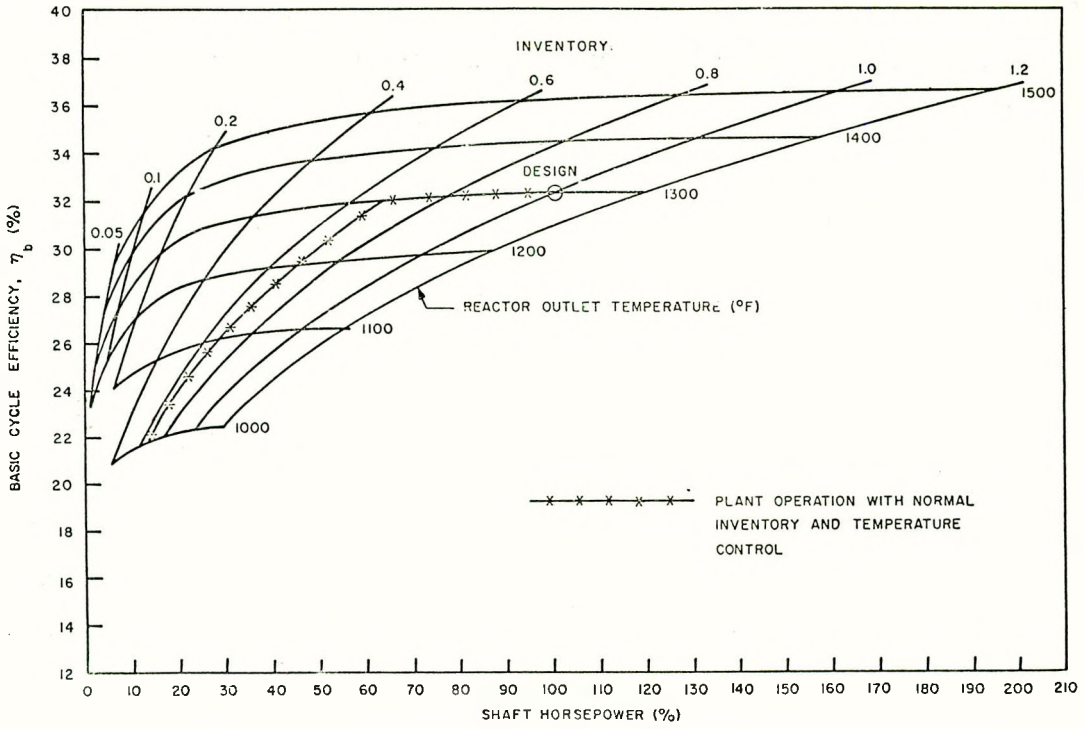


Fig. 8-14 - MGCR Estimated Basic Cycle Efficiency at Part Load

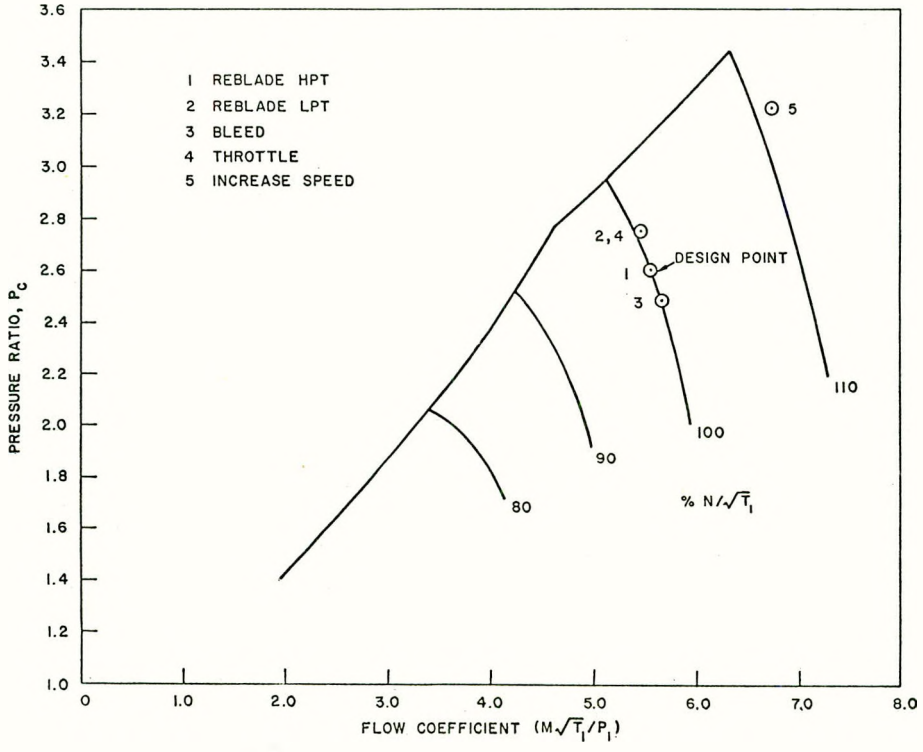


Fig. 8-15 - MGCR Operating Points for Various Plant Modifications to Permit Operation at 1,500°F

THE FRANKLIN INSTITUTE • Laboratories for Research and Development

Functions representing compressor and turbine performance at off-design points have been incorporated into the plant transient computation program of the plant[61].

Considerations for generating electrical power, for the case of electric drives for ship propulsion, have established an allowable speed variation of $\pm$ 5%. Other studies indicated that the system has satisfactory steady-state characteristics over a range of sea-water temperature from 28° to 100°F and at reduced reactor power levels, reduced plant inventories, and reduced reactor outlet temperatures.

Transient analysis established that at full load the turbine throttle valve can be moved from full open to shut in 5 seconds with a tolerable variation in compressor shaft speed. It is anticipated that equally satisfactory performance will result from closing and opening the turbine throttle valve under other load conditions[61].

A computer program designed to study the transient behavior of the high-pressure turbine drive (HPD) has indicated that this plant is controllable if certain refinements are made in the control system. The HPD plant, however, does not seem to have as much inherent stability as the low-pressure drive (LPD) plant.

Basically, there is no difference in the method of controlling the high-pressure drive and the low-pressure drive plants. In each case, four items require control:

(a) power turbine output,
(b) turbo-compressor speed,
(c) reactor outlet temperature, and
(d) reactor power level

The control elements for these items are, respectively:

(a) power turbine throttle valve,
(b) power turbine bypass valve,

(c) reactor control rods, and

(d) accumulator inlet and outlet valves (density change of coolant in system).

The minor refinements required in the control system for the high-pressure drive plant may be traced to the increased sensitivity of this system to bypassing of the power turbine. In the low-pressure drive, bypassing results in a greater pressure ratio for the compressor turbine, thus providing more power. Bypassing in the high-pressure drive provides the compressor turbine with both increased pressure ratio and increased inlet temperature. The inlet temperature changes rapidly as the bypass valve is opened so that its rate of opening must be carefully modulated (by means of proportional control, i.e., rate of valve motion proportional to speed deviation) to maintain turbocompressor speed. For the low-pressure drive, the requirement is less severe and the bypass valve may be actuated by a constant speed motor with on-off control.

The low-pressure turbine in the high-pressure drive plant cannot run for extended periods at the increased inlet temperature which results from bypassing. This imposes the requirement for an interlock which lowers the set point on reactor outlet temperature as the power turbine throttle valve is closed. Such a device would not be required for the low-pressure drive.

When shut, the bypass valve cannot control against increases in turbo-compressor speed. Compressor bypass is required to prevent such overspeed. Originally, in the low pressure-drive, this was envisioned as a safety device (as opposed to a control element) which, when tripped, would result in plant shutdown. The high-pressure drive, however, has shown a greater tendency to overspeed during ordered reactor power reductions when the bypass valve is shut. Under these circumstances, control against overspeed must be provided by means of an additional control valve for compressor bypass. This additional control valve may

possibly be necessary under certain conditions in the low-pressure drive plant. Its use, however, would be less frequent.

Studies on transient conditions showed the controllability of the high-pressure drive plant in cases such as

(a) maneuvering with bypass,

(b) ordered reduction in reactor power level, and

(c) ordered reduction in reactor outlet temperature.

Emergency conditions such as overspeed, loss of cooling water, and reactor scram, should have no more serious consequences in the high-pressure drive plant than in the low-pressure drive plant.

Further transient studies will include modifications accounting for[71]

(a) addition of bleed flows to conform with full-load program,

(b) use of compressible flow relationships for the flow through valves,

(c) addition of bearing friction in equations for shaft acceleration, and

(d) addition of a time delay in the equations describing rod motion as a function of temperature error.

During the second quarter of 1961, the MGCR turbo-machinery design effort was concentrated on modifying the present design to provide for raising operational capability from 1300°F to 1500°F maximum temperature. Other than substituting different materials in the blades and disks, redesigning of the crossover zone is the major requirement for reaching 1500°F operational capability.

In the new design, the bearing housing is supported by four radial struts carried by cantilevered beams attached to the blade ring. The beams provide flexibility for thermal differential expansion in the radial direction. The structure is stiff enough to confine normal rotor vibration to the bearing oil film proper.

Oil and gas lines (for seals) which pass through the radial struts are supported so as to be independently flexible.

Studies have indicated that with 10% of the gas flow bypassing both turbines, compressor bleed temperatures of 1500°F could be reached with the machinery matched for 1300°F operation. To obtain the full potential of 1500°F, operation will require matching the blade path of the machine for this purpose. It has been determined that this is most easily achieved by adjusting the compressor turbine flow characteristics. To convert from 1300°F to 1500°F requires increasing the gas flow capability of the compressor turbine by replacing the stationary vane assemblies. The part-load performance of the plant when matched at 1500°F is shown in Figure 8-16[11]. Machinery characteristics except for level have not changed significantly.

Consideration was given to suitable reversing gears for the MGCR. The various reversing schemes that were investigated included clutched reversing gears, reversing turbines, a radial inflow turbine with movable nozzles, controllable-pitch propellers, and turboelectric drives. Of these, turboelectric drive and controllable-pitch propeller are being considered for the MGCR. An electric drive offers following advantages:

(a) The generator can be used as a power source for cargo pumping (tanker).

(b) The arrangement of the unit is flexible, because the turbo-generator location is independent of the propelling-motor location.

(c) Propeller reversal is accomplished quickly and easily without changing the direction of turbine rotation.

(d) Maximum power is available for system operation.

(e) Propeller vibrations are not transmitted to the turbine.

(f) There are no design limitations on the amount of power transmitted.

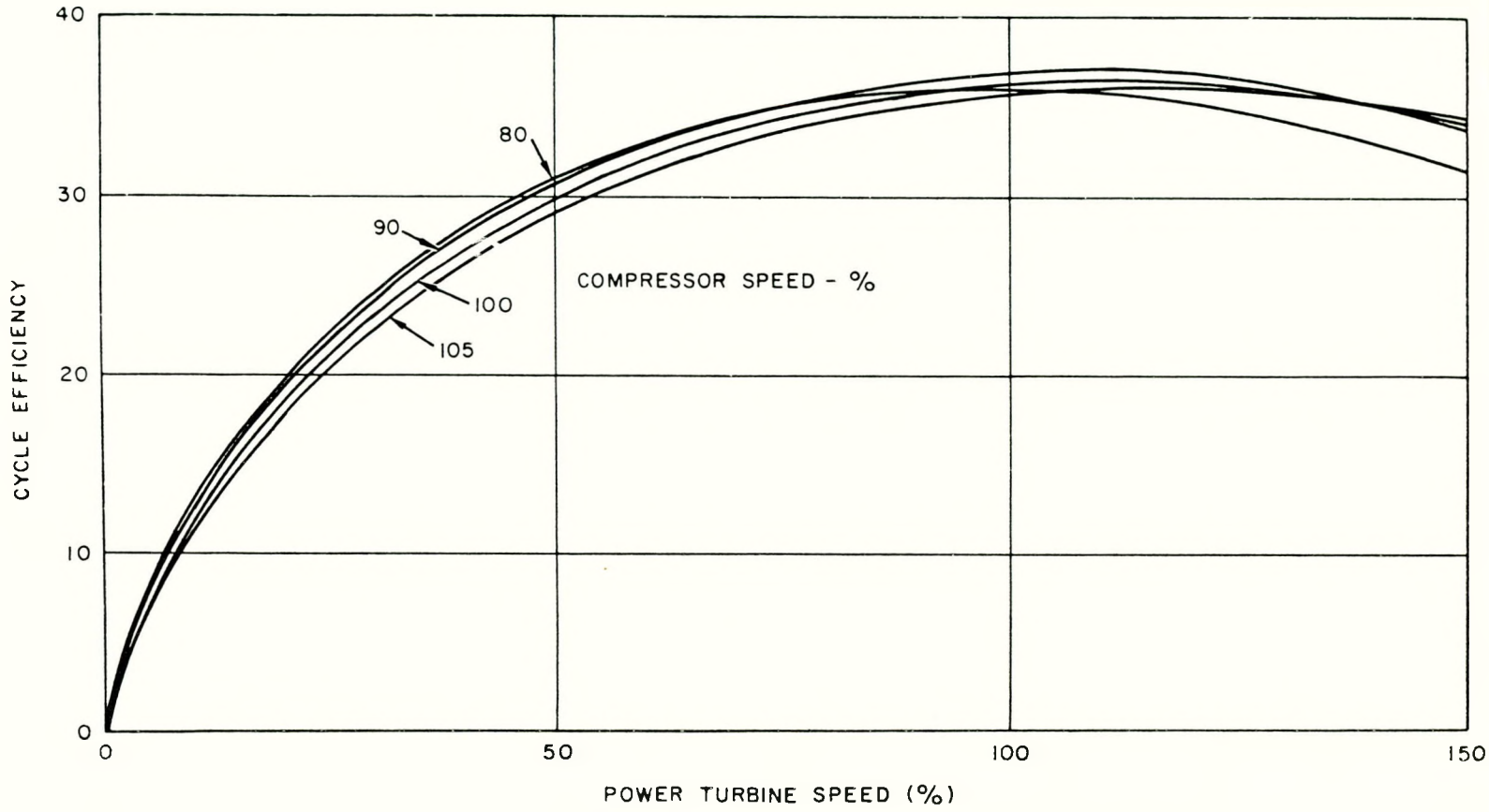


Fig. 8-16 - MGCR Program - High Pressure Drive Design, Part Load Performance

Motors may be used in tandem or parallel in order to reach any power level desired. One turbogenerator can supply power to several motors.

(g) The turboelectric system is known to be highly reliable and to require little maintenance. All maintenance can be accomplished without dry docking.

The initial cost of the controllable-pitch propeller is somewhat lower than that of the turboelectric drive, but this device has not yet been developed in the required size. The reversing turbine concept is considered impractical because the idle turbine would have to operate in a low-pressure space to avoid high parasitic losses. The design of such a space would pose difficult and expensive valving, sealing, and evacuation problems.[61]

8.5 Regulation of Closed Cycle Turbine

Fluctuations in the developed output of closed cycle gas-turbine power plants can be regulated by simply changing the quantity of gas in circulation within the system. Hence, the cycle efficiency of a constant-speed machine does not change with changes in load because the pressures at every point in the cycle vary in the same ratio, while gas temperatures and flow velocities remain unaltered. It is only the density of the coolant gas that is varied to effect a change in power.

This inherent characteristic yields a fundamentally simple power plant control system. When plant load drops, gas is withdrawn from the cycle to maintain, for example, a constant speed. Conversely, for an increase in load, gas is added to the cycle in response to the same signal. When a gas other than air is employed as the working medium, it is necessary to avoid blowoff by use of a storage tank or tanks for the accumulation of working fluid not in circulation in the power plant system.

The fundamentals of this control system can be depicted schematically as the pressure and temperature quadrants shown in Fig. 8-17[109].

THE FRANKLIN INSTITUTE - Laboratories for Research and Development
1-A2392-5

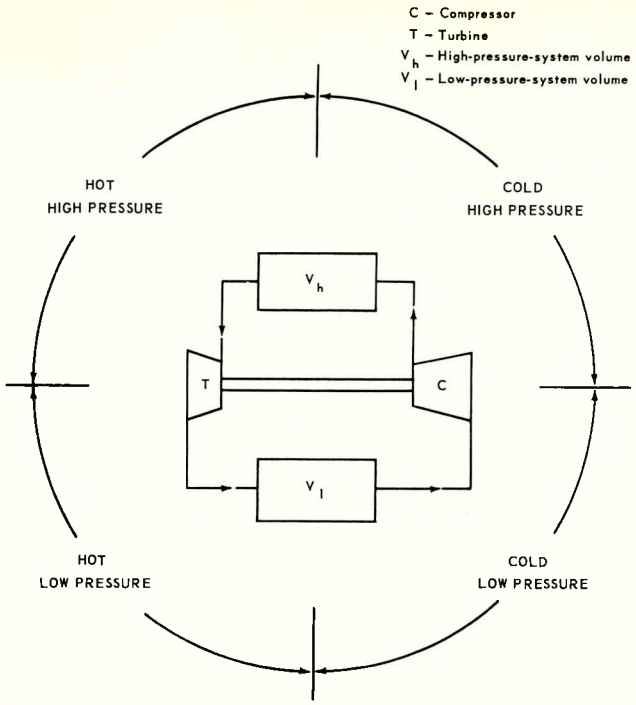


Fig. 8-17 - Closed-Gas-Cycle Temperature - Pressure Quadrants

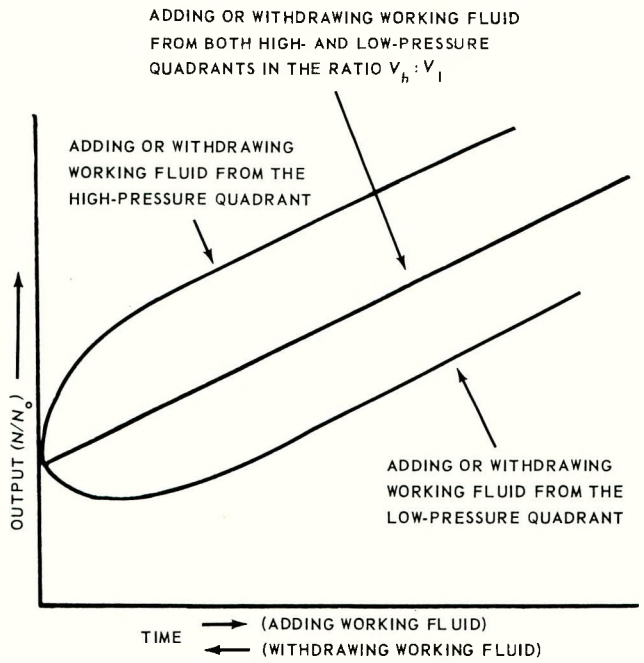


Fig. 8-18 - Time Rate of Change in Output as a Function of the System Quadrant in Which Fluid is Introduced or Withdrawn

It is advantageous from both practical and system-response considerations to effect withdrawal and addition of working fluid from the cold, high-pressure quadrant. It is also advantageous to bypass the turbine system if an almost instantaneous reduction in power is desired. This system response rate becomes primarily associated with sensing and valve-operation time constants and with the flow rates at which fluid can be added or subtracted from the system.

During the initial operating condition and the operating condition after a change in output has occurred, all pressures in the cycle are in the same ratio to one another. However, during the period of transition, pressure ratios are not the same. The pressures do not change with equal rapidity in all parts of the cycle because the pressure in that part of the cycle in which working fluid is withdrawn or admitted will approach the new conditions more rapidly than pressures at other points. Thus, if working fluid is introduced between the compressor discharge and turbine inlet, the turbine-compressor flow ratio and the expansion ratio across the turbine will be temporarily increased. The result is a momentary increase in output before system pressures are equalized and the compressor-turbine system is again in balance. Conversely, if working fluid is introduced between the turbine discharge and compressor inlet, the pressure ratio across the turbine and turbine-compressor flow ratio would be decreased and there would be a temporary decrease in output until the system conditions stabilized. Figure 8-18[109] illustrates these phenomena. This characteristic of the plant is important for the practical execution of load changes; for, by adding and withdrawing working fluid from the high-pressure side of the system, a "momentary effect" is achieved and faster regulation can be brought about. Also, adding or withdrawing gas on the cold, high-pressure side of the system simplifies valve consideration, although greater pressures are required for the addition of gas.

The effect of changes in system weight flow on net power output is shown in Figure 8-19[109]. (Special nomenclature here is N = power and g = weight flow. For other symbols, see Figure 8-20).

The power output of the turbine, N_T, and power required for the compressor, N_c, are plotted in relation to the weight of working gas flowing through these units, g_T for the turbine and g_c for the compressor. The normal point, N, corresponds to a turbine output $\overline{NQ}$, and compressor input $\overline{PQ}$. The differnece, $\overline{NP}$, represents the normal useful output. If the weight of the working medium flowing through the turbine were reduced by opening a bypass line around the turbine, thereby reducing the high pressure level and the compressor pressure ratio, the turbine output would be reduced to a value corresponding to the distance $\overline{RT}$ while the compressor power would change to $\overline{SU}$. Thus, because of the different slopes of these lines, it is possible to reduce the effective output to zero by a slight reduction in weight flow through the turbine. The practical significance of this characteristic is realized in the use of a system bypass to reduce the output instantaneously in the event of a load dump. It makes no difference in execution whether the bypass is around the turbine or the compressor. The latter is preferred from the valving standpoint because it is in the cold part of the system, but interrupting the flow through the reactor quickly may not be a tolerable situation.

In power plants using a gas other than air as the working fluid, it is necessary to use both a receiver and an accumulator for handling the working gas, as shown in Figure 8-20[109]. In this design, the pressure in the receiver is maintained at a level less than that in the high-pressure system so that a reduction in power is effected immediately upon opening of the exhaust valve, E. Conversely, the pressure in the accumulator is maintained at a level higher than the then-existing pressure in the high-pressure system so that an increase in power is effected immediately upon opening of the admission valve, A. Required pressures in the receiver and accumulator are maintained by a transfer compressor, C_t. The course of pressures in high-pressure system, low-pressure system, receiver, and accumulator are shown in Figure 8-21[109].

Although the foregoing method of regulating closed-cycle

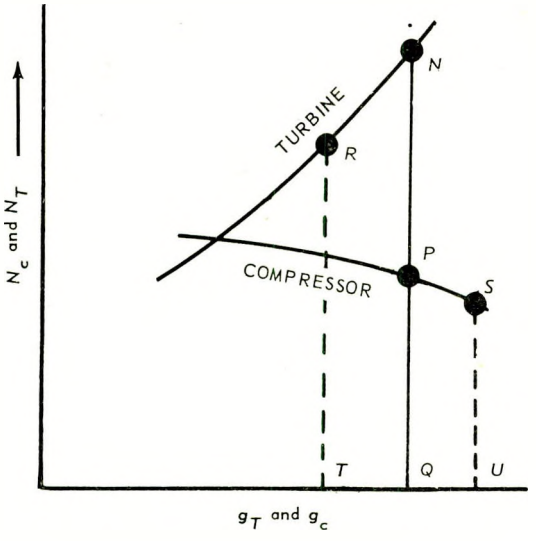


Fig. 8-19 - Effect of Changes in System Weight Flow on Net Power Output

C – Compressor
T – Turbine
V_h – High pressure system volume
V_l – Low pressure system volume
E – Exhaust valve
A – Admission valve
P – Compressor bypass valve
V_r – Receiver
V_a – Accumulator
C_t – Transfer compressor

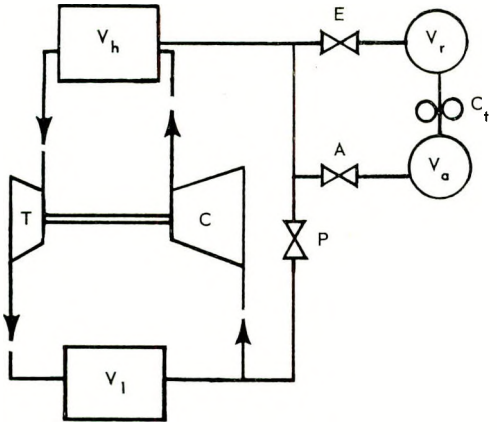


Fig. 8-20 - Closed-Cycle Gas-Turbine Nuclear Power Plant with Receiver and Accumulator

P_a = Accumulator pressure
P_h = High-pressure-system pressure
P_l = Low-pressure-system pressure
P_r = Receiver pressure

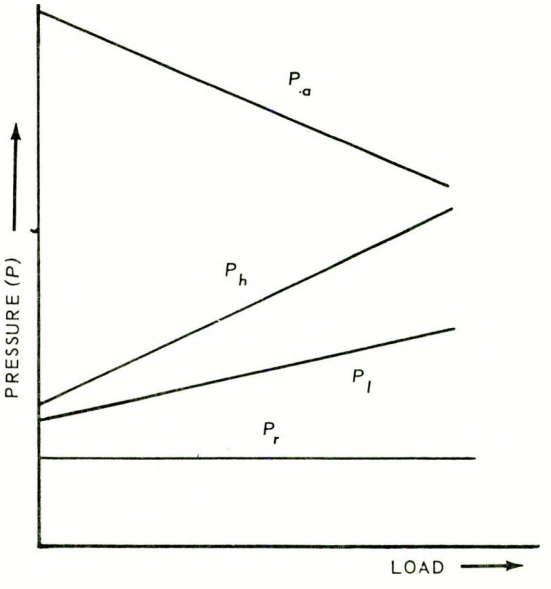


Fig. 8-21 - System Pressure Variations With Load

THE FRANKLIN INSTITUTE • Laboratories for Research and Development
F-A2392-6

gas-turbine power plants by variable pressure (i.e., variable flow) allows the reactor control to be slower acting than the over-all system response rate, regulation in response to load variations may still impose reactor control design difficulties. To avoid reactor fuel-element temperature surges, and especially an overtemperature condition, a rapid response of the reactor controls would be required unless the heat capacity of the reactor heat-generating materials is large.

An alternative method of power plant control that is better from the reactor point of view involves use of electrical control and constant-pressure operation. Variations in demand load are sensed, and compensation is made by wasting electrical energy in a dump system consisting of a set of resistors. Thus, automatic accommodations are made for instantaneous increases in demand load. The reactor fuel element temperatures remain constant with load variation, and no demand is placed on the reactor control system other than adjustment to overcome burnup. Although this method of control results in reduced over-all power plant efficiency and more costly electrical equipment, the plant is made completely automatic, fast-acting, simple, and highly reliable. Only rugged electrical equipment is affected by changes in external load.

If variable pressure regulation is used,high over-all plant efficiency can be maintained because the reactor input can be reduced at part-load conditions. A combination of both methods of control satisfies all requirements; i.e., instantaneous load variations would be controlled by the electrical dump system, and gross longer-term changes would be controlled by the accumulator-receiver components that vary the system pressure level.

THE FRANKLIN INSTITUTE • Laboratories for Research and Development

9. OPERATIONAL STABILITY

Some indications about operational stability of a compressor working in conjunction with a turbine are given in Section 7, where stability means matching of both machines on the surge-free side of the compressor characteristic. Similarly, in Section 8.1, qualitative statements are made about the influence of the cycle arrangement in compound systems on the matched regions of compressors and turbines in part-load operation, and here again stability means operation of compressors to the right side of the surge line in the compressor characteristic.

Such static consideration of stability is insufficient for complete system analysis. As is well known, self-excited oscillations in air flow, called surging, can occur in systems incorporating compressors. During these vibrations, air flow pulsates and power fluctuates, and surging can lead to the destruction of the compressor. Approximate stability conditions and some graphical and analytical methods of calculation were established sometime ago for systems incorporating a compressor. However, the effects of concentrated and distributed resistances in the system external to the compressor on stability and self-excited oscillations were not considered. In the following, Bodner and Kazakevitch[119] established the conditions for stability and self-excitation in distributed systems including a compressor as a non-linear element. The conditions for excitation of the basic frequency or its harmonics were also determined. The expressions derived indicate how to increase the surge margin of a system.

The basic one-dimensional equations of motion and the boundary conditions for flow in a parallel duct, incorporating wall frictional losses and internal viscous friction, are the hydrodynamic equations and the equation of state. Boundary conditions were expressed assuming the open ends of the duct to be loaded by acoustic impedances as factors to

perturbations in the volumetric flow. For investigation of small oscillations, the basic non-linear equations were linearized. The variation of the derivative of the pressure ratio with respect to discharge volumetric flow served as a basis for investigating self-excited oscillations of the system. The natural frequencies and the decrement of the system are determined by the parameters of the external system and by the compressor characteristics. The stability of the system can be established by the sign of the decrement δ. Also self-excitation occurs at the basic natural frequency and its harmonics. The frequency for which $\delta = 0$ will also be excited. The margin of stability can be increased by lengthening the inlet duct, reducing the cross-section of ducts, and by loading the open ends of the ducts by impedances matched to those of the ducts[119]

The next step would be to make a similar investigation for a turbine in a duct system and then to match both systems together. So far nothing is known about the existance of a stability analysis of this kind for a complete turbo-compressor set in a cycle.

Coming back to the surge phenomenon of a separate compressor, this information is covered in special literature (see also Report NY-9790 on Circulators).[37] Because of interstage-matching imperfections, multi-stage, axial-flow compressors have a less wide region of stable operation than single-stage machines; again, single-stage axials have a lesser stable range than single-stage radial compressors. In practical turbine design, it is expected that compressor pressure ratios over 5 could lead to troubles because of stalling during starting.[120]

Such troubles, for example, occurred on GE 8500-hp gas turbine for locomotives, which have a compression ratio of about 6. However, compressor pulsations could be eliminated by increasing the size of the first-stage nozzle opening and by modifying the combustion chamber line (see Section 2.3.4). In cases where high compression ratios must be applied, regulating stator blades are provided in some of the first

stages of the compressor to get stable operation in the low-mass-flow regions. Also interstage air bleed is used to increase the mass-flow of the compressor. If required, the energy of the bleed air can be partly regained in recuperation turbines (expanders).[42] An experimental study made on the influence of tip clearance on stall of compressor blades showed that the blade loading was maximum at a distance from the tip clearance but the clearance was found to relieve the pressure gradient in general and to retard stalling.[121]

In a study on wide-range axial compressors, an illustrative example is given concerning which stages stall when.[92] A compressor was selected for consideration which had an excellent peak efficiency (92 per cent polytropic) in a test when mounted on a single shaft with a turbine. The efficiency plateau of the compressor was far away from the design point and little attempt was made to match the turbine to enable the compressor to run at high efficiency because the running line was already close to the surge line at low to medium speeds. Blow-off valves were used for safety during starting. It could be seen from the test that the last stage never operated at an incidence higher than the design value, while the first stage was mostly at a positive stalling incidence. Some details of the test follow.

A single-shaft gas turbine at full speed changes through a certain range of pressure ratio (or temperature ratio) between no load and full load, and in this range the last stage changes from near choking conditions, to design-point conditions while the incidence on the first stage changes only slightly.

For simultaneous changes of pressure ratio and speed as would occur with a compressor pumping against a constant resistance, or with a change of machine load for a two-shaft gas turbine, the incidence on the last stage changes less rapidly, but in the chart, Fig. 9-1, appears to reach negative stall before the first stage has run into positive stall.

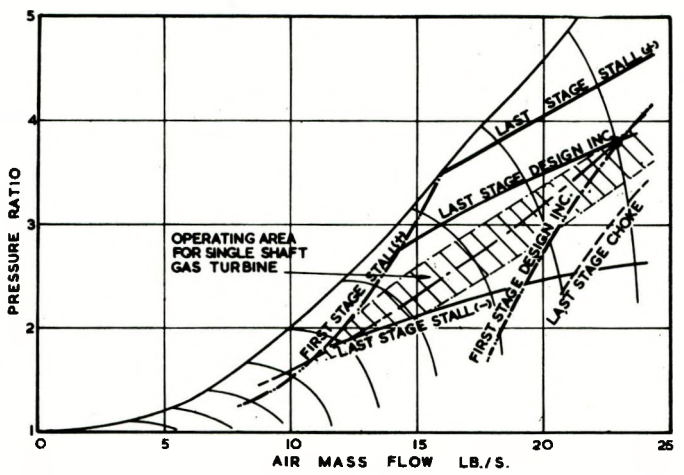


Fig. 9-1 - Blade Incidences for a Small Axial Compressor

a special type of surge. The analysis showed that the pressure rise of the unstalled part of the blade row during stall propagation will be nearly the maximum obtainable pressure rise of the blade row, but the flow velocity inside the stall cell will be extremely small. It was found that under certain conditions, two stable flow regions are possible, one axisymmetric and one much stronger stable region with rotating stall cells. This explains the hysteresis found between axisymmetric and stall-cell flows. Results of analysis are generally confirmed by observations. A somewhat unexpected result of the analysis is that instability can occur in turbine cascades. The propagation velocity of stall cells was also determined by analysis.[122]

A survey of experimental and theoretical work done on stall propagation was made by Emmons, Kronauer, and Rockett, covering a period of 8 years, starting with the discovery of this type of surge during the winter 1949-1950.[123] A rotating-stall survey in connection with blade-vibration investigation was conducted at the Lewis Flight Propulsion Laboratory on a modified production turbojet engine incorporating a 13-stage axial-flow compressor with a design pressure ratio of approximately 7 at a sealevel airflow of 120 lb/sec. Interstage bleed systems were installed over the fifth and tenth rotor stages. The maximum vibratory stresses without bleed occurred at 60 and 68 per cent of rated speed in the first and second stages, respectively. Bleeding eliminated resonance of blades. The fifth-stage bleed required a lower flow rate to eliminate vibrations in the rotating-stall-excited rotor-blade than the tenth stage.[124]

10. STRUCTURAL INTEGRITY

10.1 Materials

The complexity of factors which determine the structural integrity of a part for a required life is considerable. Material, part shape, type of loading cycle, temperature and temperature distribution, compatibility of the material with ambient conditions, among other factors, influence the structural integrity. The designer has to find a compromise to meet the requirements. He has to apply recognized methods of analysis and has to adapt available test results to conditions of his design. Where applicable test information is not sufficiently available, the designer uses "good engineering judgement," simplifies problems, extrapolates, or makes experiments if he is allowed to. After all, only operational experience enables one to make a final judgement on a design.

Let us discuss a few of the factors which determine the structural integrity of some essential parts of gas turbomachinery. (See also Report NYO 9793 on Structural Materials[6]).

Gas-turbine blades and wheels require good resistance to creep for long periods at high stresses, operating in extreme cases at 1800°F. In the temperature range of 1500°F to about 2000°F, superalloys have been widely adopted because they are able to withstand high stresses for long periods of time at these temperatures and because they have become available in a wide variety of the required forms. Refractory metals, on the other hand, are still not in the production stage and will not enjoy wide usage until their technology is mastered.

A significant expansion of the operating limits of superalloys has been brought about in the past few years with the development of over a dozen new nickel-base and cobalt-base materials. Some of these alloys are fabricable into sheets, while others are suitable only for precision casting.[125]

THE FRANKLIN INSTITUTE • Laboratories for Research and Development

In Britain, the Nimonic series of high-temperature alloys has been produced by air-melting techniques in the past. It is, however, generally accepted that melting in vacuum results in the development of even better high-temperature properties, especially if the composition of the alloys is adjusted to take advantage of the higher purity that can be maintained by this technique. Henry Wiggin & Co. Ltd. have reported that their development of alloys shows sufficient promise to initiate work on quantity production. A considerable amount of investigation has been carried out in the Research Laboratories of The Mond Nickel Co. Ltd., and, as a result, five alloys have so far been found to be worthy of further development. The experimental wrought alloys are M14V, M15V and M16V, and the experimental casting alloys, M4VC and M6VC. A special feature of M4VC alloy, produced by vacuum-melting techniques, is the high degree of reproducibility of its stress vs. rupture properties. For example, the standard deviations are less than half those of Nimocast 258 high-temperature casting alloy which is produced by normal air melting. If successful, the wrought alloys will probably be added to the Nimonic series of high-temperature alloys, while the casting materials would be marked as Nimocast high-temperature casting alloys.

Materials used in the high-temperature regions of the gas turbine represent the limiting factors in gas-turbine development. A given turbine may operate successfully with little field maintenance of hot sections parts; however, an increase of inlet temperature of 50°F can increase the deterioration of hot parts to an impractical level[126].

The selection of materials depends on the particular application of the gas-turbine because of differences in life requirements in different applications. A key consideration affecting design is the temperature of the turbine-inlet gas on which the efficiency of a given installation depends. Industrial turbines, and gas-turbines for most intended nuclear power plants, must be capable of operating

continuously for periods as long as several years without overhaul on inspection; 100,000 hours has been mentioned as a required life of such turbines.

Blade and disk alloys used in industrial turbines were originally selected on the basis of test data and experience gained in other high-temperature service. As test information and field experience is accumulating for operating turbine sets, laboratory evaluation of stronger series of alloys is under way which permits the design of new higher performance gas turbines.[126] W545 disks and Inco 713-C blades are currently available. Coupled with cooling they provide possibilities for further growth of industrial gas-turbine potential.

The first-stage rotating blades in service currently experience gas temperatures near 1300°F and newer units near 1400°F with slightly lower metal temperatures because of cooling effects. The parts must have sufficient creep strength to resist the temperatures at design stresses for many years. For a given stress, operating temperatures may be increased if the required service time can be reduced. This is shown by creep-rupture curves.

It has been the design philosophy to build a reaction type of gas turbine with relatively smaller disks, thus favoring the disk stresses. High strength-high temperature alloys are used in the disks to withstand gas-stress temperatures with the effects of turbine cooling further enhancing disk life.

The integrity of disks from the standpoint of internal soundness is of great importance. The soundness of a finished disk is quite dependent on the quality of the ingots from which the billets and final forgings are produced. The requirements of relatively small disks results in less tendency toward chemical segregation and metal separations in the starting ingots as smaller ingots may be used as raw material.

The disk material used initially in the first stages of the turbine was 19-9DL alloy. This material is strengthened by warm working; hence, large disks cannot be strengthened adequately for high-stress applications. Discaloy alloy is a stronger material which is strengthened by heat-treatment and hence has replaced the 19-9DL material.[126]

Westinghouse Electric Co. has performed tests on the effect of environment on the creep-rupture properties of metals to meet the specific requirements of the closed-cycle turbomachinery of the Maritime Gas Cooled Reactor, with helium as coolant. The military lightweight gas-cooled reactor ML-1 will use nitrogen as coolant with an addition of 0.5 % by volume of oxygen because it was found experimentally that by this addition nitriding of type 318 stainless steel, used for the cladding of fuel elements in this reactor, could be prevented.[127]

Ceramics have not yet come into practical use as structural materials for turbomachinery, except for coating of blades in some instances. Ceramics are characterized by inherent brittleness and high sensitivity to mechanical shock and often to thermal shock but are highly resistant to erosion and generally to oxidation. Metals and alloys usually possess adequate ductility and mechanical shock resistance but lose their strength at lower temperatures than do ceramics. Considerable effort has been devoted, particularly in the United States, to developing ceramics and mixtures of ceramics and metals, cermets, in the hope that the latter may combine the high temperature strength of ceramics with the ductility of metals. The development of ceramics and cermets is in no way ended and, with better understanding of the atomic structure and of the bonding which exists between particles, it seems probable that high-strength materials, resistant to mechanical and thermal shock will eventually emerge.

Meanwhile, prospects of utilizing ceramics and cermets in such applications as gas turbines would be enhanced if design engineers were to find it possible to adapt their design to accommodate the stronger but more brittle materials that are being produced.

Tests have been made at the Lewis Research Center of NASA with cermet turbine stator blades. After 52 hours at an average of turbine-inlet-gas temperature of 2000°F, one of the group of four cermet blades fractured probably because of end loads resulting from thermal distortion of the spacer band of the nozzle diaphragm. Improved design would preclude this cause of failure. Figure 10-1[128] shows such a fractured blade, illustrating also its shape and cross-section. Figure 10-2[128] shows cermet-blade assembly after 52 hours and 15 minutes operation at an average gas temperature of 2000°F.

Use of inert working media, such as helium or neon, may permit the development of a graphite turbine or perhaps a molybdenum alloy taking advantage of the strengthening due to insoluble hard particles, such as aluminum-oxide.[63]

10.2 Life, Temperature, and Load

At the high temperatures, to which vital parts of gas-turbines are exposed, relatively small changes in temperature cause considerable changes in the creep-rupture time of the employed materials. When the same materials are used, a turbine design based on higher temperature may lead to better efficiency, smaller dimensions, and lower capital investment costs. On the other hand, with a lower selected operation temperature, operational costs will decrease, because blade or disk replacements will be needed less frequently, and availability factor of the installation will increase. Generally, when information is supplied about operating temperatures of turbines, at least blade design life should be indicated also.

Figure 10-3[129] shows a plot of temperature vs. creep-life for Nimonic 80A for a stress of 20 kg/mm^2 and a limiting strain of 0.2 per cent. The curve shows that if turbine blading would be designed for 700°C inlet temperature at a stress of 20 kg/mm^2 with a limiting creep-strain of 0.2 per cent, a reduction of the inlet temperature to 660°C

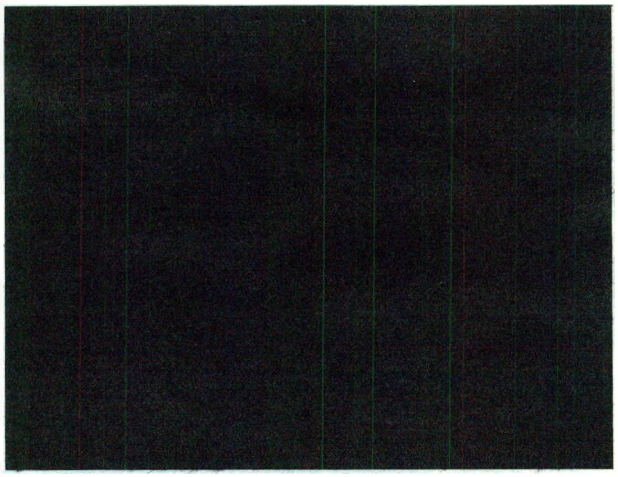


Fig. 10-1 - Oxidation of Surfaces of a Fractured Cermet Blade

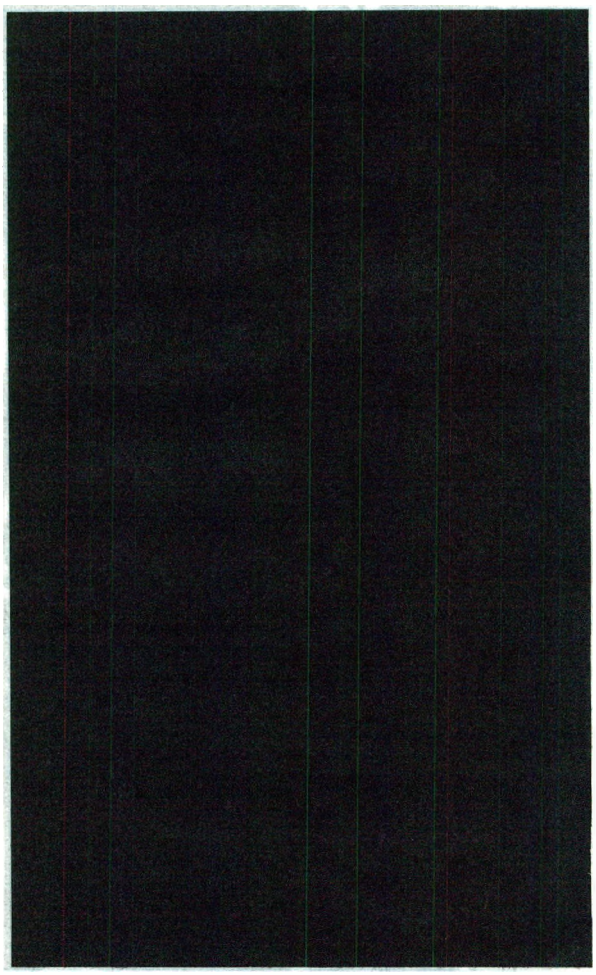


Fig 10-2 - Cermet Blades After 52 Hours and 15 Minutes at an Average Gas Temperature of 2000°F

THE FRANKLIN INSTITUTE • Laboratories for Research and Development

would increase the life from 2500 to 8000 hours. Depending on cycle conditions, turbine inlet temperature can be related to load. However, an analytical determination of such a relation would hardly be reliable. Figure 10-4[129] gives such a relation between turbine first-stage blading life and related load, obtained from measurements on an English Electric EM27P gas turbine. The turbine blading of this unit was designed for 40,000 hours life at full load.[129] The time between overhauls is specified at 10,000 hours.[18] Turbine inlet temperature at full load is 1430°F.[39]

A well-known feature of simple-cycle gas turbines is that turbine temperature falls when load is reduced. By reducing the "full-load" output to approximately 90 per cent of its original value, the creep life of the turbine blading can frequently be extended three or four fold in such installations.[16]

An important factor in assessing blading life is the possibility of peak temperatures occurring at certain points in the turbine annulus, giving rise to local hot spots in the fixed blading.[16] For gas turbines with maximum and cruise-ratings, as in maritime operation, the overhaul life of the engine will depend upon the length of the time it is operated at powers above the cruise rating, and additionally on the number of starts for short-time operated units.

10.3 Mechanical Stress

10.3.1 General

Stresses may be determined analytically or experimentally, and failure criteria must be established to judge the safety or life of a design. However, we cannot elaborate on these problems here. Our main intent is to furnish some data on stresses used in designs together with some pertinent information.

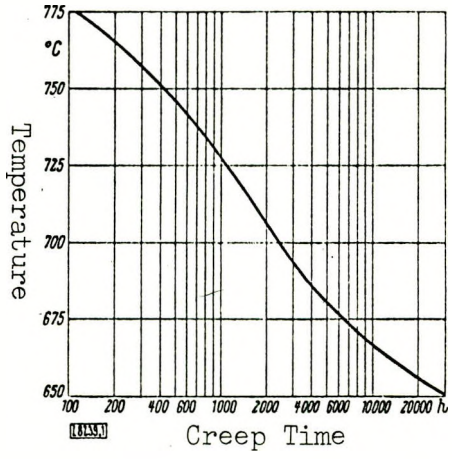


Fig. 10-3 - Temperature vs. Creep-Time From Nimonic 80A at 20 kg/mm^2 Stress and 0.2% Creep

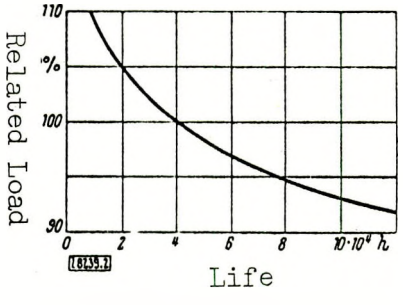


Fig. 10-4 - Relation Between Life of Gas-Turbine EM27P Blading and Related Load

THE FRANKLIN INSTITUTE • Laboratories for Research and Development

F-A2392-6

Special consideration was given to the turbocompressor sets for the Army nuclear power package ML-1, the components of which will now be discussed.

10.3.2 Clark Bros. Co. CSN-1 T-C Set

Stress values throughout the machine have been limited to values which should ensure that the life of the machine will satisfy the requirement of 50,000 hours operation before replacement of major components becomes necessary. Major components may be considered as rotating elements and stationary blading, although this may be limited to turbine blades and disks, should it prove feasible to interchange turbine disks and compressor rotor bodies.

Normal low temperature parts are designed for stresses well below the yield point of the material even when considering the specified condition of 125% overspeed. This will give stress values in the rotating components of approximately 156% of the normal stresses at the design speed of 22,000 rpm.

High temperature parts are designed on the stress-rupture characteristic of the materials rather than a specified creep rate during a given time. The premise of stress rupture has really considerably greater significance than creep strength, as the primary consideration should be the length of time which a material will sustain a given stress level at a given temperature before fracture rather than how much the material will creep or elongate.

A glance at the stress distribution versus radius for the turbine rotor blading (Figs. 10-5[21] and 10-6[21]) shows that the stress falls rapidly with radius even though shrouds are fitted to the blades. From this stress distribution, it can be seen that the creep rate for the material along the length of the blade is a complex function, even assuming that the temperature is constant. It would be not feasible to

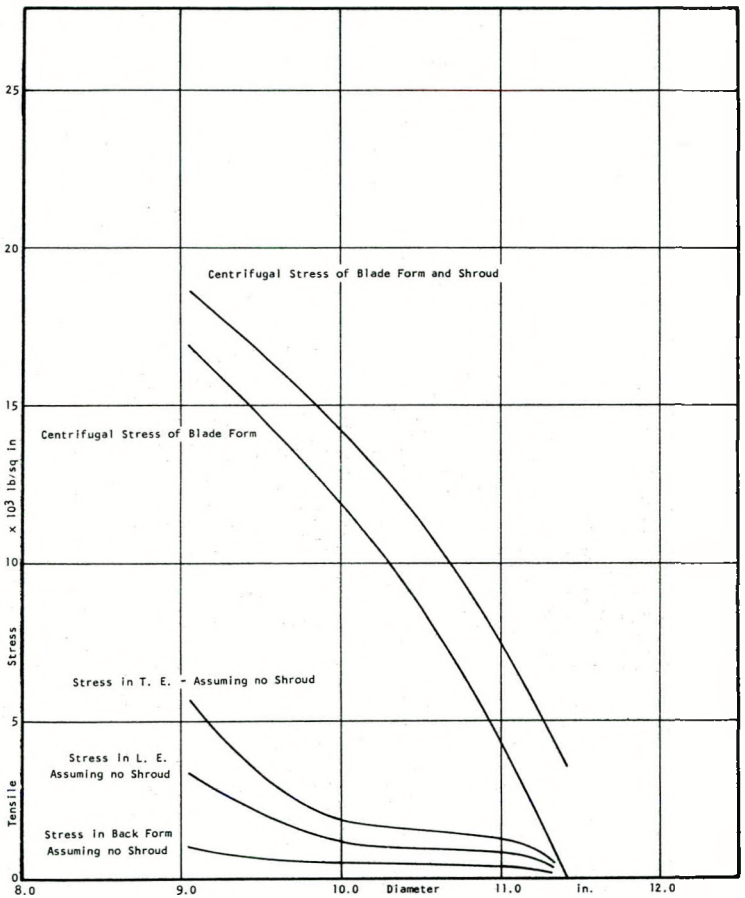


Fig. 10-5 - Clark Turbine Blade, Stress vs. Diameter, Stage 1

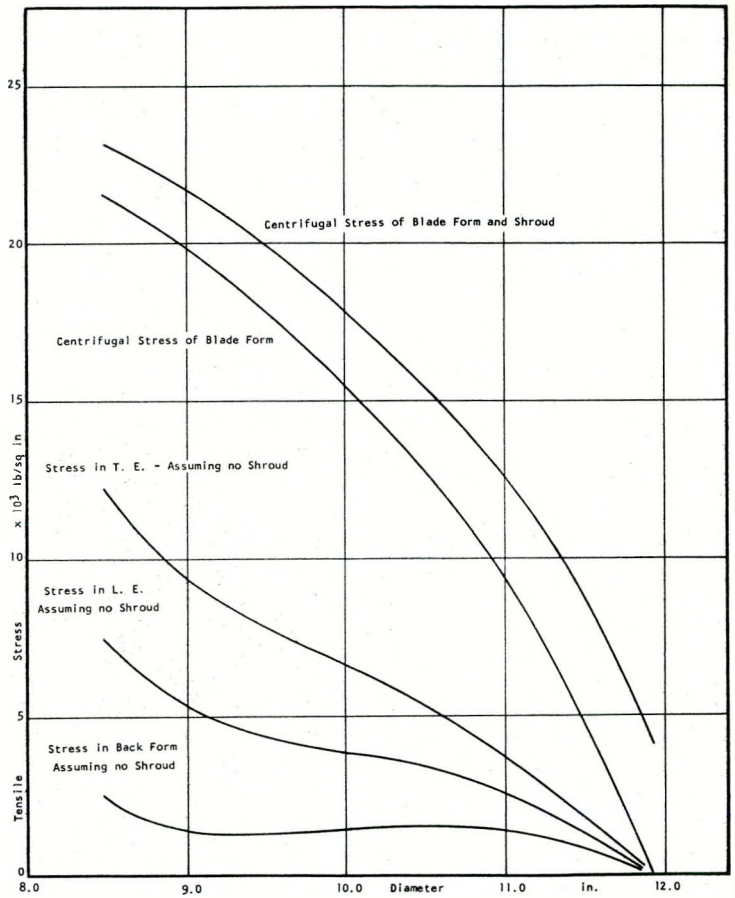


Fig 10-6 - Clark Turbine Blade, Stress vs. Diameter, Stage 2

attempt to determine how much useful life remained in the blade by measuring the length of the blades or diameter of the rotor at specified periods of time, as this would involve a more intimate knowledge of the stress and temperature distributions than is possible. For example, supposing that a blade showed a creep of 1% over 100% of its length, it would be impossible to say whether this had occurred uniformly over the length of the blade (in which case there would still be considerable life left in the blade) or whether the entire increase in length had occurred over the inner 25% of the blade length. In the second case it would mean that in the inner 25% of the blade 4% creep had taken place, and that failure was relatively imminent. This is of course a very simplified example of a complicated process, but it serves to illustrate the extreme complexity of designing a machine of this nature on the basis of creep life.

Figs. 10-7[21] and 10-8[21] show the stress distribution versus diameter in the compressor rotor blades for Stage 1 and Stage 11. The pure centrifugal stress for the blade form is shown for each case, and additional stress lines are shown for the leading edge, trailing edge, and back form caused by gas bending stress, assuming 0.007 in/in offset of the center of gravity of the sections. To determine the total stress in the blade form at any particular point, the centrifugal stress and gas bending stresses should be added algebraically taking note of sign.

The value of 0.007 in/in offset of the blade form center of gravity was chosen to give more or less optimum distribution of stress over the blade form, i.e., maximum tensile stress in back form where it is possible to obtain greatest degree of quality control and minimum tensile stress in leading and trailing edges where stress concentrating defects are most likely to occur during manufacture or be caused by ingestion of foreign material into the machine.

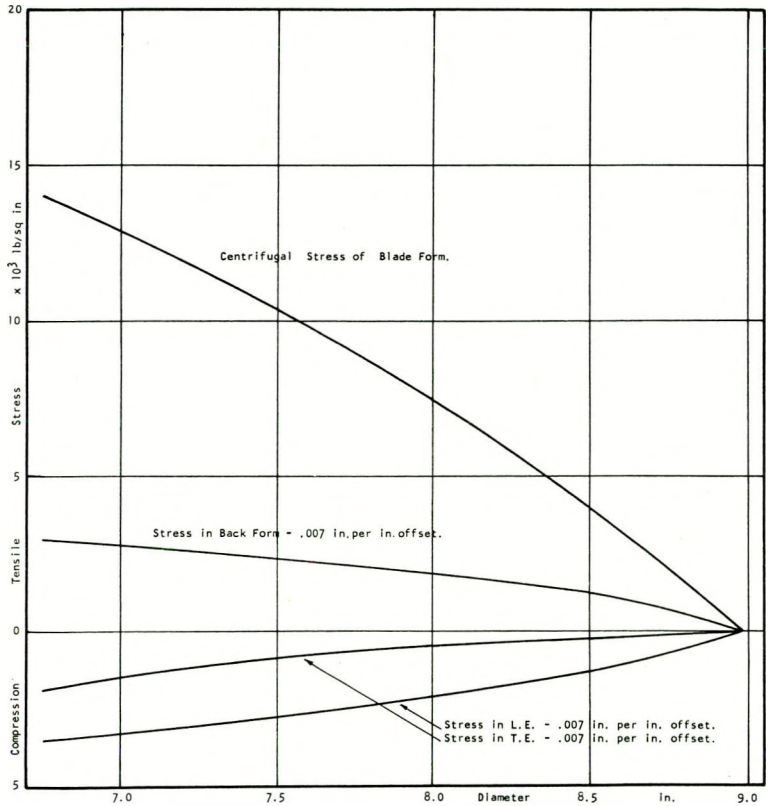


Fig. 10-7 - Clark Compressor Blade, Stress vs. Diameter, Stage 1

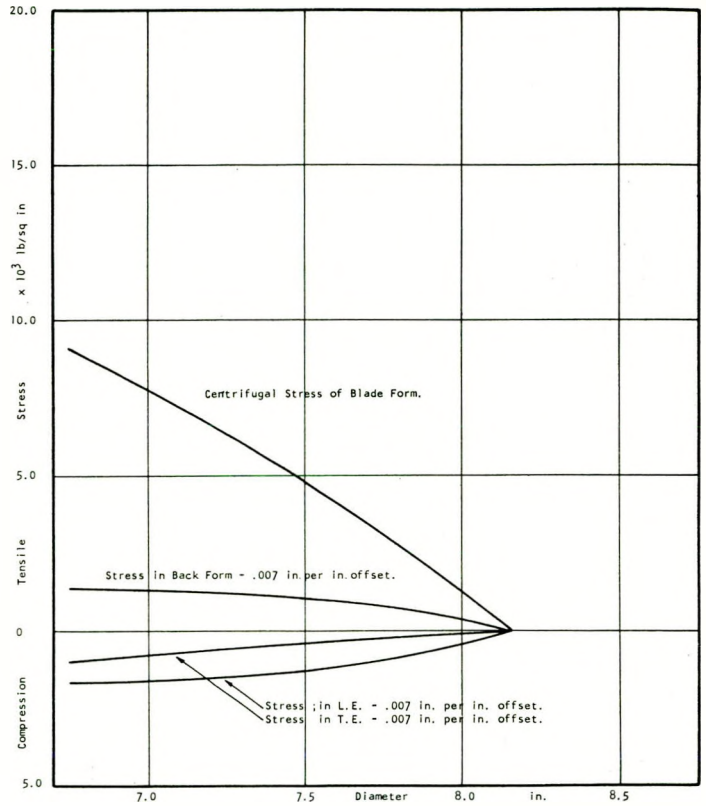


Fig. 10-8 - Clark Compressor Blade, Stress vs. Diameter, Stage 11

Figs. 10-5 and 10-6 show the stress distribution versus diameter for the turbine rotor blades. As for the compressor blade stresses, the stress due to centrifugal force is shown separately from the stress due to gas bending. Here, however, the stress due to gas bending is rather more complex, as the figures shown are for a rotor blade without shrouding. The shroud will exert some influence on the gas bending stress as it will act as a semi-rigid end fixing, but it is impossible to ascertain how much influence it will have. The curves presented, therefore, are pessimistic compared to the true stresses which will exist in practice.

Another point which should be noticed is that no offset of the turbine blades has been postulated. Again, the basic reason for this is that the shroud will help considerably to damp out or prevent appreciably resonant blade vibrations occurring so that possible stress concentrating defects are less serious.

Fig. 10-9[21] shows the stress distribution versus radius for the compressor rotor body, and Fig. 10-10[21] shows the stress distributions for the 2nd stage turbine disk. Parameters of temperature distribution with radius are included in Fig. 10-10 indicating the effect of temperature gradients on disk stress. While it is not possible to predict the temperature distribution in the disks between center and rim accurately, it is not anticipated that these will be in excess of 200°F.

Fig. 10-11[21] gives an overall picture of the stresses in the major parts of the rotating assembly, and the figures quoted are reasonably representative. Although the stress figures for the 2nd stage turbine rotor disk are higher than for the 1st stage, it should be realized that:

(a) No account is taken of the stub shaft integrally forged with the 2nd stage disk, and

(b) The metal temperatures for the 2nd stage disk should be lower because of the heat drop through the 1st wheel.

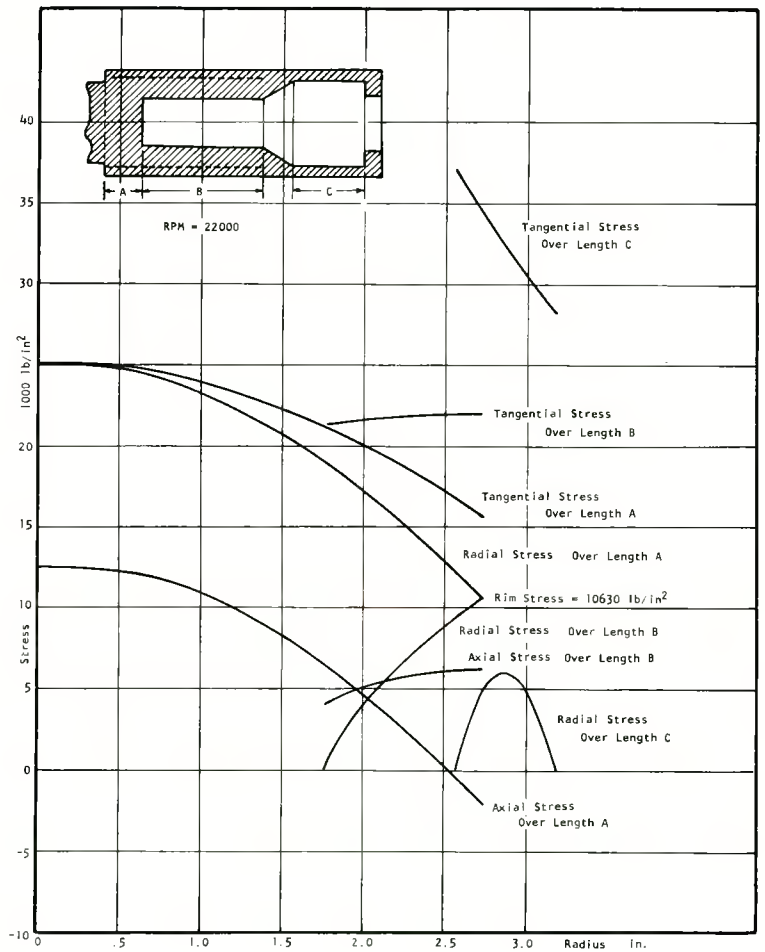


Fig. 10-9 - Clark Compressor Rotor, Stress vs. Radius

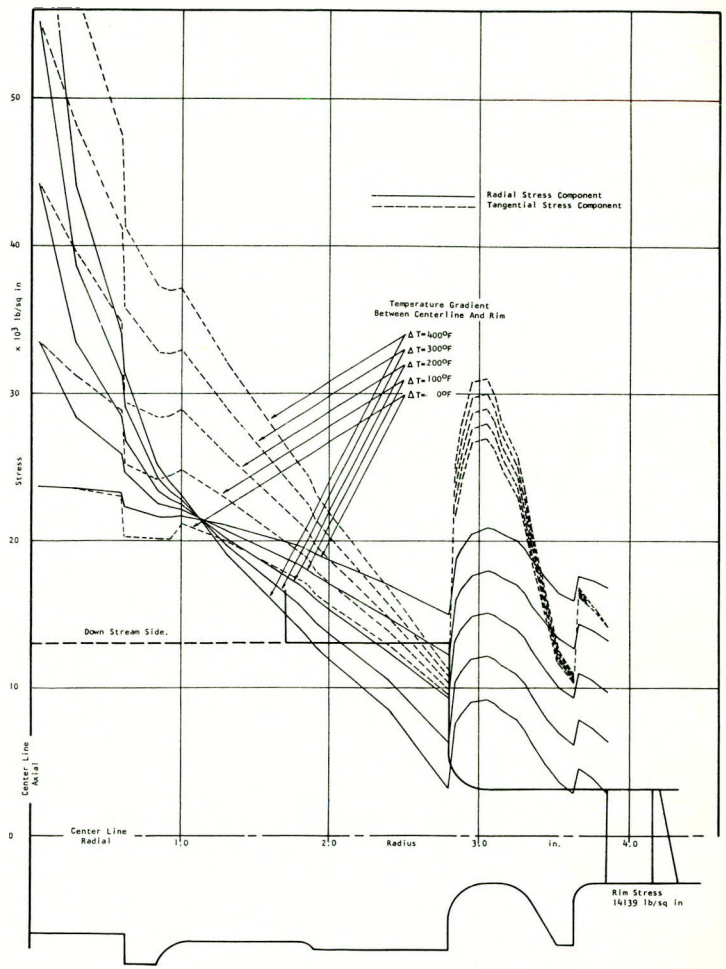


Fig. 10-10 - Clark Turbine Disk, Stress vs. Radius, Stage 2

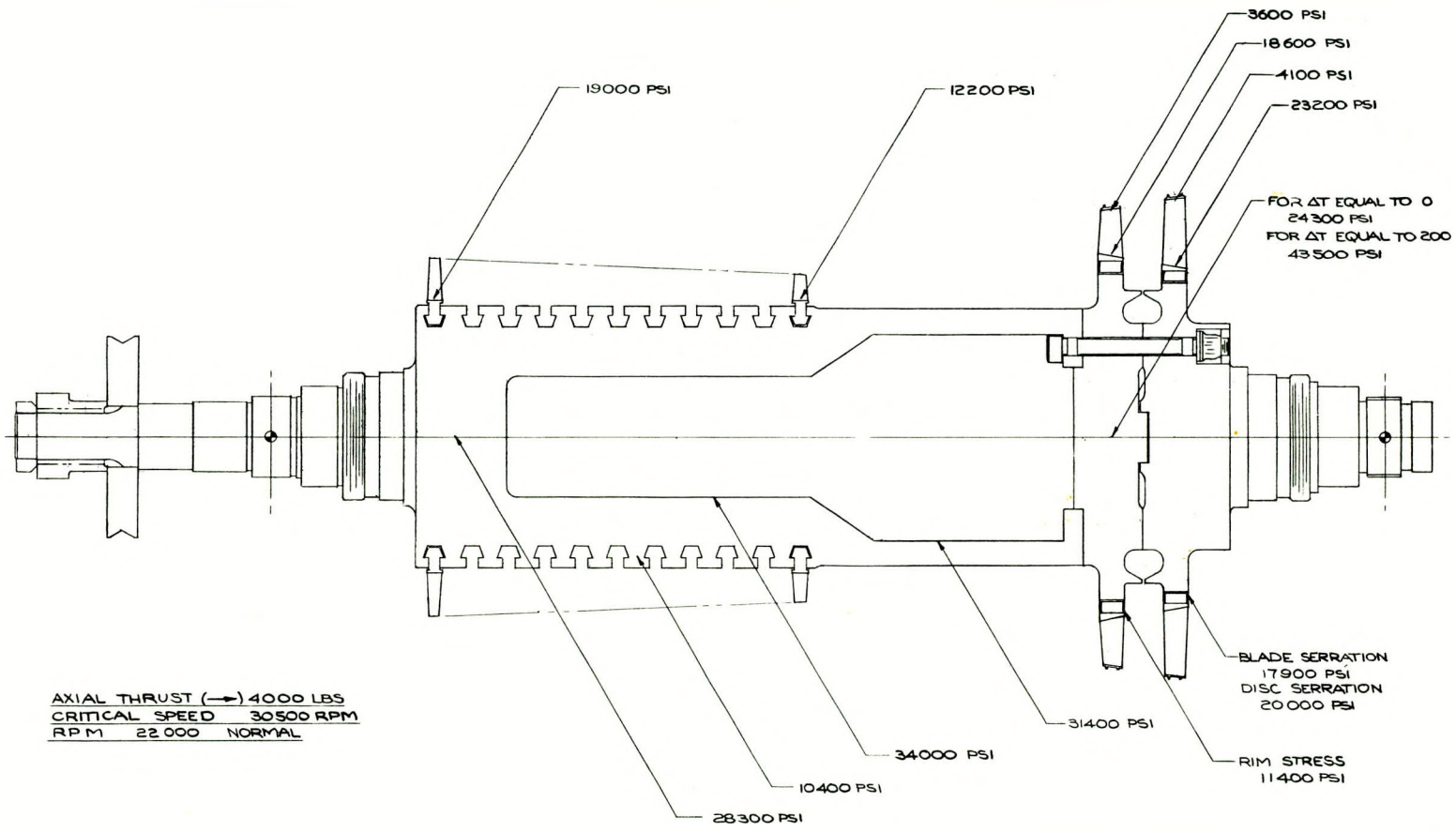


Fig. 10-11 - Clark Rotor Shaft Stress Picture

Figures 10-12 to 10-15[21] show the stress-to-rupture diagrams vs. temperature, in 50,000 hours for the more important materials used.

10.3.2 Stratos TCS-670 T-C Set

For all stress calculations for the machine, a factor of safety of three to six was used. For materials subjected to 1000°F or higher, the factor of safety was applied to the creep strength rather than the yield strength. The creep strength is based on one per cent creep in 10,000 hours, the maximum period for which data are available. It should be noted that with the safety factor applied, the actual creep in 10,000 hours is negligible.[22] It might be noted also that such procedure, if required from running clearance considerations, would only be satisfactory if some correlation has been used with data warranting a creep-rupture life of 50,000 hours with an adequate margin of safety.

The calculated stress values for the 1st stage compressor wheel are shown in Figure 10-16[22] and for the 1st stage turbine disk in Figure 10-17.[22] Compressor and turbine wheel stresses were calculated by an extension of Donath's method, adapted for a digital computer. Provision was made to include temperature variations at different radii and the changes in material physical properties due to these variations.

In calculating stresses in shrouded wheels, the effect of shroud and blade loading has been applied to the disk to produce the stresses plotted. The shroud stresses plotted are those for the shroud and blades with no restraint from the disk. As the disk does restrain the shroud, through the blades, the actual stresses are considerably lower than those plotted. The plotted disk stresses reflect the effect of shroud and blade loading on the disk.[22]

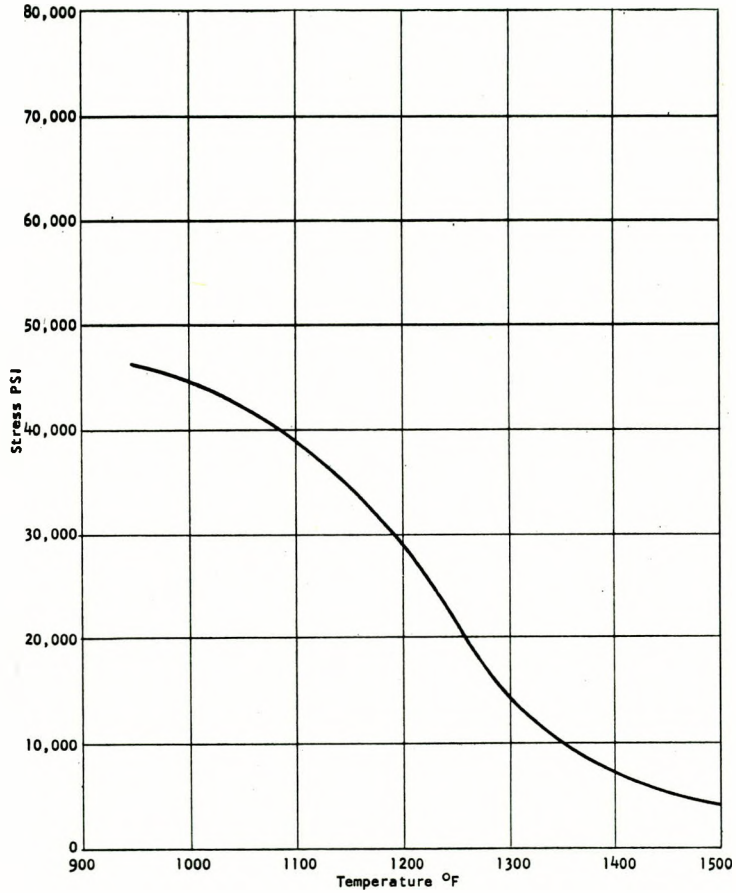


Fig. 10-12 - Stress to Rupture in 50,000 Hours vs. Temperature for 19-9 DL

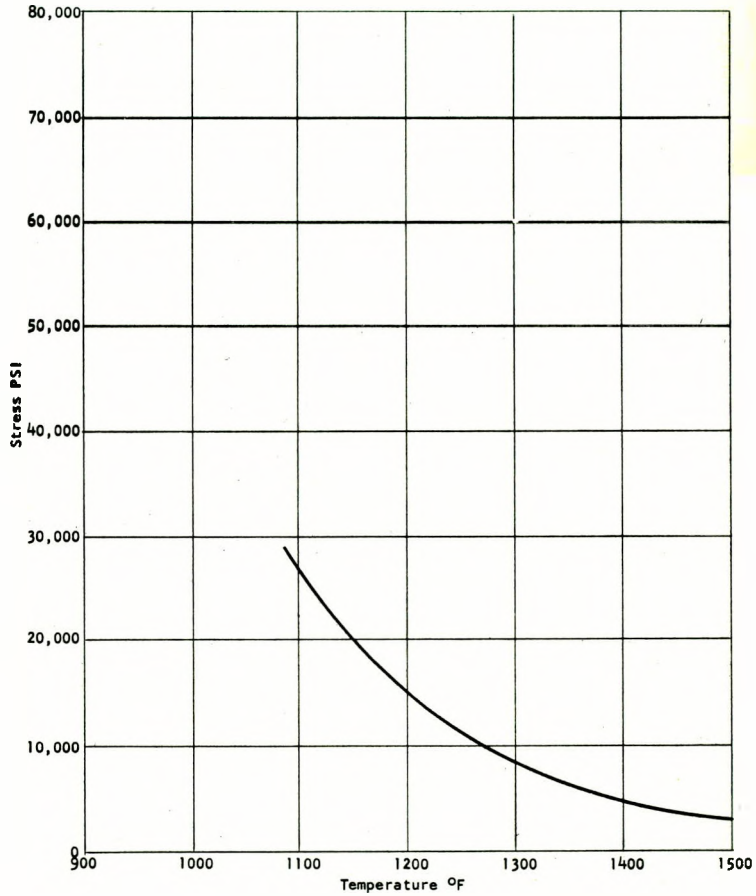


Fig. 10-13 - Stress to Rupture in 50,000 Hours vs. Temperature for Type 316 Stainless Steel

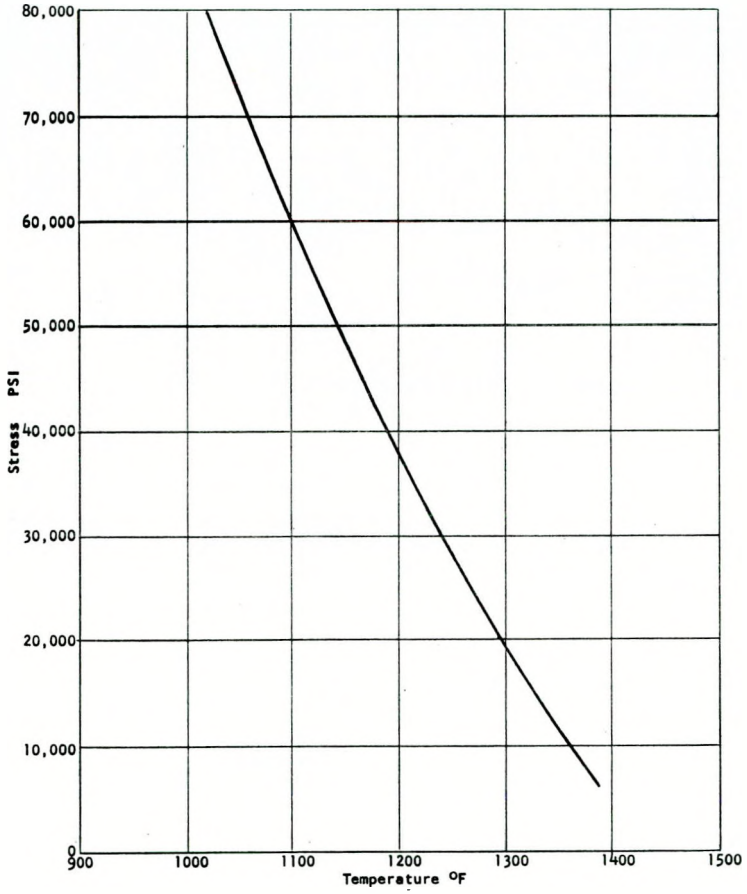


Fig. 10-14 - Stress to Rupture in 50,000 Hours vs. Temperature for Incoloy 901

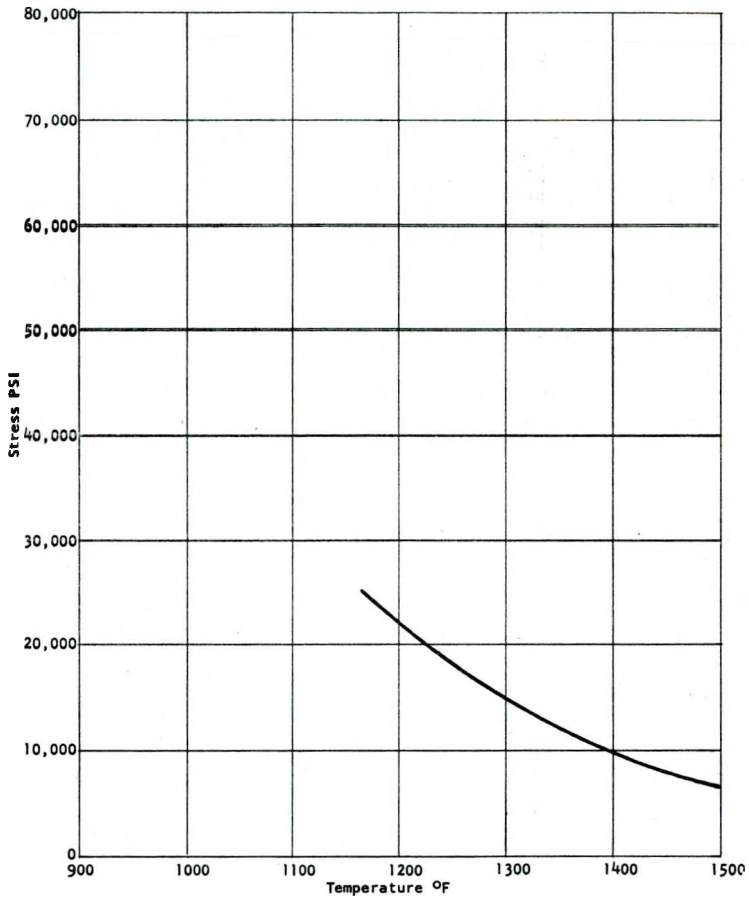


Fig. 10-15 - Stress to Rupture in 50,000 Hours vs. Temperature for N-155

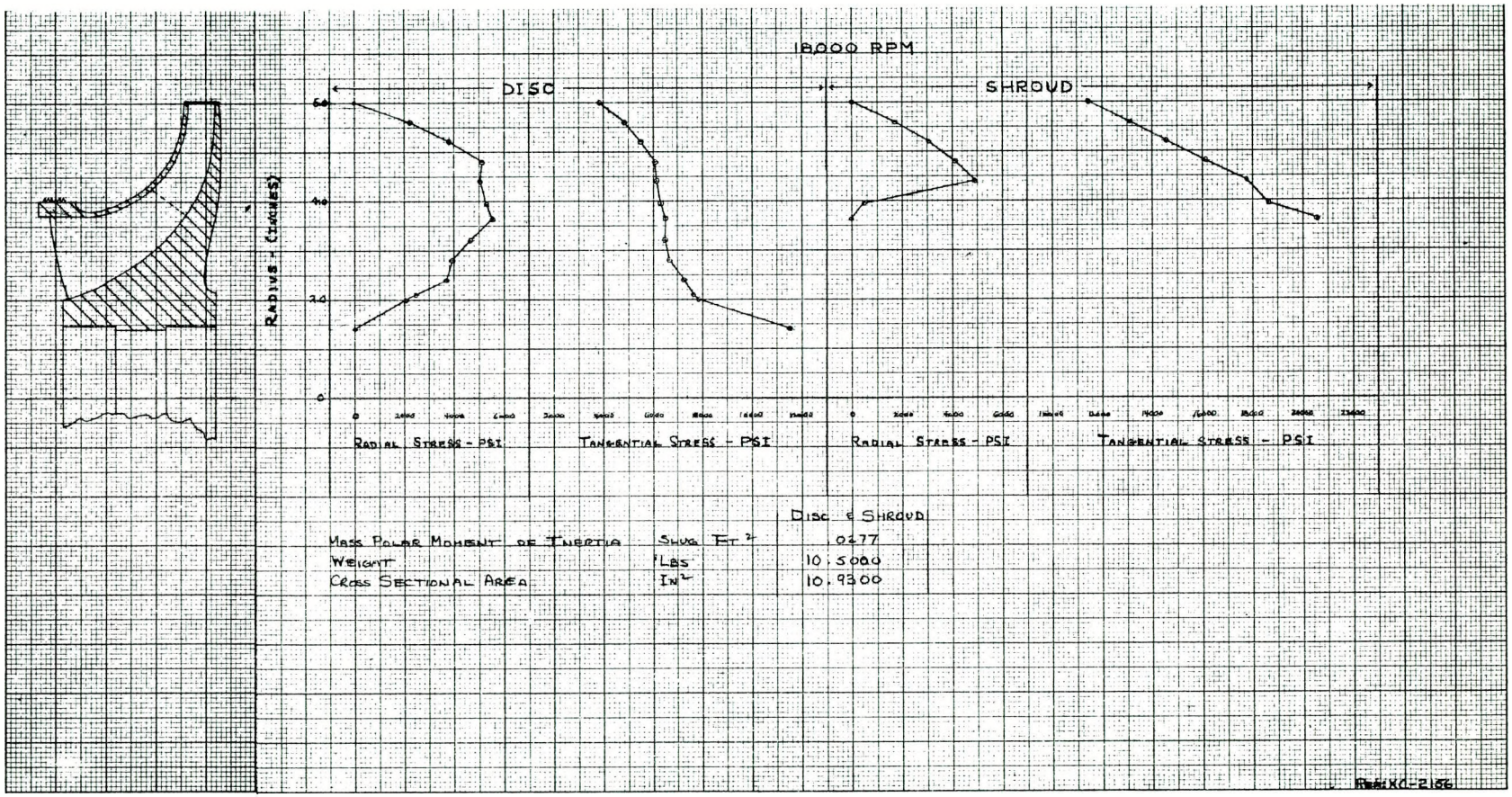


Fig. 10-16 - Stress Values in Stratos Compressor Wheel, 1st Stage

Data from Stratos Division, Fairchild Corp.,
Report SRC-104

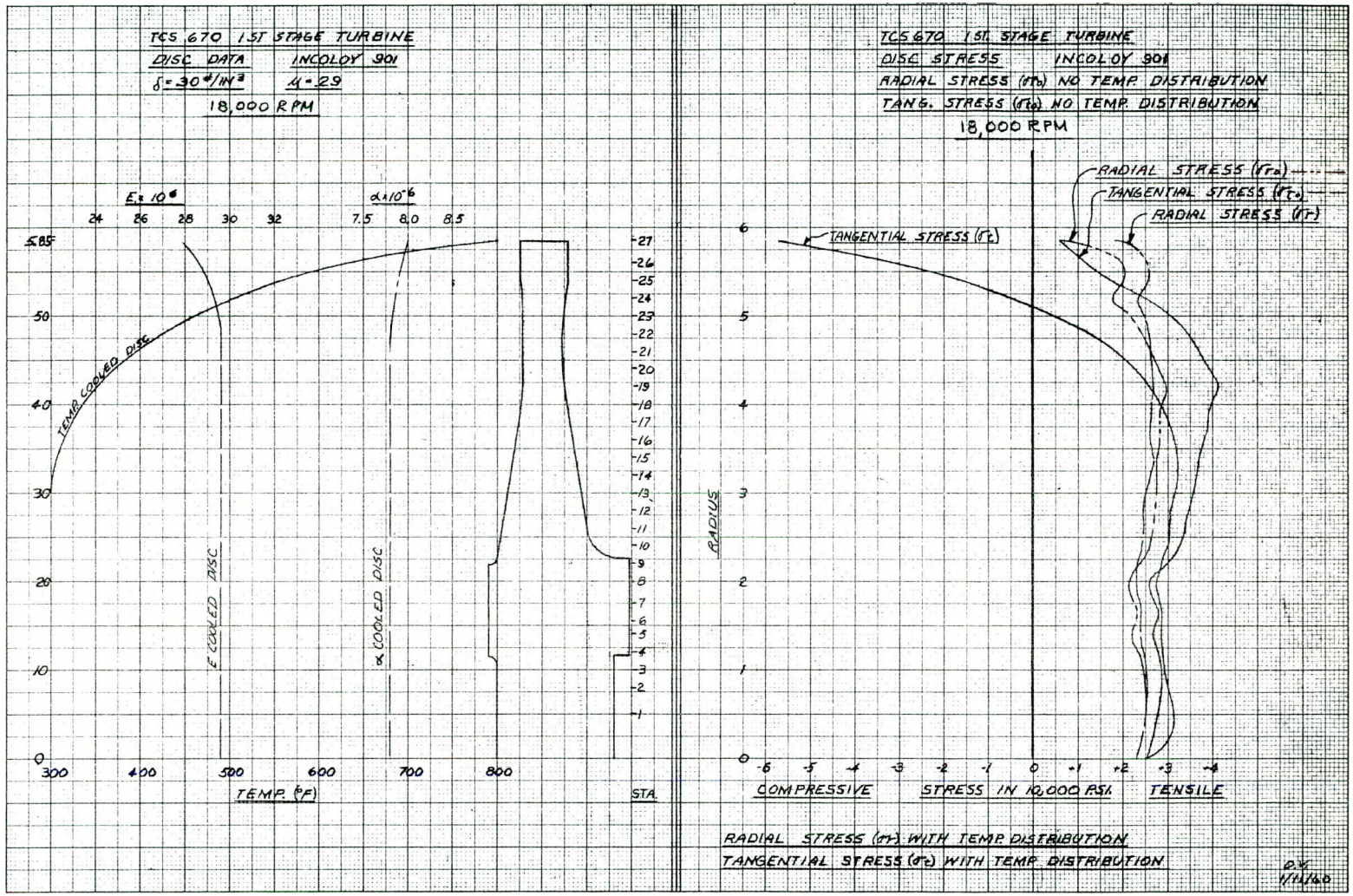


Fig. 10-17 - Stress Values in Stratos Turbine Disk, 1st Stage

Data from Stratos Division, Fairchild Corp.,
Report SRC-104

Studies on the turbomachinery for the Maritime Gas Cooled Reactor brought to attention that in any closed-cycle gas turbine the blade-bending stresses tend to be an appreciably larger portion of the total stress than in open-cycle gas turbines. In comparing carbon dioxide with helium as working fluids, the vibratory stress in the CO_2 machine is as much as 40% of the total blading stress, whereas for helium it is approximately 10% of the total with blades of similar aspect ratio. Although the bending stress levels can be adjusted by changing the blade chords, the centrifugal stress cannot. The centrifugal stress levels with carbon-dioxide are about one-half those of helium. The stress levels in the rotating disks are appreciably lower with carbon-dioxide because of the low design rpm. For helium, which is not Mach number limited, the design is based on the stress level in the turbine disks and therefore the disk material is used at its maximum capability. The disk stress level in the He machine is approximately twice that of the CO_2 machine. Typical stress levels are shown in Table 10-1[1], including comparative figures for a modern industrial gas-turbine.

Table 10-1

TYPICAL TURBINE BLADE AND DISK STRESS LEVELS

	Cycles			
	He 1000 psia	CO_2 1000 psia	CO_2 2000 psia	Industrial gas turbine*
Blade centrifugal stress, psi	31,100	14,500	18,500	34,900
Blade vibratory stress, psi	3,000	10,300	8,600	1,760
Blade total stress, psi	34,100	24,800	27,100	36,660
Disk average tangential stress psi	39,900	15,480	16,000	27,300
Relative Mach number	~ 0.4	~ 0.8	------	------

*It might be noted that disk stresses in aircraft gas turbines may be as high as 100,000 psi.

Let us add some additional stress considerations concerning radial-flow impellers. The stresses in the blades of such impellers can be high. They are less subject to calculation because of the frequently complicated blade shapes. Stress coat methods are used in such cases to determine the actual stresses. One of the consequences of the high speeds of turbomachines are the high stresses caused by the centrifugal forces as illustrated by Figure 10-18[83] which shows lines of constant radial and tangential stresses in the disk and hub of an aluminum impeller running at a rim speed which is well above the continuous duty operating speed. For this particular disk design, local yielding of the material takes place in the shaded area of the figure.

For some years, there has been a widely accepted rule of thumb that 800 feet per second is about the maximum tip speed for closed, riveted compressor wheels. The demand for higher heads in efficient, high-specific-speed wheels has led to new designs for which much higher tip speeds can safely be used. The ultimate in strength for closed wheels is the forged-welded design. In this type wheel, part of the blades are formed in the hub forging and part in the side plate forging. The two parts are then jointed by automatic, full penetration welding at the middle of the blade.

The great increase in strength of the forged-welded wheel is primarily due to the stronger blade attachment and the elimination of stress concentration at the rivet holes. Although the same strength steel is used, the factor of safety in the disks of a welded wheel is over twice that in riveted wheels at the same tip speed and the blade attachment is at least four times as strong as the rivets. Because of this additional strength in the blade attachment, in a welded wheel some of the load is transferred from the side plate to the lower-stressed hub and thus further reduces the stresses in the side plate.

A more striking comparison between riveted and welded wheels is shown in Figure 10-19[81] where the stresses in a riveted wheel at 787 feet per second tip speed are compared with those in a welded wheel at 1000 feet per second tip speed. At this higher tip speed, the welded wheel will deliver about 60 per cent more work (head) than the riveted wheel. Its maximum stress is 50,000 pounds per square inch at the side plate bore, while the maximum stress in the riveted wheel is 77,000 pounds per square inch at the first side plate rivet hole. Although delivering 60 per cent more work, the welded wheel is thus some 54 per cent safer than the riveted wheel. It is clear that the old 800 feet per second limit for riveted wheels was well chosen and that, by the same standards, the welded wheel is still loafing at 1000 feet per second.

With the advent of high pressure ratios under continuous duty conditions, the impeller metal temperatures will increase also and the high-temperature properties of impeller materials have to be considered carefully. Figure 10-20[83] shows, for example, two calculated life-to-rupture versus speed curves for an impeller based on long-time creep-to-rupture data of a particular aluminum alloy and foundry process. The two curves are for two different designs and are calculated taking into account the heat transfer between impeller and air which is heated while flowing through the impeller and undergoing compression.

Let us next consider blade-root fixings of high-temperature steels. Tests show that the stress figures obtained from creep tests are not the only important consideration in assessing the strength of blade root fixings, but that the strength may be reduced by as much as 50% if the steel has not the ductility required by the structural design employed. They also show how important it is to select not only a suitable metal but also a suitable shape of root, which will ensure that no inadmissible peak stresses occur. The dimensions of blade roots must accordingly not be based on the creep curve alone, but on the creep figures multiplied by

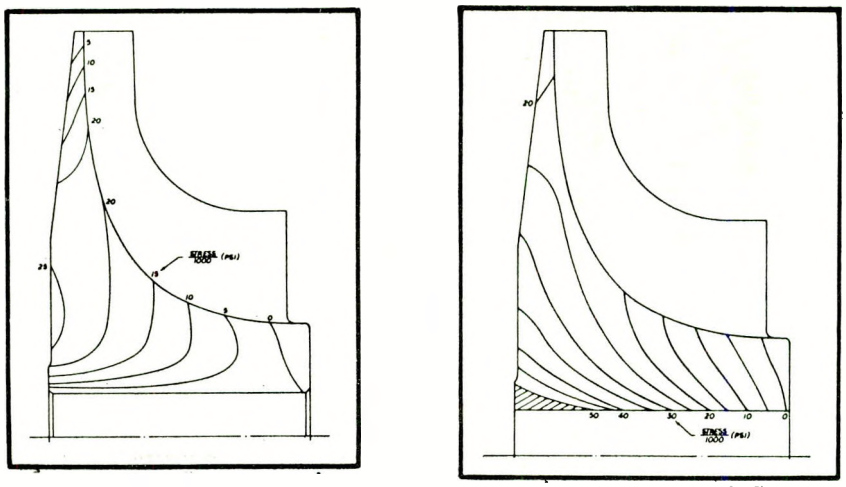


Fig. 10-18 - Stresses in Impeller at Overspeed

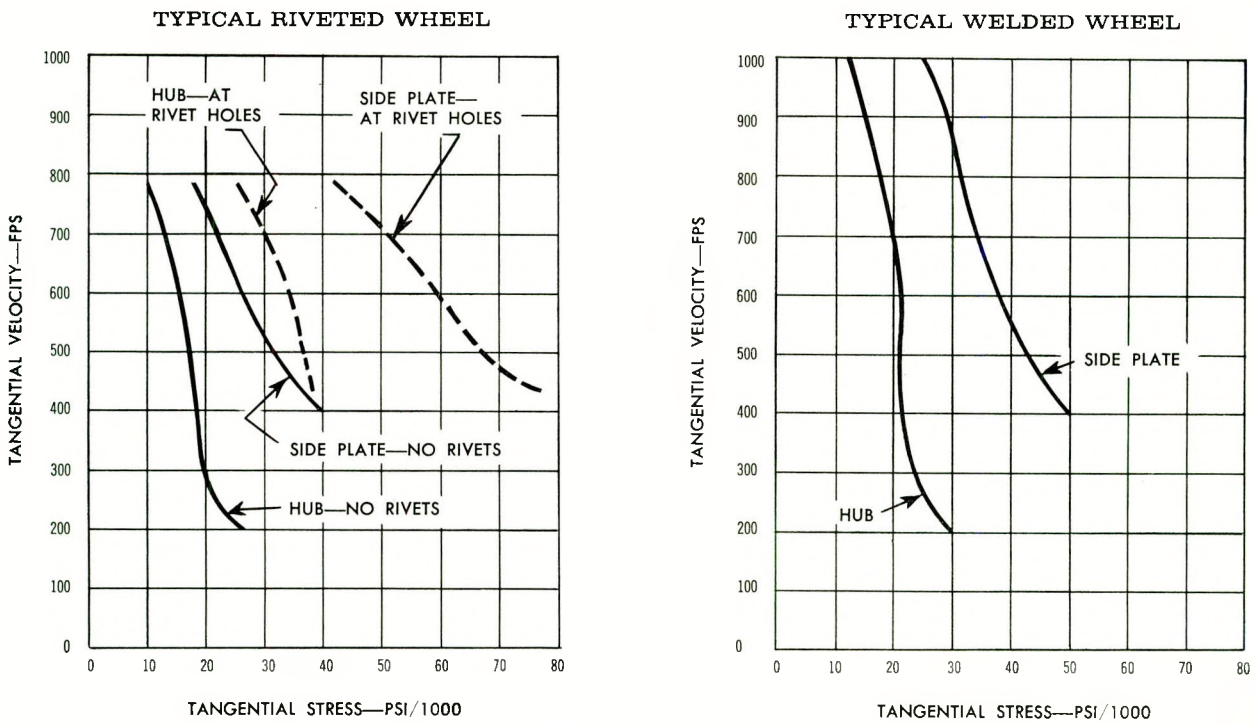


Fig. 10-19 - Wheel Stresses

THE FRANKLIN INSTITUTE • Laboratories for Research and Development
I-A2392-2

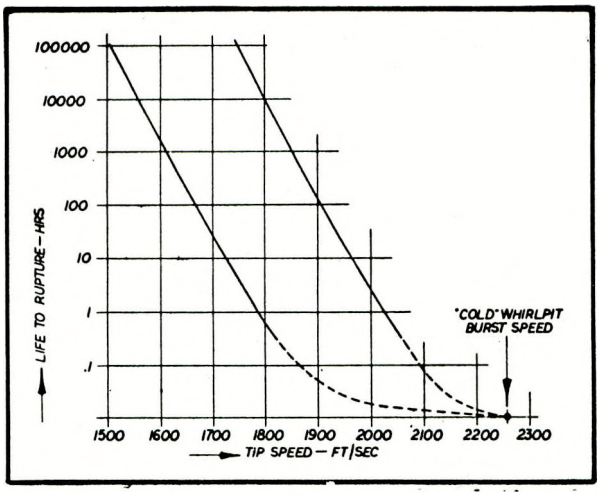
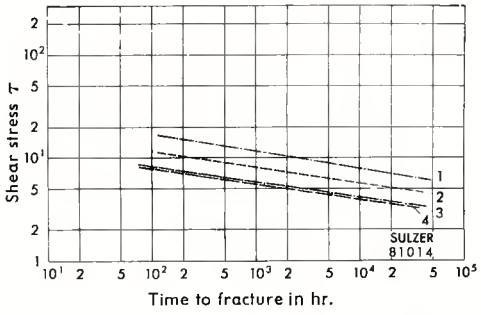


Fig. 10-20 - Typical Life-Speed Relationship for Aluminum Impeller



Curve	Specimen	Steel	Condition
1	Plain bar	1a	Hot worked
2	Plain bar	1	Solution treated
3	Model No. 2	1a	Hot worked
4	Model No. 2	1	Solution treated

Fig. 10-21 - Strength of Blade Root Fixings of Model No. 2, Steel No. 1, at 710°C

the quality figures. If this is not done, the conclusions drawn may be quite wrong, as will appear from the following example. Blade root model No. 2 was prepared with steel No. 1 in the solution treated and hot-worked conditions. Hot working raises considerably the shear stress required for a given time to fracture of plain specimens as can be seen from Fig. 10-21.[130] At the same time, however, the notch sensitivity of the metal is also increased, and this causes a drop in the quality figure. The creep curves of this blade root at the nominal shear stress are plotted for both conditions of the steel in the figure. It is evident from this graph that the gain in strength due to hot working has been completely lost again on account of the increase in the notch sensitivity. It is true that the notch sensitivity in the hot-worked state decreases at longer times, so that improvement might still be possible. This effect also depends greatly on the degree of hot working and on the metal used. The example is quoted only to demonstrate the great importance of embrittlement due to notch sensitivity in the structural design of blade root fixings.

10.4 Thermal Stress

A detailed temperature analysis of a gas turbine is needed for the following three reasons.[131]

(a) The strength properties of the material used in all structure and rotating components are a function of temperature.

(b) Relative displacement of rotating and stationary parts during start and shutdown is important because the efficiency of the engine is dependent on turbine and compressor-shroud clearance which must be kept to a minimum. The turbine structure should be free to expand without constraint from the adjacent structure at a different temperature or rate of thermal expansion.

(c) The thermal stresses in rotating components and structure are a function of the steady state and transient temperature gradients in the parts. Experience has shown that knowledge of the complete temperature distribution during the operating cycle is necessary in the design state to avoid failure of critical components due to thermal stress, during the development state.

Adequate evaluation of thermal stresses is of greater significance in high-temperature aircraft turbines compared with industrial turbines which operate under more moderate conditions of load and temperature. Consideration must be given to the effect of thermal shock which is likely to occur when quick starting is required or where the turbine is subjected to rapid load changes. Such effects are necessarily considered in the operation of turbines in transport service but are not particularly significant with relation to commercial turbines running under sustained loads for long periods of time.[35]

Transient heat-conduction equations of convective heat transfer, and several methods for solution of these equations in irregularly shaped bodies have been developed. Such methods include an electrolytic tank, analog computer, and a digital computer, each of these methods having their advantages and disadvantages.[131]

Figure 10-22[131] shows a crack in a turbine blade. Because of the nature of the crack and its location, it was diagnosed by an analysis on the analog computer as resulting from the transient thermal stresses in the blade during starting. Figure 10-23[131] shows the established temperature distribution, and Figure 10-24[131] the stress distribution at 4 seconds. Figure 10-25[131] is a plot of the maximum stress in the blade versus time. The maximum stress of 70,000 psi was reached after 4 seconds. By doubling the blade-tip thickness to 0.080 inches, the maximum stress was later reduced to 19,000 psi (see second plot in Figure 10-25).

It is interesting to note that the most difficult term to evaluate in the thermal problems is the heat-transfer coefficient. However, the thermal stresses are dependent on temperature gradients, which are not significantly affected by rather large variations in the heat transfer coefficient. A comparison of electrolytic-tank solution and an analog-computer solution of the steady-state temperature distribution in a radial turbine wheel has shown that a rather coarse network used on

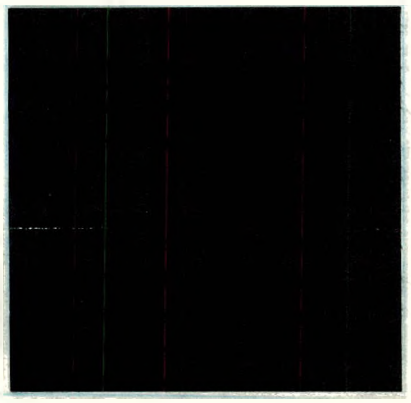


Fig. 10-22 - Cracks in Turbine Bucket

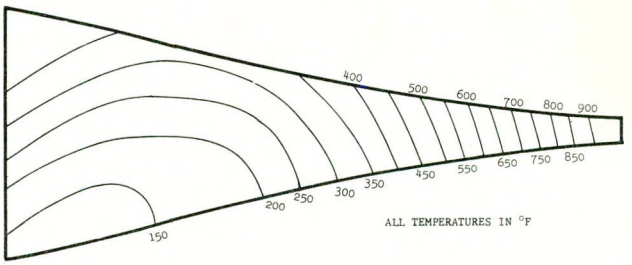


Fig. 10-23 - Temperature Distribution for Original Blade at 4 Seconds

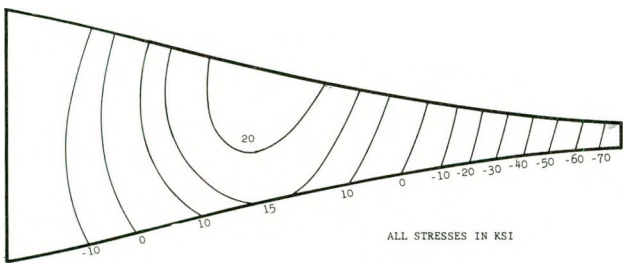


Fig. 10-24 - Stress Distribution for Original Blade at 4 Seconds

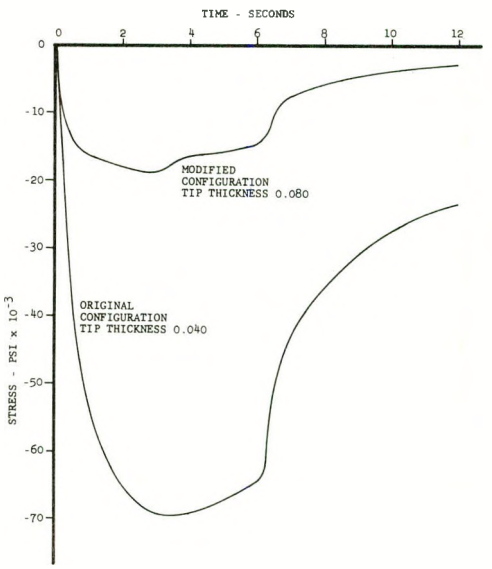


Fig. 10-25 - Maximum Blade Stress

the analog-computer solution did not differ greatly from the solution on the electrolytic tank, which indicates good approximations to the temperature distributions can be obtained with a coarse grid for the finite-difference solutions.[131]

10.5 Fatigue

The complex combination of variables contributing to failure of gas-turbine blades during engine operation prevents an accurate prediction of either the bucket life or the mode of failure based on laboratory test data alone. For example, in one engine of high centrifugal bucket stress (J33) the modes of failure were found to be primarily stress-rupture and mechanical fatigue. In the J47 engine, with a relatively low centrifugal bucket stress, the primary mode of bucket failure was shown to be thermal-stress fatigue cracking at the leading edge.[132] Thermal-stress fatigue cracking has been observed in turbine buckets in several investigations. This type of failure was shown to be primarily due to thermal stresses generated during engine start. It was also shown that rated-speed operation between engine starts markedly reduced the number of starts necessary to cause cracking of the bucket materials investigated.[133]

Figure 10-26[132] shows typical buckets cracked by thermal-fatigue. Increased operating time between starts permits substantial increases in accumulated rated-speed time before bucket cracking occurs. Thus, increased bucket life, in terms of operating hours, may be obtained by decreasing the frequency of starting.[133] According to tests, thermal stress fatigue cracks do not progress rapidly by stress-rupture to cause fracture of buckets. Buckets fractured by progression due to mechanical fatigue of a crack initiated by stress-fatigue. Buckets were observed which ran with cracks for as long as 63 hours without fracture.[132]

One of the tests was conducted with a turbine wheel containing 81 test buckets. The turbine wheel was installed in a J47-25 modified engine and operated for repeated cycles of 15 minutes at rated speed of 7950 rpm with a 1700°F bucket temperature and about 5 minutes at idle speed of 3000 rpm. Engine operation was continuous except for stops necessary for maintenance and repairs. Thermal-stress fatigue cracking occurred in buckets of all alloy groups investigated: investment cast buckets of alloys Sel-1, B&B, and Inconel 713, and forged buckets of Udimet 500.[133]

Figure 10-27[133] shows bucket stress and temperature distributions at rated conditions. Figure 10-28[133] gives the number of starts and operating hours when cracks were first found in each bucket. Since only two buckets fractured in 357 hours of operation at 1700°F, it appears that the alloy groups investigated possess considerable potential as bucket materials for advanced-temperature operation if thermal-stress fatigue failures can be minimized.

10.6 Vibration

For many years, it was considered highly desirable that a compressor operate well below its first critical speed. As speeds increased and more stages were added, it became impossible to design aerodynamically good passages, maintain tolerable stresses, and still have a stiff shaft. Figure 10-29[61] shows a stiff shaft rotor which has rather poor proportions because of the large shaft necessary to raise the first critical speed above the running speed. A flexible shaft in the same rotor would have been as shown by the dashed lines. With this smaller shaft, the wheel stresses would have been about 15 per cent lower, the wheel inlet Mach numbers also about 15 per cent lower and the performance appreciably better.

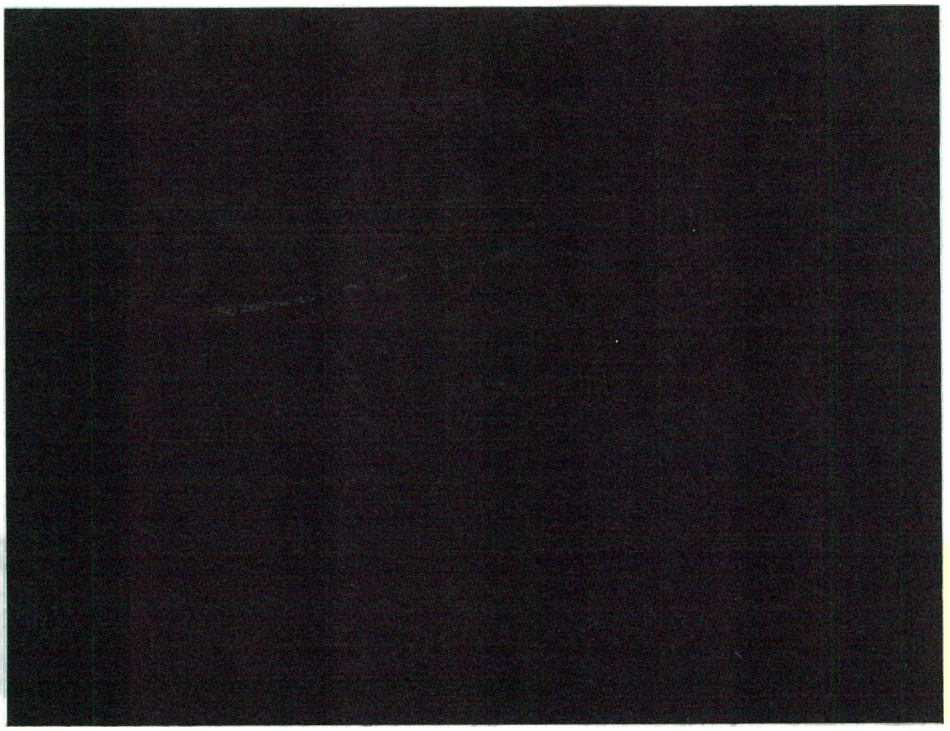


Fig. 10-26 - Typical Buckets Cracked by Thermal-Fatigue

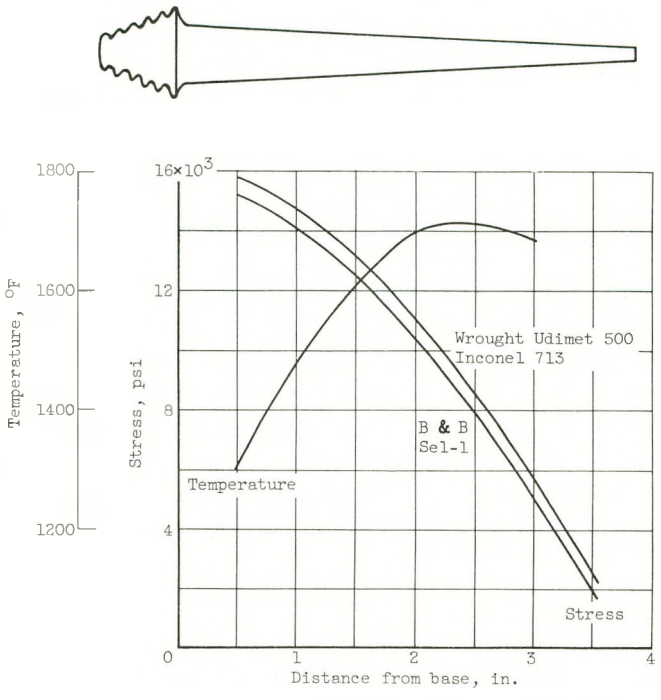


Fig. 10-27 - Bucket Stress and Temperature Distributions at Rated Conditions

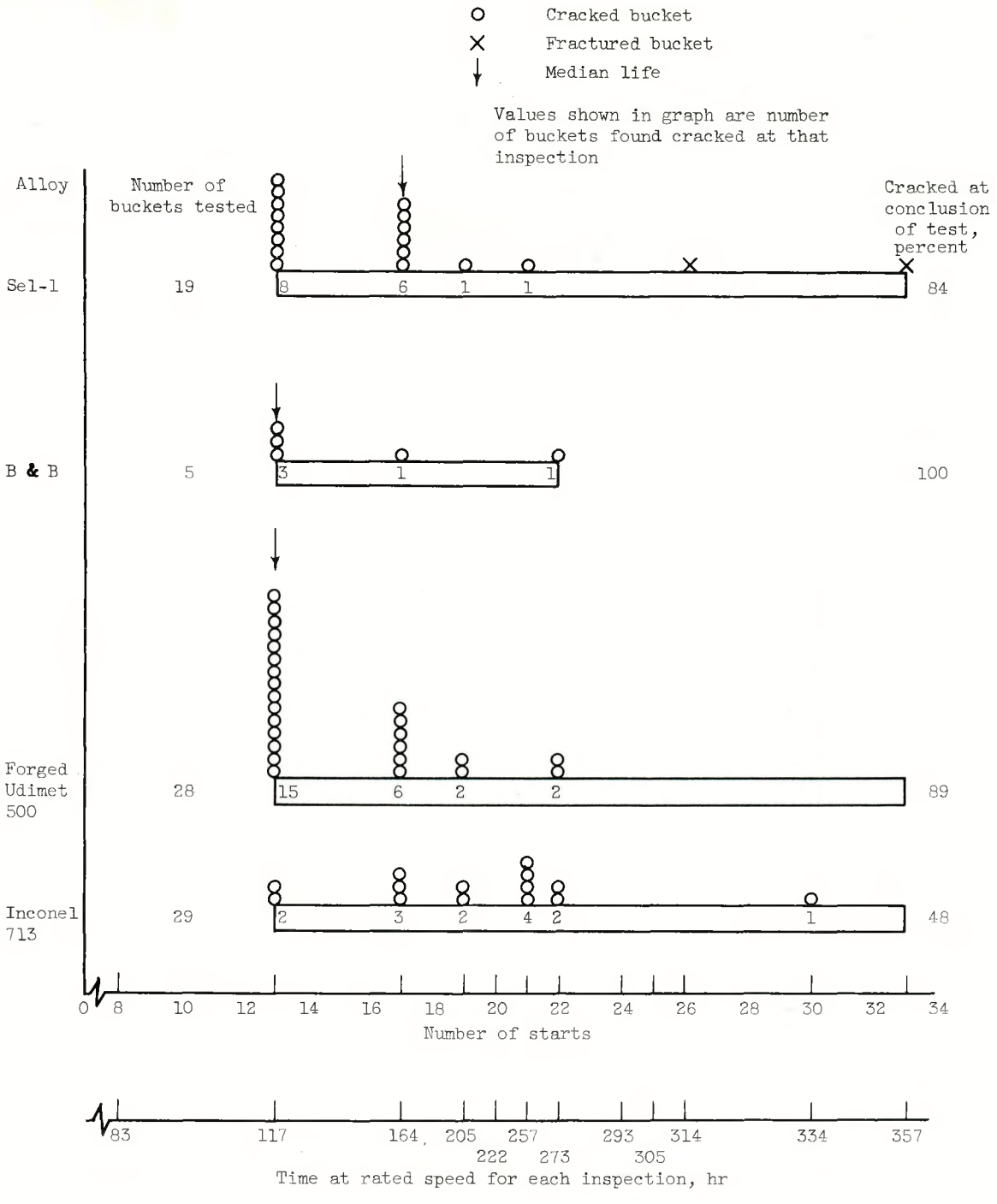


Fig. 10-28 - Number of Starts and Operating Hours When Cracks were First Found in Each Bucket

With proper balancing and assembly of a rotor, it has been found that the first critical speed is usually detectable only with precision instruments. Continued operation in or through this critical speed is of no concern and is common practice in many compressors and turbines.

As speeds increase further and still more stages are added, attention to the second critical speed becomes necessary. In high speed rotors, an accurate calculation of the second critical speed must include the effect of shaft support flexibility. Figure 10-30[81] shows the relation between the actual second critical speed and that calculated for rigid shaft supports in a typical multistage compressor. It can be seen that the difference between the rigid support value and the actual value is about 20 per cent at 10,000 rpm and increases rapidly at higher speeds. A similar relation exists between the first critical speed and the rigid support value, but first critical speeds are usually low enough so that the effect of support flexibility is insignificant. Thus, the ratio between first and second critical speeds also varies with speed, as shown in Figure 10-31.[81]

Experience has shown that with proper balancing and assembly of a motor, operation in or through the second critical speed, as well as the first, causes no significant disturbance and is no cause for concern. Figure 10-32[81] shows shaft vibration versus speed for several typical compressors. No attempt to stay away from the critical speeds is necessary. It is clear that the measure of a good machine is smooth, vibration-free operation not the location of its critical speeds.

The influence of the rotor on the main engine structure is a function of both rotor unbalance and transmissibility of this unbalance through the supporting members. There may be several unanticipated combinations of structural elements that can be excited in the operating range of the engine and the problem of altering the structure to remove these resonances could prove difficult. Elimination of the source of

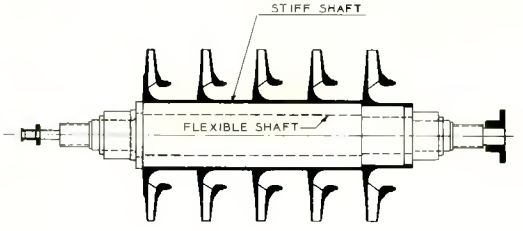


Fig. 10-29 - Relative Proportions of Stiff and Flexible Shafts

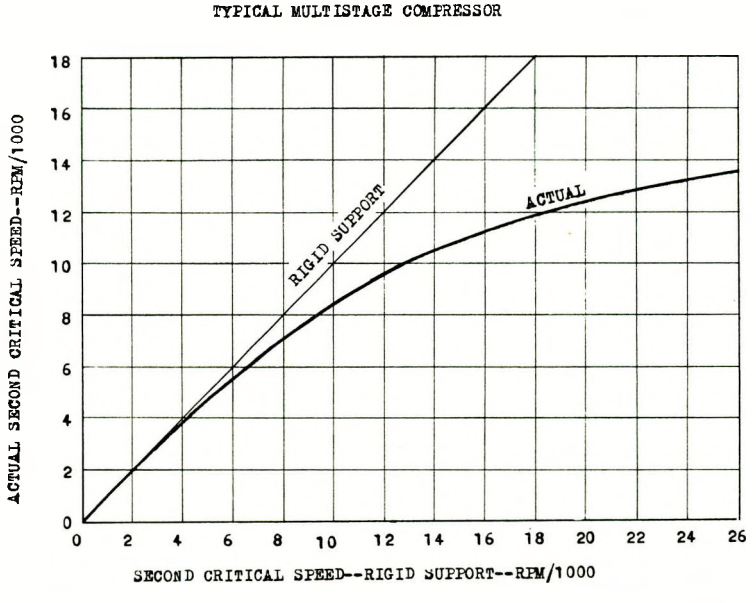


Fig 10-30 - Effect of Rotor Support Flexibility on Second Critical Speed

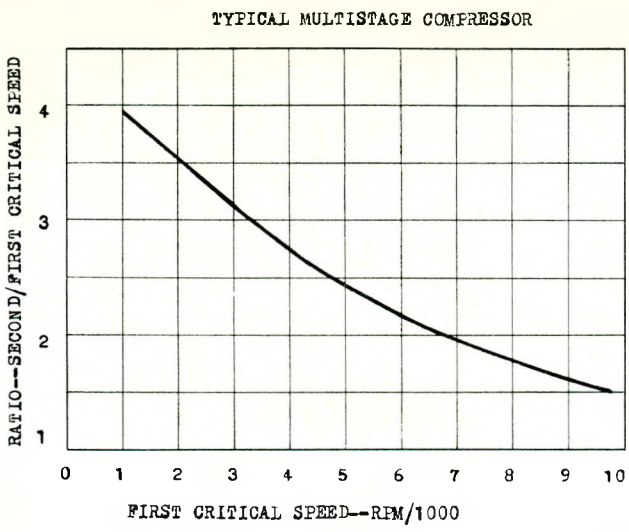


Fig. 10-31 - Relation Between First and Second Critical Speeds

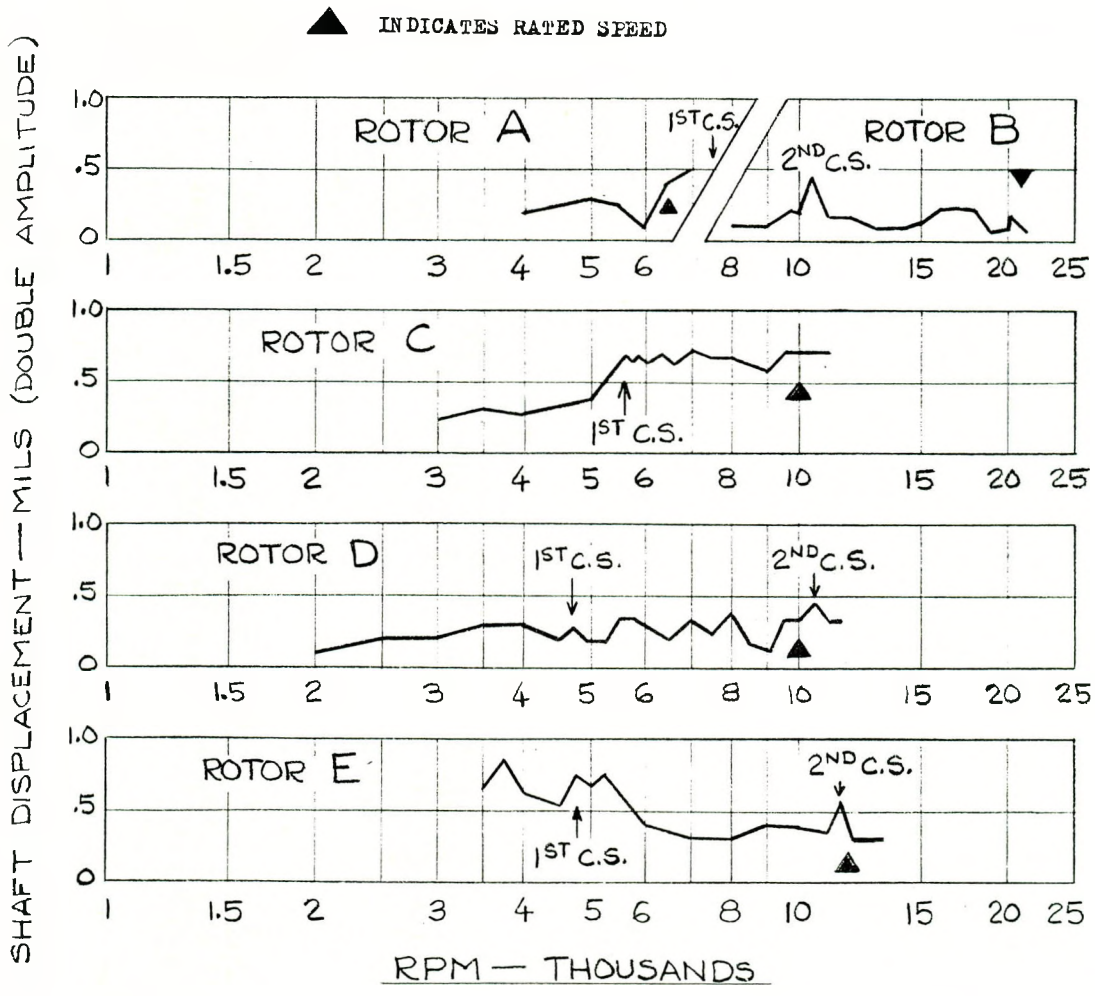


Fig. 10-32 - Vibration of Typical Compressor Rotors

excitation is therefore the most expedient means of preventing these vibrations. Assuming that the rotor is balanced as closely as possible, the only further improvement to be obtained must be through isolation of the rotor from the engine framework. Fortunately, this requirement is automatically satisfied through the use of the soft rotor suspension spring system, which allows the rotor to spin about its principal axis above the first two critical speeds with negligible transmission of force to the main stator.

Continental's practice[134] of utilizing a very stiff main rotor shaft minimizes the tendency to go out of balance at high operating speeds, thereby reducing the amount of mass shift required to accommodate unbalance due to inertial forced deflections. During a series of balancing experiments with a J69 engine employing a spring cage mounting system, it was found that 3.62 oz/in unbalance in the turbine rotor (equivalent to loss of half a bucket) caused an increase in maximum vibration level from 0.32 mils to 0.8 mils, peak to peak, at maximum engine speed of 21,700 rpm. This vibration amplitude amounts to an acceptable 5-g loading. If carried on rigid bearings this unbalance would amount to a rotating force of approximately 3000 lb.

In one test of the spring cage effectiveness on the Model 217-5 turboshaft engine, the flexibility of the rear bearing cage was removed by eliminating the deflection clearance. In spite of close balance of the rotor, vibrational levels increased by a factor of 10 - 20 times. Running experience with the standard rotor suspension system has resulted in very smooth operation throughout the operating range.

In cases where design conditions force normal operation above the first critical speed, manufacturers have their own experience how far they would judge they can go safely. Westinghouse Electric Corporation established a ratio (Design point speed/First critical speed = 2.8) and tries to avoid higher values.[135]

THE FRANKLIN INSTITUTE • Laboratories for Research and Development

T-62302-6

Critical speed calculations are required for each design and manufacturers submit such calculations to the customers. The customer usually stipulates whether the design should be a stiff-shaft design, i.e. whether the engine should operate at all times below its first critical speed. In evaluating critical speed calculations, discussions may arise regarding the necessity of taking into account bearing flexibility, oil film damping, and other refinements. Experience of the manufacturer plays a major part in such discussions. Let us cite a brief discussion of the critical speed analysis of the rotor configuration of the turbo-compressor set CSN-1 for the Army nuclear power package ML-1 as supplied by the manufacturer, Clark Bros. Co.[21]

Rotor configurations from 3600 rpm to 75,000 rpm have been designed for various duties, and experience has shown that the method used for critical speed calculation is adequate when a minimum critical speed of 110% of overspeed is specified. It should be pointed out that it is difficult to determine the actual critical experimentally. This is because modern balancing methods leave extremely small residual unbalance of the shaft, hence low vibration levels exist even at the critical. Independent calculations for critical speed may be made from information given in shear force and bending moment diagram and from detail drawings of rotor shaft and bearing supports as they become available.

An interference diagram for the compressor rotor blades is shown in Fig. 10-33.[21] While not applicable to "critical" speed in the generally accepted sense, it is an area where operation of the T-C set should be restricted if any important interference occurs. In actual fact, calculations indicate that the blade natural frequencies are outside the range of deleterious interference.

The critical speed calculation is performed on the IBM-650 computer and is based on a method outlined by M. A. Prohl.[136] The particular program used is suitable for use with two bearing configurations

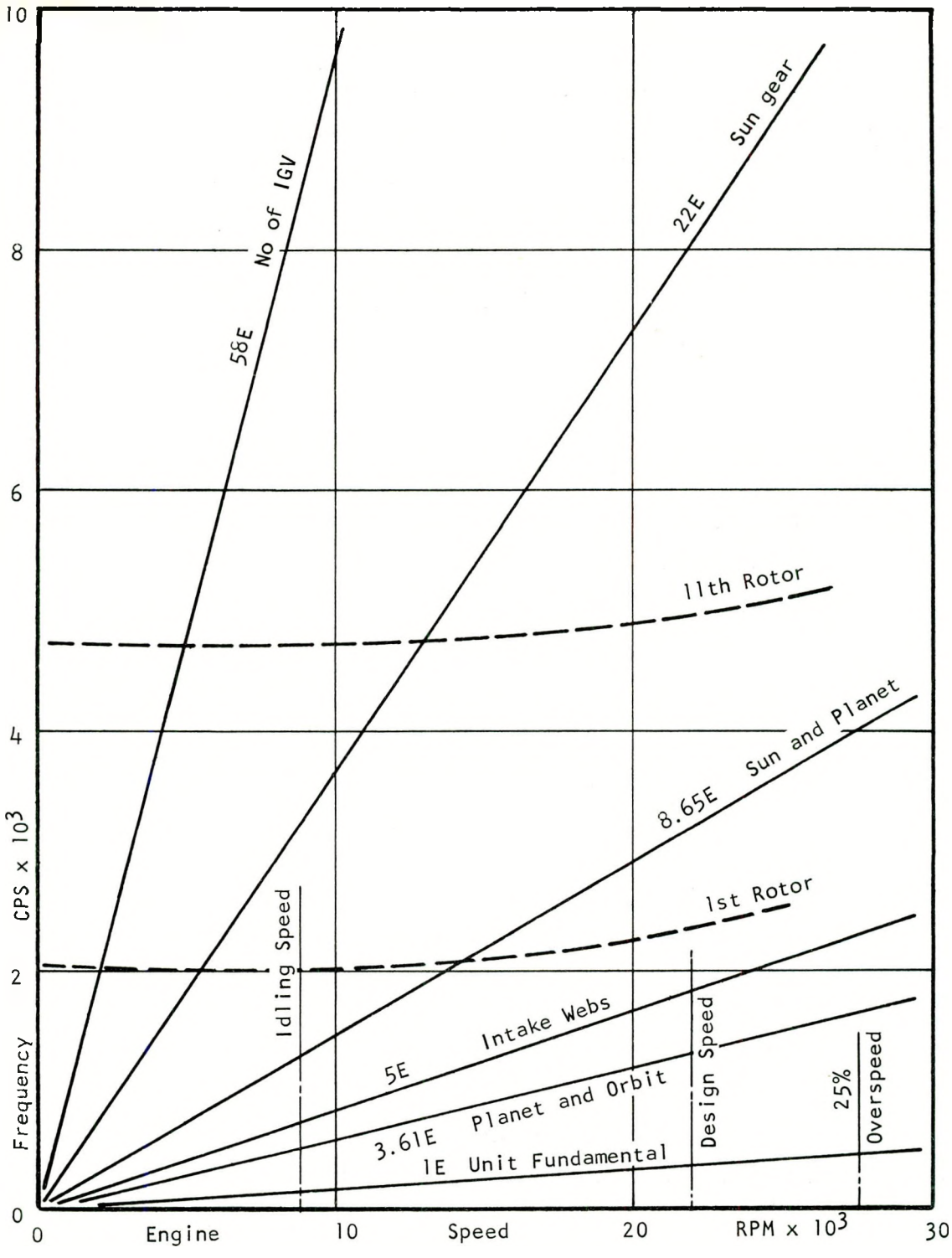


Fig. 10-33 - Clark Compressor Blade Interference Diagram

with or without extending part over the bearings at each end, and includes the gyroscopic moment. The calculation requires that the rotor be split up into 70 arbitrary sections; 20 of these to occur at each overhanging end of the shaft, the remaining 30 to occur between the bearings. Selected speeds are given as input data to the IBM-650, the calculation performed, and the residual bending moment for each given speed read as the result. This residual bending moment is then plotted versus speed, and the point of intersection of the drive end speed axis determines the critical speed.

Several calculations were performed to determine which parameter has the most important bearing on critical speed; it was found that for this particular rotor configuration, the most important parameter was the distance between bearings. An increase of 3% in bearing centerline distance results in a decrease in critical speed of approximately 10 percent.

Final critical speed calculations on the rotor give a calculated critical speed of 30,500 rpm compared with the specification requirements of 30,800 rpm, a discrepancy of less than 1%. In view of the arbitrary nature of selecting the specification requirement that the critical speed should be 140% above the normal running speed, the present calculated critical speed is considered satisfactory.

Shear force and bending moment diagrams for the rotor are shown in Fig. 10-34.[21]

Fig. 10-33 shows the natural frequency range of the compressor rotor blades including the centrifugal stiffening effect. Note that there is no significant interference pattern within the running speed of the machine which can cause "critical" speed problems.

Calculations have not been made at this time on the turbine blades as they are shrouded, making it difficult to predict the resonant frequency of the blade under rotating and loaded conditions accurately.

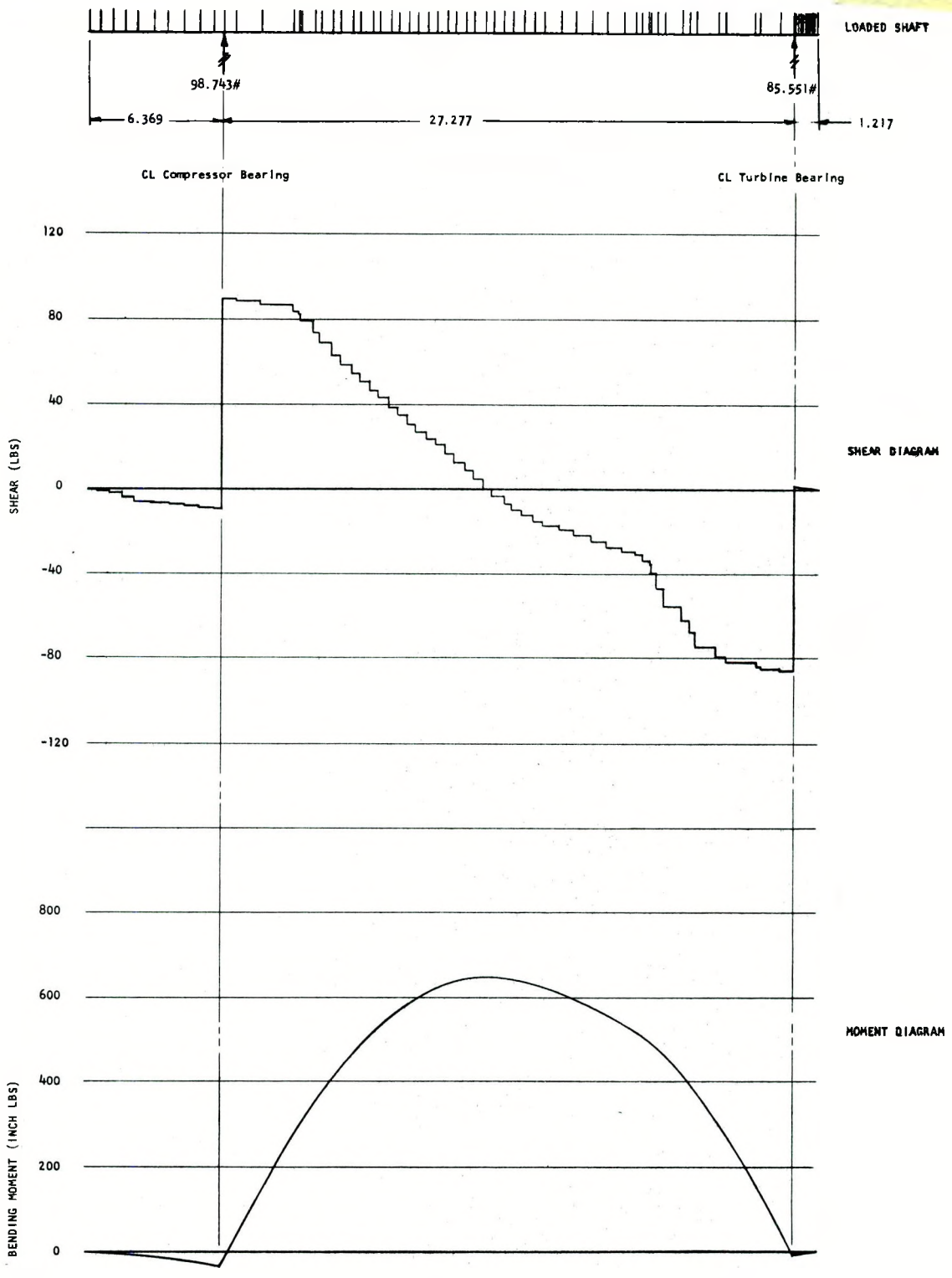


Fig. 10-34 - Clark Rotor Shaft Shear and Moment Diagram

No difficulty with shrouded rotors has been experienced in the past due to interference wakes, and no difficulty is anticipated in this present design, especially in view of the very stiff section of the rotors.[21]

Stratos Division, Fairchild Corp., supplied information on the method they applied to determine the critical speed of the TCS-670 unit for the same Army nuclear power package ML-1 as follows.[22]

The first critical speed of the turbine compressor set with no load on the stub shaft is 29,600 rpm. The method used to obtain the critical speed is an extension of a Holzer-type of iteration as modified by M. A. Prohl.[136] In order to apply the numerical calculation method of this paper, the actual rotor must be transformed into an idealized equivalent system consisting of a series of disks connected by sections of elastic but massless shaft. The mass of these disks and their spacing are chosen so as to approximate the distribution of mass in the actual rotor. Likewise, the bending flexibility of the connecting sections of shaft is taken so as to correspond to the actual flexibility of the rotor.

The method allows for flexible bearing supports and the effects of the mass moments of inertia of any attached disks. Calculations are performed on two IBM-650 data processing systems augmented by floating decimal attachments and index registers. In transforming the actual shaft to the idealized system necessary for calculation the following assumptions have been made:

(a) No coupling load is considered at this time, but will be included when the final reduction gear to turbine-compressor set coupling is selected.

(b) The bearing spring rate is taken as "infinite". It has been Stratos' experience that this gives the best representation with the accurately machined, balanced shaft and carefully aligned tilting shoe bearings used in this machine. While

the tilting journal pads do offer some automatic adjustment for bearing bore misalignment, it has been found that maintaining bearing bore accuracy produces a smoother running bearing. Similarly, the thrust pads bear against a fixed ring accurately located in the unit.

(c) Unity rigidity factors are used for the spacers. The shaft draw bolt is sized sufficiently strong to keep the shaft spacers in full contact despite the maximum bending loads imposed upon the shaft.

The moments of inertia of the rotating elements are listed in Table 10-2[22]. Those for the turbine wheels (including blades and retainers) and the compressor wheels have been found by torsional pendulum measurement of the TCS560 wheels, which are nearly identical to those for the TCS670. The total shaft weight is 123 pounds, located 9.75 inches from the rear of the second stage turbine wheel. The data sheet used for calculating the shaft critical speed is shown as Table 10-3[22].

The following symbols are used on Table 10-3:

R_o - Outer radius of shaft effective in resisting bending.

R_i - Inside radius of shaft effective in resisting bending.

$W_{addit.}$ - Excess weight at station other than that of cylinder of given inner and outer radii and density.

ΔX - Distance to right to next station.

G - Shear modulus

J - Polar moment of inertia in excess to that of cylinder of given inner and outer radii.

E - Young's modulus.

K_n - Bearing spring rate in pounds per inch.

Density - 0.283 pounds per cubic inch.

The first two numbers of the data are 50 more than the power that ten must be raised to in order to obtain the proper decimal place.

Example: 502275 = 2.275

4985 = 0.85

Table 10-2

SHAFT COMPONENT DATA FOR CALCULATING CRITICAL SPEED OF STRATOS SHAFT

Part Name and Item No.	Mass Moment of Inertia (ft. lb. sec. ^{2})	Weight	Location of C. G.
1. Stub Shaft	.0014	4.5	
2. Shaft	.013	32.7	
3. Labyrinth	.00130	2.5	
5. Journal	.00048	1.1	
8. Compressor Wheel	.0236	10.1	1.3 from rear of wheel
7 and 11. Tie Bolt Ass'y.	.00034	2.66	
12. Labyrinth	.00432	6.7	
19? ~~14.~~ Compressor Wheel	.0176	8.3	1.2 from rear of wheel
21. Labyrinth	.00195	2.8	
36. Turbine Wheel and Blades	.0738	24	at center of wheel
37. Turbine Wheel and Blades	.0800	25	at center of wheel
42 Washer	.00003	.31	

Total shaft weight 123 pounds, located 9.75 from rear of second stage turbine wheel. Drawing CL-296, Revision A, is drawn full size and may be scaled for calculations.

Data from Stratos Division, Fairchild Corp., Report SRC-104

Table 10-3

INPUT SHEET FOR COMPUTING CRITICAL SPEED
OF STRATOS SHAFT

RESEARCH COMPUTING CENTER
STRATOS DIVISION

BRG BRG

DATA FOR CARD PROGRAMMED CALCULATOR
IDENTIFICATION:

PROBLEM CRITICAL SPEED SHAFT TCS670
PROJECT. NO. 62-980
SHEET 1 OF 1

STATION	R_o (IN.)	R_i (IN.)	W_n (EXCESS) (LB)	ΔX_r (IN.)	G_n (LB/SQIN)	J_n (SLUG-IN²)	E_n (LB/SQIN)	K_n LB/IN	DIST FROM BACK OF WHEEL
0	5.02275	0	5.08750	5.01410	5.71200	4.92250	5.72900	0	0
1	5.02275	0	5.11750	5.01410	5.71200	4.94500	5.72900	0	1.41
2	5.02275	5.01440	5.08750	5.01180	5.71200	4.92250	5.72900	0	2.82
3	5.02400	4.98200	0	5.01240	5.71200	0	5.72900	0	4.00
4	5.01500	4.98200	0	5.01450	5.71200	0	5.72900	0	5.24
5	5.01500	4.98200	0	5.01720	5.71200	0	5.72900	5.81000	6.69
6	5.02560	4.98200	0	4.94400	5.71200	0	5.72900	0	8.41
7	5.02000	4.98200	0	5.01360	5.71200	0	5.72900	0	8.81
8	5.02000	4.98200	0	5.01000	5.71200	0	5.72900	0	10.17
9	5.02460	4.98200	5.01410	5.01700	5.65440	0	5.71400	0	11.17
10	5.02000	4.98200	0	4.97000	5.66220	0	5.71566	0	12.87
11	5.02000	4.98200	0	5.03540	5.71200	0	5.72900	0	13.57
12	5.02000	4.98200	0	5.01000	5.71200	0	5.72900	0	17.11
13	5.02460	4.98200	5.02710	5.02000	5.65440	0	5.71400	0	18.11
14	5.02000	4.98200	0	4.93500	5.66220	0	5.71566	0	20.11
15	5.01650	4.98200	0	5.02200	5.71200	0	5.72900	0	20.96
16	5.01500	4.98200	0	4.99500	5.71200	0	5.72900	0	22.66
17	5.01500	0	0	5.01170	5.71200	0	5.72900	5.81000	23.61
18	5.01500	0	0	5.03040	5.71200	0	5.72900	0	24.78
19	5.01500	0	0	5.01720	5.71200	0	5.72900	0	27.82
5a	5.01500	4.98200	0	5.01720	5.71200	0	5.72900	5.46250	
5b	5.01500	4.98200	0	5.01720	5.71200	0	5.72900	5.51250	
5c	5.01500	4.98200	0	5.01720	5.71200	0	5.72900	5.52500	
5d	5.01500	4.98200	0	5.01720	5.71200	0	5.72900	5.65000	
17a	5.01500	0	0	5.01170	5.71200	0	5.72900	5.46250	
17b	5.01500	0	0	5.01170	5.71200	0	5.72900	5.51250	
17c	5.01500	0	0	5.01170	5.71200	0	5.72900	5.52500	
17d	5.01500	0	0	5.01170	5.71200	0	5.72900	5.65000	
19a	5.01500	0	5.11000	0	5.71200	0	5.72900	0	
19b	5.01500	0	5.12000	0	5.71200	0	5.72900	0	
19c	5.01500	0	5.13000	0	5.71200	0	5.72900	0	
density	4.92830								
	5.3/2		3	3	38	536		521	

CTR 1 CTR 2 CTR 3 CTR 4 CTR 5 CTR 6 CTR 7 CTR 8

E 108 (4/56)

PREP. BY RSD
DATE 1-9-60

Data from Stratos Division, Fairchild Corp., Report SRC-104

Zero station is taken at the exit side of the second-stage turbine wheel. The values of E and G used at the portion of the shaft where an aluminium wheel has been clamped on the steel shaft have been adjusted to reflect the differences in moduli due to the composite nature of the section. The alternate values of stations 5 and 17 listed are input for various spring rates. Those of station 19 are for various coupling loads.[22]

During development of new turbine engines, vibration problems play an important part. Sound engineering judgment is necessary to evaluate a design during tests where the complexity of simultaneous phenomena must be deciphered to detect the real reasons of some observed abnormal behavior and to find an appropriate remedy for it. As an illustration of how observations lead to decisions, and of how improvements can be made regarding vibrations during tests, the pertinent part of the development of a 3500-hp marine gas turbine, performed by the Utica Division, Curtiss-Wright Corporation, is described.[17]

A serious development problem came to light after 117 hours of operation of the gas generator while compressor performance was being evaluated. A sudden reduction of oil flow to the No. 2 bearing was noted on the flow meter to this area and an emergency stop was made. On inspecting the bearing, it was discovered that the pin retaining the spherical bearing in its housing had failed in shear after apparently severe pounding thus allowing the spherical to rotate and cut off the oil supply (see Fig. 10-35[17]). A previous similar failure of a retaining pin in the No. 3 bearing had resulted in the use of larger pins. However, in this case, 10 of the 12 mid-frame bearing-support bolts retaining the mid-frame bearing housing to the engine backbone had failed in fatigue, and there was also evidence of pounding of the pin retaining the No. 3 bearing spherical. Critical frequencies of the gas-generator shaft were determined with the shaft freely suspended, clamped at the journals and installed in the engine frame. The results of these tests are shown in Figures 10-36 to 10-38[17]. Note that all modes of importance have nodes close to the No. 2 bearing.

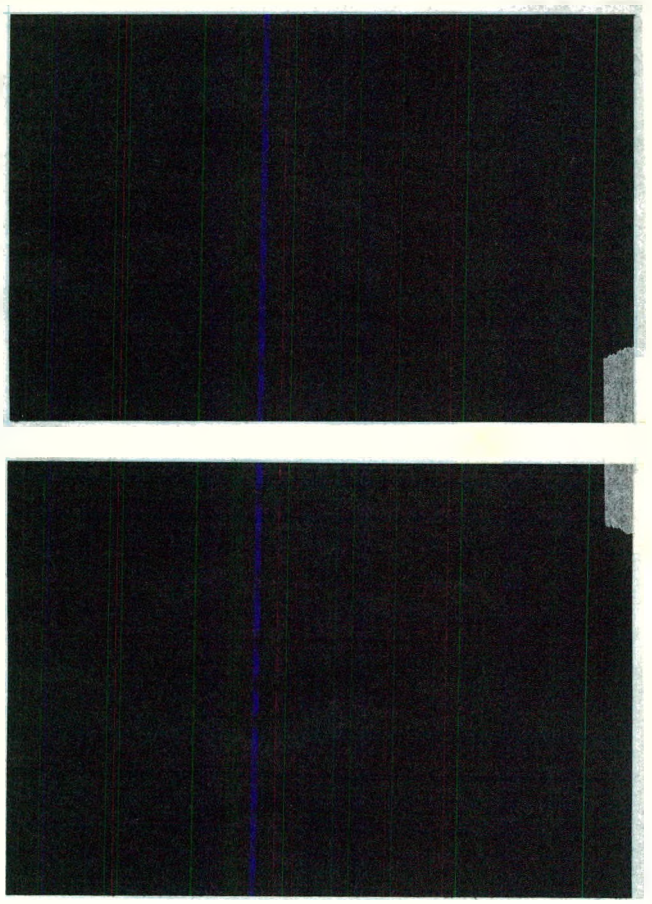


Fig. 10-35 - Spherical Bearing Retaining Pin and Hole Damage

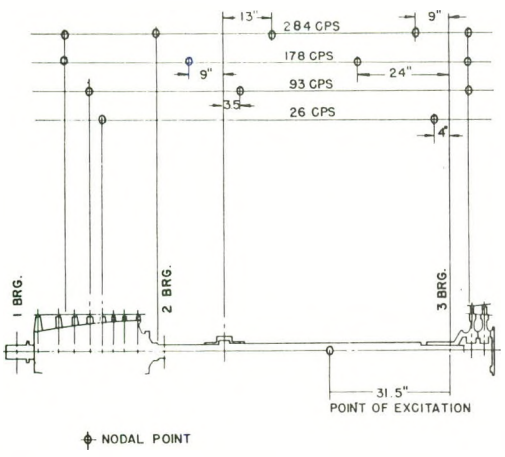


Fig. 10-36 - Frequency Response of Gas-Generator Rotor Assembly in "Free" Condition

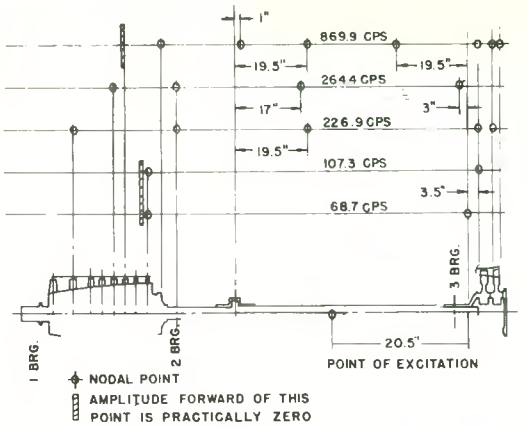


Fig. 10-37 - Frequency Response of Gas-Generator Rotor Assembly in "Fixed" Condition

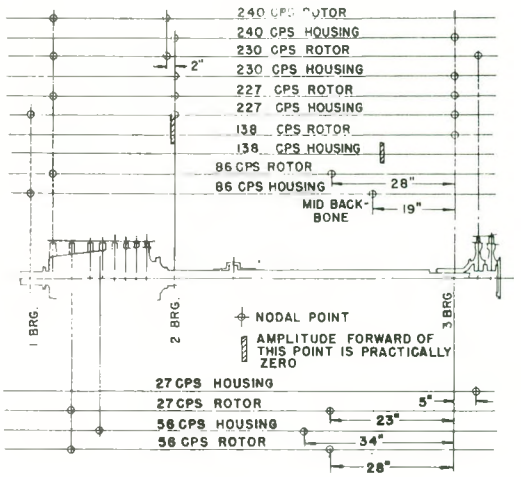


Fig. 10-38 - Frequency Response of Gas-Generator Rotor Assembly as Installed in Engine

Consequently, a critical frequency did not explain the evidence of considerable motion at the bearing housing. No rapid increase in vibration level had been observed with increased speed and since subsequent engine-vibration tests showed that no subharmonics of engine speed were present the possibility of bearing oil-film instability was rejected. Calculations showed that the temperature difference between the spherical and its housing would allow a clearance of 0.014 in. at full speed. It was hypothesized that this permitted the spherical to recess in its housing, striking the retaining pin once every revolution and causing the failure of the pin. The eccentric motion of the rotor under these circumstances resulted in a large rotating force which was responsible for the failure of the housing retaining bolts.

In subsequent models, the spherical housing was replaced by housings of Minovar, whose much lower coefficient of expansion minimized the clearance at full speed to less than 0.004 in. As an added precaution, the detail around the housing-support flange was modified to include a clamp ring to stiffen the flange. This permitted the use of longer bolts, the number being increased from 12 to 24. The bolts were designed with spherical washers under their heads to eliminate stress concentration under the head due to localized bending. Confirmatory tests in which the spherical retaining pin, bearing housing, and bolts were all strain gaged showed that these modifications were successful in eliminating vibration.

The new components have continued to operate successfully for 400 hours. The material of the No. 3 bearing spherical housing was changed to Minovar at the same time. Running experience has confirmed that pin pounding has been eliminated at this point also. One of the interesting by-products of this problem was the revelation of a number of rather complex vibratory modes in which shaft and backbone moved together and which would have been extremely difficult to predict in advance by analytical techniques.

One of these vibration modes in the static condition had a frequency of 230 cps and occurred at the top end of the running range which is 1400 rpm. The pressure loads on the disk resulted in an axial load (11272 lb) which stiffened the shaft sufficiently to raise the critical frequency out of the running range. The introduction of heavier compressor-turbine disks of lower stress resulted in a lowering of this frequency to a speed where the lower pressure loading of the compressor and turbine resulted in much less shaft stiffening. When the arrangement was run, a high vibration was encountered between 11,000 and 12,000 rpm. This problem was solved by using a larger diameter shaft with an integral turbine flange instead of a separate stub shaft for turbine mounting. The inherently higher critical frequency of the new shaft and the elimination of the flexibility of the mechanical joint between main and stub shafts disposed of the offending critical speed. The original and final designs of the shaft are shown in Figure 10-39.[17]

In general, blades of compressors are more likely to fail by fatigue due to vibration. Determination of natural frequencies of blades and disks is therefore an essential part for judgment whether critical vibrations may occur. Fig. 10-40[83] shows nodal lines of blade disk vibrations of a radial impeller as produced on a shaker table. Figure 10-41[83] gives the whole spectrum of natural frequencies of the blades and the disk of one such impeller. An impeller with its blades represents a rather complicated part with a large number of different basic and coupled modes of vibration. In some unfavorable configurations one may always get resonance. Fortunately, however, not all of these modes are critical. Figure 10-42[83] shows an impeller with slightly backward curved blades with strain gages mounted in some critical areas for a test to record blade vibration amplitudes under running conditions. Figure 10-43 gives a nodal pattern of six nodal diameters and one circular node indicated on a disk at 1015 cps (Orenda).

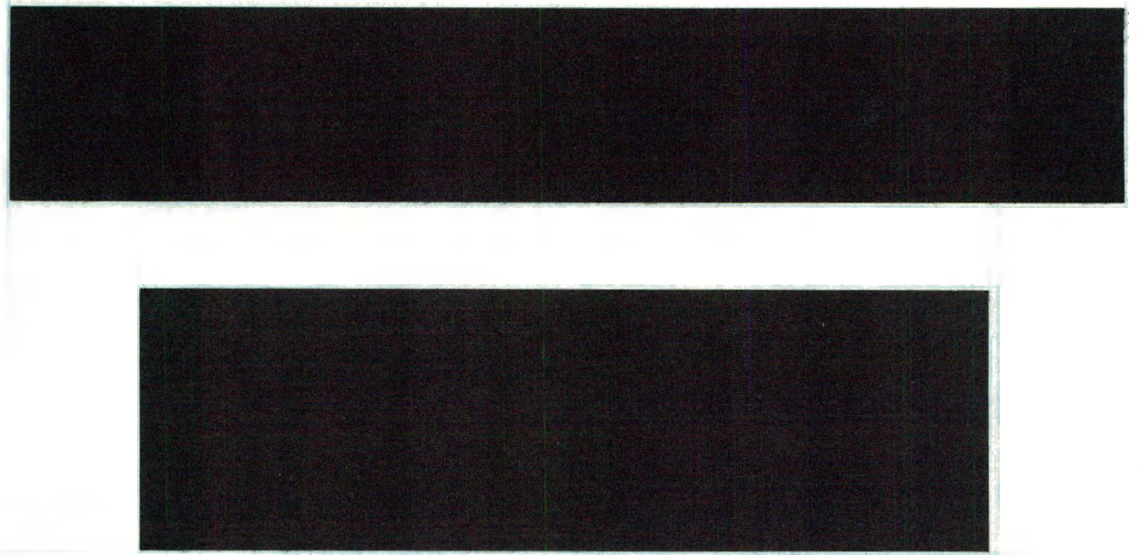


Fig. 10-39 - Original and Redesigned Compressor-Turbine Shafts

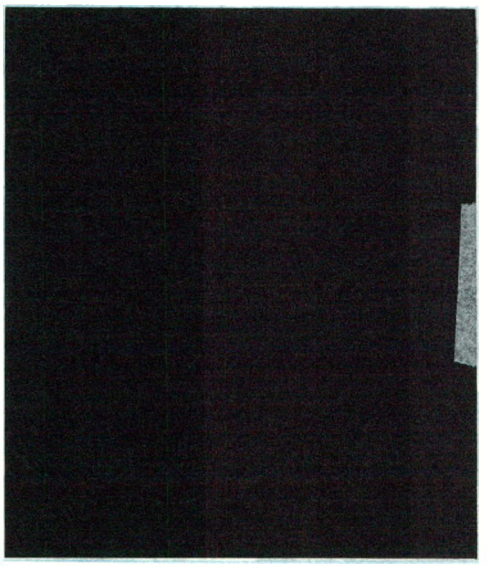


Fig. 10-40 - Nodal Lines of Blade and Disk Vibrations

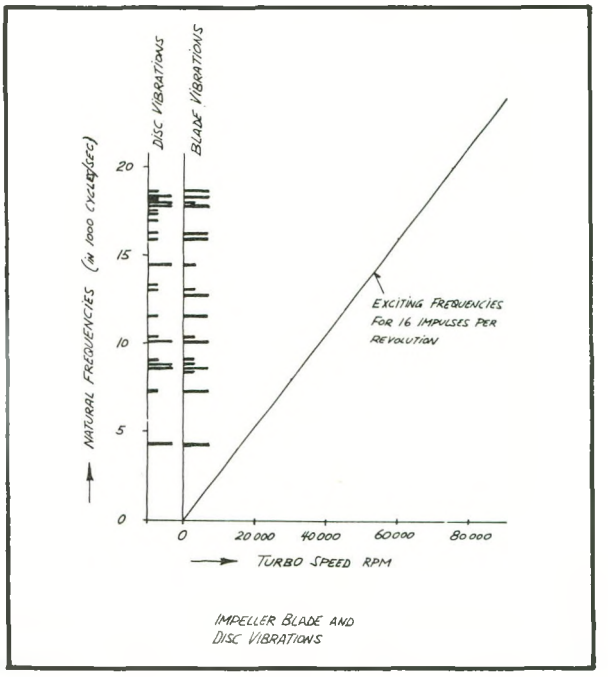


Fig. 10-41 - Spectrum of Natural Impeller Vibration Frequencies



Fig. 10-42 - Impeller with Mounted Strain Gages

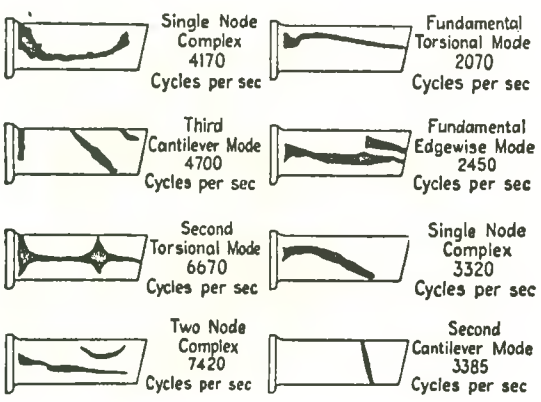


Fig. 10-44 - Principal Modes of Vibration of W2/850 Turbine Blades



Fig. 10-43 - A Nodal Pattern of Six Nodal Diameters and one Circular Node Indicated on a Disk at 1015 CPS

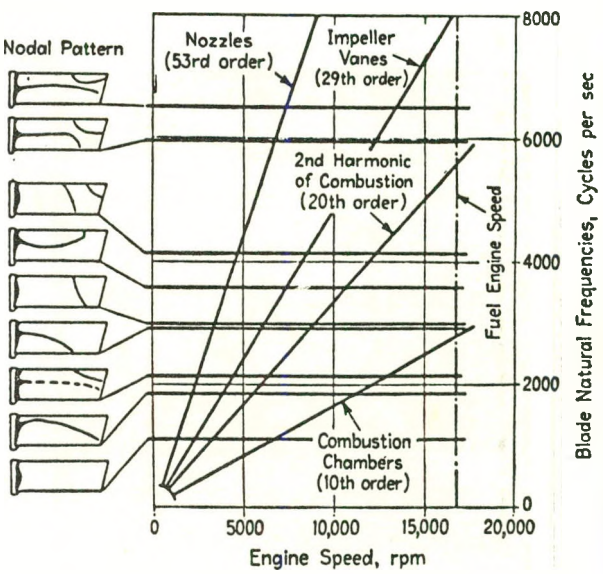


Fig. 10-45 - Interference Diagram for W2/850 Turbine Blades at 700°C

The excitation of turbine blades in the engine is provided by[114]

(a) Combustion chambers (fundamental and harmonics),
(b) Nozzle or stator blades, and
(c) Compressor.

In the base of compressor blades, it is provided by

(d) Spider at the intake, and
(e) Stator blades.

As a consequence of unmatched operation at off-design conditions, stall phenomena in a compressor (surge, rotating stall) can excite serious compressor blade vibrations, but these are transient conditions. Also, they can be governed by regulating stator vanes or by interstage bleed.[124]

A periodic exciting force having a frequency of vibration equal to one of the blade vibration modes will cause the blade to vibrate in resonance. Sustained vibration of this sort can ultimately produce fatigue failure. The exciting forces may be fairly numerous, although the most significant are the result of aerodynamic disturbances associated with flow through nozzles or stationary blade rows, impeller vanes, and combustion chambers. Some excitation may be caused by disk vibration and disturbances originating in gear pumps, gear drives, etc. The non-uniform velocity distribution of fluid across stationary blade passages produces essentially a series of jets corresponding to the number of vanes. As a rotating blade passes through these jets it receives a series of impulses from the gas stream. The frequency of the exciting force, in cycles per second, is equal to the product of wheel speed (rps) and the number of stationary vanes.

Resonance of forced vibration of the rotating blade will occur when the frequency of one of the vibration modes of the blade equals the frequency of the exciting force. There is a classical illustrative example of investigations on blade vibration of the British Whittle W2/850 gas turbine jet unit.[114] Figures 10-44[35] and 10-45[35] show the principal modes of vibration of W2/850 turbine blades.

Figure 10-45 shows a 53rd order excitation produced by the 53 stationary nozzles. The ten combustion chambers and twenty-nine impeller vanes are respectively responsible for the 10th and 29th orders of excitation. For example, at an engine speed of 12,000 rpm, the 10th order excitation occurs at 2000 cycles per second, which is close to the frequency of the first torsional mode and the fundamental edgewise mode. A change in speed of about 800 rpm in either direction will bring the blade into resonance. Thus, considering the several orders of excitation and modes of vibration, a relatively large number of possibilities exist for blade vibration. The designer must attempt to avoid all possibilities of serious vibration through alteration in blade design or changes in the excitation order. (See also compressor blade interference diagram for the Clark CSN-1 T-C set in Figure 10-33.)

The blade root design has influence on the decay of transient vibrations, and the fir-tree root was found to have particularly favorable dampening properties[48]. Furthermore, it is sometimes advantageous to use blade materials with large hysteresis damping even at a sacrifice of fatigue strength. However, it must be noted that the damping capacity of metals usually decreases as the temperature increases.

The alternative of changing the natural frequency will usually be found to be impractical if many equal vibrating members are involved because of the close tuning required.

Shroud rings on top of the blades are an effective means for changing natural frequencies and for increasing damping. However, it is an undesirable design complication.

11. TURBINE COOLING

11.1 General

The advantages of increasing turbine-inlet temperature beyond material-imposed limitations by cooling the blading have been recognized for some time. In the early 1930's, unsuccessful attempts were made in Germany and in this country to develop turbosuperchargers with hollow air-cooled turbine blading. During World War II, the shortage of high-temperature materials in Germany forced the use of cooled turbine blading in operational jet engines. However, the performance of these turbines was low, primarily because of the crudeness of blading design resulting in poor utilization of the cooling air. Since the end of the war, NASA has been working extensively in the field of turbine cooling to determine the fundamentals underlying efficient cooling[51].

Figure 11-1[51] shows the effect of turbine-inlet temperature on thrust and specific fuel consumption for both the dry and reheat versions of a 7.0:1 cycle-pressure-ratio jet engine at a flight Mach number of 2.5 in the stratosphere. Also shown are predicted cooling flow and efficiency depreciation. In the temperature range of 1500 to 2500°F, there is no appreciable change in the thrust of the reheat engine, but the dry engine exhibits an increase of 168 per cent. Specific fuel consumption decreases about 10 per cent for both reheat and dry engines.

Figure 11-2[51] shows the same data for the sea-level static operation of a high-pressure-ratio turboshaft engine. Increase of turbine-inlet temperature by 42 per cent from present-day material-limit temperatures (1600 to 1700°F) will increase the equivalent shaft horsepower by 78 per cent and reduce the specific fuel consumption by 4 per cent. This can be accomplished with about 12.6 per cent of cooling air.

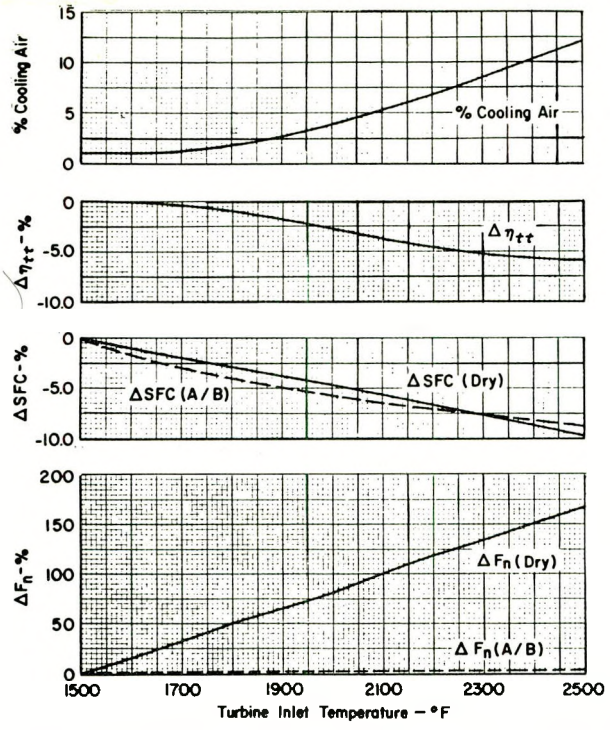


Fig. 11-1 - Jet Engine Performance as a Function of Turbine Inlet Temperature

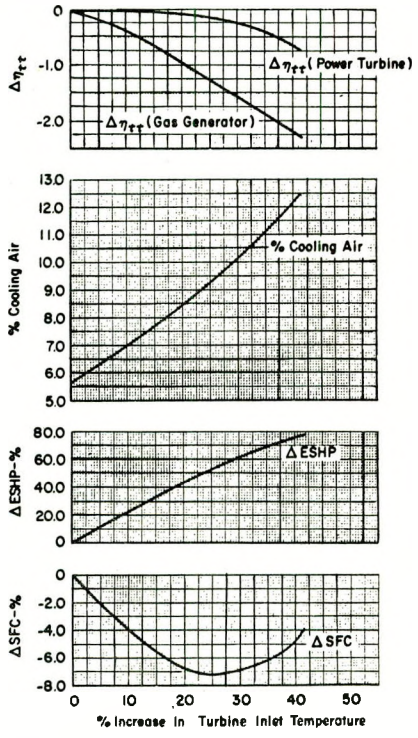


Fig. 11-2 - Turboshaft Engine Performance as a Function of Turbine Inlet Temperature

The improvement in engine performance, as a consequence of convective air cooling, cannot be had for nothing. Some of the disadvantages are:[51]

(a) Increased mechanical complexity of the turbine, including blading design, sealing design, means of getting the cooling air to the turbine, and so on.

(b) Increased manufacturing cost of the turbine.

(c) Reduction in turbine efficiency because of aerodynamic design compromises to effect good cooling, such as solidity reduction and thicker blading, and re-entry of the cooling air into the gas stream.

Although the gains of cooling are now recognized and the fundamentals understood, little success has been achieved. There are no operational jet engines utilizing turbine cooling advantageously.[51] Lack of use, however, can be explained. The jet engine performance shown in Figure 11-1 is for flight conditions which present about the strongest case possible for higher turbine inlet temperatures. At lower flight speeds, particularly at subsonic speeds, increased turbine inlet temperatures result in increased specific fuel consumption. Since subsonic flight speeds were of prime interest to engine manufacturers for several years after World War II, there was no strong desire to build engines to withstand higher temperatures. The primary purpose of turbine cooling research at that time was not to increase temperatures but to provide a means of using fewer strategic materials in the hot parts of the turbine. Since the material supply was found to be adequate for all expected needs, the necessity of turbine cooling did not arise.

Now that aircraft are flying at high supersonic speeds, there is a real advantage to increase turbine inlet temperature. Turbine cooling permits these higher temperatures which provide an efficient means of improving performance of the turbo-prop and turbo-shaft engines. There is little doubt that industrial gas turbines will benefit, after more experience is gained, from research and development in the field of turbine-blade cooling, primarily aimed for aircraft engines.

11.2 Blade Cooling

NASA started investigations on cooling of turbine blades in 1945 and extensive theoretical and experimental work has been performed since. The factors that were found to require study were those needed to determine some of the performance aspects of a cooled-turbine power plant, such as the losses caused by cooling, the net power output, the quantity of coolant required for adequate cooling, etc. Design conditions can also be obtained from these factors, for example, the speed at which the engine can be operated satisfactorily, the gas temperature that can be used, the limiting length of the blade trailing edge section, and the limiting length of the blade critical section.

The required factors can be enumerated as follows:[137]

(a) Convection heat-transfer coefficient from blade to coolant.

(b) Convection heat-transfer coefficient from gas to blade.

(c) Radiation heat-transfer coefficient for heat radiated to outside blade surface.

(d) Radiation heat-transfer coefficient from blade to insert inside blade.

(e) Gas temperature affecting heat transfer (effective gas temperature).

(f) Blade-metal temperature.

(g) Coolant temperature affecting heat transfer (effective coolant temperature).

The complexity of the basic problems may be described as follows. All problems of convection heat transfer are problems of flow of heat through the boundary layer. Consequently, it would be supposed that setting up the equations for the flow of fluid and the temperature variation in the boundary layer could establish the heat-transfer

coefficient laws. Dryden has set up the equations for both laminar and turbulent flows. For laminar flow, nine equations, five of which are differential equations, result with nine unknown terms. Up to the present, little progress has been made in the solution of this formidable problem. Simple problems, such as for flow through a pipe and across flat plates, with the assumption that the flow is one-dimensional or two-dimensional and many other assumptions, have given rise to a solution of the equations that fits experimental results fairly closely. For turbulent flow, the equations are more difficult, the fluctuating-velocity terms and their equations enter into the problem in addition to equations of the type for laminar flow. Consequently, the theory of heat transfer in eddying flow is unsatisfactory at present.

As in many other fields of technical physics where the differential equations governing the phenomena are such that their solution is impractical, if not altogether impossible, experimental techniques aided by the method of dimensional analysis based on the π theorem have proved a valuable tool in the treatment of heat-transfer problems. By use of such an analysis, the Nusselt Number, which involves the convection heat-transfer coefficient, can be shown to be a function of the parameters given in the following equation

$$Nu = \psi \left[Re,\ Pr,\ Gr,\ Ma,\ \frac{k_f(T - T_f)}{\mu_f C_f^2}\ \beta(T - T_f),\ \frac{d}{L} \right]$$

where

Nu = Nusselt number
Re = Reynolds number
Gr = Grashof number
Ma = Mach number
k_f = thermal conductivity of fluid
T = temperature of any heated or cooled section
T_f = mean fluid temperature
μ_f = viscosity of fluid
C_f = velocity of fluid
β = coefficient of thermal expansion of fluid
d = hydraulic diameter
L = length of any passage

For general forced-convection heat-transfer problems encountered in the past, the foregoing equation reduces to

$$Nu = f(Re, Pr)$$

the other terms having little or no effect.

For cooled turbines, many factors may invalidate to some extent the heat-transfer-coefficient laws already established. One factor is that the flow through the turbine is thought to be different from the flow for which the laws were established. Obviously, the flow conditions in a turbine are different from those in a static rig. In any rig, the wakes from the nozzles influence conditions downstream; in the rotating rig an additional effect due to relative motion between nozzles and turbine blades is encountered. Radial pressure gradients result from turbine rotation as well as from the turning action of the blades. Because of the high rotational speeds, centrifugal forces on the gas particles are thousands of times greater than the normal force of gravity. Radial pressure gradients are therefore more pronounced, and cross flow is greater than in a static rig. Centrifugal forces affect the cooling-passage boundary layer as well as the gases on the outer surface of the blade.

Another effect that has been generally neglected but is of particular importance in the turbine is the Grashof Number effect, which evaluates natural convection. For the turbine, the gravity term for the coolant can become about 10,000 to 50,000 times that of the earth's force of gravity because of the rotation of the turbine. Consequently, the Grashof Number value for natural-convection circulation assumes proportions never before experienced and will probably be included in any equation for the inside convection heat-transfer coefficient of turbine blades. Radiation also plays a prominent part in the transfer of heat in a turbine. A difficult effect to determine and for which no data exist is the geometry factor that enters the radiation-coefficient equation.

Evidence exists that, as the gas proceeds along the blade, the temperature of the gas adjacent to the blade surface, which affects the heat transfer, decreases because of the action of the coolant on the blade. Thus the laws of the variation of gas temperature around the blade must be established. Recourse may be had to boundary-layer theory for this problem, but again the solutions are difficult and have to be established. Experimental investigations are about the quickest solution.

At the end of World War II various references became available on work the Germans had been conducting. The agreement between these results and those of NASA was excellent.

It was learned that the practice of blowing air through hollow blades was in general use on the latest types of German engine. Temperatures of about 1550 to 1650°F. could be attained therewith, even though the heat-resisting quality of the material used was not equal to that of American turbine materials. Also considered, and tested in a static cascade of blades, was the use of a thin layer of cold air flowing out of slits in the blade and along the outside blade surface. This method is called "film cooling". This protective layer acted as a shield between the hot gases and the blade surface. A favorable cooling effect with a small amount of air was obtained. The greatest water-cooling progress was made with a single-stage turbine that ran in continuous operation at a turbine-inlet temperature of 2,200°F. with a cooling process devised by Dr. Ernst Schmidt of the Hermann Goering Institute.[137]

Analytical studies were performed by NASA with some simplifying assumptions, with regard to three possible methods of conduction cooling: (a) rim cooling, in which the temperature of the rim of the turbine disk is reduced by the cooling medium and the solid blades are cooled by conduction of heat to the rim: (b) hollow blade air cooling, in which air is passed through hollow turbine blades and heat flows through the thin metal shell forming the turbine-blade contours to the air and

(c) liquid cooling, in which liquid is circulated through passages formed in the turbine blades and disks and heat flows through the metal to the cooling fluid.

Before any experimental work was done, it was recognized in these studies that rim cooling allows little increase in effective gas temperature over that obtained without cooling but that blade life can be increased appreciably with the small decreases in blade temperature caused by rim cooling. Furthermore, analyses gave the expectancy that at a Mach number of 0.6, an effective increase of about 500°F can be obtained with hollow-blade air cooling and an increase of about 650°F with air cooling when an invert is placed in the hollow blade. Liquid-cooled high-melting-point alloy-steel turbines appeared to be able to operate at turbine-inlet temperatures near those obtainable with present-day fuels.

The desirability of doing experimental work with stationary and rotating cascades was early recognized. The advantage of being able to apply data from static cascade rigs, which are simple to construct and operate, to turbine design is evident. The applicability of the data is determined by checking against data from rotating cascades of blades. Rotating cascades of blades were expected to shed considerable light on such factors as boundary-layer flow with centrifugal forces and under radial pressure variations on both inside and outside surfaces of the blades, natural convection effects tending to augment the internal heat-transfer coefficient, compressibility temperature-rise effects in cooling-air passages, actual losses incident to pumping air through blades, and relative losses of various discharge methods (i.e., from tip, with and without controlled vector, or into boundary layer). None of these vital factors can be handled in static cascades. Results of some of the experiments are given in the following sub-sections.[137]

THE FRANKLIN INSTITUTE • Laboratories for Research and Development

F-A2392-4

11.3 Convective Air Cooling

When air-cooling is incorporated in an engine, the entire engine design must be considered so that the air will be utilized most effectively. A possible engine configuration is shown in Figure 11-3.[138] Three of the principles used in air-cooled turbine blades are illustrated in Figure 11-4.[138]

The most conventional air-cooling method used in all heat-transfer processes as well as in air-cooled turbine blades is convection cooling shown in Fig. 11-4a. With this method it is desirable to increase the heat-transfer surface area on the heat-rejection side of the blade by means of fins. In film cooling, Fig. 11-4b, a film of cool air is introduced through slots to form an insulating layer between the hot gases and the cooled surface. The thermal conductivity of air is low so that it is a good insulation medium, but the effectiveness of the layer of the air is lost some distance downstream of the slot because of mixing with the hot gases. This disadvantage is eliminated by transpiration-cooling, the most effective method of air cooling known at present Fig. 11-4c, because air is continuously passed through the entire area of a porous surface.

Air-cooled blades utilizing these cooling methods, whose comparative effectiveness was studied, are illustrated in Figure 11-5[139] with the approximate year of their development. Figure 11-6[138] shows a sketch of a transpiration-cooled blade utilizing orifices in the base for metering cooling air.

The design and manufacture of transpiration-cooled blades is difficult because the coolant-flow rate is a function of permeability of the shell and the pressures inside and outside of the blade. Because of the high-pressure gradients on the outside of the shell, a metering device is required at the blade base to meter air to each of the passages formed by the strut and the porous shell. The air can be

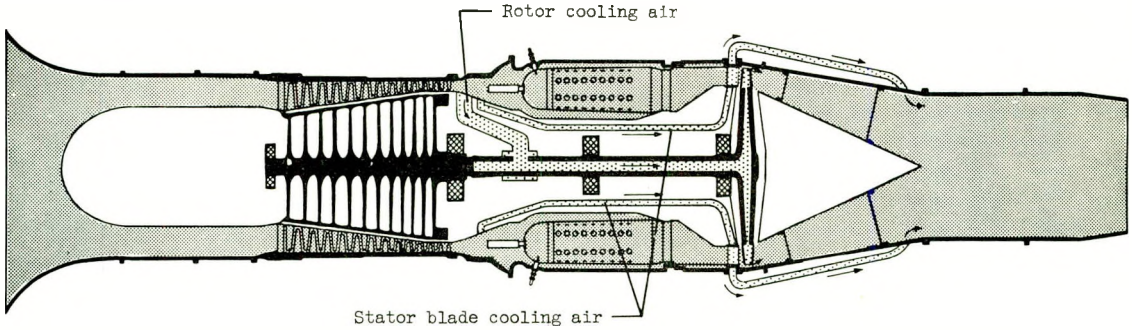
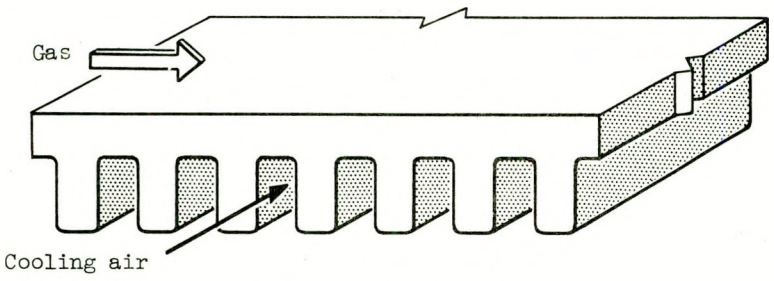
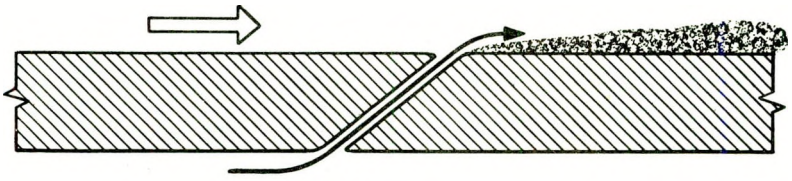


Fig. 11-3 - Cross Section of Air-Cooled Turbojet Engine



(a) Convection cooling.



(b) Film cooling.



(c) Transpiration cooling.

Fig. 11-4 - Three Methods of Air-Cooling Turbine Blades

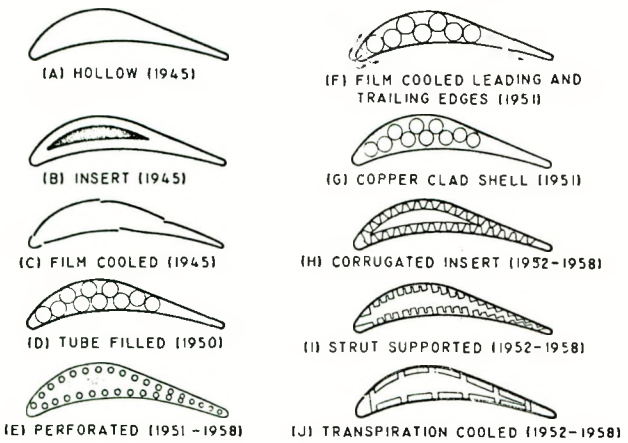


Fig. 11-5 - Air Cooled Turbine Blade Configurations

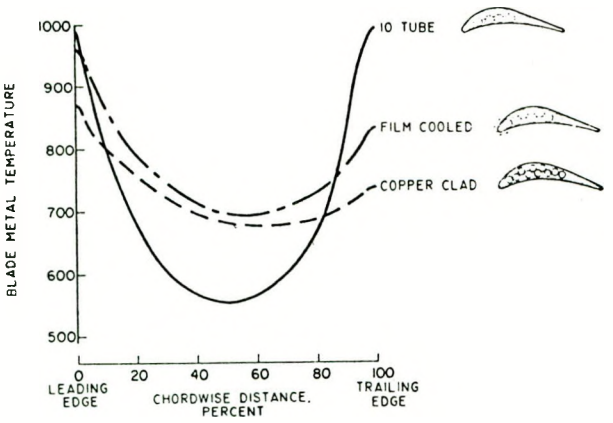


Fig. 11-7 - Effect on Metal Temperature of Special Methods of Cooling Leading and Trailing Blade Edges

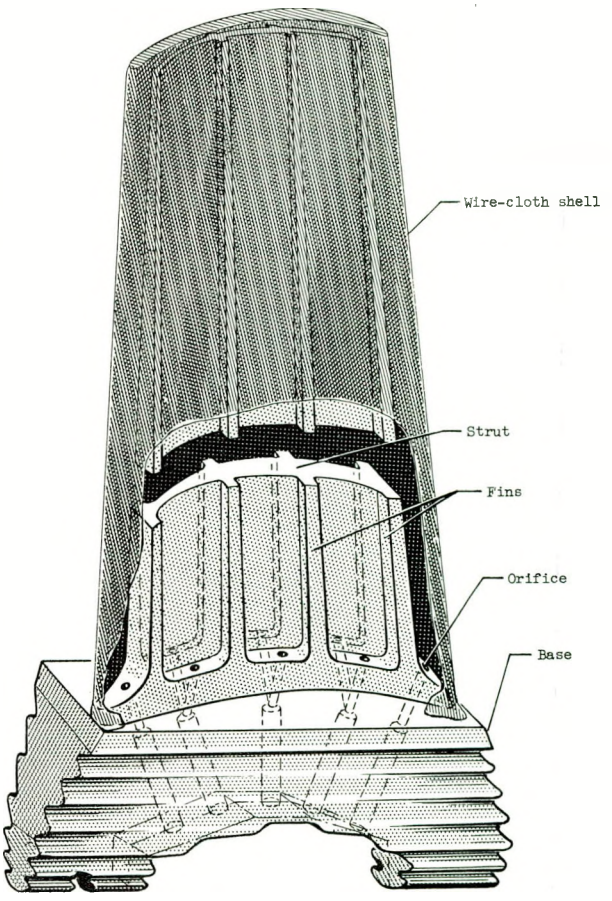


Fig. 11-6 - Transpiration-Cooled Blade Utilizing Orifices in Base for Metering Cooling Air

metered by orifices as shown in Fig. 11-6. Shell permeability must also be controlled very carefully in order to get the proper flow distribution of the coolant that will result in uniform cooling.[139]

The hollow, insert, and film-cooled blades, Figs. 11-5 (A) to (C) were used or considered for use in engines by the Germans prior to 1945. The cooling effectiveness of the hollow blade is so low that excessive quantities of cooling air are required. An insert in the interior of the blade, Fig. (B), improves the cooling effectiveness by increasing the coolant velocity at the expense of increasing the pressure loss for a given flow rate. By proper placing of an adequate number of slots in the blade wall, Fig. (C), film cooling will provide good cooling, but durability of this type of blade has been found to be poor.

The tube-filled blade, Fig. (D), was an early attempt by NASA to build an air-cooled blade with additional surface area brazed in place in the coolant passage in order to improve the cooling effectiveness. Although more recent blade developments have led to superior blade configurations, much valuable information has been obtained from the tube-filled configuration, and experience was gained in the operation of air-cooled turbine blades made of nonstrategic materials. Suitable coatings for inhibiting oxidation of low-alloy steels have been reported.

There has been a reluctance on the part of some engineers to utilize a brazed structure in turbine blades. The perforated blade, Fig. (E), overcomes this objection because it does not rely on brazing. Instead, a number of holes are provided near the periphery of solid blades by drilling, casting, or other methods. Considerable research has been conducted both in England and the U.S. on this type of blade which, although a more homogeneous structure, is usually heavier, resulting in higher disk stresses and generally less blade taper is feasible so that the blade stresses are higher than for some of the brazed blades.

Adequate cooling of the leading and trailing edges can be a problem with almost any configuration. In an attempt to improve cooling effectiveness in these regions of the tube-filled blade, film-cooling, Fig. (F), and copper-clad shells, Fig. (G), were investigated. The copper-clad blade is a type of structure similar to that of copper-clad kitchen utensils in which the copper spreads the heat over the entire area of the utensil. In the case of cooled turbine blades, the copper cladding is on the inner surface of the blade shell.

The effects on reduction of temperatures of turbine-blade leading and trailing edges are shown by the experimental data in Fig. 11-7.[139] It will be noted that the blade-temperature gradients can be reduced by use of film-cooled and copper-clad blades, but the leading and trailing-edge cooling is done at the expense of increased temperatures in the mid-chord region of the blades. The film-cooled blade shown operated only slightly cooler at the leading edge than did the 10-tube blade. The amount of cooling obtained in this region is a function of the configuration and the relative pressures on the inside and outside of the blade. At higher flow rates, this cooling becomes more effective because a greater portion of the air is bled from the slots. The blade must be designed specifically for the application for which it is intended, and the coolant supply pressure must be higher than the stagnation pressure at the blade leading edge. More effective leading-edge cooling has been found in other film-cooled blades. Durability of this type of blade was found to be a serious problem. Because of durability difficulties in turbine rotors, blades such as shown in Figs. (C) and (F) would probably be more successful when applied to stators, provided that cooling air pressure is sufficiently high.

As shown in Fig. 11-8[139] use of plain hollow blades is very impractical for cooled turbines because the coolant-flow requirements are exorbitant. On the other extreme is the transpiration-cooled turbine blade which ideally requires only small amounts of coolant even

for large increases in turbine-inlet temperature. In practice, however, the excellent cooling of the transpiration-cooled blade has not been demonstrated because of difficulties in obtaining uniformity of flow over the blade surface. In order to keep local areas from over heating, coolant flows have had to be high and, as a result, other areas are much overcooled. Further development in methods of precisely controlling shell permeability is required to overcome this difficulty in transpiration-cooled blades.

The use of air-cooled turbine blades will require a different type of turbine-rotor construction from that in current use. There is, however, considerable freedom in the type of design possible. Two main types of turbine rotors are the split disk and the shrouded disk, Fig. 11-9[139]. With either type of construction, the cooling air can be supplied from the upstream direction, the downstream direction, or through a hollow turbine shaft. With any of these possible types of construction, internal vanes are required in the turbine rotor to direct and help pump the cooling air out to the blades. Results of experimental tests with the type of disk configuration shown in Fig. 11-9 indicate that disk cooling will be adequate with the amount of air required for blade cooling.

Fig. 11-10[139] shows two types of impeller-vane configurations that have been investigated in air-cooled turbine disks. The experimental results showed that there was little or no advantage in providing the curved inducer section in the vanes as shown in Fig. 11-10(B). For a given coolant-flow rate, the vane configuration did not affect the supply pressure required significantly. Further, it was found that the efficiency of such an impeller system in the turbine disks has a negligible effect on engine performance.

General Electric Company, in an effort to design and develop a convective air-cooled turbine and test facility, arrived at the following heat-transfer considerations.[51]

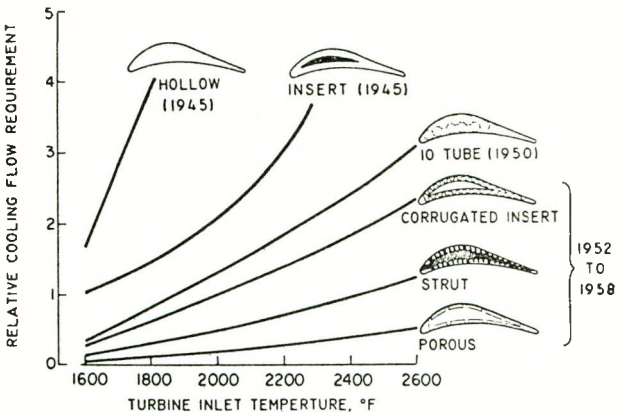
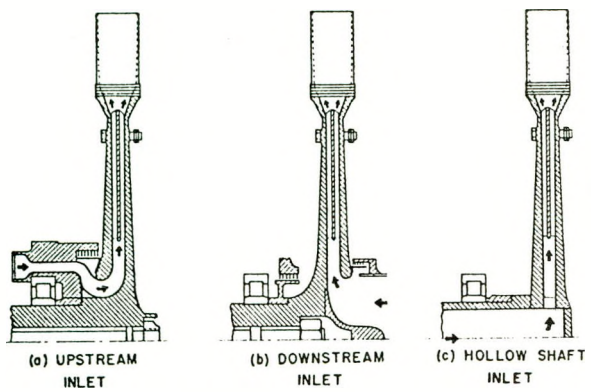
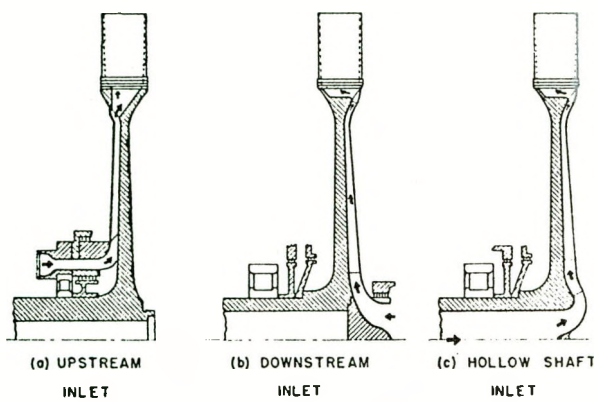


Fig. 11-8 - Comparison of Relative Coolant Flow Requirements for Several Types of Air-Cooled Turbine Blades



Split Disk Type



Shrouded Type

Fig. 11-9 - Air-Cooled Turbine-Disk Configurations

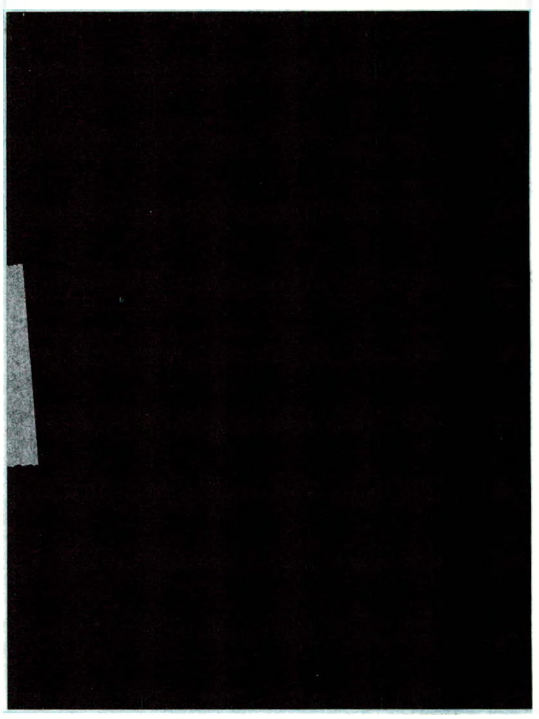


Fig. 11-10 - Impeller Vanes for Air-Cooled Turbine Disks

In the design of any air-cooled turbine, economic use of the cooling air requires that the external surface area of blading swept by the hot gas be reduced as far as possible and that the number of blades be held to a minimum. In addition, the number of stages should be reduced to a minimum and the relative bucket temperature be held down, which means reducing blade reaction. To obtain good cooling-passage configuration within the blade, rounder leading edges and thicker trailing edges than have been used in the past must be employed. All of these requirements, to achieve good cooling with a minimum of cooling air, tend to reduce the expansion efficiency of the turbine. In addition, expelling the cooling air from the blade rows back into the main gas stream and extracting heat from the gas stream might well affect the performance adversely. Although the importance of turbine efficiency diminished with increasing turbine temperatures, efficiency cannot be discounted where efficient part-load operation is required. Hence, the designer is faced with the problem of compromising the aero-thermodynamic design to effect good cooling without materially reducing efficiency. Table 11-1[51] shows the percentage difference, for several important blade parameters, between the normal and air-cooled versions of the tested turbine.

Table 11-1

COMPARISON BETWEEN NORMAL AND AIR-COOLED TURBINE BLADING

Compared Value of Blading	Percentage Change for Air-Cooled as Compared to Normal	
	Nozzle	Bucket
Root Axial Width	+ 25.5	+ 37.0
Number of Blades	- 18.6	- 39.6
Leading Edge Radius	+ 50.0	+ 33.3
Trailing Edge Radius	+ 50.0	+ 66.7
Solidity	0	- 18.7

In the interest of good cooling, the number of blades in each row was reduced, and in the interest of high efficiency, the chord was increased. Reducing the number of blades reduces the external cooling surface and increases the cooling flow to each blade. The increased cooling flow per blade results in higher Reynolds numbers in the internal cooling passages, insuring that the flow is turbulent over as wide a range as possible with higher internal film coefficients. In addition, larger cooling passages are required, a fact which eases the manufacturing problem.

Figure 11-11[51] shows cross-sections of air-cooled blading of the type tested. The nozzle blade is of the shell-insert type. Compressor discharge air enters the blade at the tip and fills the interior of the insert. The air flows upstream through holes in the insert leading edge, impinging on the skin leading edge. Then the air turns 180° and flows axially along the section and pressure sides through passages on each side formed by skin and insert. Finally, the cooling air is expelled to the main gas stream through slots in the trailing edge. This type of design was selected because it provides good cooling for the critical leading and trailing edges and offers the opportunity of improving performance by filling the trailing-edge wake.

The bucket consists of a cast stand with a brazed sheet-metal skin. Compressor discharge air enters the forward wheel space and flows radially outward to the tip, where it is expelled to the main gas stream. This type of design was chosen because of manufacturing ease and low cost, good insulation of the load-carrying strut, ability to control cooling-air-passage configuration and potential growth. A schematic of the cooling-air flow path is shown in Figure 11-12.[51]

In general, the leading-edge section of the turbine blade is the most difficult portion to cool because of the high heat flux and the restricted space available for placing internal coolant passages at this location. Early attempts to improve the cooling of the

THE FRANKLIN INSTITUTE - Laboratories for Research and Development

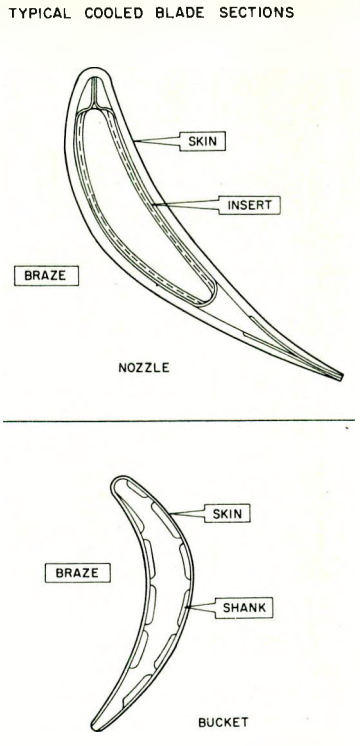


Fig. 11-11 - Air-Cooled Blade Cross Sections

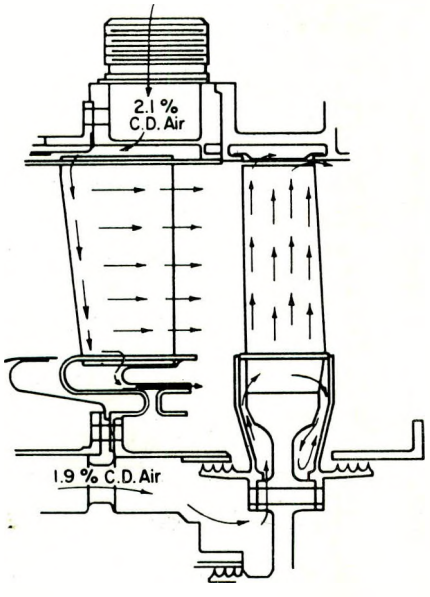


Fig. 11-12 - Cooling-Air Flow Path in Blading

leading-edge region with copper cladding on the inner surface of the shell and with film-cooling of the immediate leading-edge area through spanwise slots were not satisfactory.[46] The first method reduced the structural integrity of the blade by increasing the stress level, and the second method subjected the blade to vibrating failure from the addition of slots. However, use of chord-wise leading-edge tip caps to divert the discharge of coolant for the leading-edge passages to a lower-pressure region toward the rear of the blade chord has been shown to be effective at low coolant rates.[140] The blades could operate satisfactorily with a turbine-inlet temperature of 2000°F and a coolant flow of 3 per cent of engine mass flow or less, with an average chordwise temperature limit of 1400°F.

Figure 11-13[140] shows the schematic view of the most successful type of blade investigated. Later tests were even more successful. An air-cooled turbine with corrugated-insert type stator and rotor blades was operated in a modified production-model engine, having a split-disk turbine rotor. Results indicated that operation of turbojet engines at turbine-inlet temperatures up to 2500°F appears to be feasible. Combustors and turbine stator blades, in addition to turbine rotor blades, were critical components at these temperature levels. An average chordwise rotor blade temperature of 1300°F was maintained with a coolant-to-gas weight-flow ratio of about 0.022 when the average turbine inlet temperature was 2500°F and coolant inlet temperature was 260°F.

An average blade temperature of 1300°F would result in a stress-ratio factor (allowable to actual stress) of about 2.45 at the critical one-third-span location. Leading-edge caps on the turbine rotor blade improved the cooling of the low average coolant-flow ratios (0.02 or less). Data obtained were not conclusive enough to make a definite selection of optimum tip cap length, but indications were that the longest cap (0.55 chord) resulted in the lowest average blade temperature. Figure 11-14[46] shows the type of blades tested, and Figure 11-15[46] the arrangement in the assembly.

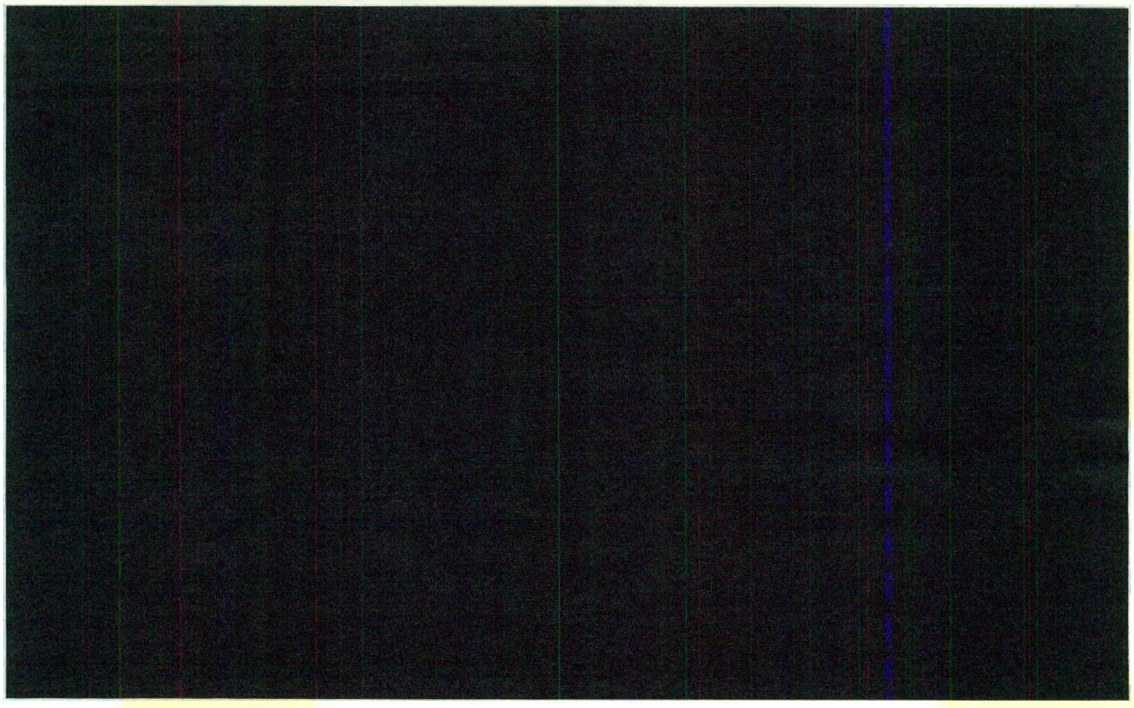


Fig. 11-13 - Slanted-Conrugation Tip-Capped Blade

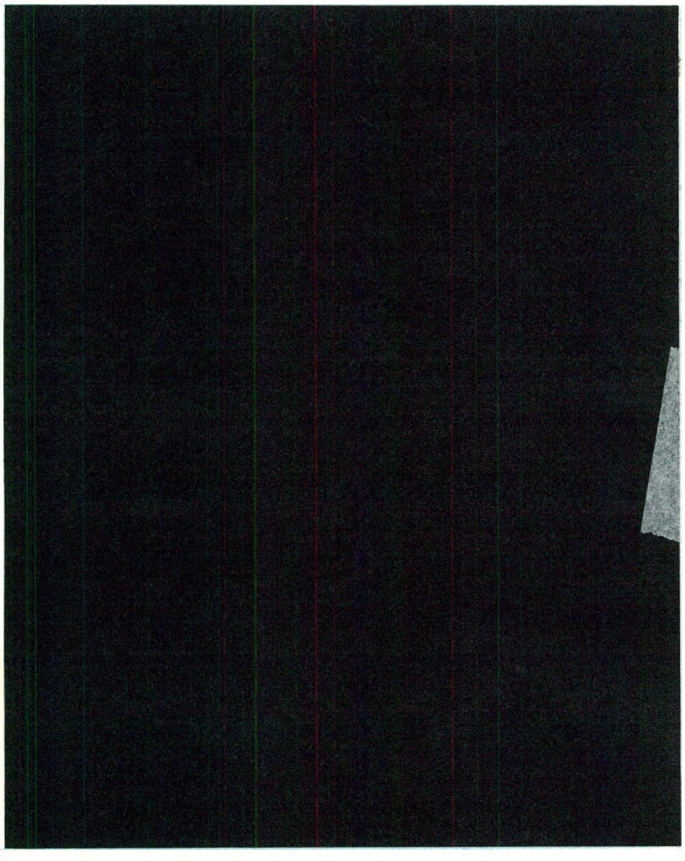


Fig. 11-14 - Air-Cooled Corrugated-Insert Turbine Rotor Blade with Leading-Edge Tip Cap

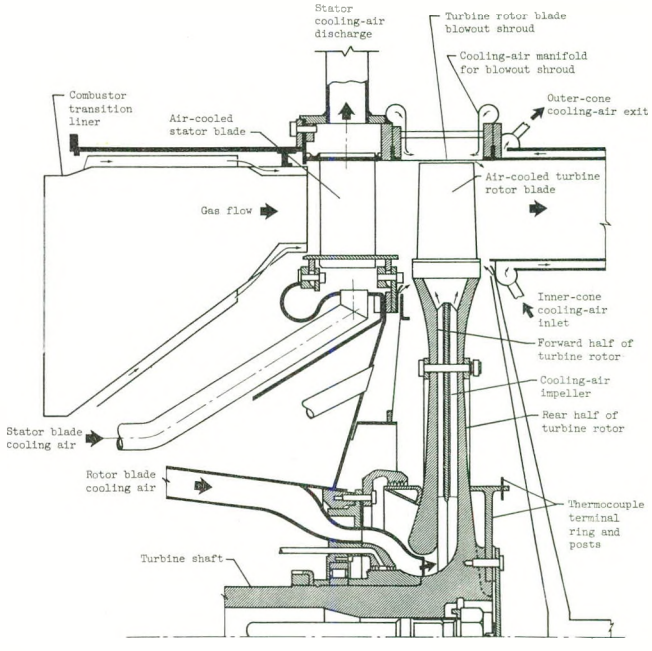


Fig. 11-15 - Air-Cooled Turbine Component and Adjacent Parts

11.4 Water Cooling

Internally water-cooled turbines have been operated in this country and in Europe, a logical method because of the excellent heat-transfer characteristics of water. Water as a turbine coolant, however, has one serious disadvantage, the boiling point is so low that, unless the entire coolant system is under high pressurization, the turbine is overcooled and the heat-rejection rates are excessive. A further disadvantage occurs in aircraft at high-flight speeds because the ram-air temperature exceeds the boiling temperature of water at normal pressures, and heat rejection in a ram-air heat exchanger becomes difficult. The ram-air temperature reaches 212°F at a flight Mach number of about 1.2 at standard sea-level conditions and at a Mach number of about 1.9 in the stratosphere.

Pressurization of the entire coolant system, would offer relief, but in order to pressurize the system to a point where water could be at a temperature that would not result in overcooling of the turbine, the system would have to be pressurized to approximately 3000 psi. A method of eliminating this difficulty would be to use special coolants such as Dowtherm or liquid metals with higher boiling points than water at normal pressure level.

The design of liquid-coolant systems requires a knowledge of heat-transfer coefficients for forced and free convection and the temperature gradients to be expected in the blade metal. Considerable experimental and analytical data have been obtained that are applicable to liquid-cooled turbines.

The British have given thought to the use of a thermosiphon liquid-coolant system for turbine blades, where the small amount of coolant placed in the turbine is not enough to fill the blade-coolant passages. The coolant evaporates in the blades and the vapor is passed over a heat exchanger and condensed. The condensate then flows back to

the turbine blades to be evaporated again. This system holds promise for some applications. Its primary advantage over other types of liquid-coolant systems is that the internal pressures in the blades can be considerably lower.

Water-spray cooling offers possibilities for certain limited applications where a boost in power is required for short periods of time. Spray cooling for prolonged periods of time, however, results in excessive liquid consumption because the water used as a coolant is lost. Using this method of cooling the rotor blades alone permits the turbine-inlet temperature to be increased to the point where the stator blades provide a limitation.

For relatively small rotor blades, the temperature can be reduced adequately by spraying water onto the blade from a few (up to 8) stationary circumferential locations. However, because of low water velocities relative to the gas and turbine-wheel velocities, the coolant supplied from stationary locations impinges on the blades near the leading edges only and cooling may not be provided at the trailing edges of large rotor blades. This difficulty can be overcome by supplying water spray from rotating orifice at the blade base. Thermal shock to the blades when the water is introduced has been found to be a problem. Some materials are much better than others, but nearly all blades of turbojet-engine size eventually fail after some given number of shock cycles.

To increase turbine-inlet temperatures above the limit imposed by uncooled stator blades using water spray as a coolant would involve additional complications and larger total coolant flows would be required. The total flow would be about 2 to 4 times the weight-flow rate of fuel required for a single-stage engine. For multistage engines the flow weights would probably be higher yet.

Consideration has been given to fuel injection ahead of the turbine for afterburner use. Although few experimental temperature data are available, it is not believed that the quantities of fuel required for suitable afterburning temperatures would be adequate for use in cooling turbine blades. Water would still have to be injected to augment the cooling from the fuel spray.

Water-spray cooling would probably be most beneficial during take-off of aircraft having marginal take-off power. For such a case, the turbine-inlet temperature could be raised a few hundred degrees. The water used for cooling would be expended during the take-off run, and the weight of the coolant would not have to be carried during the remainder of the flight. This method of cooling would also be useful for short bursts of emergency power during flight.[139]

11.5 Experimental Cooled Turbines

One of the objectives, for which turbine blade cooling is needed, is the development of an efficient gas turbine that utilizes few or none of the so-called strategic materials (nickel, chromium, molybdenum, tungsten, cobalt, columbium, beryllium). The Solar Aircraft Company conducted some experiments along this line. A three-stage turbine rotor was to be cooled with a closed cooling system. Methods of stator cooling were optional. From combined cycle and cooling considerations, the turbine inlet temperature was set at 1750°F. The components of this turbine were designed of nonstrategic, low-alloy steels. As coolant, water was selected for the rotor and a forced-convection system established. To eliminate boiling within the cooling passages where pressure was not available, fluid temperatures had to be kept below 200°F. At this temperature, the low turbine blade temperatures resulted in an excessive amount of heat being extracted by the coolant, with the effect that over-all performance dropped by about 20 per cent. Because of material limitations, temperatures in highly stressed regions had to be maintained

below 800°F, and peak metal temperatures limited to about 1100°F. The calculated variation of coolant temperature rise with flow for each of the three stages is given in Figure 11-16.[141]

Air cooling was selected for the stators, as it appeared that heat-transfer losses could be minimized. Water, having too high a conductivity, would over-cool the stators. Inasmuch as stress levels are lower in the stators, higher temperatures could be tolerated. The stators were designed to use air at a pressure comparable to the second-stage bleed of the compressor. The stator blades were designed with internal extended surfaces. Figures 11-17 to 11-22[141] illustrate the general design of coolant passages. The cycle design data are given in Table 11-2.[141]

Table 11-2

CYCLE DESIGN DATA, COOLED TURBINE

Ambient pressure	psia	14.7
Ambient temperature	deg F	80.0
Air-flow rate	lb/sec	6.57
Compressor inlet pressure drop	in H_2O	4.0
Compressor pressure ratio		4.87:1
Combustor pressure drop	per cent of inlet pressure	3.0
Combustion efficiency	per cent	95.0
Turbine inlet temperature	deg F	1750
Turbine inlet pressure	psia	68.8
Turbine gas flow rate	lb/sec	6.5
Turbine back pressure	in H_2O	10.0

THE FRANKLIN INSTITUTE • Laboratories for Research and Development

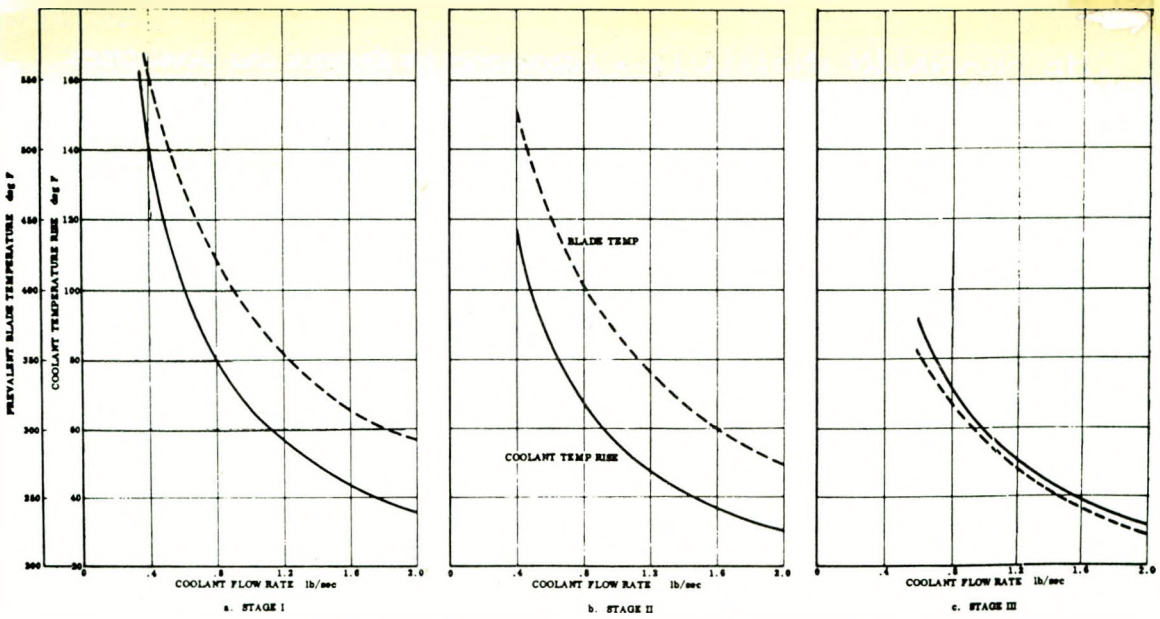


Fig. 11-16 - Variation of Coolant Temperature Rise and Prevalnet Blade Temperature With Coolant Flow Rate

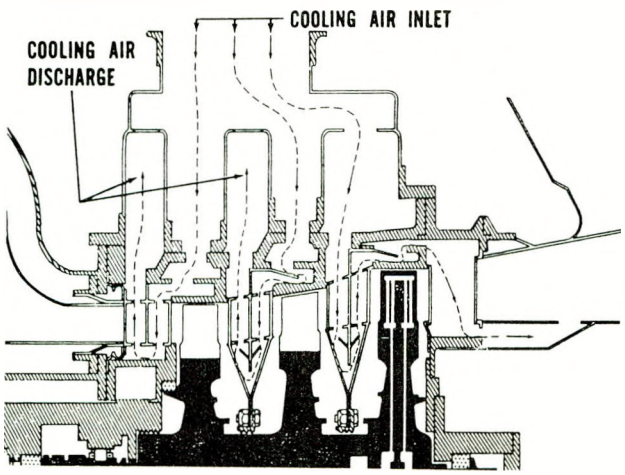


Fig. 11-17 - Cross Section of Turbine Showing Cooling Air-Flow Path

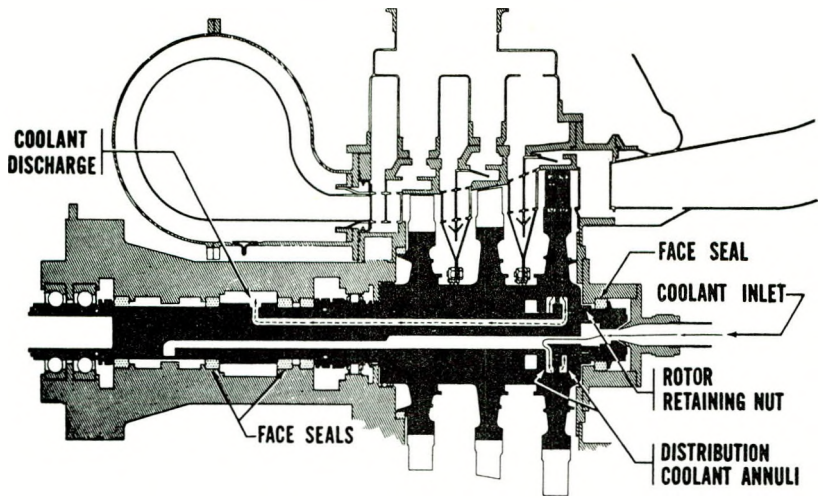


Fig. 11-18 - Cross Section of Rotor Assembly Showing Cooling Passages

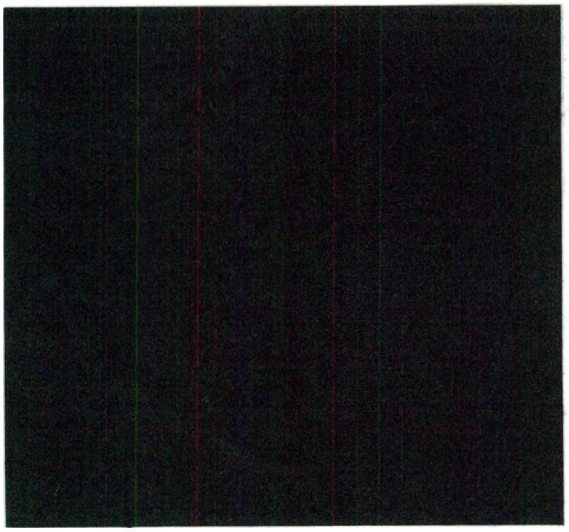


Fig. 11-19 - Three Stage Rotor Assembly - Radial Coolant Inlet

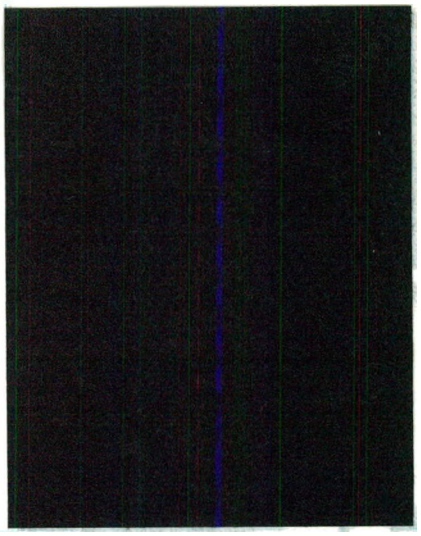


Fig. 11-21 - Section Through First-Stage Rotor Blade

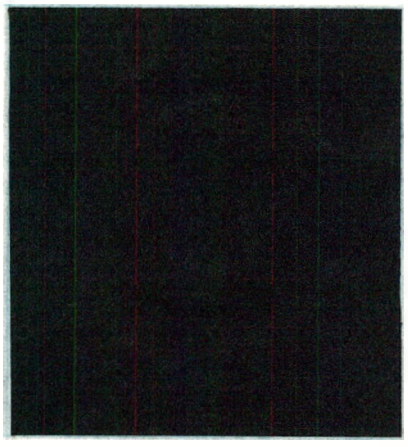


Fig. 11-20 - Cutaway of Rotor Blade Showing Cooling Passages

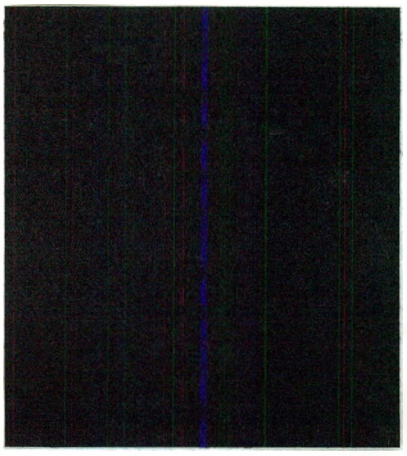


Fig. 11-22 - Section Through Stator Vane

Heat transfer calculations were used to establish coolant flow rates and heat rejection rates. The calculated cooling losses in the turbine are shown in Table 11-3[141] and the design power-plant performance is listed in Table 11-4.[141]

Table 11-3

TURBINE HEAT REJECTION RATES IN BTU/SEC

	Stage		
	I	II	III
Stator blades	26.2	15.0	12.8
Stator shrouds	28.7	14.4	9.0
Rotor blades	78.0	58.2	51.5
Rotor disks	14.9	10.8	7.9
Total	147.8	98.4	80.2

Table 11-4

DESIGN POWER-PLANT PERFORMANCE

Turbine power output	hp		1412
Compressor power	hp	864	
Cooling air power	hp	17	
Power consumed in bearings	hp	15	
Liquid coolant pumping	hp	5	
Oil pumps	hp	1	
			902
Shaft power available	hp		510
Gear Loss	hp		10
Net power	hp		500
Fuel Rate	lb/hr		479
Specific fuel consumption	lb/hp-hr		0.96
Over-all thermal efficiency	percent		14.4

A three-stage reaction turbine was designed to achieve high efficiency. For effective cooling of the rotor blade trailing edges, fairly thick trailing edges were specified. The high reaction and the low velocities in the turbine allowed these relatively thick blades to be used without excessive losses. Other than this compromise, fairly conventional design practice was used, based on free vortex flow and resulting in twisted rotor blades. The rotor blades were fabricated from precision castings. Steps in the fabrication of rotor blades include:

(a) Precision cast from low alloy steel.
(b) Anneal the casting.
(c) Drill coolant holes and manifold holes.
(d) Chromize for corrosion protection.
(e) Braze tip cap and manifold end plugs.
(f) Heat treat to tensile strength of 130,000 psi.
(g) Crush grind rotor-blade base.
(h) Braze O-ring studs into bottom of base.
(i) Pressure and flow test.

Six radial holes were used for cooling passages in the first-stage blades and four for the second and third stages. During early tests, several blades were fabricated with a copper insert in the trailing edge to reduce trailing-edge temperatures.

The fluid pressure built up in the wheel by centrifugal force is about 3000 psi in the first stage at the O-ring and about 4000 psi in the third stage. The efficiency of the radial inlet to the shaft left much to be desired, and necessary flow rates could not be obtained at design speed. Accordingly, an axial inlet was installed on the down-stream face of the shaft.

Stator vanes were fabricated of sheet metal 0.025-inch thick. The trailing edges were welded. To provide corrosion protection to the lean alloy steel, chromizing was used. The internal corrugation was rolled from 0.008-inch mild steel sheet and also chromized. A typical stator vane after brazing is shown in Figure 11-22. It had been planned to run the three-stage turbine for a total of 500 hours. However, mechanical

difficulties were such that the program was discontinued after 119 hours. At that time, the engine needed minor repairs to be operable but it was concluded that the general purposes of the program had been accomplished.

Early tests were plagued with rotor-blade failures. These failures occurred almost wholly in the blade tip caps. Alternate methods of brazing were studied and proof pressure tests up to three times operating level were performed. Blades in the first stage were especially prone to these failures. It was found that blade strength was impaired by a loss of braze fillet at the time the rotor tip diameter was ground. In the second stage, the cap was recessed so that generous fillets remained after the tip diameter was ground. The major force on the blade cap is from fluid pressure, and the fact that blades passed leak and proof pressure tests was taken to indicate that the shear area was adequate. When operating in a turbine, thermal effects caused by temperature gradients could easily produce local tension loading on the braze and result in failure.

Toward the end of the program, tip caps were welded in place. A careful technique was required to minimize burn-through and a loss of airfoil profile. In addition, the alloy used in the blades was air-hardenable, and welding cracks were frequently encountered. At the conclusion of the program, blade caps were retained adequately, but fine leaks detectable only under high pressure were found in several blades. The brazed joints in the blade manifold plugs and O-ring studs caused no problems.

The pin method of rotor-blade attachment proved to be successful. No difficulty was found with the feature. Blades were readily interchangeable, and the pin joint could withstand a large amount of abuse. Blades could be readily changed and at times were changed without rebalancing the rotor. Several pins were drilled out with a hand drill and a number of holes had drill drifts that caused uneven pin loading but no pin failures occurred.

The separate solid disks with O-ring seals proved to be practical. Individual rotors could be assembled, pressure tested, and then stacked onto the shaft. By removing the exhaust collector, the rotor disks could be readily removed. With adequate chamfers on the disk bores, the assembly could be readily made without cutting the O-rings.

Special techniques were developed for balancing the rotors. Blades were weighed individually and selected for assembly. For balancing, the entire rotor was filled with water. Filling was done by evacuating the system and then allowing the water to be drawn in. Because of the nature of the blade fabrication, some rather large out-of-balance conditions were found, and compensation would require the removal of a considerable amount of material from the rotor. This was objectionable because it removed the nickel-plating and subjected the disk to corrosion. Since, one time, holes had been drilled through the disks just below the wheel rims for instrumentation, balancing was achieved by inserting tungsten plugs.

In almost all cases for which satisfactory machine balancing was accomplished, no vibration troubles were encountered. As was noted, blades were changed on the test stand without rebalancing and ususally but not always without producing critical unbalance.

The stators were damaged by rotor-blade tip caps coming loose. Air cooling of the stators was generally inadequate. One major failure occurred with a rupture of the weld joining the cover plates to the inner shroud ring. This failure was attributed to overheating. New plates were welded into place after internal baffles were added to provide more effective internal cooling in that area.

Conventional antifriction bearings were used with good results. Some initial difficulty was encountered with the roller bearing as a result of differential thermal expansion. With the outer race in

warm housing and the inner race in contact with a cold shaft, an increase in radial clearance would take place. This resulted in loss of one bearing, and the assembly was changed to provide for a lower initial radial clearance.

After extensive research and testing various types of coolant seals in the earlier part of the program, standard carbon-face Sealol seals were selected for use in the engine. A minimum-diameter seal was selected to be compatible with the shaft design to minimize circumferential rubbing velocity. From the manufacturer's recommendation and the seal test rig experience, the flatness and surface quality of the rub ring mating face was found to be extremely critical in the effect on seal life.

Close stack-up dimensions were taken on engine assembly and shims to assure proper seal spring compression. During actual operating, many seal failures occurred. These failures were attributed either to foreign matter in the coolant, an out-of-flatness on the rub ring caused by distortion on stack-up, or excessive engine vibration. Individual seals, which were operated under ideal conditions where the mating rub ring surface was not distorted and foreign particles did not enter the system, displayed excellent wearing capabilities for long life. Because of the experimental nature of the program, seal lives of 50 hours or less were attained.

Examination of the turbine parts indicated various degrees of effectiveness of the corrosion resistant coatings. Parts in contact with the hot gas had been chromized, and generally evidence of residual surface chrome was apparent. Most of the loss in protection is believed to have resulted from excessive vapor blasting. Machined parts that had been protected with nickel plate showed similar irregular residual protection, again caused mostly by handling and cleaning.

Aerodynamically, the turbine was found to yield satisfactory performance when run with reasonable tip clearances. Because of the early failure of blade tip caps, honeycomb seals with generous clearances were used except during tests to determine performance.

Heat-transfer data for the liquid-cooled rotor indicated that design calculations were more than adequate. At the engine design point, a total heat rejection rate to the coolant of 187.7 Btu/sec had been estimated. As the measured flow rates were higher than design, the theoretical curves of rotor-blade heat transfer were used with the flow rates from the actual test to re-estimate heat-transfer rates. These results are presented in Table 11-5[141].

Table 11-5

THEORETICAL ROTOR HEAT-TRANSFER RATES FOR MEASURED FLOW

Stage	Coolant flow (lb/sec)	Blade Q (Btu/sec)	Disk Q (Btu/sec)
I	0.885	82.9	14.9
II	1.162	73.4	10.8
III	0.720	68.5	7.9
	Total	224.8	33.6

Thus, the total theoretical rotor heat rejection rate is 258.4 Btu/sec. The measured rate was 237.0 Btu/sec, 9 per cent below the theoretical value. This difference can be explained by the fact that the theoretical values were based on the shaft-power configuration, whereas the measured values were obtained with an air-bleed configuration. The lower pressure for the air-bleed configuration would produce a lower heat rejection rate. An over-all heat balance is presented in Table 11-6[141].

Table 11-6

DESIGN POINT HEAT BALANCE FROM TEST DATA

Gas flow rate	lb/sec	6.88	
Turbine inlet temperature	deg. F	1750	
Turbine outlet temperature	deg. F	1050	
Turbine enthalpy drop	Btu/Sec		1368
Shaft power output			
Compressor enthalpy rise	Btu/Sec	958	
Mechanical losses (1 per cent)		10	
		968	
Heat rejection to coolant water	Btu/Sec	237	
Heat rejection to coolant air	Btu/Sec	156	
2.7 lb/sec			
249F ΔT			
Unaccounted heat losses	Btu/Sec	7	
Total enthalpy drop, Btu/Sec			1368

Data taken during the single-state tests confirmed calculated rotor-blade temperatures. A comparison of blade temperatures with and without copper inserts is shown in Figure 11-23[141]. Inasmuch as maximum temperatures even without the insert were relatively low, it was concluded that the inserts were not necessary.

The turbine efficiency calculated from the total pressure ratio and the work output was 78 per cent, as compared to a design value of 82 per cent. The design value corresponded to the higher pressure ratio of the shaft-power machine. The measured value was obtained under bleed conditions. It is felt that the deterioration of the stator, because of damage, and the high heat loss were responsible for the lower efficiency.

For the over-all power plant, reduction of the measured performance data to conditions comparable to design for a shaft power machine resulted in an output of 488 hp at a specific fuel consumption

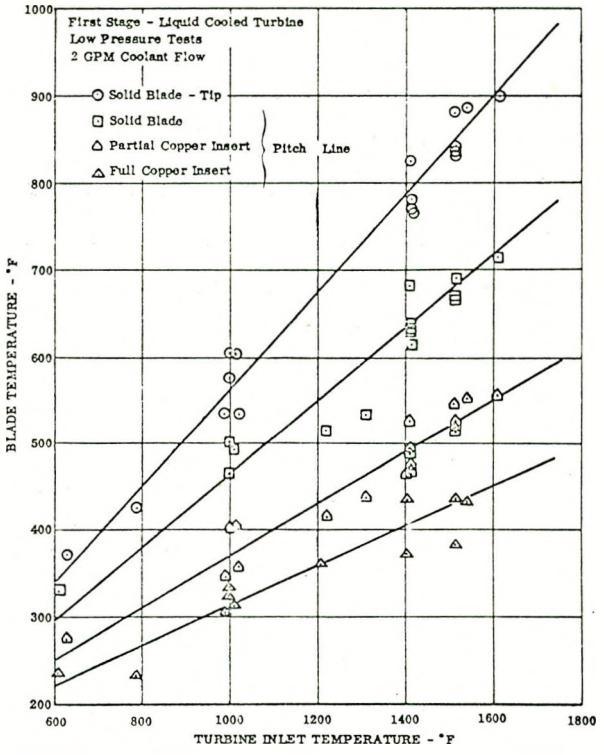


Fig. 11-23 - Rotor-Blade Trailing Edge Temperature

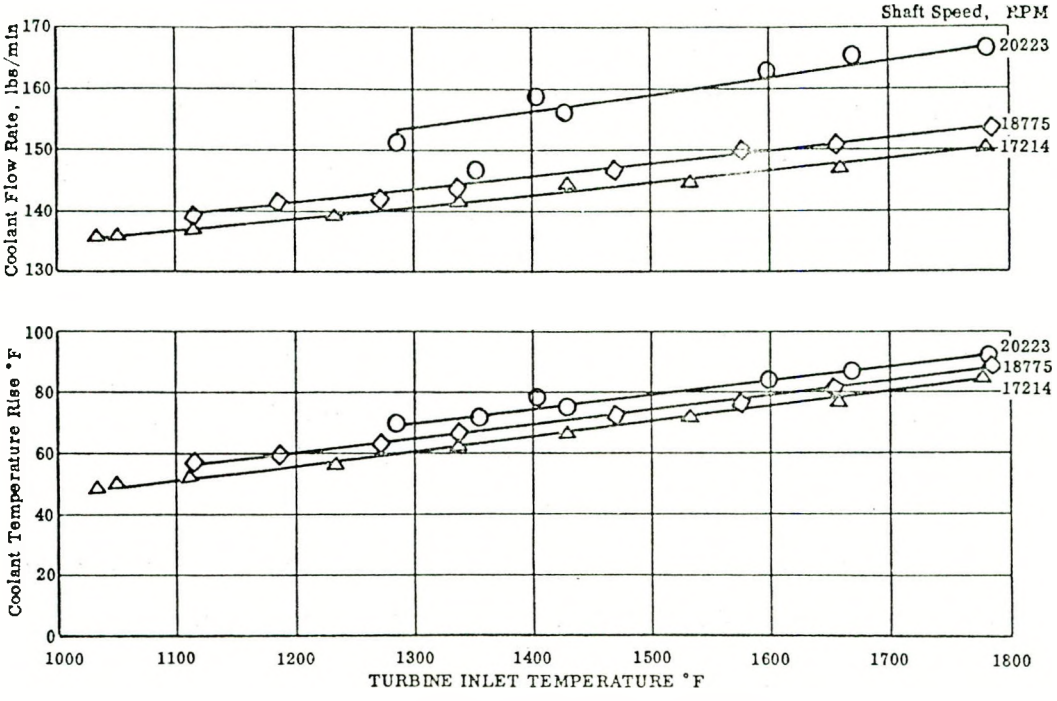


Fig. 11-24 - Cooling System Performance, Liquid Cooled Turbine

of 0.987 lb/hp-hr. This does not reflect the power required to cool the stators. At the design point, 2.7 lb/sec at 75°F and a pressure of 20 psig were supplied. This is equivalent to about 175 hp. The higher pressure was required to keep hot gas from leaking into the cooling passages. Even with this cooling air pressure, evidence of leakage was found in the sooty deposits in the cooling air collector.

A study was conducted of control methods for coolant flow rates. Although for optimum efficiency, constant blade temperatures would be desirable, a system to provide the control was considered to be too complicated. It was decided to adopt a control system that utilized natural convection pumping for control.

As the return fluid is heated, and thus is at a lower density, it can be demonstrated analytically that a net pressure rise should occur in the rotor. This pressure rise would be proportional to the coolant temperature rise and to the square of the speed. During single-stage tests, attempts were made to measure the pressure rise. At constant speed, the gas temperature was raised and the coolant flow rate adjusted to a constant value. Although the convection pumping effect can be seen to occur, its magnitude was only a fraction of that anticipated.

For the three-stage turbine, this convection pumping effect was used to provide coolant control. Fixed area orifices were installed in the discharge line. These were sized individually for each stage, but because difficulty was experienced with Stage II, it was run with a wide open discharge. Data taken during engine tests demonstrated that, as the gas temperature and coolant temperature were increased, the coolant flow rate automatically increased. These data are shown in Figure 11-24.[141]

The increase in coolant flow with coolant temperature rise and gas temperature indicates that the convection pumping effect is occurring.

Again, the magnitude is less than expected theoretically. For an increase in the coolant temperature rise from 70 to 90 degrees, the actual coolant flow rates increased 7.3 per cent, as compared with a theoretical value of 16.3 per cent.

Although the test operation of the liquid-cooled gas turbine was not carried through the scheduled number of hours, most of the design details have been adequately proved. The following conclusions were drawn.

(a) It was demonstrated that a low alloy turbine could be operated successfully at temperatures over 1700°F.

(b) Adequate corrosion protection can be given to low alloy steels for use in liquid-cooled gas turbines.

(c) Available data on heat-transfer coefficients are accurate for prediction of cooling losses and blade temperatures.

(d) High-temperature brazing can be used effectively for the fabrication of components of cooled turbines.

(e) The pin method of blade attachment is effective in producing a practical design.

(f) O-rings were satisfactory for coolant seals between shaft and disk and between disk and blades.

(g) Natural convection effects were measured though of lesser magnitude than expected theoretically.

(h) The radial coolant inlet to the shaft could not be developed satisfactorily. Additional work will be necessary to ascertain if it is feasible. The axial coolant inlet was entirely satisfactory.

(i) Face-type coolant seals can be used if cleanliness, installation accuracy, and low vibration can be maintained.

(j) The design tested did not wholly solve the stator cooling problem. The possible use of ceramic or liquid-cooled stators should be considered.

(k) The turbine inlet scroll was never successfully cooled, as high alloy liners were used. For high temperatures, turbine inlet scrolls are undesirable unless heavy, furnance-type construction can be used. An engine arrangement with a straight-through flow path is required.

The experience with this development program supports the conclusion that liquid-cooled turbines are feasible if the added weight and complication can be tolerated. Studies of reliability of gas-turbine plants have indicated that the environmental stress resulting from high temperatures is one of the major causes of malfunctions. Liquid cooling, or any cooling, can reduce the deleterious effects of high temperatures but with the penalty of added complexity. In the field of small gas turbines, the complexity does not appear to be warranted for most known applications. For larger, stationary machines, the picture may be different. With the use of high alloy steels, turbine inlet temperatures over 2000°F appear possible. With high inlet gas temperatures, exhaust gas temperatures are also high, and cycles utilizing exhaust heat recovery can show attractive theoretical performance. These findings agree with the statement made by Dr. von der Nuell in a recent paper.[142] "In general, resort should not be taken to higher working temperatures until all other methods of improvement have been exhausted, especially when such methods mean greater safety, longer life, greater freedom in materials and numerous other significant advantages."[141]

11.6 Other Cooling Methods

Another method, which might be eventually utilized, is the use of internal cooling of the turbine blades by the vaporation of water, the water being circulated by natural convection in the centrifugal field of the rotating turbine wheel.[58] It is hoped with this method to operate the turbine blades as much as 1000°F cooler than the gas stream in which they operate. Pametrada (The Parsons & Marine Engineering Turbine Research and Development Association) patents showed as early as 1953 a

proposition for designing a cooling water circuit for a liquid-cooled turbine rotor with the object of producing steam. However, in this case the evaporation is not used for blade cooling. Pametrada is continuously working on the development of a liquid-cooled gas turbine, and has recorded successful runs with inlet temperatures up to 2200°F. Sweat-cooling (through porous-walled blades) was also tried by Pametrada.[143] Unfortunately, not many details are known about this research work.

Apart from blade cooling, many turbines utilize partial cooling of disk rims (blade roots) or of the casing, to guard against creep and thermal distortion, respectively. Let us describe the cooling and internal insulation of a modern industrial gas turbine, the English Electric EM85, as an example. Figure 11-25[144] shows a cross-section through this turbine.

The design of the EM85 turbine makes use of the high turbine inlet temperatures made possible by modern blading steels. At the same time, the turbine disks and casings are protected adequately and operate at conservative temperatures. This is achieved in two ways.

First, between the combustion chamber and the turbine inlet, the gases are carried in thin shells or liners fabricated from high-grade heat-resisting alloy. These shells are subject to negligible pressures and are flexibly supported within the turbine casing. They are the only components, besides the blades and packers, actually in contact with the hot gases and their only function is that of guidance. The casings are insulated from heat radiated from the liners by an internal covering consisting of mattresses made from quartz and glass fibers contained in a stainless steel gauze.

Secondly, heat penetrating the mattresses is removed by cooling air, so that at all times the casings, which carry both pressure and mechanical stresses, are maintained at moderate temperatures. Furthermore, the rings holding the stator blades are themselves cooled, so that the whole static assembly is at a temperature well below that which is

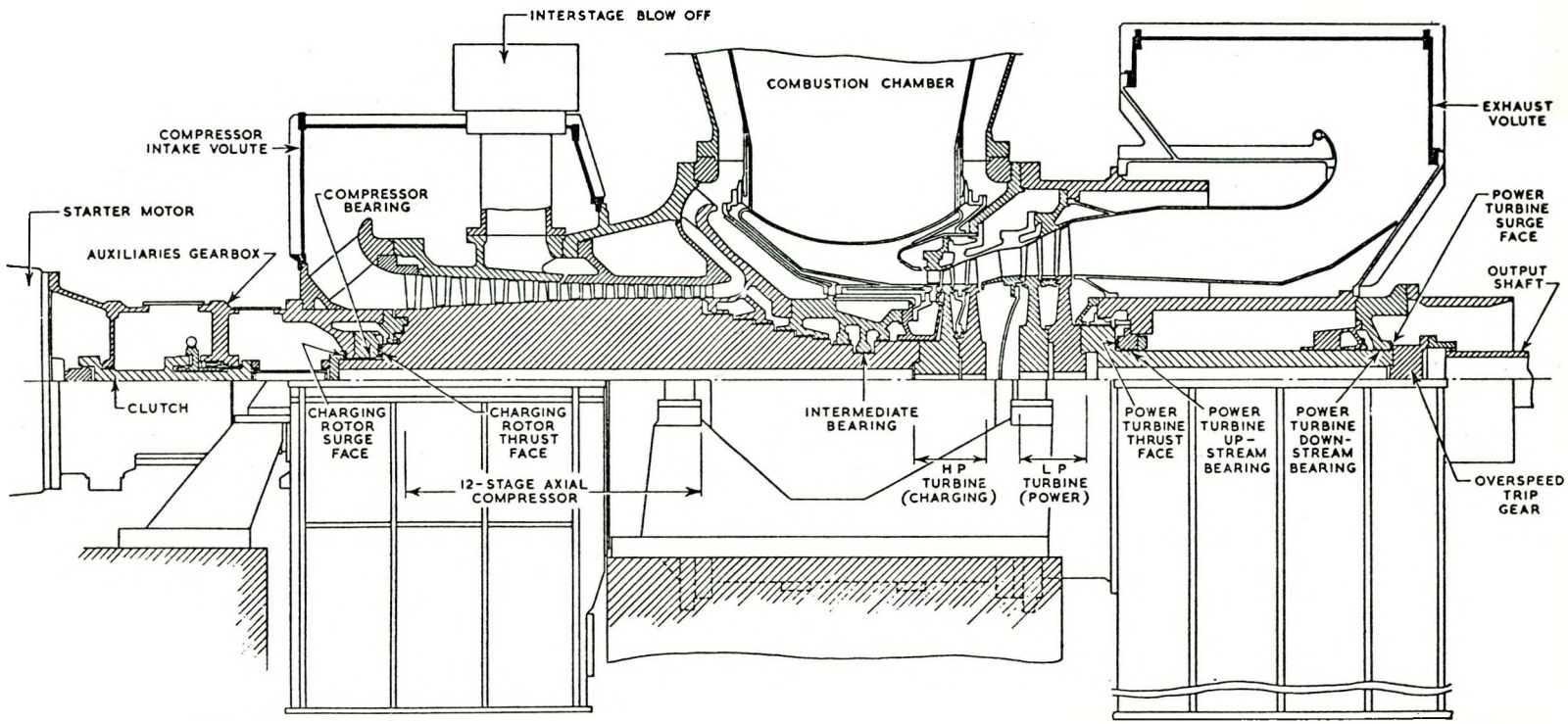


Fig. 11-25 - A Part-Sectioned View of the English Electric EM85 8,000 hp Gas Turbine

normally considered safe. Similarly, the turbine disks are cooled by air passing over both faces, and in the case of the charging turbine, air is introduced under the blade roots, thus effectively limiting the flow of heat from the hot blades to the disk. Extensive running experience of this design has shown that the disk operates at well below creep temperatures.

The hot gases leaving the combustion chamber pass into the two-stage charging turbine through a high-grade heat-resisting alloy inner shell. This shell is un-split and is enclosed in a lagging carrier containing the heat insulating mattresses referred to earlier. The turbine disks are made of high tensile ferritic alloy steel and are cooled on both faces by a part of the compressor delivery air. In addition a metered supply of compressor delivery air is passed to the bottom of the slot carrying the fir-tree blade roots. This cooling air extracts a large proportion of the heat flow entering the disk from the hot gas stream, and ensures that the portion of the rotor carrying the rotational stresses is operating at a temperature low enough to eliminate the danger of creep. It also ensures that the main parts of the disk are practically free from thermal stress during rapid load transients. The turbine rotor and stator blades themselves are not cooled, but are made in the highest available grades of heat-resisting materials and are stressed consistent with long-life operation at full load.

The turbine stator blades and diaphragms are mounted in un-split holding rings, and allowance is made for free thermal expansion, both of the blades and the holding rings themselves. Cooling air is passed between the holding rings and their mountings, preventing undue heat flow into the turbine casing. The power turbine cooling arrangements are similar to those for the charging turbine, due allowance being made for the lower operating temperatures. The power turbine stators are both un-split and the mounting is such as to allow free thermal expansion.

The power turbine casing is a mild steel fabrication with internal lagging and air cooling. The hot exhaust gas is ducted in a thin-wall fabrication mounted inside the turbine casing. The exhaust temperature is sufficiently low to allow the use of aluminium sprayed mild steel fabrications for the liner and the exhaust chamber.

The necessary temperature drop of the exhaust gases has been achieved in only four expansion stages. This is a direct result of the use of positive cooling, since due to the low disk temperature, ferritic steel can be used, permitting higher stresses and hence more work per stage. The single turbine disks are of relatively small size and are forged from billets.[144]

As another example, the air cooling system of the Orenda OT-F-2 industrial gas turbine is shown on Figure 11-26 and is summarized as follows:

A controlled internal leakage of air at the compressor outlet is used to cool the gas producer turbine rotor. The rearward flow of cooling air is guided past the disk rims and blade roots, thereby keeping heat transfer from the blades to the disks at a minimum. A second flow of cooling air, bled from the compressor fourth stage, is piped rearwards to the power turbine where it cools the rotor disk and blade roots. Air tapped from the compressor outlet passage passes over and cools the gas producer turbine inlet scrolls. Compressor air is also used to pressurize the bearing oil seals and thereby prevent leakage of lubricating oil from the bearing chambers.

Finally, let us describe the cooling and insulation system of the Clark CSN-1 closed cycle turbine-compressor set for the ML-1 Army mobile nuclear power package (see Figure 11-27).[21]

Cooling and insulation on the T-C set is accomplished by the use of cooling gas, reflective insulation and oil cooling. No attempt has been made to use blanket asbestos or glass wool type insulation because of:

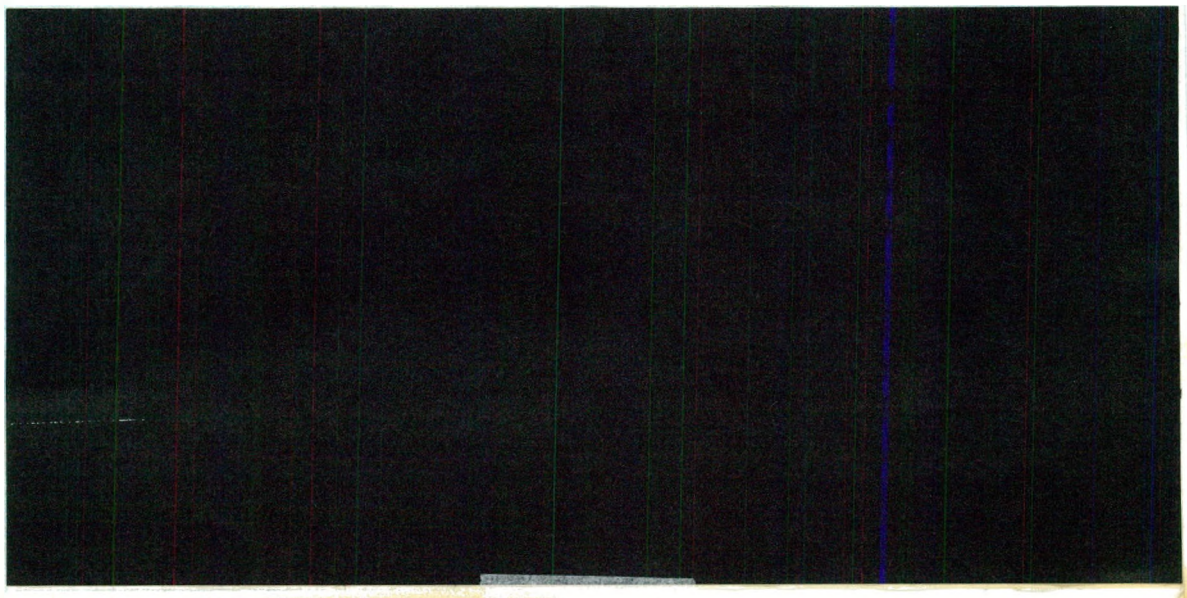


Fig. 11-26 - Air Cooling System of the Orenda OT-F-2 Industrial Gas Turbine

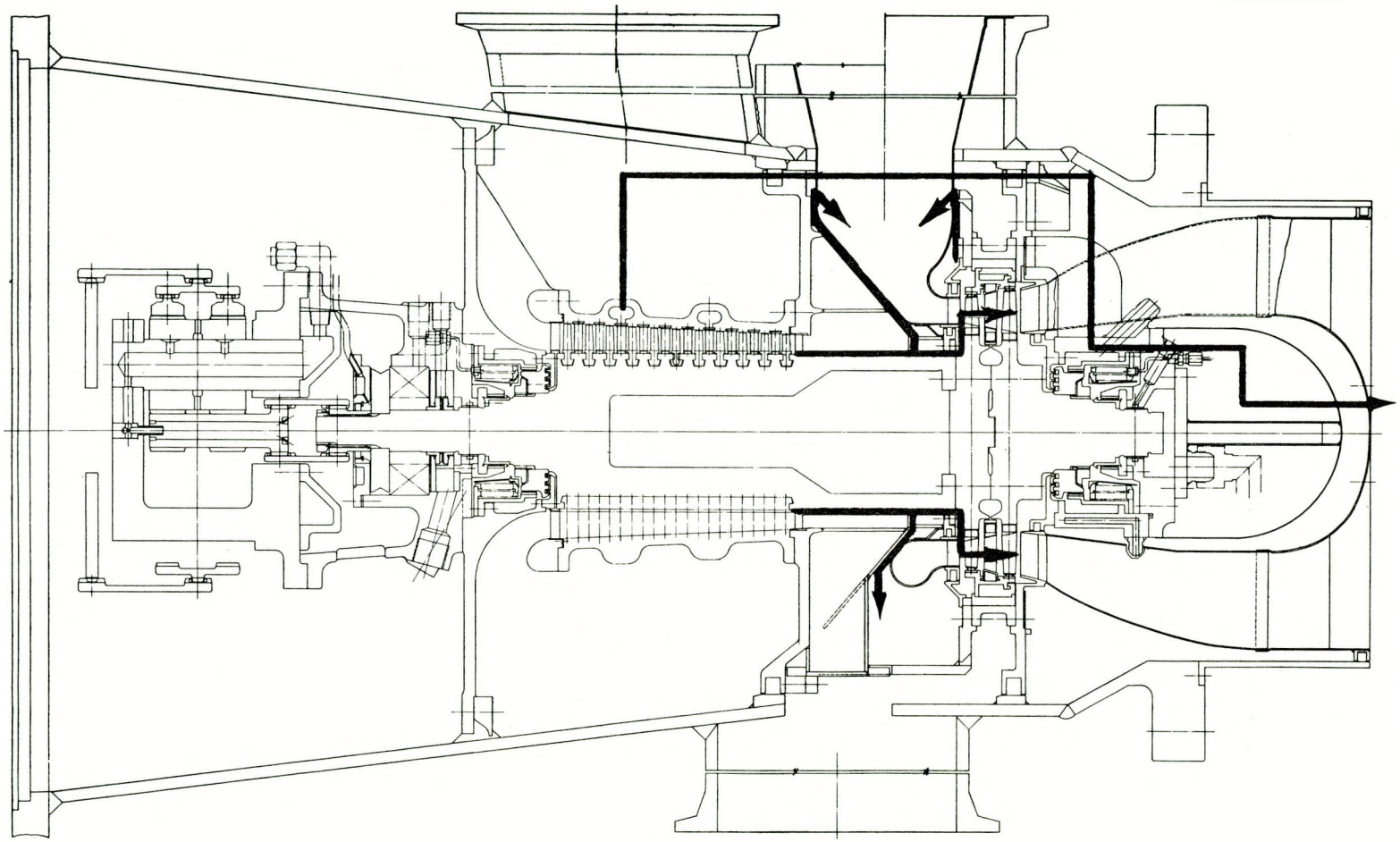


Fig. 11-27 - Turbine Compressor Set for ML-1, Cooling Gas Diagram

(a) The difficulty of removing trapped oxygen.

(b) The distinct possibility of particles breaking free of the main insulation and permeating the system.

(c) The problem of obtaining insulation of sufficiently high purity to ensure that the relatively high radiation levels would not cause trouble.

Because of the complex shape of some of the areas to be insulated and shielded, it would be advisable to manufacture a simplified mock-up of the rear bearing case (the most essential part from the cooling viewpoint) to determine the relative cooling merits of straight gas cooling versus gas cooling with multiple layers of reflective insulation. This would ensure that the most judicious use was made of the cooling gas.

The cooling system may be described as follows. Basically, nitrogen is taken from the third stage of the axial compressor through pipes, traversing the intermediate section of the unit, into the outer annulus of the exhaust. The gas then flows inwards along the tangential support arms of the bearing case. Separation of the cooling gas from the hot exhaust gas stream is accomplished by hollow aerofoil-shaped struts. The gas then passes between layers of reflective insulation surrounding the bearing case into the exhaust fairing where it passes via orifices or holes into the main system gas stream so that there is no total loss to the system.

A second cooling gas circuit starts from the compressor discharge, flows along the rotor shaft, and then by controlled leakage paths into the turbine inlet duct and first-stage nozzle blades. In going through the nozzles, the gas passes along the front face of the 1st turbine disk giving some cooling to this area. It should be pointed out that the gas is forced to flow in this direction because of the system differential pressure of approximately 9.5 psi between compressor discharge and turbine inlet. It should also be recognized that this gas is not a total loss to the system output as work is recovered from the turbine as the gas passes through it. It will, however, have the effect of reducing the average turbine inlet temperature slightly for a given reactor outlet temperature. Total cooling air flow is expected to be approximately 1/2% of the total flow in the machine.

THE FRANKLIN INSTITUTE • Laboratories for Research and Development

I-A2392-6

Because of the difficulty of predicting the effectiveness of the gas cooling of the rear bearing case accurately, provision has been made to pass 5 gpm of oil between the inner and outer walls of the rear bearing case for additional cooling. This oil makes a number of passes along the length of the bearing case before passing through closed pipes back to the oil tank.

12. DETAILS OF STRUCTURAL DESIGN

12.1 Components

This section is concerned with the description of the structural design of turbines. Individual parts are covered in Section 12.1 while the main nuclear gas turbine sets are discussed in Section 12.2. Combustors are not considered. Also not covered are bearings and seals which are the subject of Report NYO 9792[5] of this series.

12.1.1 Casings

Machines may be of either horizontal joint or vertical joint construction. Both constructions have advantages and disadvantages as follows:

HORIZONTAL JOINT UNIT

Advantages	Disadvantages
(a) The unit may be disassembled on the foundation.	(a) There is possibly greater total joint length; greater possible leakage area; possibly greater weight
(b) Smaller pieces are used; consequently there is less weight for individual handling.	
(c) Inspection and maintenance of individual components is facilitated.	
(d) Spigot dimensions of mating joints is less critical reducing machining costs.	
(e) No special jigs are required for assembly and disassembly.	

VERTICAL JOINT UNIT

Advantages	Disadvantages
(a) There is possibly less joint length; possibly reduced leakage area; possibly weight reduction.	(a) True line-up of horizontal parts is more difficult.
(b) Less casing thickness is needed for required pressure loadings.	

(b) Spindle, diaphragm and casing inspections are accomplished by lifting the unit from the bedplate or by extensive use of fixtures.

(c) Unit must be lifted as an entity, hence heavy hoisting equipment is required.

Total joint length of the horizontal or vertical joint units is a function of assembly prerequisites. A greater number of vertical joints is required to achieve axial assembly. The total linear length of either type construction may be approximately equal. Bearing and seal accessibility in the axial assembly unit may require horizontal joints in these areas.

Most of the casings used are split horizontally, except for small or short machines. For example, experience with vertically-split casings of older General Electric gas-turbines working on gas transmission lines showed that major inspection time and cost could be reduced 50 percent if the turbines had a horizontal-split casing.[29] Casings may be cast or of welded steel plate construction. Compressor casings are not subjected to high stress and temperature effects.

Where overall weight is important, frequent use is made of aluminum or magnesium alloys. In other cases, spheroidal graphite cast iron is a useful material. The addition of magnesium to cast iron causes the graphite to be formed in spheroidal form instead of the large flakes obtained when no treatment is given. Treatment leads to a doubling of the tensile strength and a considerable reduction in the brittleness. If a high degree of corrosion resistance is required in the compressor casing, stainless steel or a chromium steel could be used.

The turbine casing must be sufficiently oxidation resistant to withstand the effects of the hot gases passing through it and must be of adequate strength to avoid warping troubles. The high-alloy steels, containing about 25% chromium and 12% nickel, or the modified 18/8 steels are generally satisfactory.[39]

A cast casing has the advantage that it is more easily formed according to required flow conditions (see Figure 12-1).[145] Such a casing is also less susceptible to vibrations. On the other hand, welded-steel-plate construction is usually lighter, less subject to thermal stresses in transient conditions, and also more leak-proof. For nuclear applications, especially when helium is used as coolant, a welded casing will definitely be required. Lightweight gas-turbine units will also always demand a welded casing because of the weight requirements and favorable behavior during quick starts. Examples of various casings are shown in Figures 12-2 to 12-10.

Figure 12-2 shows a horizontally split single casing of welded construction of a Westinghouse gas-turbine. Figure 12-3 shows a horizontally split casing of a typical General Electric industrial turbine. This carbon steel casing is protected by a stainless steel lining and adequate insulation to maintain low temperatures. Nozzles and other internal parts are of stainless steel.

Figure 12-4 shows a horizontally split compressor casing of the gas turbine mentioned above. This casing is designed to resist distortion under transient operating conditions. The stator blades are made of a corrosion-resistant chrome steel. Figures 12-5 and 12-6 show the horizontally split casings and other details of a Clark multi-stage centrifugal compressor. Up to ten stages can be handled in a single casing.

Figures 12-7 and 12-8 show a Clark No. 3 vertically-split multi-stage centrifugal compressor. Open ends of the barrel are closed by removable covers or heads. A bolt ring of heavy, closely spaced

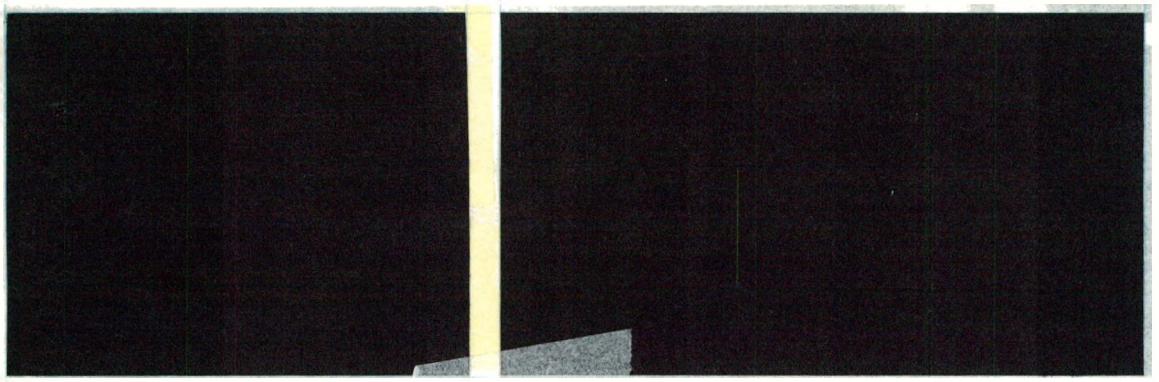


Fig 12-1 - Cast Casings of a Two-Stage Turbine

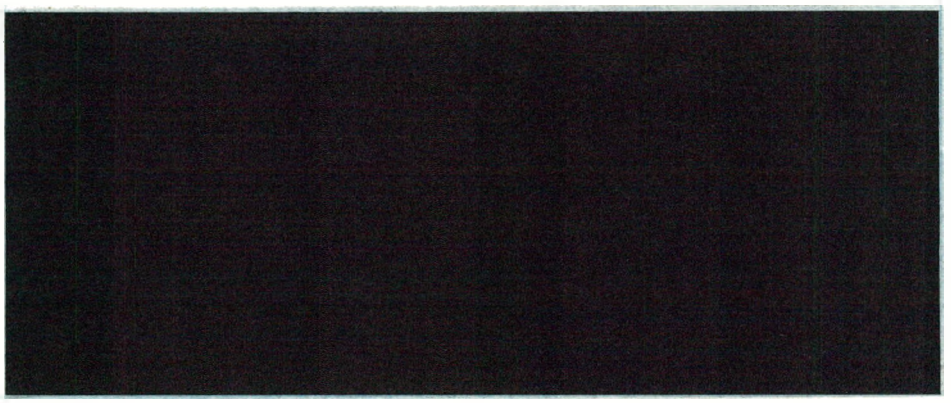


Fig. 12-2 - Simple Open-Cycle Type Westinghouse 7000 hp Gas Turbine, Showing Simplified Two-Bearing Construction

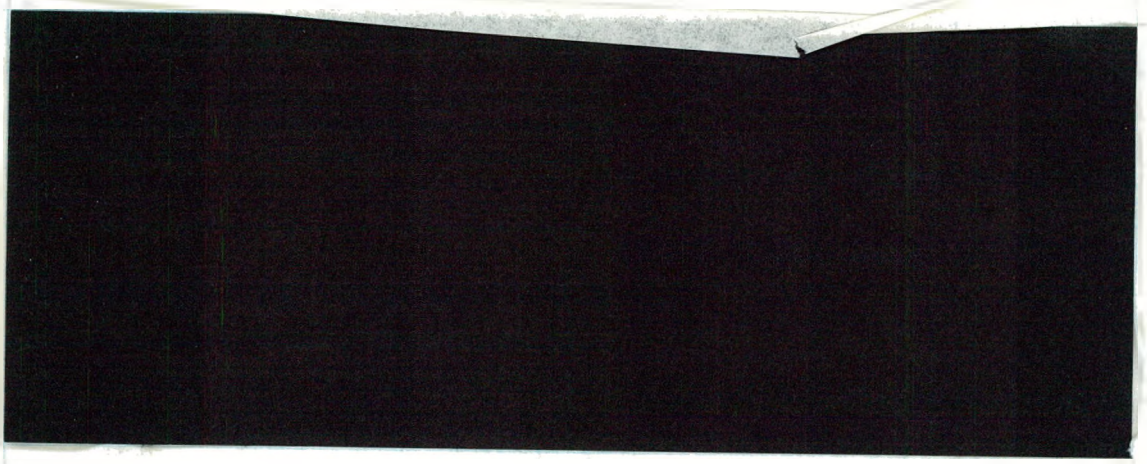


Fig. 12-3 - Turbine Casing

Fig. 12-4 - Compressor Casing

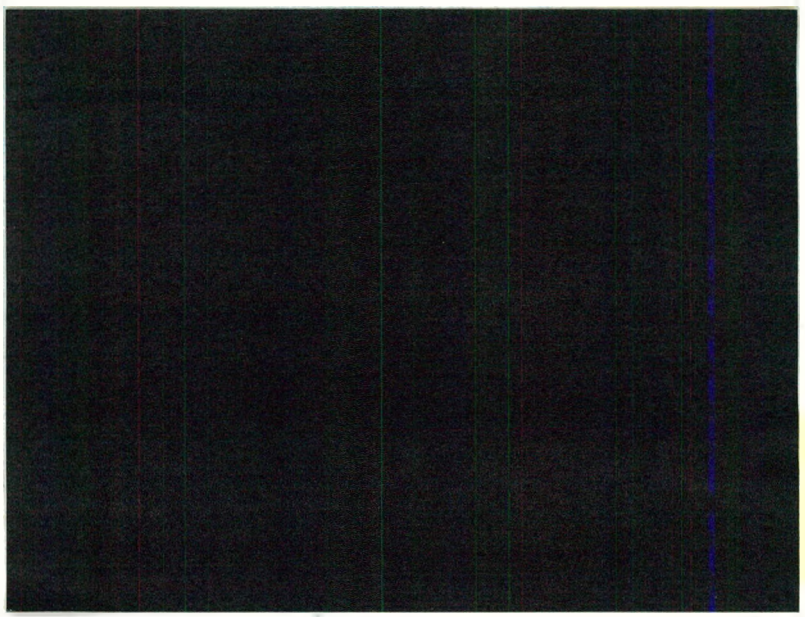


Fig. 12-5 - Cross-Section of Horizontally-Split Centrifugal Compressor-Diaphragm Cooling is Provided

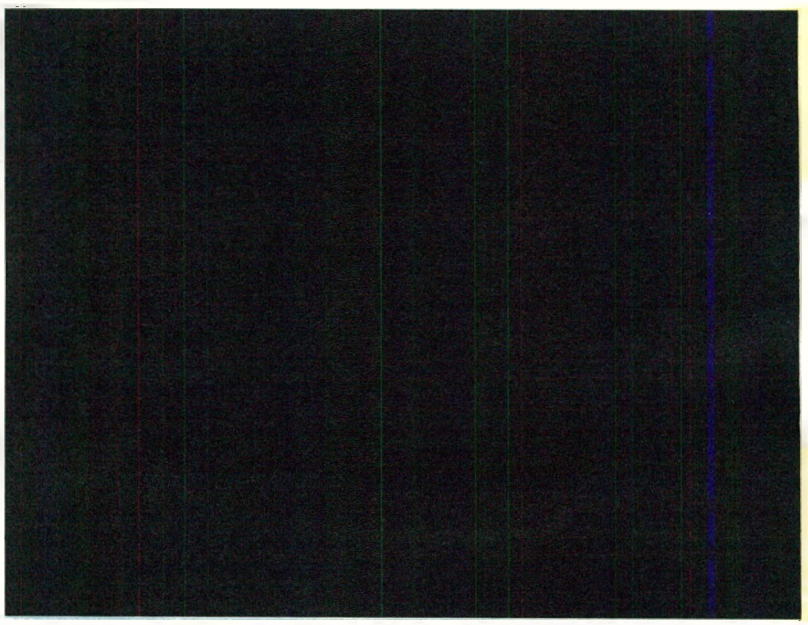


Fig. 12-6 - Clark No. 2 10-stage Horizontally-Split Multi-Stage Centrifugal Compressor

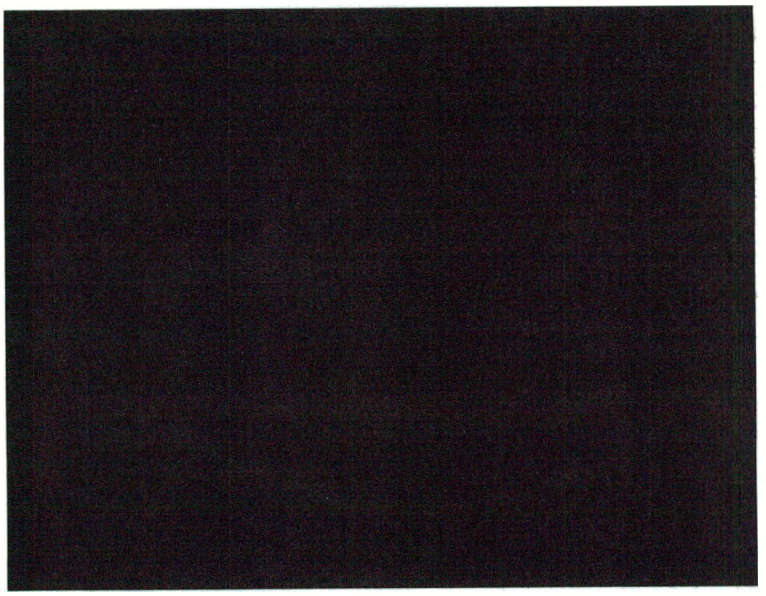


Fig. 12-7 - Cross-Section of Vertically-Split Centrifugal Compressor

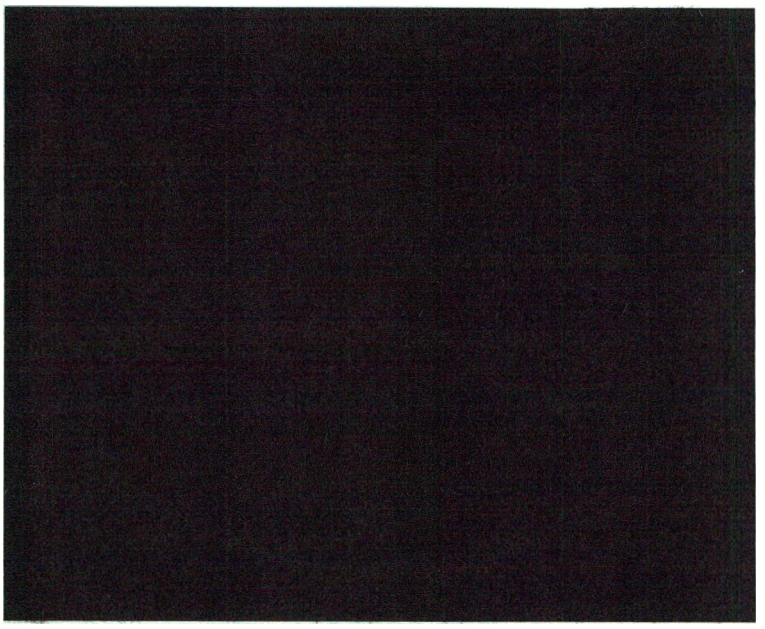


Fig. 12-8 - Vertically-Split Multi-Stage Centrifugal Compressor

studs secure the heads to the case. The inner case, which is split on the horizontal center line for greater accessibility, consists of diaphragm and guide vane components. It is readily inserted into the outer pressure-tight case as a complete assembly. Cases are of either cast or forged steel depending on the pressure level. This type of Clark vertically-split machine can operate at pressures up to 5000 psi. Clark compressor casings are made of steel or semi-steel depending on the pressure level.

Figure 12-9 shows a cross-section of a DeLaval centrifugal compressor having a vertically split casing. This compressor has been developed for high-pressure gas transmission. Finally, Figure 12-10 shows an exploded view of a DeLaval high pressure turbocharger, revealing vertically split casings for both turbine and compressor.

Some units are combined horizontal and vertical split, depending on disassembly and assembly requirements and on considerations of strength, stiffness, and tightness.

12.1.2 Rotors and Disks

Axial-flow rotors are made either from one solid forging or are composed of disks. Brown Boveri has long proposed to make turbine rotors by welding disks together. Figure 12-11[14] shows a section through the Brown Boveri experimental rotor for the St. Dizier gas turbine of Electricité de France. One suggested proposition is the formation of medium-sized rotors by flash-butt welding disks and shaft ends together, as shown in Figure 12-12.[146]

General Electric makes use of a composite disk for larger jet-engine turbine rotors, in which a strong forged disk of low-alloy steel has a rim of heat-resisting alloy welded to it. For high-temperature steam turbines, for long service, it was learned that a rotor of a single-piece forging is best. The same would apply for gas turbines,

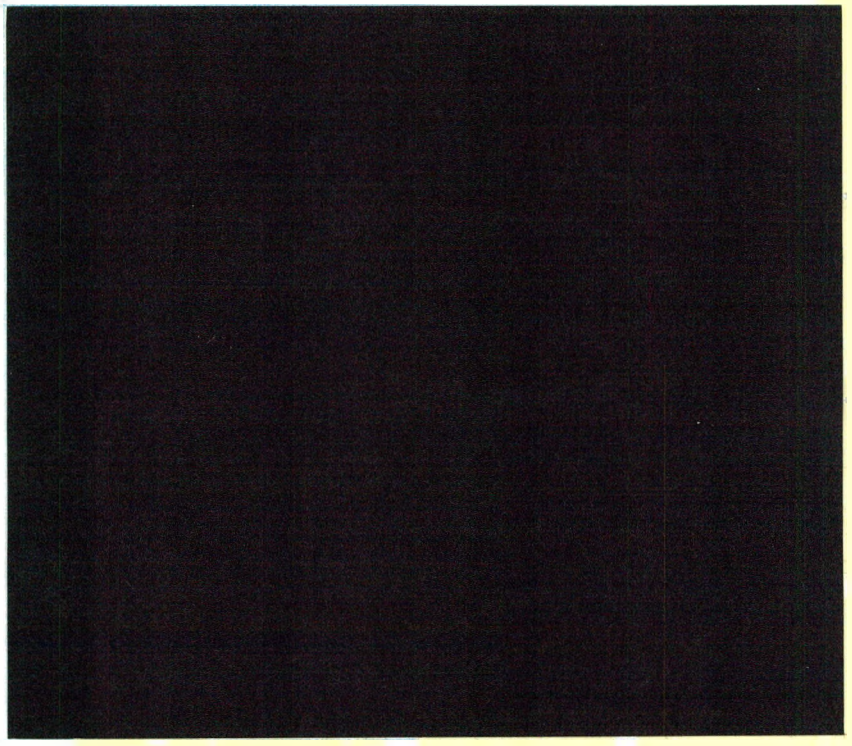


Fig. 12-9 - Cross Section of DeLaval Centrifugal Compressor

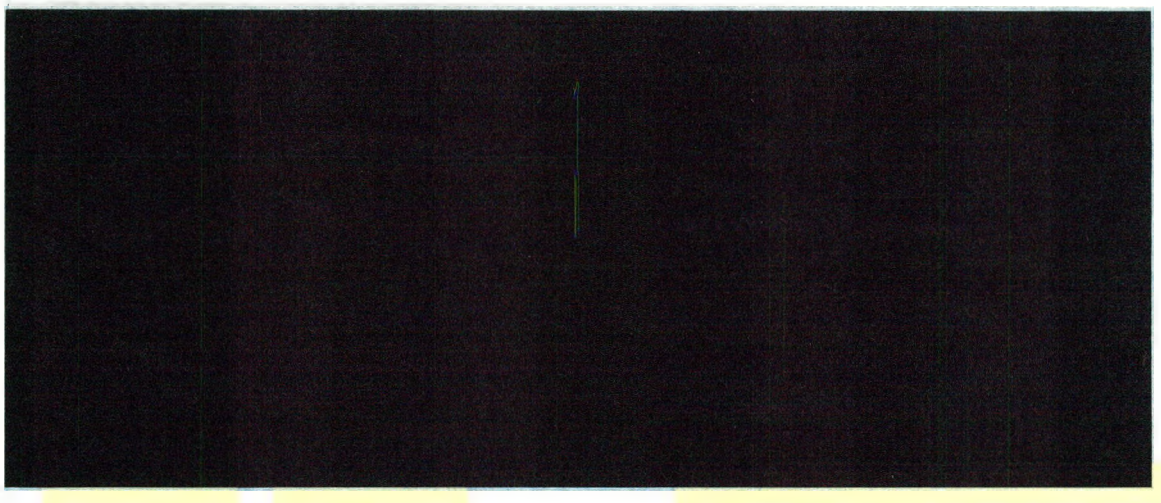


Fig. 12-10 - Exploded View of DeLaval Supercharger

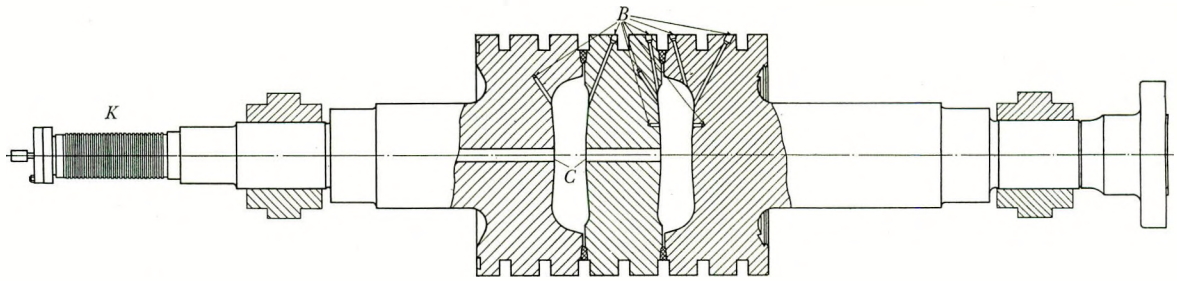


Fig. 12-11 - Section Through the Experimental Rotor for the St. Dizier Gas Turbine of Electricité de France

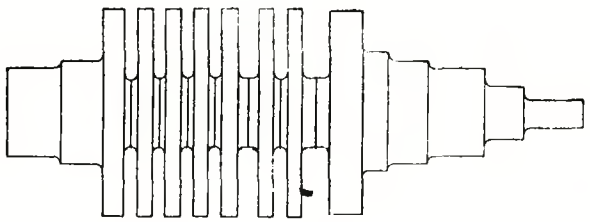


Fig. 12-12 - A Suggested Built-Up Rotor Formed by Flash-Butt-Welding Disks Together

where even higher temperatures are involved. However, it would appear that the knowledge and ability to handle larger masses of the heat-resisting alloys has not reached the stage where large reliable forgings are possible. Hence, disks have been used largely in the various gas turbines which have been built up. In the case of superchargers, and many of the jet engine and propeller drives as well, a single disk of the heat-resisting alloy is flash-butt welded to a shaft of low-alloy steel. In some cases, one or two disks are bolted to a shaft. For small and especially short-life apparatus, such disks are readily formed, and usable physical properties may be built into them by forging operations.

Much work has been done in developing alloys for disks and in producing reliable disks from those materials. These disks have been explored and tested in many ways. Both the age-hardenable and the work-hardenable alloys have been considered and used.

To secure the best load-carrying ability or strength, one must properly heat-treat or age-harden the first, and the work-hardenable alloys must be forged or worked at temperatures below those usually considered normal for forging operations. The term "hot-cold-worked" has been used to designate this. However, it appears to be true with all of our materials that when we improve the load-carrying ability by heat-treatment or by hot-cold work, we lose the ductility of the metal at high temperatures.

There has been an impression that the age-hardenable alloys stood alone in this particular respect, but a great many tests have been made to show that hot-cold-worked disks of supposedly ductile materials are also very deficient in ductility as judged by creep-rupture tests.[146]

Compressor rotors do not require high-temperature resisting materials. Thus we find solid forgings for the rotors of some axial compressors. For example, the 12-stage rotor at the compressor for the English Electric EM85 gas turbine is made from one solid forging of low-alloy nickel-chromium-molybdenum steel.[144] Circumferential T-slots are machined in the rotor to receive the blading.

The single compressor rotor of the Solar Jupiter has ten disks which are shrunken and riveted to an inner drum (see Figure 12-13) and the turbine rotor is a set of interlocking disks. Each disk is connected to the other by three radial fitted keys. The ten-stage axial-flow compressor rotor of an Orenda gas turbine is built up of spigotted steel disks, spacer rings and stub shafts, clamped together by eight through bolts. These bolts transmit drive torque to the rotor and also enable the disks and spacers to act as a rigid, large diameter shaft (see Figure 12-14).

The main requirements of rotor and disk alloys may be summarized as follows:

(a) High proof stress,
(b) Good creep strength,
(c) Oxidation resistance,
(d) Good thermal conductivity, and
(e) Low coefficient of thermal expansion

Early gas turbines used austenitic 18% chromium-8% nickel alloys, suitably modified, and the rotor and disks were forged as a single unit. It was later realized, however, that by efficient cooling the maximum temperature in the rotor could be kept below 1000°F, thus permitting the use, in certain cases, of ferritic alloys. At the present time, therefore, both types of alloy are in use, according to the type of turbine concerned. Table 12-1 indicates the alloys used most frequently for turbine disks and rotors at the present time. However, other alloys have been developed and used in specific instances.

Note also that turbine disks were successfully made by General Electric Co. of an austenitic alloy rim being welded to a ferritic hub (Ni-Cr-Mo steel). Table 12-2[39] indicates the advantages and disadvantages of ferritic and austenitic alloys.

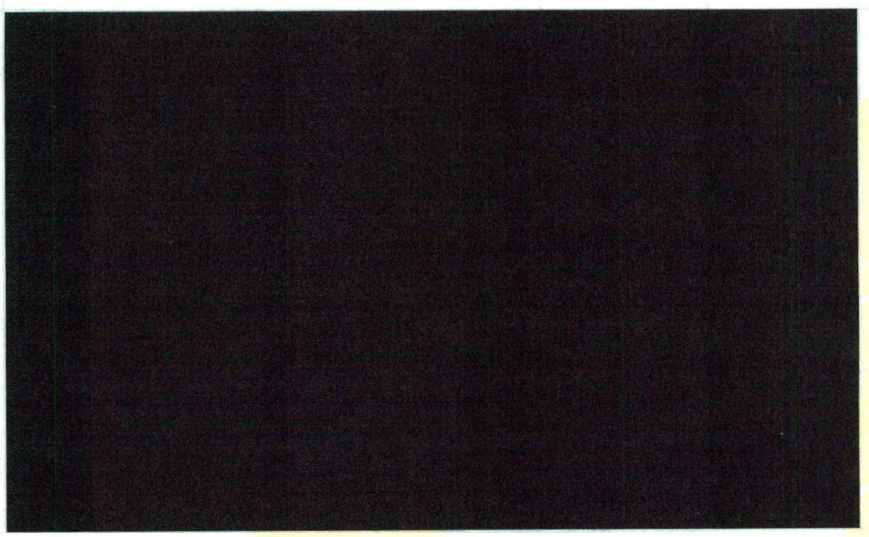


Fig. 12-13 - Solar Jupiter Engine Compressor Rotor

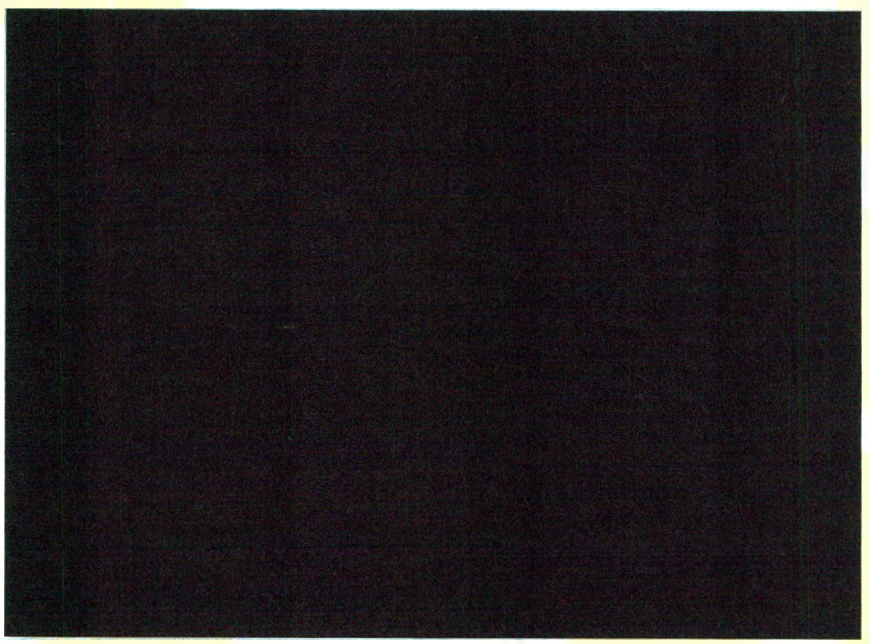


Fig. 12-14 - Built-Up Compressor Rotor of the Orenda OT-F-2 Industrial Gas Turbine

Table 12-1

MATERIALS USED FOR TURBINE DISKS AND ROTORS

America

Of the many American alloys, the following are a few:

19-9DL, Discaloy, 16-25-6, W 545, Incoloy 901

Great Britain

Ferritic Alloys

Molybdenum-vanadium steels-e.g. Mova.

1% chrome-molybdenum steels-e.g. Hecla 153.

1% chrome-molybdenum-vanadium steels-e.g. H.51.

3% chrome-molybdenum-vanadium steels-EN.40 type.

3% chrome-molybdenum-vanadium-tungsten steels-e.g. Chrom Va-W.

12% Chromium steels-e.g. F.G., H.G.T.4, H.46, Silver Fox 11, etc.

Austenitic Alloys

18% chromium-8% nickel type-e.g. F.C.B. (T).

Nickel-chromium steels-e.g. R.20, G.56.

Nickel-chromium-cobalt steels-e.g. G.18B, Res 326.

Cobalt-nickel-chromium alloys-e.g. G.32.

Nickel-chromium alloys-e.g. Nimonic 80, 80A and 90.

Table 12-2

ADVANTAGES AND DISADVANTAGES OF FERRITIC AND AUSTENITIC ALLOYS

FERRITIC

Advantages	Disadvantages
1. Good ductility.	
2. High proof and maximum stresses, at lower temperatures.	1. More susceptible to loss of strength if design temperature is exceeded.
3. Lower coefficient of thermal expansion.	2. Poor weldability, and complete heat-treatment required after welding.
4. Higher thermal conductivity.	3. Poor oxidation resistance.
5. Good forgeability.	4. More liable to segregation during casting.
6. Good machining properties.	
7. Structural quality, especially the central portion of the ingot.	
8. Lower cost, about one-quarter to one-half that of a similar austenitic disk.	
9. Lower strategic metal content.	

AUSTENITIC

1. Superior hot-strength properties.	1. Require a large amount of strategic elements.
2. Better oxidation resistance.	2. More difficult to forge.
3. More easily welded and need only be stress-relieved after welding.	3. Greater cost, due to 1 and 2
	4. Tendency to solidify in ingot with central unsoundness.

12.1.3 Radial-Flow Impellers

In compressors, according to application, impellers are open radial, inducer-type, or closed. The standard design is an open radial, the inducer-type design incorporates inlet scoops which help maintain efficiency at higher flow conditions, and the closed impeller with backward leaning blades offers greater flexibility of design over a wider range of flow and head. Elliott Co. uses the following design practice: the open radial impeller is cast or forged and milled to accurate profiles; the inducer-type impeller is similar to the open radial design but includes welded-on inlet scoops; the closed impeller is made up of a forged backplate onto which blades are welded. A forged cover plate is then welded into position. No rivets are used which might impede flow or accumulate foreign material (see Figure12-15). Elliott single-stage impellers are available from 700 to 100,000 cfm and greater.

The impellers of DeLaval multi-stage compressors are of the enclosed type. Impeller parts are fabricated from heat-treated forgings and joined by counter rivets or special welding techniques. Hubs and side plates are usually made of a special hammer-forged nickel steel alloy. Where the impeller passages are wide, the blades are separate 11-13% chrome steel forgings as illustrated in Figure 12-16.

Figure 12-17 shows a DeLaval riveted impeller. Where impeller passages are narrow, the blades are milled directly from the hub forging as illustrated in Figure 12-18. Rivets are of 11-13% chrome steel hand-worked to assure tightness. Construction of the impellers may be welded, depending on size: for large impellers the blades are separate forgings, fillet-welded to the hub and sideplate; for others, the blades are milled partly from the hub and partly from the sideplate, and butt-welded down the center (Figure 12-19).[81]



Fig. 12-15 - Elliott Co. Radial Compressor Impellers

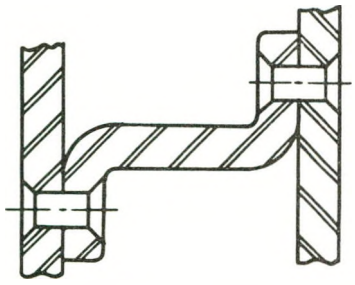


Fig. 12-16 - Section Through DeLaval Impeller Showing Separate Forged Blades

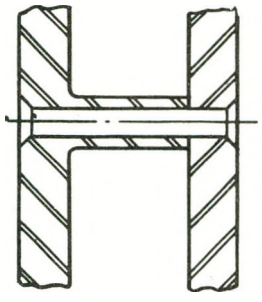


Fig. 12-18 - Section Through DeLaval Impeller Showing Blade Milled from Hub Forging

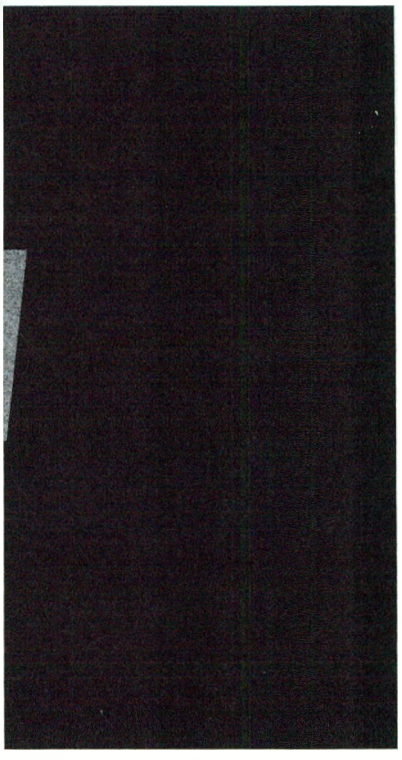


Fig. 12-17 - DeLaval Riveted Centrifugal Compressor

The welds are full penetration welds and are performed as submerged arc welding. The thickness of the forgings prevents distortion during welding. After welding is completed, the impeller is stress relieved at 1100°F. Before final machining and grinding, the welds are checked by magnafluxing. Figure 12-20[61] shows a complete welded DeLaval impeller. Such welded impellers are used for tip speeds up to 1000 fps. The impellers are individually balanced and shrunk and keyed to the shaft.

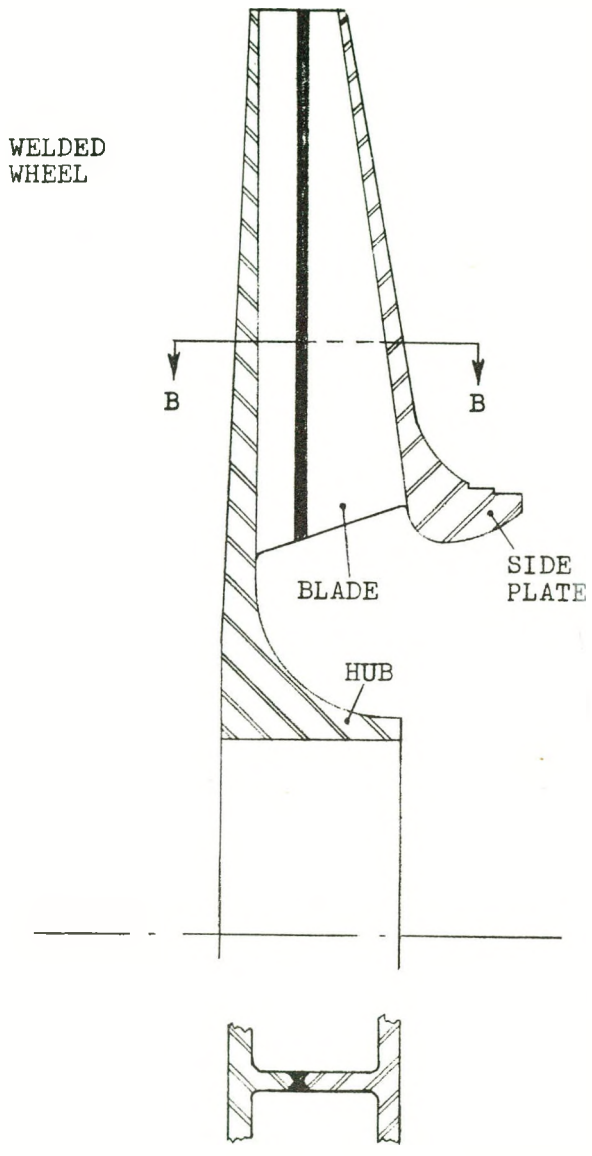
Clark builds four basic types of impellers: milled, fabricated, welded and cast. The kind used is determined primarily by the size of the unit, by the gas being handled, and by the specific application (see Figure 12-21).

Most applications use fabricated impellers. Disk and cover halves of the impellers are of forged alloy steel. Die-formed chrome alloy vanes are attached to the disk and cover halves by chrome alloy rivets. The milled type is machined from a solid disk forging. Disk and cover halves are joined by rivets which pass through the milled vanes. Flush riveting is achieved by use of countersunk rivet holes. The outer surfaces of the impellers are ground smooth. After assembly, impellers are individually tested for strength and balance. Impellers are keyed to the shaft and the complete rotor tested. For smaller units, impellers are frequently precision cast of aluminum alloys.

Radial inflow turbine rotors are made only for small power gas turbines. They are made as one-piece rotors, i.e., turbine blades and turbine hub, made from highly heat-resisting alloys, are an integral structure. Usually such rotors are integrally cast by such methods as investment casting. Figure 12-22[147] shows such a rotor (diameter, 125 mm) cast of Cr-Ni-Mo steel and butt-welded to the shaft.

12.1.4 Turbine Blading

Probably more thought and more effort have been placed on blading and blade materials than on any other component parts (See also Section 10.1 and Report NYO 9793[6] on Structural Materials).



Fig, 12-19 - Sections Showing DeLaval Impeller, Forged and Machined in Halves and Welded Together

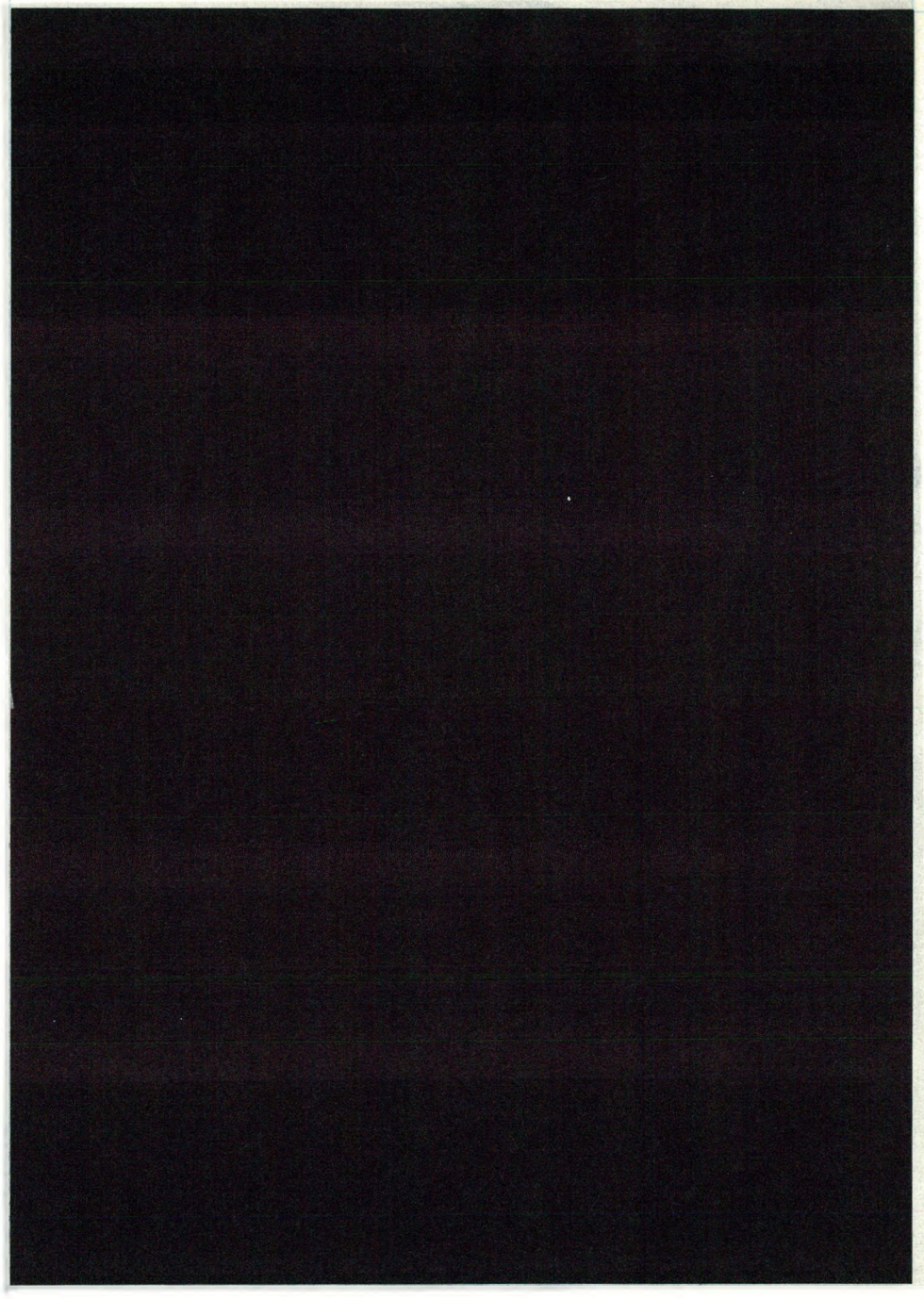


Fig. 12-20 - DeLaval Welded Compressor Wheel

Solid Blades

The design of a gas-turbine blade is made in the light of the known creep and fatigue properties of the material to be used, and of the expected life of the engine. A turbine blade is a relatively complex shape, involving many machining operations in its development from a simple bar, and considerable attention has therefore been paid to methods of producing blades in order to minimize the amount of machining necessary, the object being to produce a perfectly satisfactory component in the most economical manner.

Several American and Swiss gas turbines have successfully used precision-cast rotor blades and serious attempts have been made to introduce them in British engines.

In fact, with the introduction of welding in vacuum of the Nimomic series of high temperature alloys, cast alloys have developed even superior high-temperature properties than wrought alloys.[148] Against cast turbine blades can be said that non-destructive methods of testing, by which such components must be examined, have not yet been developed to a high enough degree as to warrant complete confidence in the absence of small defects. Precision-cast rotor blades will be used more extensively when the high-temperature properties will exceed those of the best available wrought alloy far enough that even with the application of an appreciably higher safety factor the cast component will give an advantage.

The production of rotor blades from wrought material can follow one of three main directions, as described below. A typical selection of gas-turbine rotor blades in wrought Nimonic alloys is illustrated in Figure 12-23.[149]

(a) Machining from wrought stock - This method of production is commonly applied to two types of blade. It is used for relatively small blades, which cool rapidly during forging operations so that repeated re-heating is necessary. This makes it an expensive process and, since

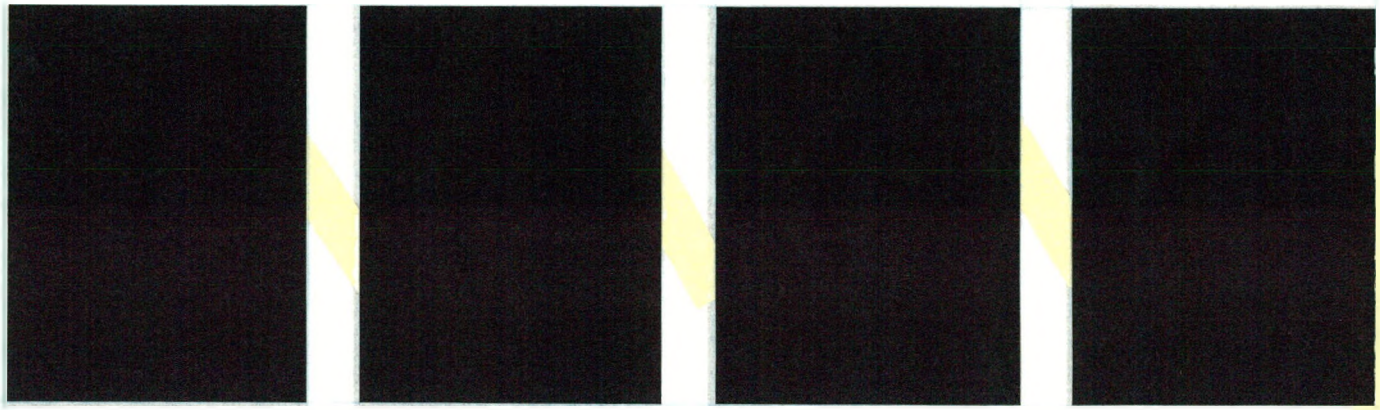


Fig. 12-21 - Clark Centrifugal Impellers

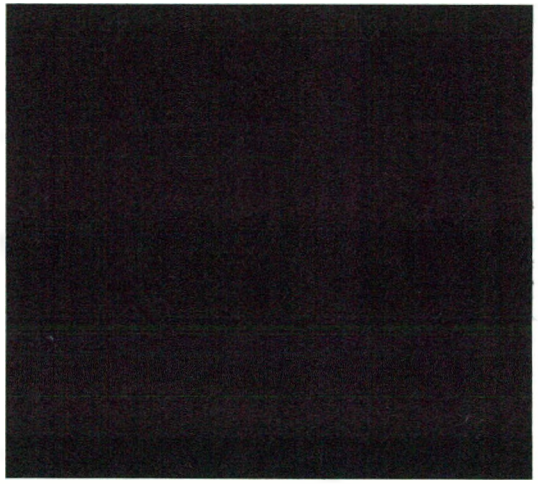


Fig. 12-22 - Integrally Cast Wheel for an Exhaust-Gas Turbine

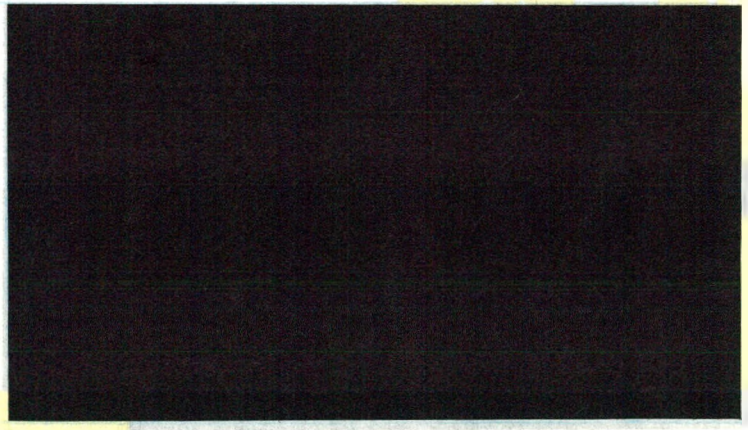


Fig. 12-23 - Selection of Gas-Turbine Rotor Blades in Nimonic Alloys

only small quantities of metal have to be removed, it is usually found to be more economical to machine from wrought stock. The other class of blade commonly produced by this method is the type used in industrial gas turbines. This is true for such gas turbine types which are being produced in relatively small quantities, where the cost of making forging dies for the blades is therefore not justified. The wrought stock from which the blades are to be machined is normally of rectangular or parallelogram section. This is usually produced by direct extrusion from cast ingots, sometimes followed by cold-rolling to refine the grain. In the larger-section material of industrial gas-turbine blades, forging may be desirable in order to break up the remains of the cast structure because low-ratio extrusion is frequently insufficient in itself to remove all traces. Generally, highly heat-resisting materials encounter serious difficulties in forging.[28]

(b) Over-size forgings - The majority of rotor blade forgings are made approximately 0.04-0.08 inches over-size on all surfaces. This is an adequate allowance to permit correction of inaccuracies of forging during machining, and has the further advantage that it allows the forging dies to wear appreciably before they need to be resized. The procedure adopted by different forgers vary considerably, but a common factor is the production of a "use" before die-forging is carried out. The forging "use" is normally in the shape of a dumb-bell and is produced either from bar stock of diameter corresponding to that of the shank of the dumb-bell or from slugs cut from bar stock of diameter corresponding to that of the ends of the dumb-bell. In the former case, the enlarged ends are produced by upsetting either on special electro-upsetting machines or on mechanical upsetting machines, for which the bars have to be heated separately. A larger diameter bar can be formed into a dumb-bell by partial extrusion followed by upsetting, by hand-forging on a hammer, or by pinch-rolling on a special machine. Conversion of the dumb-bell to the final die-forged blade is carried out in two or three

operations with intermediate reheatings. A variety of equipment has been employed successfully for the forging operations: hydraulic presses, screw or crank presses, and drop hammers. In general, a quick-acting machine is desirable in order to minimize the chilling effect of the dies.

(c) Precision forging - In some cases it is considered economically advantageous to forge to within about 0.005 inches of the finished dimensions. For forging of this type, it is normal practice to electroplate the "use" with nickel, in order to minimize the amount of intergranular oxidation occurring, for instance, in Nimonic alloys and as an aid to flow of metal in the die. Such close-tolerance forgings can frequently be finished by a process such as abrasive-band polishing, thereby avoiding expensive machining operations on the airfoil section of the blade.[149]

Figure 12-24 shows one drop-forged combination blade bucket produced for the General Electric CJ-805-23 aft-fan engine by Utica Drop Forge & Tool Division of Kelsey-Hayes. The same company developed, together with General Motors, a special cold-forming process which was used, for example, for the fabrication of the turbine and compressor blades for the Clark T-C set of the ML-1 nuclear power package.[12]

Cooled blades

Much thought has been given to hollow blades (see also Section 11.2). They have been formed by cupping and drawing from sheet metal, by forming and welding sheet metal, by forging from special shapes, and by casting.[28] One promising method which has been developed for application to the Nimonic alloys is that involving the extrusion of aerfoil sections with a number of suitably disposed elliptical-section holes parallel to the axis of the extrusion. Figure 12-25[149] shows extruded blade sections in Nimonic alloys with cooling passages. Passages are formed by drilling the cylindrical extrusion billet with the required number of holes at

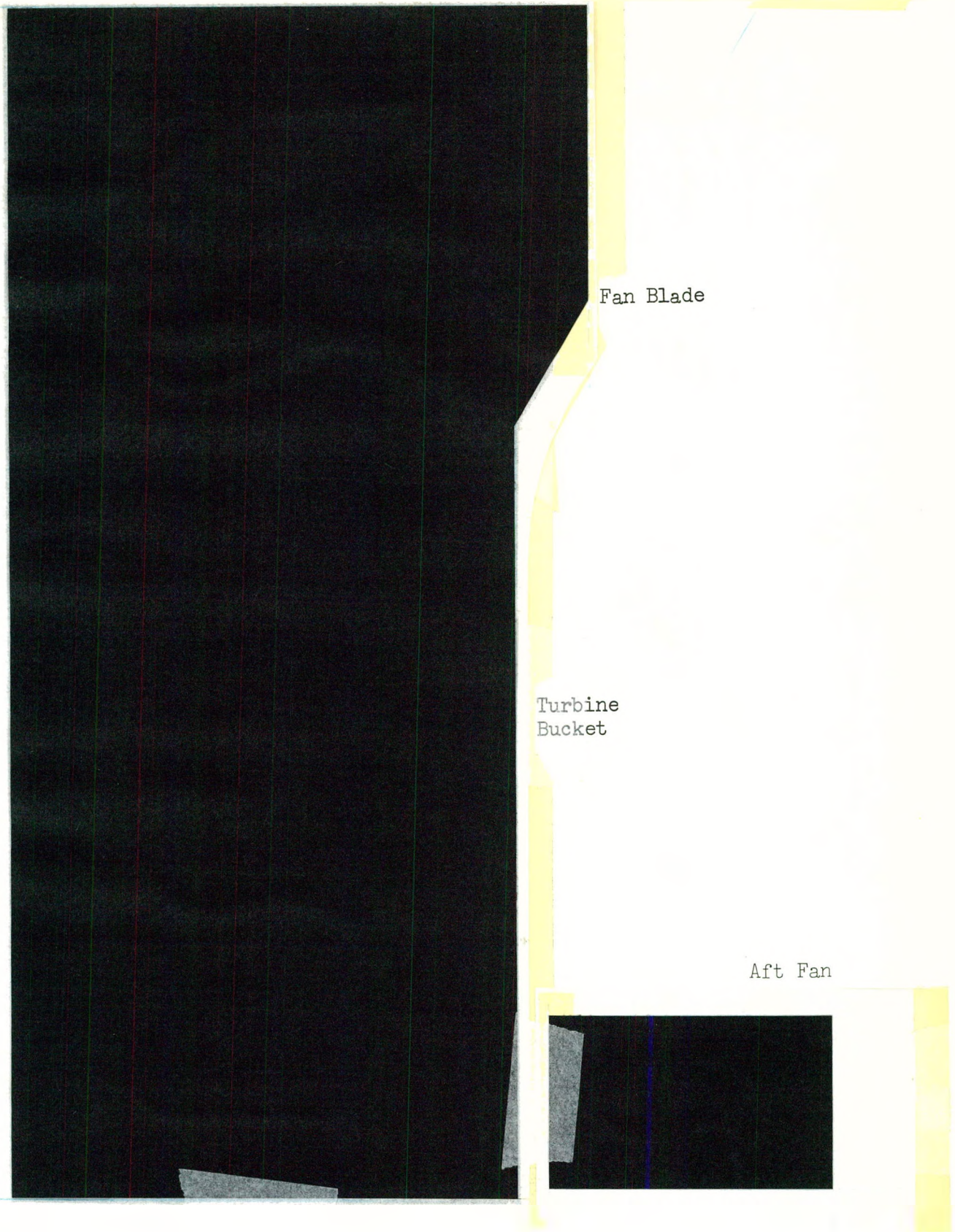


Fig. 12-24 - Combination Blade Bucket Produced for the General Electric CJ-805-23 Aft-Fan Engine

positions determined empirically, filling these holes with closely-fitting rods of a special material, the hot-working characteristics of which match those of the Nimonic alloy, and extruding the composite assembly through a suitably shaped dye. The approximately airfoil-designed extrusion is then finished close to the required size by hot or cold rolling, and cut to length. The filler material is then removed from the holes.

Constant-section extrusions of this type are suitable for stator blades, but for rotor blades, which require an integral root, a further development of the process is necessary. A billet with the necessary filled holes is first extruded to a cross-section approximating that of the root. This extrusion is then cut into short lengths, which are re-extruded singly to the required aerofoil section, but the press is stopped so that a suitable amount of material is left at the larger size to provide the root. The extrusion may finally be finished by die-forging to produce the desired taper or twist. The filler material is removed after all the hot or cold working operations are completed. Cooled blades of similar type have been produced by forging previously drilled and filled slugs, but in this case, the number of cooling holes is usually much smaller and they are located in a single line along the camber line of the aerofoil. A further method adopted for the production of experimental cooled blades has been to machine, from a normal blade forging, a blade having cooling channels in the surface and then to cover these channels with a brazed-on sheet. This method appears to be less reliable than those previously described because partial failure of the cooling could well lead to melting of the brazing alloy.

The methods outlined above have all been applied to most of the Nimonic alloys normally used for rotor blades. Other methods investigated with varying degrees of success, have included (a) casting (see Fig 12-26[147]), in which case the necessary cooling holes are introduced by the use of fine silica tubing as cores which are subsequently dissolved out in molten alkali, and (b) pressing and sintering of blades

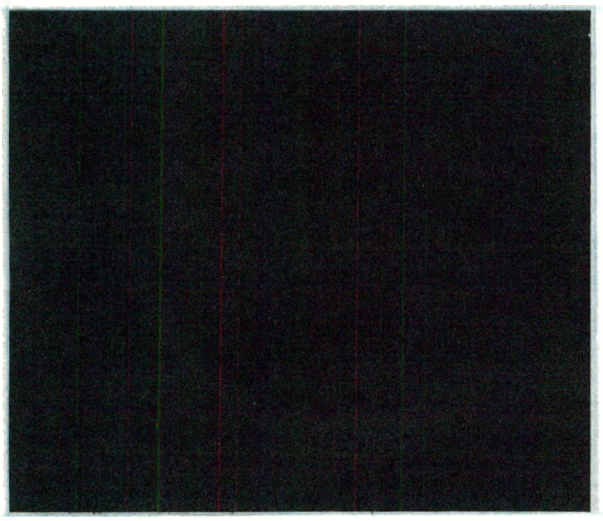


Fig. 12-25 - Extruded Blade Sections In Nimonic Alloys with Cooling Passages

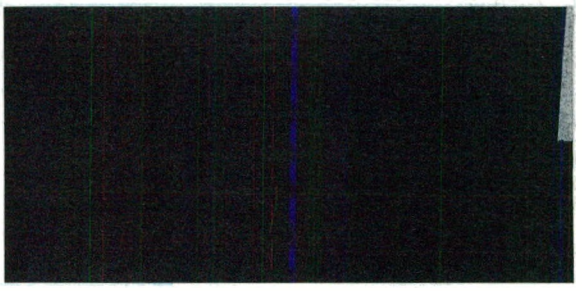


Fig. 12-26 - Case Hollow Stator Blades for Jet Engine (Diam. 140 mm)

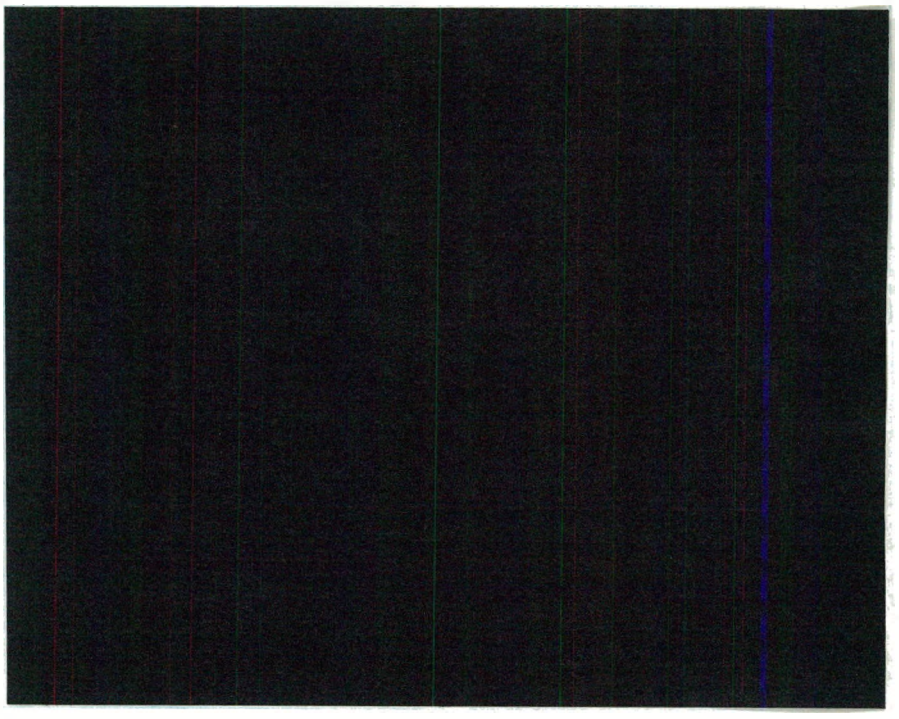


Fig. 12-27 - Internal Airfoil Designs for Maximum Blade Heat Transfer

from powdered alloys, with production of the holes by the inclusion in the required positions of cadmium wires which are subsequently evaporated in vacuum. Both these methods suffer from the disadvantage that the material from which the blade is made does not, at the present stage of development, have the reliability and strength properties of the normal wrought alloy. Other methods to produce a hollow blade are by cupping and drawing from sheet metal, and by forging and welding sheet metal.

The General Motors Corporation developed a new thin-wall hollow airfoil by casting the shell and strut as one piece in order to avoid objectionable features of fabrication and to reduce the cost of manufacture.[150] The lost wax investment method was the process selected as being most adaptable, and the foundry research and development work was done by the Fabricast Plant of the GMC Central Foundry Division. For the benefit of those persons who may not be familiar with the lost wax process, a brief step by step description is in order:

(a) The wax pattern is formed in a die made from bronze, steel, or soft metal. The cavity reproduces the desired cast contour with shrinkage allowances, and incorporates core prints to locate the preformed core within the cavity.

(b) The preformed core is placed in one-half of the injection die and the die closed.

(c) Wax is injected into the cavity and covers all of the core except the ends which are left exposed to hold the core in the investment mold material.

(d) The wax patterns are cleaned, inspected and assembled onto a combination pouring basin and riser.

(e) This assembly is then dipped in a thin slurry covered with stucco grain, and the slurry dried. The assembly is then attached to a metal plate with wax, and the metal flask or can is placed around it. The plate to flask junction is sealed with wax.

(f) Investment material, premixed with binder, is poured into the flask. After a period of time the binder undergoes a chemical reaction which causes the investment slurry to gel or set up into a solid mass.

(g) The mold is then passed through a continuous oven where the wax is melted out and the investment material preheated to 1900°F. This takes approximately 12 hours.

(h) The preheated mold is removed from the oven and clamped onto an induction furnace crucible, in which has been melted a weighed charge of metal which is just sufficient to fill the mold cavity. The furnace and mold are then rolled over to transfer the molten metal from the crucible to the mold.

(i) After cooling the castings are removed from the investment material, the riser is cut off, the casting sand-blasted, and the core removed prior to inspection and subsequent machining.

Satisfactory cores were molded from American Lava Corporation Alsimag 145 ceramic material, then dried and fired on setter blocks made from the same material, to provide compatible shrinkage. Several setter block designs were tried before a satisfactory combination was found.

Using these cores, a sufficient quantity of turbine blades were cast to make laboratory and single burner rig tests and provide for actual engine running. Similar ceramic cores of the pedestal design were made for the associated air cooled stator vanes, and parts made for test rig and engine use. During a ten hour endurance run, with the pedestal type of internal geometry, and with gas temperatures cycling between 1785°F and 2060°F, no detrimental heat effects were encountered. Theoretical calculations predict that with a total of 3% of compressor air used for cooling, a 25% increase can be gained in bhp with a reduction of 4.5% in specific fuel consumption.

The success of the pedestal type core design led to the development of the internal fin configuration, wherein the weight of the fins, unlike the pedestal type, would be transferred back to the base platform

instead of loading the shell, and the heat transferability would be increased to a maximum efficiency, while at the same time permitting control of the heat gradient across the airfoil. Work on this design was started with a 0.020 thick fin on a 0.020 spacing and a common air space 0.020 wide in the center (Figure 12-27[150]). This was considered to be the minimum practical thickness to which a reliable core could be made.

The inspection of complex hollow structures is rather difficult because of restrictions which prevent use of conventional instruments. To overcome this difficulty, it has been determined that the use of radioactive materials can be used if proper techniques are evolved into standard procedures. Such a technique was developed to accurately determine the wall thickness of hollow airfoils containing internal cross pedestals and fins within a plus or minus 0.001-inch tolerance. The procedure involves holding the airfoil in a fixture which also positions a small geiger tube equipped with a lead collimator. The fixture is located in a glove box to protect the operator. An aqueous 1 M HCl acid solution containing the isotope Samarium 153 Oxide (Sm_2153_{03}) is injected into the airfoil with a hypodermic syringe. The radiation attenuation is measured by the geiger tube. Pulses from the tube are counted on an Atomic Scale. The counts in a specified time are then converted to actual thickness measurements. Several spot measurements are made by repositioning the geiger tube. This procedure is currently being used in the Allison Applied Physics Isotope Laboratory as a routine check of air cooled turbine airfoils of this type.

It was concluded that:

(a) Investment casting with preformed soluable ceramic cores is a practical and economical method for making hollow air cooled airfoils with intricate geometry, which will have long endurance life.

(b) Any of the presently used heavy alloys can be cast with an internal air passage geometry selected by the airfoil designer.

(c) Hollow airfoil wall thicknesses can be cast to a controlled thickness as low as 0.020 inch, and can be solution machined to further reduce the thickness if desired.

(d) Twisted, tapered and dumbell type internal passage configurations can be economically produced in production quantities.

(e) Parts may be inspected to plus or minus 0.001 inch without difficulty.

(f) Similar parts such as fuel controls, thermocouple probes, Pitot tubes, etc., can be economically made by the soluable ceramic core method.

(g) Vacuum and centrifugal castings can be readily produced.

(h) Electric analog computation may be used to good advantage in establishing the heat transfer geometry required.

Hollow blades merit attention. They offer three advantages: they will result in the use of lesser quantities of scarce materials; they can result in lower stresses; and they provide for air or other cooling which is desirable from the materials standpoint. There are blading problems, of course. For example, many blades will have to be shrouded. Integral shrouds on blades have some limitations. The heat-resisting alloys do not cold-rivet at all, and hot-riveting methods are being developed. The welding of blades to disks is practical but needs further development.[146]

12.1.5 Integral Rotors

Small turbine rotors are sometimes produced as integral units. Figure 12-28[149] shows a gas-turbine rotor of Rover Gas Turbines Ltd. with integrally machined blades. Figure 12-29[147] represents a rotor for a Sulzer exhaust-gas turbine with integrally cast blades, of Sulzer alloy WF178. Finally, integrally cast blade rings, welded to a combined hub and disk of lower alloy are used by the Chrysler Corporation for the development of an automotive gas turbine (see Figure 12-30[10]).

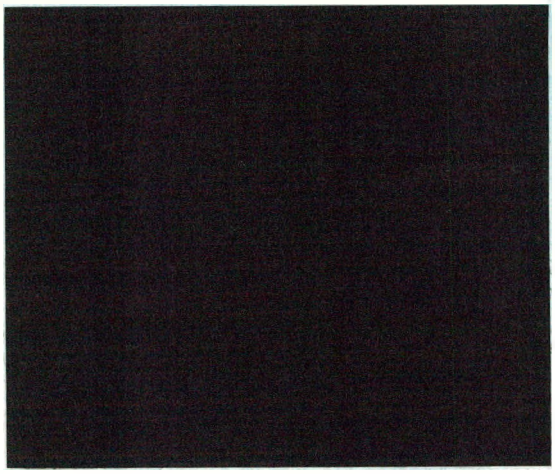


Fig. 12-28 - Rover Gas-Turbine Rotor with Integrally Machined Blades

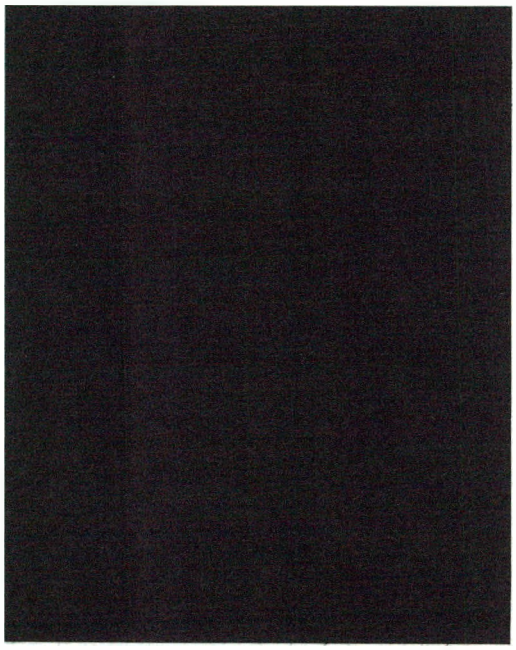


Fig. 12-29 - Sulzer Wheel of an Exhaust-Gas Turbine with Cast Blades

Table 12-3[39] lists some of the materials now in use as gas-turbine blading alloys.

Table 12-3

BLADE MATERIALS

America

Medium-alloy steels-e.g. 19-9DL, Discaloy, 24.
Nickel-chromium-cobalt alloys-e.g. N-155, S.590, S.816.
Nickel-chromium alloys-e.g. K.42B, Inconel X, Hastelloy B and C, Inco 713-C.
Cobalt-based alloys (e.g. Vitallium or Haynes Stellite 21, 422-19, 6059 and X.40-all used in the cast condition).

Great Britain

Low-alloy steels-coolest stages of certain industrial turbines only.
Medium-alloy steels-e.g. F.C.B. (T), Rex 326, G.40.
Nickel-chromium-cobalt alloys-e.g. Hecla EM.20 and MM.20, G.32 and G.42B.
Nickel-chromium alloys-e.g. Nimonic 80, 80A, 90, 95 and 100.

While American manufacturers favor precision cast blades, British practice generally has been to use forged rotor blades. The British preference for forged blades arises from the, until recently, much greater uniformity in the properties of blades produced in this way. The cast cobalt alloys, however, are among the most creep-resistant alloys available and it is generally found that American gas turbines using these alloys run at higher temperatures than usual. Several alloys are available in England for producing cast turbine rotor blades, e.g. G.34, Hecla EM.35 and MM.35, but little use has been made of them so far in this position. The present trend toward the use of shroud rings on the rotor blades will, however, encourage the use of these alloys, because the greater damping-out of vibrations that this will achieve will make the lower fatigue strength of cast blades of less importance.

The Nimonic alloys have so far provided the vast majority of British aircraft turbine rotor blades. Those which have found the most extensive use until recently are Nimonic 80, 80A and 90. Nimonic 95 and 100 are fairly recent developments and are mainly designed for short-life requirements at fairly high temperatures.

While the nickel alloys, are, without doubt, superior to all the iron-base alloys at the highest operating temperatures, the much greater initial cost of nickel alloy blades frequently restricts their use in land and marine turbines to the hottest stages. This may be illustrated by reference to the recent 2500 kw power sets built by the B.T.H. Co. Ltd., for the East African Power and Lighting Co. Here there are nine stages of rotor and stator blades, the first stage being Nimonic 80, the second Rex 326 and the rest F.C.B. (T), for both types of blade.

It was mentioned above that the cast cobalt alloys have greater creep resistance than any of the heat-resisting steels or other wrought heat-resisting alloys. The metallurgical structure of these alloys is similar to that of a cored solid solution with the minor phases present in the interdendritic region. It is interesting to note that if such a structure is annealed at a high temperature so that homogenization takes place, the alloy will lose a large proportion of its creep strength. Consequently the cast alloys are usually put into service with no prior heat-treatment[39].

12.1.6 Stator Blading

The primary requirements for the stator blades, or inlet guide vanes of gas turbines are resistance to oxidation and to thermal shock. The first-stage inlet guide vanes reach the highest temperature attained by a metallic component of a gas turbine, and although the applied stress is small, being only that due to the gas pressure, the inlet vanes are subject to severe buckling and cracking due to the stresses developed by the rapid changes of temperature. The temperature changes occur

principally on starting or shutting down the engine, and particularly in aircraft turbines in which rapid accelerations or decelerations occur, severe stresses ensue.

A wide variety of different alloys and methods of production are adopted for these components. The alloys used in Great Britain range from the simpler stainless steels in the cooler stages, through the higher alloy steels, e.g., 25% chromium-20% nickel, in intermediate conditions, to the Nimonic alloys in the hottest region. In American turbines alloys such as S.590, N-195, Hastelloy C, Inconel X and Haynes Stellite 21 are frequently used. A certain amount of research work has been carried out, and is still in progress, to develop nozzle guide vanes from either wholly refractory materials or metal-ceramic combinations. For example, Pametrada are experimenting with zircon plus $2\frac{1}{2}\%$ chromic oxide and silicon carbide blades, while in America Kentanium is promising[39]. For aircraft engines and for the smaller industrial gas turbines, most stator blades are made by precision casting and among the alloys used, including austenitic steels, cobalt-base alloys, and nickel-base alloys, the Nimonic alloys play an important part. Nimocast 75, 80 and 90 have all been used for these components and although their casting characteristics are such as to necessitate carefully developed production techniques, followed by the most searching methods of non-destructive inspection, very satisfactory cast blades have been produced. Figure 12-31[149] shows a selection of gas-turbine stator blades precision-cast in Nimonic alloys.

A method for one-piece investment casting of small gas-turbine engine diaphragms has been developed by Austenal Co. in this country.

12.1.7 Compressor Blading

Similar to the turbine blades, the manufacturing of compressor blades may be performed by machining from rolled stock, by drop-forging, by casting; or they can be integrally machined or cast with their respective disks. All of these methods are being used, depending on the

particular design. Compressor working temperatures are well below those of turbines, so that particular material difficulties do not arise.

For the compressor blading, the main requirements are:

(a) Good resistance to creep at temperatures up to 390-570°F because the temperature of the air may rise to this level during compression.

(b) Good fatigue resistance.

(c) Ease of fabrication.

(d) In cases where the overall weight of the unit is important, such as the aircraft gas turbine compressor, the specific gravity of the material should be low.

(e) For marine purposes, and certain land-based turbines, the compressor blading should have good corrosion-resisting properties.

In the aircraft field, wrought aluminium alloys and, to a lesser extent, cast magnesium alloys are proving to be extremely satisfactory. Their low density keeps the overall weight of the compressor down, and their ease of fabrication, when compared with steel, allows the entire rotating section of the compressor to be forged or even cast as a single unit where the design makes this possible. The creep strength of alloys based on these two metals have been much improved recently, and they are now capable of short-time operation up to the 480-660°F required: "short-time" in such cases usually refers to periods of operation from a few hundred to 1000 or 2000 hours. Where lives of several years are called for, these alloys are not suitable. Such alloys have a high resistance to corrosion, particularly of the intercrystalline type, to which the thin trailing edges of the blades are most susceptible. The natural corrosion resistance of an aluminium alloy is greatly enhanced by an electro-chemical treatment, generally referred to as anodizing, which produces a highly-protective film of aluminium oxide on the surface.

The aluminium alloys are readily forged, particularly in the annealed condition and require little or no surface cleaning afterwards. The cast aluminium alloys have so far had little or no application in the gas turbine in situations where both temperature and stress will be encountered, but they are frequently used for casings, etc., in aircraft gas turbines. They lose their mechanical properties rapidly when heated to 300-400°F for prolonged periods.

Magnesium alloys are relative newcomers to the metallurgical field. The high inflammability of magnesium and the difficult production of the pure metal delayed its use until recent years and, consequently, the application of magnesium alloys to the gas turbine is rather limited at the present time.

The recently developed titanium alloys are now appearing in commercial production, though the total annual world output is still only a few thousand tons. The considerable interest which has arisen in the application of titanium alloys springs from a number of desirable properties, particularly the possibility of tensile strengths in the region of 85 ton/in^2 with only half the specific gravity of steel. Because of the rather rapid loss of strength, and susceptibility to excessive oxidation as the temperature increases, however, the useful limit to titanium alloys is probably only in the region of 930°F. The properties of titanium alloys, therefore, are roughly intermediate between those of aluminium or magnesium and the ferritic steels. Extensive use of titanium in an aircraft gas turbine compressor can effect a saving in weight of approximately 20% of the total engine weight, a real advantage.

In certain conditions, the resistance of titanium to corrosion is higher than that of stainless steel, particularly to that caused by sea-water. Its application in the compressor of marine gas turbines should, therefore, prove particularly attractive because the moisture-laden sea air is detrimental to many metals. In its fatigue properties,

titanium is similar to steel in that it possesses a definite fatigue limit, i.e., the application of reversed stresses below about 30% of the ultimate tensile strength is unlikely to lead to failure.

In marine and land-based gas turbines, weight is not such an important consideration as in the aircraft engine and long-term reliability, particularly resistance to fatigue, becomes a prime factor. Furthermore the higher pressure ratios available from an axial compressor make this design more attractive than the centrifugal type. Consequently, these engines generally use the heavier but much stronger alloys such as aluminium bronze, copper-nickel alloys, low-alloy steel and stainless iron or steel.

Substantial numbers of both moving and stationary blades are manufactured from aluminium bronze, a copper alloy containing from 5% to 11% aluminium, together with iron, nickel and manganese in varying proportions. This material is readily formed into blade shape by precision forging and the surface finish is so good after this operation that little further treatment is required. The specific gravity is approximately 7.5. An alloy containing 10% aluminium, 5% iron and 5% nickel (e.g. Hidurax 1/12A) has particularly good creep strength. At the temperature encountered in the compressor, the thin surface film of alumina formed on these alloys provides a high degree of corrosion resistance.

In certain gas turbines where a high compression ratio is required, a steel may be necessary for the compressor blading. Several types of steel are used, ranging from mild steel to the stainless materials. The greater density is offset by the much higher resistance to fatigue stresses.

The corrosion resistance of stainless iron and steel, however, is frequently required and these are the most popular ferrous alloys for compressor blading. Stainless iron blading has been used for a

number of years in steam turbine manufacture, the composition being about 12% chromium with the carbon content being kept as low as possible. Ferritic steels of the 12% chromium type and austenitic steels of the stabilized 18% chromium-8% nickel type are also widely used.

The manufacture of blading in these materials is conveniently carried out by precision casting or precision forging. A mechanical or electrolytic polishing process is usually employed as a final operation to ensure freedom from surface flaws, the presence of which would impair the fatigue properties of the blade.[39]

12.1.8 Blade Fastenings

Rotor

Considerable thought has been given to the design of blade roots for proper attachment to the supporting disk. A.T. Colwell and R.E. Cummings recommend the fir tree attachment as the best of ten methods presented for comparison.[35] Other sources confirm this statement.[48] The fir tree is by far the most employed attachment for turbine blades. Sometimes turbine blades are fastened to the disk by a bulbroot attachment, called also DeLaval attachment (see Figure 12-41).

For compressor blades, the fir tree attachment is also frequently used. However, other attachments, as T-roots or dovetail roots, have also a wide application here. In some compressors, the long blades have fir tree roots, and the short blades are dovetailed. Hinge attachments, threaded root attachments, or others are less frequently encountered. Locking devices are provided in each type of fastening. Fir tree roots can be locked, for instance, by peened-over pins.

Stator

Two alternative installation methods are most frequent:

(a) The cylinder may be grooved to receive the blades directly. The blades would have some T-shaped or dovetailed root to fit the corresponding cylinder grooves. Seals are secured to the inner shroud to form the diaphragm ring.

(b) Stationary blades can be welded into punched inner and outer shrouds to form half-diaphragms. Rectangular or T-shaped slots conforming to the diaphragm outer shroud are machined in the cylinder. Inner shrouds are sometimes omitted.

Diaphragms may be held in place by screws or strips at the horizontal joint or by bolting through the casing to the outer shroud.

While the use of shroud rings on the moving blades of the turbine is usually undesirable from weight consideration, they are frequently used on the stator blades to prevent warping and bending. The materials of shroud rings are generally the same as those used in the blades themselves to avoid differential expansion effects. Figure 12-32[17] shows a turbine interstage half-diaphragm of a 3500 hp marine gas turbine. These components have the second-stage turbine nozzles mounted on their periphery. The nozzles are brazed together in groups at the outside diameter. Each group is pin-mounted to the turbine casing with radial clearance allowed for thermal expansion of the whole assembly. This permits accurate centering of the assembly in the casing. The nozzles are brazed individually to the diaphragm, the outer rim of which is keyhole slotted between each nozzle. By this means, the temperature gradient in the diaphragm cannot result in high stresses in the diaphragm rim. Cover patches are brazed over the keyhole slots to prevent air flow through them.

Figure 12-33[151] shows a fixed stator-vane ring of the General Electric T58 turboshaft-engine compressor. The fixed stator-vane rings are built in 180° segments, of two stages each, and slip into tee slots in the casing. The fixed stator-vane rings are made of constant-section strip stock, stabbed into the rings, and brazed as an assembly. This design permits field replacement of stator-vane rings by simply removing half the casing, slipping out the ring, and slipping in a new ring. The inlet guide vanes and first-stage stator of this compressor are shrouded to make them more rugged and to increase their resistance to foreign-object damage.



Fig. 12-30 - Integrally Cast Turbine-Blade Rings Welded to a Combined Hub and Disk of Lower Alloy

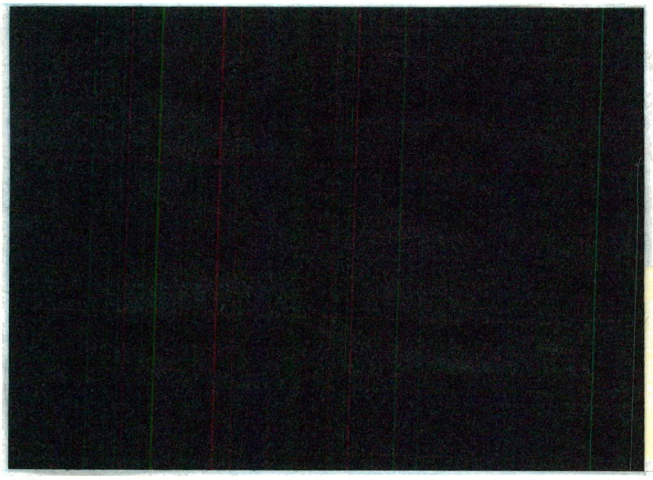


Fig. 12-31 - Selection of Gas-Turbine Stator Blades Precision-Case in Nimocast Alloys

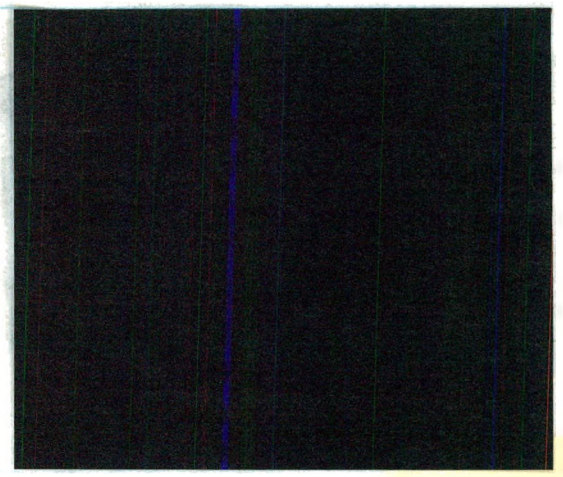


Fig. 12-33 - T58 Fixed Stator-Vane Ring

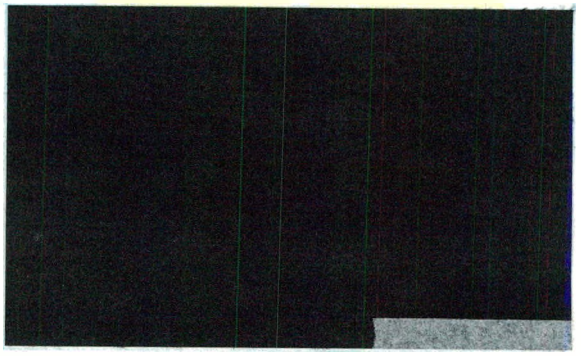


Fig. 12-32 - Compressor-Turbine Interstage-Seal Diaphragm and Nozzle-Vane Assembly

THE FRANKLIN INSTITUTE • Laboratories for Research and Development

12.1.9 Bolts

Many parts of the turbine have to be inspected at regular intervals and it is therefore preferable to fasten the casings or cover plates in position with bolts. Since the pressure inside the turbine is of the order of several atmospheres, these bolts are under stress and if they do not perform satisfactorily, the hot gases would tend to leak out at the joined faces instead of passing on energy to the turbine. Bolts are also used in certain turbines for fastening the disks to the main rotor shaft. For moderate temperature conditions the chromium-molybdenum, chromium-molybdenum-silicon and chromium-molybdenum-vanadium steels are generally used while Nimonic or equivalent alloys are suitable for use under more stringent conditions.[39]

12.2 Gas Turbine Sets

12.2.1 Clark Model CSN-1, Axial-Flow T-C Set for ML-1

Little was known about the performance characteristics or specifications governing the remainder of the components in the cycle during design of the T-C set for the ML-1. Hence, the compressor had an additional stage added to it. This would enable the T-C set to be operated at a slightly higher pressure ratio should it be required. If not required, it will be a comparatively simple matter to delete the last stage. A description of the set follows.

The T-C set is shown in Figure 12-34.[69] Figures 12-35 to 12-38[21] show a number of key features. A selected parts list is given in Table 12-4[21] while component weights are given in Table 12-5[21]. Fig. 12-39[26] shows the Clark CSN-1 turbocompressor set during assembly.

The principal components of the axial flow T-C set are: a rotor assembly on which are mounted the rotor blades for the axial compressor and turbine; a bearing housing for the compressor; the compressor inlet; the stator assembly for the compressor; the bearing housing for

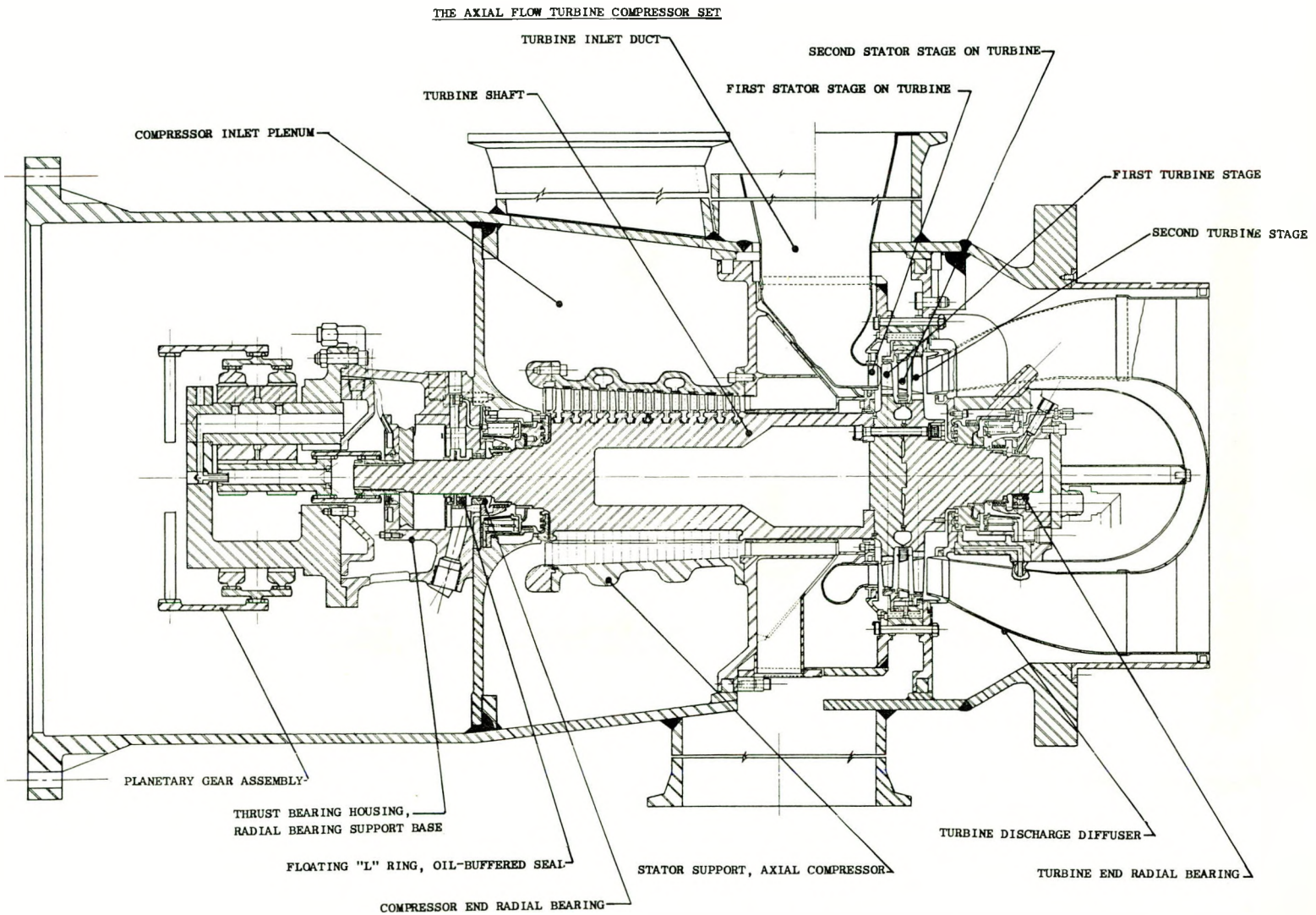


Fig 12-34 - Clark Axial Flow Turbine Compressor Set for the ML-1

THE FRANKLIN INSTITUTE • Laboratories for Research and Development
I-A2392-6

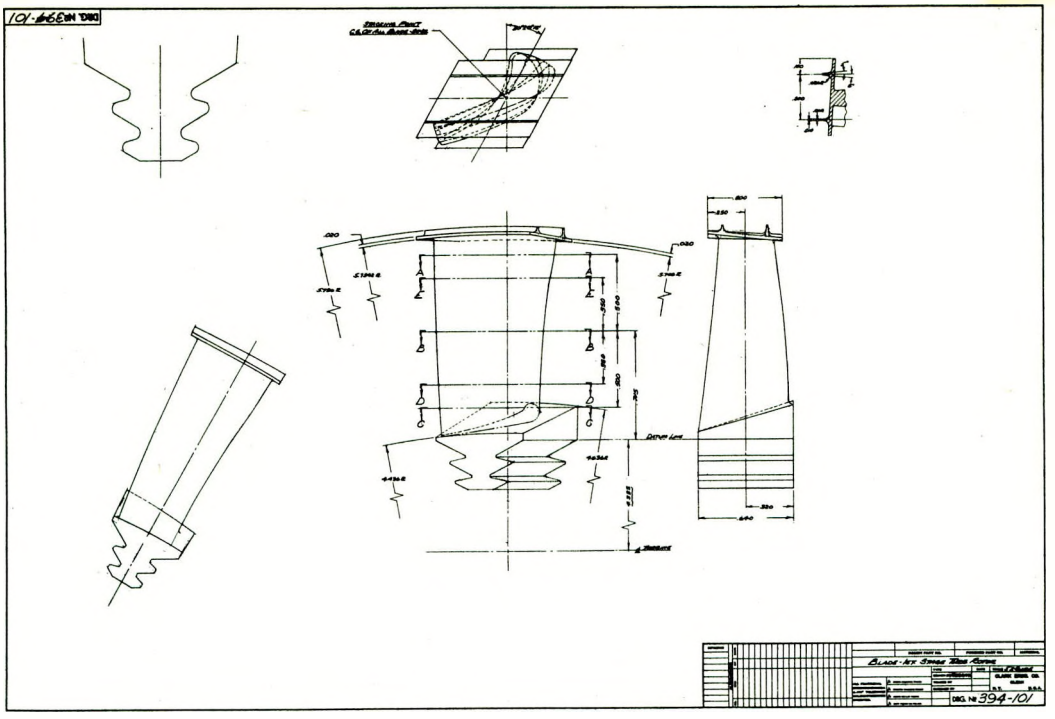


Fig. 12-35 - Clark T-C Set for ML-1 Blade- 1st Stage Turbine Rotor

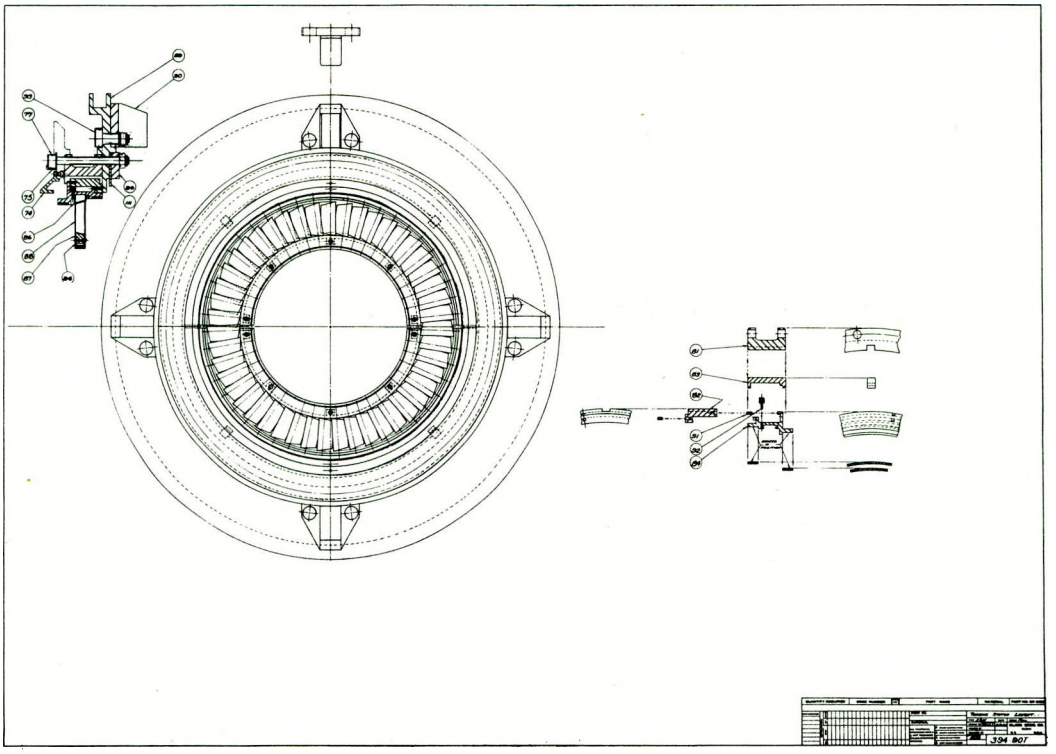


Fig. 12-36 - Clark T-C Set for ML-1 Turbine Stator Layout

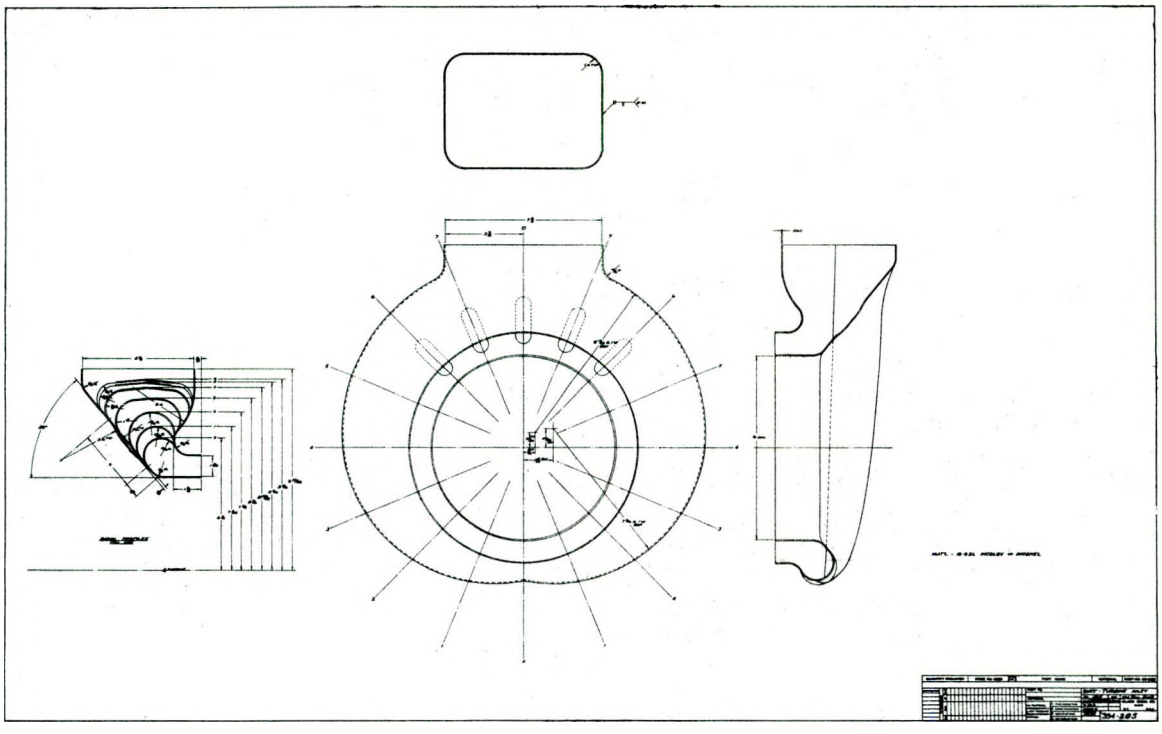


Fig. 12-37 - Clark T-C Set for ML-1, Duct-Turbine Inlet

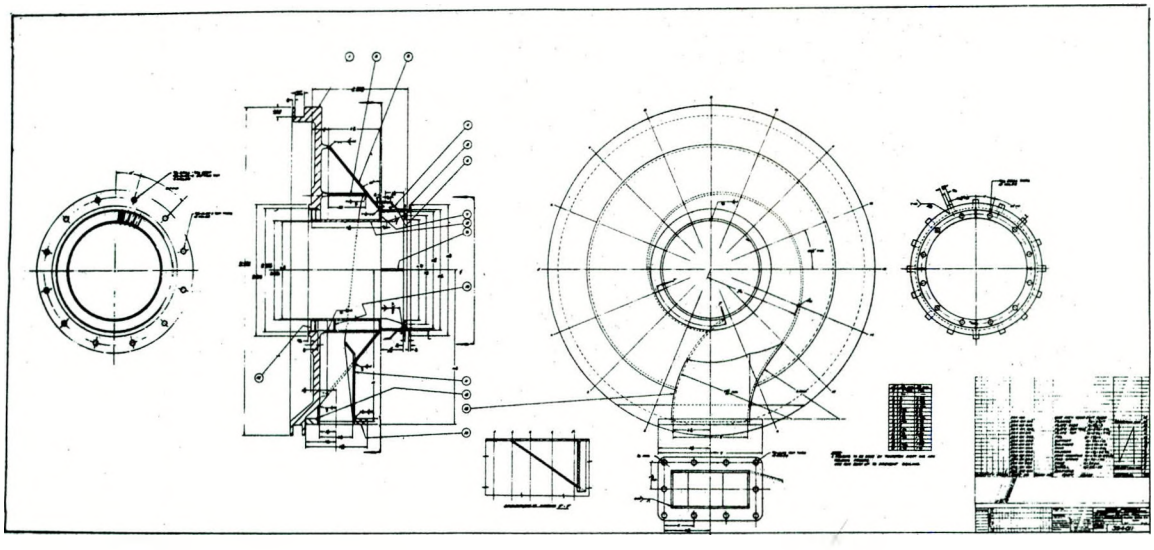


Fig. 12-38 - Clark T-C Set for ML-1, Compressor Discharge Volute Assembly



Fig. 12-39 - Clark CSN-1 Turbo-Compressor Set During Assembly

the turbine; the turbine exhaust annulus; and the reduction gear assembly. The T-C set, complete with the reduction gear assembly, is structurally self-supporting and is housed in a barrel-type pressure container 52-in. long by 28-in. in diameter. The total weight of the set, including the pressure container is 2000 lb. (The T-C set is shown in Figure 12-34.)

The main shaft and compressor rotor is a single forging. The forged compressor rotor blades are mounted in circumferential grooves in the rotor. The first-stage turbine rotor disk, and the second-stage turbine disk including the stub shaft, also forgings, are bolted to the compressor rotor. Pilot diameters on each part maintain concentricity, and radial pins transmit torque. The forged, shrouded turbine-rotor blades are mounted in broached fir tree slots in the rotor disks. Two cylindrical labyrinths and one radial labyrinth seal, at each end of the shaft, control gas leakage and prevent leakage of oil into the nitrogen loop. The cylindrical labyrinths are opposite to a stainless-steel honeycomb seal which is brazed to the case. The plain radial bearings are of babbitt to ensure long life. The thrust bearing is a tilting-pad bearing, similar to the Kingsbury bearing, sized to accommodate the 4000-lb axial load for the long life required. The lubrication system includes filters rated to remove particles above 25 microns. All the bearings are replaceable to facilitate maintenance.

The cast steel compressor-bearing housing contains compressor journal bearing, thrust bearing, part of the labyrinth seal, and carries the necessary connections for lubricating oil supply and drain. The stationary planet carrier of the reduction gear is bolted to a conical projection from this bearing housing. The bearing housing is bolted to the compressor inlet.

The compressor inlet is a steel casting which serves as a mounting for the shutdown seal and two labyrinth seals. In addition, when it is bolted to the inlet bearing housing, the compressor inlet supports the T-C set. Clean nitrogen from the compressor bleeds

is supplied to the labyrinth seals through internal porting in the casting. The compressor inlet is bolted by its outer flange to the barrel and separates the compressor inlet plenum from the gearbox. It provides structural support for the turbine-compressor set.

The compressor stator case is a two-piece steel casting to facilitate assembly. The case incorporates cored manifolds to permit high-pressure gas to be bled from the 3rd or 7th stages. The stator blades are cut from a rolled strip, with a blade section common to all stages. The blades are furnace-brazed into half-ring assemblies which are slid into grooves cut in the stator case.

The reduction gear consists of the internal parts of a standard DeLaval-Stoeckicht planetary reduction gear. To reduce weight, the standard gear case has been eliminated. The case around the turbine and compressor has been extended over the reduction gear assembly so the case can be bolted to the alternator. The high-speed sun gear is coupled to the rotor of the T-C set by a short sleeve with internal teeth. This sleeve can accommodate 0.002-in. of misalignment due to dimensional tolerances between the planet carrier and bearing housing. The pressure container around the whole T-C set and gearbox is provided with lubricating oil supply and drain connections. These external connections are at the alternator end of the pressure container.

The compressor-discharge volute bolts to the compressor case and seals with a piston-ring-type seal at the outer case. The volute assembly separates the compressor inlet from the compressor discharge and turbine inlet region. A labyrinth seal is provided in the volute assembly to control gas leakage between compressor discharge and turbine inlet. The intermediate case bolts to the compressor discharge volute assembly and to the turbine stator assembly. This case has two perforations to allow access to the turbine inlet volute and the compressor discharge volute.

The turbine stator assembly includes a diaphragm separating the turbine inlet-compressor discharge area from the turbine discharge. The stator blades are held in split-ring assemblies which are supported to allow radial expansion. The four arms supporting the hub assembly bolt to the turbine diaphragm and four keys are bolted to the support for the bearing at the turbine stub-shaft. The keys fit into keyways fastened to the outer case and provide for axial and radial expansion of the T-C set relative to the outer pressure case.

The oil-cooled bearing hub contains two cylindrical labyrinths, one radial labyrinth and a shut-off seal. Suitable inlet and outlet connections are provided to supply nitrogen to the labyrinth seals and the oil supply and drain lines.

Hub support arms and plumbing lines pass through the turbine exhaust diffuser annulus. Fairings, provided around the support arms and the plumbing lines for insulation and streamlining, divide the exhaust diffuser into four flow passages. The annulus is reformed downstream of the support arms. An extension sleeve is bolted on the turbine exhaust flange to protect the diffuser. This arrangement permits a piston-ring-type seal, located at the end of the diffuser, to control the amount of cooling flow through this area[69].

12.2.1 Stratos Model TCS-670 Radial-Flow T-C Set for ML-1

The design approach by Stratos for this unit has been governed by two primary considerations:

(a) The unit should require a minimum of maintenance during the expected life of 50,000 hours and

(b) The efficiencies of turbine and compressor should be as high as possible with no sacrifice in reliability.

Table 12-4

SELECTED PART LIST FOR CLARK T-C SET OF THE ML-1

Compressor Inlet

Item	Title	Mat'l	No. Req.	Remarks
1	Annulus - Comp. Inlet	Low Carb. Steel	1	Castings
2	Seal Assy. - Comp. Shutdown	AM 350 Bellows	1	17-4 PH End Plates (Purchased from Koppers Co.)
3	Bearing - 2" Precision Journal	Babbitt-lined Stl. backed	1	
4	Pin - Journal Bearing Lock	SAE 1020		
5	Housing - Comp. Bearing	Low Carb. Steel	1	Casting
6	Labyrinth Comp. Face	Bronze	1	
7	Bearing - 5" Thrust		1	Purchased from Waukesha
8	Seal Thrust Bearing	Bronze	1	
9	Plate Assy. - Thrust	Babbitt Faced	1	Low Carb. Stl. Fab.
10	Pin - Thrust Brg. Seal	SAE 4140	1	
11	Seal Ring ("L" Seal)	Silicone Ring	2	
12	Retaining Ring	SAE 1065	1	Purchased Part

Turbine Rotor

13	Blade - 1st Stage Turbine Rotor	N. 155	47	Forging
14	Blade - 2nd Stage Turbine Rotor	N. 155	47	Forging
15	Tab - Turbine Rotor Blade Lock	304 S.S.	94	Sheet
16	Bolt - Turbine Rotor	N. 155	6	Threads Silver-Plated
17	Clip - Turb. Rotor Bolt	304 S.S.	6	Sheet
18	Cover - Turb. Rotor Bolt	N. 155	6	Threads Silver-Plated

Table 12-4 (Cont.)

SELECTED PART LIST FOR CLARK T-C SET OF THE ML-1

Turbine Rotor

Item	Title	Mat'l	No. Req.	Remarks
19	Plug - Balancing		12	Threads Silver-Plated
20	Pin - Torque	N. 155	8	
21	Disc. 1st Stage Turbine Rotor	Incoloy 901	1	Forging
22	Disc. 2nd Stage Turbine Rotor	Incoloy 901	1	Forging with Haynes alloy hard faced Journal
26	Ring - Turbine Labyrinth	SAE 4340	1	
	Compressor Rotor			
23	Shim-Compr. Rotor Blade	Inconel Wire	671	
24	Shaft - Comp. Rotor	SAE 4340	1	Forging
25	Sleeve - Labyrinth	SAE 4340	2	
27	Ring - Compr. Labyrinth	SAE 4340	1	
28	Nut - Laby. Ring Retaining	SAE 4340	2	
29	Key - Thrust Collar	SAE 1030	1	
30	Blade - Comp. Rotor 1st to 11th Stages	403 S.S.	671	61 of each Stage
31	Washer - Lock	304 S.S.	2	
32	Pin - Compr. Rotor Blade	SAE 4140	11	
33	Nut - Shaft	SAE 4140	1	Purchased 001-351
34	Washer Lock	SAE 1060	1	Purchased
35	Collar - Thrust	SAE 1060	1	
	Compressor Stator			
36	Case - Compr. Stator	Low Carb. Steel	1	Cast in Identical Halves
37	Blade Assy. - Compr. Stator (St. 1-10)		10	Brazed assy. 2 half rings per stage
38	Blade-Compr. Stator(St.1-10)	403 S.S.	580	58 Per Stage
39	Vane Assy. - Compr. inlet Guide		1	Brazed assy. 2 halves
40	Vane - Compr. inlet Guide	403 S.S.	58	
41	Vane Assy.-Compr. Exit Guide		1	Brazed assy. 2 halves
42	Vane - Compr. Exit Guide	403 S.S.	58	
43	Pin-Inlet Guide Locating	SAE 4140	2	

THE FRANKLIN INSTITUTE • Laboratories for Research and Development
F-A2372-6

Table 12-4 (Cont.)

SELECTED PART LIST FOR CLARK T-C SET OF THE ML-1

Turbine Stator

Item	Title	Mat'l	No. Req.	Remarks
44	Blade - 1st St. Turb. Stator	N. 155 or 19.9 DL	47	Cast or Rolled
45	Ring - Inner 1st St. Turbine Stator	19.9 DL	1	Sheet
46	Ring - Outer 1st St. Turbine Stator	19.9 DL	1	Sheet
47	Duct Sub. Assy. - Turbine Inlet	19.9 DL Incoloy or Inconel	1	
55	Ring - Turb. Stator Seal	304 S.S.	1	
56	Clip - Stator Bolt	304 S.S.	36	
57	Duct. Turb. Inlet Outer	19.9 DL Incoloy or Inconel	1	
58	Retainer - Turb. Inlet Outer Seal	19.9 DL Incoloy or Inconel	1	
59	Ring - Turb. Inlet Inner Sealing	19.9 DL Incoloy or Inconel	1	
49	Seal - Turb. Inlet Outer	#3 Ni-resist	1	
50	Seal - Turb. Inlet Inner	#3 Ni-resist	1	

Compressor Discharge

48	Seal Assy. - Compr. Disch.	316 S.S. Honeycomb	1	Brazed assy. 316 S.S. Ring
51	Seal - High Pressure	AMS 7310	1	
52	Diaphragm - Compr. Disch.		1	ASTM-A-296 Grade CFBM Casting
53	Volute Sub. Assy. - Compr. Discharge	304 S.S.	1	Fabricated
54	Case - Intermediate	304 S.S.	1	Fabricated

Table 12-4 (Continued)

SELECTED PART LIST FOR CLARK T-C SET OF THE ML-1

Turbine Stator

Item	Title	Mat'l	No. Req.	Remarks
60	Ring - Turb. Stator Mtg. (R&H Mach.)	18.8 S.S.	1	
61	Ring - Turb. Stator Aligning (R&H Mach.)	18.8 S.S.	1	
62	Ring - Turb. Stator Carrier	316.S.S.	1	Brazed assy. with 316 S.S. Honeycomb
63	Blade Assy. - 2nd St. Turb. Stator		1	Brazed assy. 2 halves
64	Blade - 2nd St. Turb. Stator	N. 155 or 19.9 DL	47	
65	Diaphragm - Turb. Stator	18.8 S.S.	1	
66	Key - T.C. Set Support		4	Haynes alloy Hard-faced
67	Pin - Stator Carrier Locating	N. 155	4	
68	Pin - Turb. Stator Locating	N. 155	2	
69	Seal - High Pressure	#3 Ni-resist	1	

Turbine Discharge

70	Sleeve Assy. - Seal	Carb. Stl. Sleeve	1	Brazed assy. with 316 S.S. Honeycomb
71	Collector Assy.	Carb. Stl. Sleeve	1	Brazed assy. with 316 S.S. Honeycomb
72	Seal Assy. - Turb. Shut Down	AM 350 Bellows	1	17-4 PH end plates (Purch. from Koppers)
73	Support - Turb. Bearing	18.8 S.S.	1	
74	Bearing - 2" Precision Journal	Babbitt Lined Stl. Backed	1	
75	Pin - Journal Bearing Lock	SAE 1020	1	
76	Cover - Turb. Bearing Housing	18.8 S.S.	1	

THE FRANKLIN INSTITUTE • Laboratories for Research and Development

T-42903-6

Table 12-4 (Continued)

SELECTED PART LIST FOR CLARK T-C SET OF THE ML-1

Turbine Discharge

Item	Title	Mat'l	No. Req.	Remarks
77	Seal - Turb. Disch. Inner	Koppers K-6E Allowed Grayiron	1	Purchased
78	Seal - Turb. Disch. Outer	Koppers K-6E Allowed Grayiron	1	Purchased
79	Segment - Turb. Disch. Retainer	304 S.S.	4	
80	Ring - Turb. Disch. Inner	304 S.S.	1	
81	Ring - Turb. Disch. Outer	304 S.S.	1	
82	Radiation Shield Assy.	304 S.S.	1	
83	Nozzle Details - Turb. Discharge	304 S.S.	1	
84	Seal Ring - Turb. Brg. Housing	S.S.	1	Purchased
85	Seal Ring - Brg. Housing Cover	S.S.	1	Purchased
86	Guard - Turbine Disch.	304 S.S.	1	

Table 12-5

WEIGHT OF MAJOR COMPONENTS IN CLARK T-C SET FOR THE ML-1 (POUNDS)

Barrel Case	1015
Compressor Inlet Bulkhead	136
Compressor Case (including Stator Rings)	60
Compressor Discharge Duct	94
Turbine Inlet Duct	19
Planetary Gear	260
Rotor Shaft	184
Turbine Stator Housing (including Stator Ring)	75
Turbine Bearing Case and Seal Assembly	53
Compressor Bearing Case, Thrust Bearing and Seal Assembly	70
	1966
Piping and Miscellaneous Items	34
Total Weight	2000

The present unit is an improved version of Stratos Model TCS-560. All stressed members in the turbine are constructed of materials with maximum resistance to nitriding (cylce coolant is nitrogen). Because of the materials selected and the moderate temperatures of the design, no provision was necessary for cooling either turbine nozzles or turbine wheel blades. The materials used for each major part of the machine are listed in Table 12-6.[22] The highest temperature to which each part will be subjected is stated and tensile and yield strengths for each stressed part at this temperature are tabulated.

A description of the set follows. The T-C set is shown in Figure 12-40[69], Figure 12-41 and 12-42[22] show the key features. Figure 12-43[113] shows the stratos turbine-compressor set (TCS-670) from the turbine discharge end and from the gearbox end.

The radial-flow T-C set is a reaction-type, two-stage, axial-flow turbine coupled to a two-stage radial compressor mounted on the same shaft (Figure 12-40). The turbine is designed with a constant blade-root diameter of 12.14-in. The mean diameters of the first- and second-stage rotors are 12.90-in. and 13.20-in. respectively. Each turbine rotor has 83 blades. The nozzle rings each have 79 blades.

The construction features of the turbine are as follows: The turbine support structure is cylindrical, without horizontal joints, to avoid thermal distortion. Axial thermal distortion is minimized by locating the thrust bearing immediately inboard of the overhung turbine rotors. The turbine-nozzle ring assembly supports the stator assembly and the wheel shroud rings. The turbine-nozzle ring assembly and inner-stage diaphragm are supported by a conical member mounted to, and located by, the thrust bearing support structure. The turbine inlet duct, a non-structural member, has been designed to minimize heat losses. The hollow wall of this duct will be evacuated to further reduce heat transfer. An extension of this duct is a heat shield between the turbine wheels and bearing.

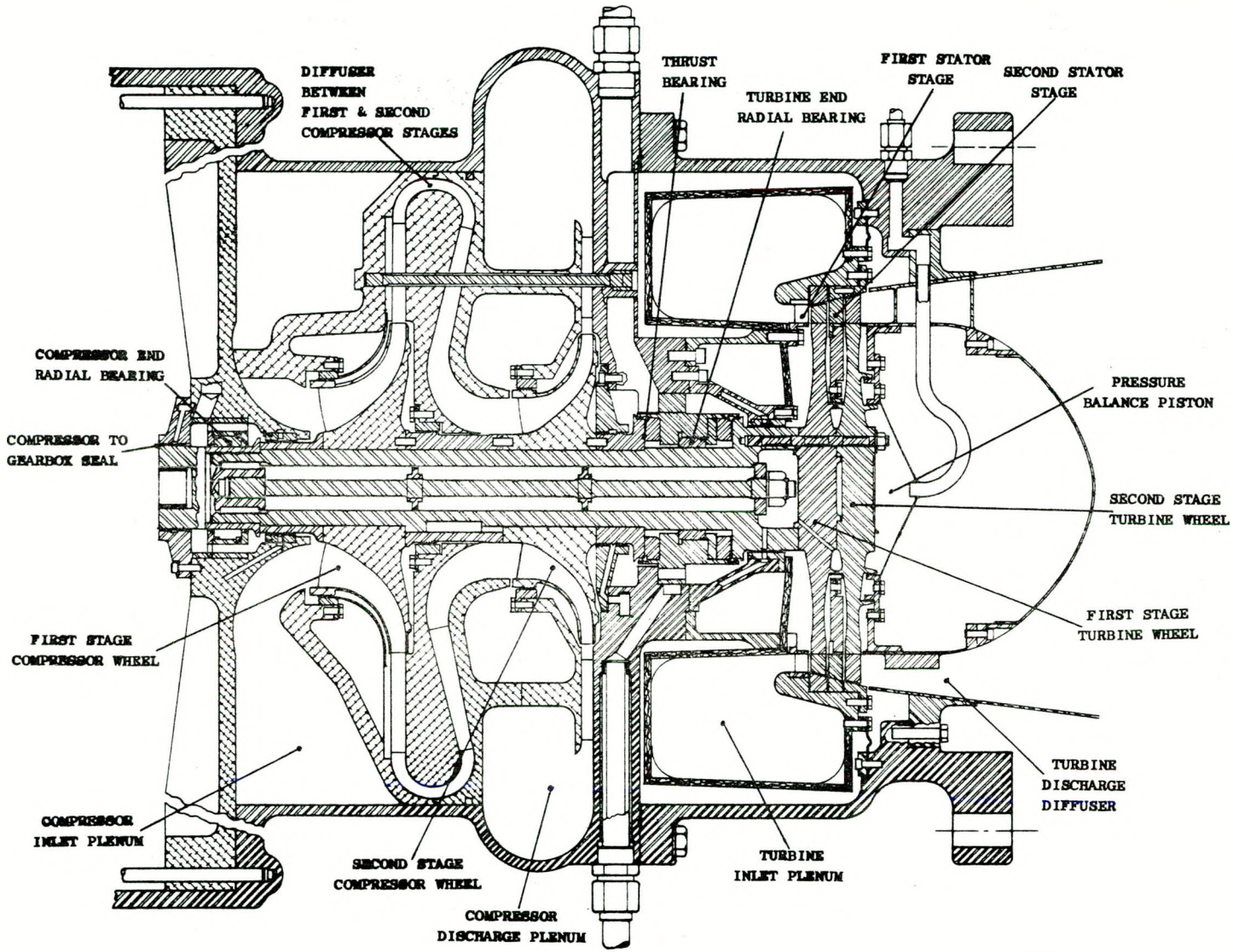


Fig. 12-40 - Stratos Radial Flow Turbine Compressor Set for ML-1

Data from Stratos Division, Fairchild Corp.,
Report SRC-104

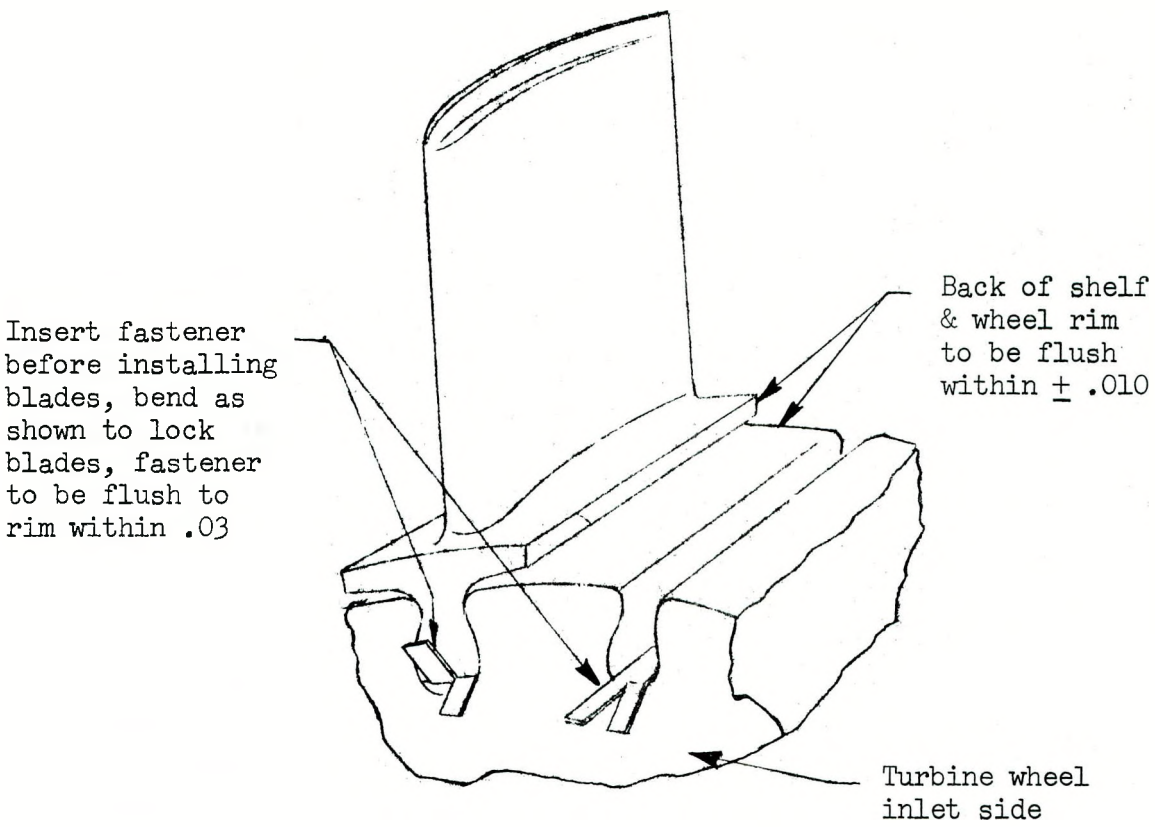


Fig. 12-41 - Stratos T-C Set for ML-1, Second-Stage Turbine Wheel

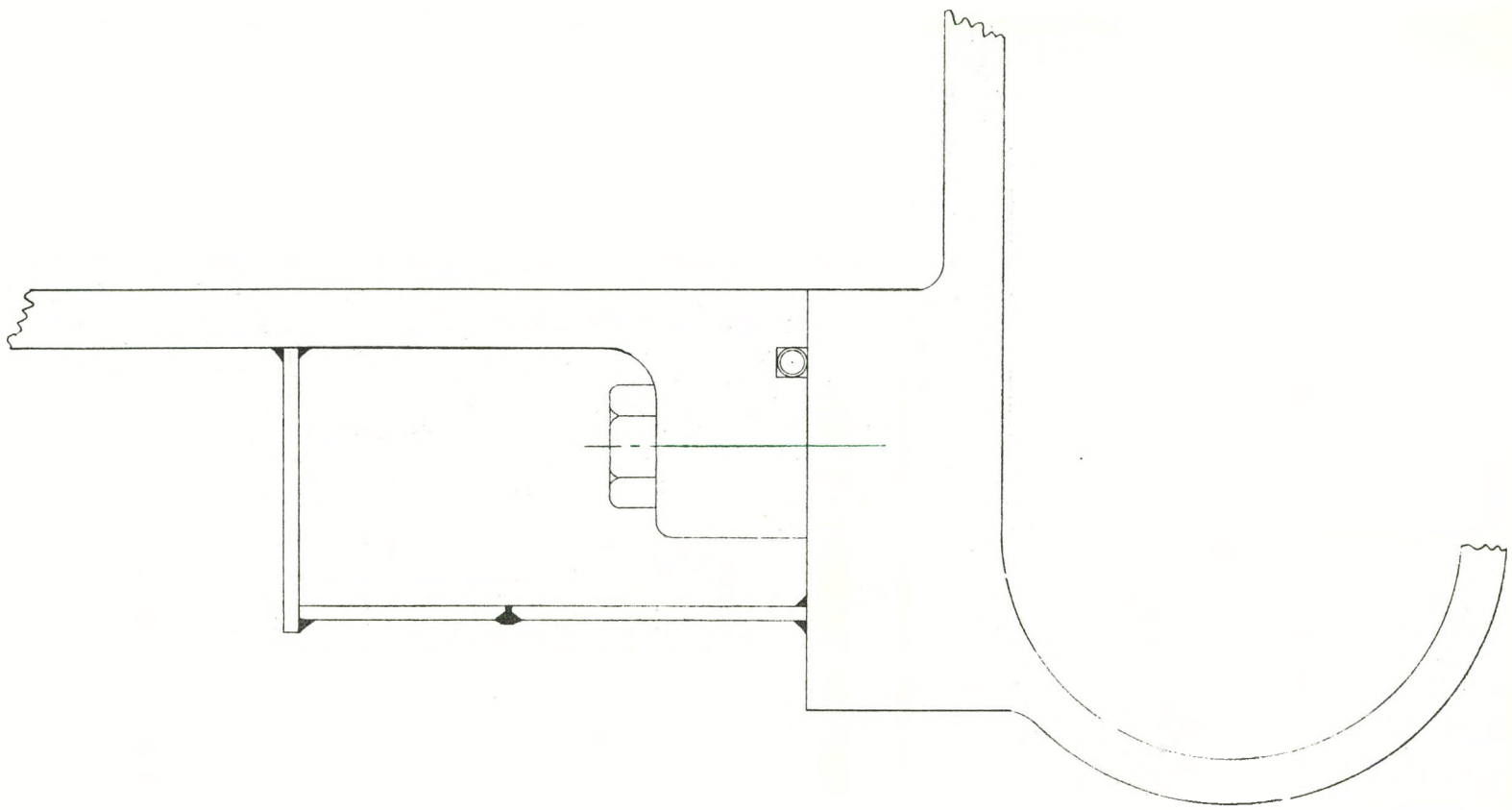
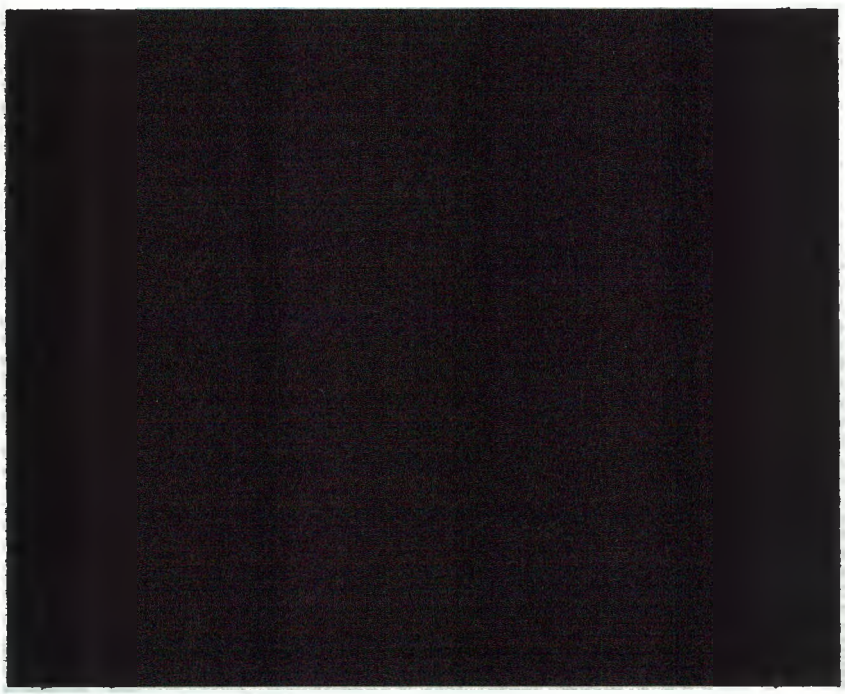


Fig. 12-42 - Stratos T-C Set for ML-1, Turbine Flange Seal



The Turbine Discharge End.



The Gearbox End.

Fig. 12-43 - Stratos T-C Set TCS-670

The barrel-type main housing of the T-C set is cast in stainless steel. The main bearing support is cast into the main housing. The compressor bearing is installed in the gearbox housing. The turbine and compressor wheels, mounted on a common shaft, are supported by two tilting-pad radial bearings. Tilting-pad thrust and anti-thrust bearings are also included. The T-C set is flange-mounted to a recuperator without other supports. Three lugs are provided on each housing casting to aid in handling. All stressed members in the turbine are constructed of nitriding-resistant materials.

The turbine rotors are Incology 901 forgings. The rotor blades are precision cast in Inco 713 alloy, a modified form of Inconel "X". The blades are assembled to the rotors with bulbroot attachments. The nozzle blades are precision cast in Inconel. The nozzle rings and interstage diaphragm are welded assemblies. The turbine rotors are bolted to the flanged ends of the hollow rotor shaft.

An external connection is provided to supply working gas (at separately controlled pressure) to a balance chamber fitted to the downstream side of the second-stage turbine wheel. This balance chamber exerts a thrust on the main shaft proportional to the controlled pressure, reducing the load to insure axial stability. Gas passes through the balance chamber labyrinths and along the second-stage turbine rotor, serving to cool it.

Working gas is supplied under pressure to the cavity inside the flanged end of the shaft. This gas flows through drilled holes in the first-stage turbine rotor and through the turbine inter-stage labyrinth. A close-fitting wheel shroud directs this gas along side both rotors. Thus, the gas cools both the labyrinth and the rotors.

Lubricating oil is supplied to the turbine end bearing through a double-walled feed passage. Seal-cooling gas passes through the outer portion of the passage and insulates the bearing lubricating oil from the housing, thus a minimum of heat is picked up by the oil at the back end of the unit.

Since axial length available at the turbine exit is limited, a set of vortex generator vanes is installed in the turbine exhaust to diffuse the gas discharge. Tests of these vortex generator vanes have shown that satisfactory diffusion can be achieved.

The compressor wheel diameters are 11.9 and 11.2-in. with eye diameters of 7.4 and 6.7-in. Twelve full-length and twelve half-length blades are used in each impeller.

The compressor support structure is cylindrical to ensure accurate alignment of the inter-stage passages, diffusers, and seals. The shrouded impellers are precision cast in aluminum. The inter-stage baffle plates, diffusers and return guide vanes are fully-machined aluminum castings. The compressor wheels are pinned to shaft spacers which are, in turn, keyed to the rotor shaft.

Incorporated within the main turbine-compressor housing is a complete reduction gear unit. Power from the T-C set is transmitted to a helical pinion. The pinion is mounted directly on the T-C set shaft. The helix angle was chosen so that the gear thrust will be opposed to the normal turbine thrust. Meshing with the pinion are three secondary reduction gears on shafts, equally spaced around the pinion center. Helical pinions on three shafts mate with the low-speed gear. A double reduction gear was chosen. Radial loads normally found in a straight double reduction system are balanced out by locating the pinions equally around the center of the high-speed gear. Load sharing of the gears is ensured by axial shimming to obtain uniform tooth contact. A drive shaft at right angles to main shaft is provided to supply the auxiliary power take-off for the lubricating oil pump. The main support plate for the gearing pilots into the main turbine-compressor housing and carries the compressor end bearing of the turbine-compressor set. The secondary gearbox supports are pinned to the main support plate. Gear units are removable as complete assemblies. Gearbox supports are aluminum alloy castings. Gears are manufactured from certified alloy steel forgings. Gear profiles are precision generated by grinding.[69]

The alternator is housed in a gas-tight case, flange-mounted to the gearbox case. Also enclosed in the gas-tight case is a 480-volt line-to-line, 3-phase, 60-cycle 50 hp starting motor mounted on a generator shaft. This starting motor is capable of rotating the T-C set and alternator up to rated speed.

The lubrication system supplies oil to the turbine-compressor set, including gearbox and alternator. Oil is supplied to the system by a gear-type pump driven by the gearbox at 1800 rpm. An auxiliary pump (motor-driven) provides lubrication during start and stop operation to prevent bearing damage. Regulators are utilized to maintain a pressure differential of 30 psi across the bearings.

The dual filtration circuit (parallel connected) provides 25 micron oil filtration with a provision to permit changing each element during operation. Oil is passed through an air-cooled oil cooler on the discharge side of the pump to reduce the oil temperature to approximately 150°F. The cooler is capable of removing 293,000 Btu/hr.

The entry of bearing lubricating oil into the gas cycle is prevented by two stages of labyrinth seals at each bearing on the T-C set shaft. Seals are supplied with regulated nitrogen from the compressor discharge through external connections. The oil in the bearing exit cavities is maintained at a lower pressure and, therefore, cannot enter the working gas. Individual feeds and drains are provided for each bearing, and individual feeds and vents are provided for each seal. It therefore is possible to hold each bearing cavity and its adjacent seals at any desired pressure level.

Nitrogen is supplied to the labyrinth seal by an auxiliary compressor during startup and shutdown when main compressor gas is not available. When the system compressor develops a minimum of 45 psia, the auxiliary compressor will automatically shut off.

Table 12-6

TABLE OF MATERIALS, STRATOS T-C SET FOR ML-1

Part No.	Part Name	Material and Condition	Temp. °F	Tensile Strength At Temp. lbs./sq. in.	Yield Strength At Temp. lbs./sq. in.
1	Stub Shaft	SAE 4340 C-32-36	150°F	150,000	130,000
2	Rotor Shaft	SAE 4340	400°F	111,000	99,000
3	Labyrinth	CRES 410 C-28-34	150°F	90,000	68,000
4	Seal Ass'y	CRES 410 C-28-34 Lead Lined	150°F	*	*
5	Journal	SAE 4340 C-32-36	150°F	90,000	68,000
6	Bearing Support	Al Al 355-T51	150°F	26,000	21,000
7	Tie Bolt Damper	SAE 4340 Annealed	200°F	111,000	99,000
8	Wheel	Al Al 355-T71	210°F	30,000	25,000
9	Seal Ass'y	CRES 303 Lead Lined	210°F	*	*
10	Inlet Hsg.	Al Al 355-T6	250°F	30,600	25,000
11	Tie Bolt	SAE 4340 C-32-36	400°F	150,000	130,000
12	Labyrinth	CRES 410 C-28-34	270°F	90,000	68,000
13	Seal Ass'y	CRES 410 C-28-34 Lead Lined	210°F	*	*
14	Diffuser	Al Al 6061-T6	270°F	32,000	30,000
15	Passage Guide	Al Al 355-T6	270°F	30,000	25,000
16	Guide Vane	Al Al 355-T6	380°F	14,600	12,000
17	Bolt	SAE 4340 C32-36	380°F	150,000	130,000
18	Seal Ass'y	CRES 303 Lead Lined	325°F	*	*
19	Wheel	Al Al 355-T71	325°F	25,750	21,000
20	Diffuser	Al Al 355-T6	380°F	14,600	12,000
21	Labyrinth	CRES 410 C-28-34	400°F	80,000	60,000
22	Seal Ass'y	CRES 410 C-28-34 Lead Lined	400°F	*	*

Data from Stratos Division of Fairchild Engine & Airplane Corp., Report SRC-104

12.2.3 MGCR Turbomachinery

No hardware has been so far made for the MGCR turbomachinery except for models of four compressor stages and two turbine stages which are presently being tested. Figure 12-44[75] shows the second stage model turbine disk assembly. However, the preliminary design of the prototype plant has been completed and a general description of the machinery can be given. Figures 12-45 to 12-51[55] show pieces of machinery of Westinghouse commercial designs as typical examples. Detailed design, where applicable, will follow existing Westinghouse commercial designs. Major design features of components are given below.

Spindle Construction

The compressor rotors may be manufactured in several ways. Two of these are:

(a) Alloy steel disks, shrunk on a solid shaft (see Figure 12-45), and

(b) A solid alloy steel forging (drum construction).

In both configurations, the blades are forged alloy steel, suitably tapered and twisted to insure good aerodynamic performance. Side entry roots hold the blades in the rotor and permit replacement without disturbing other blades. Each blade is individually locked in place by a spring-loaded pin which engages both blade and rotor disk. Westinghouse commercial designs use ball type blade roots in the compressor.

The turbine rotor is of built-up construction consisting of forged alloy steel disks held together by means of curvic couplings and through bolts (see Figures 12-46 and 12-47). The curvic coupling is a toothed connection member with teeth spaced circumferentially around the face of the rotor disk. On one disk face, the teeth are hour-glass shaped and on the mating disk face, the teeth are barrel shaped. When the disks are engaged, the teeth mate to form a highly accurate, simply constructed, torque transmitting joint.

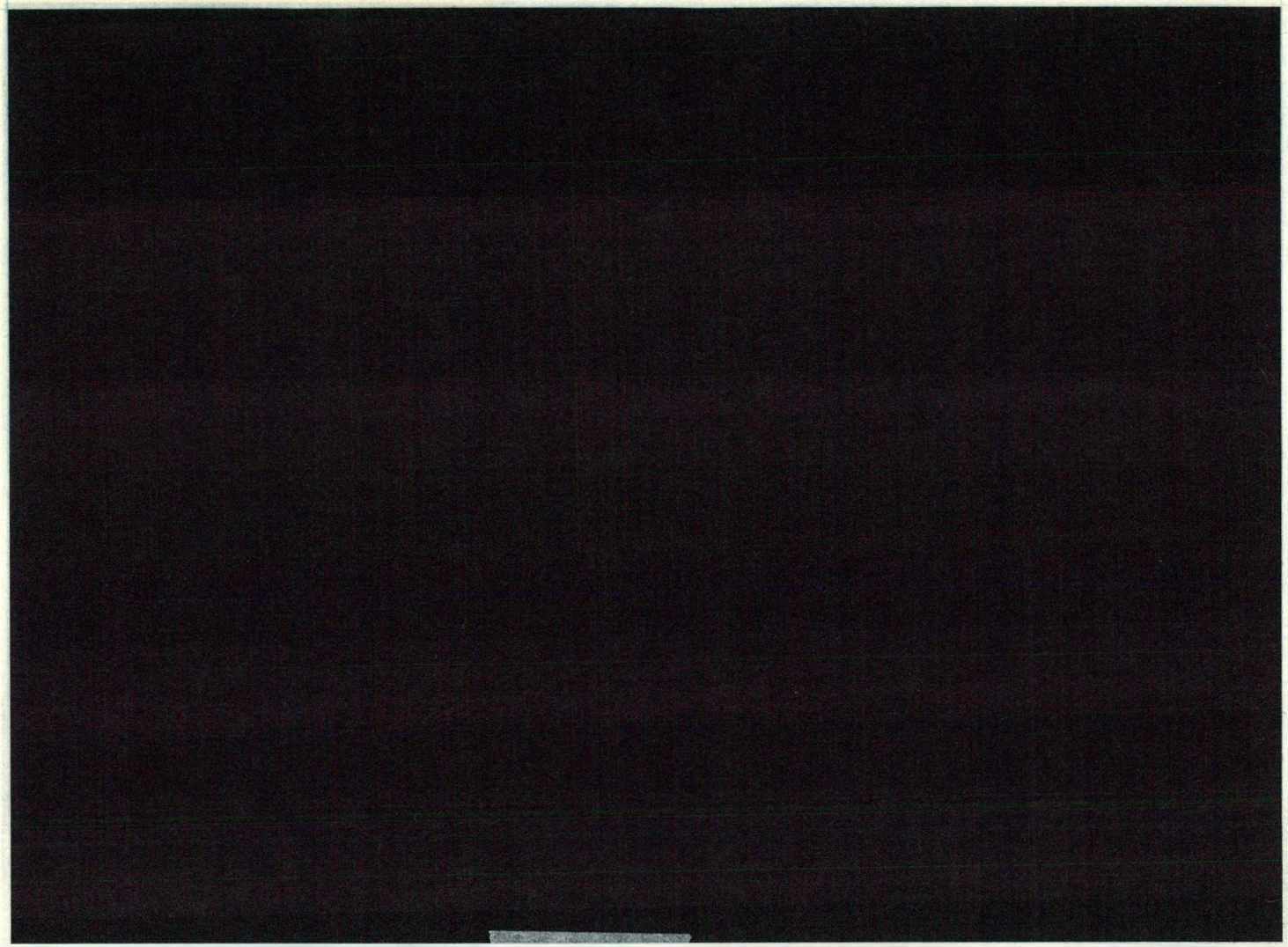


Fig. 12-44 - Second Stage Disk Assembly for MGCR

THE FRANKLIN INSTITUTE • Laboratories for Research and Development

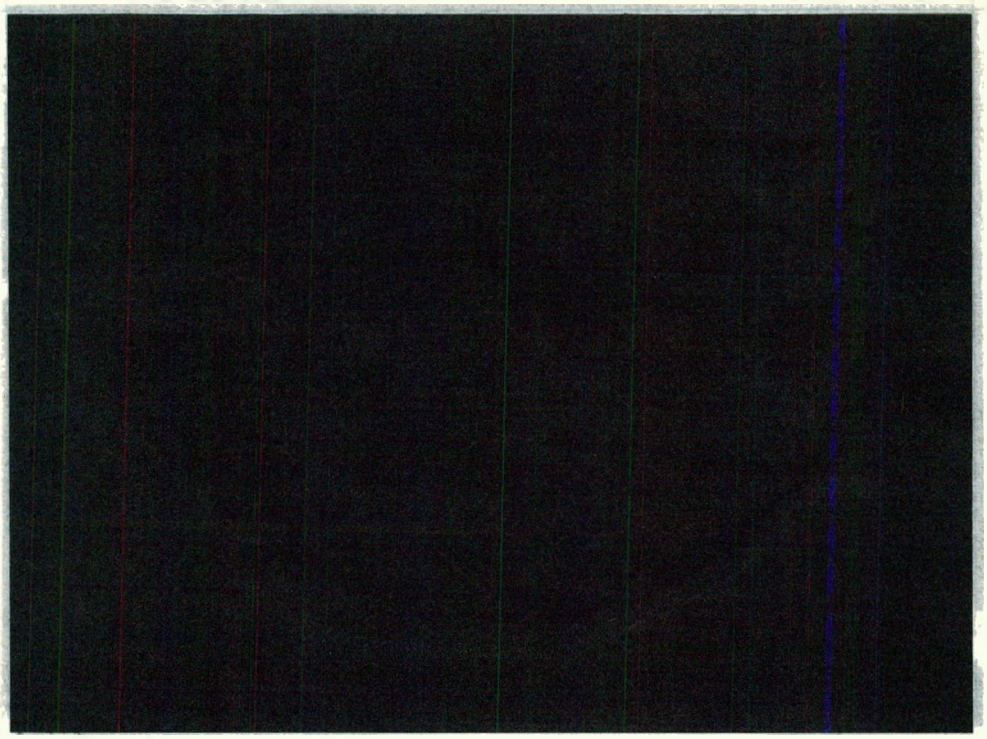


Fig. 12-45 - Westinghouse Compressor Disk and Shaft Assembly Installation of Compressor Blades

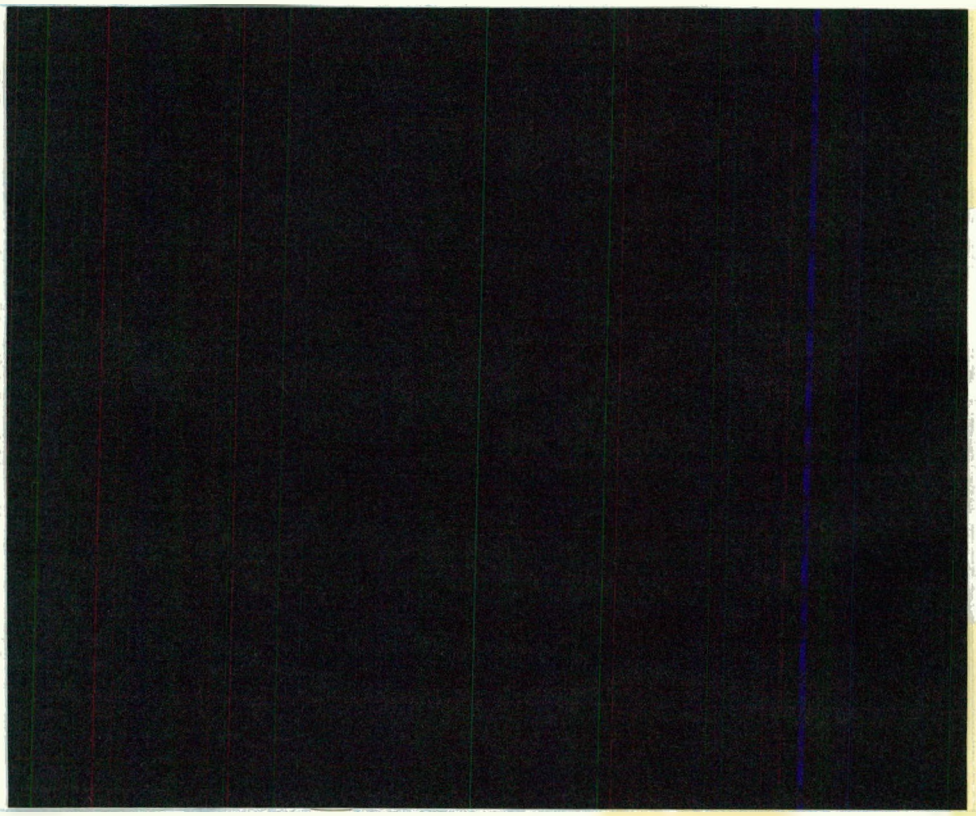


Fig. 12-46 - Westinghouse Turbine Wheel Assemblies Showing Curvic Coupling Connection Between Rotating Stages

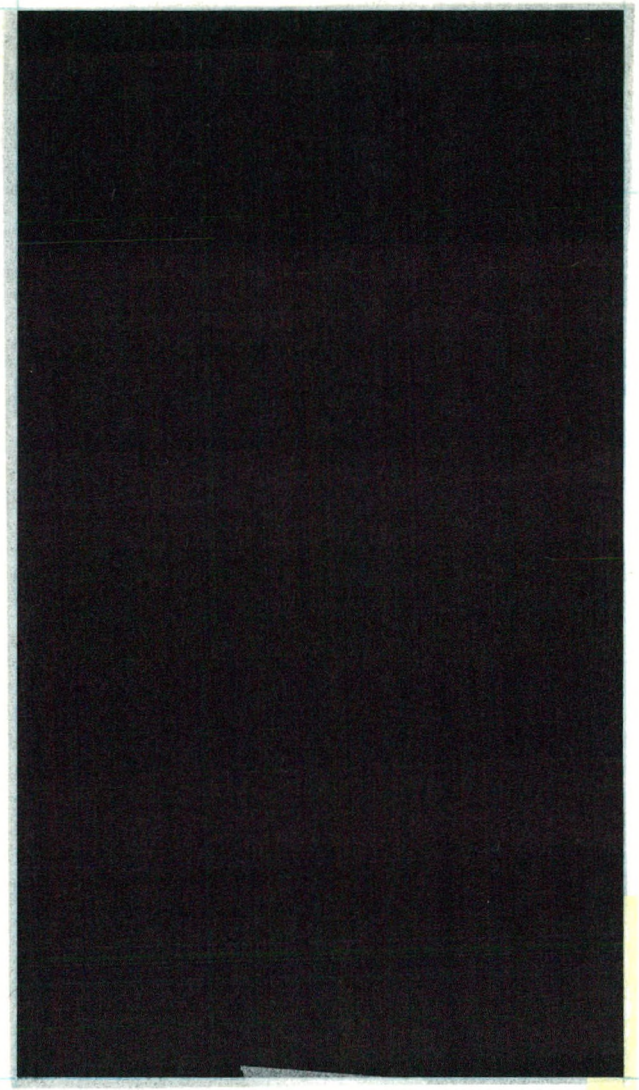


Fig. 12-47 - Westinghouse Turbine Disk and Torque Assembly of Through Bolts and Blades

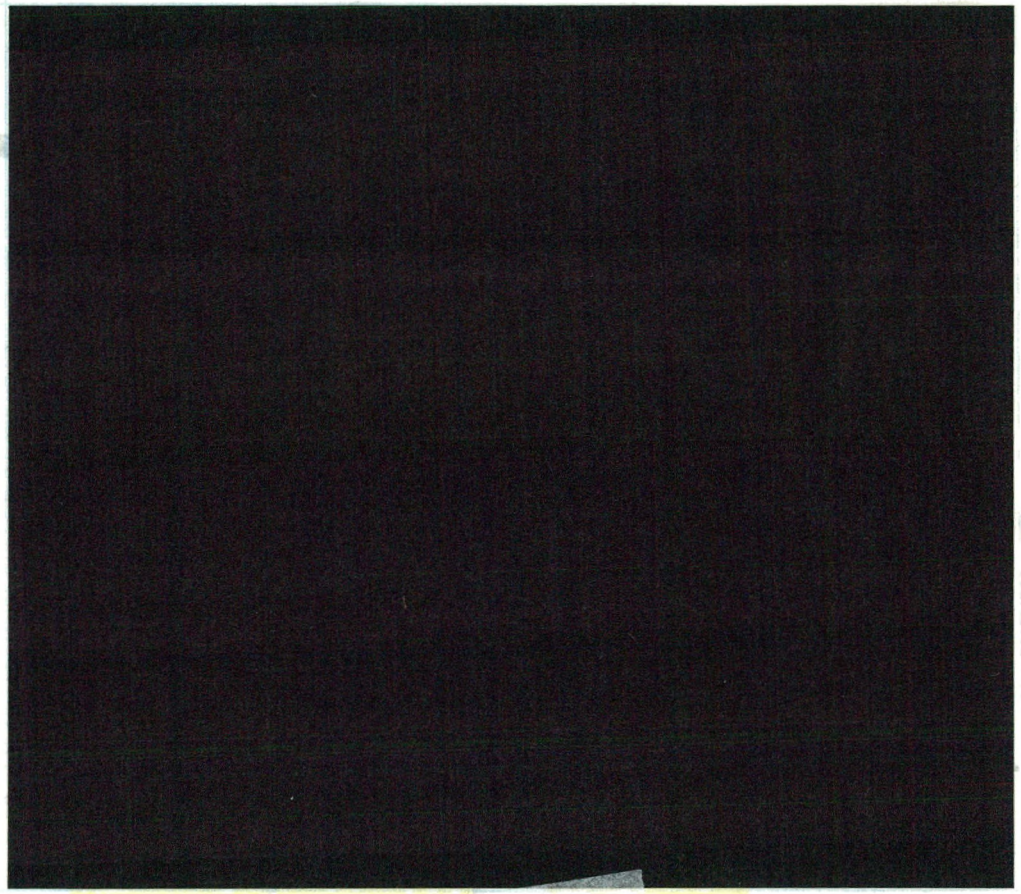


Fig. 12-48 - Westinghouse Turbine Blades, Fir-Tree Root

FRANKLIN INSTITUTE . Laboratories for Research and Development

The turbine rotating blades are forged from high-alloy (heat resisting) steel. Blade roots are held in grooves cut across the periphery of the rotor disks. Westinghouse commercial designs use the serrated or fir tree type attachment for blades in the turbine (see Figure 12-48). Turbine blades are installed axially and may be locked individually or as a row. The blades in each row may be removed or installed without disturbing blades in adjacent rows. Turbine and compressor rotors (excluding the power turbine) are rigidly connected by means of a torque tube (see Figure 12-49).

Spindle Balance and Stacking

The compressor and turbine rotor subassemblies are individually stacked and balanced. The subassemblies are then joined as one assembly and balanced. This type of construction permits replacement of either turbine or compressor rotor subassembly without special fixtures. With the relative runouts within prescribed limits, the complete rotor assembly can be dynamically balanced in the gas turbine proper. Assembly of the turbine rotor requires special fixtures to maintain prescribed runouts and is considered to be a factory operation.

Turbine Blading Proportions

The blading will have low aspect and high thickness-to chord ratios with high unit pressures and small unit diameters. Thus, the blades will be short and relatively thick. Westinghouse design practice for high efficiency turbine blading uses an almost pure impulse section at the blade root increasing in reaction toward the tip.

Stator Blading Construction

The stator blades may be manufactured by one of three processes: stainless steel strip rolled and punched, cast, or forged. A diaphragm has been worked in between compressor and turbine, which will reduce external pressure-stress on the turbine scroll and facilitate control of cooling gas to the turbine. External piping connections have

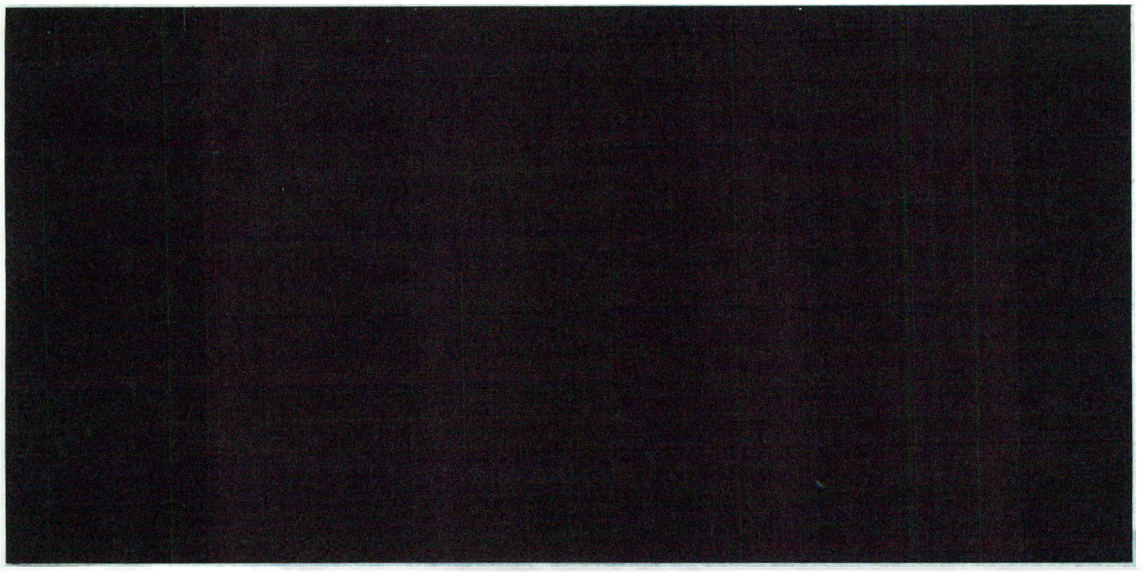


Fig. 12-49 - Westinghouse Compressor-Turbine Assembly

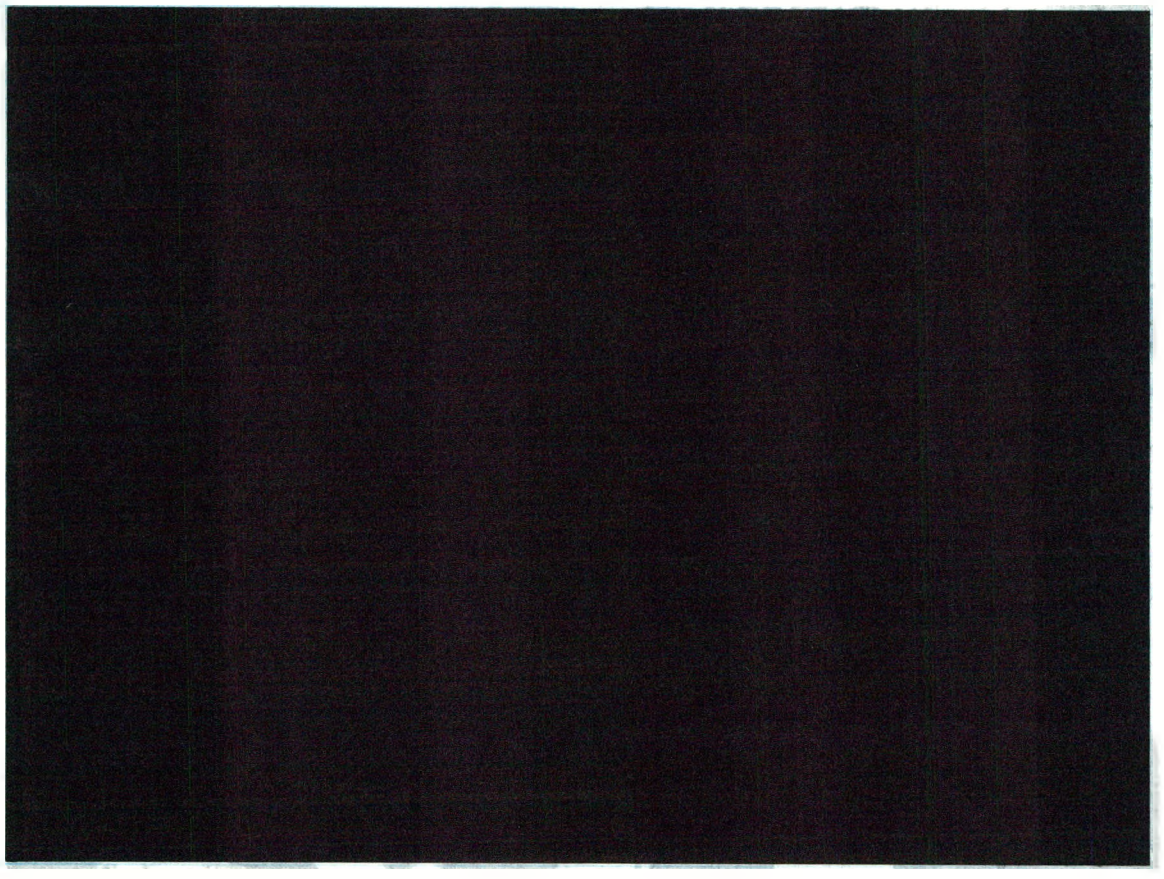


Fig. 12-50 - Westinghouse Compressor Cylinder Base Assembly Showing Vane Assembly Construction and Installation

all been moved to the bottom half of the casing to make a more compact piping arrangement and to permit ready removal of the upper half of the casing. They can be rolled in place (see Figure 12-50). Diaphragms may be held in place by screws or strips at the horizontal joint or by bolting through the casing to the outer shroud.

Casings

All casings will be castings or weldments of materials consistent with individual pressure and temperature requirements. A few representative casing flange and wall thicknesses are tabulated below. A pressure of 2000 psi would require larger, more specialized bolting.

Location	1000 psi	2000 psi
H.P. Turbine Inlet	7 in.	11 in.
H.P. Turbine Discharge	4 in.	6-1/2 in.
H.P. Compressor Discharge	4 in.	6-1/2 in.

Casing studies have indicated that horizontal joints will be satisfactory in most sections of the machine from the standpoints of tightness, strength, and total length of joint. This construction is greatly preferred for reasons of access and assembly. High-pressure compressor and high-pressure turbine are combined in a horizontally split section of casing (in the version of LPT-drive). Low-pressure compressor and low-pressure turbine retain vertically split, or barrel-type, casings except at the bearings.[73]

Casing Sealing Arrangements

Experience with high-pressure joints on steam turbines may be directly applied to closed-cycle gas turbine plants. Pressure sealed joints, stepped and lapped joints, are examples of several types in use. It must be realized that even the most perfect mechanical joint is subject to some leakage with time. A direct approach to full sealing is the use of the best available joint with seal welding.

Support Arrangement

A large amount of longitudinal and vertical expansion of the unit must be compensated for in the supporting system. The system must maintain proper axial alignment, and, at the same time, maintain rigidity for pitching, rolling, and yawing loads. Westinghouse will supply the support system integral with the casings.

Pipe expansion and deflection problems may dictate, to some degree, the location of support members. The flexible support(s) would be located under those casings that would provide span requirements and least thermal expansion problems.

The in-line and separate power turbine units will require different support locations. In the in-line unit, the fixed support would be located under the high-pressure turbine casing and the flexible supports under the low-pressure compressor and low-pressure turbine casings. Figure 12-48 shows such support arrangement for a study with low-pressure turbine drive, CO_2 as coolant, and 2000 psia maximum cycle pressure.

In the separate Power Turbine Unit, the fixed support for the low-pressure, high-pressure compressor and high-pressure turbine assembly (assuming low-pressure turbine drive) would be located under the high-pressure turbine casing, and the flexible support, under the low-pressure compressor casing. The separate fixed support for the power turbine would be located at the exhaust and near the main reduction gear and the flexible support would be under the turbine inlet.

Piping, Flange Sizes and Locations

Approximate pipe and flange sizes with centerline locations from the power turbine drive coupling (low-pressure turbine drive version) are tabulated in Table 12-7.[55]

Table 12-7

PIPING, FLANGE SIZES AND LOCATIONS
FOR 1000 PSIA AND 2000 PSIA CO_2 PLANTS (FOR MGCR)
(Ratings Conform to ASA Standards)

Location	Pipe Size (in.)	Sched.	Flange Rating (#)	Flange Thickness (in.)	Distance From Power Drive Coupling Face
1) L.P. Compressor Inlet from Pre-cooler					
1000 psia	24	Std.	150	1 - 7/8	19'7"
2000 psia	18	Std.	600	3 - 1/4	17'4 - 1/2"
2) L.P. Compressor Discharge to Intercooler					
1000 psia	18	Std.	300	2 - 3/8	17'0 - 1/2"
2000 psia	12	60	900	3 - 1/8	14'5 - 1/2"
3) H.P. Compr. Inlet from Intercooler					
1000 psia	16	Std.	300	2 - 1/4	12'0"
2000 psia	10	60	900	2 - 3/4	9'11 - 1/2"
4) H.P. Compr. Discharge to Regenerator					
1000 psia	24	100	600	4	6'2"
2000 psia	8	xxStrong	2500	6 - 1/2	4'5 - 1/2"
5) Inlet from Reactor to H.P. Turbine					
1000 psia	26	140	2500	12	4'2"
2000 psia	16 O.D.	Special	2500	10	4'5 - 1/2"
6) Exhaust to Regenera-tor from L.P. Turbine					
1000 psia	28	Std.	600	4 - 3/8	2'10"
2000 psia	26	30	600	4 - 1/4	2'3"

Materials based on useage in present Westinghouse commercial gas turbine units are:[55]

Compressor Casings	Carbon Steel
Compressor Cylinder	Carbon Steel
Compressor Blades	12% Cr Steel
Compressor Disks	SAE 4147
Compressor Spindle	Alloy Steel
Torque Tube	Alloy Steel
Turbine Casings	Alloy Steel
Turbine Cylinder	18-8 Stainless Steel
Turbine Disks	Discaloy
Turbine Blades	Inconel "X"
Diaphragm Vanes	25-20 Stainless Steel
Diaphragm Shrouds	25-20 Stainless Steel

The use of helium for powering a turbine is a departure from the usual oxidizing and corroding atmosphere of combustion gases. Consequently, any effects on the behavior of materials in a helium atmosphere would have to be known to insure confidence in design and manufacture of the equipment. In addition, high strength alloys, required for components, subjected to more severe operating conditions of temperature and pressure should be commercially available, possess metallurgical stability, and exhibit long-time strength at elevated temperatures. Among the materials selected for investigation were those which provided excellent service in conventional Westinghouse gas-turbine application. Inconel X, D979, W545 and Discaloy possessed allowable stress limits which appeared suitable for disks in the low-temperature portions of the system, in particular, the low-pressure turbine and the compressors. Higher strength alloys, for example, INCO 713C, and INCO 700 are considered for blades for the high-temperature turbine.

Consideration of these requirements led to the investigation for compatibility and suitability in a helium atmosphere of these and other materials for the reactor core, pressure vessel internals, turbine and compressor disks and blading, ducting, and valves.[152]

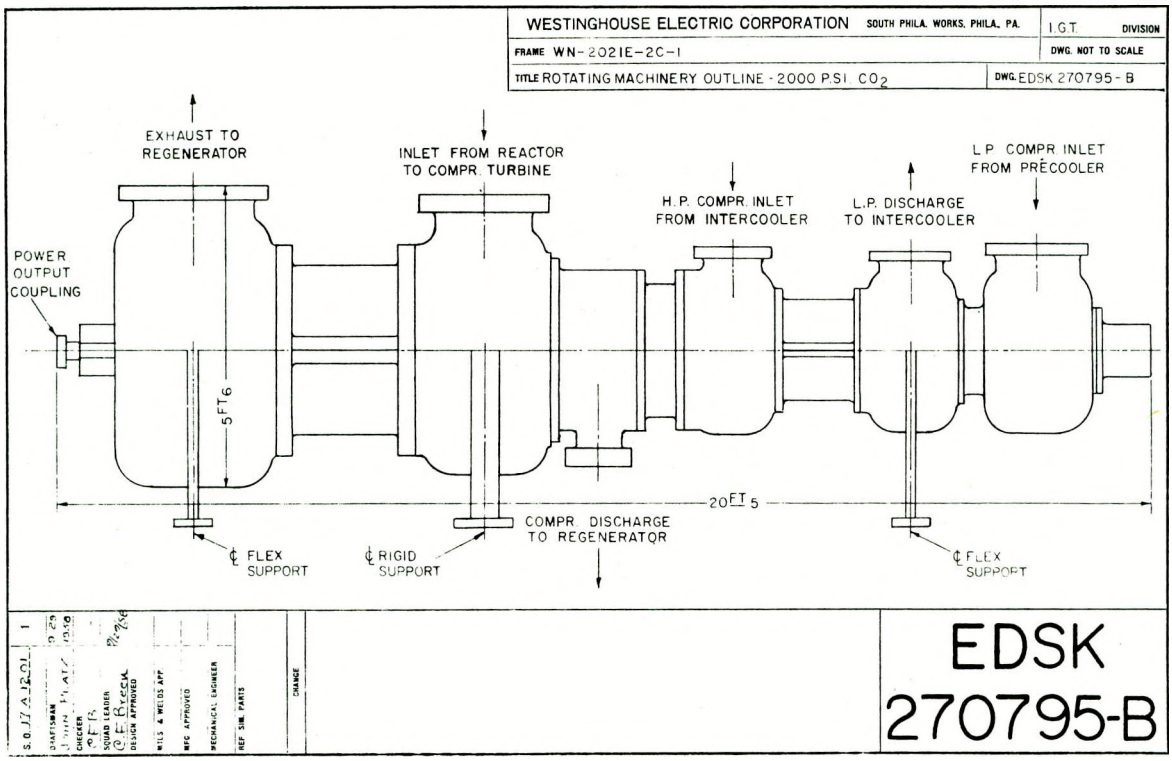


Fig. 12-51 - Support Arrangement for MGCR Machinery

13. AVAILABILITY AND CAPABILITY

13.1 Manufacturers' Information

We selected about 40 gas-turbine manufacturers and a number of manufacturers, making compressors as separate units, and contacted them directly to obtain first-hand information. A part of the received information is contained in special data sheets which we prepared. Data Sheets A contain information availability and Data Sheets B contain information on capability of a given manufacturer. The response to the inquiry was about 60% and contained mostly less information than requested. We also had to style much of the information to fit our Data Sheets. Thirty-one such sheets are included in Section 3.4. Additional information received is utilized throughout this text.

The performance requirements indicated in Data Sheets B are consistent for four selected cycles and for two gases, helium and molecular nitrogen, corresponding to four reactor outlet temperatures, 1300, 1500, 1700, and 2000°F, representative of present reactor possibilities at 1300°F and of future development at higher temperatures. A discussion of why these requirements were selected is contained in NYO Report 9787[2] on cycles.

Table 13-1 (in Section 3.4) lists present gas-turbine manufacturers. We believe that the list includes most of the important manufacturers. Compressor manufacturers are not listed separately because turbine manufacturers usually produce their own compressors for a complete turbine-compressor set. Exceptions may exist where positive displacement compressors are used, such as the free-piston type or others, which will probably not be applied to nuclear gas-turbines.

Let us say a few words about the Data Sheets (in Section 3.4) which are otherwise self-explanatory.

(a) Data Sheets (File Number) 1 and 2 are typical of those compressor manufacturers who are not interested in being engaged in the nuclear field.

(b) Clark Bros. Co. is represented by four Data Sheets, 3, 4, 5, and 6. Sheets 3 and 4 cover the turbine-compressor set CSN-1 for the Army mobile, low-power reactor ML-1, while Sheets 5 and 6 show the capability of the manufacturer.

(c) General Electric Co. submitted data sheets 7, 8, and 9. Sheet 7 gives data about a HP test compressor, and sheets 8 and 9 indicate G.E.'s capability. According to indicated mass flows, G.E. feels confident to design gas-turbine units for the indicated closed cycle conditions up to a capacity of about 150 Mw.

The Gas Turbine Department of G.E. has experience primarily with long-life turbo-machinery components for transportation, industrial, marine, and electric utility industries. G.E. has performed a considerable number of design studies of gas turbine systems for both nuclear and fossile fuel energy sources. In the period of 1947 through 1950, under contract with the Bureau of Ships, a development was performed by G.E., in which closed-cycle gas turbine components were developed for a classified Navy project. G.E. has been developing a direct-cycle nuclear-powered aircraft engine at Evendale and in Idaho.

(d) Neratoom represents various Dutch manufacturers. Sheets 10 and 11 deal only with compressors. Gas-turbine information was delayed and is not included here.

(e) Orenda Engines Limited indicate their capabilities on Sheets 12 and 13 and consider approximately 110 Mw to be the upper limit of one unit they would be capable of constructing, which needs a certain amount of development to satisfy the closed-cycle requirements. However, such development work will be required by any firm, whether it is explicitly stated or not.

(f) Rocketdyne Div. of North American Aviation indicates on Sheets 14 and 15 plainly that they can design according to the specified closed cycles but must spend development effort, which they feel they are capable to perform.

(g) SNECMA presents Sheets 16, 17, 18, and 19. Sheets 16 and 17 describe some of their products, and Sheets 18 and 19 express their capabilities. Compressors are mentioned up to large units but not turbines.

(h) Solar Aircraft Co. states their capability in compressor and turbine construction on Sheets 20 to 23.

(i) Stratos Div. of Fairchild Corp. presents on Sheets 24 and 25 data for the turbo-compressor set TCS560, which was designed for the GTTF (Gas Turbine Test Facility) at Fort Belvior, Va. Data Sheets 26 and 27 give data of the TCS 670 turbo-compressor set for the Army mobile, low-power reactor ML-1.

(j) Westinghouse Electric Corp. submitted Sheets 28, 29, 30, and 31. Sheets 28 and 29 describe the WN-202-IE turbo-compressor machinery for the MGCR Project (Maritime Gas-Cooled Reactor) with the high-pressure turbine drive arrangement, based on results of preliminary design. Sheets 30 and 31 show the capability of Westinghouse, which feels able to design closed-cycle units up to 200 Mw capacity.

(k) Escher Wyss Ltd. describes on Sheets 32 and 33 a 23 Mw closed-cycle helium unit, and on sheets 34,35 indicates the capability to design closed-cycle 50 Mw turbo-compressor sets. Escher Wyss states that their calculations are not in agreement with optimum pressure ratios and pressure losses assumed by The Franklin Institute for Data Sheets B, which were determined for maximum thermal efficiency of representative cycles. To this may be added that an optimization of a cycle is a complex problem which is not determined by thermal efficiency alone.

13.2 Future Development

Major areas in the nuclear gas-turbine power machinery requiring development are seals and bearings,[5] materials[6], and special valves.[7] Seal development presents about the same problems as those for circulators in the primary gas-loop of nuclear steam power plants, except that gas-turbine seals are larger in diameter because of the

larger shaft size, and will consequently have higher rubbing speeds. The fact that circulator seals will operate at higher differential pressure as suggested by some, does not need to be true in all cases.[1]

Development work in aerodynamics of the turbomachinery is needed especially when gases other than air will be used as, for example, helium. Particularly the compressor stage-work should be carefully selected. Gas-turbine plant efficiency is very sensitive to compressor and turbine efficiencies because about 2/3 of the work output of the turbine is used to drive the compressors (see Charts B-30 and B-31 in NYO Report 9787 on Cycles).[2]

The principal material-selection problems occur in the high-pressure gas turbine and in the reactor outlet duct. Because the requirements of the gas-turbine blading are no more severe than for commercial industrial gas turbines, they should present no major problems unless material properties drop substantially in the selected coolant atmosphere, as, for instance, has been observed with some materials in helium.[6]

Future development will doubtless tend to apply higher reactor outlet temperatures to improve the efficiency of the gas-turbine power plant and make it really competitive with nuclear steam plants. At the present time, it is mainly a reactor problem to obtain such higher temperatures. While it is the prevailing opinion in Britain that the time has not yet come for a gas-turbine in nuclear power plants, in this country, a positive effort is made (ML-1, MGCR) to gain experience, which will be used to advantage when higher reactor outlet temperatures will become available.

13.3 Limiting Factors

For turbomachinery in general, limitations of volume rates, and therefore of size, are dictated on the high side by fabrication and handling facilities, and on the low side by the efficiency of the machine and by critical speed. No exact limits can be indicated. In high-pressure

closed cycles, pressure and temperature both may impose restrictions on the maximum feasible size of the pressure casing. To get an idea of the sizes involved with the constantly increasing outputs of single units, Table 13-2[48] lists tip diameters of rotors according to a study of Escher Wyss for closed-cycle machinery.

Table 13-2

APPROXIMATE DIAMETERS OF CLOSED-CYCLE TURBOMACHINERY RUNNERS FOR DIFFERENT OUTPUTS

Output, Mw	6	12	25	50	100
Max. Cycle pressure, psia	600	600	850	850	850
Max. diameters of impellers (axial design), mm					
HPT	432	483	662	890	1200
LPT	790	1000	1270	1780	2200
HPC	254	305	408	510	690
LPC	535	765	840	1350	1650

According to Escher Wyss, the dimensions may change slightly because of changes in speed or changes of system pressure level or because of use of a different blading, a different degree of reaction for the turbine, or of radial compressors instead of axials.

An investigation of a Russian 300-Mw gas-turbine plant project (see Figure 2-49) showed the following mean stage diameters and blade sizes (see Table 13-3).[48]

Table 13-3

COMPRESSOR AND TURBINE DATA FOR RUSSIAN 300 MW GAS-TURBINE PLANT

Rotor	Stage	Blade Size (mm) Height	Chord	Mean Diam.
Compressor C1	First	775	240	2325
Compressor C5	First	88	99	1044
Compressor C5	Last	60	99	1016
Turbine T4	Last	757	141	3030
Turbine T1	First	137	121	750

The manufacturers' information in Section 13.4 indicates that large outputs of a single, closed-cycle, gas-turbine unit are judged to be within manufacturing capabilities. The upper limits are deduced from indicated flow rates to be approximately as follows:

Escher Wyss	50 Mw
General Electric	150 Mw
Orenda	110 Mw
Westinghouse Electric	200 Mw

At present, the largest open-cycle gas turbine in the world has been built by DeLaval Ljungstrom, Finspang, Sweeden.[13] It has a maximum output of 40 Mw at 25°F and a weight of 900,000 lb, including accessories and heat exchanger.

Very large compressors have also been built. For example, Allis Chalmers' largest compressor has an inlet volume flow rate of 4,300,000 cfm of air and a 150,000-hp drive. Such volume flow would correspond to approximately 5400 lb/sec of mass flow. A smaller compressor for NASA, designed and built by Allis Chalmers, York Works, is shown on Figures 13-1 and 13-2. This compressor has an inlet volume flow of 2,250,000 cfm, and is driven by 3 electric motors, totalling 89,000 hp, at a maximum speed of 900 rpm.



Fig. 13-1 - Allis Chalmers 2,250,000 cfm Axial Flow Compressor for NASA During Assembly

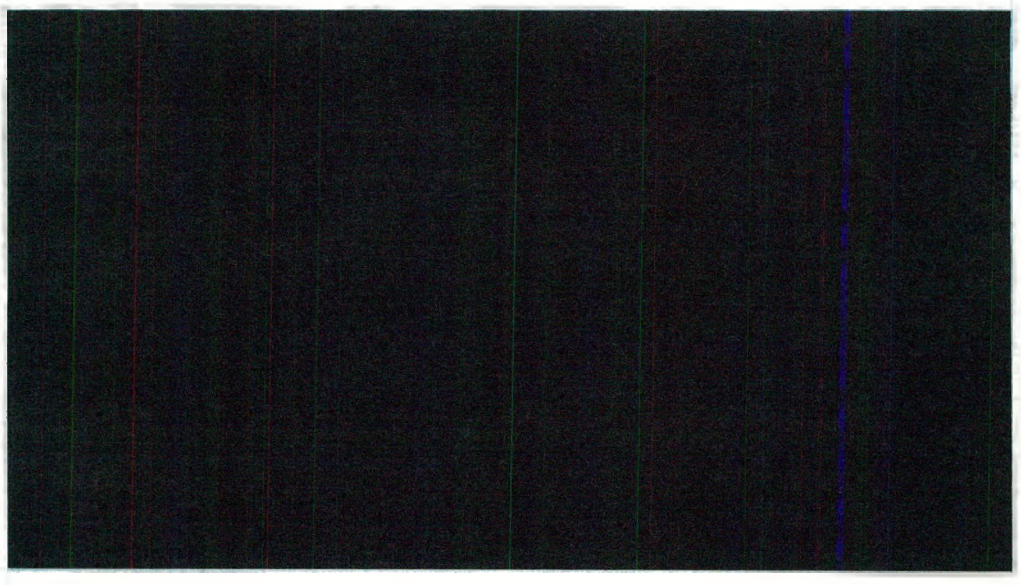


Fig. 13-2 - Allis Chalmers 2,250,000 cfm Axial Flow Compressor for NASA. Rotor on a 42-Foot Vertical Boring Mill at the York Works

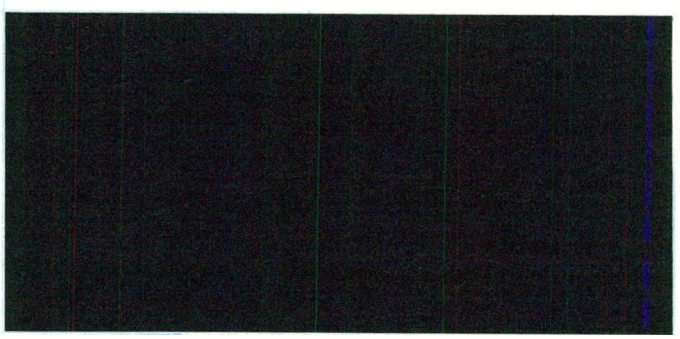


Fig. 13-3 - AiResearch Twenty-Horsepower Turbine Wheel Compared With the Size of a Silver Dollar

The lowest limits for volume flow are set by what is considered to be an acceptable efficiency which, at small sizes, rapidly decreases with decreasing size because of a decrease in Reynolds number, increase in relative surface roughness, and increase in relative running clearances. An increase in speed with decreasing size may also set a limit because of critical speed values. There are no sharp limits for the smallest size, which depends also on the purpose of the machine. For power machinery considered in this report, the smallest sizes are of less interest. Manufacturer's information in Section 13.4 indicates various smallest mass flows, from which corresponding sizes could be deduced. Solar Aircraft Co. directly indicates smallest recommended tip diameters of runners:

For radial compressors, 6.25 inches, and
For axial compressors, 10.0 inches.

High-pressure turbine wheels, where friction losses can be recovered as reheat and utilized for further expansion, can be smaller but still remain efficient. In general, any increases of entropy in the region of high temperatures are less detrimental to cycle efficiency than similar losses in the region of low temperatures.

Figure 13-3 shows one small turbine runner built by AiResearch, which still does not represent the smallest unit ever built. The same company has produced small air turbines in large quantities for special purposes, rotating at speeds of 100,000 rpm and faster. No information is available about the efficiency of such small runners.

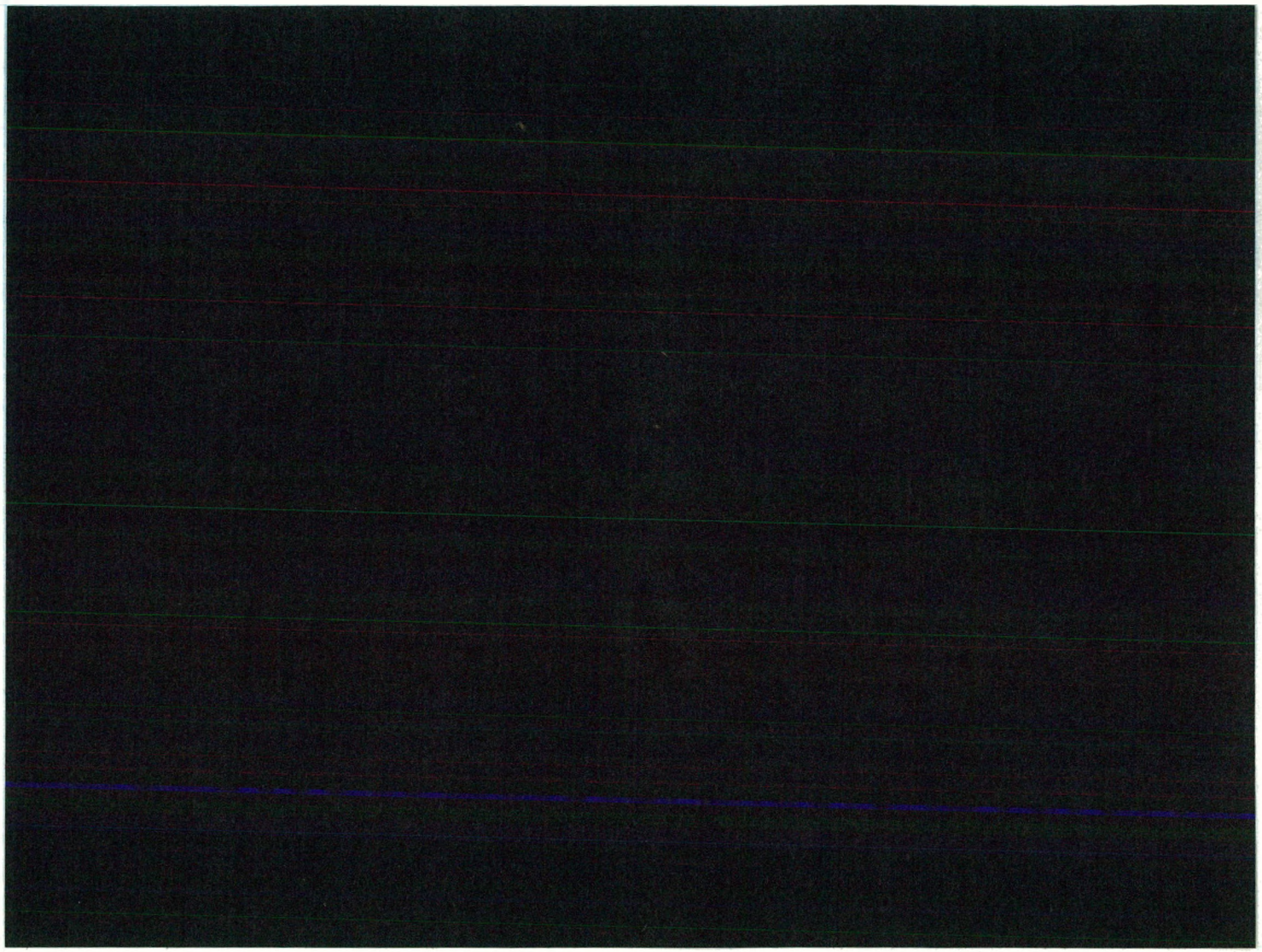


Fig. 13-4 - DeLaval Ljungstrom Turbine Co.
40 Mw Gas Turbine Plant

THE FRANKLIN INSTITUTE • Laboratories for Research and Development

13.4 List of Manufacturers, Turbine and Compressor Data Sheets

Table 13-1

LIST OF GAS-TURBINE MANUFACTURERS

1. AiResearch Manufacturing Div., The Garret Corporation
   Phoenix, Arizona.
   35-200 hp - AS, O, SP, W

2. W. H. Allen & Co., Ltd., Bedford, England
   0.115 - 0.885 Mw - APU, G, M

3. Allgemeine Elektrizitaets-Gesellschaft, (AEG)
   Berlin - Grunewald, Germany
   5.44 Mw - BF

4. Allis Chalmers Mfg. Co.
   Milwaukee, Wisconsin
   Experimental Gas Turbines

5. Allison Div. of General Motors Corporation
   Indianapolis, Ind.
   175-3730 hp - AC, Ap, Au, G, GC, M, D, W

6. Associated Electrical Industries, Ltd. (Includes Metropolitan Vickers Corp.)
   Manchester, England
   1.95 - 13.5 Mw - AC, G, GC, M, D

7. Blackburn Engines Ltd.
   Brough, England
   359-815 hp - Aj, Ap, APU, AS

8. BMW Triebwerke
   Munich, Allach, West Germany

9. Boeing Airplane Company, Industrial Products Division
   Seattle, Washington
   195-500 hp - Ap, AS

10. Bristol Siddeley Engines Ltd.
    Filton, Bristol, England
    3400-4165 hp - Ab, Ap, G, M

11. British Thompson - Houston Co.
    Rugby, England
    1200 - 5500 hp - M

12. Brown Bovery and Co., Ltd.
Baden, Switzerland
1.6 - 22.2 Mw - G, BF, L, P, SP

13. John Brown & Co., Ltd. (Escher Wyss Licensee)
Clydebank, Scotland
2.0 - 2.2 Mw - G

14. Canadian Westinghouse Co.
Hamilton, Ontario
8500 hp - GC

15. Cantieri del Tirreno (Clark Bros. Co. Licensee)
Genoa, Italy
8000 - 9300 hp - AC, E, G, GC, M, O, P, Pr, W

16. Chrysler Corporation
Detroit, Michigan
140-225 hp - Au

17. Clark Bros. Co., Division of Dresser Industries, Inc.
Olean, N. Y.
8000 - 10,000 hp - AC, E, G, GC, M, O, P, Pr, W

18. Continental Aviation and Engineering Corporation
Detroit, Michigan
190 - 1375 hp - Aj, Ap, AS, SP

19. Cooper-Bessemer Corporation
Mount Vernon, Ohio
10500 hp - G, GC, L, M, Pr

20. Daimler-Benz AG
Stuttgart, West Germany
260 - 300 hp - Au, P

21. DeHavilland Engine Co., Ltd. (Part of Hawker Siddeley Group)
Leavesden near Watford, Herts, England
- Aj

22. DeLaval Ljungström Turbine Co.
Finspång, Sweden
7.5 - 40 Mw - AC, G, GC

23. Elliott Co., Div. of Carrier Corporation
Jeannette, Pensylvania
750-30,000 scfm - AS, GC and Experimental Gas Turbines

24. English Electric Co., Ltd.
London, and Whetstone, England
1280 - 27,600 hp - Ap, AC, AS, G, GC, L, M, O, P, W

25. Escher Wyss Ltd.
Zurich, Switzerland
2 - 25 Mw - AC, G, GC

26. FIAT Stabilimento Grandi Motori
Torino, Italy
5.85 - 32 Mw - G

27. Ford Motor Company
Detroit, Michigan
300 hp - Au

28. Franco Tosi S. P. A. (Associated Electrical Industries Licensee)
Legnano, Italy
up to 6000 hp - AC, G, GC, O

29. Hispano-Marep (T.H.M.)
Paris, France
3000 - 6000 hp - I

30. Fuji Denki (Escher Wyss Licensee)
Tokyo, Japan
10 Mw - G

31. General Electric Co.
Lynn, Cincinnati and Schenectady, USA
858 - 33,000 hp - Aa, Aj, Ap, G, I, M, PL, SP

32. Gutehoffnungshuette (Escher Wyss Licensee)
Sterkrade, West Germany
9500 hp - G

33. Hawker Siddeley Brush Turbines, Ltd. (Clark Bros. Co. Licensee)
Gloucester, England
8000 - 9300 hp - AC, E, G, GC, M, O, P, Pr, W

34. Ishikanajima Shibaura Turbine Co.
Tokyo, Japan
1.6 - 4.9 Mw - G

35. B. C. Jet Engines Ltd.
Vancouver, Canada
350 hp max. - AC, APU, AS, G, H, M, P, W

36. Klockner-Humboldt-Deutz AG
Oberursel, Germany
80 hp - APU, G, P, W

37. Lycoming Division of Avco Corporation
Stratford, Conn.
700 - 1850 - Ap, H, I, M, SP

38. Maschinenfabrik Augsburg - Nurnberg A. G. (MAN)
Augsburg, Germany
7500 hp - G

39. D. Napier & Sons Ltd.
London, England
1280 - 2910 hp - Ap

40. Nordberg Mfg. Co.
Milwaukee, Wisconsin
Manufacturer on subcontract basis.

41. Nuove Reggiane (Associated Electrical Industries licensee)
Reggio Emilia, Italy
up to 6000 hp - M

42. Oerlikon Engineering Co.
(Dpt. for turbines & compressors associated with
Escher Wyss Co. in Zurich since 1959)
Zurich, Switzerland
989 hp - G

43. Orenda Engines Ltd.
Toronto, Canada
6200 - 8300 hp - G, GC, M

44. C. A. Parsons and Co., Ltd.
Newcastle upon Tyne, England
2710 - 21,430 hp - G, GC, O, W

45. Pratt & Whitney Aircraft
East Hartford, Conn.
350 - 18,000 hp - Af, Aj, Ap, AS, G, GC, GG, M, O, SP

46. Rateau A. C. B.
La Courneuve (Seine), France
3300 hp and other - M, Aj and other
(The American Instrument Company is agent for Rateau in USA)

47. Rocketdyne, Div. of North American Aviation
Canoga Park, California
Potential Manufacturer

48. Alsthom, Sté.de Constructions Électriques
e Mécaniques
Paris, France
- M

49. Spencer Turbine Company
Hartford, Connecticut
- AC

50. Rolls-Royce Ltd.
Derby, England
1432 - 16,500 hp - Ab, Aj, Ap

51. Rover Gas Turbines Ltd.
Solihull, Warwickshire, England
60 - 90 hp - Ap, APU, G, I, M, P

52. Ruston & Hornsby Ltd.
Lincoln, England
430 - 1260 hp - AC, AS, G, GC, L, M, O, P, Pr, W

53. Siemens Schuckertwerke AG, (SSW)
Mühlheim, Ruhr
3.0 - 21.0 Mw - BF, G, I

54. Société des Forges et Ateliers du Creusot, Usines Schneider
(Westinghouse licensee)
Paris, France

55. Societé Nationale d' Etude et de Construction de
Moteurs d' Aviation, (SNECMA)
Paris, France
12,000 hp - APU, G

56. Solar Aircraft Co.
San Diego, California
50 - 1080 hp - Ap, APU, AS, G, GC, M, O, P, Pr, W

57. Stratos Division, Fairchild-Stratos Corp.
Bay Shore, Long Island, New York

58. Sulzer Bros. Ltd.
Winterthur, Switzerland
4100 - 35,000 hp AC, APU, BF, G, GC, O, W

59. Turbines Hispano Marep
Paris, France
2800 - 4380 hp - AC, G, GC, L, M, O, P, W

60. Turbomeca
Bordes, France
210-2420 hp - Aj, Ap, AS, SP

61. Utica Division, Curtiss-Wright Corporation
Utica, New York
50 - 4000 hp - APU, AS, Au, G, I, L, M, P

62. Vector Corporation
Troy, Michigan
75 hp - I, G

63. Waukesha Motor Company (In collabor. with Williams Research Corp.)
Waukesha, Wis.
400 hp - Au, I, M, O, SP

64. Westinghouse Electric Corporation
Lester, Penna.
1375 - 30,000 hp - AC, AS, BF, E, G, GC, GG, M, O, Pr, W

65. Williams Research Corporation
Walled Lake, Michigan
70 - 400 hp - Aj, Au, I, M, O, SP

SYMBOLS:

Aa = Aft Fan Jet
Ab = Bypass Jet
AC = Air Compressor Drive
Af = Forward Fan Jet
Aj = Pure Jet
Ap = Prop Turbine
APU = Auxiliary Power Unit
AS = Air Supply
Au = Automotive
BF = Blast Furnace
E = Extraction Unit
G = Generator Drive
GC = Gas Compressor Drive
GG = Gas Generator
H = Helicopter
I = Industrial
L = Locomotive
M = Marine
O = Oil Pump Drive
P = Portable
PL = Peak Load
Pr = Process
SP = Shaft Power
W = Water Pump Drive

Manufacturer & Address	Compressor
American Standard Industrial Division Detroit 32, Michigan	DATA SHEET A Franklin Institute File No. 1

Report by: R. B. Smith Title: Appn. Engineer Date: 11-28-60

Describe already designed or manufactured compressor suitable for the primary loop of a high temperature gas-cooled nuclear power plant but with the following approximate restrictions:

Compression ratio 1.2 to 6
Flow rate 5 lb/sec and up for He, and 23 lb/sec and up for N_2
Inlet pressure at least 100 psia

1. TYPE. Manufacturer's designation: Single Stage Compressor

☒ centrifugal, ☐ axial, ☐ other: _____

2. ACTUAL PERFORMANCE PARAMETERS		Gases				
		He	N_2	Air		
Inlet pressure,	psia			* 44.0		
Inlet temperature,	°F			130.0		
Outlet pressure,	psia			55.9		
Outlet temperature,	°F			186.0		
Flow rate,	lb/sec			109.5		
Number of stages				1		
Speed,	rpm			4700		
Shaft horsepower				2100		

3. DRIVE	Turbine
4. COOLING	None
5. LUBRICATION	Oil
6. BEARINGS	Sleeve
7. SEAL AT SHAFT PENETRATION	Carbon Rings
8. SIZE & WEIGHT, lb	30,000

9. SPECIAL FEATURES:

10. NOTES: * Rated Conditions: Other operating points to 400 PSIA and 400°F from 700 RPM to 5200 RPM

List bulletins or other descriptive material accompanying this sheet.

Manufacturer & Address	Compressor
American Standard Industrial Division Detroit 32, Michigan	DATA SHEET B
	Franklin Institute File No. 2

Report by: R. B. Smith Title: Appn. Engineer Date: 11-28-60

Indicate capability to design and manufacture compressors suitable for the primary loop of high temperature gas-cooled nuclear power plants for the data below

1. TYPE. ☐ centrifugal, ☐ axial, ☐ other: _____

Performance parameters		He				N_2			
Inlet pressure,	psia	373	348	326	297	274	251	230	204
Inlet temperature,	°F	100	100	100	100	100	100	100	100
Total compression ratio		2.68	2.87	3.07	3.37	3.65	3.99	4.35	4.90
Range of flow rates,	lb/sec								
Number of units in series									
Can be designed based on present experience of manufacturer:		☐	☐	☐	☐	☐	☐	☐	☐
Can be designed but needs development:		☐	☐	☐	☐	☐	☐	☐	☐
Cannot be considered at present conditions:		☒	☒	☒	☒	☒	☒	☒	☒

Notes: a. When design needs development indicate what: _____

b. Indicate in the above table the range of flow rates considered practicable and the number of units in series.

c. Indicate limiting factors: _____

2. CAPABILITY TO CONDUCT PARTICULAR DEVELOPMENT:

3. ACTUAL DEVELOPMENT WORK:

4. EXTRAORDINARY FABRICATION FACILITIES:

5. EXTRAORDINARY TESTING FACILITIES:

6. NOTES:

List bulletins or other descriptive material accompanying this sheet.

Manufacturer & Address Clark Bros. Co. Div. Dresser Industries, Inc. Olean, New York	Compressor DATA SHEET A Franklin Institute File No. 3

Report by: Title: Date:

Describe already designed or manufactured compressor suitable for the primary loop of a high temperature gas-cooled nuclear power plant but with the following approximate restrictions:

Compression ratio 1.2 to 6
Flow rate 5 lb/sec and up for He, and 23 lb/sec and up for N_2
Inlet pressure at least 100 psia

1. TYPE. Manufacturer's designation: CSN-1

☐ centrifugal, ☒ axial, ☐ other:

2. ACTUAL PERFORMANCE PARAMETERS		Gases				
		He	N_2			
Inlet pressure,	psia		116.2			
Inlet temperature,	°F		132.9			
Outlet pressure,	psia		321.3			
Outlet temperature,	°F		369.7			
Flow rate,	lb/sec		25.7			
Number of stages			11			
Speed,	rpm		22,000			
Shaft horsepower			2220			

3. DRIVE	Common shaft with turbine
4. COOLING	Lubricating oil to air
5. LUBRICATION	Forced feed system with flow controlled by differential regulators
6. BEARINGS	
7. SEAL AT SHAFT PENETRATION	Oil film with buffer gas.
8. SIZE & WEIGHT, lb	Total Turb.-Compr. Set 36" dia. x 56" long 2000 lb

9. SPECIAL FEATURES:

10. NOTES: Compressor is part of complete turbine-compressor set for ML-1.

List bulletins or other descriptive material accompanying this sheet.

Manufacturer & Address	Gas Turbine
Clark Bros. Co. Div. Dresser Industries, Inc. Olean, New York	DATA SHEET A
	Franklin Institute File No. 4

Report by: Title: Date:

Describe already designed or manufactured gas turbine suitable for the primary loop of a high temperature gas-cooled nuclear power plant but with the following approximate restrictions:

Expansion ratio 1.2 to 6
Flow rate 5 lb/sec and up for He, and 23 lb/sec and up for N_2
Inlet temperature above 1100°F
Outlet pressure at least 100 psia

1. TYPE. Manufacturer's designation: CSN-1

☒ axial, ☐ radial, ☐ other:

2. ACTUAL PERFORMANCE PARAMETERS		Gases				
		He	N_2			
Inlet pressure,	psia		290.4			
Inlet temperature,	°F		1193.5			
Outlet pressure,	psia		120			
Outlet temperature,	°F		899.2			
Flow rate,	lb/sec		25.2			
Number of stages			2			
Speed,	rpm		22,000			
Shaft horsepower						

3. STARTING	Electric motor generator set
4. COOLING	Lubricating oil to air
5. LUBRICATION	Forced feed system with flow controlled by differential regulators
6. BEARINGS	Sleeve
7. SEAL AT SHAFT PENETRATION	Oil film with buffer gas.
8. SIZE & Weight, lb	Total Turb.-Compr. Set 36" dia. x 56" long, 2000 lb

9. SPECIAL FEATURES:

10. NOTES: Turbine is part of complete Turbine-Compressor Set for ML-1.

List bulletins or other descriptive material accompanying this sheet.

Manufacturer & Address	Compressor
Clark Bros. Co. Div. Dresser Industries, Inc. Olean, New York	DATA SHEET B
	Franklin Institute File No. 5
Report by:	Title: Date: 12-8-60

Indicate capability to design and manufacture compressors suitable for the primary loop of high temperature gas-cooled nuclear power plants for the data below

1. TYPE. ☒ centrifugal, ☒ axial, ☐ other: _____

Performance parameters		He				N_2			
Inlet pressure,	psia	373	348	326	297	274	251	230	204
Inlet temperature,	°F	100	100	100	100	100	100	100	100
Total compression ratio		2.68	2.87	3.07	3.37	3.65	3.99	4.35	4.90
Range of flow rates,		1000 cfm & up							
No. of compressor cases		← 3 - 4 →				← 1 →			
Stages (centrifugal)									
Number of in series		← 15 - 30 →				← 5 - 7 →			
Can be designed based on present experience of manufacturer:		☒	☒	☒	☒	☒	☒	☒	☒
Can be designed but needs development:		☐	☐	☐	☐	☐	☐	☐	☐
Cannot be considered at present conditions:		☐	☐	☐	☐	☐	☐	☐	☐

Notes: a. When design needs development indicate what: _____

b. Indicate in the above table the range of flow rates considered practicable and the number of units in series.

c. Indicate limiting factors: _____

2. CAPABILITY TO CONDUCT PARTICULAR DEVELOPMENT:

3. ACTUAL DEVELOPMENT WORK:

4. EXTRAORDINARY FABRICATION FACILITIES:

5. EXTRAORDINARY TESTING FACILITIES:

6. NOTES:
Can use existing equipment.

List bulletins or other descriptive material accompanying this sheet.

Manufacturer & Address	Gas Turbine
Clark Bros. Co. Div. Dresser Industries, Inc. Olean, New York	DATA SHEET B
	Franklin Institute File No. 6

Report by: Title: Date: 12-8-60

Indicate capability to design and manufacture gas turbines suitable for the primary loop of high temperature gas-cooled nuclear power plants for the data below

1. TYPE. ☒ axial, ☒ radial, ☐ other: _____

Performance parameters		He				N_2			
Inlet pressure,	psia	925	925	925	925	925	925	925	925
Inlet temperature,	°F	1300	1500	1700	2000	1300	1500	1700	2000
Total expansion ratio		2.37	2.54	2.71	2.97	3.22	3.52	3.84	4.32
Range of flow rates	20 lb/sec	and up							
Number of units in series						2	2	3	
Lifetime									
Can be designed based on present experience of manufacturer:		☐	☐	☐	☐	☒	☐	☐	☐
Can be designed but needs development:		☒	☒	☒	☐	☐	☒	☒	☐
Cannot be considered at present conditions:		☐	☐	☐	☒	☐	☐	☐	☒

Notes: a. When design needs development indicate what: new concept

b. Indicate in the above table the range of flow rates considered practicable, the number of units in series, and the expected lifetime.

c. Indicate limiting factors: Temperature & Stress

2. CAPABILITY TO CONDUCT PARTICULAR DEVELOPMENT:

Yes

3. ACTUAL DEVELOPMENT WORK:

4. EXTRAORDINARY FABRICATION FACILITIES:

5. EXTRAORDINARY TESTING FACILITIES:

6. NOTES:

List bulletins or other descriptive material accompanying this sheet.

Manufacturer & Address	Compressor
General Electric Company Gas Turbine Department Schenectady, N.Y.	DATA SHEET A Franklin Institute File No. 7

Report by: R.L. Hendrickson **Title:** Mgr., Systems Engineering **Date:** March 16, 1961

Describe already designed or manufactured compressor suitable for the primary loop of a high temperature gas-cooled nuclear power plant but with the following approximate restrictions:

Compression ratio 1.2 to 6
Flow rate 5 lb/sec and up for He, and 23 lb/sec and up for N_2
Inlet pressure at least 100 psia

1. TYPE. Manufacturer's designation: HP Test Compressor

☐ centrifugal, ☒ axial, ☐ other: _____

2. ACTUAL PERFORMANCE PARAMETERS		Gases				
		He	N_2	CO_2		
Inlet pressure,	psia		61.3	133.5		
Inlet temperature,	°F		71	71		
Outlet pressure,	psia		239	510		
Outlet temperature,	°F		*	*		
Flow rate,	lb/sec		31.9	83.6		
Number of stages			11	11		
Speed,	rpm		18600	14800		
Shaft horsepower			3260	5460		
*Overall adiabatic efficiency of design			78%	78%		

3. DRIVE	Normal: Gas Turbine Test: 6000 HP D.E. Steam Tb. and Gear
4. COOLING	Andale Co. water cooler 500 GPM CO_2 performance 95% effectiveness
5. LUBRICATION	Forced feed oil
6. BEARINGS	3 Lube journal bearings - tapered load thrust
7. SEAL AT SHAFT PENETRATION	Oil ring seals fed from special seal oil system with CO_2 detraining system.
8. SIZE & WEIGHT, lb	11.6" Stator casing inside diameter
9. SPECIAL FEATURES:	Adjustable inlet guide vanes. Design for air and CO_2 operation.

10. NOTES: GED 3603, GED 3546 - GER -1488

KCH-9761173 - Instrumentation Diagram and Typical Values

List bulletins or other descriptive material accompanying this sheet.

Manufacturer & Address	Compressor
General Electric Company Gas Turbine Department Schenectady, N.Y.	DATA SHEET B
	Franklin Institute File No. 8

Report by: R.L. Hendrickson Title: Mgr, Systems Engineering Date: March 16, 1961

Indicate capability to design and manufacture compressors suitable for the primary loop of high temperature gas-cooled nuclear power plants for the data below

1. TYPE. ☐ centrifugal, ☒ axial, ☐ other: _____

Performance parameters		He				N_2			
Inlet pressure,	psia	373	348	326	297	274	251	230	204
Inlet temperature,	°F	100	100	100	100	100	100	100	100
Total compression ratio		2.68	2.87	3.07	3.37	3.65	3.99	4.35	4.90
Range of flow rates,	lb/sec	60/600	60/600	50/500	50/500	400/4000	400/4000	300/3000	300/3000
Number of units in series		2	2	2	2	1 or 2	1 or 2	1 or 2	1 or 2
Can be designed based on present experience of manufacturer:		☐	☐	☐	☐	☐	☐	☐	☐
Can be designed but needs development:		☒	☒	☒	☒	☒	☒	☒	☒
Cannot be considered at present conditions:		☐	☐	☐	☐	☐	☐	☐	☐

Notes: a. When design needs development indicate what: Check out of Seal System, Hydrostatic Test, Blade Fatigue Life (strain gauge measurements)

b. Indicate in the above table the range of flow rates considered practicable and the number of units in series.

c. Indicate limiting factors: Inadequate experience with blade vibration and excitation to be expected at high pressures. Maximum casing diameter of current experience is 66.6".

2. CAPABILITY TO CONDUCT PARTICULAR DEVELOPMENT:

Depending upon schedules, general timing of projects, Department employees 50 to 100 Gas Turbine Engineers.

3. ACTUAL DEVELOPMENT WORK:

General Development of Marine, Industrial, Elect. Utility -Gas Turbine.

4. EXTRAORDINARY FABRICATION FACILITIES:

Gas Turbine Factory

5. EXTRAORDINARY TESTING FACILITIES:

6. NOTES:

GED 3603, GED 3546

List bulletins or other descriptive material accompanying this sheet.

Manufacturer & Address	Gas Turbine
General Electric Company Gas Turbine Department Schenectady, N.Y.	DATA SHEET B Franklin Institute File No. 9

Report by: R.L. Hendrickson **Title:** Mgr. Systems Engineering **Date:** March 16, 1961

Indicate capability to design and manufacture gas turbines suitable for the primary loop of high temperature gas-cooled nuclear power plants for the data below

1. TYPE. ☒ axial, ☐ radial, ☐ other: _____

Performance parameters		He				N_2			
Inlet pressure,	psia	925	925	925	925	925	925	925	925
Inlet temperature,	°F	1300	1500	1700	2000	1300	1500	1700	2000
Total expansion ratio		2.37	2.54	2.71	2.97	3.22	3.52	3.84	4.32
Range of flow rates	lb/sec	60/600	60/600	50/500	50/500	400/4000	400/4000	300/3000	300/3000
Number of units in series		1 or 2	1 or 2			1 or 2	1 or 2		
Lifetime - hours		10^5	10^5	10^4		10^5	10^5	10^4	
Can be designed based on present experience of manufacturer:		☒	☒	☐	☐	☒	☒	☐	☐
Can be designed but needs development:		☐	☐	☒	☐	☐	☐	☒	☐
Cannot be considered at present conditions:		☐	☐	☐	☒	☐	☐	☐	☒

Notes: a. When design needs development indicate what: Seal System, Hydrostatic Test, Blade Fatigue and rupture life at elevated pressure and temp.

b. Indicate in the above table the range of flow rates considered practicable, the number of units in series, and the expected lifetime.

c. Indicate limiting factors: Inadequate experience with blade vibration and excitation to be expected at high pressures. Maximum tip diameter of current experience is 85".

2. CAPABILITY TO CONDUCT PARTICULAR DEVELOPMENT:

Depending upon schedules, general timing of projects, Department employees 50 to 100 Gas Turbine Engineers

3. ACTUAL DEVELOPMENT WORK:

General Development of Marine, Industrial, Elec. Utility - Gas Turbine

4. EXTRAORDINARY FABRICATION FACILITIES:

Gas Turbine Factory

5. EXTRAORDINARY TESTING FACILITIES:

6. NOTES:

GED 3603, GED 3546

List bulletins or other descriptive material accompanying this sheet.

Manufacturer & Address N.V. Neratoom and participants, Noordeinde 38, Den Haag, Holland.	Compressor DATA SHEET A Franklin Institute File No. 10

Report by: Title: Date:

Describe already designed or manufactured compressor suitable for the primary loop of a high temperature gas-cooled nuclear power plant but with the following approximate restrictions:

Compression ratio 1.2 to 6
Flow rate 5 lb/sec and up for He, and 23 lb/sec and up for N_2
Inlet pressure at least 100 psia

1. TYPE. Manufacturer's designation: W.S.

☐ centrifugal, ☒ axial, ☐ other: _____

2. ACTUAL PERFORMANCE PARAMETERS		Gases				
		He	N_2	Air		
Inlet pressure,	psia			14,36		
Inlet temperature,	^oF			86		
Outlet pressure,	psia			78,98		
Outlet temperature,	^oF			480		
Flow rate,	lb/sec			71,2		
Number of stages				19		
Speed,	rpm			5000		
Shaft horsepower				9900		

3. DRIVE	Gasturbine
4. COOLING	None
5. LUBRICATION	Oil
6. BEARINGS	Journal bearings
7. SEAL AT SHAFT PENETRATION	Labyrinth seal
8. SIZE & WEIGHT, lb	11 ft long, 2500 lbs.
9. SPECIAL FEATURES:	Axial compressor.

10. NOTES:

List bulletins or other descriptive material accompanying this sheet.

Manufacturer & Address	Compressor
N.V. Neratoom and participants, Noordeinde 38, Den Haag, Holland.	DATA SHEET B
	Franklin Institute File No. 11

Report by: Title: Date:

Indicate capability to design and manufacture compressors suitable for the primary loop of high temperature gas-cooled nuclear power plants for the data below

1. TYPE. ☒ centrifugal, ☒ axial, ☐ other: _____

Performance parameters		He				N_2			
Inlet pressure,	psia	373	348	326	297	274	251	230	204
Inlet temperature,	°F	100	100	100	100	100	100	100	100
Total compression ratio		2.68	2.87	3.07	3.37	3.65	3.99	4.35	4.90
Range of flow rates,	lb/sec								
Number of units in series									
Can be designed based on present experience of manufacturer:		☐	☐	☐	☐	☐	☐	☐	☐
Can be designed but needs development:		☒	☒	☒	☒	☒	☒	☒	☒
Cannot be considered at present conditions:		☐	☐	☐	☐	☐	☐	☐	☐

Notes: a. When design needs development indicate what: shaft seals

b. Indicate in the above table the range of flow rates considered practicable and the number of units in series.

c. Indicate limiting factors: _____

2. CAPABILITY TO CONDUCT PARTICULAR DEVELOPMENT:

available

3. ACTUAL DEVELOPMENT WORK:

Compressor for open seal gasturbines

4. EXTRAORDINARY FABRICATION FACILITIES:

none

5. EXTRAORDINARY TESTING FACILITIES:

none

6. NOTES:

List bulletins or other descriptive material accompanying this sheet.

Manufacturer & Address

Orenda Engines Limited,
Box 4015,
Terminal 'A' Toronto

Compressor

DATA SHEET B

Franklin Institute File No. 12

Report by: J. J. Conrath Title: Senior Engineer Date: Nov. 21/60

Indicate capability to design and manufacture compressors suitable for the primary loop of high temperature gas-cooled nuclear power plants for the data below

1. TYPE. centrifugal, x axial, other: _____

Performance parameters		He				N_2			
Inlet pressure,	psia	373	348	326	297	274	251	230	204
Inlet temperature,	°F	100	100	100	100	100	100	100	100
Total compression ratio		2.68	2.87	3.07	3.37	3.65	3.99	4.35	4.90
Range of flow rates,	lb/sec	40 to 900 ⟶				100 to 1600 ⟶			

Number of units in series	2 ⟶				1 ⟶			
Can be designed based on present experience of manufacturer:	☐	☐	☐	☐	☐	☐	☐	☐
Can be designed but needs development:	☒	☒	☒	☒	☒	☒	☒	☒
Cannot be considered at present conditions:	☐	☐	☐	☐	☐	☐	☐	☐

Notes: a. When design needs development indicate what: Seals and Aerodynamic

b. Indicate in the above table the range of flow rates considered practicable and the number of units in series.

c. Indicate limiting factors: Flows limited by reasonable axial MN Nos. & compressor practical Geometry in terms of casing diameters and blade height.

2. CAPABILITY TO CONDUCT PARTICULAR DEVELOPMENT: Have staff available that are experienced in designing suitable development equipment and carrying out development program.

3. ACTUAL DEVELOPMENT WORK: Have developed axial compressors for 3 aircraft Jet Engines.

4. EXTRAORDINARY FABRICATION FACILITIES: Manufacturing shop and tool room equipped for precision manufacture and quality control suitable for the standards of aircraft gas turbines.

5. EXTRAORDINARY TESTING FACILITIES: Materials, aerodynamic, Instrument and mechanical testing laboratories available for all aspects of this programme.

6. NOTES: Brochures on Orenda Engines Ltd. (1) Facilities and Service (2) Laboratory Facilities (3) Manufacturing Facilities.

List bulletins or other descriptive material accompanying this sheet.

Manufacturer & Address	Gas Turbine
Orenda Engines Limited, Box 4015, Terminal 'A' Toronto	DATA SHEET B Franklin Institute File No. 13

Report by: J. J. Conrath **Title:** Senior Engineer **Date:** Nov. 21/60

Indicate capability to design and manufacture gas turbines suitable for the primary loop of high temperature gas-cooled nuclear power plants for the data below

1. TYPE. ☒ **axial,** ☐ **radial,** ☐ **other:** _____

Performance parameters	He				N_2			
Inlet pressure, psia	925	925	925	925	925	925	925	925
Inlet temperature, °F	1300	1500	1700	2000	1300	1500	1700	2000
Total expansion ratio	2.37	2.54	2.71	2.97	3.22	3.52	3.84	4.32
Range of flow rates (Min) lb/sec	20	→	→*		40	→	→*	
Range of flow rates (Max) lb/sec	439	384	362*		728	645	580*	
				*Requires 150°F Blade Cooling				
Number of units in series	1	→	→		1	→	→	
Lifetime	30 yrs	→	→		30 yrs	→	→	
Can be designed based on present experience of manufacturer:	☐	☐	☐	☐	☐	☐	☐	☐
Can be designed but needs development:	☒	☒	☒	☐	☒	☒	☒	☐
Cannot be considered at present conditions:	☐	☐	☐	☒	☐	☐	☐	☒

Notes: **a.** When design needs development indicate what: Seals, Aerodynamic and Blade Cooling

b. Indicate in the above table the range of flow rates considered practicable, the number of units in series, and the expected lifetime.

c. Indicate limiting factors: Blade stresses (Detail Analysis may impose changes on above performance parameters)

2. CAPABILITY TO CONDUCT PARTICULAR DEVELOPMENT: Have staff available that are experienced in designing suitable development equipment and carrying out development work.

3. ACTUAL DEVELOPMENT WORK: Have developed axial turbines for 3 aircraft jet engines.

4. EXTRAORDINARY FABRICATION FACILITIES: Manufacturing, shop and Tool Room equipped for precision manufacture and quality control suitable for the standards of aircraft gas turbines.

5. EXTRAORDINARY TESTING FACILITIES: Materials, Aerodynamic, Instrument and Mechanical testing Laboratories available for all aspects of this program.

6. NOTES: Brochures on Orenda Engines Ltd. (1) Facilities and service (2) Laboratory Facilities (3) Manufacturing Facilities

List bulletins or other descriptive material accompanying this sheet.

Manufacturer & Address	Compressor
Rocketdyne a Division of North American Aviation, Inc. 6633 Canoga Ave., Canoga Park, Calif.	DATA SHEET B Franklin Institute File No. 14

Report by: Title: Date: 11-28-60

Indicate capability to design and manufacture compressors suitable for the primary loop of high temperature gas-cooled nuclear power plants for the data below

1. TYPE. ☒ centrifugal, ☒ axial, ☒ other: _____

Performance parameters		He				N_2			
Inlet pressure,	psia	373	348	326	297	274	251	230	204
Inlet temperature,	°F	100	100	100	100	100	100	100	100
Total compression ratio		2.68	2.87	3.07	3.37	3.65	3.99	4.35	4.90
Range of flow rates,	lb/sec								
Number of units in series									
Can be designed based on present experience of manufacturer:		☐	☐	☐	☐	☐	☐	☐	☐
Can be designed but needs development:		☒	☒	☒	☒	☒	☒	☒	☒
Cannot be considered at present conditions:		☐	☐	☐	☐	☐	☐	☐	☐

Notes: a. When design needs development indicate what: _____

b. Indicate in the above table the range of flow rates considered practicable and the number of units in series.

c. Indicate limiting factors: _____

2. CAPABILITY TO CONDUCT PARTICULAR DEVELOPMENT:

3. ACTUAL DEVELOPMENT WORK:

4. EXTRAORDINARY FABRICATION FACILITIES:

5. EXTRAORDINARY TESTING FACILITIES:

6. NOTES:

List bulletins or other descriptive material accompanying this sheet.

Manufacturer & Address 150, Boulev. Haussmann, Paris VIII Societe Nationale d'Etude et de Coustr. de Moteurs d'Aviation	Compressor DATA SHEET A Franklin Institute File No. 16

Report by: Title: Date:

Describe already designed or manufactured compressor suitable for the primary loop of a high temperature gas-cooled nuclear power plant but with the following approximate restrictions:

Compression ratio 1.2 to 6
Flow rate 5 lb/sec and up for He, and 23 lb/sec and up for N_2
Inlet pressure at least 100 psia

1. TYPE. Manufacturer's designation: _____

☒ centrifugal, ☐ axial, ☐ other: _____

2. ACTUAL PERFORMANCE PARAMETERS		Gases				
		He	N_2	air		
Inlet pressure,	psia			14,7		
Inlet temperature,	°F			59		
Outlet pressure,	psia			88,2		
Outlet temperature,	°F			486		
Flow rate,	lb/sec			2,9		
Number of stages				2		
Speed,	rpm			44 500		
Shaft horsepower				425		

3. DRIVE	Moteur électrique ou turbine à gaz
4. COOLING	Pas de refroidissement intermédiaire
5. LUBRICATION	Classique - Huile ordinaire
6. BEARINGS	Roulements ou paliers lisses - piston d'équilibrage
7. SEAL AT SHAFT PENETRATION	Arbre cannelé - Multiplicateur
8. SIZE & WEIGHT, lb	D maxi = longueur = 12,5" ; poids = 90 lbs

9. SPECIAL FEATURES:

10. NOTES:

List bulletins or other descriptive material accompanying this sheet.

Manufacturer & Address S.N.E.C.M.A SOCIETE NATIONALE D'ETUDE ET DE CONSTRUCTION DE MOTEURS D'AVIATION 150, Boulevard Haussmann - PARIS - (VIIIème) FRANCE	Gas Turbine DATA SHEET A Franklin Institute File No. 17
Report by:	Title: Date: 9/1/1961

Describe already designed or manufactured gas turbine suitable for the primary loop of a high temperature gas-cooled nuclear power plant but with the following approximate restrictions:

Expansion ratio 1.2 to 6
Flow rate 5 lb/sec and up for He, and 23 lb/sec and up for N_2
Inlet temperature above 1100°F
Outlet pressure at least 100 psia

1. TYPE. Manufacturer's designation: _____

☒ axial, ☐ radial, ☐ other: axial

2. ACTUAL PERFORMANCE PARAMETERS		Gases				
		He	N_2	Air	Air	Air
Inlet pressure,	psia			330	230	230
Inlet temperature,	°F			1,520	1,100	1,100
Outlet pressure,	psia			100	100	100
Outlet temperature,	°F					
Flow rate,	lb/sec			9	20	35
Number of stages				2	2	2
Speed,	rpm			50,000	24,000	18,000
Shaft horsepower				1,500	1,700	3,000

3. STARTING	
4. COOLING	
5. LUBRICATION	
6. BEARINGS	
7. SEAL AT SHAFT PENETRATION	
8. SIZE & Weight, lb	

9. SPECIAL FEATURES:

10. NOTES:

List bulletins or other descriptive material accompanying this sheet.

Manufacturer & Address	Gas Turbine
Rocketdyne, a Division of North American Aviation, Inc. 6633 Canoga Ave., Canoga Park, Calif.	DATA SHEET B
	Franklin Institute File No. 15

Report by: Title: Date: 11-28-60

Indicate capability to design and manufacture gas turbines suitable for the primary loop of high temperature gas-cooled nuclear power plants for the data below

1. TYPE. ☐ axial, ☐ radial, ☐ other: _____

Performance parameters		He				N_2			
Inlet pressure,	psia	925	925	925	925	925	925	925	925
Inlet temperature,	°F	1300	1500	1700	2000	1300	1500	1700	2000
Total expansion ratio		2.37	2.54	2.71	2.97	3.22	3.52	3.84	4.32
Range of flow rates	lb/sec								
Number of units in series									
Lifetime									
Can be designed based on present experience of manufacturer:		☐	☐	☐	☐	☐	☐	☐	☐
Can be designed but needs development:		☒	☒	☒	☒	☒	☒	☒	☒
Cannot be considered at present conditions:		☐	☐	☐	☐	☐	☐	☐	☐

Notes: a. When design needs development indicate what: _____

b. Indicate in the above table the range of flow rates considered practicable, the number of units in series, and the expected lifetime.

c. Indicate limiting factors: _____

2. CAPABILITY TO CONDUCT PARTICULAR DEVELOPMENT:

3. ACTUAL DEVELOPMENT WORK:

4. EXTRAORDINARY FABRICATION FACILITIES:

5. EXTRAORDINARY TESTING FACILITIES:

6. NOTES:

List bulletins or other descriptive material accompanying this sheet.

Manufacturer & Address	Compressor
Soc. Nationale D'Étude et de Constr. De Moteurs D'Aviation 150, Boulev. Haussmann, Paris VIII[e]	DATA SHEET B Franklin Institute File No. 18

Report by: Title: Date:

Indicate capability to design and manufacture compressors suitable for the primary loop of high temperature gas-cooled nuclear power plants for the data below

1. TYPE. ☒ centrifugal, ☒ axial, ☐ other: _____

Performance parameters		He				N_2			
Inlet pressure,	psia	373	348	326	297	274	251	230	204
Inlet temperature,	°F	100	100	100	100	100	100	100	100
Total compression ratio		2.68	2.87	3.07	3.37	3.65	3.99	4.35	4.90
Range of flow rates,	lb/sec	10	→	→	8	25	→	→	19
		↓			↓	↓			↓
		1300	→	→	1000	3300	→	→	2500
Number of units in series									
Can be designed based on present experience of manufacturer:		☐	☐	☐	☐	☒	☒	☒	☒
Can be designed but needs development:		☒	☒	☒	☒	☐	☐	☐	☐
Cannot be considered at present conditions:		☐	☐	☐	☐	☐	☐	☐	☐

Notes: a. When design needs development indicate what: _____

b. Indicate in the above table the range of flow rates considered practicable and the number of units in series.

c. Indicate limiting factors: _____

2. CAPABILITY TO CONDUCT PARTICULAR DEVELOPMENT:

3. ACTUAL DEVELOPMENT WORK:

4. EXTRAORDINARY FABRICATION FACILITIES:

5. EXTRAORDINARY TESTING FACILITIES:

6. NOTES:

List bulletins or other descriptive material accompanying this sheet.

Manufacturer & Address S.N.E.C.M.A SOCIETE NATIONALE D'ETUDE ET DE CONSTRUCTION DE MOTEURS D'AVIATION 150, Bd Haussmann - PARIS - (VIII) FRANCE	Gas Turbine DATA SHEET B Franklin Institute File No. 19
Report by:	Title: Date: 9/1/1961

Indicate capability to design and manufacture gas turbines suitable for the primary loop of high temperature gas-cooled nuclear power plants for the data below

1. TYPE. ☐ axial, ☐ radial, ☐ other: _____

Performance parameters		He				N_2			
Inlet pressure,	psia	925	925	925	925	925	925	925	925
Inlet temperature,	°F	1300	1500	1700	2000	1300	1500	1700	2000
Total expansion ratio		2.37	2.54	2.71	2.97	3.22	3.52	3.84	4.32
Range of flow rates	lb/sec	1,10	1,15	1,20	1,25	3,20	3,30	3,40	3,50
Con be designed with single-stage		X	X	X	X				
Number of units in series		2	2	2	2	2	2	2	2
Lifetime									
Can be designed based on present experience of manufacturer:		☒	☒	☒	☒	☒	☒	☒	☒
Can be designed but needs development:		☐	☐	☐	☐	☐	☐	☐	☐
Cannot be considered at present conditions:		☐	☐	☐	☐	☐	☐	☐	☐

Notes: a. When design needs development indicate what: _____

b. Indicate in the above table the range of flow rates considered practicable, the number of units in series, and the expected lifetime.

c. Indicate limiting factors: Length of blades
Rational speed based on present experience of manufacturer 60,000 rpm

2. CAPABILITY TO CONDUCT PARTICULAR DEVELOPMENT:

3. ACTUAL DEVELOPMENT WORK:

4. EXTRAORDINARY FABRICATION FACILITIES:

5. EXTRAORDINARY TESTING FACILITIES:

6. NOTES:

List bulletins or other descriptive material accompanying this sheet.

Manufacturer & Address	Compressor
Solar Aircraft Co. 2200 Pacific Hwy. San Diego 12, Calif.	DATA SHEET B Franklin Institute File No. 20

Report by: Title: Date:

Indicate capability to design and manufacture compressors suitable for the primary loop of high temperature gas-cooled nuclear power plants for the data below

1. TYPE. ☒ centrifugal, ☐ axial, ☐ other: _____

Performance parameters		He				N_2			
Inlet pressure,	psia	373	348	326	297	274	251	230	204
Inlet temperature,	°F	100	100	100	100	100	100	100	100
Total compression ratio		2.68	2.87	3.07	3.37	3.65	3.99	4.35	4.90
Range of flow rates,	lb/sec				*	> 35	> 33	> 31	> .29
*6.25 in. dia. tip Minimum Recommended		Multi Staging of Radial Compressors not feasible because of length, efficiency & critical speed with He.							
Number of units in series						2	2	2	2
Can be designed based on present experience of manufacturer:		☐	☐	☐	☐	☒	☒	☒	☒
Can be designed but needs development:		☐	☐	☐	☐	☐	☐	☐	☐
Cannot be considered at present conditions:		☐	☐	☐	☐	☐	☐	☐	☐

Notes: a. When design needs development indicate what: _____

b. Indicate in the above table the range of flow rates considered practicable and the number of units in series.

c. Indicate limiting factors: _____

2. CAPABILITY TO CONDUCT PARTICULAR DEVELOPMENT:

100%

3. ACTUAL DEVELOPMENT WORK:

Bearings & Seals.

4. EXTRAORDINARY FABRICATION FACILITIES:

5. EXTRAORDINARY TESTING FACILITIES:

6. NOTES:

List bulletins or other descriptive material accompanying this sheet.

Manufacturer & Address Solar Aircraft Co. 2200 Pacific Hwy. San Diego 12, Calif.	Compressor DATA SHEET B Franklin Institute File No. 21

Report by: Title: Date:

Indicate capability to design and manufacture compressors suitable for the primary loop of high temperature gas-cooled nuclear power plants for the data below

1. TYPE. ☐ centrifugal, ☒ axial, ☐ other: _____

Performance parameters		He				N_2			
Inlet pressure,	psia	373	348	326	297	274	251	230	204
Inlet temperature,	°F	100	100	100	100	100	100	100	100
Total compression ratio		2.68	2.87	3.07	3.37	3.65	3.99	4.35	4.90
Range of flow rates,	lb/sec*	>58	>53	>50	>46	>208	>190	>170	>165
*10 in. dia. axial comp. Minimum Recommended									
Number of units in series (Stages)		19	20	21	23	7	8	8	9
Can be designed based on present experience of manufacturer:		☒	☒	☒	☒	☒	☒	☒	☒
Can be designed but needs development:		☐	☐	☐	☐	☐	☐	☐	☐
Cannot be considered at present conditions:		☐	☐	☐	☐	☐	☐	☐	☐

Notes: a. When design needs development indicate what: _____

b. Indicate in the above table the range of flow rates considered practicable and the number of units in series.

c. Indicate limiting factors: _____

2. CAPABILITY TO CONDUCT PARTICULAR DEVELOPMENT:

100%

3. ACTUAL DEVELOPMENT WORK:

Bearings & Seals

4. EXTRAORDINARY FABRICATION FACILITIES:

1500 HP ~ 25000 RPM Compressor Drive-Stand.

5. EXTRAORDINARY TESTING FACILITIES:

6. NOTES:

List bulletins or other descriptive material accompanying this sheet.

Manufacturer & Address Solar Aircraft Co. 2200 Pacific Hwy. San Diego 12, Calif.	Gas Turbine DATA SHEET B Franklin Institute File No. 22

Report by: Title: Date:

Indicate capability to design and manufacture gas turbines suitable for the primary loop of high temperature gas-cooled nuclear power plants for the data below

1. TYPE. ☐ axial, ☒ radial, ☐ other: _____

Performance parameters		He				N_2			
Inlet pressure,	psia	925	925	925	925	925	925	925	925
Inlet temperature,	°F	1300	1500	1700	2000	1300	1500	1700	2000
Total expansion ratio		2.37	2.54	2.71	2.97	3.22	3.52	3.84	4.32
Range of flow rates	lb/sec					35	33	31	29
		Multi Staging of Radial Turbines is not recommended							
Number of units in series (Stages)						1	1	1	1
Lifetime									?
Can be designed based on present experience of manufacturer:		☐	☐	☐	☐	☒	☒	☒	☐
Can be designed but needs development:		☐	☐	☐	☐	☐	☐	☐	☐
Cannot be considered at present conditions:		☐	☐	☐	☐	☐	☐	☐	☒

Notes: a. When design needs development indicate what: _____

b. Indicate in the above table the range of flow rates considered practicable, the number of units in series, and the expected lifetime.

c. Indicate limiting factors: _____

2. CAPABILITY TO CONDUCT PARTICULAR DEVELOPMENT:

100%

3. ACTUAL DEVELOPMENT WORK:

Bearings & Seals.

4. EXTRAORDINARY FABRICATION FACILITIES:

5. EXTRAORDINARY TESTING FACILITIES:

6. NOTES:

List bulletins or other descriptive material accompanying this sheet.

Manufacturer & Address	Gas Turbine
Solar Aircraft Co. 2200 Pacific Hwy. San Diego 12, Calif.	DATA SHEET B
	Franklin Institute File No. 23

Report by: Title: Date:

Indicate capability to design and manufacture gas turbines suitable for the primary loop of high temperature gas-cooled nuclear power plants for the data below

1. TYPE. ☒ axial, ☐ radial, ☐ other: _____

Performance parameters		He				N_2			
Inlet pressure,	psia	925	925	925	925	925	925	925	925
Inlet temperature,	F	1300	1500	1700	2000	1300	1500	1700	2000
Total expansion ratio		2.37	2.54	2.71	2.97	3.22	3.52	3.84	4.32
Range of flow rates	lb/sec	> 58	> 53	> 50	> 46	>208	> 190	> 170	> 165
Number of units in series (stages)		6	7	7	8	3	3	3	3
Lifetime					?				?
Can be designed based on present experience of manufacturer:		☒	☒	☒	☐	☒	☒	☒	☐
Can be designed but needs development:		☐	☐	☐	☐	☐	☐	☐	☐
Cannot be considered at present conditions:		☐	☐	☐	☒	☐	☐	☐	☒

Notes: a. When design needs development indicate what: _____

b. Indicate in the above table the range of flow rates considered practicable, the number of units in series, and the expected lifetime.

c. Indicate limiting factors: _____

2. CAPABILITY TO CONDUCT PARTICULAR DEVELOPMENT:

100%

3. ACTUAL DEVELOPMENT WORK:

Bearings & Seals.

4. EXTRAORDINARY FABRICATION FACILITIES:

5. EXTRAORDINARY TESTING FACILITIES:

6. NOTES:

List bulletins or other descriptive material accompanying this sheet.

Manufacturer & Address	Compressor
Stratos, Division of Fairchild Engine and Airplane Corp. Long Island, N.Y.	DATA SHEET A Franklin Institute File No. 24
Report by:	Title: Date:

Describe already designed or manufactured compressor suitable for the primary loop of a high temperature gas-cooled nuclear power plant but with the following approximate restrictions:

Compression ratio 1.2 to 6
Flow rate 5 lb/sec and up for He, and 23 lb/sec and up for N_2
Inlet pressure at least 100 psia

1. TYPE. Manufacturer's designation: TCS 560

☒ centrifugal, ☐ axial, ☐ other: _____

2. ACTUAL PERFORMANCE PARAMETERS		Gases				
		He	N_2			
Inlet pressure,	psia		68.6			
Inlet temperature,	°F		100			
Outlet pressure,	psia		188.5			
Outlet temperature,	°F					
Flow rate,	lb/sec		16.6			
Number of stages			2			
Speed,	rpm		18,000			
Shaft horsepower			1350			

3. DRIVE	Common Shaft with Turbine
4. COOLING	Lubricating oil to air
5. LUBRICATION	Forced Feed System with Flow Controlled by Differential Regulators
6. BEARINGS	
7. SEAL AT SHAFT PENETRATION	oil Film with Buffer Gas.
8. SIZE & WEIGHT, lb	

9. SPECIAL FEATURES:

10. NOTES: Compressor is Part of Complete Turbine-Compressor Set for GTTF

List bulletins or other descriptive material accompanying this sheet.

Manufacturer & Address	Gas Turbine
Stratos Division of Fairchild Engine and Airplane Corp. Long Island, N.Y.	DATA SHEET A Franklin Institute File No. 25

Report by: Title: Date:

Describe already designed or manufactured gas turbine suitable for the primary loop of a high temperature gas-cooled nuclear power plant but with the following approximate restrictions:

Expansion ratio 1.2 to 6
Flow rate 5 lb/sec and up for He, and 23 lb/sec and up for N_2
Inlet temperature above 1100°F
Outlet pressure at least 100 psia

1. TYPE. Manufacturer's designation: TCS 560

☐ axial, ☐ radial, ☐ other:

2. ACTUAL PERFORMANCE PARAMETERS		Gases				
		He	N_2			
Inlet pressure,	psia		183			
Inlet temperature,	°F		1150			
Outlet pressure,	psia		71.5			
Outlet temperature,	°F		848			
Flow rate,	lb/sec		16.6			
Number of stages			2			
Speed,	rpm		18,000			
Shaft horsepower			1906			

3. STARTING	El. Motor
4. COOLING	Lubricating oil to air
5. LUBRICATION	Forced Feed System with Flow Controlled by Differential Regulators
6. BEARINGS	
7. SEAL AT SHAFT PENETRATION	Oil Film with Buffer Gas.
8. SIZE & Weight, lb	

9. SPECIAL FEATURES:

10. NOTES: Turbine is Part of Complete Turbine-Compressor Set for GTTF

List bulletins or other descriptive material accompanying this sheet.

Manufacturer & Address	Compressor
Stratos Division of Fairchild Engine and Airplane Corp. Long Island, N.Y.	DATA SHEET A
	Franklin Institute File No. 26

Report by: **Title:** **Date:**

Describe already designed or manufactured compressor suitable for the primary loop of a high temperature gas-cooled nuclear power plant but with the following approximate restrictions:

Compression ratio 1.2 to 6
Flow rate 5 lb/sec and up for He, and 23 lb/sec and up for N_2
Inlet pressure at least 100 psia

1. TYPE. Manufacturer's designation: TCS 670

☒ centrifugal, ☐ axial, ☐ other: _____

2. ACTUAL PERFORMANCE PARAMETERS		Gases				
		He	N_2			
Inlet pressure,	psia		118.2			
Inlet temperature,	°F		133.7			
Outlet pressure,	psia		322.8			
Outlet temperature,	°F		368.4			
Flow rate,	lb/sec		26.0			
Number of stages			2			
Speed,	rpm		18,000			
Shaft horsepower						

3. DRIVE	Common Shaft with Turbine
4. COOLING	Lubricating Oil to Air
5. LUBRICATION	Forced Feed System with Flow Controlled by Differential Regulators
6. BEARINGS	
7. SEAL AT SHAFT PENETRATION	Oil Film with Buffer Gas.
8. SIZE & WEIGHT, lb	

9. SPECIAL FEATURES:

10. NOTES: Compressor is Part of Complete Turbine-Compressor Set for ML-1

List bulletins or other descriptive material accompanying this sheet.

Manufacturer & Address	Gas Turbine
Stratos Division of Fairchild Engine and Airplane Corp. Long Island, N.Y.	DATA SHEET A
	Franklin Institute File No. 27

Report by: **Title:** **Date:**

Describe already designed or manufactured gas turbine suitable for the primary loop of a high temperature gas-cooled nuclear power plant but with the following approximate restrictions:

Expansion ratio 1.2 to 6
Flow rate 5 lb/sec and up for He, and 23 lb/sec and up for N_2
Inlet temperature above 1100°F
Outlet pressure at least 100 psia

1. TYPE. Manufacturer's designation: TCS 670

☒ axial, ☐ radial, ☐ other: _____

2. ACTUAL PERFORMANCE PARAMETERS		Gases				
		He	N_2			
Inlet pressure,	psia		291.8			
Inlet temperature,	°F		1193.5			
Outlet pressure,	psia		122			
Outlet temperature,	°F		907.8			
Flow rate,	lb/sec		25.3			
Number of stages			2			
Speed,	rpm		18,000			
Shaft horsepower						

3. STARTING	El.
4. COOLING	Lubricating Oil to Air
5. LUBRICATION	Forced Feed System with Flow Controlled by Differential Regulators
6. BEARINGS	
7. SEAL AT SHAFT PENETRATION	Oil Film with Buffer Gas
8. SIZE & Weight, lb	

9. SPECIAL FEATURES:

10. NOTES: Turbine is Part of Complete Turbine-Compressor Set for ML-1

List bulletins or other descriptive material accompanying this sheet.

Manufacturer & Address	Compressor
Westinghouse Electric Corporation Lester, Pennsylvania	DATA SHEET A
	Franklin Institute File No. 28

Report by: P. A. Berman **Title:** Des. Engr. **Date:** 12/19/60

Describe already designed or manufactured compressor suitable for the primary loop of a high temperature gas-cooled nuclear power plant but with the following approximate restrictions:

Compression ratio 1.2 to 6
Flow rate 5 lb/sec and up for He, and 23 lb/sec and up for N_2
Inlet pressure at least 100 psia

1. TYPE. Manufacturer's designation: WN-202-IE

☐ centrifugal, ☒ axial, ☐ other: _____

2. ACTUAL PERFORMANCE PARAMETERS		Gases				
		He	N_2	He		
Inlet pressure,	psia	445		680		
Inlet temperature,	°F	85		85		
Outlet pressure,	psia	690		1,155		
Outlet temperature,	°F	206		236		
Flow rate,	lb/sec	112		112		
Number of stages		15		25		
Speed,	rpm	12,000		12,000		
Shaft horsepower						

3. DRIVE	
4. COOLING	
5. LUBRICATION	Oil
6. BEARINGS	Pad Type
7. SEAL AT SHAFT PENETRATION	Oil Barrier
8. SIZE & WEIGHT, lb	

9. SPECIAL FEATURES:

10. NOTES:
Preliminary Design Completed

List bulletins or other descriptive material accompanying this sheet.

Manufacturer & Address	Gas Turbine
Westinghouse Electric Corporation Lester, Pennsylvania	DATA SHEET A
	Franklin Institute File No. 29

Report by: P. A. Berman **Title:** Des. Engr. **Date:** 12/19/60

Describe already designed or manufactured gas turbine suitable for the primary loop of a high temperature gas-cooled nuclear power plant but with the following approximate restrictions:

Expansion ratio 1.2 to 6
Flow rate 5 lb/sec and up for He, and 23 lb/sec and up for N_2
Inlet temperature above 1100°F
Outlet pressure at least 100 psia

1. TYPE. Manufacturer's designation: WN-202-IE

☒ axial, ☐ radial, ☐ other: _____

2. ACTUAL PERFORMANCE PARAMETERS		Gases				
		He	N_2	He		
Inlet pressure,	psia	1,080		814		
Inlet temperature,	°F	1300		1110		
Outlet pressure,	psia	820		460		
Outlet temperature,	°F	1120		825		
Flow rate,	lb/sec	112		112		
Number of stages		9		7		
Speed,	rpm	8140		12,000		
Shaft horsepower		32,000		56,000		

3. STARTING	
4. COOLING	
5. LUBRICATION	Oil
6. BEARINGS	Pad Type
7. SEAL AT SHAFT PENETRATION	Oil Barrier
8. SIZE & Weight, lb	

9. SPECIAL FEATURES:

10. NOTES:
Preliminary Design Completed

List bulletins or other descriptive material accompanying this sheet.

Manufacturer & Address	Compressor
Westinghouse Electric Corporation Lester, Pennsylvania	DATA SHEET B
	Franklin Institute File No. 30

Report by: P. A. Berman Title: Des. Engr. Date: 12/19/60

Indicate capability to design and manufacture compressors suitable for the primary loop of high temperature gas-cooled nuclear power plants for the data below

1. TYPE. ☐ centrifugal, ☒ axial, ☐ other: _____

Performance parameters		He				N_2			
Inlet pressure,	psia	373	348	326	297	274	251	230	204
Inlet temperature,	°F	100	100	100	100	100	100	100	100
Total compression ratio		2.68	2.87	3.07	3.37	3.65	3.99	4.35	4.90
Range of flow rates,	lb/sec	100	to	800		400	to	3200	
Number of units in series									
Can be designed based on present experience of manufacturer:		☒	☒	☒	☒	☒	☒	☒	☒
Can be designed but needs development:		☐	☐	☐	☐	☐	☐	☐	☐
Cannot be considered at present conditions:		☐	☐	☐	☐	☐	☐	☐	☐

Notes: a. When design needs development indicate what: Verification Tests of design needed

b. Indicate in the above table the range of flow rates considered practicable and the number of units in series.

c. Indicate limiting factors: Low limit on axial machines is disc diameter and critical speeds

2. CAPABILITY TO CONDUCT PARTICULAR DEVELOPMENT:

Facilities available to conduct compressor development

3. ACTUAL DEVELOPMENT WORK:

Development work in process on MGCR compressors

4. EXTRAORDINARY FABRICATION FACILITIES:

5. EXTRAORDINARY TESTING FACILITIES:

6. NOTES:

List bulletins or other descriptive material accompanying this sheet.

Manufacturer & Address	Gas Turbine
Westinghouse Electric Corporation Lester, Pennsylvania	DATA SHEET B
	Franklin Institute File No. 31

Report by: P. A. Berman **Title:** Design Engineer **Date:** 12/19/60

Indicate capability to design and manufacture gas turbines suitable for the primary loop of high temperature gas-cooled nuclear power plants for the data below

1. TYPE. ☒ axial, ☐ radial, ☐ other: _____

Performance parameters		He				N_2			
Inlet pressure,	psia	925	925	925	925	925	925	925	925
Inlet temperature,	°F	1300	1500	1700	2000	1300	1500	1700	2000
Total expansion ratio		2.37	2.54	2.71	2.97	3.22	3.52	3.84	4.32
Range of flow rates	lb/sec	100	to	800		400	to	3200	
Number of units in series									
Lifetime		100,000 hr design, 30,000 hr blade life @1500°F							
Can be designed based on present experience of manufacturer:		☒	☒	☐	☐	☒	☒	☐	☐
Can be designed but needs development:		☐	☐	☒	☐	☐	☐	☒	☐
Cannot be considered at present conditions:		☐	☐	☐	☒	☐	☐	☐	☒

Notes: a. When design needs development indicate what: Materials and Component Cooling

b. Indicate in the above table the range of flow rates considered practicable, the number of units in series, and the expected lifetime.

c. Indicate limiting factors: Materials at high temperatures

2. CAPABILITY TO CONDUCT PARTICULAR DEVELOPMENT:

All facilities available to Conduct Development

3. ACTUAL DEVELOPMENT WORK:

Development work in process on MGCR turbine

4. EXTRAORDINARY FABRICATION FACILITIES:

5. EXTRAORDINARY TESTING FACILITIES:

6. NOTES:

List bulletins or other descriptive material accompanying this sheet.

Manufacturer & Address	Compressor
ESCHER WYSS Ltd. Zürich	DATA SHEET A Franklin Institute File No. 32

Report by:	Title:	Date:

Describe already designed or manufactured compressor suitable for the primary loop of a high temperature gas-cooled nuclear power plant

1. TYPE. Manufacturer's designation: _____

☒ centrifugal, ☒ axial, ☐ other: _____

2. ACTUAL PERFORMANCE PARAMETERS		Gases				
		He	N_2	Air		
Inlet pressure,	psia	388				
Inlet temperature,	°F	100				
Outlet pressure,	psia	853		Closed cycle		
Outlet temperature,	°F	224		compressor for air		
Flow rate,	lb/sec	77		2 MW (radial)		
				up to 20 MW		
Number of stages		6+8		axial		
Speed,	rpm	17'000				
Shaft horsepower	MW	23				
Intercooler		1				

3. DRIVE	HP Turbine
4. COOLING	intercooled
5. LUBRICATION	gas
6. BEARINGS	hydrostatic gas bearings for He
7. SEAL AT SHAFT PENETRATION	no
8. SIZE & WEIGHT, lb	

9. SPECIAL FEATURES: special blading for high pressure ratio per stage

10. NOTES:

List bulletins or other descriptive material accompanying this sheet.

Manufacturer & Address	Gas Turbine
ESCHER WYSS Ltd. Zürich	DATA SHEET A
	Franklin Institute File No. 33

Report by:	Title:	Date:

Describe already designed or manufactured gas turbine suitable for the primary loop of a high temperature gas-cooled nuclear power plant

1. TYPE. Manufacturer's designation: _____

☒ axial, ☐ radial, ☐ other: _____

2. ACTUAL PERFORMANCE PARAMETERS		Gases				
		He	N_2	3)		
Inlet pressure,	psia	805				
Inlet temperature,	°F	1300				
Outlet pressure,	psia	400		all type of c.c.		
Outlet temperature,	°F	909		air turbines		
Flow rate,	lb/sec	77		up to 20 MW el.		
Number of stages		4+4				
Speed,	rpm	17000 ~~9500~~				
Shaft horsepower	MW	23/16				

3. STARTING	Electromot. or open cycle G.T.
4. COOLING	partial blade root gas cooling
5. LUBRICATION	gas
6. BEARINGS	hydrostatic gas b.
7. SEAL AT SHAFT PENETRATION	gland and sealing gas for power turbine
8. SIZE & Weight, lb	depends design, 1,2 casings
9. SPECIAL FEATURES:	HP turbine on integral shaft with HP compressor (TUCO)

10. NOTES:

List bulletins or other descriptive material accompanying this sheet.

Manufacturer & Address	Compressor
ESCHER WYSS Ltd. Zürich	DATA SHEET B
	Franklin Institute File No. 34

Report by: Title: Date:

Indicate capability to design and manufacture compressors suitable for the primary loop of high temperature gas cooled nuclear power plants for the data below

1. TYPE. ☐ centrifugal, ☒ axial, ☐ other: _____

Performance parameters		He				N_2			
Inlet pressure,	psia	373	348	326	297	274	251	230	204
Inlet temperature,	°F	100	100	100	100	100	100	100	100
Total compression ratio		2.68	2.87	3.07	3.37	3.65	3.99	4.35	4.90
Range of flow rates,	lb/sec	200	100			200	200		
Number of units in series		2	2			2	2	2	2
Can be designed based on present experience of manufacturer:		☒	☐	☐	☐	☒	☒	☐	☐
Can be designed but needs development:		☐	☒	☐	☐	☐	☐	☒	☒
Cannot be considered at present conditions:		☐	☐	☒	☒	☐	☐	☐	☐

Notes: a. When design needs development indicate what: shaft arrangement, critical speed, matching with turbine

b. Indicate in the above table the range of flow rates considered practicable and the number of units in series.

c. Indicate limiting factors: No. of stages on one shaft and critical speed

2. CAPABILITY TO CONDUCT PARTICULAR DEVELOPMENT:)

3. ACTUAL DEVELOPMENT WORK:) see recuperator sheet

4. EXTRAORDINARY FABRICATION FACILITIES:
available

5. EXTRAORDINARY TESTING FACILITIES:
single and two stage axial facility

6. NOTES: ESCHER WYSS calculations are not in agreement with optimum pressure ratios indicated.

List bulletins or other descriptive material accompanying this sheet.

Manufacturer & Address	Gas Turbine
ESCHER WYSS Ltd. Zürich	DATA SHEET B
	Franklin Institute File No. 35

Report by: Title: Date:

Indicate capability to design and manufacture gas turbines suitable for the primary loop of high temperature gas-cooled nuclear power plants for the data below

1. TYPE. ☒ axial, ☐ radial, ☐ other: _____

Performance parameters		He				N_2			
Inlet pressure,	psia	925	925	925	925	925	925	925	925
Inlet temperature,	°F	1300	1500	1700	2000	1300	1500	1700	2000
Total expansion ratio		2.37	2.54	2.71	2.97	3.22	3.52	3.84	4.32
Range of flow rates	lb/sec	200	100			200	200		
Number of units in series		1 or 2				1 or 2			
Lifetime	h	100000	100000	50000		100000	50000		
Can be designed based on present experience of manufacturer:		☒	☒	☐	☐	☒	☒	☐	☐
Can be designed but needs development:		☐	☐	☒	☐	☐	☐	☒	☒
Cannot be considered at present conditions:		☐	☐	☐	☒	☐	☐	☐	☒

Notes: a. When design needs development indicate what: shaft, rotor or drum cooling - plant arrangement

b. Indicate in the above table the range of flow rates considered practicable, the number of units in series, and the expected lifetime.

c. Indicate limiting factors: rotor design and cooling forgings for rotor, double wall pipes insulation, gas impurities for Mo alloys

2. CAPABILITY TO CONDUCT PARTICULAR DEVELOPMENT:) see recuperator sheet

3. ACTUAL DEVELOPMENT WORK:

4. EXTRAORDINARY FABRICATION FACILITIES:

steam- and gas-turbine manufacturing

5. EXTRAORDINARY TESTING FACILITIES:

turbine blade test fac.

6. NOTES: pressure ratios and pressure losses are not in agreement with ESCHER WYSS optimization

List bulletins or other descriptive material accompanying this sheet.

14. TEST FACILITIES

Each gas turbine manufacturer has his own test facilities, and usually, the larger the manufacturing plant, the larger and more elaborate the test facilities. Apart from such facilities located at manufacturing plants, there are special research centers in which gas turbine tests are performed, sponsored by the Government or by interested member firms. One such typical research center is, for example, the Parsons and Marine Engineering, Turbine and Development Association's (Pametrada) Research Station, Wallsend, Northumberland, England. This research station has run an experimental gas turbine at temperatures up to 2200°F, applying cooling to the blades. The station is also engaged in development work. However, this is not directly connected with nuclear applications.

Nuclear application of gas-turbines is a new idea which was started in this country. The first gas-turbine nuclear power plant in the world is the ML-1. The firms supplying the turbine-compressor sets for this power plant (Clark Bros. Co. and Stratos Division Fairchild-Stratos Corp.) can test the sets at their test installations only in an open-cycle arrangement and have so far made such tests only at partial load conditions. Figures 14-1 and 14-2 show the test arrangement at the Clark Bros. plant. An auxiliary turbo-compressor set is provided for starting the turbine of the CSN-1 set under test.

The Stratos arrangement for testing the TCS 670 is shown in Figure 14-3. Another Gas Turbine Test Facility is at Ft. Belvoir, Va. This facility has been in operation since 1959 and was, in the beginning, used as an open-cycle gas-turbine supporting facility, however, without noteworthy success. Later, it was developed into a facility for testing power conversion equipment for the Army Gas Cooled Reactor Systems Program (AGCRSP). The flow diagram of the new facility is shown in Figure 14-4 with the installed turbine-compressor set TCS 560 of Stratos. This available unit has been used for

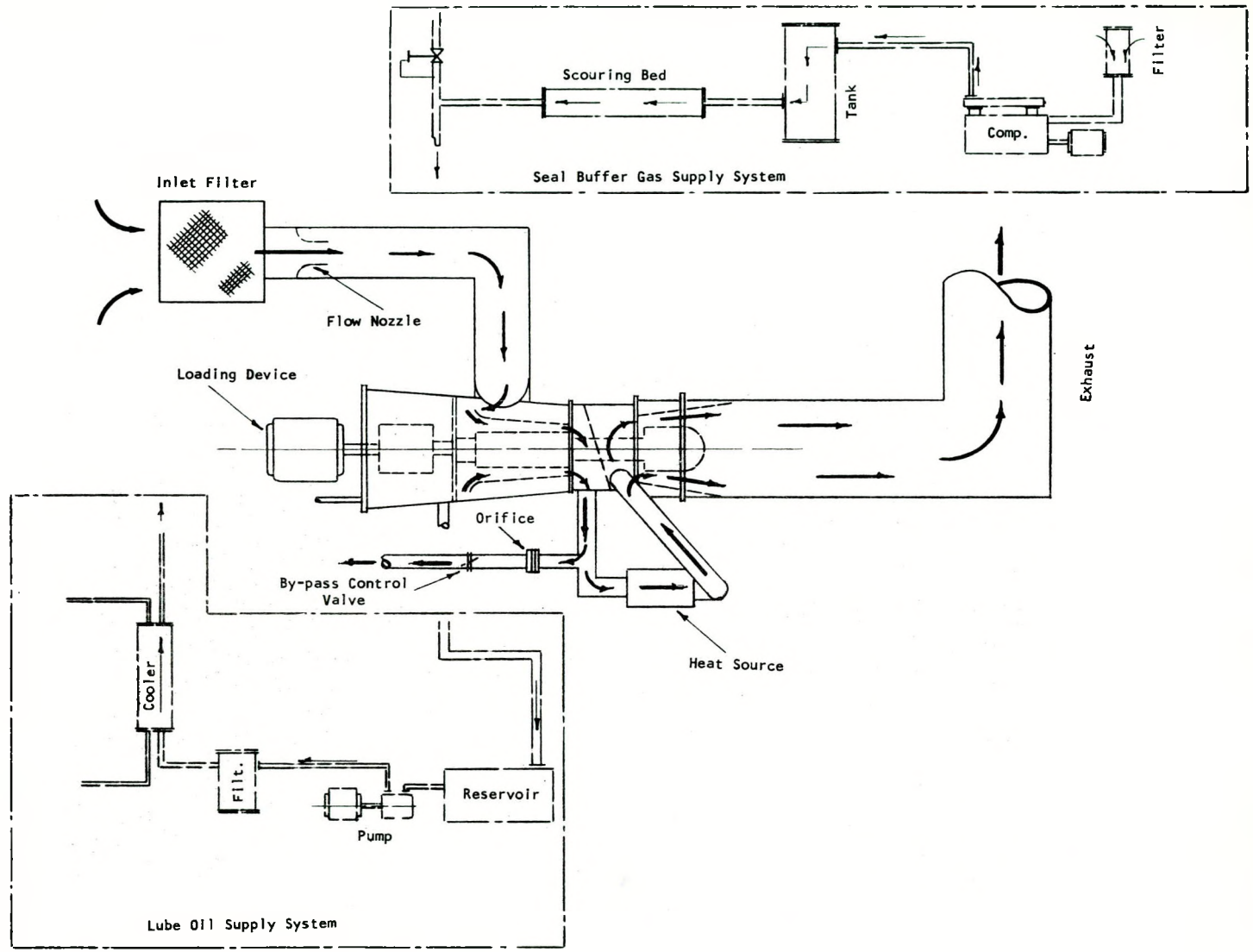


Fig. 14-1 - Open Cycle Test Facility at Clark Bros. Co.

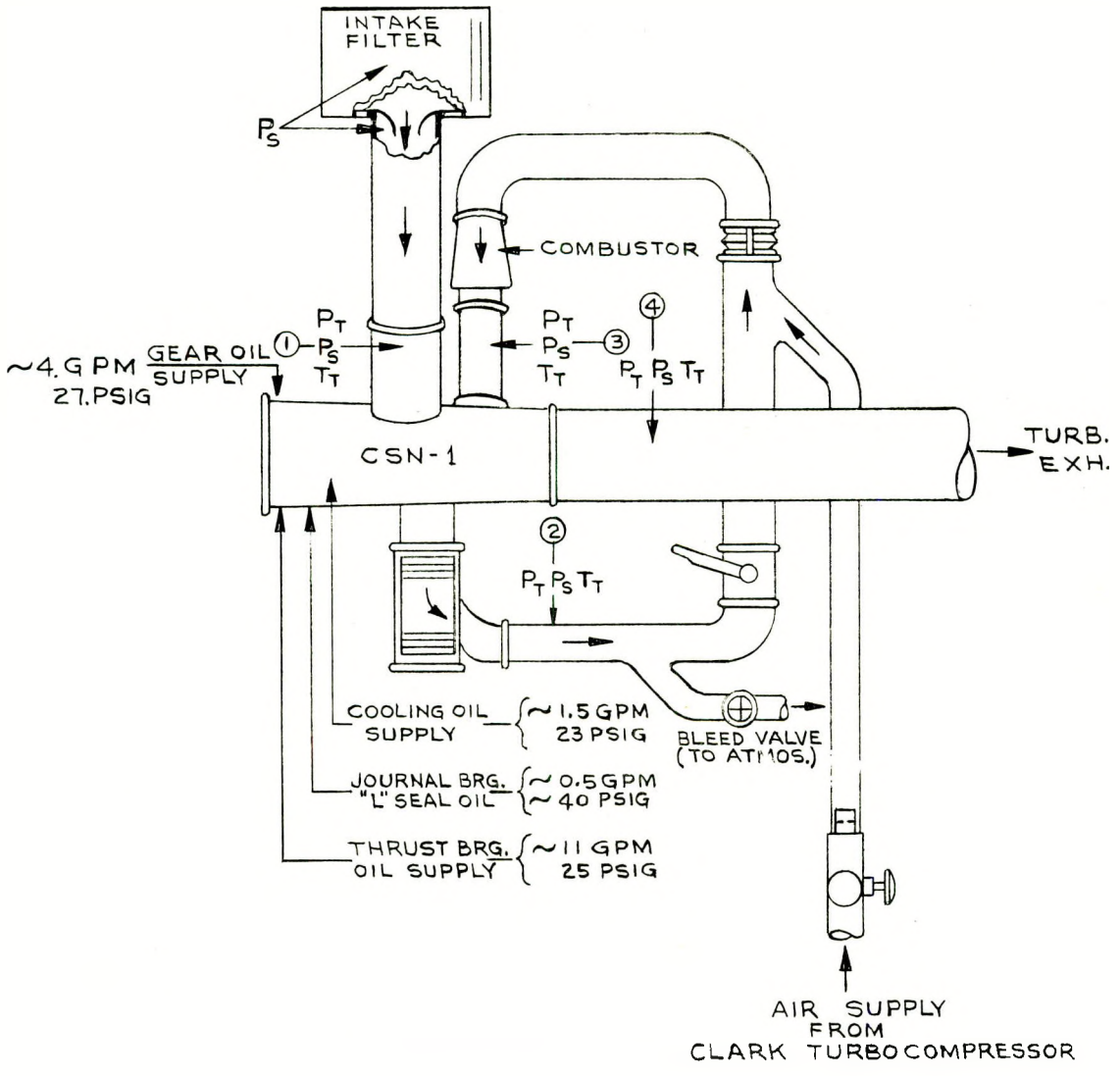


Fig. 14-2 - Clark Bros. Co. CSN-1 Turbine Compressor Test Installation

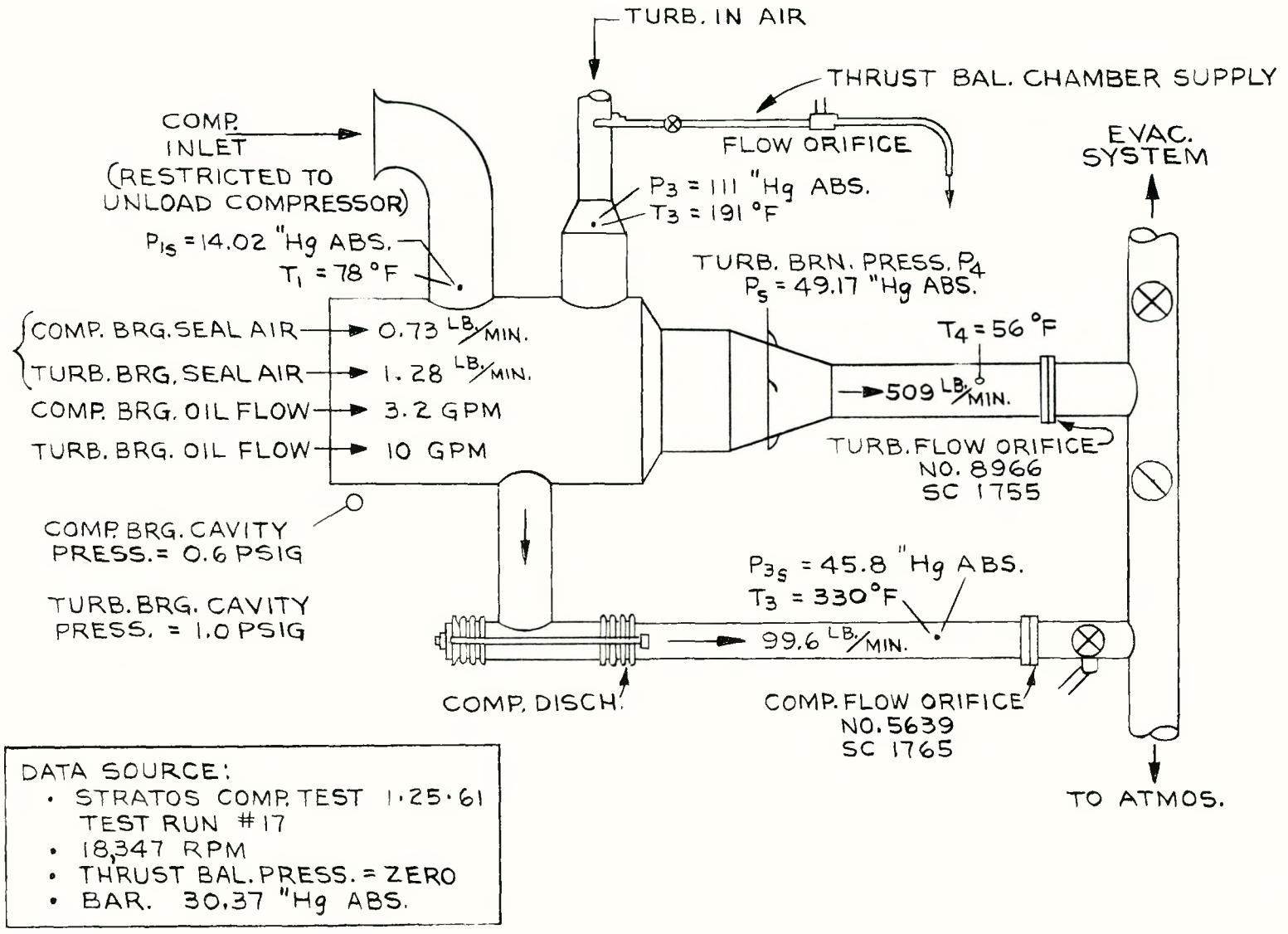


Fig. 14-3 - Stratos Test Arrangement for TCS-670

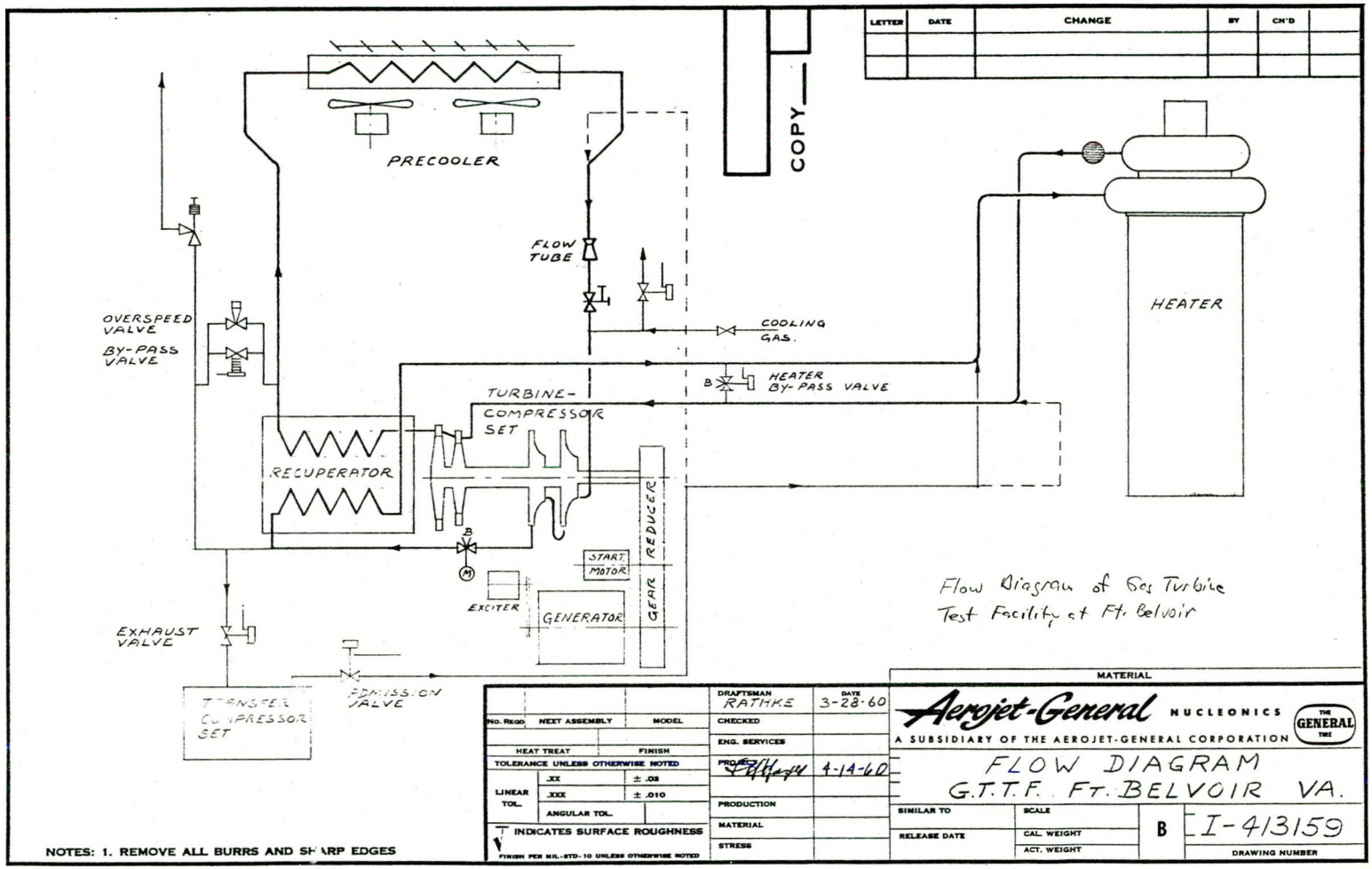


Fig. 14-4 - Flow Diagram of Gas Turbine Test Facility at Ft. Belvoir

development of cycle components similar to such for CSN-1 and TCS 670. However, each turbo-compressor to be tested will generally require different components at the testing facility, corresponding to the thermal power of the set and layout of the various circuits, such as the lubricating oil or seal system.

Primarily, at the test facility the feasibility of turbo-compressor sets similar to such as needed for the ML-1 will have to be established. Efficiency will be established by measurements leading to heat balance values. After this task, the behavior at transient conditions will be investigated, and reliability tests made in a series of runs presumably totalling about 500 hours. During the preliminary tests with the TCS 560 installed, the necessity arose to replace the original cast aluminium casing of the set with a new casing of stainless steel because of severe distortion of the former by differential thermal expansion which was not sufficiently taken care of in the design concept of TCS 560. All test runs of the TCS 560 at the Test Facility to date were made only under partial load conditions at a maximum inlet temperature to the turbine of 1200°F and at approximately 200 psi maximum cycle pressure. During future tests, the load will be applied by rheostats in the electrical circuit of a driven generator. Recording gages are being installed for all important test readings.

The reactor is simulated by a primary heat exchanger, heated in its primary loop by two kerosene burners: one small for heating up to approximately 300°F at a maximum rate of 15°F per minute, to keep low thermal stresses, and one large to be able to reach the 1200°F in the power loop at steady operation and rated output. The large burner alone would not operate stably in the heat-up range. The heating equipment is of commercial type for a heat duty of 9.5×10^6 Btu/hr. It was furnished by Thermal Research and Engineers of Conshohocken, Pa. The

primary heat exchanger is of U-shap bent-tube and shell type. Difficulties were observed because the primary passages of the heat exchanger fouled by oil burning residuals. It is intended to add cleaning ingredients to the fuel. The recuperator is of the pin-fin type and was furnished by Ferrotherm, Cleveland. It has a temperature effectiveness of about 80%. The working fluid is 99.5% pure nitrogen.

According to the experience of test peronnnel, sealing and bearing problems and problems related to stable operation at transient conditions are the most difficult ones. It was experienced at the Test Facility that keeping of the lubrication oil from entering into the loop is mainly an operational problem, which can be controlled by maintaining proper pressure of sealing gas. This control is intended to be made automatic in the future. The gear reducer is a Western Gear Co. make, and practically no difficulties were observed with it. The electric starting motor is connected to the gear by a "Formsprag" coupling which cuts the motor out at 14,000 rpm when the TCS 560 becomes self-sustained. The connection of the gear-box output shaft to the load generator is provided by a "Falk" type coupling. Between the gear box and the turbo-compressor set, a sier-Bath coupling is used. Control valves are furnished by the Annin Co., and for the piping, instead of bolted flanges, Marman clamps are used satisfactorily.

Useful test data will be provided by Aerojet-General Nucleonics (designer of ML-1) operating the Test Facility with the TCS 560 which will shorten the development time for the final equipment of ML-1[12,153].

The second nuclear gas-turbine plant being developed is the Maritime Gas Cooled Reactor project, the turbomachinery for which is being developed by the Westinghouse Electric Corporation. So far, the tests being performed at Westinghouse for the MGCR turbo-machinery are of a preliminary nature. Compressor and turbine stage tests are underway in the variable-density tunnel at Westinghouse. A four-stage compressor

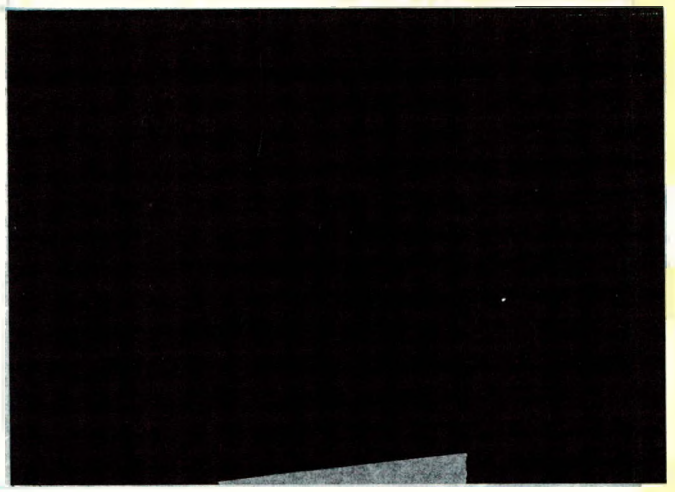


Fig. 14-5 - Large GE, Regenerative-Cycle, One-Shaft Gas Turbine on Factory Test

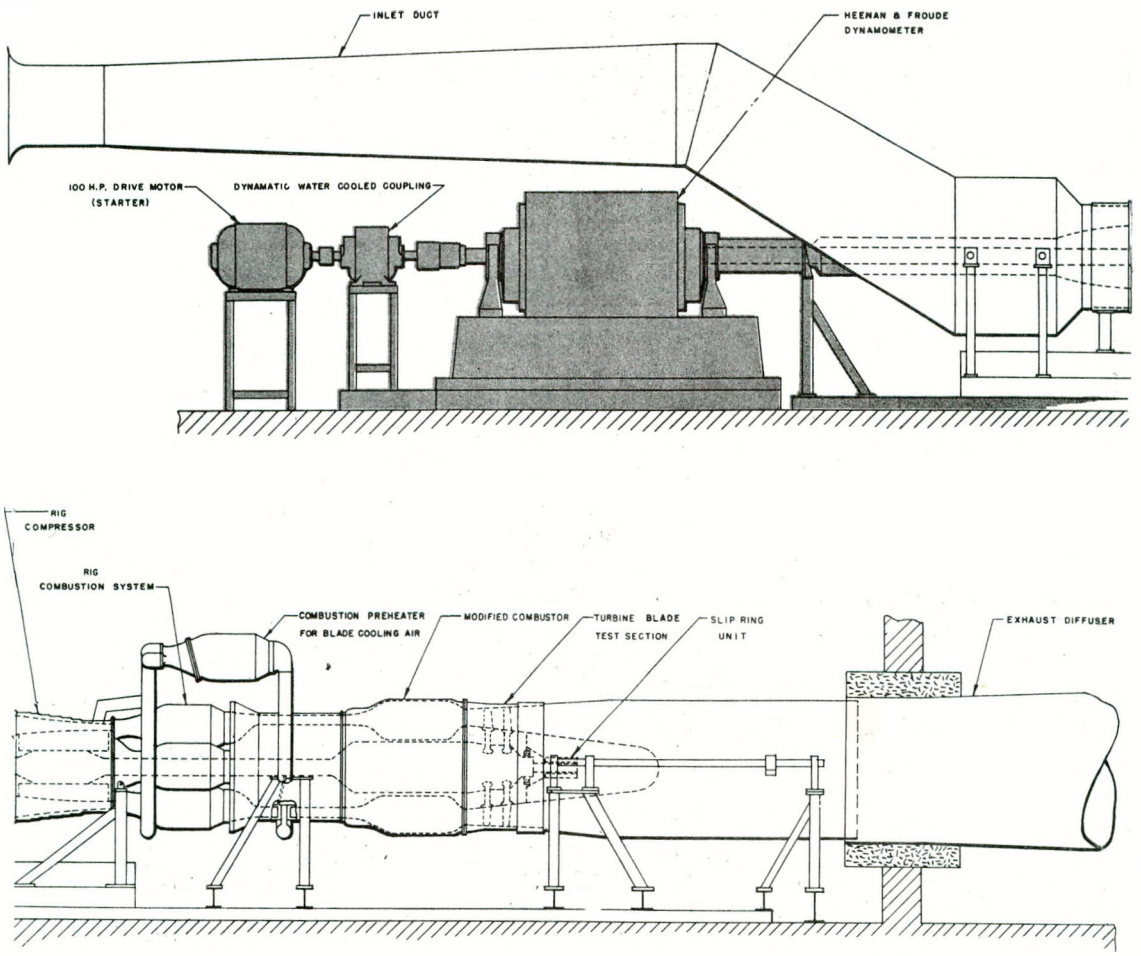


Fig. 14-6 - Orenda Rotating Blade-Cooling Rig

model has provided data which gives the pressure coefficient and efficiency as a function of flow coefficient.[71] Compressor model tests were conducted to study effects of stage loading in the compressor. Similarly, single-stage turbine tests are in progress. Only after the EBOR(Experimental Beryllium Oxide Reactor) is completed will the MGCRT(Maritime Gas-Cooled Reactor Test) start in which the turbomachinery will be utilized. MGCRT will serve as a test for the final sea-going unit.[11] No specific description of the test arrangement is available at the present time.

There is a difference between component tests needed for development and acceptance tests of a production unit to be delivered to the customer. The latter do not require cycle components pertaining to the facility but certainly need space, foundations, extra instrumentation, and in many cases power absorbers and some cooling water supply if inter-cooled compressor stages are provided. Figure 14-5[29] shows a large General Electric gas turbine on factory test.

As an example of a special test facility, the Orenda rotating-blade cooling rig is shown in Figure 14-6. This is essentially a turbine test rig but is specifically designed to develop various types of cooled turbine blades both as to mechanical reliability and performance. Evaluated on this rig are the more promising blade designs as determined by testing on the static blade cooling rig. Preheated air is supplied by an upstream slave unit consisting of a rig compressor which pumps air through a rig combustion system and modified combustor in series. The air so delivered to the turbine simulates a high altitude flight condition. After expanding through the turbine the gases are cooled with a water spray and passed through an outlet silencer.

The rig is driven by the test turbine, but to allow for mismatching of this turbine with the rig compressor, excess power is absorbed by a Heenan and Froude eddy current dynamometer which is capable of absorbing 6000 hp at speeds between 5000 and 9000 rpm. The rig is

protected by special speed trips. Blade cooling and root cooling air may be drawn from the ducting downstream of the rig compressor or alternatively from the main air manifold and raised to the required delivery temperature in the combustion preheater. It is reintroduced to the rig through radial tubes in the duct upstream of the modified combustor, and fed through an axial passage to the blade cooling and root cooling system.

The turbine test unit is heavily instrumented for the recording of blade temperature and vibration stresses by thermocouples and strain gages which produce signals that are transmitted through a water-cooled slip-ring unit in the tailcone to the recording instruments.

The turbine test unit is designed to duplicate closely the design of the rotating components so that gas loads, speeds, and vibratory forces are the same as those on an engine under altitude conditions. Provision is made for visual examination of the test blades and for removal and replacement of the first row of blades.

Georgs Novickis

Georgs Novickis
Senior Research Engineer

Reviewed by:

K R Stearns

K. R. Stearns, Manager
Applied Mechanics Laboratory

N R Droulard

N. R. Droulard
Technical Director

Approved by:

F. L. Jackson

Francis L. Jackson
Director of Laboratories

REFERENCES

1. "Evaluation of Coolants and Moderators for the Maritime Gas-Cooled Reactor," General Dynamics Corp., Report GA-570, December 10, 1958.

2. Novickis, G., Zudans, Z., "Survey of Component Requirements and Availability for Gas-Cooled Nuclear Reactor Power Plants: Direct Closed Cycles," The Franklin Institute, Report I-A2392-2, NYO Report No. 9787, November 1961.

3. "Information Meeting on Gas-Cooled Power Reactors," ORNL October 21-22, 1958, AEC Report TID-7564, December 1958.

4. "Practical Examples of Utilizing the Waste Heat of Gas Turbines in Combined Installations," Brown Boveri Review, Vol. 47, December 1960, pp. 800-825.

5. Malanoski, S. B., Fuller, D. D., "Survey of Component Requirements and Availability for Gas-Cooled Nuclear Reactor Power Plants: Bearings and Seals," The Franklin Institute, Report I-A2392-8, NYO Report 9792, June 1961.

6. Yen, T. C., "Survey of Component Requirements and Availability for Gas-Cooled Nuclear Reactor Power Plants: Structural Materials," The Franklin Institute, Report I-A2392-13, NYO Report No. 9793, June 1961.

7. Novickis, G., "Survey of Component Requirements and Availability for Gas-Cooled Nuclear Reactor Power Plants: Vessels and Supports, Valves, Expansion Joints, and Pipes," The Franklin Institute, Report I-A2392-4, NYO Report 9788.

8. Armstrong, R. H., "Gas-Cooled Reactors in the USA, A Survey and Recommendations," Argonne National Laboratory, Report ANL-6255, November 1960.

9. Gas Turbine, Vol. 1, November - December, 1960, "Russians Explore Gas Turbine Field," pp. 14, 15, 31.

10. "Gas-Turbine Progress Meeting, Proceedings," Department of Defense, Office of Fuels, Materials and Ordnance, Office of Director of Defense Research and Engineering, Washington 25, D. C., April 6-7, 1959.

11. "Maritime Gas-Cooled Reactor Program," General Dynamics Corp. Quarterly Progress Report for period ending June 30, 1961, Report GA-2372, Contract AT(04-3)-187.

12. "Army Gas-Cooled Reactor Systems Program," Aerojet-General Nucleonics Semiannual Progress Report, January through June 1960, Report No. IDO-28558, Contract AT(10-1)-880, July 31, 1960.

13. "Gas Turbine Specifications - 1961," Gas Turbine, Vol. 2, January-February 1961, pp. 51 to 512.

14. "Brown Boveri Gas Turbines for an Inlet Temperature of 750°C," Brown Boveri Review, January-February 1960, pp. 35-64.

15. "Solid-Fuel Gas Turbine Plants," Keller, C., Gaehler, W., Gas Turbine, Vol. 2, July-August 1961, pp. 24-26.

16. Harris, F. R., "A 7500 hp Gas Turbine for Naval Boost Propulsion," ASME Paper 61-GTP-5, March 5-9, 1961.

17. Knowles, D. W., "Development of a 3500 hp Marine Gas Turbine," ASME Misc. Paper 59-A-199, November 29 - December 4, 1959.

18. "Chrysler's Automotive Turbine," Gas Turbine, Vol. 2, July-August, 1961, p. 23.

19. "GE's Turbine Accessory Lineup," Gas Turbine, Vol. 2, January-February 1961, pp. 28-29.

20. Pearson, H., "Trends in Aircraft Propulsion," Jnl. of the Royal Aeronautical Soc., Vol. 65, June 1961, pp. 373-385.

21. "A Design Study of a Closed Cycle Gas Turbine Compressor Set for ML-1," Clark Bros. Co., Final Report, March 23, 1960.

22. "Stratos Model TCS-670 Turbine-Compressor Set for Closed Cycle Gas Turbine Power Plant," Stratos, A Division of Fairchild Engine and Airplane Corp., Final Design Report SRC-104, March 8, 1960.

23. Skrotzky, B. G. A., "Industrial and Central Station (1958 Gas Turbine Progress Report)," Trans. ASME, Series A, Vol. 81, July 1959, pp. 344-351.

24. Sawyer, J. W., Simpson, H.M., "Marine 1958 Gas Turbine Progress Report," Trans. ASME, Series A, Vol. 81, July 1959, pp. 311-343.

25. Sawyer, R. T., "Introduction, 1958 Gas Turbine Progress Report," Trans. ASME, Series A, Vol. 81, July 1959, pp. 215-219.

26. Toesca, R. A. M., "An Integrated Turbo/Generator Unit," Gas Turbine, Vol. 2, September-October 1961, p.28.

27. James, R. K., "Seapower: Gas Turbines Add Fighting Punch," ASME Paper 61-GTP-10, March 5-9, 1961.

28. Honaker, C. M., Bruce, D. F., "25000 KW Mene Grande Gas Turbine Installation," ASME Paper 59-A-191, November 29 - December 4, 1959.

29. McLean, H.D., "Operating Experience of General Electric Gas Turbines," Contributed by the Gas Turbine Power Division for Presentation at the ASME Gas Turbine Power Conference and Exhibit, Washington, D. C., March 2-6, 1958.

30. Gas Turbine, (Various notes of articles in this issue), March-April 1962.

31. Keller, C., Gaehler, W., "The Coal-Burning Closed-Cycle Gas Turbine," Contributed for presentation at the Gas Turbine Power Conference, Washington, D. C., ASME Paper No. 61-GTP-2, March 5-9, 1961.

32. Baxter, A. D., "Recent British Technical Progress in Aeronautics, Part Two Engine Design," Aircraft Engineering, Vol. 33, September 1961.

33. "BS75 - Ein Zweikresistriebwerk für Kurzstreckenflugzeuge," Motortechnische Zeitschrift, Vol. 22, October 1961.

34. Rees, H., "Running Experience with Gas-Turbine Locomotives of 8500 hp," Gas & Oil Power, Vol. LVI, March, 1961.

35. Sorensen, H. A., Gas Turbines, Ronald Press, New York, 1951.

36. Dyment, J. T., Eden, J. J., "Engine Maintenance," Gas Turbine, Vol. 2, November - December 1961, pp. 30, 31.

37. Novickis, G., "Survey of Component Requirements and Availability for Gas-Cooled Nuclear Reactor Power Plants: Circulators," The Franklin Institute, Report I-A2392-5, NYO Report 9790, August 1961.

38. Moult, E. S., Pearson, H., "The Relative Merits of Centrifugal and Axial Compressors for Aircraft Gas Turbines," Jnl. of the Royal Aeronautical Soc., Vol. 55, March 1951.

39. Lucas, G., Pollock, J. F., Gas Turbine Materials, The MacMillan Company, New York, 1958.

40. Connell, W.,"Gas Turbine Burns Coal Slurry," Gas Turbine, Vol. 2, May - June, pp.28, 29.

41. Rahnke, C. J., Carmody, R. H., "The Combined Transonic Axial and Centrifugal Stage Compressor," SAE Preprint 268D for 1961 SAE International Congress, January 9-13, 1961.

42. Dibelius, G., "Mehrstufige Turboverdichter," Chemie-Ing.-Techn., Vol. 31, 1959.

43. Vincent, E. T., The Theory and Design of Gas Turbines and Jet Engines, McGraw-Hill Book Co., New York, 1950.

44. Jennings, B. H., Rogers, W. L., Gas Turbine Analysis and Practice, McGraw-Hill Book Co., New York, 1953.

45. Silvern, D. H., Balje, O. E., "A Study of High Energy Level, Low Power Output Turbines," Sunstrand Turbo Div. Report AMF/TD 1196, Contract NONR-2292(00), April 9, 1958, (AD-161323).

46. Cochran, R. P., Dengler, R. P., "Experimental Investigation of an Air-Cooled Turbine Operating in a Turbojet Engine at Turbine Inlet Temperatures up to 2500°F," NASA Technical Note D-1046, July 1961.

47. Mallinson, D. H., Lewis, W. G. E., "The Part Load Performance of Various Gas-Turbine Engine Schemes," Proc. Inst. Mech. Engrs., Vol. 159, 1948.

48. Kruschik, J., Die Gasturbine, Springer-Verlag, Vienna, 1952.

49. Seippel, C., Bereuter, R., "The Theory of Combined Steam and Gas Turbine Installations," Brown Boveri Review, Vol. 47, December 1960.

50. "Chrysler Refires the Turbine Turmoil," Machine Design, Vol. 34, January 18, 1962, p. 24, 28.

51. Weatherwax, W. F., "Design and Development of a Convective Air-Cooled Turbine and Test Facility," Trans. ASME, Series A, Vol. 83, January 1961, pp. 9-18.

52. Strub, R. A., "Turbomachines for Nuclear Power Plants," Sulzer Technical Review 1958, No. 3, pp. 59-69.

53. Godwin, R. P., Dennison, E. S., "Nuclear 1958 Gas Turbine Progress Report," Trans. ASME, Series A, Vol. 81, July 1959, pp. 352-359.

54. Zudans, Z., Goff, J. A., "Survey of Component Requirements and Availability for Gas-Cooled Nuclear Reactor Power Plants: Coolants," The Franklin Institute, Report I-A2392-1, NYO Report 9786, August 1961.

55. "Power Plant Design, Materials, and Seal Design Studies," Westinghouse Electric Corporation, Steam Division, Engineering Report GTM-46, Maritime Gas-Cooled Reactor Project, Contract AT(04-3)-187, October 13-15, 1958.

56. Johnson, J. R., "High Temperature Gas Cycle Reactor Power Systems," ASME Paper 57-A-274, December 1-6, 1957.

57. "Gas Cycle Reactors for Power," Nucleonics, Vol. 14, March 1956, pp. 33-66.

58. Thompson, A. S., "Gas-Cooled Nuclear Reactor Study," Studebaker-Packard Corporation, Detroit, Report AECU-3559, Contract AT(30-3)-214, July 31, 1956.

59. "15 Mw Gas-Cooled Closed-Cycle Reactor Power System Study," Ford Instrument Co., Final Report FICO-101, Volumes 1 and 2, Contract AT(30-3)-215, April 1, 1957.

60. Hammond, R. P., et al., "Turret: A High Temperature Gas-Cycle Reactor Proposal," Los Alamos Scientific Laboratory, Report LA-2198, Contract W-7405-Eng-36, January 23, 1958.

61. "Maritime Gas-Cooled Reactor Program," General Dynamics Corp., Quarterly Progress Report for the period ending December 31, 1959 Report GA-1195, Contract AT(04-3)-187.

62. "Army Gas-Cooled Reactor Systems Program; ML-1 Components Design Report," Aerojet-General Nucleonics, Report AGN TM-378, Contract AT (01)-880, July 1960.

63. "Gas-Cooled Ceramic Power Breeder Reactor. Reactor Design and Feasibility Problem," AEC Research and Development Report CF-54-8-235, August, 1954.

64. "Nuclear Power and Gas Turbines-2, Joint U.S. Swiss Design Study," Atomics and Nuclear Energy, Vol. 8, March 1957, pp. 86-92.

65. Daniels, F., "Small Gas Cycle Reactor Offers Economic Promise," Nucleonics Vol. 14, March 1956.

66. Baljé, O. E., "A Study on Design Criteria and Matching of Turbomachines, Part A - Similarity Relations and Design Criteria of Turbines," ASME Paper 60-WA-230, November 27 - December 2, 1960.

67. Robinson, S. T., "Influence of Working-Fluid Characteristics on the Design of the Closed-Cycle Gas Turbine," ASME Paper 57-GTP-13, March 18-21, 1957.

68. Frankfort, J. H., "A Conceptual Study of a 100 KW Gas-Cooled Reactor Power Plant for a Remote Location," Walter Kidde Nuclear Laboratories, Inc., Report WKNL-46(Del.), May 31, 1955, Contract AT(11-1)-339.

69. "Army Gas-Cooled Reactor Systems Program," Aerojet-General Nucleonics, The ML-1 Design Report IDO-28550, Contract AT(10-1) -880, May 16, 1960.

70. "Preliminary Hazards Summary Report for the ML-1 Nuclear Power Plant," Aerojet-General Nucleonics, Report IDO-28537, Contract AT(10-1)-880, April 22, 1959.

71. "Maritime Gas-Cooled Reactor Program," General Dynamics Corp., Quarterly Progress Report for the period ending September 30, 1960, Report GA-1738, Contract AT(04-3)-187.

72. "Maritime Gas-Cooled Reactor Program," General Dynamics Corp., Quarterly Progress Report for the period ending March 31, 1959, Report GA-1030, Contract AT(04-3)-187.

73. "Maritime Gas-Cooled Reactor Program," General Dynamics Corp., Quarterly Progress Report for the period ending June 30, 1959, Report GA-1099, Contract AT(04-3)-187.

74. "Maritime Gas-Cooled Reactor Program," General Dynamics Corp., Quarterly Progress Report for the period ending September 30, 1959, Report GA-1183, Contract AT(04-3)-187.

75. "Maritime Gas-Cooled Reactor Program," General Dynamics Corp., Quarterly Progress Report for the period ending March 31, 1960, Report GA-1259, Contract AT(04-3)-187.

76. Vavra, M. H., Aero-Thermodynamics and Flow in Turbomachines, John Wiley & Sons, New York, 1960.

77. Weske, J. R., "Fluid Dynamics Aspects of Axial Flow Compressors and Turbines," Jnl. of the Aeronautical Society, Vol. 42, 1947, pp. 651-656.

78. Flugel, G., "Der optimal erreichbare Wirkungsgrad von Stromungs-maschinen," Z.d. VDI, Vol. 96, 1954, pp. 752 - 755.

79. Eck, B., Ventilatoren, Springer, Berlin 2, Ed., 1952, p. 92.

80. Pantell, E., "Versuche uber Scheibenreibung," Forsch.-Ing. Wes., Vol. 16, 1950, pp. 97-108.

81. Koenig, C. F., "Modern Design in Heavy Duty Centrifugal Compressors," Paper presented as part of the Compressor Symposium at the ASME Winter Annual Meeting, 1960.

82. Dallenbach, F., "The Aerodynamic Design and Performance of Centrifugal and Mixed-Flow Compressors," SAE Preprint 268A for 1961 SAE International Congress, January 9-13, 1961.

83. Egli, H., "Basic Design of Turbochargers for Diesel Engines," AiResearch Industrial Division, The Garrett Corp., 1959.

84. Klapproth, J. F., "A Review of Supersonic Compressor Development," Trans. ASME, Series A, Vol. 83, 1961, pp. 258-268.

85. Rodgers, Colin, "Influence of Impeller and Diffuser Characteristics and Matching on Radial Compressor Performance," SAE Preprint 268B for 1961 SAE International Congress, January 9-13, 1961.

86. Amann, C. A., Nordenson, G. E., "The Role of the Compressor in Limiting Automotive Gas Turbine Acceleration," SAE Preprint 268F for 1961 SAE International Congress, January 9-13, 1961.

87. Stahler, F., "Transonic Flow Problems in Centrifugal Compressors," SAE Preprint 268C for 1961 SAE International Congress, January 9-13, 1961.

88. Lieblein, S., Johnsen, I.A., "Resumé of Transonic-Compressor Research at NACA Lewis Laboratory," Trans. ASME, Series A, Vol. 83, July 1961, pp. 219-234.

89. Miller, G. R., Lewis, G. W., Jr., and Hartmann, M. J., "Shock Losses in Transonic Compressor Blade Rows," Trans. ASME, Series A, Vol. 83, 1961, pp. 235-242.

90. Serovy, K., Anderson, E. W., "Method for Predicting Off-Design Performance of Axial-Flow Compressor Blade Rows," NASA Technical Note D-110, August 1959.

91. Goldstein, A. W., Schacht, R. L., "Relation Between Flow Range and Other Compressor-Stage Characteristics," NACA Research Memorandum E58B24, May 20, 1958.

92. Wilson, D., "Patterning Stage Characteristics for Wide Range Axial Compressors," ASME Paper 60-WA-113, November 27 - December 2, 1960.

93. Millar, D. O., "Considerations in the Design of Extreme Range Axial Compressors," ASME Paper 60-WA-176, November 27, - December 2, 1960.

94. Brown, L. E., Groh, F. G., "Use of Experimental Interstage Performance Data to Obtain Optimum Performance of Multistage Axial Compressors," ASME Paper 61-GTP-3, March 5-9, 1961.

95. Bullock, R. O., "Critical High Lights in the Development of Transonic Compressor," Trans. ASME, Series A, Vol. 83, 1961, pp. 243-257.

96. Savage, M., Boxer, E., and Erwin, J. R., "Resumé of Compressor Research at NACA Langley Laboratory," Trans. ASME, Series A, Vol. 83, 1961, pp.269-285.

97. Geye, R. P., Lucas, J. G., "Investigation of Effects of Reynolds Number on Over-all Performance of an Eight-Stage Axial-Flow Research Compressor With Two Transonic Inlet Stages," NACA Research Memorandum E56L11a, February 15, 1957.

98. Sievers, G. K., Geye, R. P., Lucas, J. G., "Investigation of Reynolds Number Effect on Performance of an Eight-Stage Axial-Flow Research Compressor With Long-and Medium-Chord Lengths in the Two Transonic Inlet Stages," NACA Research Memorandum E57J30, February 18, 1958.

99. Sievers, G. K., Geye, R.P., Lucas, J. G. "Preliminary of Over-All Performance of an Eight-Stage Axial-Flow Research Compressor With Two Long-Chord Transonic Inlet Stages," NACA Research Memorandum E57H14, February 10, 1958.

100. Creagh, J. W. R., "Performance Characteristics of an Axial-Flow Transonic Compressor Operating up to Tip Relative Mach Number of 1.34," NACA Research Memorandum E56D27, August 1956.

101. Wichert, K. E., "Some Investigations Into Transonic Axial-Flow Compressors With High Stage Load Coefficients and Low Degrees of Reaction," Trans. ASME, Series A, Vol. 83, 1961, pp. 286-290.

102. King, J. A., "The J83 Seven-Stage Transonic Compressor," Trans. ASME, Series A, Vol. 83, 1961, pp. 291-302.

103. Kovach, K., Sandercock, D. M., "Aerodynamic Design and Performance of Five-Stage Transonic Axial-Flow Compressor," Trans. ASME, Series A, Vol. 83, 1961, pp. 303-321.

104. Swan, W. C., "A Practical Method of Predicting Transonic-Compressor Performance," Trans. ASME, Series A, Vol. 83, 1961, pp. 322-330.

105. Wilcox, W. W., Tysl, E. R., Hartmann, M. J., "Resumé on the Supersonic-Compressor Research at NACA Lewis Laboratory," ASME Paper 58-A-177, September 17, 1958.

106. Baumgartner, F., Amsler, R., "Presentation of a Blade-Design Method for Axial-Flow Turbines, Including Design and Test Results of a Typical Axial-Flow Stage," Trans. ASME, Series A, Vol. 82, 1960, pp. 19-26.

107. Knoernschild, E. M., "The Radial Turbine For Low Specific Speeds and Low Velocity Factors," Trans. ASME, Series A, Vol. 83, 1961, pp. 1-8.

108. "Maritime Gas-Cooled Reactor Program," General Dynamics Corp., Quarterly Progress Report for the period ending March 31, 1961, Report GA-2178, Contract AT(04-3)-137.

109. Szekely, T., "Closed-Cycle Gas Turbine Nuclear Power Plants," General Electric, Atomic Prod. Div., Cin., Report APEX 410, Contracts AF33(038)-21102 and AT(11-1)-171, February 1957.

110. Reiher, Dieter, "Untersuchung bestimmter gasförminger Stoffe als Arbeitsmittel in geschlossenen Gasturbinen in Verbindung mit der Ausnutzung der Atomkernergie," MTZ, Vol. 22, October 1961. PP. 390-397

111. Baljé, O. E., "A Study on Design Criteria and Matching of Turbomachines - Part B - Compressor and Pump Performance and Matching of Turbocomponents," ASME Paper 60-WA-231, November 27 - December 2, 1960.

112. Buehning, P. G., "Uber das Verhalten von extrem Schnellaeufigen Axialmaschinen," VDI Forshungsheft 468, 1958.

113. "Semiannual Progress Report 1 January through 30 June 1961," Aerojet General Nucleonics, Report IDO-28573, August 10, 1961.

114. Adams, H. T., Elements of Internal Combustion Turbine Theory, Cambridge, University Press, 1949.

115. Rebeske, J. J., Jr., Dugan, J. F., "Matched Performance Characteristics of a 16-Stage Axial-Flow Compressor and a 3-Stage Turbine," NACA Research Memorandum E52H18, April 28, 1953.

116. Hodge, J., Cycles and Performance Estimation, Butterworths Scientific Publications, London, 1955.

117. Stys, Z. S., "Large Gas Turbines for Central Station Application," AIEE Paper 58-164, February 2-7, 1958.

118. Stys, Z. S., "4000 Kw Gas-Turbine Power Plant, Mayaguez, Puerto Rico, " ASME Miscel. Paper 59-GTP-11, March 8-11, 1959.

119. Bodner, V.A., Kazakevich, V. V., "On the Stability of Compressors as Non-Linear Elements in Distributed Systems," (Izv. Akad. Nauk, OTN Energ.; Automat., Vol. 44, pp. 116-125, 1959, U.S.S.R., Moscow) Translated by E. P. Tyrrell, J. Dunham, University of Cambridge, issued November 1960 by Technical Information and Library Services, Ministry of Aviation.

120. "St. Dizier Gas-Turbine Station of Electricité de France," Brown Boveri Review, January-February 1960, pp. 37-42.

121. Khabbaz, G., Senoo, Y., "The Influence of Tip Clearance on Stall Limits of a Rectilinear Cascade of Compressor Blades," Trans. ASME, Series D., Vol. 83, 1961, pp. 371-378.

122. Ershov, V. N., Pavlenko, G. V., "Rotating Stall in an Axial Compressor Stage," (Izv VUZ, Aviat. Tekh., Vol. 3, pp. 64-71, 1959, U. S. S. R.), Translated by E. P. Tyrrell, J. Dunham, University of Cambridge, issued November 1960, by Technical Information and Library Services, Ministry of Aviation.

123. Emmons, H. W., Kronauer, R. E., Rockett, J. A., "A Survey of Stall Propagation - Experiment and Theory," Trans. ASME, Series D, Vol. 81, 1959 p. 409.

124. Calvert, H. F., Johnson, D. F., Lucas, J. G., "Effect of Interstage Bleed on Rotating Stall and Blade Vibration in a 13-Stage Axial-Flow Compressor in a Turbojet Engine," NACA Research Memorandum E56106, January 17, 1957.

125. "Recent Developments in Superalloys," DMIC Memorandum No. 64, Defense Metals Information Center, Battelle Memorial Institute, September 8, 1960, (O.T.S. Document No. PB 161214).

126. Gayley, H. B., "Materials Keep Pace with Industrial Gas-Turbine Needs," ASME Paper 61-GTP-15, March 5-9, 1961.

127. "The ORNL Gas-Cooled Reactor - Advanced Concepts," ORNL Report 2510, Contract W-7405-Eng-26.

128. Chiarito, P. T., Johnston, J. R., "Experimental Evaluation of Cerment Turbine Stator Blades for Use at Elevated Gas Temperatures," NASA Memorandum 2-13-59E, February 1959.

129. Gasparovic, N., "Belastung und Lebensdauer der Gasturbine", Z.d. VDI, 1957, pp. 23- 24.

130. Seizfried, W., "Investigations into Blade Root Fixings of High-Temperature Steels," Sulzer Technical Review, 1958, pp. 34-52.

131. Nimwegen, R. R., "Transient Temperatures and Thermal Stress Problems in Small Gas Turbines," ASME Paper 61-GTP-13, March 5-9, 1961.

132. Signorelli, R. A., Johnston, J. R., Weeton, J. W., "Thermal-Stress Fatigue Cracking of Turbine Buckets Operated at 1700°F in a Turbojet Engine with Frequent Starts and Stops," NASA Technical Note D-125, October, 1959.

133. Signorelli, R. A., Johnston, J. R., Water, W. J. "Thermal-Stress Fatigue Cracking of Turbine Buckets Operated at 1700°F in a Turbojet Engine with Long Periods of Operating between Starts," NASA Technical Note D-272, February 1960.

134. Hamburg, Glenn, Parkinson, Jon, "Gas Turbine Shaft Dynamics," SAE Preprint 382B of 1961 Summer Meeting.

135. "Maritime Gas-Cooled Reactor Program," General Dynamics Corp., Quarterly Progress Report for period ending December 31, 1958, Report GA-744, Contract AT(04-3)-187.

136. Prohl, M. A., "A General Method for Calculating Critical Speed of Flexible Rotors," Trans. ASME, Vol. 12, September 1945.

137. Ellerbrock, H., Jr., "NACA Investigations of Gas-Turbine-Blade Cooling," Jnl. of the Aeronautical Sciences, Vol. 15, December 1948.

138. Esgar, J. B., Ziemer, R. R., "Review of Status, Methods, and Potentials of Gas-Turbine Air-Cooling," NACA Research Memorandum E54123, February 23, 1955.

139. Esgar, J. B., "Turbine Cooling," Trans. ASME, Series A, Vol. 81, 1959, pp. 226-233.

140. Calvert, H. F., Meyer, A. J., Jr., Morgan, W. C.,"Air-Cooled Turbine Blades with Tip Cap for Improved Leading-Edge Cooling," NASA Memorandum 2-9-59E, February 1959.

141. Alpert, S., Grey, R. E., Flaschar, W. O., "Development of a Three-Stage Liquid-Cooled Gas Turbine," Trans. ASME, Series A, Vol. 82, pp. 1-9.

142. Von der Nuell, W. T., "General Design, Considerations for Smaller Gas Turbines," Trans. ASME, Vol. 80, 1958, p. 941.

143. "Progress Report for Year 1959," Parsons and Marine Engineering Turbine Research and Development Association, Pametrada Research Station, Wallsend, England.

144. "English Electric EM85 Gas Turbine," Gas and Oil Power, Vol. LV, April 1960, pp. 83-87.

145. "Ruckblick auf die Entwicklung der Brown Bovery Konstruktionen im Jahre 1944, Section IC Verbrennungs-Turbinen," Brown Boveri Mitteilungen, January - February 1945, pp. 8-10.

146. Mochel, N. L., "Metallurgical Considerations of Gas Turbines," Trans. ASME, Vol. 69, August 1947, pp. 561-568.

147. "Sulzer Investment Cast Turbo Rotors and Blades," Sulzer Technical Review, 1958, pp. 19-33.

148. "Back-Room Alloys for Gas Turbines," Gas and Oil Power, Vol. LV, January 1960, pp. 9-10.

149. Betteridge, W., The Nimonic Alloys, Edward Arnold Pub. Ltd., London, 1959.

150. McCormick, H. L., "Evolution of the Cast Internally Cooled Gas Turbine Airfoil," SAE Preprint 280B for the 1961 SAE International Congress, January 9-13, 1961.

151. Thorson, M. H., "Design and Development of a Transonic Compressor for General Electric's T58 Turboshaft Engine," ASME Paper 60-WA-171, November 27 - December 2, 1960.

152. Resnick, B. T., "Technical Considerations in the Development of a Maritime Gas-Cooled System," ASME Paper 61-GTP-14, March 5-9, 1961.

153. "Army Gas-Cooled Reactor Systems Program," Aerojet-General Nucleonics, Monthly Progress Report for February 1959, Report IDO-28538, March 1959.

GENERAL USEFUL REFERENCES

Oak Ridge National Laboratory, "Rotating Machinery for Gas-Cooled Reactor Application," Report TID-7631, Proceedings of Meeting held April 2-4, 1962.

Miskell, R. V., "Effects of Major Parameters on Cycle Efficiency and Cost for a Gas-Cooled Reactor Turbine Power Plant," Union Carbide Corp., Report Y-1396 (TID-4500), Contract W-7405-Eng-26, June 19, 1962.